Megataxa 011 (1): 001–261
https://www.mapress.com/mt
Copyright © 2024 Magnolia Press

ISSN 2703-3082 (print edition)
MEGATAXA
ISSN 2703-3090 (online edition)

https://doi.org/10.11646/megataxa.11.1.1
http://zoobank.org/urn:lsid:zoobank.org:pub:5F42E7FE-C154-4979-9691-E6F74BBBBC10

MEGATAXA

11

Systematics and palaeobiology of kangaroos of the late Cenozoic genus *Protemnodon* (Marsupialia, Macropodidae)

ISAAC A.R. KERR*, AARON B. CAMENS, JACOB D. VAN ZOELEN, TREVOR H. WORTHY & GAVIN J. PRIDEAUX

College of Science and Engineering, Flinders University, Bedford Park, South Australia, Australia, 5042

Isaac A.R. Kerr: isaac.kerr@flinders.edu.au; https://orcid.org/0000-0002-8242-8195
Aaron B. Camens: aaron.camens@flinders.edu.au; https://orcid.org/0000-0003-0464-0665
Jacob D. van Zoelen: jacob.vanzoelen@flinders.edu.au; https://orcid.org/0000-0003-2952-8549
Trevor H. Worthy: trevor.worthy@flinders.edu.au; https://orcid.org/0000-0001-7047-4680
Gavin J. Prideaux: gavin.prideaux@flinders.edu.au; https://orcid.org/0000-0002-9958-0265
**Corresponding author*

Magnolia Press
Auckland, New Zealand

Submitted: 29 Aug. 2023; accepted by Z.-Q. Zhang: 22 Mar. 2024; published: 15 Apr. 2024

Licensed under Creative Commons Attribution-N.C. 4.0 International https://creativecommons.org/licenses/by-nc/4.0/

ISAAC A.R. KERR, AARON B. CAMENS, JACOB D. VAN ZOELEN, TREVOR H. WORTHY & GAVIN J. PRIDEAUX
Systematics and palaeobiology of kangaroos of the late Cenozoic genus *Protemnodon* (Marsupialia, Macropodidae)
(*Megataxa* 11)

261 pp.; 30 cm.

15 April 2024

ISBN 978-1-77973-032-9 (Paperback)

ISBN 978-1-77973-033-6 (Online edition)

FIRST PUBLISHED IN 2024 BY

Magnolia Press

P.O. Box 41-383

Auckland 1041

New Zealand

e-mail: megataxa@mapress.com

https://www.mapress.com/mt

© 2024 Magnolia Press

All rights reserved.

ISSN 2703-3082 (Print edition)

ISSN 2703-3090 (Online edition)

Table of Contents

Abstract 3
Introduction 3
Materials and methods 5
Fossil occurrences (Figs 1 & 2) 5
Taxonomic and ecomorphological methods 5
Phylogenetic methods 9
Systematic palaeontology 9
Protemnodon anak Owen, 1874 10
Protemnodon mamkurra sp. nov. 59
Protemnodon viator sp. nov. 100
Protemnodon tumbuna Flannery *et al.*, 1983 141
Remarks: 155
Protemnodon dawsonae sp. nov. 156
Remarks: 169
Protemnodon otibandus Plane, 1967 169
Remarks: 187
Holotypes of P. chinchillaensis ***and*** P. devisi 187
Identities of P. otibandus ***and*** P. chinchillaensis 187
Protemnodon snewini Bartholomai, 1978 188
Remarks: 189
Status of other species previously referred to *Protemnodon* 189
Australian Pleistocene species 189
Nombe nombe 191
Pliocene species 193
Results 194
Skeletal dimensions and proportions 194
Phylogenetic analysis 212
Distributions 214
Discussion 217
Taxonomic implications 217
Phylogenetic relationships 217
Diet 218
Neck morphology 218
Locomotion 218
Body size and mass 225
Palaeoecology 226
Conclusion 228
Acknowledgements 229
Funding 229
Author contributions 229
References 229
Comparative figures 239
Additional tables 249

Abstract

Species of the kangaroo genus *Protemnodon* were common members of late Cenozoic communities across Australia and New Guinea until their extinction in the late Pleistocene. However, since the genus was first raised 150 years ago, it has proven difficult to diagnose, as have the species allocated to it. This is due primarily to the incompleteness of the type material and a heavy reliance on cheek tooth size and slight variations in premolar form. Along with the rare association between cranial and postcranial material, this has hampered understanding of the palaeobiology of these large-bodied kangaroos. Here we review and re-diagnose *Protemnodon*, recognising a total of seven species and providing a hypothesis of species interrelationships. The following new synonymies are made: *Protemnodon chinchillaensis* is synonymised with *P. otibandus* and *P. hopei* with *P. tumbuna*. The following are considered *nomina dubia*: *Protemnodon brehus*, *P. roechus*, *P. mimas*, *P. antaeus*, and *P. devisi*. We reveal that the morphology of the cheek dentition is not as consistently useful for differentiating species of *Protemnodon* as features of the cranium and postcranial skeleton. As a whole, the species share anatomical features that reflect stability and power in the limb joints, yet they differ in body proportions, and axial and limb morphology. This we interpret as showing locomotory adaptations to different habitats. Of the three Pliocene species, *Protemnodon snewini* is interpreted as a medium- to high-geared hopper, suggesting proficiency in more open environments, whereas *P. dawsonae* **sp. nov.** we infer to have been a medium-geared inhabitant of eastern Australian forests and woodlands. *Protemnodon otibandus*, with a range extending through the woodlands and forests of eastern Australia into the rainforests of eastern New Guinea, displays adaptations to slower hopping. Its Pleistocene descendant, *P. tumbuna*, is convergent on the morphology of modern New Guinea forest wallabies, and was likely facultatively quadrupedal. Of the three Australian Pleistocene species, the long-necked *P. anak* is hypothesised to have been a large, medium-geared, eastern Australian species, and *P. mamkurra* **sp. nov.** a robust, low-geared resident of well-wooded southern Australia habitats. By contrast, *P. viator* **sp. nov.** was larger but more gracile, suggested to be a medium- to high-geared species convergent in some traits on large extant kangaroos. This and a wide inland distribution point to adeptness in open, arid environments. *Protemnodon mamkurra* **sp. nov.** and *P. viator* **sp. nov.** occupy the morphospace previously occupied by *P. roechus* and *P. brehus*. Overall, the species of *Protemnodon* exhibit a degree of ecomorphological variation suggestive of a broader array of ecological adaptations than hitherto envisioned.

Keywords: Australia, New Guinea, Biogeography, Quaternary, Phylogeny, Morphology, Adaptation, Megafauna

Introduction

The family Macropodidae (kangaroos, wallabies, and their kin) is a diverse group of living marsupials from Australia and New Guinea, with representatives in nearly all terrestrial ecosystems (Frith & Calaby 1969; Maynes 1989). The evolutionary origins of Macropodidae lie in the widespread forests of late Oligocene–early Miocene Australia, in the form of small, terrestrial or scansorial herbivores (Long *et al.* 2002; Travouillon *et al.* 2014) that moved by either bounding quadrupedally or hopping bipedally (Janis *et al.* 2016). By the Pliocene, two subfamilies were the most widespread and diverse: the short-faced, now-extinct, browsing (dicot-consuming) sthenurines (Prideaux 2004; Arman 2017), some of whom may have stridden bipedally (Janis *et al.* 2014), and the bipedally

hopping macropodines (Prideaux & Warburton 2010). The crown tribe Macropodini, which contains the large, grazing (grass-eating) and mixed-feeding (consuming a grass/dicot combination) kangaroos (Dawson 1989; Jarman & Phillips 1989; Prideaux & Warburton 2010; Cascini *et al.* 2019), radiated rapidly in response to the spread of grasslands across much of Australia in the mid-Pliocene (Couzens & Prideaux 2018). This grassland expansion likely drove the evolution of grazing- and open-habitat-related features such as large body size, faster and more efficient bipedal saltation, and higher-crowned molars (Helgen *et al.* 2006; Prideaux & Warburton 2010; Mitchell *et al.* 2018). This broad vision of the evolutionary direction of Macropodini, however, overlooks a small number of taxa that do not have clear grazing adaptations, for example *Congruus kitcheneri* (Flannery, 1989), which is hypothesised to have secondarily developed arboreality (Warburton & Prideaux 2021). Species of the macropodin genus *Protemnodon* Owen, 1874 have long been considered palaeoecologically varied (Bartholomai 1973; Archer *et al.* 1994; Menzies & Ballard 1994; Helgen *et al.* 2006; Kear *et al.* 2008), but this is primarily based on incomplete and fragmentary dental remains with limited postcranial associations.

Many studies have identified specimens only to genus level or demonstrated reluctance in allocating material, often despite possession of more intact and complete specimens than the relevant type material (see *e.g.*, Flannery 1984; Flannery & Gott 1984; Pledge 1990, 1992; Louys & Price 2015; Hocknull *et al.* 2007; Montanari *et al*. 2013; Hocknull *et al.* 2020), and thus utilise terms like '*Protemnodon* sp.' or 'the large Pleistocene Australian species of *Protemnodon*'. This demonstrates a lack of clarity and utility in the diagnoses of the species, regardless of the quality of the material in question. Difficulty in identifying material that is accepted as *Protemnodon* to species level has hamstrung palaeoecological investigations and the ecomorphology of most species remains unclear and understudied.

The position of *Protemnodon* within Macropodini is now well established by both molecular (Llamas *et al.* 2015; Cascini *et al.* 2019) and morphological (Prideaux & Warburton 2010) data. Within *Protemnodon*, the evolutionary relationships have not been investigated. It was suggested by Flannery (1994), based on geographic ranges and on the similarity of the dentition, that the two species from the Pleistocene of New Guinea were descended from the sole Pliocene New Guinean species, but for the remainder of the species there is no published phylogenetic hypothesis.

Fossils of *Protemnodon* from the Pliocene and Pleistocene have been found across much of continental Australia and New Guinea (Dawson 2004; Webb 2008). Species are thought to have ranged between 50 and 170 kilograms adult body mass, making the larger specimens among the heaviest kangaroos to have existed (Helgen *et al.* 2006; Wagstaffe *et al.* 2022). Members of *Protemnodon* have been described as having hindlimb proportions similar to those seen in the specialised bipedal hopping species of *Notamacropus* Dawson & Flannery, 1985 and *Macropus* Shaw, 1790, but with more robust hindlimb elements and shorter and stouter tarsals, implying adaptation to slower movement over shorter distances (Kear *et al.* 2008). Further, differences in hindlimb proportions between the species of *Protemnodon* have been used to imply that locomotory patterns varied, with those inhabiting New Guinea described as having adaptations to slow, possibly quadrupedal, locomotion, in contrast to the Australian species, which were purportedly higher-geared (that is, faster and more efficient hoppers) (Archer *et al.* 1994; Flannery 1994; Kear *et al.* 2008). More recent studies have challenged the latter idea to an extent, interpreting a slow and probably quadrupedal gait for the Australian Pleistocene species of *Protemnodon* (Janis *et al.* 2020; Jones *et al.* 2021; Wagstaffe *et al.* 2022; Janis *et al.* 2023) despite trace fossils attributed to *Protemnodon* indicating a hopping gait (Belperio & Fotheringham 1990; Carey *et al.* 2011).

At the outset of the present study, *Protemnodon* formally contained the following ten species: *Protemnodon anak* Owen, 1874, *Protemnodon brehus* (Owen, 1874), *Protemnodon roechus* Owen, 1874, *Protemnodon otibandus* Plane, 1967, *Protemnodon chinchillaensis* Bartholomai, 1973, *Protemnodon devisi* Bartholomai, 1973, *Protemnodon snewini* Bartholomai, 1978, *Protemnodon tumbuna* Flannery *et al.*, 1983, *Protemnodon nombe* Flannery *et al.*, 1983, and *Protemnodon hopei* Flannery, 1992a. Owen (1874, 1877) described five species of *Protemnodon* from localities in eastern Australia. Later, Lydekker (1887) reallocated '*Sthenurus*' *brehus* Owen, 1874 to *Protemnodon*, resulting in a total of six species accepted at the end of the 19th century. Initiated by Trouessart (1904), and followed by Tate & Archbold (1937) and Raven (1929), *Protemnodon* was considered to contain some species of *Wallabia* Trouessart, 1904, due to similarity in their cheek teeth. Stirton (1963) removed all extant species from *Protemnodon*, reestablishing *Protemnodon* as a genus containing only extinct species, an arrangement since unanimously accepted. Stirton included a comprehensive review of the taxonomic history of the genus, which clarified and stabilised its identity.

The addition of further species to *Protemnodon* began with the description by Plane (1967) of *P. otibandus* and *P. buloloensis* Plane, 1967 from the late Pliocene Papua New Guinean Otibanda Formation. Bartholomai (1973) reviewed the material from the Australian Pleistocene, accepting three species (*P. anak*, *P. brehus* and *P. roechus*) and describing *P. chinchillaensis* and *P. devisi* from the Pliocene Chinchilla Sand In eastern Australia. Understanding of the geographical and temporal spread of the genus continued to improve: Bartholomai (1978) described *P. snewini* from the early Pliocene Allingham Fm. in northeastern Australia; Flannery *et al.* (1983) described *P. tumbuna* and *P. nombe* from the late Pleistocene Nombe Rockshelter of Papua New Guinea; Flannery (1992a) added *P. hopei* from Pleistocene West Papua; and Dawson *et al.* (1999) described *P. bandharr* Dawson, Muirhead & Wroe, 1999 from the Pliocene Big Sink deposit in eastern Australia in a partial review of the taxonomy of the genus, Dawson (2004) removed '*P.*' *bandharr* and '*P.*' *buloloensis* from *Protemnodon*, placing them into a new genus, *Silvaroo* Dawson,

2004. The identity of *Protemnodon* and its species has since remained unchanged. In the period following the last complete review of the genus, various associated specimens including multiple complete skeletons have been discovered from the Australian Pleistocene, including from, and Lake Callabonna in South Australia. This new material, much of which is described and figured for the first time here, provided the basis for our review of *Protemnodon*. With analyses conducted as part of this review, *Protemnodon nombe* was moved by Kerr & Prideaux (2022) to a new monotypic genus, *Nombe* Kerr & Prideaux, 2022.

With the discovery of better-preserved fossils, including associated and articulated skeletons, it became clear that the current species-level taxonomy was unstable and required systematic revision. Therefore, the chief objectives of this taxonomic review were to revise and improve the diagnosis of the genus *Protemnodon*; and to re-examine the validity of each currently recognised species using comparative dental and skeletal morphology, with a focus on better-preserved and associated fossils. We also conduct a morphological cladistic analysis and present hypothesised evolutionary relationships within *Protemnodon*, incorporating a range of discrete craniodental and postcranial osteological characters. Supplementing this review, a further objective is to make functional inferences about the locomotory capabilities of species of *Protemnodon* based on biomechanical principles and comparisons with extant macropodines. We combine functional morphological deductions with an improved understanding of species geographic distributions to make inferences about the palaeoecology of the species of *Protemnodon*.

Materials and methods

Fossil occurrences (Figs 1 & 2)

Taxonomic and ecomorphological methods

Format of the review

A list of all synonyms—*nomina nuda*, junior synonyms and misidentifications—accompanies each taxonomic group. The formats of the *nomina* listed are as follows: for primary synonyms, the complete *nomen* including genus, species author and date, separated by a colon from the full reference; for secondary synonyms (different generic combinations, incorrect referrals, or spelling errors), the binomial and author are separated by a semicolon from the reference to that usage, *e.g.*, *Halmaturus anak* (Owen); Krefft (1875). All taxonomically significant material that was undescribed and is attributable to a species is used in the revised taxon diagnoses, where relevant. Descriptions and comparisons are deliberately rigid and grid-like in structure for ease of navigation by readers. The amount of morphological difference or variation deemed 'acceptable' within a taxon in this study will be informed primarily by the variation seen within the sample of the easily recognised and relatively well-sampled type species, *P. anak*, as well as by the variation seen within the sample of extant taxa (see below). Diagnoses are arranged with synapomorphies first in the case of the generic diagnosis and autapomorphies first for species diagnoses, followed by lists of differences to similar taxa arranged by body section. Where an element is not known for one or more species, the generic diagnosis has been made on the basis of the species for which that element is known.

The Pleistocene species are dealt with first, beginning with the type species, followed by the Pliocene species. A section discussing taxonomic acts and arguments concerning taxa considered *nomina dubia* etc. is situated after the generic diagnosis, titled 'Status of other species of *Protemnodon'. Protemnodon snewini* is not redescribed, as no new material is known for the species and the definition remains largely unchanged. It is included in the comparative figures. The dentitions of *P. tumbuna* and *P. otibandus* are not redescribed, as their original descriptions suffice.

Referred specimens

The 'Referred specimens' listing in the 'Systematic palaeontology' section includes all specimens that are here referred to a taxon following direct observations. All specimens previously listed for a species in a publication were examined where possible; only those that were directly observed and had their identity confirmed are listed in Referred specimens. We examined material widely, including in almost all main Australian museums and several international collections, as detailed below under 'Data collection'.

Included and comparative taxa

Detailed comparisons were made with the following macropodine taxa: *Congruus kitcheneri*, *Macropus fuliginosus* Desmarest, 1817, *Osphranter rufus* (Desmarest, 1822) and *Wallabia bicolor* (Desmarest, 1804). For a list of compared specimens, see Appendix Table 1. Morphological comparisons of all possible elements were made between all species of *Protemnodon*. Dental, cranial, and skeletal morphological comparisons focused on *C. kitcheneri* and *W. bicolor* on the basis of their taxonomic and morphological similarity, and for palaeoecological comparison. *Macropus fuliginosus* and *O. rufus* were compared due to the similarity of particular elements, to compare and contrast palaeobiological adaptations, and, due to the larger sample size available for specimens of these two species, to help gauge allometric changes in species of *Protemnodon*.

Data collection

Specimens from the collections of the following Australian institutions/collections were analysed: Western Australian Museum (WAM), Perth; South Australian Museum (SAMA P/M) and Flinders University Vertebrate Collection (FUR), Adelaide; Museums Victoria (NMV P),

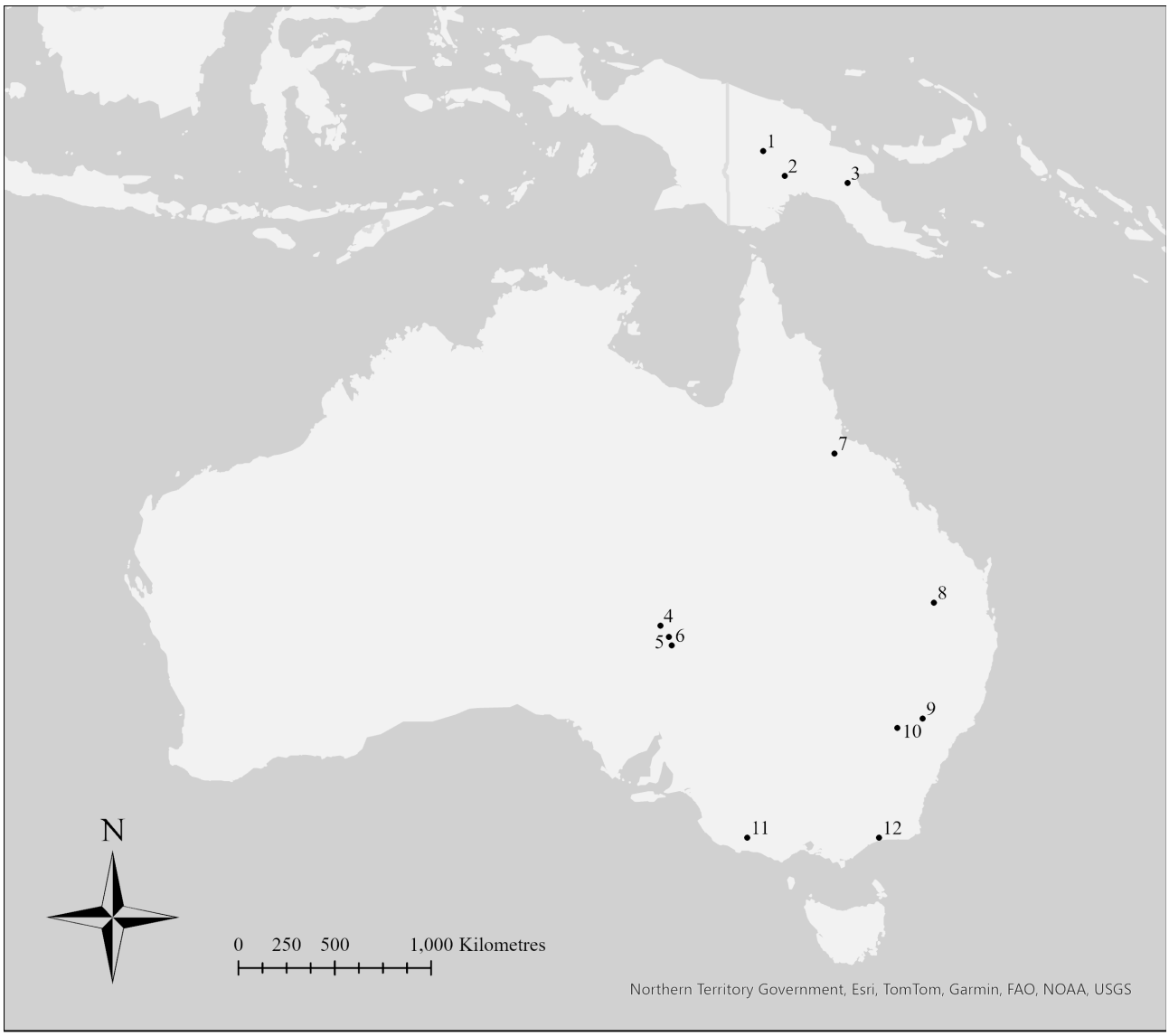

- **Pliocene localities yielding material of *Protemnodon***

FIGURE 1. map showing locations of Pliocene deposits in Australia and New Guinea yielding material of species of *Protemnodon*, including that not confidently referable to species level. 1, Mogorafugwa, Hela Province; 2, Lower Kikori River, Gulf Province; 3, Otibanda, Morobe Province; 4, Toolapinna Waterhole, Warburton River; 5, Site 4, Lake Kanunka; 6, Lawson–Daily Quarry, Lake Palankarinna; 7, Bluff Downs, Allingham; 8, Rifle Range/Sand Scree locality/Chinchilla, Chinchilla Sands; 9, Bow, Hunter Valley; 10, Big Sink, Wellington Valley; 11, Hamilton, Glenelg Shire; 12, Lake Tyers, East Gippsland Shire.

Melbourne; Queensland Museum (QM F/JM), Brisbane; Australian Museum (AM F), Sydney; Queen Victoria Museum and Art Gallery (QVM GFV), Launceston; and Australian National Wildlife Collection (ANWC M) and GeoScience Australia (CPC), Canberra. Specimens were analysed from the following international institutions: Papua New Guinea National Museum and Art Gallery (PNG/PM/NCA), Port Moresby, Papua New Guinea; University of California Museum of Paleontology (UCMP), Berkeley, California, USA; Smithsonian National Museum of Natural History (NMNH PAL), Washington D.C., USA; American Museum of Natural History (AMNH FM), New York, USA; and the Natural History Museum (NMHUK PVOR/PVM), London, UK. Specimens were also included from the private collection of Mr Ian Sobbe (IS V), Clifton, Queensland. Scanning priority was given to more complete, better-preserved, associated, and/or taxonomically significant specimens. For this reason some fragmentary material from museum collections was not scanned and photographed.

A subset of the best-preserved specimens was photographed using a Canon EOS 5DSR with 100 mm and 35 mm lenses, processed in image-processing application Capture One 21 Pro 12.4.1 and compiled ('focus stacked') in image-compilation program Zerene Stacker 1.04. Three-dimensional surface scans were collected from all specimens for which scanning permissions were obtained, with a Shining 3D 'EinScan Pro+ Handheld' scanner and

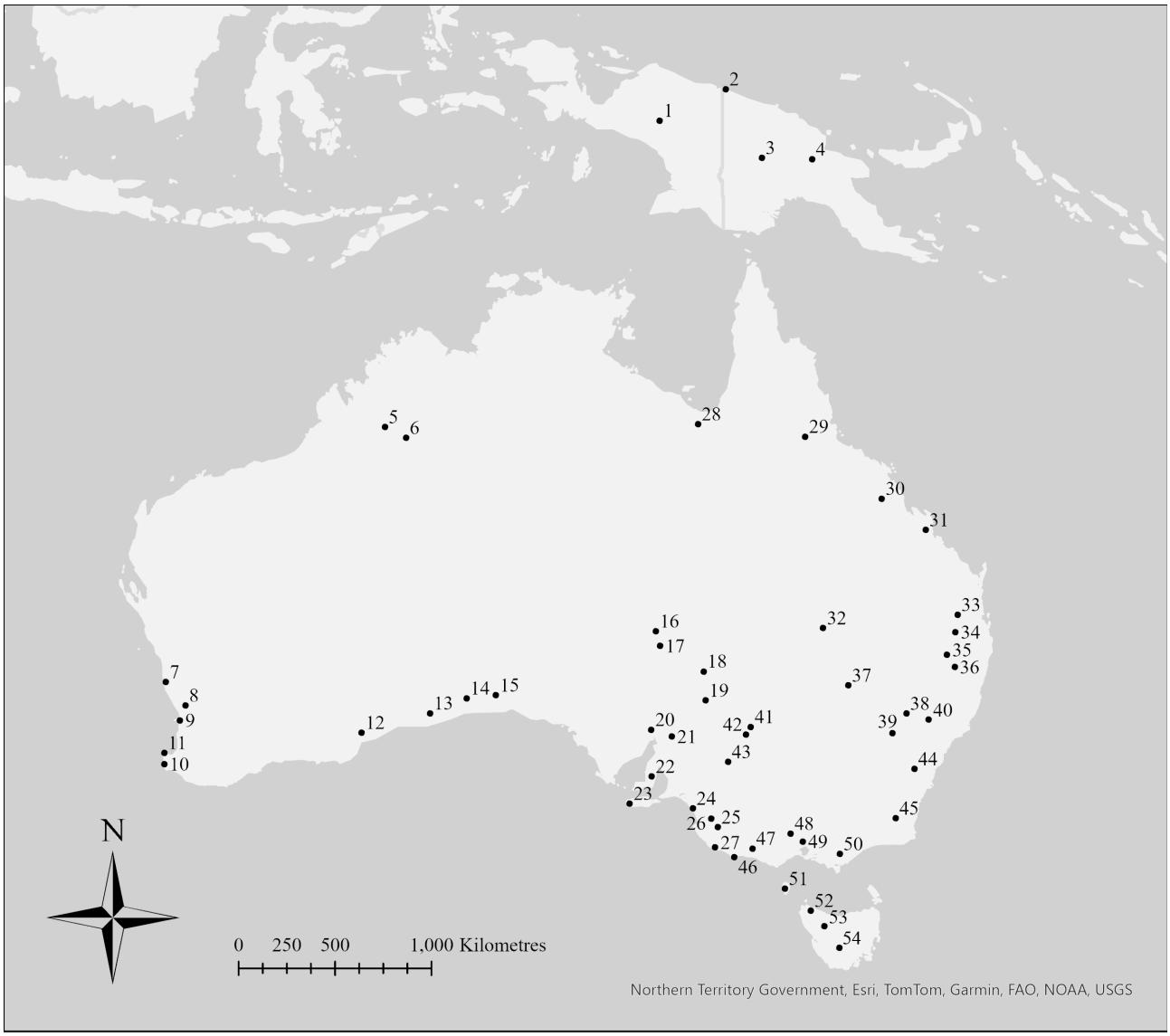

- **Pleistocene localities yielding material of *Protemnodon***

FIGURE 2. map showing locations of Pleistocene deposits in Australia and New Guinea yielding any material of species of *Protemnodon*, including that not confidently referable to species level. 1, West Baliem River/Kelangurr Cave; 2, Lachitu Cave; 3, Haeapugua Basin/Pureni; 4, Nombe Rockshelter; 5, Quanbun Station; 6, Christmas Creek; 7, Hastings Cave; 8, Gingin; 9, Leighton marshalling yards, Perth; 10, Devil's Lair/Kudjal Yolgah Cave/Mammoth Cave/Strong's Cave/Tight Entrance Cave; 11, Crystal Cave; 12, Balladonia Station; 13, Madura Cave/Horseshoe Cave; 14, Last Tree Cave/Leaena's Breath Cave; 15, Moonera Station; 16, Keekalanna Soakage/Lookout/Pompapillina/Whip Well, Warburton River; 17, Cooper's Last/Kutjitara Waterhole/ Malkuni Waterhole/Piranna Waterhole/Site 072/Site 072b/Site 073/Site 075/Sleeping Dog Cliff/Waralamanko Waterhole, Cooper Creek; 18, Lake Callabonna; 19, Billeroo Creek; 20, Dempsey's Lake/ Boolcunda Creek, Port Augusta; 21, Baldina Creek/Black Rock Gravel Pit, Burra; 22, Curramulka Town Well Cave; 23, Rocky River; 24, Salt Creek; 25, Comaum Forest Cave/Henschke's Quarry Cave/Robertson Cave; 26, Cave A/213/Goulden's Hole/Green Waterhole Cave/Kilsby's Hole; 27, Blanche Cave/Specimen Cave/Victoria Fossil Cave/Wombat Cave; 28, Floraville; 29, Wyandotte Creek; 30, South Walker Creek; 31, Mt Etna; 32, Nulla Station; 33, Emu Creek/Thorndale; 34, Condamine River/Gowrie Creek/Hodgson Creek/King's Creek/Umbiram Creek, Darling Downs; 35, Russenden Cave, Texas Caves; 36, Bingara/Dundee; 37, Cuddie Springs; 38, Lake Keepit/Mullaley/Weetalibah; 39, Wellington Caves; 40, Warrah Creek/Cuan Station; 41, Lake Menindee; 42, Lake Tandou; 43, Bone Gulch/Fisherman's Cliff/Lake Victoria; 44, Wombeyan Caves; 45, Teapot Creek; 46, Nelson Bay; 47, Childer's Cove/North Tarrone/Spring Creek; 48, Lake Weeranganuk/Bald Hills/Lake Colongulac/Lake Milangil; 49, Bacchus Marsh/Batesford Quarry/Dog Rocks/Jackson's Creek / Lancefield Swamp/Merri & Bone Creeks/Dry Creek; 50, Morwell Coal Mine; 51, King Island; 52, Scotchtown Cave; 53, Bone Aven (CP213), Mt Cripps; 54, 'no-name cave' (JF155), Florentine River valley.

tripod and turntable. Use of the tripod and turntable allowed 'fixed scans' of specimens smaller than ~300 mm across, accurate to 240 microns. Hand-held or 'rapid' scans were taken of specimens larger than ~300 mm, which are accurate to 700 microns. Specimens for which scanning permission could not be obtained were photographed and measured. Point cloud scan files (.rge) were processed ('meshed') into triangle meshes (.stl) in EinScan Software V3.0 before being imported into the 3D mesh processing application MeshLab 2020.03 (Cignoni *et al.* 2008) for digital collection of measurements and morphological descriptions. Files in MeshLab were viewed at 40.8 FOV (field of view) for consistency and to best imitate the appearance of physical fossils. Three-dimensional graphics program Blender 2.90.1 (Blender Online Community 2018) was used to rearticulate associated specimens and to render high-quality images of scans for figures in orthographic view.

The digital rendering of images of surface scanned specimens used to produce many of the figures herein is not a traditional method of displaying the morphology of palaeontological specimens. However, it is increasingly widely used, and is considered reasonable here due to: 1, the utility of the 3D nature of the scans, which can be viewed from any angle and accurately measured, and many of which are accessible online via MorphoSource.org; and 2, the logistical challenges presented by reviewing all material of species of *Protemnodon*, specimens of which number in the thousands and are spread across more than 14 institutions in five countries. The surface scan images are used only where focus-stacked photographs could not be obtained. To help clarify terminology and morphological features, line drawings accompany the photographs/surface scan images of an element the first time it is described within the paper. Line drawings are also given for articulated specimens deemed especially significant.

Locations shown in generic and specific distributions are taken from the describing study where available, or represent an approximate location. They are not intended to illustrate an exact location, but to give an idea of geographic range. Different sites are conflated into a single point in various cases to prevent the map from becoming too cluttered. Oldest and youngest dates provided for each species are in reference to the few dated sites and dated specimens, made with reference to FosSahul 2.0 (Peters *et al.* 2019) and Prideaux (2006). The vast majority of sites yielding material of *Protemnodon* have not been directly dated, and so we consider it unlikely that these dates represent the full temporal range of the species.

Skeletal dimensions and proportions

Element measurements targeted total articular lengths and minimum widths across shafts for examination of robustness and length ratios, relative positions of significant muscular attachments, and heights and widths of articular facets. Measurements of the dentary were adapted from Plane (1967). Dental measurements targeted lengths, maximum widths across anterior and posterior lophs/lophids, and posterior lophid crown heights, following the method of Prideaux (2004). Physical measurements were taken with Absolute Digimatic digital callipers and digital measurements were taken using point-to-point measurements on MeshLab 2020.03.

In the case of the femur, the maximum length typically measured by palaeontologists is from the tip of the greater trochanter to either the trochlea or the distal margin of the medial condyle. Only one femoral specimen of *Protemnodon* preserves a complete greater trochanter, so for the purposes of examining hindlimb dimensions and proportions, femoral length was taken from the centre of the articular surface of the femoral head to the distal extremity of the medial condyle, following Dawson *et al.* (2015).

Discrete and continuous data were arranged in Microsoft Excel 2019 16.0.6742.2048. The data computation and analysis program RStudio 1.1.463 (RStudio Team 2020), using R x64 3.6.2 with packages 'ggplot2', 'dplyr', 'tidyr' and 'RColorBrewer', was used to produce plots of absolute and relative craniodental and postcranial dimensions to visualise continuous specimen data. Principal Component Analyses (PCA) were not undertaken due to the high percentage of missing data in the dataset. The complete morphometric dataset is available in the Supplementary Information, along with a subset showing the ranges (minimum–maximum) for each measurement by species.

Terminology and abbreviations

Sequential numeration of the dentition follows Flower (1867), Wilson & Hill (1897), and Luckett (1993). Dental nomenclature follows Prideaux (2004). Upper and lower dentitions are designated using upper and lower case, *e.g.*, M2 (upper second molar) or i1 (lower first incisor). The two deciduous premolars, those replaced by the permanent third premolar, are referred to as dp2/DP2 and dp3/DP3 (lower/upper). Postcranial nomenclature follows Warburton *et al.* (2019), neurocranial nomenclature follows Beck *et al.* (2022), and where necessary, terminology more specific to species of *Protemnodon* follows Stirton (1963). Nomenclature of muscle attachment areas follow Warburton (2009) for jaw musculature, Warburton *et al.* (2013) and Hopwood (1974) for the forelimb, Hopwood & Butterfield (1990) and Warburton *et al.* (2012) for the hindlimb, and Dawson *et al.* (2014) for the tail.

Descriptions of the cheek teeth are made in occlusal view unless otherwise stated. Depth or the condition of being deep refers to craniocaudal dimensions, unless describing the degree of concavity of a fossa or foramen. In descriptions of the manus, palmar is used to refer to the direction of the underside of the manus, while plantar is used to refer to the direction of the underside of the pes. Proximal/distal are used in descriptions of the digits (metacarpals/metatarsals and phalanges) of the manus and pes, but anterior/posterior are used for the same directions in descriptions of the carpals, and cranial/caudal in the tarsals. This was done to avoid confusion in elements with differing proximal/distal directions, such as the pisiform

or the calcaneus. The terminal phalanx of the digits is referred to as the distal phalanx, rather than ungual. Left and right are abbreviated to 'L' and 'R', and where both sides of an element are present in a specimen 'LR' is used. 'Fm.' is used for geological formations.

Phylogenetic methods

Included taxa

The phylogenetic analysis included: the seven species of *Protemnodon* recognised herein, *C. kitcheneri*, *W. bicolor*, *O. rufus*, *M. fuliginosus*, with *Thylogale billardierii* (Desmarest, 1822) as an outgroup taxon. *Congruus kitcheneri* and *W. bicolor* were included due to the close relationship between these taxa and *Protemnodon* (Stirton 1963; Prideaux & Warburton 2010; Cooke *et al.* 2015; Cascini *et al.* 2019; Warburton & Prideaux 2021). *Macropus fuliginosus* and *O. rufus* were included as they are members of the crown '*Macropus*' complex (Cascini *et al.* 2019; Celik *et al.* 2019) and to help identify homoplasious characteristics associated with adaptations to open habitats in derived species of *Protemnodon*. *Thylogale billardierii* was selected as the outgroup taxon because it is a relatively unspecialised (as opposed to, for example, *Dendrolagus* Müller, 1840 or *Petrogale* Gray, 1837) non-macropodin macropodine (Prideaux & Warburton 2010; Cascini *et al.* 2019; Westerman *et al.* 2022). For a list of phylogenetic reference specimens, see Appendix Table 2.

Character selection

States for a total of 85 discrete characters (39 craniodental and 46 postcranial) were scored from direct observation of physical specimens or of 3D scans. Characters were identified from observation and/or mensuration, identified from the literature (*e.g.*, in studies of macropodid myology), or taken or reworked from Prideaux & Warburton (2010). New characters were informed by features shown to be taxonomically significant among species of *Protemnodon* in the taxonomic analysis. The best-known parts of the skeleton for the species of *Protemnodon* are the teeth, the dentary, and the hindlimbs, particularly the pes. Some postcranial material is known for all species of *Protemnodon*, but the material of the species from the Pliocene is broadly more fragmentary and less well-preserved. This had some effect on the selection of characters, with a slight bias toward features of more commonly preserved areas of the body. For a detailed list of characters, states, and their source and justification, see Appendix Table 3.

Strong sexual dimorphism in body size and proportions is well-known in large, extant macropodine species and is associated with inter-male competition for mating rights (Ganslosser 1989; Jarman 1989). This dimorphism is most pronounced in the proportions and musculature of the forelimbs, particularly of the humerus, as powerful forelimbs are key in the ritualised 'boxing' bouts between males (Jarman 1989; Warburton *et al.* 2013). Due to the confounding effects of positive allometry and of larger musculature on the morphology of much of the humerus, osteological characteristics pertaining to the musculature of the upper forelimb were not included in the matrix. Sexual dimorphism in species of *Protemnodon* is to be discussed in an upcoming publication.

Analysis

The character matrix was edited in the biological data organisation and analysis program Mesquite v3.70 (Maddison & Maddison 2021). A parsimony analysis was undertaken using a New Technology search in command-line TNT v1.5 software (Goloboff *et al.* 2008). Characters were unweighted and unordered (non-additive). The 'BBREAK+TBR' branch-swapping search method in TNT was used (100,000 trees held, 10,000 replications, ten starting trees for each replication). Nodes with <50% bootstrap support were collapsed into polytomies. The most parsimonious trees, a strict consensus tree, and bootstrap and jacknife values, were generated and exported to tree-editing program FigTree v1.4.4 and to Adobe Illustrator v25.4.1 for formatting. The character matrix is available in the Supplementary Information.

Systematic palaeontology

Class MAMMALIA Linnaeus, 1758

Order DIPROTODONTIA Owen, 1866

Suborder MACROPODIFORMES Kirsch *et al.*, 1997

Superfamily MACROPODOIDEA Gray, 1821

Family MACROPODIDAE Gray, 1821

Subfamily MACROPODINAE Gray, 1821
Tribe MACROPODINI Gray, 1821

Genus *PROTEMNODON* Owen, 1874

Protemnodon Owen, 1873; *Proc. Roy. Soc. Lond*. 21, p. 128 (*nomen nudum*).

Protemnodon Owen, 1874: *Phil. Trans. Roy. Soc.* 164, p. 274–275.

Type species: *Protemnodon anak* Owen, 1874, p. 278.

Revised diagnosis:

Within Macropodinae, the species of *Protemnodon* most closely resemble those of *Congruus* McNamara, 1994 and *Wallabia* in craniodental features. Species of *Protemnodon* differ from all known macropodines in having: an ilium with a highly reduced cranial iliac spine, a craniocaudally deeper caudal iliac spine and an associated deeply concave gluteal fossa; and a middle pedal phalanx IV that is short, broad, and highly dorsoplantarly compressed, with its shaft only slightly narrower than the distal end.

Protemnodon *vs* Congruus

Species of *Protemnodon* and *Congruus* share 14 thoracic and five lumbar vertebrae to the exclusion of all other macropodines, which have 13 and six, respectively. Dentally, the species of *Protemnodon* are distinguished from those of *Congruus* by having longer premolars relative to molars and a more dorsally inclined lower incisor. Species of *Protemnodon* differ from species of *Congruus* in the following cranial attributes: cranium larger and more robust; premaxilla lacks an anterior sulcus within the nasal cavity, and is taller and more robust anteriorly; nasal less domed and less anteriorly projected; larger masseteric process; thicker, less laterally projected orbital lip on jugal; taller zygomatic arch; foramen ovale with a single anteroposterior ridge abutting the medial margin, rather than being abutted at the anterior by a shallow but distinct anteroposterior groove; occipital condyles that project posteriorly well beyond the posterior margin of the nuchal crest and occiput; and a broader foramen magnum relative to occipital height and width. The dentary of the species of *Protemnodon* differs from those of *Congruus* in its more inflected diastema, more posteriorly situated mental foramen, and deeper medial pterygoid fossa with higher posterior margin.

The forelimb differs by having: humerus more robust, with more dorsally projected greater and lesser tubercles and a deeper proximal shaft that deepens proximally; proximal ulna more transversely compressed; more elongate metacarpals; and manual phalanges considerably more dorsopalmarly compressed, particularly the distal phalanges. Within the hindlimb, species of *Protemnodon* are distinguished from those of *Congruus* by: a pelvis with a broader ilium and a smaller, blunter iliopubic eminence; straighter femur in dorsal view with a larger, more dorsally deflected head, more distally extensive lesser trochanteric ridge, less medially displaced quadratus tubercle, and a more proximally situated lateral gastrocnemial fossa; tibia with a deeper, flatter and more distinct distal fibular facet; talus with a more caudoplantarly extensive navicular facet, and a cuboid facet on the navicular head; a taller, narrower navicular; a more robust metatarsal IV; metatarsal V with a proximal plantar groove present, larger lateral plantar tuberosity and medial plantar tubercle, and lacking a slight kink of the arch of the shaft immediately proximal to midpoint in lateral view; and dorsoplantarly shorter distal phalanges with a more rounded dorsal peak and a less plantarly curved shaft.

Protemnodon *vs* Wallabia

Besides greater size, species of *Protemnodon* differ from those of *Wallabia bicolor* in the following ways. Their dentitions are distinguished by: P3 with larger posterolingual basin relative to length of P3; and upper molars with postparacrista and premetacrista that curve or deflect lingually toward the centre of the interloph valley, rather than continuing straight from the cones along the buccal margin of the lophs to merge above the buccal edge of interloph valley. The cranium differs in: a more ventrally projected anterior part of the premaxilla; nasal less convex and less anteriorly projected; masseteric process anteroposteriorly shorter and more ventrally projected; occipital condyles that project posteriorly well beyond the posterior margins of the nuchal crest and occiput; foramen magnum broader relative to the posterior cranium height; a more raised anteroposterior ridge meeting the medial margin of the foramen ovale; and a more laterally projected postglenoid process.

The forelimb differs in its humerus with a more medially projected humeral head, lower (less raised) and less elongate deltoid tuberosity, straighter pectoral crest, and a broader lateral supracondylar ridge; and ulna with olecranon lacking cranial deflection. The manus differs in its deeper, squarer capitatum. The hindlimb differs in its pelvis with broader ilium and more rounded, less projected iliopubic eminence; and femur with larger, more dorsally deflected femoral head and less dorsoventrally compressed distal shaft. The pes is differentiated by: calcaneus with a broader medial talar facet; talus with a more rounded posterior plantar process in medial view; metatarsal IV more robust; metatarsal V with larger proximolateral process relative to metatarsal V length; and broader pedal phalanges relative to length.

Etymology:

Greek, neutral gender; *pro* (before), *temno* (to cut), *odous* (tooth). '…in reference to the sectorial form of the anterior molar or premolar' (Owen 1874, p. 274).

Remarks:

We contend that *Protemnodon anak* was designated the type species for the genus by Owen (1874) when he described *Protemnodon mimas* Owen, 1874 on the page following the description of *P. anak*: "The postbasal ridge though narrow is definite; the parabasal ridge is proportionately as well developed as in *Protemnodon Anak*; its 'link' also, and that of the two chief lobes, are more distinct than in the type species" (Owen 1874, p. 278). Here, Owen clearly referred to *P. anak* as the type species, demonstrating his intent, not otherwise stated, that *P. anak* be given this status, *contra* Mahoney & Ride (1975), who stated that *P. anak* is the type species 'by subsequent designation... by Simpson, 1930'.

Protemnodon anak Owen, 1874

Macropus anak (Owen, 1859): *Quart. J. Geol. Soc. Lond*. 15, p. 185 (*nomen nudum*).

Protemnodon anak Owen, 1873: *Proc. Roy. Soc. Lond*. 21, p. 128 (*nomen nudum*).

Protemnodon anak Owen, 1874: *Phil. Trans. Roy. Soc.* 164, p. 277. See also Owen (1877) pp. 428–430, pl. 85, figs 1–4 & 7–14); Etheridge & Jack (1892), p. 677; Raven (1929), p. 255; Simpson (1930), p. 76; Tate & Archbold (1937), p. 410; Tate (1948), p. 297; Troughton (1957), p. 187; Stirton (1963), p. 137, fig. 13a; Bartholomai (1973), pp. 318–330, pl. 9–12; Hope (1973), pp. 167, 182; Dawson (1985), p. 66, table 1; Helgen *et al.* (2006), p. 303, appendix 2; Jones *et al.* (2021), p. 36; Janis *et al.* (2023), figs 2–4, SI table 1.

Protemnodon og Owen, 1874: *Phil. Trans. Roy. Soc.* 164, p. 277,

pl. 25, figs 5–6. See also Owen (1877), p. 430, pl. 85, figs 5–6; Etheridge & Jack (1892), p. 678; Palmer (1904), p. 883; Simpson (1930), p. 76; Stirton (1963), p. 139, fig. 13b.

Halmaturus anak (Owen); Krefft (1875), p. 208; De Vis (1895) (*partim*), pp. 104–109, pl. 17, figs 5–10.

Sthenurus atlas (Owen); Owen (1876) (*partim.*), pp. 210–212, pl. 25, fig. 2, pl. 26, fig. 4. Not *Sthenurus atlas* (Owen, 1838).

Macropus anak (Owen); Flower (1884), p. 715; Lydekker (1887), pp. 214–218; Lydekker (1894), p. 257; Lydekker (1896), p. 257; Palmer (1904), p. 883.

Procoptodon goliah Owen; Owen (1876), pl. 23, fig. 4. Not *Procoptodon goliah* (Owen, 1845).

Holotype:
NHMUK PVM1895 partial L dentary containing p3–m4, missing sections immediately anterior to p3 and from 10 mm posterior to m4, ventral margin intact below m2–m4. Figured in Owen (1874), pl. 25, fig. 1.

Type locality:
Pleistocene fluviatile deposits in Darling Downs, southeast Queensland. Exact locality unknown; described by Owen (1874, p. 276) as 'freshwater deposits exposed in the beds of creeks in Darling Downs'.

Paratype(s):
None.

Referred specimens:

South Australia

Malkuni Waterhole, Cooper Creek: SAMA P53058 L premaxilla fragment; SAMA P25052 partial R maxilla; SAMA P25049 partial R dentary; SAMA P25063 partial R dentary; SAMA P25031 L calcaneus; SAMA P54627 L proximal pedal phalanx IV.

Waralamanko Waterhole, Cooper Creek: SAMA P25185 partial R dentary.

Lower Cooper Creek (site unknown): UCMP 47924 partial L dentary.

Main Fossil Chamber, Victoria Fossil Cave, Naracoorte: SAMA P28172 partial juvenile R maxilla.

Queensland

Hodgson Creek/Umbiram Creek, Darling Downs: IS V653 R metatarsal V.

Wyandotte Creek, Greenvale: NMV P184050 partial juvenile R dentary.

Pearson Bed, King's Creek: IS V122 cranium; IS V127 partial cranium; IS V637 partial cranium.

Sobbe Bed, King's Creek: IS V657 partial cranium; IS V593 juvenile R dentary.

Sutton Bed, King's Creek: IS V126 cranium; IS V590 juvenile L dentary.

Darling Downs (site unknown): QM F616 partial cranium; QM F3007 L dentary; QM F3034 R dentary; QM F4712 partial juvenile L maxilla; QM F5045 partial R maxilla; QM '1065' R calcaneus; QM '8771/XXII2' L calcaneus. AM F19648 splanchnocranium; AM F30688 partial L maxilla; AM F30691 partial R dentary. AMNH FM19256 splanchnocranium; AMNH FM19288 L dentary; AMNH FM19257 L dentary; AMNH FM32747 R dentary. NHMUK PVM48 R maxilla; NHMUK PVM2261 P3 and M1; NHMUK PVM2262 partial L maxilla and LR premaxillae; NHMUK PVOR47838 partial splanchnocranium; NHMUK PVOR38751 partial L maxilla; NHMUK PVM2258 L dentary; NHMUK PVM3451 partial L dentary; NHMUK PVM5006 partial R dentary; NHMUK PVOR10068 R dentary; NHMUK PVOR38753 partial L dentary; NHMUK PVOR40009 R dentary fragment; NHMUK PVOR40010 partial L dentary; NHMUK PVOR48423 R dentary; NHMUK PVOR47854 L i1; NHMUK PVOR47829 R calcaneus. QVM1990 GFV50 partial L maxilla; QVM1990 GFV82 R dentary.

Gowrie Creek, Darling Downs (site unknown): AM F2221 partial cranium. QM F651 partial LR premaxillae; QM F4896 partial L maxilla and L dentary; QM F4900 partial R dentary. NHMUK PVOR50064b partial maxilla; NHMUK PVOR35963 partial L dentary; NHMUK PVOR35964 partial L dentary; NHMUK PVOR35967 R dentary fragment; NHMUK PVOR50060 partial L dentary.

King's Creek, Darling Downs (site unknown): UCMP 53292 partial R dentary.

Pilton, Darling Downs (site unknown): QM F5028 partial R premaxilla; QM F3017 partial R dentary.

New South Wales

Cox's Creek, Tambar Springs: AM F112005 partial L maxilla.

Cuan Station, Scone: AM F7238 partial R dentary.

Dundee: AM F39813 L dentary fragments.

Weetalibah: AM F2343 L dentary.

Site 51, Lake Victoria: NMV P28273a partial L dentary.

Wellington Caves, Wellington (site unknown): AM F17599 premaxilla; AM F18894 partial premaxilla; AM F30599 partial L maxilla; AM F47055 partial LR maxillae; AM F47070 partial maxilla; AM F18904 partial L dentary; AM F18905 juvenile R dentary; AM F104750 L calcaneus; AM F104754 L calcaneus. UCMP 57375 R dentary.

Lake Menindee (site unknown): AM F19649 partial R dentary.

Victoria

Nelson Bay, Portland: NMV P215986 partial L maxilla; NMV P200471 L DP2; NMV P252398 R i1.

Childers Cove: NMV P230263 partial DP3.

Northeast shore, Lake Weeranganuk: NMV P162930 L humerus and partial L scapula, radius and ulna.

Batesford Quarry, Moorabool Viaduct Sands: NMV P201869 partial juvenile LR dentaries.

Locality 477, Lancefield Swamp South: NMV P177784 partial R dentary.

Locality 1534, Lancefield Swamp: NMV P31340 partial L dentary.

Lancefield Swamp, Lancefield (site unknown): NMV

P31588 partial L dentary; NMV P31614 partial R dentary; NMV P43701 partial L dentary; NMV P200720 partial R dentary; NMV P240498 L calcaneus; NMV P240564 L calcaneus; NMV P240605 L calcaneus; NMV P40509 R metatarsal V.

Firehole No. 2, Morwell Mine, Hazelwood: NMV P42532 partial cranium; NMV P39101 cranium, partial LR dentaries, cervical vertebrae C2–7, partial R scapula, L humeral fragments, ulnar fragments, radius, R tibia, LR calcanei, and L cuboid and metatarsals IV and V; NMV P39105 partial cranium, LR dentaries, partial atlas and axis vertebrae, partial sacrum, R humerus, LR ulnae, R radius, metacarpal IV and proximal, middle and distal manual phalanges IV, tibial and fibular fragments, R calcaneus, cuboid, talus, metatarsals IV, V, proximal pedal phalanx IV and proximal, middle and distal phalanges V, and L middle and distal phalanges IV; NMV P159917 L femur, tibia and calcaneus, R metatarsals IV, V, and distal pedal phalanx IV; NMV P159917b L calcaneal fragment, cuboid and metatarsals IV and V, and proximal pedal phalanx IV.

Morwell Mine, Hazelwood (site unknown): NMV P188455.2 juvenile cranium and mandible; NMV P39118 partial L maxilla, partial R dentary, partial sacrum, caudal vertebra, LR femora, tibial and femoral fragments, and L calcaneus, cuboid, talus, and metatarsals IV and V; NMV P39128 partial R maxilla, premaxilla and dentary; NMV P39134 caudal vertebra Ca13?, R metatarsal IV L proximal pedal phalanx IV and R proximal, middle and distal phalanges V; NMV P209937 R calcaneus and metatarsals IV and V; NMV P39132 R tibial fragments, L calcaneus, cuboid, metatarsals IV, V and proximal pedal phalanx IV, and R proximal, middle and distal phalanges IV and middle and distal phalanges V.

Dry Creek, Keilor: NMV P29632 partial LR dentaries; NMV P29554 partial L dentary.

Tasmania

Egg Lagoon, King Island: NMV P30786 partial R maxilla and partial LR dentary fragments.

South East Lagoon, King Island: QVM2019 GFV0002 L dentary; QVM2019 GFV0003 partial juvenile R dentary.

Scotchtown Cave, Smithton: QVM 1992 GFV0203 partial R dentary; QVM1996 GFV7 partial R dentary; QVM1996 GFV 08 partial L dentary; QVM1996 GFV12 partial juvenile L dentary; QVM1996 GFV13 L i1.

Revised specific diagnosis:

Protemnodon anak is distinguished from its congeners by several unique dental and skeletal characteristics and by its combination of other osteological characteristics. *Protemnodon anak* is differentiated from all members of the genus for which this part of the cranium is known by having a more anteriorly extensive masseteric ridge of the jugal (anterior jugal ridge). The dentition of *P. anak* is distinguished from all congeners by the following characteristics: a P3 narrower relative to length, with more raised, angular, distinct and dorsoventrally aligned ridgelets on the buccal surface of the main crest, and a distinctly jagged lingual crest that terminates short of the lingual base of the anterior cusp; and a p3 with more raised, angular and distinct ridgelets. The axial skeleton is differentiated from all members of the genus that preserve an axial skeleton by having an elongate axis vertebra (C2), with the caudal extremity of the centrum strongly caudally projected, and the postzygopophyses large and elongate; cervical vertebrae (C3–7) elongate, with large, elongate pre- and postzygopophyses, and a strongly caudoventrally projected caudal extremity of the centra. The forelimb is distinguished from all other species of *Protemnodon* in having a more elongate, proximally deeper, and strongly transversely compressed ulna that is distinctly recurved in lateral view. The pes is differentiated from all other species of *Protemnodon* except *P. otibandus* by having a calcaneus with a fibular facet with distinct margins and a rounded, caudally projected caudal component, and from all other species of *Protemnodon* in having the middle pedal phalanx IV with a far broader proximal than distal end, due to lateral and medial flaring of the proximal plantar (flexor) tubercles.

Protemnodon anak is most similar in cranial morphology to *Protemnodon mamkurra* **sp. nov.** and *P. viator* **sp. nov.** The cranium is further distinguished from those of *P. mamkurra* **sp. nov.** and *P. viator* **sp. nov.** in having straighter, relatively more dorsally situated occipital condyles. It additionally differs from *P. mamkurra* **sp. nov.** in having a dorsoventrally lower rostrum and narrower occipital condyles, and is further distinguished from *P. viator* **sp. nov.** by having rounder, less dorsoposteriorly slanted orbits in lateral view. The dentary of *P. anak* is most similar to that of *P. mamkurra* **sp. nov.**, *P. viator* **sp. nov.**, *P. dawsonae* **sp. nov.**, and *P. otibandus*, but differs from these species in having a less dorsally deflected diastema, and further from *P. otibandus* in having a broader, more robust anterior dentary below the diastema. The dentary further differs from that of *P. viator* **sp. nov.** in having a proportionally shallower mandibular corpus when fully grown.

Protemnodon anak is similar in dental morphology to *P. mamkurra* **sp. nov.**, *P. viator* **sp. nov.**, *P. otibandus*, and *P. snewini*. The dentition of *P. anak* further differs from that of *P. otibandus* and *P. snewini* in being higher crowned; from *P. otibandus* in having a squarer, relatively anteroposteriorly shorter occlusal surface of I1 when worn and relatively narrower molars; and from *P. snewini* in having a P3 with a narrower posterior relative to anterior width, and a broader, more robust i1. It is further distinguished from *P. mamkurra* **sp. nov.** and *P. viator* **sp. nov.** in having: a narrower I1 relative to the length of the I3; a relatively narrower DP2, particularly across the anterior cusp; a DP3 with a distinct, raised preprotocrista forming the lingual half of an incomplete protoloph; relatively narrower upper molars with a higher preparacrista; less robust i1 with thinner, more raised dorsobuccal and ventrolingual crests; p3 with fewer,

lower, and less distinct, transverse ridgelets on main crest; and lower molars with straighter lophid margins, and higher, more distinct cristid obliqua when unworn or slightly worn.

Protemnodon anak is most similar in aspects of skeletal morphology to *P. mamkurra* **sp. nov.**, *P. viator* **sp. nov.**, *P. snewini*, and *P. otibandus*. The axial skeleton of *P. anak* further differs from that of *P. mamkurra* **sp. nov.** and *P. viator* **sp. nov.** in having: an axis vertebra with a more elongate and less dorsally deflected dens, flatter and less dorsolaterally orientated cranial articular surfaces, and a spinous process with more level dorsal margin, much smaller caudal projection, and a more elongate base; and cervical vertebrae with a narrower caudal extremity of the centra. The cervical vertebrae further differ from those of *P. mamkurra* **sp. nov.** in having more rounded vertebral canals, and from *P. viator* **sp. nov.** in being taller and relatively narrower, with a taller cranial extremity of the centra and a taller caudal extremity of the centra lacking a slightly bilobed ventral margin.

The forelimb of *P. anak* differs from those of *P. mamkurra* **sp. nov.** and *P. viator* **sp. nov.** in having: a scapula with a more medially extensive scapular spine; a more elongate humerus with a longer and more deeply concave bicipital groove and a longer pectoral crest; and an ulna with a more cylindrical distal shaft. The forelimb further differs from *P. mamkurra* **sp. nov.** in having: a humerus with a more rounded, less pointed proximal peak on the lateral supracondylar ridge; a more elongate radius; and distal manual phalanges with shorter, less dorsopalmarly compressed shafts. It further differs from *P. viator* **sp. nov.** in having: a radius with a more distally situated cranial ridge; a shorter and more robust metacarpal IV with a vertical rather than dorsomedially tilted hamatal facet and a distally facing (rather than laterally facing) metacarpal V facet; proximal manual phalanges with deeper, more V-shaped trochleae; and distal manual phalanges with less palmarly curved shafts.

The hindlimb differs from those of *P. mamkurra* **sp. nov.** and *P. viator* **sp. nov.** in having a femur with a shallower trochlea. It further differs from *P. mamkurra* **sp. nov.** in having: a femur with a more raised proximolateral ridge and a broader and higher lateral trochlear crest; and a more gracile tibia that is longer relative to femoral length. It further differs from *P. viator* **sp. nov.** in having: a shorter tibia relative to femoral length; a more gracile femur with a less medially projected lesser trochanter, a more curved lesser trochanteric ridge such that the conjunction of the ridges at the lesser trochanter is broadly more curved, a broader and more rounded trochlea, and a relatively broader, lower medial trochlear crest; and a more robust tibia with a more distinct peak of the cnemial crest. The pes of *P. anak* differs from those of *P. mamkurra* **sp. nov.** and *P. viator* **sp. nov.** in having: a metatarsal V with a larger, more proximally projected medial plantar tubercle; shorter, more robust pedal phalanges; and a proximal phalanx IV with a less distinct waist. The pes further differs from *P. mamkurra* **sp. nov.** in having: a less robust calcaneus with a more rounded sustentaculum tali in medial view, a more caudally situated and distinctly separate lateral talar facet relative to the medial talar facet, and less bulbous talar and fibular facets; a talus with a narrower navicular facet more aligned in the sagittal plane; a cuboid with a narrower metatarsal V facet, a more plantarly projected lateral plantar tubercle and a narrower, deeper flexor groove; a more transversely compressed metatarsal V; and distal pedal phalanges IV and V lacking V-shaped indentations in the transverse margins of the proximal surface. It further differs from *P. viator* **sp. nov.** in having: a broader and more robust calcaneus with a domed calcaneal tuberosity; a shorter, broader cuboid with a larger metatarsal V facet and a smaller medial plantar tubercle; a dorsoplantarly shorter, broader metatarsal V with a broader and more concave cuboid facet; and distal pedal phalanges IV and V with more rounded, less triangular dorsal peaks.

The hindlimb of *P. anak* is further differentiated from that of *P. snewini* in having a more robust tibia with a relatively longer cnemial crest with a less distinct distal peak, and a longer proximolateral crest relative to total length. The pes is differentiated by having: a talus with a small indentation between the cranial margin of the medial trochlear crest and the talar head; a cuboid with the dorsal and plantar metatarsal IV facets continuous with one another and the facet for metatarsal V larger and more distinct; a more elongate metatarsal IV with a relative longer plantar ridge, continuous dorsal and plantar cuboid facets, and a more plantolaterally situated proximal cuboid fossa; and distal phalanx IV with a more rounded dorsal peak.

The forelimb of *P. anak* further differs from that of *P. otibandus* in that: both the capitulum and ulnar facet of the humerus are relatively larger and more distally projected; the ulna has a shorter olecranon process relative to ulnar length with a larger ventromedial eminence and a shallower proximomedial flexor fossa; the caudomedial surface of the distal shaft of the radius is less flattened and the distal end is less transversely compressed. The manus differs from *P. otibandus* in having less palmarly curved distal phalanges. The hindlimb is further differentiated by its femur with a shallower and broader trochlea and a relatively lower and more rounded medial trochlear crest. The pes differs as follows: calcaneus larger and taller with a less medially displaced head; talus with a narrower navicular facet and smaller medial malleolus, both more aligned in the sagittal plane, and in lacking a small tubercle plantar to the medial malleolus on the medial surface; cuboid taller, with more plantarly projected plantar tubercles and the dorsal and plantar metatarsal IV facets continuous with one another; more gracile metatarsal IV with a more raised plantar ridge, the dorsal and plantar cuboid facets continuous, and the shaft broadening more distally; metatarsal V with a larger proximolateral process and a larger, more proximomedially projected medial plantar tubercle; distal phalanx IV with a more pointed dorsal peak; and proximal phalanx V with a more distinct waist.

Etymology:
In reference to a biblical giant named *Anak*.

Description and comparisons:

Cranium and dentition

Cranium (Figs 3–5): large, narrow and elongate. Rostrum narrow, low, and rounded in cross-section, with a shallow buccinator fossa. Diastema elongate, ~70% of rostral length, consists of slightly more maxilla than premaxilla. Premaxilla anteroventrally projected; ventral part narrows gradually anterior to the maxilla, but broadens slightly around I3, before forming a narrow, rounded anterior extremity; ventral width is subequal to maximum width across the nasal cavity. Incisor-bearing component of the premaxilla is robust, broadest ventrally and shallowly concave, contributing ~50% of the ventral length from the anterior tip to the premaxilla–maxilla suture. Ventral premaxilla–maxilla suture angled posterolaterally, and the lateral premaxilla–maxilla suture extends straight dorsally before curving smoothly posteriorly toward posterior of nasal. Incisive foramina elongate, more posteriorly positioned relative to the incisors in mature individuals, with, in ventral view, a tapering channel extending anteriorly and curving laterally from them toward I3. Shallow buccinator fossa smoothly concave and quite tall with depth gently decreasing anteriorly; extends dorsally from the ventral margin of the diastema to one-third of maxilla height and anteriorly from the anterior side of the P3/DP2 to between the premaxilla–maxilla suture and the base of the I3. Infraorbital foramen large, narrow, and opens anteriorly, positioned dorsal to P3/DP2, well anterior of orbit. Nasal narrow, elongate, and slightly convex dorsally, with linear lateral suture; projects anteriorly past anterodorsal margin of premaxilla and tapers to a shared medial point. Frontal strongly concave at the midpoint of the temporal fossa in dorsal view, broadens anteriorly and flares over orbits.

Lateral cranium. Lacrimal quite large, extends anteriorly well onto lateral side of splanchnocranium, and gently projects laterally; has a small dorsoposterior foramen and larger anteroventral foramen, both dorsoposteriorly bordered by a rounded tubercle. A ventral orbital lip (masseteric ridge of the jugal, for the dorsal margin of the origin of the intermediate masseter; see Warburton 2009) projects laterally from the dorsal margin of the zygomatic process; this extends anteriorly into a thin, low ridge to the anterior margin of the jugal (Fig. 5b), with occasional small, pointed eminences projecting anteriorly from the anterior tip (see IS V126 and NMV P39105). Temporal fossa elongate, broadest at midpoint, and slanted gently anteroventrally into orbit in lateral view. Orbit large and round in lateral view (Fig. 5b). Masseteric process composed solely of maxilla; moderately enlarged and ventrolaterally projected, with ~90° posterior rotation of tip. Jugal rises gently at its posterior end and bifurcates around the anterior tip of the zygomatic arch into a short, broad dorsomedial part (the postorbital process), and a ventrolaterally situated posterior part that extends almost to the postglenoid process; a low ridge extends posteriorly from the ventral orbital lip on the lateral surface of the posterior part. Zygomatic arch is orientated dorsoposteriorly at 30–40° to axis of molar row; zygomatic process of squamosal tall posteriorly, with the lateral surface tilted slightly dorsally, dorsal margin smoothly convex in lateral view, tapering anteriorly to a point between the postorbital process and the posterior part of the jugal.

Palatal region. Palatine thick, broad, and lacking fenestrae, with a narrow, elongate anterolateral foramen level with the anterior of the M3; small, rounded posterolateral foramen posteriorly adjacent to the M4; lateral margin tapers gently anteriorly before forming a linear transverse maxilla–palatine suture level with abutment of M2–M3; posterior margin concave. Maxillary foramen quite large, round, and opens posteriorly into a broad, rounded valley. Sphenopalatine foramen small and round, situated immediately posteromedial to the maxillary foramen. Pterygoid crest thin and elongate, with the anterior peak tall and slightly posteriorly deflected; pterygoid (anteromedial) wing of the alisphenoid thick, laterally flared, abuts the lateral margin of the pterygoid crest, curves gently posteromedially to form a low anteroposterior ridge.

Dorsal and posterior cranium. Parietals broad and smoothly convex. Temporal (sagittal) crests, in young individuals, are separate low, rounded crests (for dorsal edge of m. temporalis) extending anteriorly from lateral margins of interparietal to merge with supraorbital crests; with age, crests migrate medially to partially merge posteriorly at the anterior margin of the interparietal; with advancing age, the merging point advances anteriorly and the height of the crest increases gently. Interparietal small and approximately triangular, tapers to a point anteriorly. Nuchal crest low in young individuals, becomes thicker and flares dorsoposteriorly with age; extends ventrolaterally into the mastoid-petrosal crest and bifurcates around the mastoid foramen into the lateral margin of a short, laterally flared mastoid process with a small ventrolateral tubercle and, ventrally, into the lateral side of a short, broad paroccipital process. Supraoccipital subequal in height and width in posterior view, with a slight posterior curve ventrally; dorsolateral margin rounded, dorsal margin flattened, abuts interparietal; supraoccipital foramina broad and fairly shallow; medial ridge very low and broad. Foramen magnum large, broad, oval and moderately dorsoventrally compressed, with slight divot in centre of dorsal margin. Occipital condyles tall, fairly narrow and narrowing slightly ventrally, and straight to gently ventromedially curved, with convex lateral margins; projected posterolaterally and tilted slightly laterally in posterior view; situated lateral to and extending slightly dorsal to dorsal margin of foramen magnum.

Neurocranial region. Neurocranium elongate and dorsoventrally compressed. Basioccipital broad and smoothly convex, with a very low or absent medial ridge and a broad, shallow lateral depression immediately medial to the crest on the paroccipital wing of the alisphenoid. Paroccipital process with tip, posterior and medial basal components formed from the exoccipital; posterolateral basal component formed from the mastoid; anterior basal component contributed by the paroccipital wing of the alisphenoid; a thick, dorsoventrally aligned crest projects

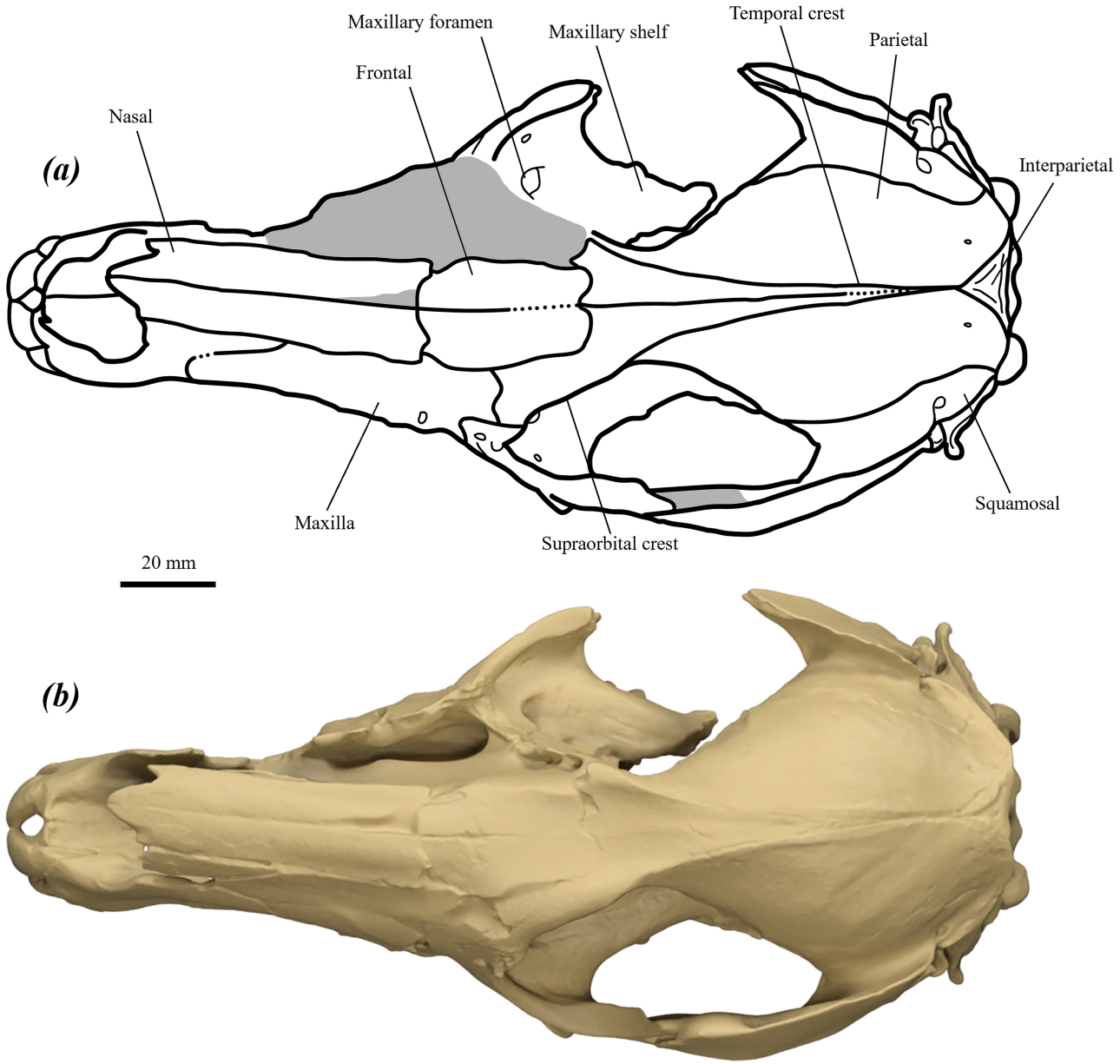

FIGURE 3. (a) line drawing, and (b) surface scan image of cranium of *Protemnodon anak* specimen IS V122 in dorsal view.

anteromedially from the base of the paroccipital process immediately posterior to the eustachian canal and anteriorly abuts the deep, rounded posterior lacerate foramen set into the medial base of the paroccipital process. Medial pterygoid origin thin, tall and curving anteromedially to continue anteriorly into the pterygoid crest. Pterygoid fossa deep and elongate, bordered laterally by a low, narrow, rounded anteroposterior ridge that extends posteriorly from base of pterygoid wing of alisphenoid to abut the medial margin of the foramen ovale; anterolateral surface of body of alisphenoid broad and flat to gently convex. Glenoid fossa broad, flat, abuts the postglenoid process posteriorly. Postglenoid process fairly broad, ventrally rounded in lateral view and angled anterolaterally in ventral view, its posteromedial component extends ventrally into, and is semi-fused with, the lateral tip of the anterior process of the ectotympanic, to form a deep, anterior-facing ventral postglenoid foramen along the medial margin. Ectotympanic has a large, rugose anterior process that projects ventromedial to the postglenoid process; ectotympanic around external auditory meatus rugose, approximately cylindrical, angled posterolaterally with a slight dorsal tilt, not projected laterally beyond the lateral margin of the anterior process.

The cranium of *P. anak* differs from those of compared taxa in having the masseteric ridge of the jugal extend anteriorly into an anterior jugal ridge (Fig. 5a & b). The cranium differs further from that of *P. mamkurra* **sp. nov.** in being relatively narrower, with a dorsoventrally lower rostrum, taller, straighter and narrower occipital condyles situated more dorsally relative to the foramen magnum, and a more posteriorly curved exoccipital; from *P. viator* **sp. nov.** in being relatively narrower, with relatively slightly longer

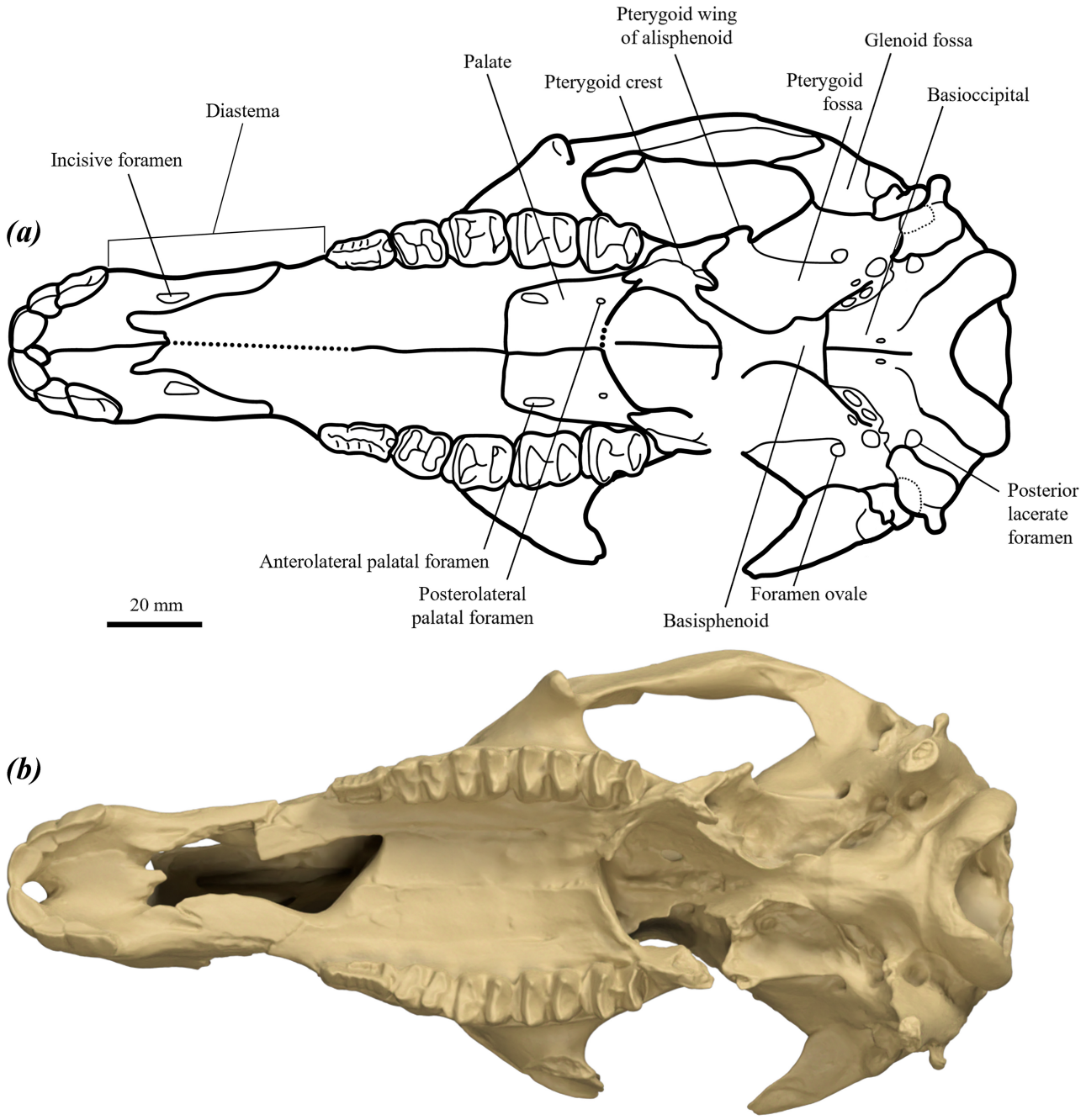

FIGURE 4. (a) line drawing, and (b) surface scan image of cranium of *P. anak* IS V122 in ventral (palatal) view.

diastema, more rounded postglenoid process in lateral view and straighter occipital condyles that are more dorsally situated in adults; from *C. kitcheneri* in being larger, broader, more robust, and lacking a bony 'pocket' of the premaxilla within the nasal cavity, with less domed and less anteriorly projecting nasal, taller and more robust anterior component of the premaxilla, larger masseteric process, taller zygomatic arch, broader foramen magnum relative to posterior cranium height, occipital condyles that project posteriorly well beyond the posterior margins of the nuchal crest and occiput, a single anteroposterior ridge meeting the medial margin of the foramen ovale and a less laterally extensive anterior process of the ectotympanic relative to the external auditory meatus; and from *W. bicolor* in being much larger, with a more ventrally projected anterior component of the premaxilla, less convex, less anteriorly projected nasal, anteroposteriorly shorter and more ventrally projected masseteric process, occipital condyles that project posteriorly well beyond the posterior margins of the nuchal crest and occiput, broader foramen magnum relative to posterior cranium height, more raised anteroposterior ridge meeting the medial margin of the foramen ovale and a more laterally projected postglenoid process.

Upper dentition (Figs 6–8): I1: fairly broad, robust and arcuate. Thick buccal enamel extends around to the edges of the lingual surface, from which it recedes with age. Buccal surface gently to moderately convex and smooth,

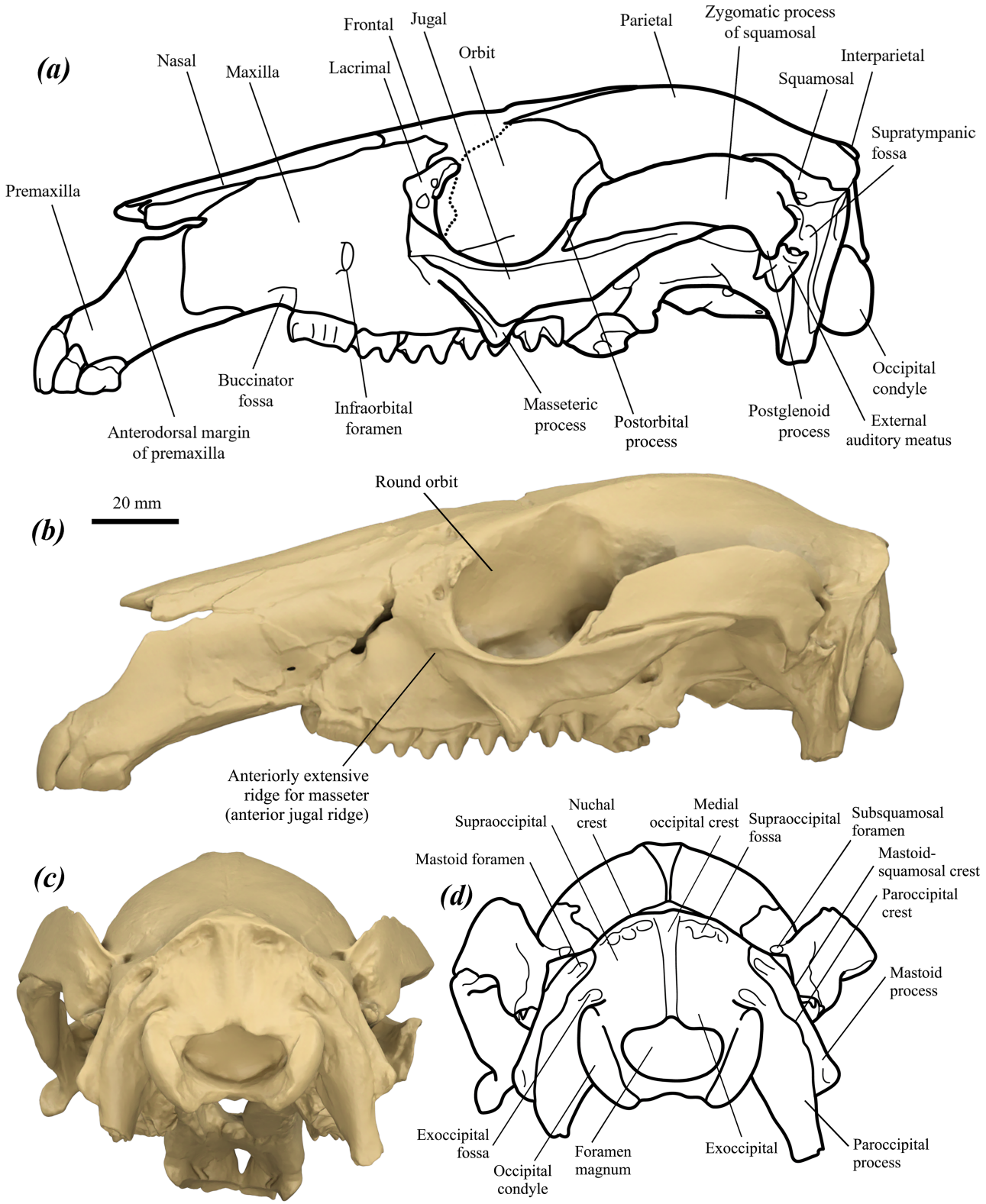

FIGURE 5. cranium of *P. anak* specimen IS V122: (a, d) line drawings and (b, c) surface scan images in (a, b) lateral view, and (c, d) posterior view. Paroccipital processes (c, d) are damaged, missing their ventral portion.

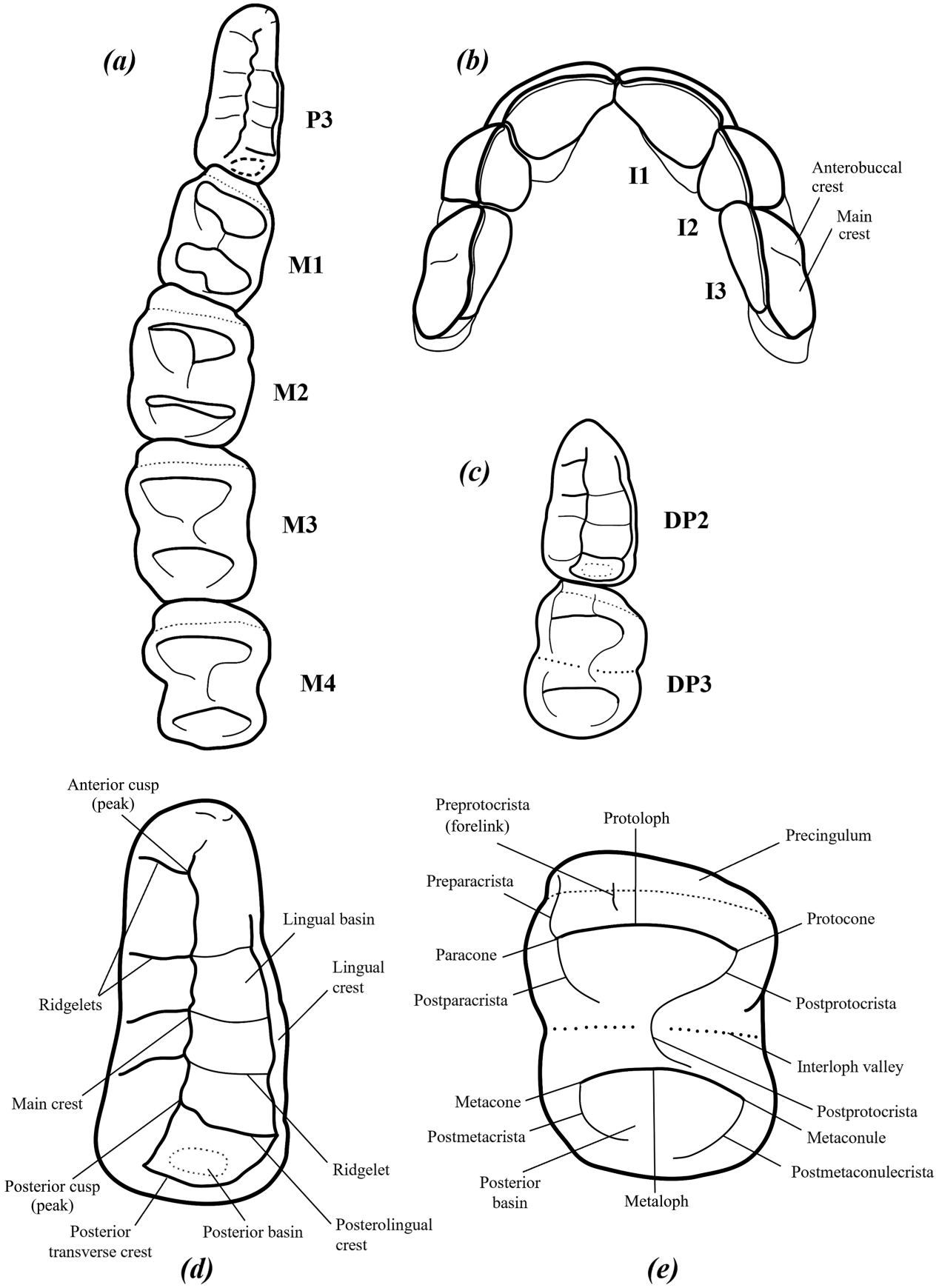

FIGURE 6. line drawings of upper dentition of *P. anak* (based on IS V122) in occlusal view: (a) upper cheek teeth, P3–M4, (b) upper incisors, I1–3, (c) deciduous premolars, DP2–3, (d) P3, and (e) upper third molar, M3. Tooth designation is indicated in (a–c).

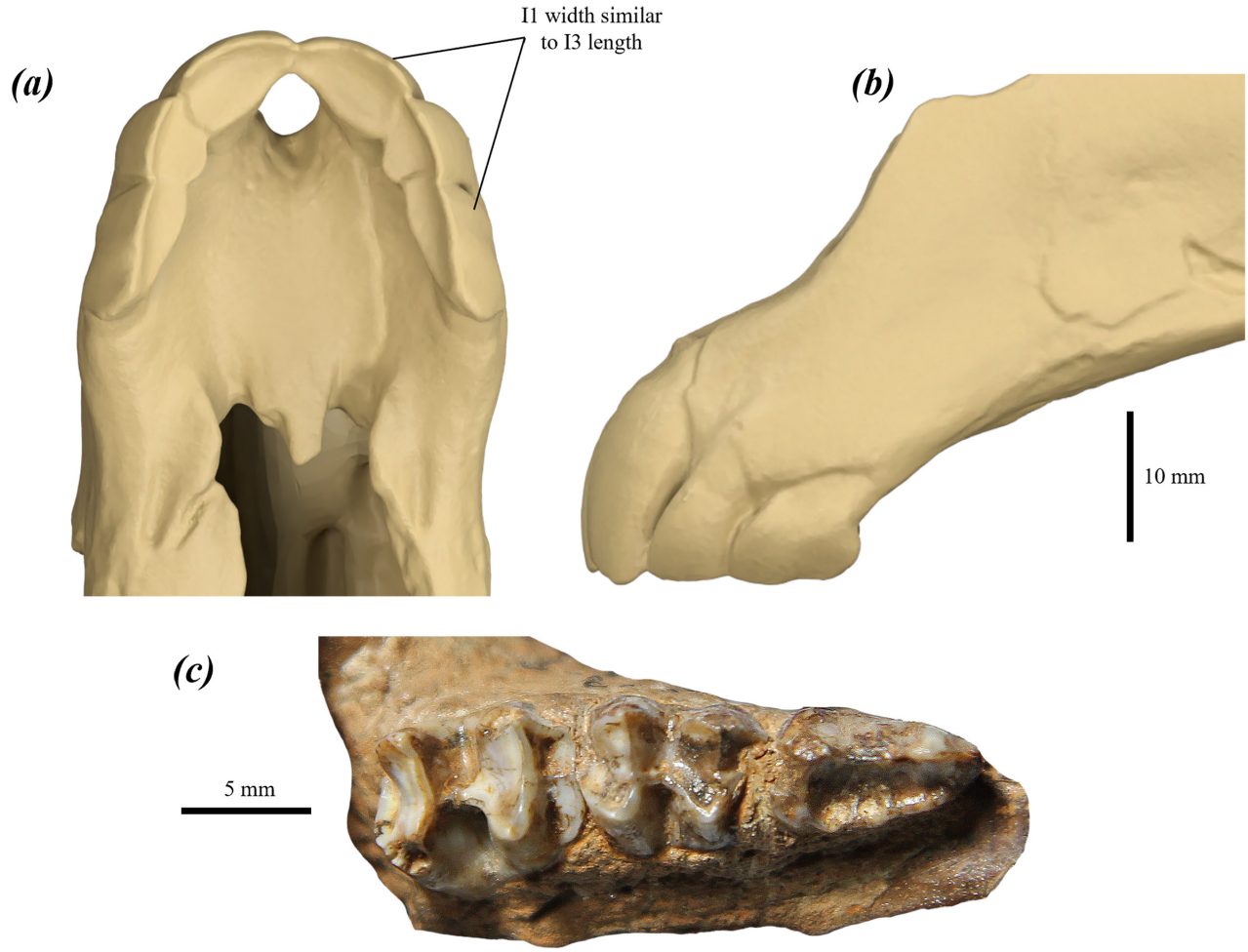

FIGURE 7. surface scan images of upper dentition of *P. anak*: (a–b) left and right I1–3 of IS V122 in (a) occlusal, and (b) left lateral views; and (c) right DP2–3 and M1 of SAMA P28172 in occlusal view.

with a very shallow, dorsoventrally aligned groove in unworn to slightly worn I1. Occlusal surface approaches rectangular in slightly worn I1, becomes oval and forms a slight anterior buccal enamel lip with age. I2: slightly elongate and narrow, with a slight secondary posterolingual crest when unworn; smaller than I1 and I3 and wears relatively quickly, becoming short and broad. I3: elongate, transversely compressed, approaching triangular in buccal view, and slightly long to slightly shorter than width of I1 (Fig. 7a), becomes shorter with wear. A large, gently buccally convex main crest curves anterolingually to be lingual to posterior margin of smaller anterobuccal crest in unworn to slightly worn specimens. Anterobuccal crest is around half the length of the main crest and removed by moderate wear, leaving a slight dorsoventrally aligned groove in the buccal enamel.

The cheek teeth are high-crowned. DP2: morphologically very similar to the P3 but anteroposteriorly truncated; fairly narrow and approaching triangular in occlusal view, broadens posteriorly and narrows to rounded point anteriorly, with thickened peaks over the anterior and posterior roots linked by a high main crest. Main crest blade-like and anteroposteriorly orientated with occasional very slight buccal curve at posterior end; crest jagged to gently undulating in buccal view, with two or three raised, dorsoventrally aligned transverse ridgelets on the buccal face, mirrored on the lingual face by relatively lower ridgelets transecting lingual valley. Lingual crest low, extends from immediately posterior to the lingual base of the anterior cusp, to meet the small posterolingual peak (cuspule); lingually borders a fairly broad, anteriorly tapering lingual basin. A small posterior basin abuts the posterior margin, sits between the posterior and posterolingual peaks, and removed by a small amount of wear. DP3: molariform, with the protoloph and metaloph narrower than the swollen loph bases; anterior loph slightly longer and narrower than the posterior loph (Fig. 7e). Precingulum moderately anteriorly projected, slightly narrower than the anterior loph, merges buccally with a thick, distinct, straight preparacrista. Protoloph generally gently U-shaped or V-shaped in posterior view; protoloph is incompletely formed, wherein the raised, distinct preprotocrista (forelink) extends up from the centre of the precingulum and curves lingually up to the protocone, and the paracrista descends from the paracone, thins and

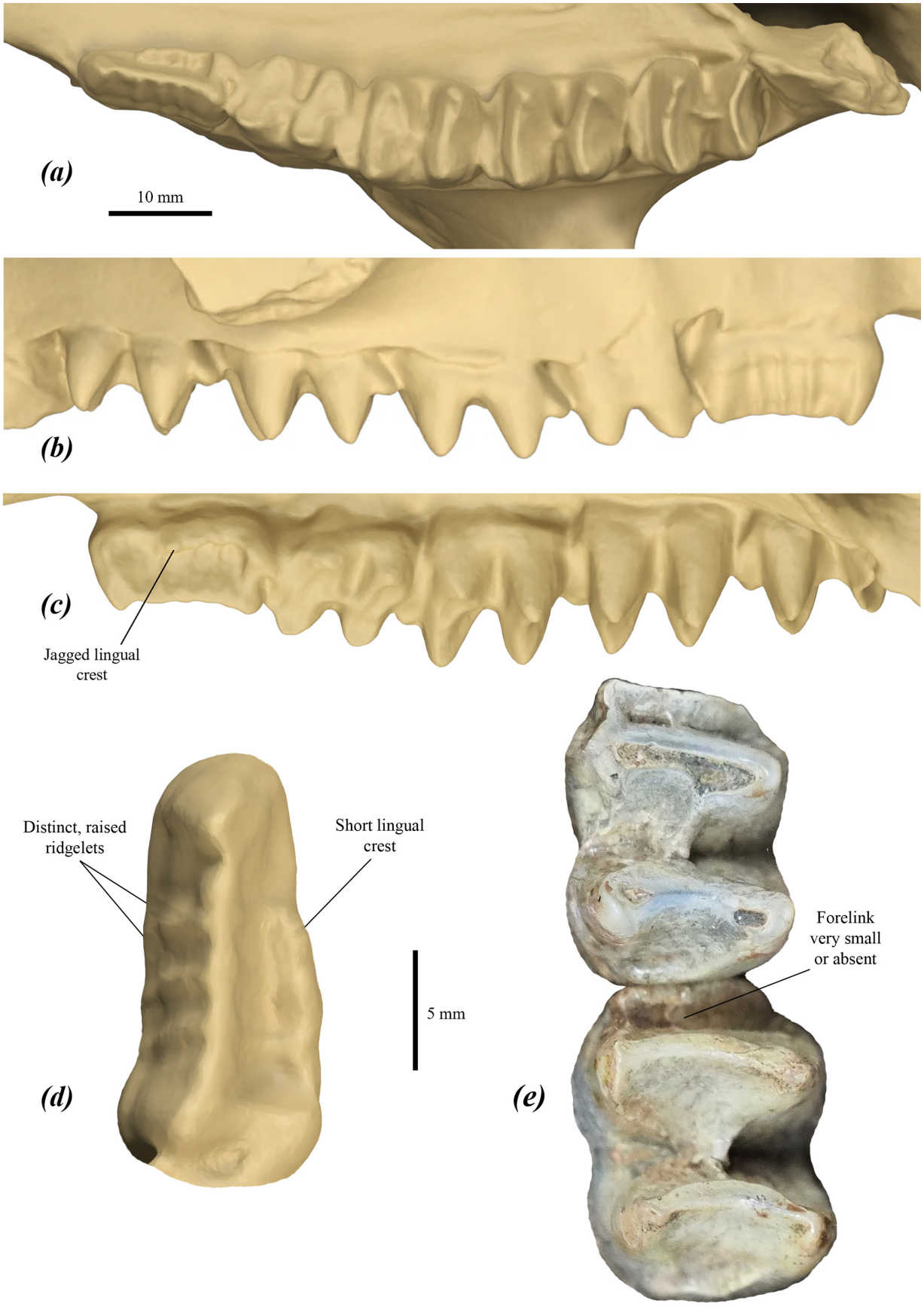

FIGURE 8. right upper cheek dentition of *P. anak*: (a–c) P3–M4 of IS V122 in (a) occlusal, (b) buccal, and (c) lingual views; and occlusal views of (d) P3 of IS V122, and (e) M2–3 of AM F2221.

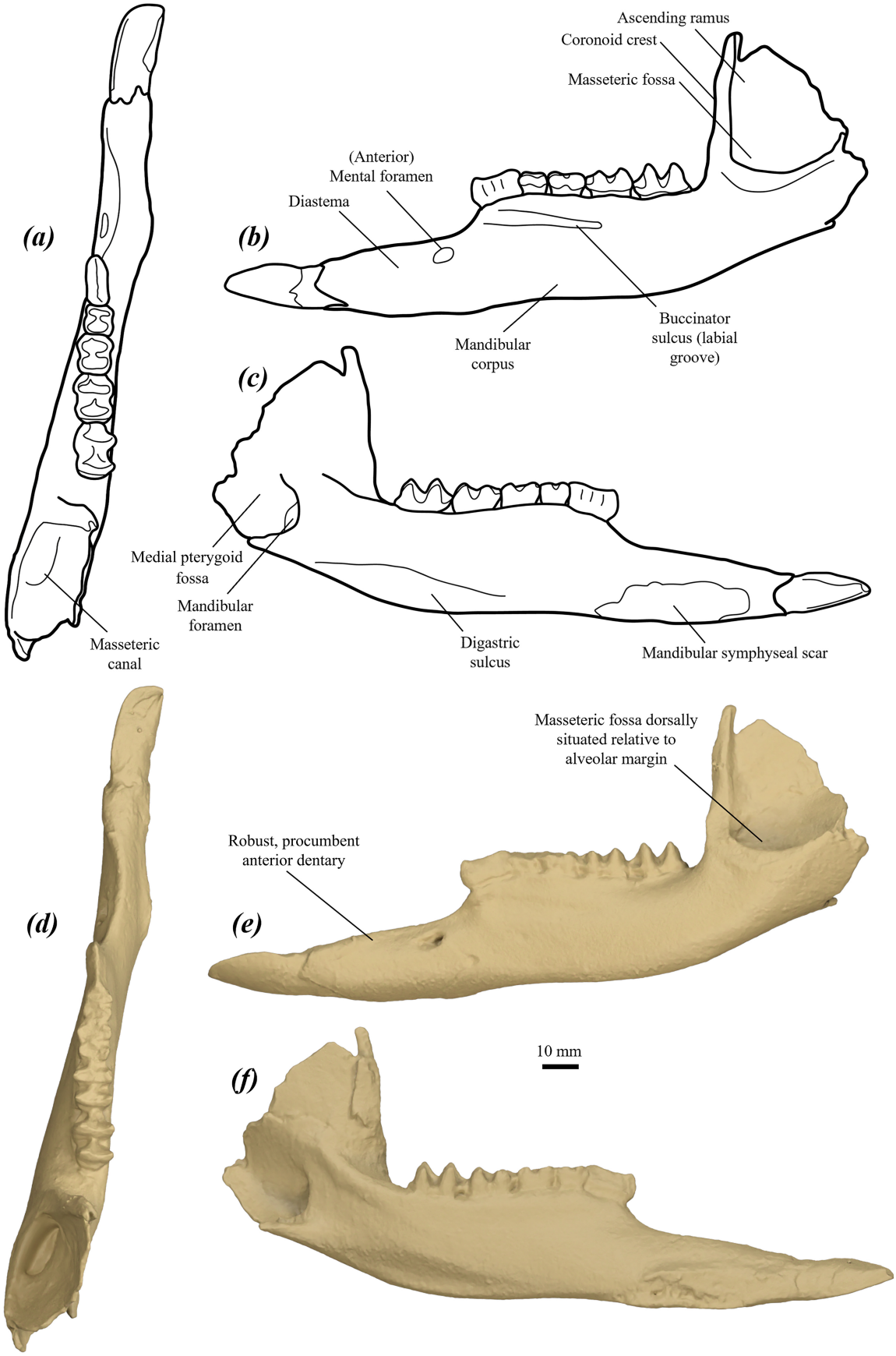

FIGURE 9. left dentary of *P. anak* NMV P39105: line drawings (a–c) and surface scan images (d–f) in (a, d) occlusal, (b, e) buccal, and (c, f) lingual views.

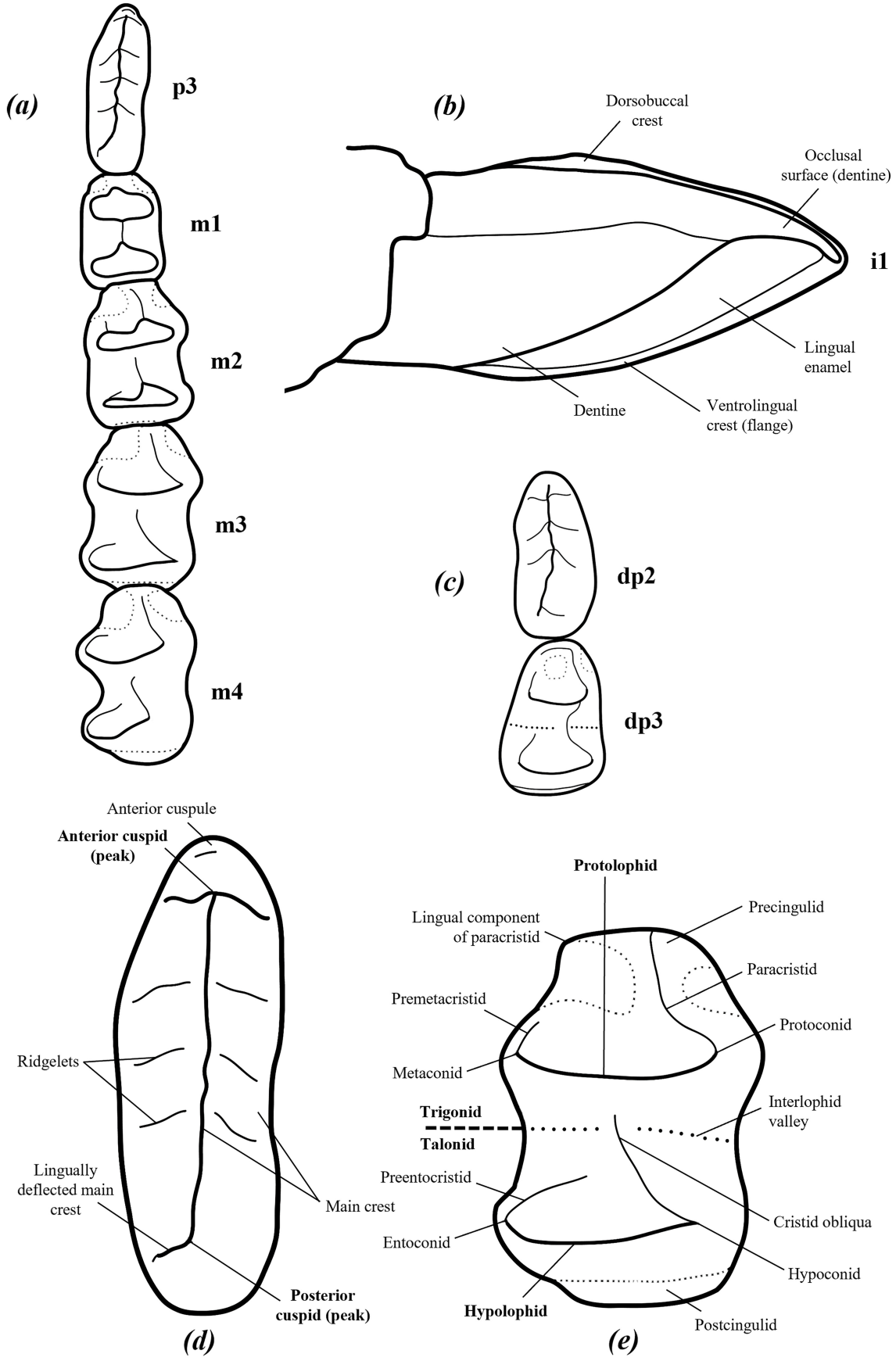

FIGURE 10. line drawings of the lower dentition of *P. anak*: (a) right lower cheek teeth, p3–m4; (b) lower incisor, i1; (c) deciduous premolars, dp2–3, (d) lower premolar, p3, and (e) lower third molar, m3. All in occlusal view except for (b), which is in lingual/medial view. Tooth designation indicated in (a–c).

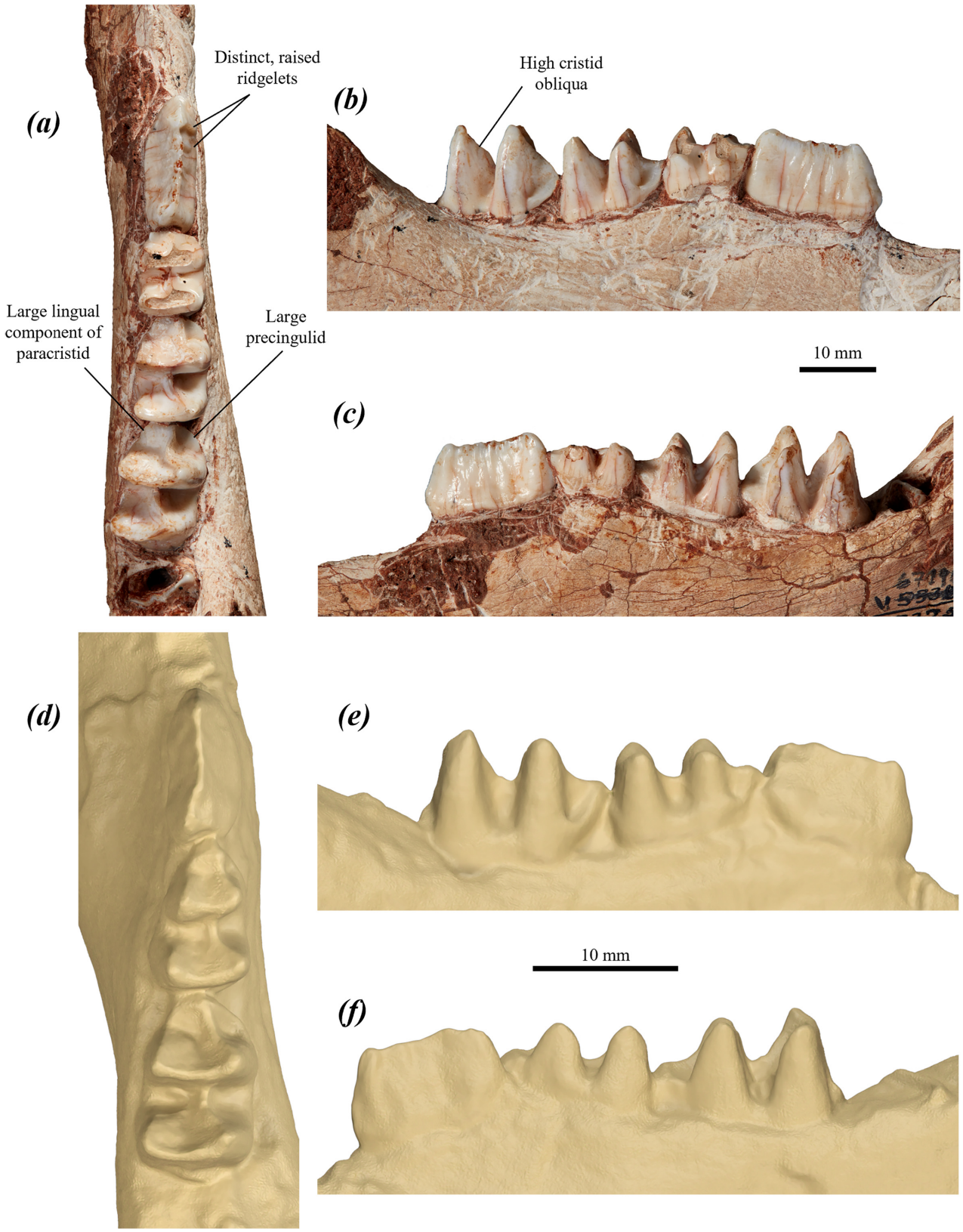

FIGURE 11. right lower dentition of *P. anak*: (a–c) p3–m3 and unerupted m4 of UCMP 57375 in (a) occlusal, (b) buccal, (c) lingual views; and (d–f) surface scan images of right dp2–3 and m1 of AMNH FM32747 in (d) occlusal, (e) buccal, and (f) lingual views.

merges into the lingual edge of the high, curved preprotocrista; this feature is removed by light wear. Postparacrista thin, raised and distinct, extends straight from the paracone to the buccal margin of the interloph valley or curves gently lingually. Postprotocrista thin, raised and distinct, angled buccally as it descends into the interloph valley; lifts again as very low, thin crest, occasionally extends to metaconule. Metaloph level or gently V-shaped in posterior view. Premetacrista occasionally present, thin and indistinct, extending from the metacone to meet the postparacrista in the interloph valley. Postmetaconulecrista thick, curves gently toward the midline of the tooth and merges into the posterior face of the metaloph.

P3: large, elongate, tapers to a rounded point anteriorly, broadest across the posterior; variably curves buccally toward posterior, with the posterior component slightly swollen or expanded buccally; rounded posteriorly. Pointed peaks over the anterior and posterior cusps are linked by a high main crest. The main crest is blade-like and roughly anteroposteriorly orientated, with a variable degree of posterobuccal curvature in occlusal view; crest jagged in buccal view with three or four distinct, raised, angular and dorsoventrally aligned transverse ridgelets on the buccal surface extending to the crest (Fig. 8d), mirrored on the lingual face by relatively lower, rapidly wearing ridgelets that intersect the lingual valley. Anterior cusp slightly broader than the middle section of the tooth, with a tall, pointed peak; in some specimens (*e.g.* NHMUK PVM48), there are one or two small, low, rounded cuspules on the anterior or anterolingual base of the anterior cusp. A jagged, low to very low lingual crest extends from the lingual base of the anterior cusp to the secondary posterolingual peak (Fig. 8c & d); lingually borders a broad, anteriorly tapering lingual valley. Main posterior cusp tall and rounded. Posterolingual peak pointed, lower than the posterior cusp and linked to the lingual surface of the posterior component of the main crest by a thin transverse crest; anteriorly borders the posterior basin. Posterior basin small, abuts the posterior margin of the tooth, sits between the main and posterolingual peaks, and is posteriorly bordered by a short, moderately low posterior transverse crest that rapidly accumulates wear.

Molars: rounded-rectangular in occlusal view; the interloph valley is slightly narrower than the lophs, though occasionally broader in M1 and very rarely in M2; buccal margins of the lophs slightly to moderately convex in posterior view, particularly the anterior lophs, with the protoloph and the metaloph both narrower than the corresponding trigonid base; unworn protolophs and metalophs are gently concave posteriorly in occlusal view. The precingulum is generally fairly broad but narrower than the anterior loph, moderately anteriorly projected and medially tilted, generally becoming slightly larger, broader and more projected toward M4, flat, broad and shelf-like when worn; M1–M3 occasionally have a slight, short preprotocrista on the precingulum. Preparacrista thin but distinct in M1, slightly less so in M2, and typically low and indistinct in M3 and M4. Postparacrista generally short and weakly developed, arises from the paracone but typically does not extend to the interloph valley (Fig. 8e). Postprotocrista relatively broader, much more distinct and more raised, particularly in the interloph valley; curves from the protocone to around the midpoint of the interloph valley; in some specimens, continues to the metaconule as a very low, indistinct crest. Premetacrista extremely slight or absent. Postmetaconulecrista quite thick and raised, arises from the metaconule and curves dorsobuccally to form a small, oblique shelf beneath the posterior basin. Postmetacrista lower, shorter and less distinct, arises from the metacone, deflects lingually to merge into the buccal margin of the posterior basin or into the posterior margin of the postmetaconulecrista.

The upper dentition of *P. anak* differs from that of all other species of *Protemnodon* in having a P3 with higher, more distinct transverse ridgelets on the buccal surface of the main crest and in the lingual valley, and a less anteriorly extensive lingual crest that is more jagged and less smoothly undulating in lingual view. It differs further from that of *P. mamkurra* **sp. nov.** and *P. viator* **sp. nov.** in having a relatively narrower DP2–3, DP3 with the preprotocrista extending to the protocone to form half of an incomplete protoloph, a relatively narrower P3, and molars with a higher, more distinct preparacrista; additionally differs from *P. viator* **sp. nov.** in being generally slightly smaller and in having a narrower I1 relative to the length of I3; from *P. tumbuna* in being higher crowned, with relatively narrower P3 across the anterior cusp and relatively narrower molars with a larger precingulum; from *P. dawsonae* in having generally smaller P3 and relatively narrower molars with a broader protolophid relative to the trigonid base when unworn; from *P. otibandus* in being higher crowned, with a less rounded, relatively anteroposteriorly shorter occlusal surface of I1 when worn, and relatively narrower P3 across the anterior cusp; from *P. snewini* in being larger and higher crowned, with P3 with more posterobuccal swelling; from *C. kitcheneri* in being larger and higher crowned, with larger incisors relative to the size of the cranium, more elongate P3 with more numerous ridgelets on the buccal face of the main crest and a less anteriorly extensive lingual crest, and relatively slightly narrower molars; and from *W. bicolor* in being larger and higher crowned, with relatively broader I1, P3 generally longer relative to molar length with more raised, more distinct buccal ridgelets and a less anteriorly extensive lingual crest, and relatively narrower molars with more anteriorly prominent precingulum, less distinct postparacrista and thicker postprotocrista distinctly extending to the protocone, rather than merging into the centre of the posterior surface of the protoloph.

Dentary (Fig. 9): anterior dentary (section ventral to the diastema) is robust and procumbent, slightly ventrally deflected relative to molar row (Fig. 9e); diastema long, with length increasing with age; height of the anterior dentary is between two-thirds and three-quarters of the maximum height of the mandibular corpus. Mental foramen round to oval, opens dorsolaterally to anterolaterally, positioned between one-quarter and one-fifth of depth below the dorsal margin, around one-third

of diastema length from dp2/p3. Mandibular corpus tall, slightly taller beneath m1 than m4. Buccinator sulcus (labial groove) distinct but quite shallow, extends with a slight posteroventral slant along the buccal surface of the mandibular corpus slightly ventral to the cheek teeth; extends from the anterior margin of the mandibular corpus to roughly beneath m3. Digastric sulcus generally very shallow, extends roughly from ventral to the base of the coronoid crest to ventral to m3. Coronoid crest rises at an angle of around 95–110° from the alveolar margin, straight to smoothly convex anteriorly, ascends to a pointed, posteriorly curved, anteroposteriorly short peak; some specimens with slight, rounded corner or elbow at midpoint; dorsoposterior margin of coronoid process deeply concave, curves anteroventrally before levelling out at or slightly ventral to the anterior margin of the mandibular condyle. Ascending ramus slightly concave on the lateral face and convex on the medial face.

Masseteric fossa large and shallow, situated slightly dorsal to level of alveolar margin (Fig. 9e), and bounded anteriorly and ventrally by a low ridge; posterior component deepened by a laterally projected 'shoulder' on the posterolateral base of the condylar process; margins broadly rounded to U-shaped in lateral view. Masseteric foramen oval, elongate and very narrow; situated in the anteroventral end of the masseteric fossa, abuts its anterior margin and shares the anterior component of its lateral lip. Masseteric dental canal very deep, demarcated from the mandibular foramen and the inferior dental canal by a narrow dorsal crest running anteroposteriorly. Medial pterygoid fossa deeply concave and broad, broadened posteriorly and truncated anteroposteriorly relative to the masseteric fossa; posteromedial extremity is squared and posterior margin is straight in dorsal view. Mandibular foramen large, rounded to oval, and transversely compressed; situated in the anterolateral component of the medial pterygoid fossa, at the ventral base of the medial surface of the ascending ramus, opens posteriorly and slightly medially. Angular process is a thin, elongate crest, dorsally and slightly posteriorly projected such that the posterior extremity is level with that of the mandibular condyle. Ventral margin of the dentary near linear to gently convex beneath the tooth row. Posteroventral margin of the dentary rounded and smoothly convex in lateral view, straightens dorsally to the posteroventral margin of the mandibular condyle; condylar process not posteriorly projected. Mandibular condyle smooth, oval, slightly anteroposteriorly compressed, rotated anterolaterally in dorsal view and tilted anteromedially.

With age, the dentary becomes more transversely compressed and less robust, the posterior margin of the mandibular symphyseal plate migrates slightly anteriorly relative to the premolar, the mandibular corpus becomes taller, the diastema becomes longer, the cheek tooth row becomes slightly more level, and the medial pterygoid and masseteric fossae become relatively larger (see *e.g.* juvenile NMV P188455.2 versus adult NMV P39105).

The dentary of *P. anak* differs from that of *P. mamkurra* **sp. nov.** and *P. viator* **sp. nov.** in being narrower and less robust, with a longer, less dorsally deflected diastema relative to tooth row length; from *P. tumbuna* in being generally larger and slightly less robust, with a longer diastema relative to cheek tooth row length and a slightly more anterodorsally situated mental foramen; from *P. dawsonae* in having a less dorsally deflected diastema; from *P. otibandus* in having a broader, slightly less dorsally deflected diastema and a slightly taller mandibular corpus; from *P. snewini* in being larger, taller and more robust, with a broader diastema and a relatively dorsally situated masseteric fossa; from *C. kitcheneri* in being larger and relatively taller, with a shorter, and slightly more dorsally deflected diastema below which the mandible is shallower, deeper buccinator sulcus, less posteriorly deflected coronoid crest, deeper medial pterygoid fossa with a higher posterior margin, and a more rounded, less elongate mandibular condyle; and from *W. bicolor* in being much larger, with a more distinct step between the dorsal margins of the mandibular corpus and diastema, a deeper buccinator sulcus and a larger septum partially separating the masseteric and mandibular foramina.

Lower dentition (Figs 10 & 11): i1: large, broad, and procumbent; parallel with alveolar row to slightly anterodorsally tilted. In adults, i1 is rotated buccally such that the tooth is quite broad and slants dorsobuccally to ventrolingually in cross-section, and tooth appears shovel-like. Transversely compressed and acuminate when unworn, becoming slightly shorter and rounder on the dorsal margin with wear. A thin, raised enamel crest is present along the dorsobuccal and ventrolingual margins. Thick enamel completely covers the buccal surface, with a thinner layer covering the ventral half of the lingual surface when unworn; this lingual layer tapers posteriorly such that well-worn i1s lack lingual enamel.

The tooth row is roughly straight in occlusal view; in lateral view, it is sloped slightly ventrally toward the posterior; the rate of wear along the tooth row is highly variable as a result of the variable tooth row angle (see *e.g.* NMV P39105 versus NMV P39101). dp2: morphologically very similar to p3 but is anteroposteriorly about half as long; blade-like, tall and triangular in cross-section, roughly oblong to mucronate in occlusal view; typically broadens gently to posterior or is asymmetrically swollen around the midpoint (Fig 11d). Anterior cuspid very slightly swollen, such that it is distinct from the main crest. Main crest aligned anteroposteriorly, extends from the anterior to the posterior peak and twists lingually at posterior end, with two low, indistinct, dorsoventrally aligned transverse ridgelets on the buccal and lingual surfaces. dp3: molariform, very similar to morphology of m1 but relatively narrower, with narrower trigonid relative to talonid. Both lophid crests are significantly narrower than bases, but protolophid narrows slightly more; both lophid crests are slightly convex posteriorly in occlusal view when unworn to moderately worn. Lophid bases slightly bulged buccally. Precingulid well-developed, tapers anteriorly, generally slightly narrower than the trigonid. Paracristid raised and thick but wears quickly; anterior component anterobuccally borders a small, rounded trigonid basin before curving up posterobuccally to the protoconid. Premetacristid raised and narrow, lingually

borders the trigonid basin. Postprotocristid absent or very slight. Cristid obliqua relatively taller and broader, curves posterobuccally to the hypoconid. Preentocristid low and broad, curves up from immediately lingual to the base of cristid obliqua to the entoconid.

p3: elongate and oblong in occlusal view with parallel buccal and lingual margins, or occasionally with a slight waist or a slight bulge around the midpoint; typically subequally broad across the anterior and posterior ends; tall and triangular in cross-section. Main crest blade-like, linear, anteroposteriorly aligned, with the anterior cuspid (anterior peak) pointed and the posterior cuspid (posterior peak) blunt and posteriorly rounded, twists slightly to moderately lingually past posterior cuspid; both the lingual and buccal surfaces of the main crest have three or occasionally four roughly dorsoventrally aligned ridgelets extending to the crest (Fig. 11a), such that the unworn or slightly worn crest appears jagged in buccal view. The anterior base of the anterior cuspid occasionally has a small, irregular cuspule projected slightly anteriorly or anterolingually.

Molars: high-crowned, rounded-rectangular in occlusal view, with the interlophid valley width equal to or narrower than the lophid bases. When unworn or slightly worn, the protolophid and hypolophid are posteriorly convex or have an oblique mesial kink toward the posterior; lingual component of the hypolophid is slightly posteriorly tilted, becomes straight and perpendicular to the tooth row centreline when moderately worn. Precingulid fairly large and thickened occlusally. Buccal margins of lophids slightly more convex than the lingual margins in posterior view. Paracristid thick and raised; lingual component extends straight posteriorly before the buccal component curves dorsobuccally to the protoconid. When little worn, the protoconid is taller than the metaconid and is very slightly lingually displaced by the distinctive 'folding' of the buccal enamel (see Fig. 11a). Premetacristid very low and often indistinct or absent; extends from the lingual margin of the trigonid basin to the metaconid. Cristid obliqua thick and high; arises from the midpoint to slightly buccal to the midpoint of the interlophid valley, curves very slightly buccally, and extends to the hypoconid (Fig. 11b). Preentocristid very low, broad and indistinct; arises midway between the base of the cristid obliqua and the lingual extremity of the interlophid valley and deflects slightly lingually to meet the entoconid. When little worn, the hypoconid is distinctly taller than the entoconid and is very slightly lingually displaced. Postcingulid narrow and slight on dp3–m2; slightly broader and more posteriorly projected in m3–4, occasionally only present as slight, wrinkled bulge on posterior lophid base.

The lower dentition of *P. anak* differs from that of *P. mamkurra* **sp. nov.** and *P. viator* **sp. nov.** in being generally smaller, with i1 having a more raised dorsobuccal crest and a thin ventrolingual crest, a slightly narrower dp2 relative to length, narrower p3 relative to length with more numerous, raised and distinct ridgelets on the main crest, and slightly narrower molars relative to length with a generally larger precingulid and straighter buccal lophid margins; from *P. dawsonae* **sp. nov.** in having i1 with a more raised dorsobuccal crest and a thin, raised ventrolingual crest, relatively narrower p3 with more numerous, raised and distinct ridgelets on the main crest, and molars with a generally larger precingulid and straighter buccal lophid margins; from *P. otibandus* and *P. tumbuna* in having broader, relatively larger and more buccally rotated i1, and relatively slightly narrower molars with a larger precingulid, less convex buccal lophid margins and a less distinct premetacristid; from *P. snewini* in being larger and higher crowned, with broader, more robust i1, and p3 with more numerous and more raised ridgelets on the main crest; from *C. kitcheneri* in being larger and higher crowned, with relatively larger, broader, more spatulate i1, more elongate p3 with more numerous, raised and distinct ridgelets on the main crest, and relatively slightly narrower molars with a higher paracristid, higher cristid obliqua and a postcingulid present; and from *W. bicolor* in being larger and higher crowned, with broader i1, p3 generally longer relative to molar length, and relatively narrower molars with a larger precingulid.

Axial skeleton

Atlas (C1) (Figs 12 & 13): broadens toward cranial end in dorsal view (Fig. 13e). Craniodorsal component of dorsal arch slightly cranially inclined, immediately lateral to the dorsal tubercle. Cranial articular surfaces large, oval and strongly concave, particularly dorsally, with the medial end of dorsal margin curving slightly ventrally. Caudal articular surfaces quite tall, smooth and flat to slightly concave, angled medially, with a relatively large, circular dorsal part and a smaller, narrow, ventromedially deflected and curved ventral part (Fig. 13d); ventral part thickened cranially. Only the base of the wings is known, situated on the caudal margin of dorsal component of lateral side of centrum; wings are inferred to be large, robust and caudally deflected. Lateral vertebral foramina small, rounded and facing laterally, situated immediately craniodorsal to the cranial margin of the base of the wing.

The atlas vertebra of *P. anak* differs from that of *P. mamkurra* **sp. nov.** in being craniocaudally longer; from *P. viator* **sp. nov.** in having taller and slightly less concave caudal articular surfaces; from *C. kitcheneri* in being larger, with a craniocaudally longer arch, more deeply concave and less cranially projected cranial articular processes, craniocaudally shorter and more elongate ventromedial processes, more caudoventrally situated lateral vertebral foramina (closer to the base of the wings), more medially tilted caudal articular surfaces, and lacking a broad, shallow groove extending ventrally from lateral vertebral foramina; from *O. rufus* in being larger, with a craniocaudally longer arch; from *M. fuliginosus* in being larger, with a craniocaudally longer arch, more caudoventrally situated lateral vertebral foramina and taller caudal articular surfaces; and from *W. bicolor* in being larger, with a craniocaudally longer arch and more caudally situated lateral vertebral foramina.

Axis (C2) (Figs 12a, 13a–b, & 14): large, solid, and elongate. Dens elongate, undeflected to slightly dorsally deflected, and circular in cross-section. Cranial articular surfaces large, tall and gently convex, very slightly dorsally

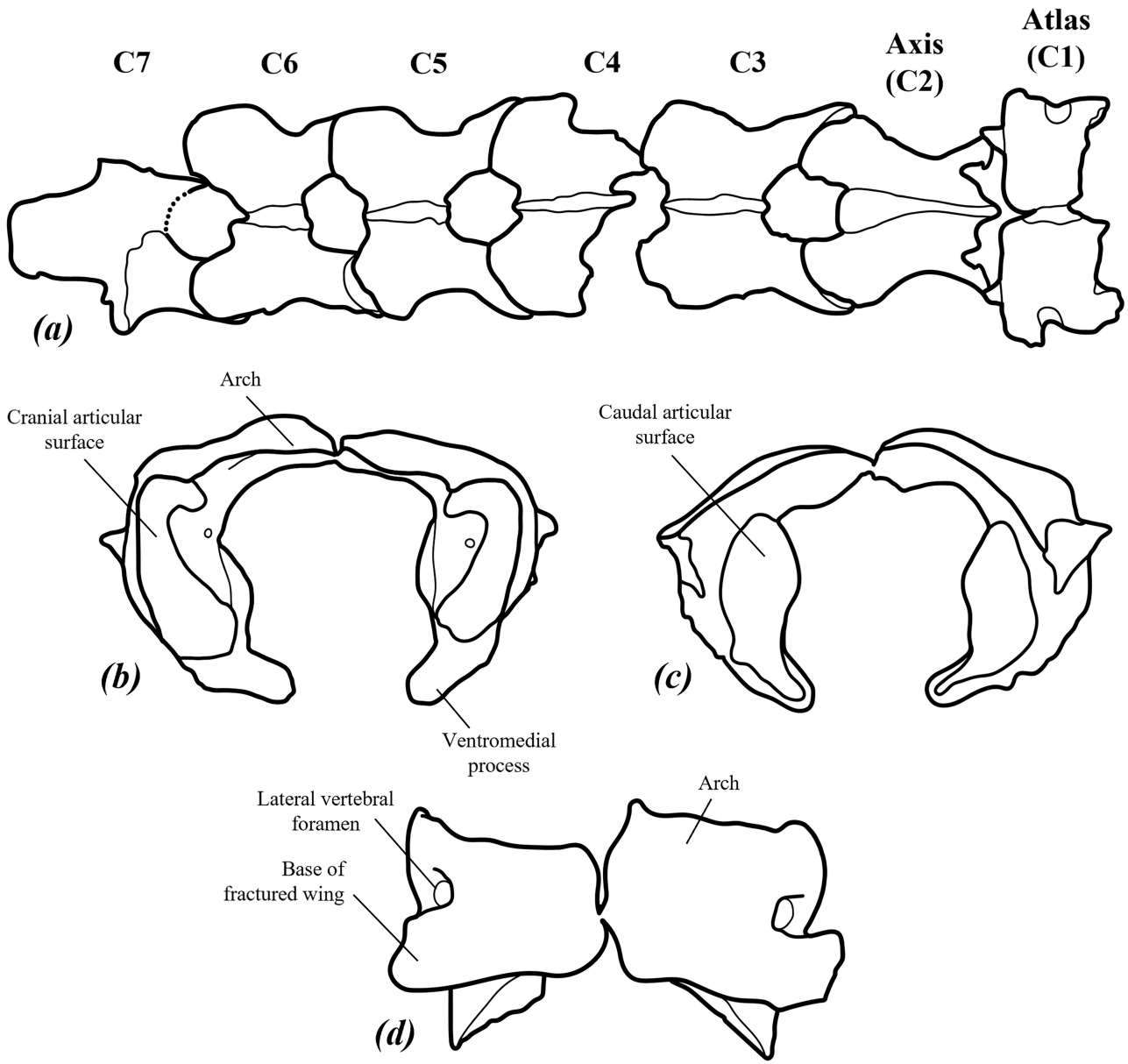

FIGURE 12. line drawings of cervical vertebrae of *P. anak* NMV P39101: (a) articulated cervical vertebrae C1–7 in dorsal view with vertebral numeration; and (b–d) atlas vertebra C1 in (b) cranial, (c) caudal, and (d) dorsal views.

tilted in lateral view, angled moderately laterally in dorsal view, with ventrolateral to dorsolateral margins smoothly rounded and dorsomedial margins linear. The arch has a concave cranial margin in lateral view. Spinous process quite low, with the base extending along the entire dorsal surface of the arch; dorsal margin level and slightly convex in lateral view (Fig. 14e), broadens distinctly toward the caudal end in dorsal view; cranial margin projected slightly beyond the cranial margin of the arch; caudal margin with large dorsal and small ventral projections extending beyond the caudal margin of the arch. The vertebral canal is roughly circular. Postzygopophyses very large, robust, craniocaudally elongate, strongly caudally projected and laterally flared; extend well beyond the caudal margins of the spinous process and dorsal arch, slightly further caudally than the caudal extremity of the centrum. Caudal articular surfaces oval, transversely compressed, tilted caudoventrally at around 45° from the dorsoventral plane. The centrum narrows to a waist between the broad cranial articular surfaces and the small, pointed transverse processes. The transverse foramen is small and rounded, possibly not enclosed laterally. Caudal extremity of the centrum very elongate, projected caudally and slightly ventrally deflected (Fig. 14e); rounded in distal cross-section, with a narrow craniocaudal ventral ridge.

The axis vertebra of *P. anak* differs from all compared taxa in being relatively and absolutely much more elongate, with a much more caudally projected caudal extremity of the centrum and larger, more elongate postzygopophyses. Further differs from that of *P. mamkurra* **sp. nov.** and *P. viator* **sp. nov.** in having a spinous process with a more level dorsal margin, much smaller caudal projection and more elongate base, a more elongate and less dorsally deflected dens, and flatter

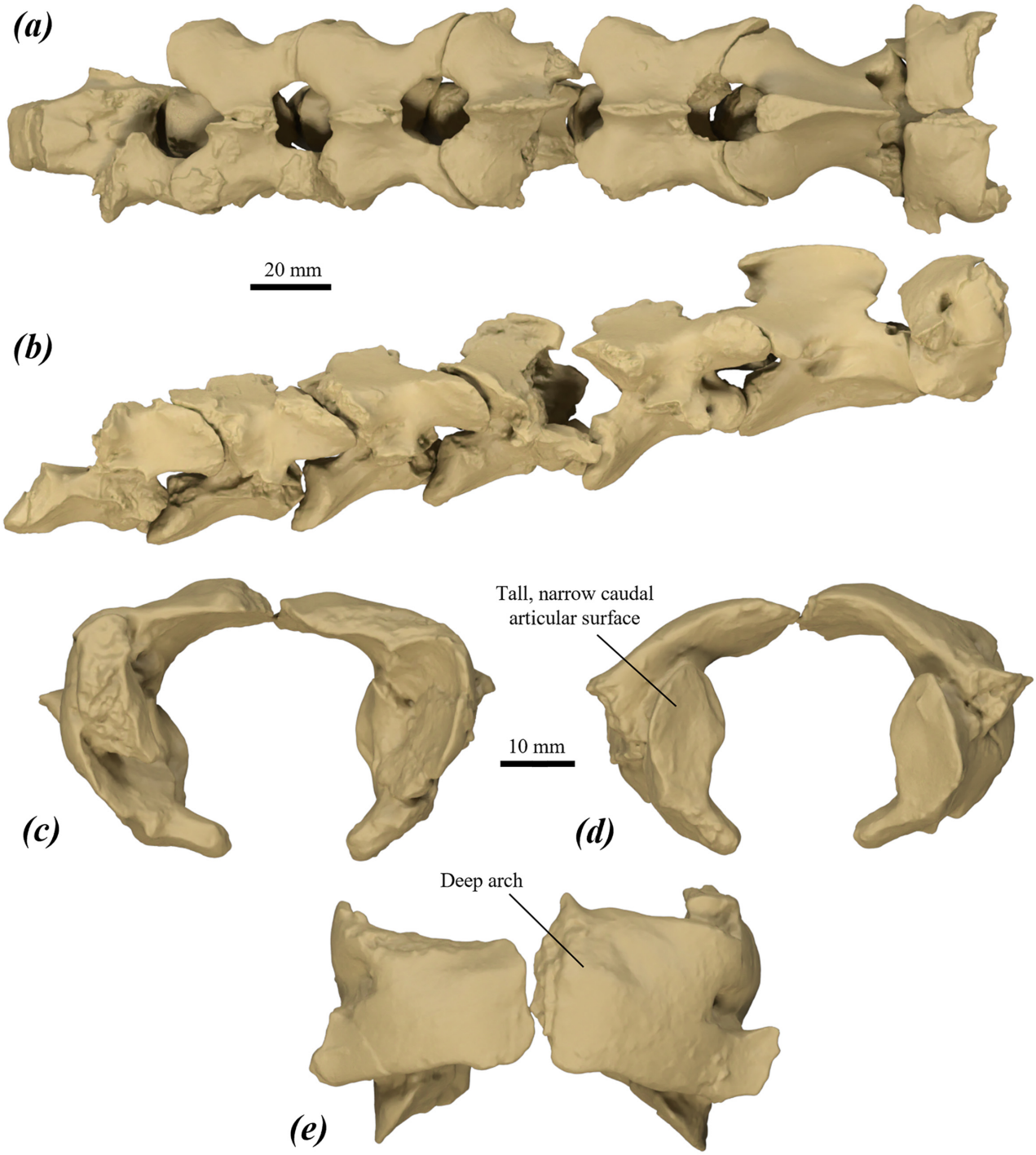

FIGURE 13. surface scan images of cervical vertebrae of *P. anak* NMV P39101: (a–b) cervical vertebrae C1–7 in (a), dorsal, and (b) lateral views; and (c–e) atlas vertebra C1 in (c) cranial, (d) caudal, and (e) dorsal views.

and less dorsolaterally tilted cranial articular surfaces; from *P. dawsonae* in having a more elongate and less dorsally deflected dens and dorsoventrally taller and less convex cranial articular surfaces; from *C. kitcheneri* in being larger, with a less dorsally deflected dens and a relatively larger caudal extremity of the centrum; from *O. rufus* in being larger, with a longer and less dorsally deflected dens, less laterally tilted cranial articular surfaces, and a spinous process with a gently convex dorsal margin and a rounded cranial margin; from *M. fuliginosus* in being larger, with a less dorsally deflected dens, relatively larger cranial articular surfaces, a and small caudal eminence present on the caudodorsal margin of the spinous process; and from *W. bicolor* in being larger, with a longer dens, taller cranial articular surfaces, the spinous process smaller relative to the centrum with a less cranially inclined dorsal margin and much smaller, less caudally projected caudal component, larger and more elongate postzygopophyses

and a more caudally projected caudal extremity of the centrum.

Cervical vertebrae (C3–7) (Figs 12a, 13a–b, & 15): large, solid, and elongate. Centrum depth decreases slightly from C3 to C7. Cranial extremity of the centrum broad, slightly dorsoventrally compressed, cranially projected and very concave in dorsal view, with the cranial surface tilted ventrally. Prezygopophyses large, broad, laterally deflected, and projected cranially, extending beyond the margins of the cranial extremity of the centrum; some narrowing occurs at base; articular surfaces very large, rounded, flat, tilted very slightly medially and strongly dorsally at around 45°; subequal in size to the vertebral canal in cranial view. Spinous process low, slightly projected cranially and caudally past the margins of the arch, with the dorsal margin gently convex in lateral view. Vertebral canal roughly circular (Fig. 15g). Arch quite thick and elongate; only the bases of the transverse processes preserved, but inferred to be short and thick, with the transverse foramina small, round, and roughly level with the dorsal margin of the cranial and caudal extremities; tubercles on the ventral bases of the transverse processes mostly abraded; bases intact in C6, inferred to be large and markedly elongate. Centrum broad relative to caudal extremities, with the craniomedial component of the ventral surface convex; a narrow medial ridge on the caudal component of the ventral surface extends to the caudal margin. Postzygopophyses robust, very large, very broad, and slightly projected caudally, with a small, pointed eminence on the cranial margins of the postzygopophyses of C3 giving a slight hooked appearance; articular surfaces large, tilted slightly laterally and strongly ventrally at around 45°, roughly round in C3, becoming more elongate dorsoventrally toward C6, with slight concavity in dorsal component of medial margin in C5–C6. Caudal extremity of the centrum large, very elongate, caudally curved, and caudoventrally projected; extends caudally beyond the margins of the postzygopophyses; outline of the articular surface is a rounded square in caudal view, and becomes taller distally in lateral view; articular surface very slightly concave.

The cervical vertebrae of *P. anak* differ from those of all compared taxa in being more elongate and having a very strongly caudoventrally projected caudal extremity of centra. Further differ from those of *P. mamkurra* in having larger, more cranially projected, and more cranially tilted prezygopophyses, more rounded vertebral canals, larger postzygopophyses and narrower caudal extremity of centra; from *P. viator* in being taller and relatively narrower, with larger pre- and postzygopophyses, taller, narrower cranial extremity of centra and taller, narrower, more caudoventrally projected caudal extremity of centra lacking a slightly bilobed ventral margin; from *P. tumbuna* in having larger and less medially tilted prezygopophyses, larger and less laterally tilted postzygopophyses, taller and narrower vertebral canals, and taller cranial extremity of centra; from *C. kitcheneri* in being larger, with more elongate and less laterally projected pre- and postzygopophyses; from *O. rufus* in being larger, with more rounded, less medially and more cranially tilted cranial articular surfaces, relatively larger and more laterally flared pre- and postzygopophyses, relatively narrower cranial extremity of centra, rounder and less domed vertebral canals and relatively narrower caudal extremity of centra; from *M. fuliginosus* in being larger, with relatively larger and more cranially projected prezygopophyses, more cranially tilted cranial articular surfaces, rounded, less domed vertebral foramina, larger, more caudally projected postzygopophyses and more caudally tilted caudal articular surfaces; and from *W. bicolor* in being larger and relatively taller and narrower, with larger prezygopophyses with more cranially tilted articular surfaces, rounder, less reniform vertebral canals, larger postzygopophyses with more caudally tilted articular surfaces and taller, narrower, more caudoventrally projected caudal extremity of centra.

Thoracic vertebra (T2?) (Fig. 16): large and tall. Cranial extremity of the centrum abraded on the lateral margins, inferred to be roughly triangular in cranial view, very slightly convex, and not cranially projected. Prezygopophyses small and projected cranially slightly beyond the margin of the cranial extremity of the centrum; articular surfaces small, smooth, flat, and oval, facing dorsolaterally at ~45° from transverse plane, situated cranial to the lateral margins of the arch. Cranial costal fovea abraded and poorly preserved. Centrum roughly triangular in cross-section, with the lateral surfaces tilted distinctly ventrally; ventral surface narrows strongly to an angular, thickened medial ridge; dorsal component broadens caudally. Spinous process very tall, transversely compressed, becoming slightly craniocaudally longer at its midpoint, and slightly cranially deflected; tip slightly thickened and rugose. Vertebral canal rounded and very slightly transversely compressed; arch robust, low, and roof-like in angle. Diapophyses quite large and robust, thickened and rugose on the lateral surfaces; a low ridge along the craniodorsal margin of the diapophyses caudodorsally bounds a broad, shallow groove over the base of the prezygopophyses (Fig. 16e). Caudal extremity of the centrum quite broad, slightly concave, and distinctly larger and taller than the cranial extremity; projected caudally slightly more than the postzygopophyses. Caudal costal fovea large and concave, covering lateral margins of the caudal extremity of the centrum, facing caudally and slightly laterally.

The T2 of *P. anak* differs from that of *C. kitcheneri* in being larger, with a slightly cranially deflected (rather than caudally deflected) spinous process and in lacking a low, rounded crest on the ventral component of the cranial margin of the spinous process; from *O. rufus*, *M. fuliginosus* and *W. bicolor* in being larger, with a slightly taller centrum and a relatively longer and slightly cranially deflected (rather than caudally deflected) spinous process not tapering to point in lateral view.

Sacrum (S1–2, 3) (Fig. 17): large, broad, robust and dorsoventrally compressed; broadest cranially and roughly triangular in dorsal view. Cranial extremity of the centrum broad, oval and distinctly dorsoventrally compressed; caudal extremity of the centrum taller and more rounded. Prezygopophyses small and elongate with a robust base,

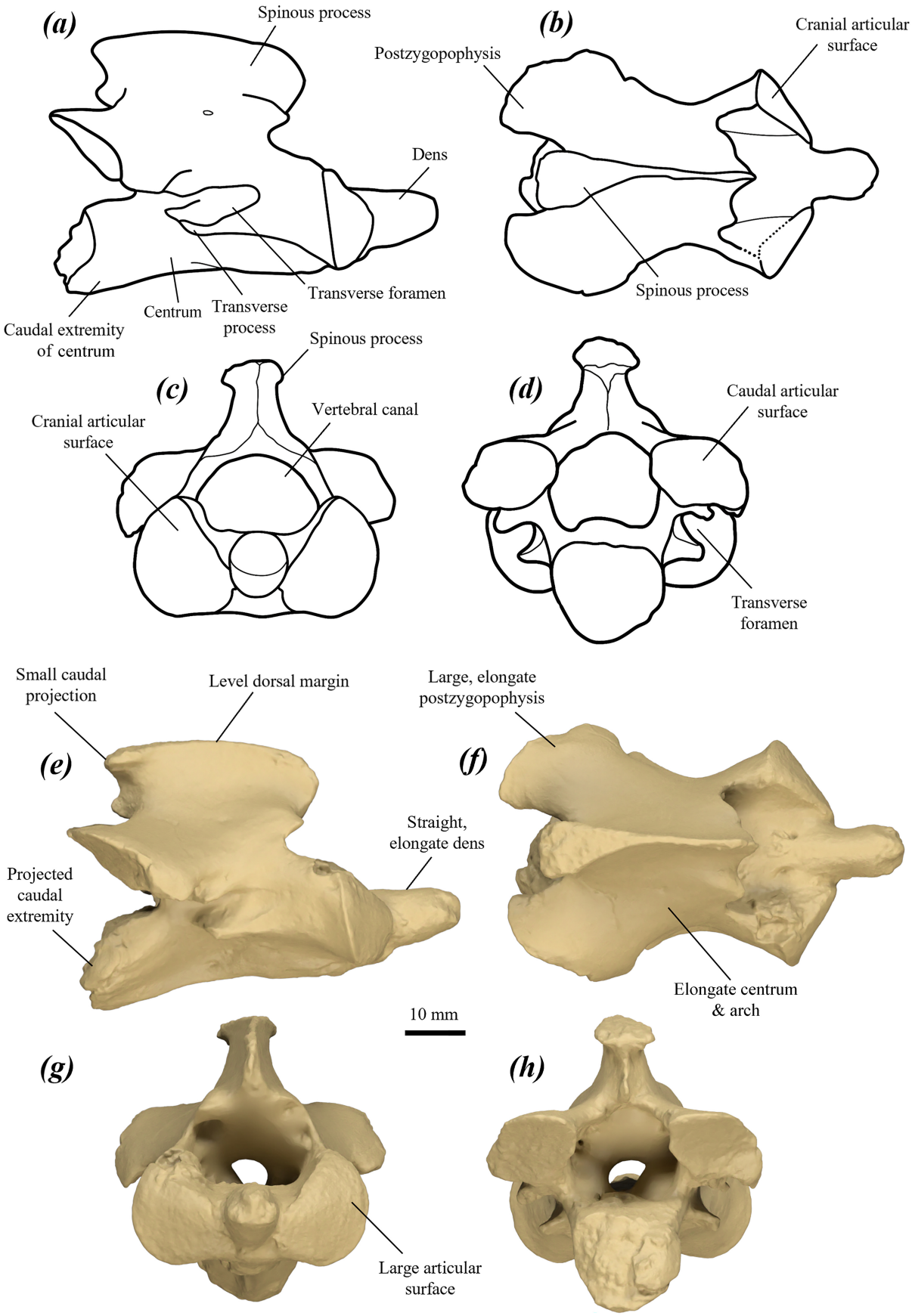

FIGURE 14. axis vertebra (C2) of *P. anak* NMV P39101.4: line drawings (a–d) and surface scan images (e–h) in: (a, e) lateral, (b, f) dorsal, (c, g) cranial, and (d, h) caudal views.

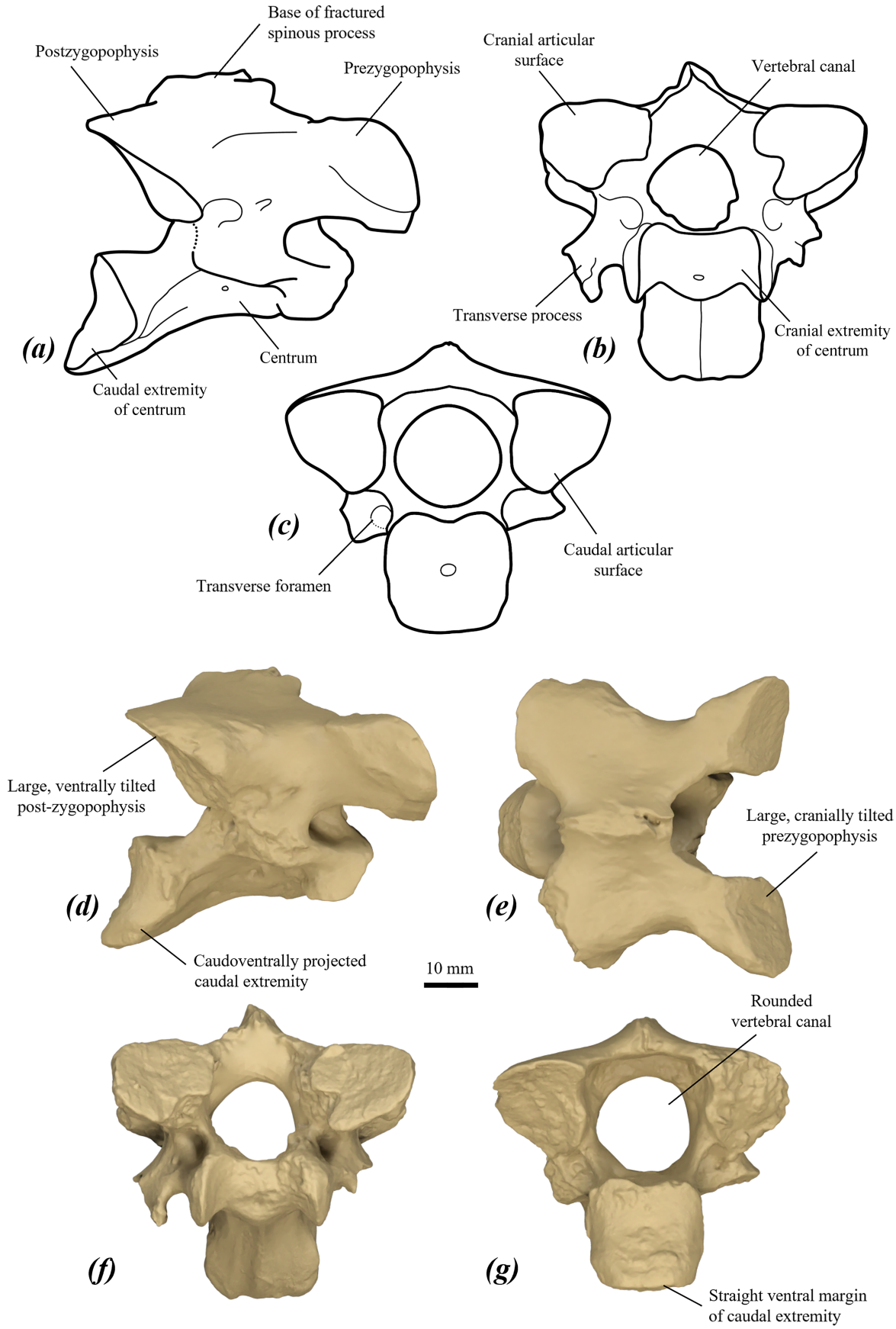

FIGURE 15. cervical vertebrae of *P. anak* NMV P39101: (a–c) line drawings in (a) right lateral, (b) cranial, and (c) caudal views; and (d–g) surface scan images in (d) right lateral, (e) dorsal, (f) cranial, and (g) caudal views. (a, b, d, f) show C3; (c, e, g) show C5.

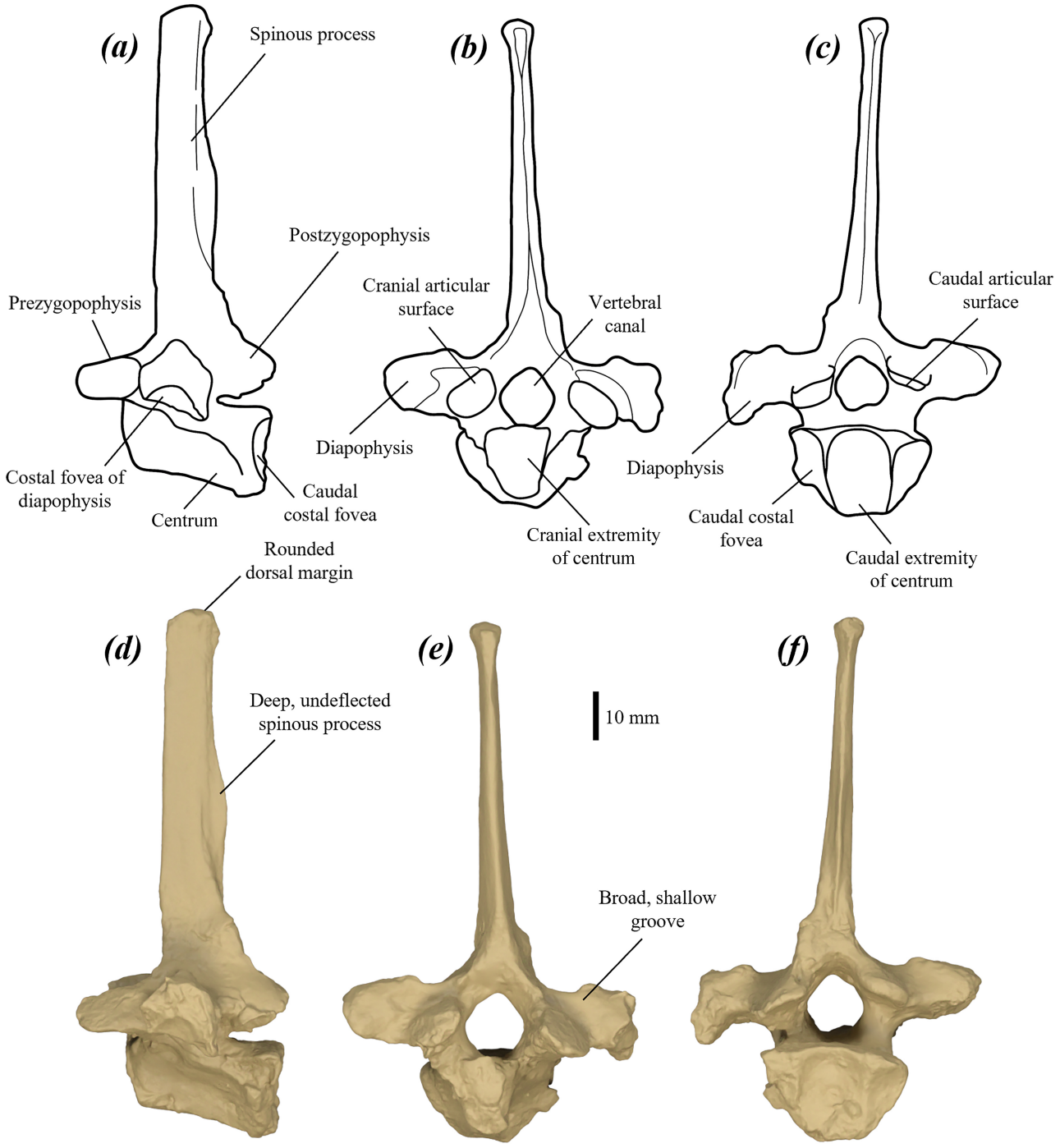

FIGURE 16. thoracic vertebra T2 of *P. anak* NMV P39105.17: line drawings (a–c) and surface scan images (d–f) in (a, d) left lateral, (b, e) cranial, and (c, f) caudal views.

project cranially beyond the cranial extremity of the centrum; articular surfaces oval, transversely compressed, slightly concave and facing dorsally with a slight medial rotation. The vertebral canal is dorsoventrally slightly compressed and roughly reniform. Wings broad, height increases to large auricular surface; a large, gently concave is fossa present against the lateral margin on the dorsal surface (Fig. 17c). Auricular surface roughly rounded and very rugose, with caudoventral margin abruptly narrowing caudally. Sacral tubercle large, oval and concave; sacral canal absent; sacral foramina quite large and rounded, with much smaller additional foramen cranially adjacent to one or both sacral foramina, only penetrating through dorsal arch. Spinous processes with bases robust; those of S1 and S2 vertebrae not fused across vertebral suture. Transverse processes: cranial part robust, moderately dorsoventrally compressed and more laterally extensive, merges with caudal margin of wings; broader, more gracile, highly dorsoventrally compressed and laterally pointed caudal part, arises craniolaterally

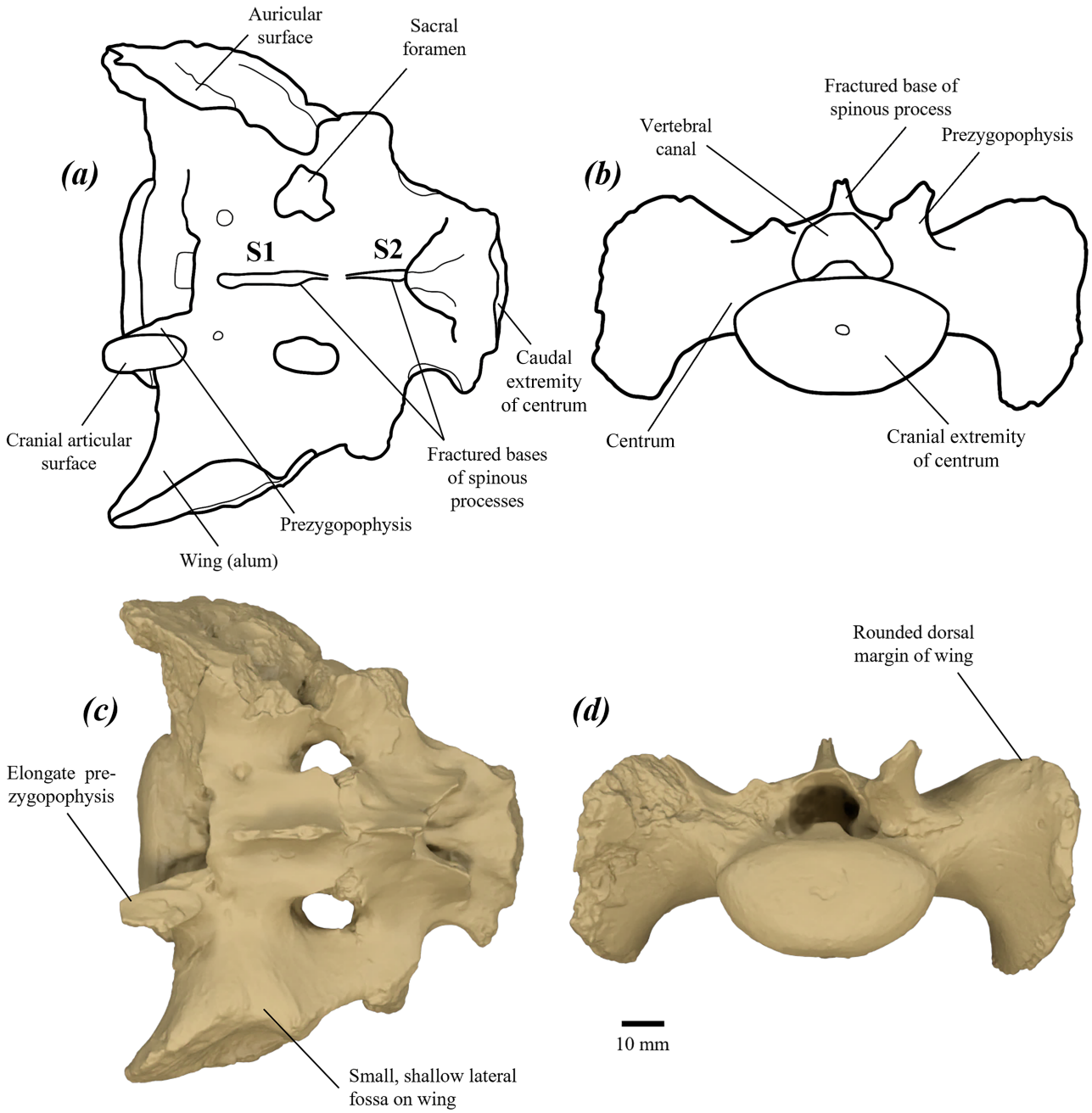

FIGURE 17. sacrum of *P. anak* specimen NMV P39105.75: line drawings (a, b) and surface scan images (c, d) in (a, c) dorsal, and (b, d) cranial views.

adjacent to caudal extremity; parts separated by dorsoventrally compressed mesial section with concave lateral margin in dorsal view. Postzygopophyses not known.

The sacrum of *P. anak* differs from that of *P. mamkurra* **sp. nov.** in having smaller, shallower fossa against lateral margin on dorsal surface of wings; from *C. kitcheneri* in being larger and more elongate, with more elongate and more cranially projected prezygopophyses; and from *O. rufus* and *M. fuliginosus* in being relatively longer, with less medially tilted cranial articular surfaces and wings with rounded (rather than pointed) cranial margins.

Caudal vertebrae (Ca6, 7 & 13?) (Fig. 18a–f): numerical position of vertebrae estimated. Large and robust, with well-developed processes, narrow slightly to a waist in dorsal view; length decreases from Ca6 to Ca13. Ca6: cranial extremity of the centrum large and roughly round with a flat dorsal margin and the caudal extremity oval, broad and dorsoventrally compressed. Mammillary processes (prezygopophyses) very tall, straight, transversely compressed, quite long craniocaudally, dorsolaterally situated and slightly more dorsally than laterally deflected in cranial view (Fig. 18f); cranial articular surfaces absent. Cranial transverse processes small, planar and laterally projected, with thin crest extending caudally along the lateral surfaces to merge with the caudal transverse processes. Caudal transverse processes very broad, dorsoventrally compressed and

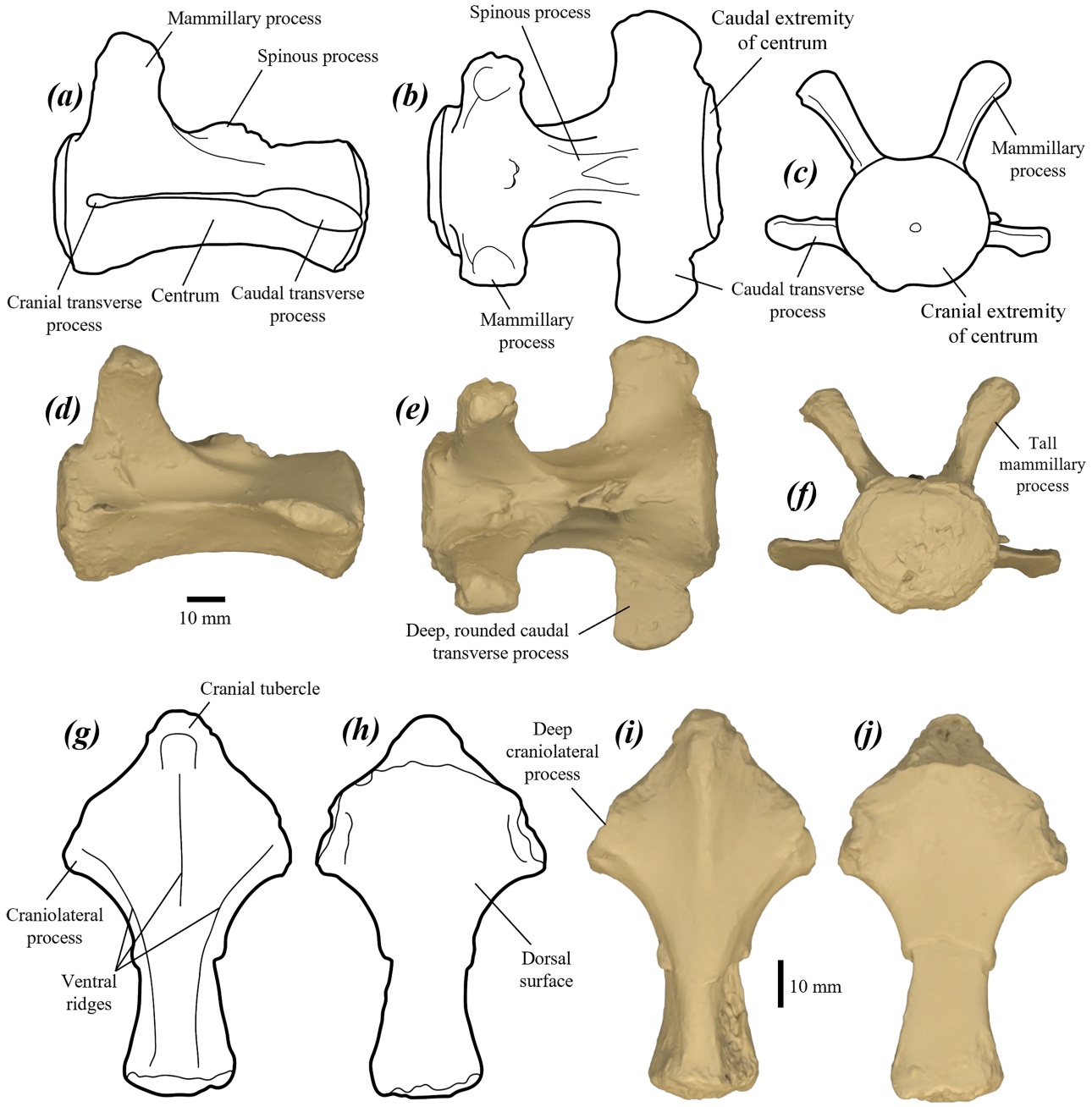

FIGURE 18. (a–c) line drawings and (d–f) surface scan images of caudal vertebra Ca6 of *P. anak* NMV P39105.24 in (a, d) left lateral, (b, e) dorsal, and (c, f) cranial views; and (g, h) line drawings and (i, j) surface scan images of manubrium of *P. anak* NMV P39101.66 in (g, i) ventral, and (h, j) dorsal views.

craniocaudally long, with depth not tapering to gently rounded lateral margins. Postzygopophyses present as very small, thin crests situated on the midpoint of the dorsal surface, abutting caudal margins of the bases of the mammillary processes. Ca7: cranial and caudal extremities of the centrum similarly round in cranial and caudal views. Mammillary processes not preserved, but their bases appear large and transversely compressed. Cranial transverse processes not preserved, but their bases appear thicker and more developed than in Ca6. Caudal transverse processes mostly abraded, but their bases appear craniocaudally shorter and less dorsoventrally compressed than in Ca6.

Ca13: cranial extremity of the centrum round to smoothly hexagonal; caudal extremity round with small concavities on dorsal and ventral margins. Mammillary processes moderately short and robust, dorsally situated, curved toward the midline and dorsomedially deflected such that the dorsal component is fused over a small, rounded vertebral canal. Cranial transverse processes thick and robust, uncompressed dorsoventrally, not extending cranially beyond margin of cranial extremity of the centrum, craniolaterally deflected in dorsal view, dorsally deflected in cranial view and smoothly extending caudally to merge with centrum around the midpoint.

Two very thin, parallel ridges extend craniocaudally along the midline of the caudal surface. Caudal transverse processes small, thickened and blunt, less elongate than cranial processes; abut caudal extremity of the centrum on the dorsal component of the lateral surfaces, dorsally deflected in caudal view; caudal ventral processes are small, thickened, blunt tubercles, projecting ventrally either side of the midpoint of the ventral margin of the caudal extremity.

The caudal vertebrae of *P. anak* differ from those of *P. mamkurra* in being generally slightly more robust and in having larger caudal transverse processes on Ca6; from *P. viator* in being generally more robust, with caudal transverse processes of Ca6 broader and with depth not tapering to tips; from *P. tumbuna* and *P. dawsonae* in being larger; from *C. kitcheneri* in being larger and more robust, with taller, straighter prezygopophyses lacking cranial deflection on Ca6, and dorsoventrally thicker, more robust transverse processes on Ca13; from *O. rufus* and *M. fuliginosus* in being generally larger and more robust, with taller mamillary processes and smaller caudal transverse processes on Ca6–7; and from *W. bicolor* in being larger and more robust, with Ca7 with larger, more dorsally deflected mammillary processes, smaller, narrower cranial transverse processes and larger, broader and less laterally tapering caudal transverse processes.

Manubrium (Fig. 18g–j): large, robust, deep and dorsoventrally compressed; roughly arrowhead- to crucifix-shaped in ventral view. Cranial extremity thickened, with a rounded tubercle on ventral surface; manubrium then broadens caudally from a rounded cranial point to squared craniolateral processes before narrowing caudally to an elongate caudal component. Craniolateral processes for articulation with clavicles rugose and thickened, rounded in lateral view; articular facets for clavicles not preserved. Dorsal surface planar, with some thickening around the craniolateral extremities. Ventral surface with broad, low ridges extending caudomedially from the craniolateral processes and a taller medial ridge from the cranial extremity, merging in the caudal part and extending to the caudal extremity; possibly attachment sites for the origin of the m. pectoralis superficialis (Warburton *et al.* 2011). Caudal component deepens caudally, narrower ventrally than dorsally and thus roughly diamond-shaped in cross-section; taller lateral surfaces possibly for the attachment of the m. subclavius (Warburton *et al.* 2011).

The manubrium of *P. anak* differs from that of *C. kitcheneri* and *O. rufus* in being larger; from *M. fuliginosus* in being larger, with a less distinct medial ventral ridge, particularly on the caudal component; and from *W. bicolor* in being larger, more robust and relatively broader, with deeper, more cranially situated craniolateral processes, a lower medial ventral ridge and a taller caudal part.

Forelimb

Scapula (Fig. 19): broad and deep; acromion not preserved in available specimen. Spine extends medially almost to medial edge (Fig. 19c), cranially inclined in lateral view; tall and thin, becoming lower medially (i.e. toward vertebral column) to merge with the scapular body short of the cranial angle. Scapular notch moderately deep and obtuse, external angle approaches 100°. Supraspinous fossa very gently concave; roughly half the size of the infraspinous fossa. Infraspinous fossa broad, deep, and gently concave. Cranial angle thickened; medial border (between the cranial and caudal angles) deep and gently convex. Caudal angle obtuse, comes to a broad, rounded point. Caudal border linear to very slightly convex, distinctly thickened relative to the infraspinous fossa and other borders; medial component and glenoid tubercle not known. Subscapular fossa slightly convex around a slight, shallow channel extending transversely, ventral and parallel to the scapular spine. Glenoid cavity large, oval and gently anteroposteriorly compressed, with cranial margin gently curving out laterally. Supraglenoid tubercle small, blunt and slightly projected laterally. Coracoid process a blunted, rounded point, slightly larger than supraglenoid tubercle, situated ventromedial to the supraglenoid tubercle and pointed anteromedioventrally.

The scapula of *P. anak* differs from that of *P. mamkurra* in having a thinner, more medially extensive scapular spine; from *P. viator* in being broader, with a thinner, more medially extensive spine; from *C. kitcheneri* in having a slightly larger supraspinous fossa relative to the infraspinous fossa, less anterolaterally projected coracoid process and glenoid tubercle, shorter and thicker coracoid process, and a rounder, less anteroposteriorly compressed glenoid fossa; from *O. rufus* in being broader than depth, with a relatively less medially extensive caudal section, more gently curved angle between the scapular notch and cranial angle, scapular notch with a wider angle, and a rounder, slightly less anteroposteriorly compressed glenoid fossa; from *M. fuliginosus* in being generally larger, with a narrower infraspinous fossa and slightly less anteroposteriorly compressed glenoid fossa; from *W. bicolor* in being larger, with a relatively less medially extensive caudal section, less medially extensive spine, broader scapular neck, and a more ventrally tilted coracoid process.

Humerus (Fig. 20): Given the probable sexual dimorphism in this element, the two very large humeri that form the basis of this description (NMV P39101 and NMV P39105, both partial skeletons) are probably those of adult males. NMV P39105 has the longest humerus known for the genus.

The humerus is large, deep, and elongate with well-developed muscle attachments; straight to very slightly curved in cranial view. Head roughly hemispherical and medially projected; similar in height to the greater tubercle. Greater tubercle large, quite tall, deep, and highly transversely compressed; crest of greater tubercle extends as tall, broad, craniomedially facing ridge merging smoothly with the pectoral crest (Fig. 20e). Lesser tubercle relatively narrower in craniomedial view and rounded in dorsal view; smoothly merges into the humeral shaft roughly midway between the head and the pectoral crest. Bicipital groove deep, distinct, and quite broad, extends distally into a broad, shallow fossa medial to the pectoral crest.

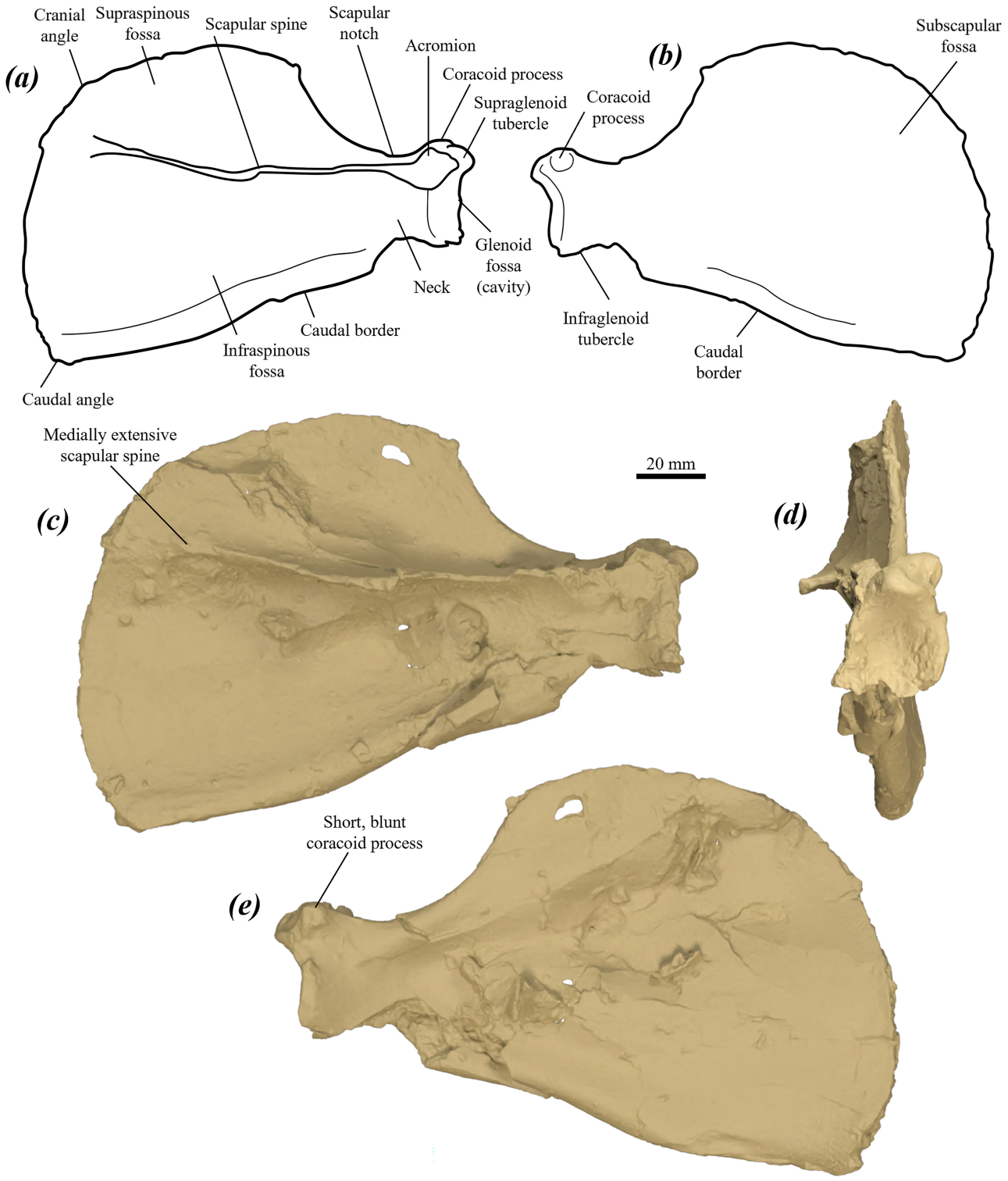

FIGURE 19. left scapula of *P. anak* specimen NMV P39101: (a–b) line drawings in (a) dorsolateral, and (b) ventromedial views; (c–e) surface scan images in (c) dorsolateral, (d) proximal/lateral, and (e) ventromedial views.

Proximal shaft robust and very deep, deepens proximally in lateral view (Fig. 20g). Deltoid tuberosity quite proximodistally short, fairly narrow in lateral view, and comes to a broadly pointed, rugose peak; positioned two-thirds of the distance from the humeral head to the peak of the pectoral crest. The teres tubercle is absent. There is a broad, rugose, muscle scar slightly proximal to the pectoral crest on the medial surface of the shaft for the insertion of the m. latissimus dorsi. Pectoral crest large, thickened, elongate, with the cranial margin rugose and rounded in lateral view and tilted distinctly laterally in cranial view. Distal component of the shaft (between pectoral crest and lateral supracondylar ridge) narrow and gracile compared to proximal shaft. Distal end broad,

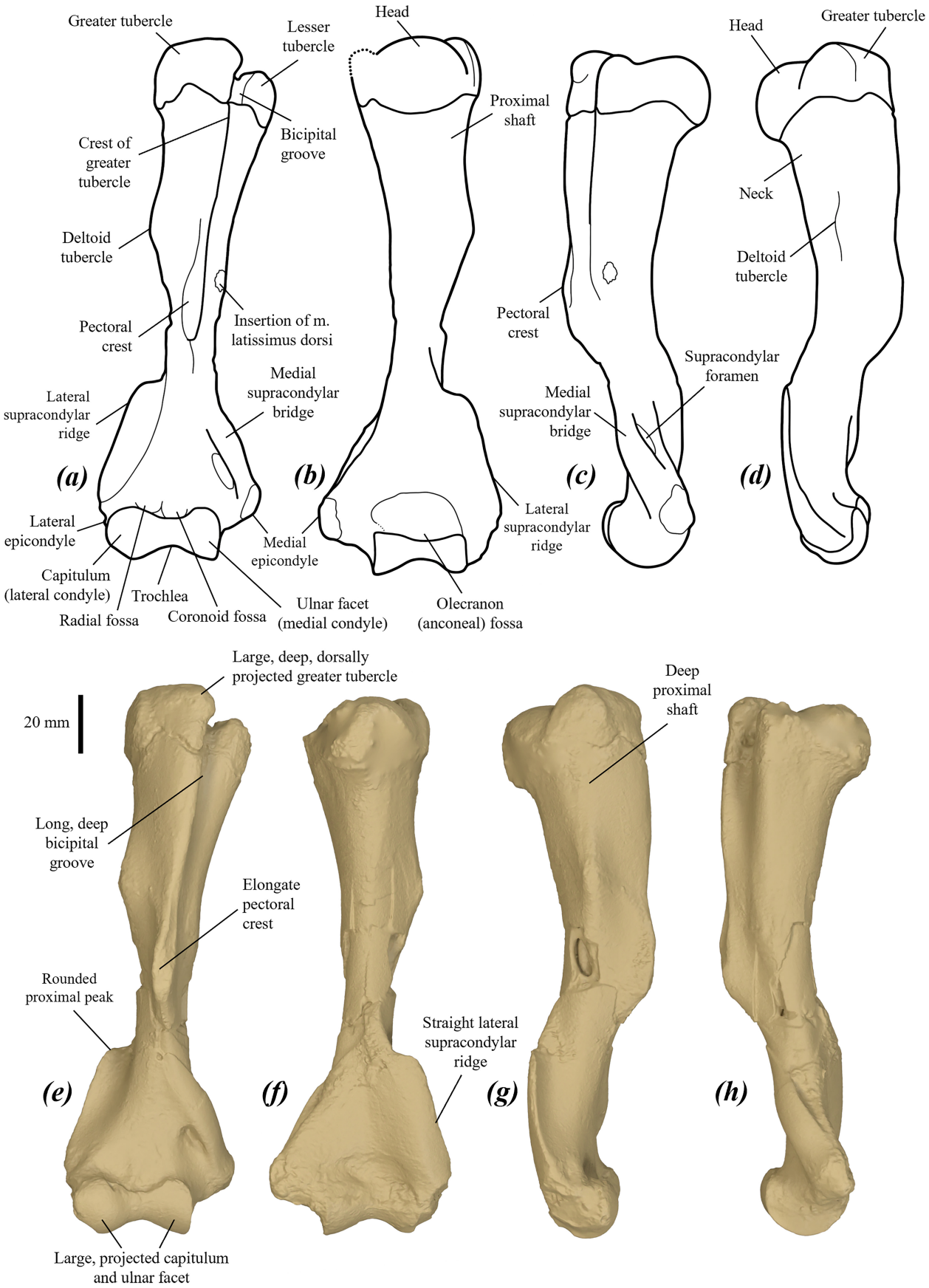

FIGURE 20. right humerus of *P. anak* NMV P39105.1: (a–d) line drawings and (e–h) surface scan images in (a, e) cranial, (b, f) caudal, (c, g) lateral, and (d, h) medial views.

rotated distinctly medially in distal view relative to shaft and proximal head. Lateral supracondylar ridge large and quite broad, broadens slightly proximally, slightly convex caudally and extending proximally with caudal tilt, such that proximal component of ridge extends around lateral surface of the shaft to merge with caudal surface; proximal peak broad with rounded tip (Fig. 20f). Capitulum (lateral condyle) and ulnar facet (medial condyle) laterally situated, abutting lateral epicondyle; capitulum slightly larger, cranially rotated and projected with lateral margin rounded; ulnar facet with the medial margin raised, straight and sharply angular; combined width roughly two-thirds of epicondylar width. Trochlea quite deep and smoothly concave. Medial epicondyle pointed and medially projected. Medial supracondylar bridge broad, thin and elongate, extends onto humeral shaft as broad, low ridge. Supracondylar foramen elongate, oval and very craniocaudally compressed. The radial fossa is small, shallow, gently concave and indistinct; coronoid fossa (supratrochlear fossa) small and shallow; olecranon fossa broad, moderately concave, with margins indistinct.

The humerus of *P. anak* differs from that of *P. mamkurra* in being longer, with a longer and more deeply concave bicipital groove, longer pectoral crest, and longer lateral supracondylar ridge with more rounded proximal peak; from *P. viator* in being longer, with longer pectoral crest, relatively slightly narrower distal end and straighter lateral margin of lateral supracondylar ridge; from *P. tumbuna* in being larger, with relatively more distally situated pectoral crest and less elongate distal end; from *P. otibandus* in being larger, with larger and more distally projected capitulum and ulnar facet; from *C. kitcheneri* in being larger and lacking a crest on the distal margin of the attachment site for the m. latissimus dorsi, with a more medially projected humeral head, larger, deeper and more dorsally projected greater tubercle, much deeper, narrower bicipital groove, deeper proximal shaft, smaller and less elongate deltoid tuberosity, lower, straighter pectoral crest, more elongate distal end, less pointed proximal peak of the lateral supracondylar ridge, and a broader medial supracondylar bridge; from *O. rufus* in having a deeper proximal shaft relative to length, with a more deeply concave bicipital groove, broader distal end and relatively shorter lateral supracondylar ridge; from *M. fuliginosus* in being larger, with a relatively larger, deeper greater tubercle, deeper proximal shaft, much deeper and more elongate bicipital groove, less elongate and less raised deltoid tuberosity, straighter and more raised pectoral crest, relatively broader distal end, less pointed proximal peak of lateral supracondylar ridge, shallower trochlea and relatively larger, more distally projected ulnar facet; and from *W. bicolor* in being larger and less laterally bowed in cranial view, with a more medially projected head, larger and more dorsally raised greater tubercle, lesser tubercle lacking dorsoventrally aligned groove on medial face, more deeply concave bicipital groove, lower, less elongate deltoid tuberosity, straighter pectoral crest, less pointed lateral supracondylar ridge, shallower radial, anconeal and olecranon fossae and relatively larger ulnar facet.

Ulna (Fig. 21): large, elongate, straight in cranial view and very deep proximally; recurved in lateral view, with proximal component curving smoothly cranially, curving slightly caudally around the midpoint and straightening distally (Fig. 21d). Olecranon quite short, index of olecranon length = 9.8 (total ulnar length/ length of olecranon from the midpoint of trochlea); slightly transversely compressed and narrowing slightly in lateral view to a blunt, squared distal end; epiphysis with a medially projected eminence on the caudomedial margin (Fig. 21f). The caudal margin beneath the humeral articulation is smoothly, gently convex. Facet for humeral articulation saddle-shaped, quite broad, with distinct but rounded trochlear notch; medial component deeply concave, situated more cranially than lateral component and proximodistally more elongate; lateral component shallow, concave and laterally projected, orientated craniolaterally and tilted laterally, with lateral margin sinusoidal in cranial view. Anconeal process mesial angle (peak) rounded and reflex. Coronoid process tall and quite narrow. Radial facet broad, gently concave, roughly semicircular and abutting the lateral three-quarters of the linear anterior margin of the lateral part of the humeral facet. Ulnar tuberosity low, narrow, quite elongate, and rugose, with the cranial and lateral components abutting the anterior margins of the coronoid process and radial facet, respectively.

Proximal part of the shaft tall and highly transversely compressed, transitions to cylindrical in the distal part (distal to midpoint), deepens very slightly to the distal end; lateral surface slightly convex proximally, becomes slightly concave beneath the radial facet, transitions to gently convex around the midpoint; medial surface gently concave proximally (proximomedial flexor fossa, partial origin of mm. flexor carpi et digitorum), becomes planar or very slightly convex beneath radial facet, with distal component gently convex. There is an indistinct, shallow, elongate, laterally tilted fossa distal to the ulnar tuberosity, from which a slightly rounded, quite tall, and distinct ridge gently arises, extends distally along dorsolateral surface of the shaft, broadens then merges with the shaft around its midpoint. Distal end has a broad and cone-shaped epiphysis, smoothly narrows to a styloid process with a narrow base curving craniolaterally, and a globular tip.

The ulna of *P. anak* differs from that of *P. mamkurra* **sp. nov.** in being more elongate and gracile, with a greater degree of recurvature in lateral view, and the distal shaft more cylindrical; from *P. viator* **sp. nov.** in being generally narrower and more elongate, with a shorter olecranon relative to ulnar length and the distal component more cylindrical; from *P. tumbuna* in being deeper and more transversely compressed; from *P. otibandus* in being proximally taller, more transversely compressed, and more cranially curved between the humeral facet and midpoint, with a shorter olecranon process with large caudomedial eminence, and a shallower proximomedial flexor fossa; from *C. kitcheneri* in being larger, straighter in cranial view, proximally much deeper and more transversely compressed, and tapering more distally in lateral view, with less rounded, less raised radial notch, less medially flared coronoid process, lower

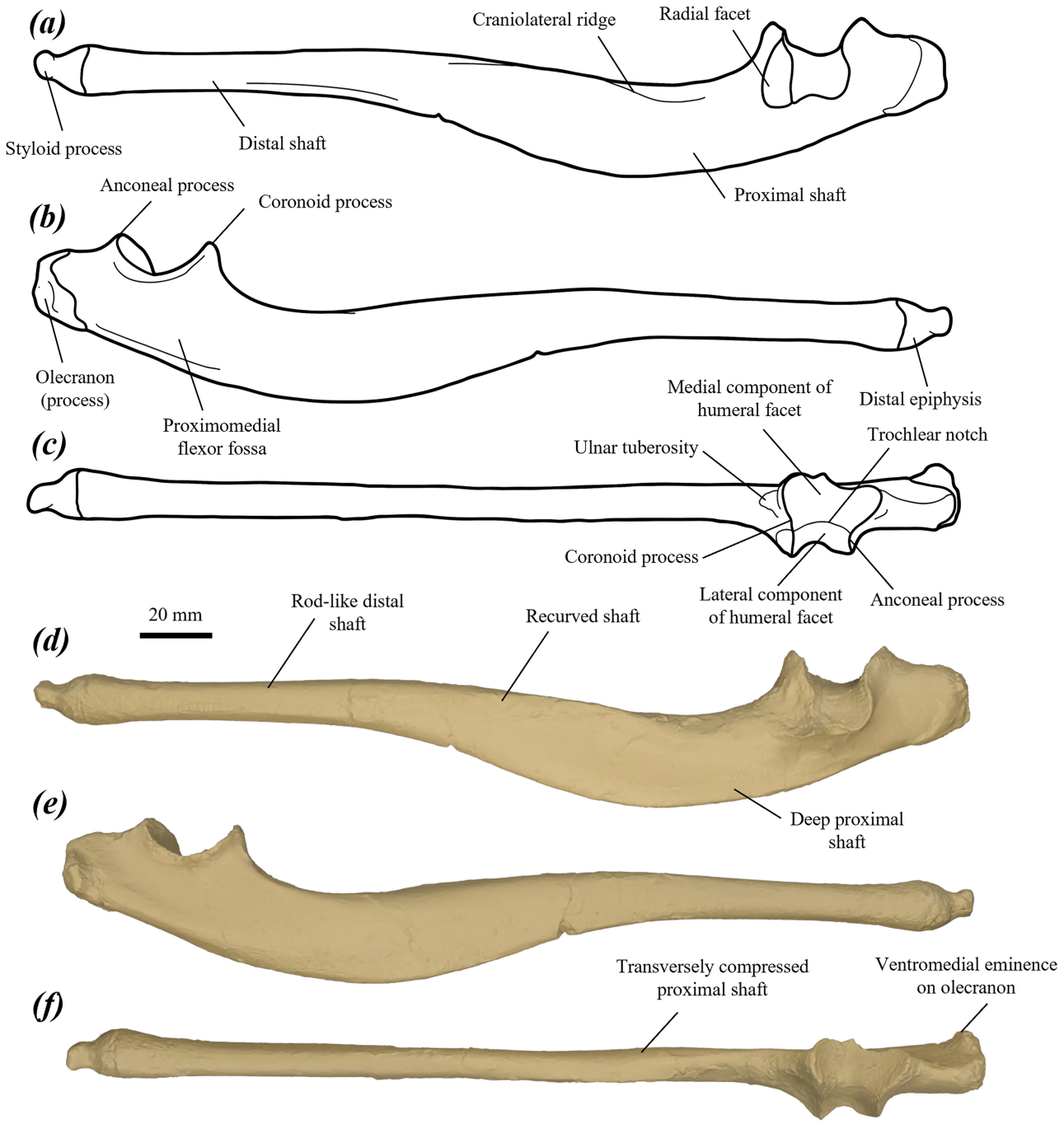

FIGURE 21. left ulna of *P. anak* NMV P39105.1: (a–c) line drawings and (d–f) surface scan images in (a, d) lateral, (b, d) medial, and (c, f) cranial views, with certain diagnostic features labelled.

and more proximally situated cranial ridge on shaft, less transversely compressed and more cylindrical distal shaft and more distally projected styloid process; from *O. rufus* in being generally larger, straighter in cranial view, more recurved in lateral view, and proximally deeper and more transversely compressed, with a more caudally deflected olecranon process, broader and less laterally tilted lateral component of the humeral facet, less bilobed lateral margin of the humeral facet, higher coronoid process, less laterally tilted radial facet, and less transversely compressed distal epiphysis; from *M. fuliginosus* in being larger, and deeper and more transversely compressed proximally, with broader and less laterally tilted lateral component of the humeral facet, less bilobed lateral margin of the humeral facet, less medially deflected and flared coronoid process, less laterally tilted radial facet, less cranially projected, less transversely compressed distal epiphysis with more distally projected styloid process; and from *W. bicolor* in being larger, and proximally slightly deeper and more transversely compressed, with a longer, less cranially deflected, and cranially unprojected olecranon, less medially flared anconeal process, lower, less medially

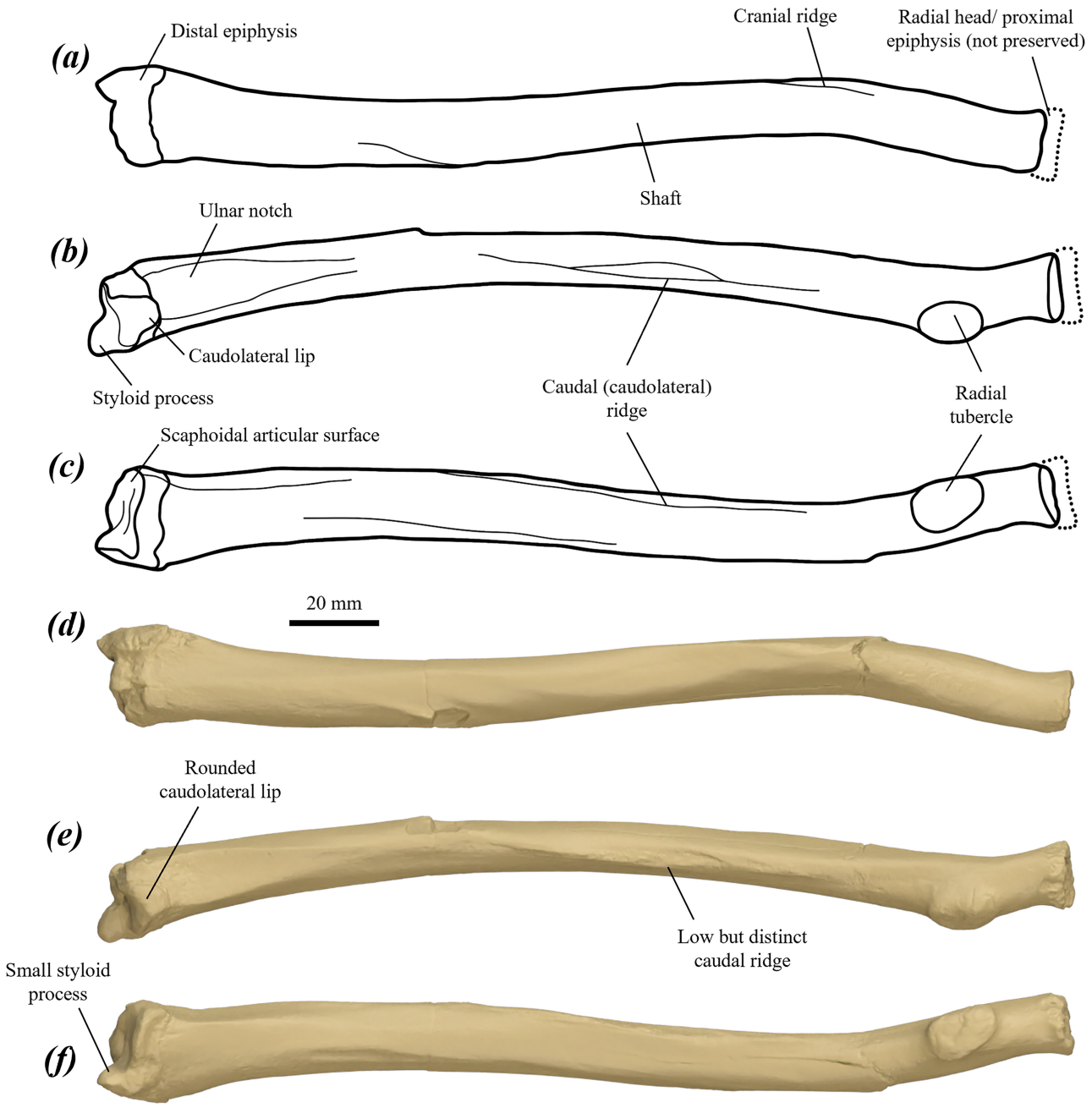

FIGURE 22. left radius of *P. anak* NMV P39101.47: (a–c) line drawings and (d–f) surface scan images in (a, e) cranial, (b, f) lateral, and (c, f) caudal views.

flared coronoid process, relatively shorter lateral component of the humeral facet, and a lower and broader cranial ridge on the shaft.

Radius (Fig. 22): large and elongate, with the shaft straight to gently caudomedially curved distal to the radial tubercle. Facet of radial head circular and smoothly concave. Radial neck has a slight waist proximal to the radial tubercle. Radial tubercle rugose, oval and gently projected caudally. Shaft cross-section is circular immediately distal to the radial tubercle, transitions to transversely compressed by the midpoint, and expands past midpoint to large distal end, becoming more cylindrical; in lateral view, it curves slightly caudally after an initial gentle cranial curve distal to the radial tubercle. The cranial ridge is a thin, elongate ridge on the craniomedial surface immediately proximal to the midpoint of the shaft; caudal ridge is relatively slightly lower and broader, caudomedial to the caudal surface (Fig. 22e), probable origin of the m. flexor digitorum profundus radiale; both ridges are higher in larger specimens. Ulnar notch broad, shallowly concave, and elongate, slowly tapers in height proximally along the caudolateral surface. Scaphoidal facet broad, slightly caudally tilted, and gently concave, with a rounded lip over the caudolateral margin, sitting caudal to a large, gently convex tubercle along cranial margin. Styloid process quite large, transversely compressed and tapering to a rounded tip.

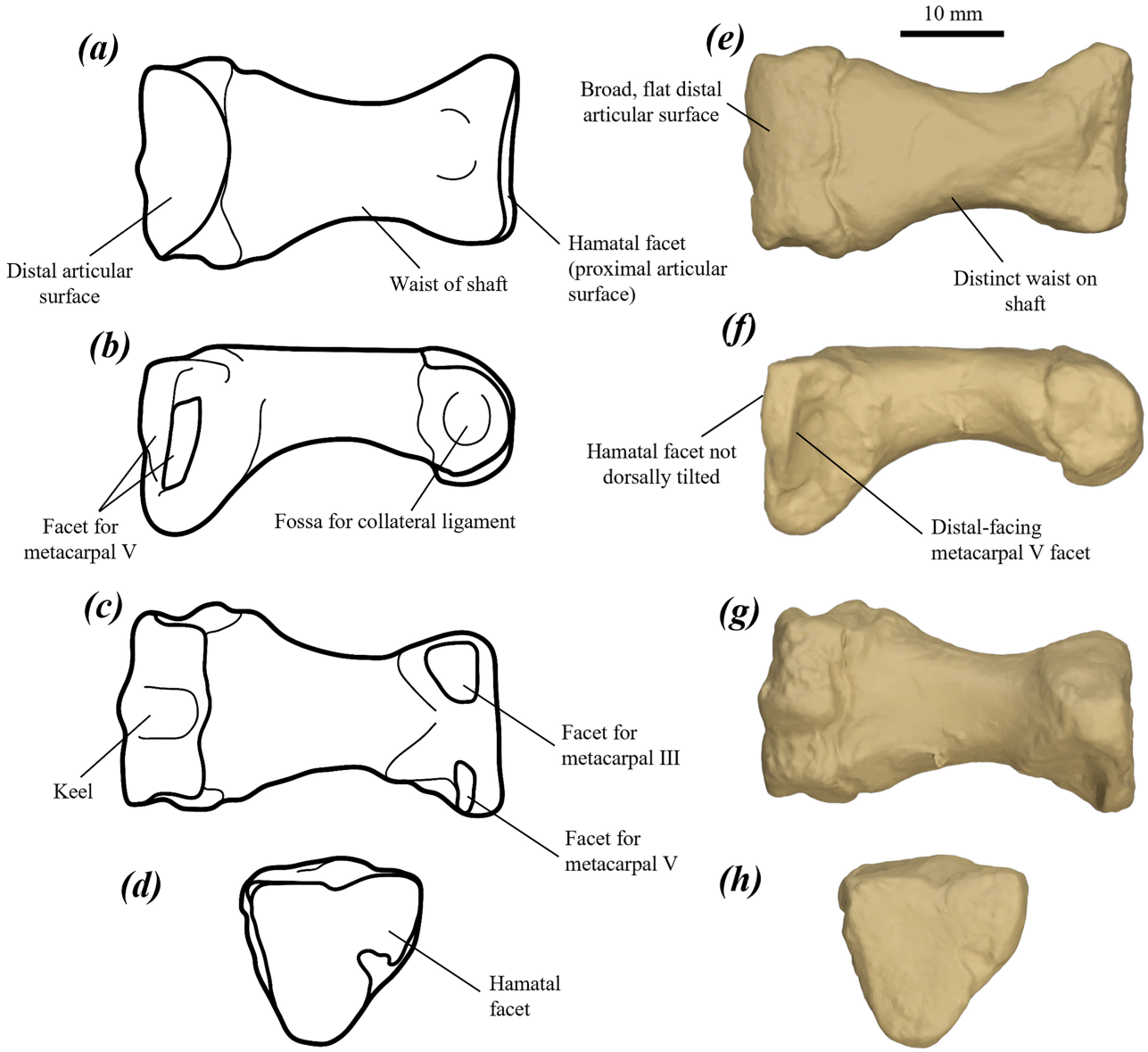

FIGURE 23. right metacarpal IV of *P. anak* NMV P39105: (a–d) line drawings and (e–h) surface scan images in (a, e) dorsal, (b, f) lateral, (c, g) palmar, and (d, h) proximal views.

The radius of *P. anak* differs from that of *P. mamkurra* in being more elongate, with the distal shaft having less craniocaudal compression and a more flattened caudomedial surface; from *P. viator* in having a slightly more distally situated cranial ridge and a more distinct caudal ridge; from *P. tumbuna* in having a smaller styloid process relative to the scaphoidal facet, more rounded distal end in distal view and more swollen cranial component of distal end; from *P. otibandus* in being generally larger, with the caudomedial surface of the distal shaft less flattened and the distal end less transversely compressed; from *C. kitcheneri* in being slightly more elongate and generally less curved, with a cranial ridge present, a considerably lower and less elongate caudal ridge, and a less cranially tilted scaphoidal facet with a rounded caudolateral lip and a low cranial tubercle both present; from *O. rufus* in being more robust, with a thinner, more raised cranial ridge, thicker, more raised caudal ridge, and a slightly more concave scaphoidal facet with rounded caudolateral lip and low cranial tubercle both present; from *M. fuliginosus* in being larger, with a more rounded, slightly more distally situated radial tubercle and more raised cranial and caudal ridges; and from *W. bicolor* in being larger, generally less curved, and lacking a caudally tilted distomedial ridge, with a higher cranial ridge, lower, less elongate caudal ridge, longer styloid process, and a scaphoidal facet with a smaller cranial tubercle.

Manus

Metacarpal IV (Fig. 23): short and very robust; tall proximally, becoming dorsopalmarly compressed distally. Proximal end flared laterally, triangular in proximal view, with a linear dorsal margin; large proximal facet for the hamatum smooth and flat. Facet for metacarpal V tall,

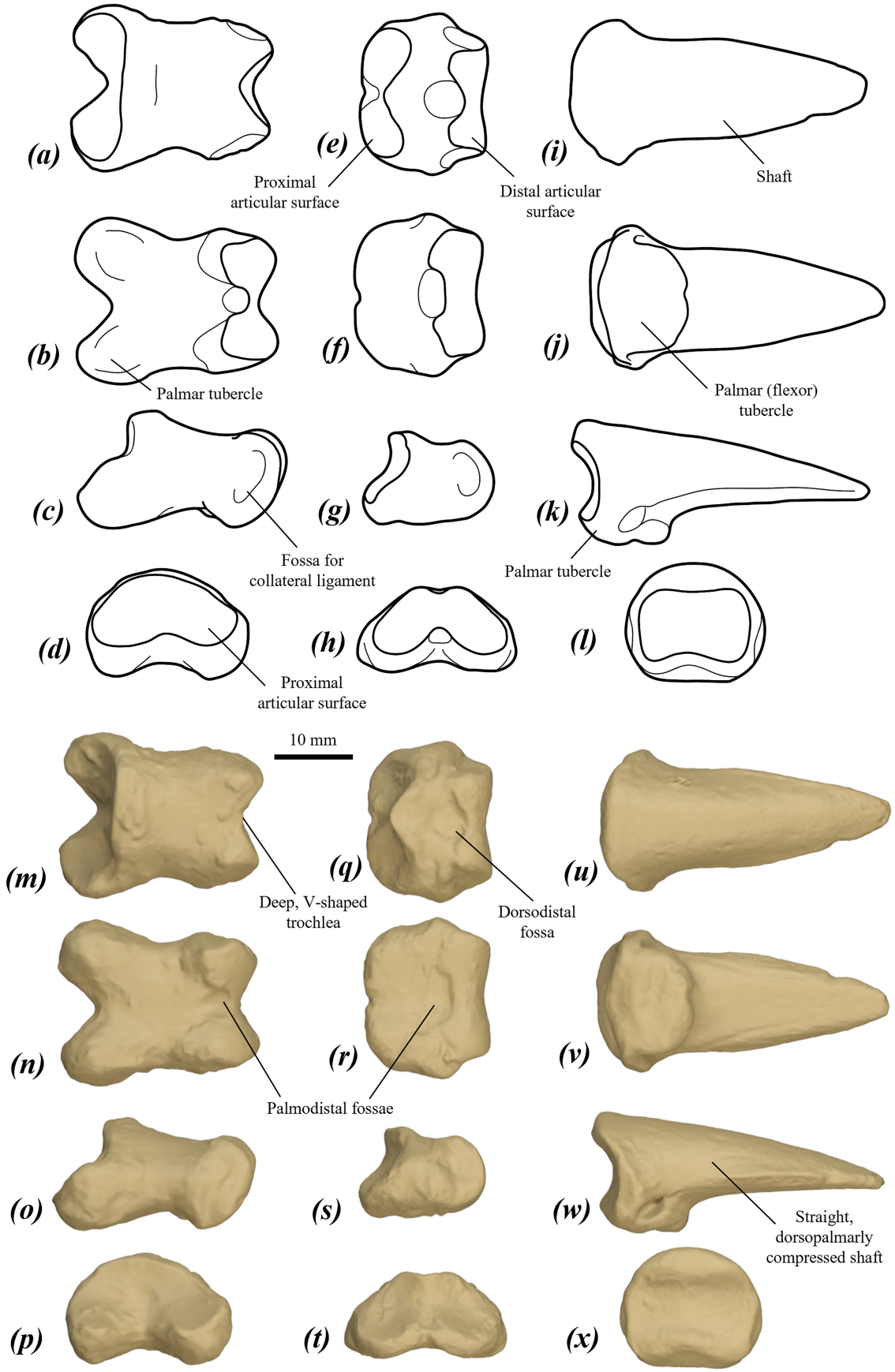

FIGURE 24. left manual phalanges III of *P. anak* specimen NMV P39105: (a–l) line drawings and (m–x) surface scan images of proximal phalanx III (a–d, m–p), middle phalanx III (e–h, q–t), and distal phalanx III (i–l, u–x) in dorsal (a, e, i, m, q, u), palmar (b, f, j, n, r, v), right lateral (c, g, k, o, s, w), and proximal (d, h, l, p, t, x) views.

narrow, very slightly concave, and distal-facing (Fig. 23f), located on the distal surface of a larger, concave fossa that opens distolaterally, on the distolateral surface of the proximal end. Facet for metacarpal III tall, narrow, and slightly convex, on the medial surface of the proximal end. Shaft narrows significantly to a waist before broadening to the distal end. Distal articular surface smoothly convex dorsopalmarly, with a prominent palmar keel. The fossae for collateral ligaments are round and shallow.

The metacarpal IV of *P. anak* is not differentiated from that of *P. mamkurra*. It differs from that of *P. viator* in being shorter and more robust, with a vertical (rather than dorsomedially tilted) hamatal facet and a distal-facing (rather than lateral-) metacarpal V facet; from *P. otibandus* in being slightly larger; from *C. kitcheneri* in having a less concave, less dorsally tilted hamatal facet, more distal facing facet for metacarpal V, narrower, more distinct waist, and a squarer, less convex distal end; from *O. rufus* and *M. fuliginosus* in being larger, and broader across distal end, with a less dorsally tilted hamatal facet and a more distal facing facet for metacarpal V; and from *W. bicolor* in being much larger and more robust, with a broader proximal end, narrower palmar component of the proximal end, less dorsally tilted proximal face, more distal facing metacarpal V facet, and a narrower waist.

Manual phalanges (Fig. 24): short, broad, dorsopalmarly compressed and tapering distally. Proximal phalanges: palmar tubercle distinctly proximally projected and articular surface distinctly dorsally tilted. Shaft narrows to a slight waist. Distal end with the distal surface distinctly palmarly tilted and the trochlea rounded-triangular (Fig. 24m). Distal articular surface with the medial and lateral sections tilted mesially and bifurcating proximopalmarly, with rounded mesial fossae against the proximopalmar and proximodorsal margins. Fossae for collateral ligaments tall, shallow and indistinct. Middle phalanges: very short, broad and dorsopalmarly compressed. Proximal articular surface slightly dorsally tilted with gently concave lateral and medial components separated by rounded medial ridge. Shaft very short, almost absent. Distal end relatively narrow, with a gently concave articular surface and rounded collateral ligament fossae. Distal phalanges: proximal surface oval, with the articular facet concave, and the palmar tubercle broad and rounded in palmar view. Shaft quite short, broad and straight (Fig. 24w), with the dorsal surface smoothly convex and the palmar surface very slightly convex.

The manual phalanges of *P. anak* differ from those of *P. mamkurra* **sp. nov.** in that the proximal phalanges have slightly deeper trochleae, and the distal phalanges have shorter, less dorsopalmarly compressed shafts; from *P. viator* **sp. nov.** in having proximal phalanges with deeper, more V-shaped trochleae and slightly more dorsally tilted proximal articular surfaces, middle phalanges with small palmodistal and dorsodistal fossae against distal articular surfaces, and distal phalanges with less palmarly curved shafts; from *P. otibandus* in being larger, with less palmarly curved distal phalanges; from *C. kitcheneri* in being significantly shorter relative to metacarpals, relatively broader and far more dorsopalmarly compressed, particularly middle and distal phalanges, with broader, less V-shaped trochleae, more dorsally tilted proximal surfaces of proximal phalanges, and dorsally rounded and unpeaked distal phalanges with no palmar curvature of the shaft; from *O. rufus* and *M. fuliginosus* in being larger and relatively broader, with proximal phalanges with distal end broader relative to proximal end, shorter, more dorsopalmarly compressed middle phalanges, and distal phalanges with shaft more dorsopalmarly compressed; and from *W. bicolor* in being much larger and relatively slightly broader, with more V-shaped trochleae on the proximal phalanges.

Hindlimb

Femur (Figs 25 & 26): large and gracile. Head large and hemispherical with an extended proximomedial margin and a robust neck; medially projected and dorsomedially deflected, positioned slightly anterior to medial base of the greater trochanter. Greater trochanter large and robust, with rounded, rugose tip. Greater trochanteric ridge broad, slightly ventrally arched, and laterally projected to form a raised, rugose proximolateral ridge on the dorsolateral margin of the proximal end (Fig. 26a); proximolateral ridge (dorsolateral margin of trochanteric ridge) becomes more raised and distally extensive with age. Trochanteric fossa extends distally to level with the peak of the lesser trochanter. Intertrochanteric ridge quite thick, distinct and ventromedially orientated, extends distomedially from the ventromedial base of the greater trochanter to the lesser trochanter. Lesser trochanter rugose and rounded, ventromedially projected; unites with the intertrochanteric crest forming a long, gently curved ridge. Lesser trochanteric ridge thickened, raised; distal portion curving slightly dorsally; extends distally as a low, indistinct ridge merging with the shaft adjacent to the quadratus tubercle in some specimens. Dorsal surface of proximal end smoothly, distinctly convex.

Femoral shaft (between the proximal end and distal epiphysis) straight, round to very slightly transversely compressed in cross-section; narrowest around one-third of length, broadens to the distal end. Quadratus tubercle (insertion of m. quadratus femoris) low, rugose, and elongate oval in shape, situated on the ventral surface of the shaft with a very slight medial displacement, at around the midpoint of the shaft. Most of the ventral surface of the distal shaft is gently medially tilted; lateral part of the ventral surface forms a shallow, elongate fossa for the partial origin of the m. flexor digitorum superficialis that extends onto the proximal surface of the lateral condyle. Distal end (distal epiphysis) large and broad. Trochlea wide and very shallow, skewed medially by a tall, broad lateral trochlear crest; medial trochlear crest considerably lower than the lateral crest (Fig. 26e). Condyles broadest across ventral surfaces, with the lateral condyle larger and broader in distal view. Intercondylar fossa has a large, broad ventral part and a smaller, rounded and slightly laterally displaced distal part. Lateral epicondyle tall and laterally projected, particularly the ventral part, with the fibular facet laterally and slightly ventrally projected; a deep, narrow fossa (lateral fibulocondylar fossa) is present

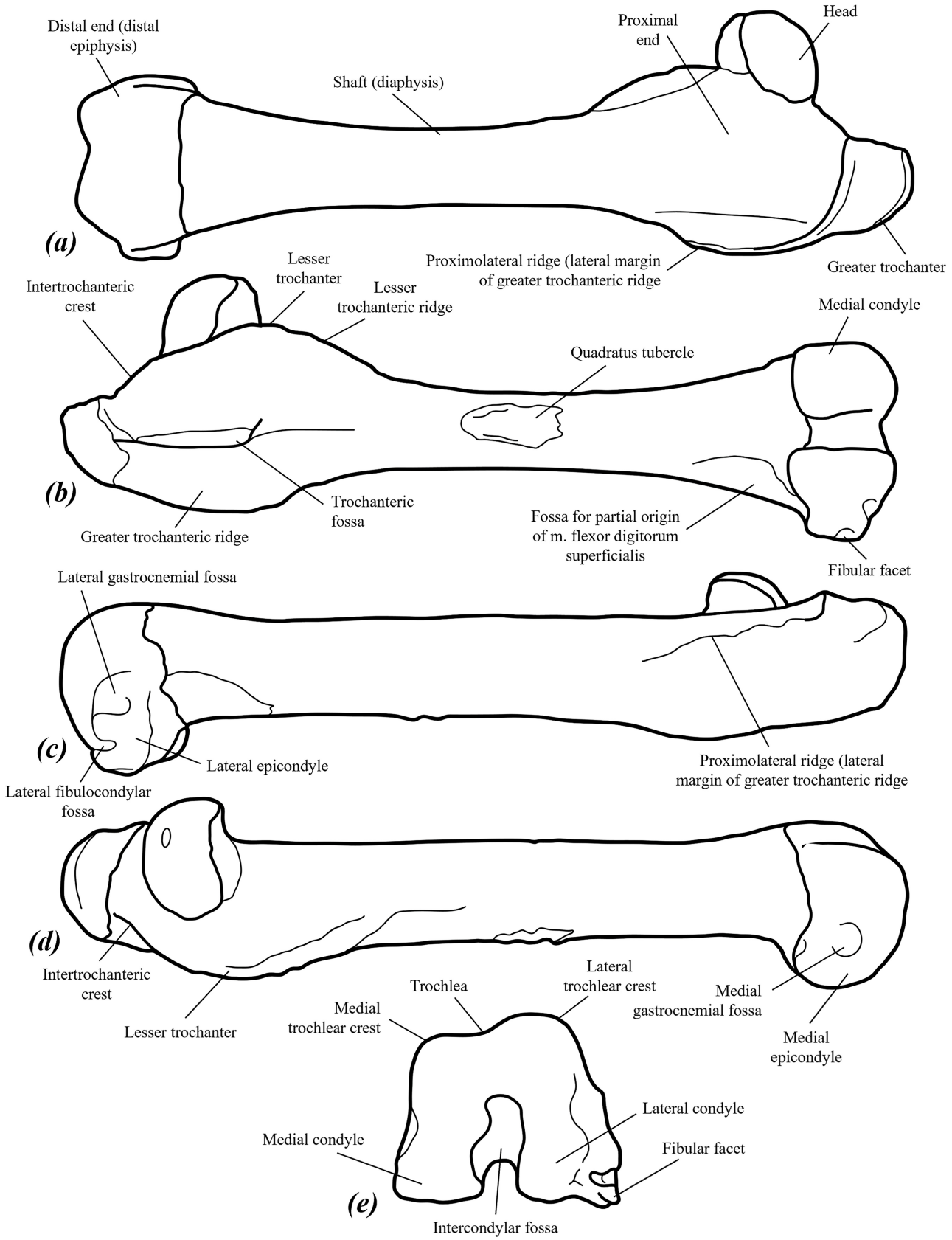

FIGURE 25. line drawings of left femur of *P. anak* NMV P159917 in: (a) dorsal, (b) ventral, (c) lateral, (d) medial, and (e) distal views.

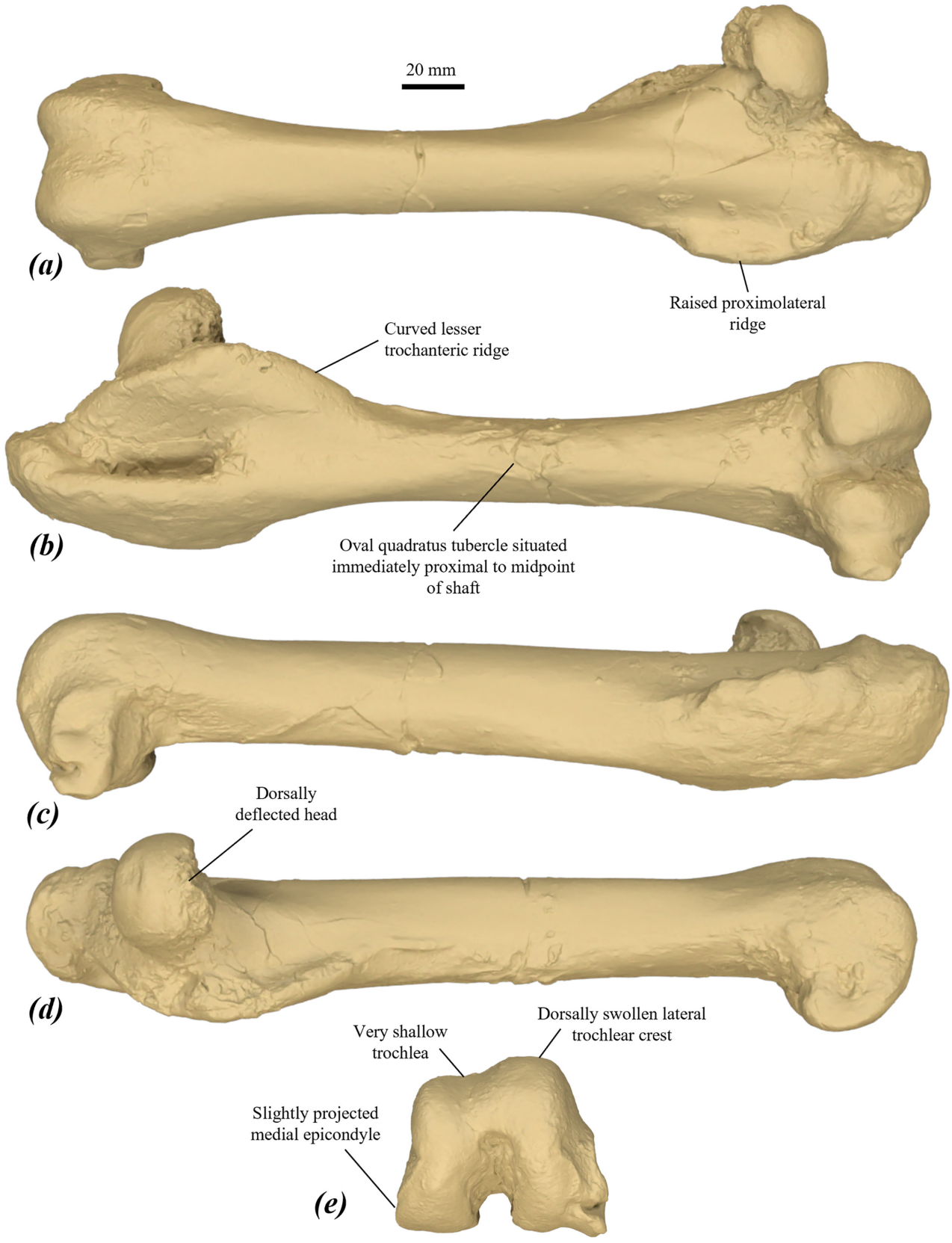

FIGURE 26. surface scan images of left femur of *P. anak* NMV P159917 in: (a) dorsal, (b) ventral, (c) lateral, (d) medial, and (e) distal views.

on the distolateral margin, separating the fibular facet and the lateral epicondyle; a broad, shallow fossa is present on the midpoint of the lateral surface for the partial origin of the m. gastrocnemius lateralis. Medial epicondyle relatively small and unprojected, with a small, rounded central fossa for the origin of the m. gastrocnemius medialis.

The femur of *P. anak* differs from that of *P. mamkurra* in being slightly more gracile, with a more dorsally deflected head, more raised proximolateral ridge, shallower trochlea, lateral trochlear crest considerably more dorsally swollen than the medial crest, and a less medially projected ventral component of the medial epicondyle; from *P. viator* in being more elongate, with a less medially projected lesser trochanter, more curved lesser trochanteric ridge such that the conjunction of the ridges at the lesser trochanter is broadly more curved and less angular, a shallower, broader trochlea, and a relatively broader, lower medial trochlear crest; from *P. tumbuna* in being more robust, with a less elongate, more proximally situated quadratus tubercle and a more dorsoventrally compressed distal shaft; from *P. otibandus* in being larger, with a shallower and broader trochlea and a lower, more rounded medial trochlear crest; from *C. kitcheneri* in being larger but more gracile, with a relatively larger, more dorsally deflected head, longer and narrower greater trochanter, more distally extensive proximolateral crest, less distally extensive trochanteric fossa relative to the position of the head, less medially displaced quadratus tubercle, straighter shaft in dorsal view, slightly shallower trochlea, and a less distally situated lateral gastrocnemial fossa; from *O. rufus* in being larger but more gracile, with a less dorsally deflected head, broader proximal end, thicker and more laterally projected proximolateral ridge, more distally extensive lesser trochanteric ridge, more distally situated quadratus tubercle, broader, less tall trochlear crests with the lateral crest relatively lower, shallower trochlea, deeper medial gastrocnemial fossa, and deeper fibulocondylar and lateral gastrocnemial fossae; from *M. fuliginosus* in being larger and more robust, with a larger greater trochanter, more dorsally deflected head, more raised proximolateral ridge, more elongate lesser trochanteric ridge, more elongate quadratus tubercle, shorter and shallower fossa for m. flexor digitorum superficialis on distoventrolateral shaft, taller, more laterally projected lateral epicondyle, and a less ventrally deflected fibular facet on the lateral condyle; and from *W. bicolor* in being larger and more robust, with a relatively larger, more dorsally deflected head, less distally extensive trochanteric fossa relative to the head, more distally extensive lesser trochanteric ridge, more raised proximolateral crest, slightly more distally situated quadratus tubercle, less dorsoventrally compressed distal shaft, relatively less tall distal epiphysis, relatively lower medial trochlear crest, shallower trochlea, larger fibular facet on the lateral condyle, and in a lacking small, rounded tubercle on the proximal margin of the lateral epicondyle.

Tibia (Figs 27–29): large and quite robust; proximal component bowed very slightly medially in cranial view, and distal component bowed very slightly laterally. Proximal epiphysis depth greater than width; intercondylar eminence tall and narrow; medial condyle narrow, deep, and slightly projected caudally; lateral condyle much shallower, smaller, and broader, with a large, concave groove (muscular groove) in the craniolateral margin. Proximal fibular facet narrow and shelf-like, orientated ~50° from sagittal plane. Cnemial crest (cranial tibial crest) deep and elongate, with an indistinct, rugose, curved distal peak (Fig. 28d); slowly thickens and merges with the shaft by its midpoint; lateral surface gently concave and medial surface very slightly convex. Proximolateral crest thin and very raised, bounds a broad, deep sulcus for the m. tibialis cranialis; extends distally to merge into the distal fibular facet on the distolateral surface. The distal fibular facet extends on the shaft's lateral surface from the midpoint to immediately proximal to the distal epiphysis. Shaft minimum diameter is at ~three-quarters of length, with diameter increasing gently to distal epiphysis. Distal epiphysis robust, with the talar trochlea slightly wider than deep; medial tuberosity robust and deep with the medial malleolus quite large, blunt, and medially projected; in some specimens the cranial section curves medially.

The tibia of *P. anak* differs from that of *P. mamkurra* in being longer and more gracile, with a more laterally curved cnemial crest and a thinner proximal component of the proximolateral crest; from *P. viator* in being more robust, with a more distinct peak on the cnemial crest, the shaft slightly curved distally in lateral view (rather than straight), and less caudal facing talar facet; from *P. tumbuna* in being longer and more gracile, with a taller, narrower intercondylar eminence, the cranial part of the proximal epiphysis not tilted cranially, a more raised proximolateral crest, and the cnemial crest shorter relative to tibial length and with a more distinct peak; from *P. otibandus* in being larger, with a relatively slightly narrower distal epiphysis; from *P. snewini* in being more robust, and having a more elongate cnemial crest with a less distinct peak, and a more elongate proximolateral crest relative to total length; from *C. kitcheneri* in being larger, with a relatively broader cranial part of the proximal epiphysis, a more elongate cnemial crest, a more elongate proximolateral crest with a narrower, more raised proximal part, and the distal shaft expanding more to the distal epiphysis; from *O. rufus* in being larger and more robust, with a proximal epiphysis with a larger muscular groove and broader, more cranially tilted cranial component, more elongate cnemial crest, deeper, more distinct distal fibular facet craniolateral, distal shaft broadening more distally, and a larger, more rounded talar trochlea; from *M. fuliginosus* in being larger and more robust, with the proximal epiphysis with lower, broader intercondylar eminence, larger muscular groove and broader, more laterally deflected and more cranially tilted cranial component, more raised proximal component of proximolateral crest, more elongate cnemial crest, deeper, more distinct distal fibular facet, distal shaft broadening more distally, and a larger, more rounded talar trochlea; and from *W. bicolor* in being larger and more robust, with a more concave proximal fibular facet, broader cnemial crest with less distinct distal peak, thicker, more raised proximolateral crest, deeper, more distinct distal fibular facet, and a more rounded talar trochlea.

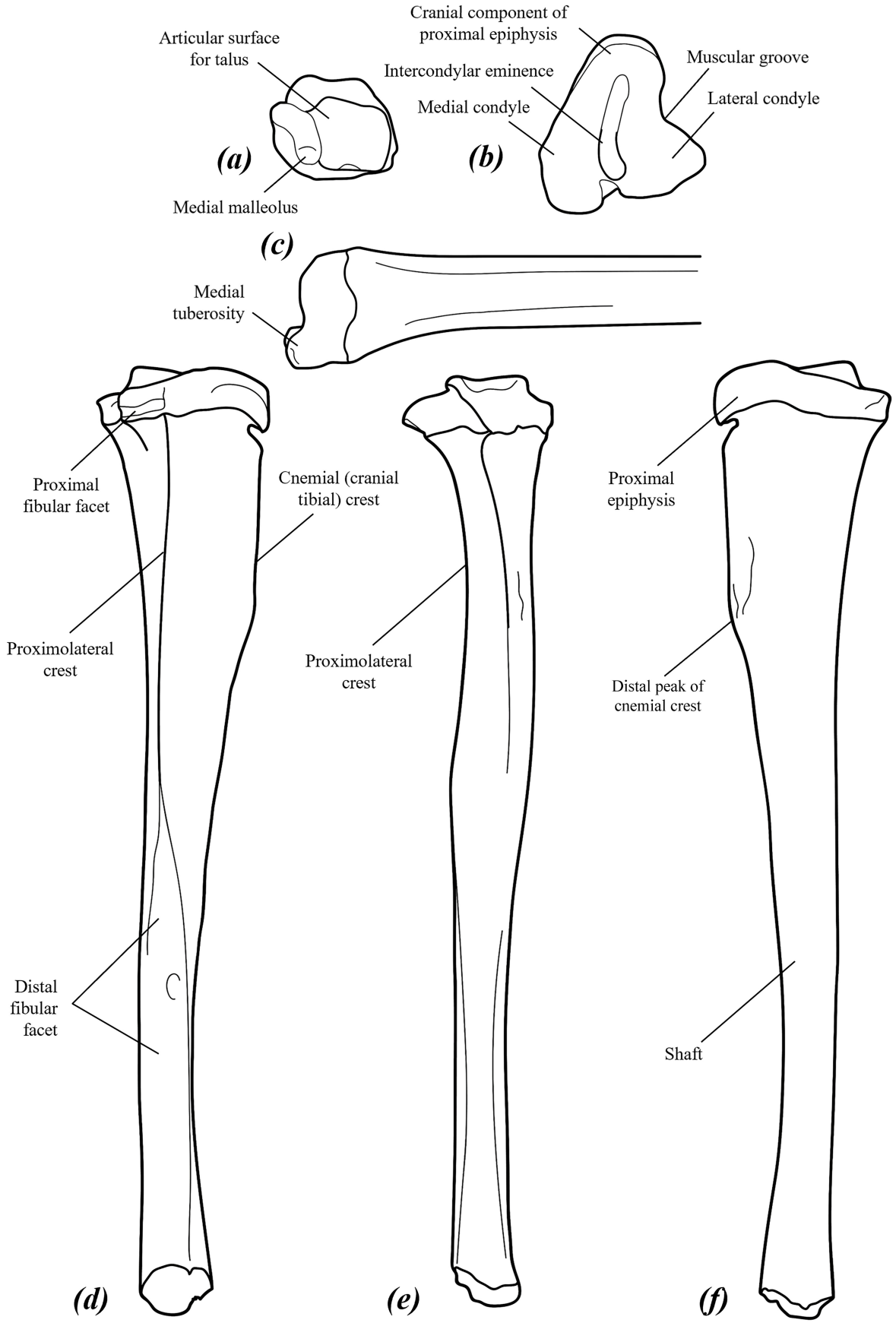

FIGURE 27. line drawings of right tibia of *P. anak*: distal epiphysis of NMV P39105 in (a) distal, and (c) caudal views; and tibia of NMV P39101.41 in (b) proximal, (d) lateral, (e) cranial, and (f) medial views.

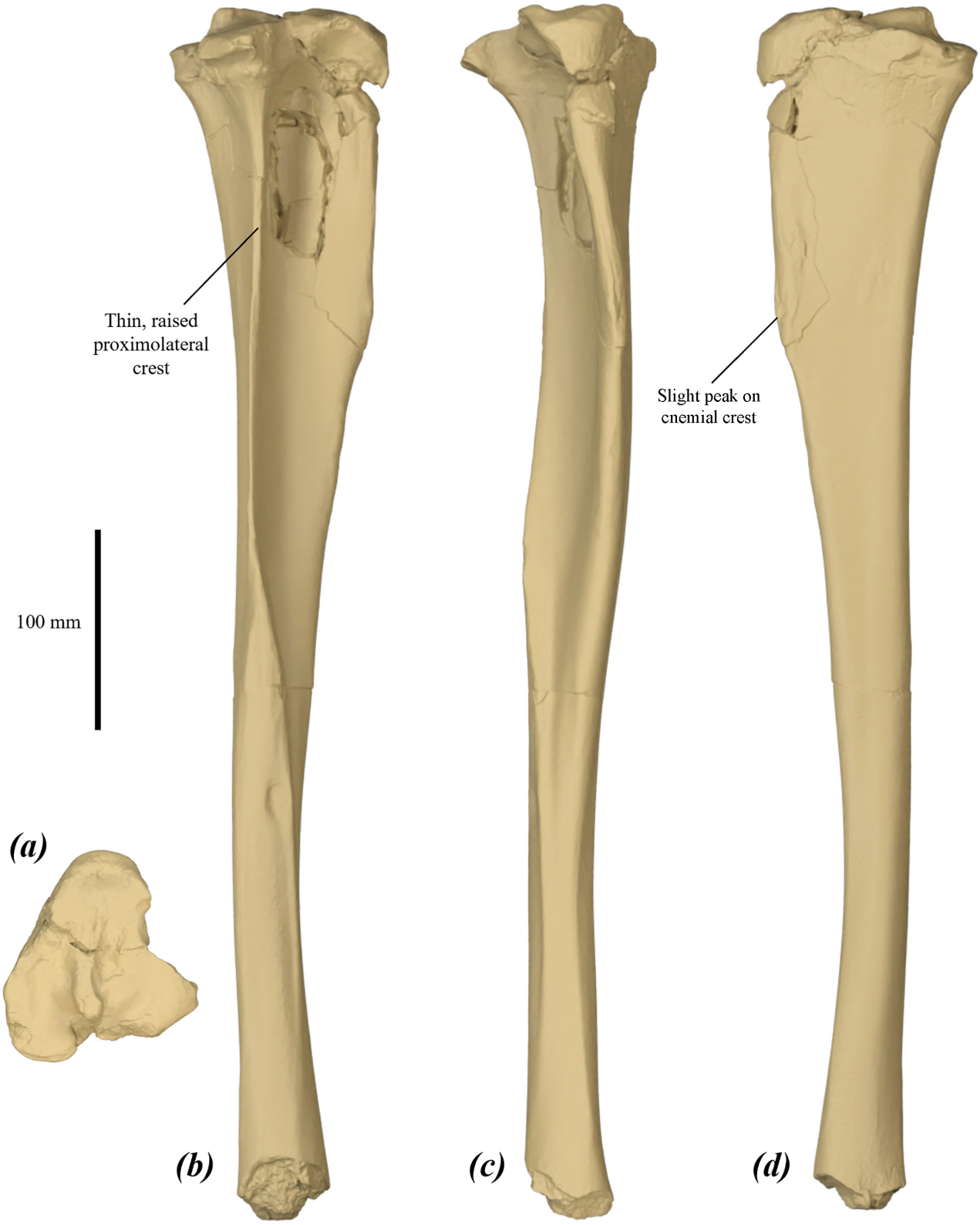

FIGURE 28. surface scan images of right tibia of *P. anak* NMV P39101.41 in: (a) proximal, (b) lateral, (c) cranial, and (d) medial views.

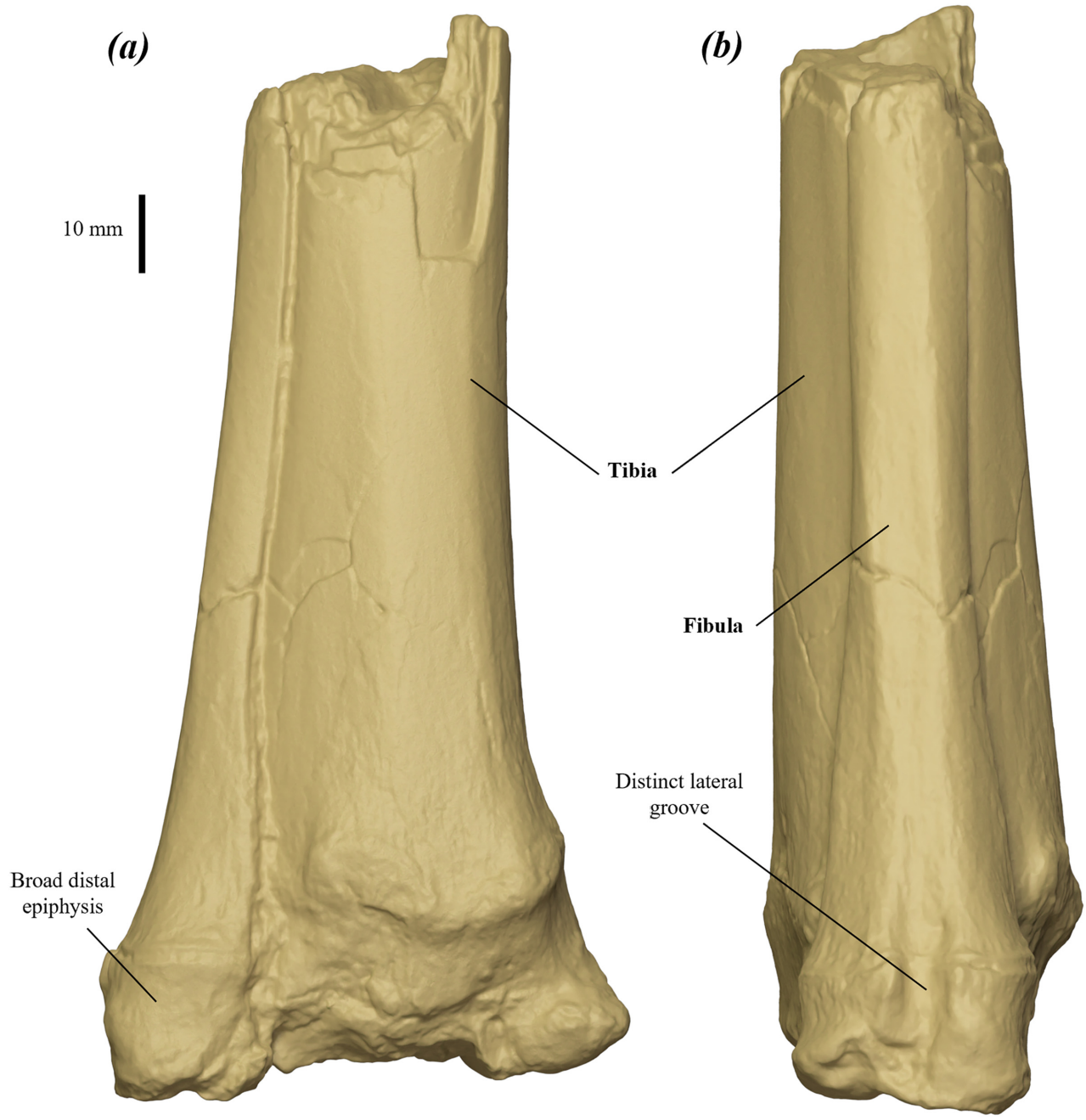

FIGURE 29. surface scan images of distal right tibia and fibula of *P. anak* NMV P39105.83 in: (a) cranial, and (b) lateral views.

Fibula (Fig. 29): proximal part not known. Distal component transversely very compressed, crescentic in cross-section, thickens and deepens to distal epiphysis. A narrow, quite deep groove extends proximodistally from immediately proximal to the distal epiphysis over the lateral surface of the epiphysis (Fig. 29b). Distal epiphysis robust, slightly compressed transversely, and oval in distal view; calcaneal facet with the caudal component deep, quite broad, gently concave, and slightly medially tilted, and the cranial component round, smoothly convex, and slightly ventrally projected.

The fibula of *P. anak* differs from that of *P. mamkurra* **sp. nov.** in being narrower; from *P. viator* **sp. nov.** in being relatively slightly broader across the distal epiphysis, with less broadening and craniocaudal tapering immediately proximal to the distal epiphysis, a more deeply concave lateral groove, and a broader, less medially slanted caudal calcaneal facet; from *C. kitcheneri* in being larger and broader distally; from *O. rufus* in being broader distally and much more robust, with a more deeply concave lateral groove on distal end and the distal epiphysis with a slightly less medially tilted caudal component of calcaneal facet; from *M. fuliginosus* in being more robust, with the distal component of the shaft deeper and more distinct, with a more deeply concave lateral groove, and the distal epiphysis relatively broader; and from *W. bicolor* in being larger.

Pes

Calcaneus (Figs 30 & 31): moderately large and robust. Calcaneal tuberosity elongate, quite tall, broadest plantarly, and domed in cross-section (Fig. 31f), increasing slightly in height and width caudally; lateral surface occasionally slightly concave caudally and deeply concave ventral to fibular facets. Caudal epiphysis tall, thickened and rugose; dome-shaped in caudal view, with a shallow transverse groove across the centre. Plantar surface very thick, rugose, and broad, becomes substantially thicker and broader with age; tapers cranially in ventral view and extends cranially to level with the cranial margin of the sustentaculum tali, with the craniomedial margin deflected laterally around the cranial plantar tubercle. Cranial plantar tubercle variable in size and shape, but generally quite small and rounded to oval; abuts or is caudally adjacent to the plantar margin of the plantomedial facet for the cuboid.

The calcaneal head is broad and robust. Sustentaculum tali large, medially projected beyond the margin of the medial talar facet, and moderately extensive caudally; varies from rounded to gently skewed cranioplantarly; flexor groove deep and broad. Medial talar facet quite small, oval, craniocaudally compressed, slightly caudal relative to the lateral talar facet, aligned laterally and occasionally craniolaterally in dorsal view, and tilted distinctly cranially in medial view; caudal margin sometimes has a rounded lip. A small ridge extends caudally from the caudolateral margin of the medial talar facet, tapers and lowers caudally; occasionally as only a slight swelling. Lateral talar facet broad, smoothly convex, roughly semicylindrical, and tapers from lateral margin to midpoint. Fibular facet quite large and bulbous, projected laterally; separated into semi-distinct cranial and caudal components which are separated by a groove on the lateral surface and linked by a narrow band of articular surface which is semicontinuous with the lateral margin of the lateral talar facet. Cranial component of fibular facet low, slightly dorsolaterally concave, craniocaudally elongate, cranially tilted and laterally projected. Caudal component of fibular facet quite large, rounded, gently convex, caudally and slightly laterally projected and facing caudally, with distinct margins (Fig. 31f).

Facet for the talar head small, abuts the medial margin of the dorsomedial cuboid facet on the medial surface of the calcaneal head. The facets for articulation with the cuboid are quite variable in morphology, particularly the plantomedial facet; dorsomedial cuboid facet roughly pentagonal in cranial view, gently convex, slightly broader and more dorsally situated than the dorsolateral facet, and separated from the dorsolateral facet by a slightly bevelled step. Dorsolateral cuboid facet tall, cranially projected, gently convex, and tilted plantarly, with the dorsal margin slanted slightly laterally; dorsolateral facet curves plantomedially such that it is continuous with the plantomedial cuboid facet. Plantomedial facet smaller than the dorsal facets, generally dorsoplantarly compressed and broad, occasionally rounded and less medially extensive; curves plantomedially from the plantar margin of the dorsolateral facet to either terminate as a small, rounded facet beneath dorsomedial facet or to extend further plantomedially and merge with the cranial plantar tubercle—occasionally, in this latter case, a small separate plantomedial facet is present beneath the dorsomedial facet (Figs 30e & 31e). A deep, oblong fossa is typically present between the dorsomedial and plantomedial cuboid facets; occasionally this fossa is absent, with the area covered by a smooth articular surface.

The calcaneus of *P. anak* differs from that of all compared species except *O. rufus* and *M. fuliginosus* in having a more rounded caudal fibular facet with more distinct margins. Further differs from that of *P. mamkurra* **sp. nov.** in being generally slightly less robust, with a more rounded sustentaculum tali, more caudally situated lateral talar facet relative to the medial talar facet, and the medial talar and fibular facets less bulbous and less dorsally projected; from *P. viator* **sp. nov.** in being broader and more robust, with a domed (rather than triangular) calcaneal tuberosity in cross-section and a relatively broader dorsolateral cuboid facet; from *P. tumbuna* in being larger and taller, with a less medially displaced calcaneal head, and a planar (rather than convex), less medially flared plantar surface; from *P. dawsonae* **sp. nov.** in being generally larger and taller, with a broader plantar surface, slightly craniocaudally deeper lateral talar facet, more rounded and distinct caudal fibular facet, and a broader flexor groove; from *P. otibandus* in being larger and taller, with a less medially displaced calcaneal head; from *C. kitcheneri* in being larger, taller and narrower, with a dorsomedial cuboid facet not tilted laterally, and a more cranially extensive plantar surface that is not rotated laterally; from *O. rufus* and *M. fuliginosus* in being larger, and broader, particularly the calcaneal tuberosity and plantar surface, with a much more medially flared sustentaculum tali, larger and more medially situated medial talar facet, much less distinct facet for the posterior plantar process of the talus, relatively broader dorsolateral cuboid facet, and the step separating the dorsal cuboid facets lower and slightly more bevelled; and from *W. bicolor* in being much larger, and relatively taller and broader, with a deeper fibular facet in dorsal view, broader medial talar facet, and a broader dorsomedial cuboid facet relative to the dorsolateral cuboid facet.

Talus (astragalus) (Fig. 32a–f): width greater than craniocaudal depth. Trochlear crests parallel, orientated very slightly laterally, and subequal in height, with the lateral crest rounded, and the medial crest slightly narrower, more pointed and extending further caudally; trochlea shallow and broad. Talar head large and craniomedially projected. Medial malleolus quite large, rounded, medially tilted, extends craniomedially along the talar head (Fig. 32d); malleolar fossa broad and quite deep. Facet for the navicular fairly broad, very tall and deep, convex, cranioplantarly facing, extends caudoplantarly to end plantar to cranial margin of medial malleolus. Facet for the cuboid located on lateral surface of talar head relatively small, craniocaudally compressed and facing laterally. Posterior plantar process large, slightly caudally projected, and broadly rounded in medial view. A broad, shallow fossa is present on the medial surface of the base of the plantar

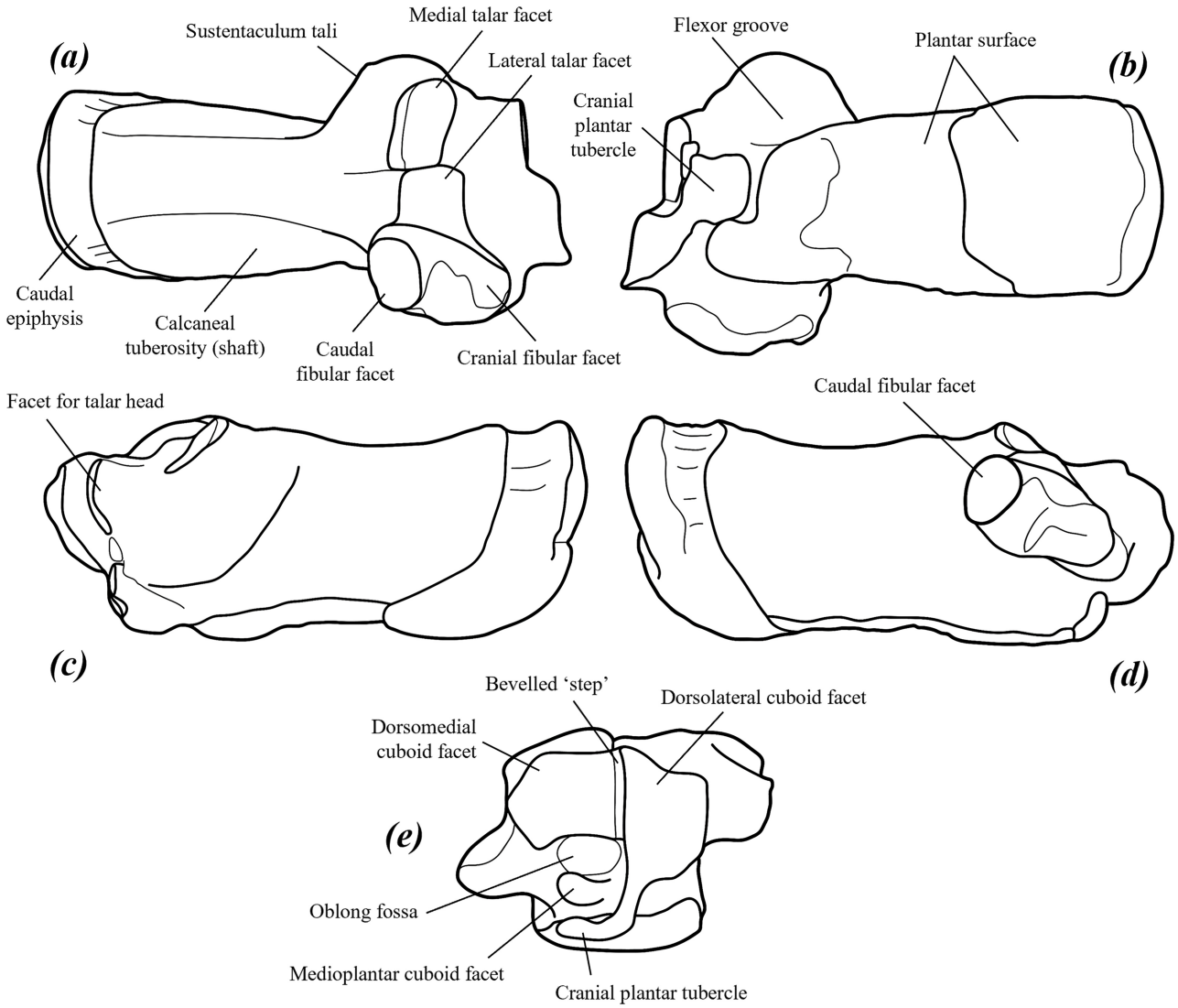

FIGURE 30. line drawings of right calcaneus of *P. anak* NMV P39101.59 in: (a) dorsal, (b) plantar, (c) medial, (d) lateral, and (e) cranial views.

process. Plantarly, the facets for articulation with the talar facets of the calcaneus are deeply concave, mirroring the morphology of the calcaneal facets; craniolateral component of medial facet smoothly convex. A small, slightly laterally projected tubercle is present on the plantar surface of the craniolateral corner of the talus, with a small articular facet for articulation with the calcaneal head situated immediately cranial to lateral calcaneal facet.

The talus of *P. anak* differs from that of *P. mamkurra* **sp. nov.** in having shallower trochlea with more medially skewed concavity, deeper malleolar fossa, less transversely aligned medial malleolus, less cranially tilted cuboid facet, and narrower navicular facet more aligned in sagittal plane; from *P. viator* **sp. nov.** in having the medial malleolus more obliquely aligned (rather than aligned in the sagittal plane), with a small indent present between the cranial margin of the medial trochlear crest and the talar head, and the concavity of the trochlea more medially skewed; from *P. otibandus* in being larger, with a narrower navicular facet and a smaller medial malleolus both more aligned in sagittal plane, and in lacking the small tubercle plantar to the medial malleolus on the medial surface; from *P. snewini* in being slightly larger, with a small indent present between the cranial margin of the medial trochlear crest and the talar head; from *C. kitcheneri* in being larger and slightly more elongate, with a shallower trochlea, broader medial trochlear crest, a cuboid facet present on the navicular head, and a more caudoplantarly extensive navicular facet; from *O. rufus* and *M. fuliginosus* in being larger and relatively broader, with a deeper, less medially skewed trochlea, a more cranially situated malleolar fossa, less medially projected medial malleolus and navicular head, and a shorter, more rounded posterior plantar process; and from *W. bicolor* in being much larger, with a more rounded medial trochlear crest and a more rounded posterior plantar process in medial view.

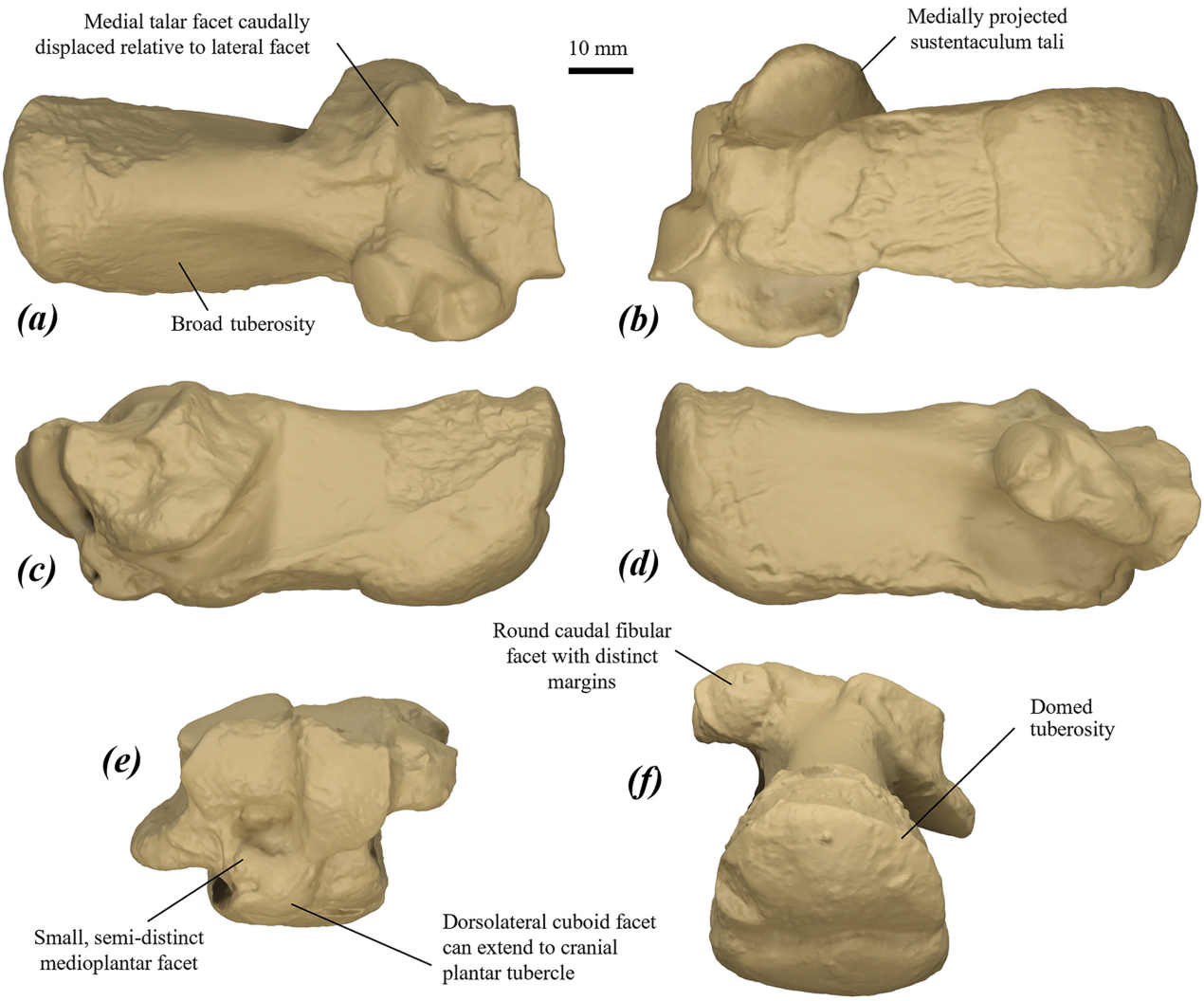

FIGURE 31. surface scan images of right calcaneus of *P. anak* NMV P39101 in: (a) dorsal, (b) plantar, (c) medial, (d) lateral, (e) cranial, and (f) caudodorsal views.

Cuboid (Fig. 32g–l): roughly rectangular in dorsal view except for the step between the dorsal calcaneal facets. Dorsomedial calcaneal facet slightly broader and dorsoplantarly shorter than the dorsolateral facet, demarked by a distinct, slightly bevelled step on the lateral margin. Plantar component of caudal surface is highly variable; the plantar continuation of dorsolateral calcaneal facet is either distinct and curves medially beneath dorsomedial calcaneal facet, or is indistinct and merges onto the caudal surface of the lateral plantar tubercule. Metatarsal IV facet occupies the entirety of the dorsal component of the cranial surface; medial part slightly convex and lateral component slightly concave, such that the dorsal margin is gently S-shaped. Metatarsal V facet broad, rounded, slightly laterally projected, incompletely separated from the metatarsal IV facet, angled plantolaterally. Lateral plantar tubercle very large, broad, oval in plantar view, and slightly laterally deflected. Medial plantar tubercle small, elongate, triangular to oval in plantar view, angled plantomedially, very small relative to the lateral plantar tubercle, and separated by a deep, quite broad flexor groove (sometimes peroneal or plantar groove) running craniocaudally. The area of articulation with the navicular on the dorsocaudal component of the medial surface is partially abraded, rugose, extends around the facet for the talar head. Facet for the ectocuneiform indistinct, dorsoplantarly tall, craniocaudally compressed, with semicontinuous dorsal and plantar parts; dorsal part abuts the medial margin of the metatarsal IV facet on the cranial margin of the medial surface; plantar part extends along the medial margin onto the medial surface of the medial plantar tubercle.

The cuboid of *P. anak* differs from that of *P. mamkurra* **sp. nov.** in having a taller, less distinct talar facet, narrower metatarsal V facet, more plantarly projected lateral plantar tubercle, and a narrower, deeper flexor groove; from *P. viator* **sp. nov.** in being generally dorsoplantarly shorter and broader, with a larger and slightly more dorsally situated metatarsal V facet, less plantarly situated plantar calcaneal facet, broader and less plantarly projected lateral plantar tubercle, and a more elongate, more medially deflected, and less plantarly projected medial plantar tubercle; from

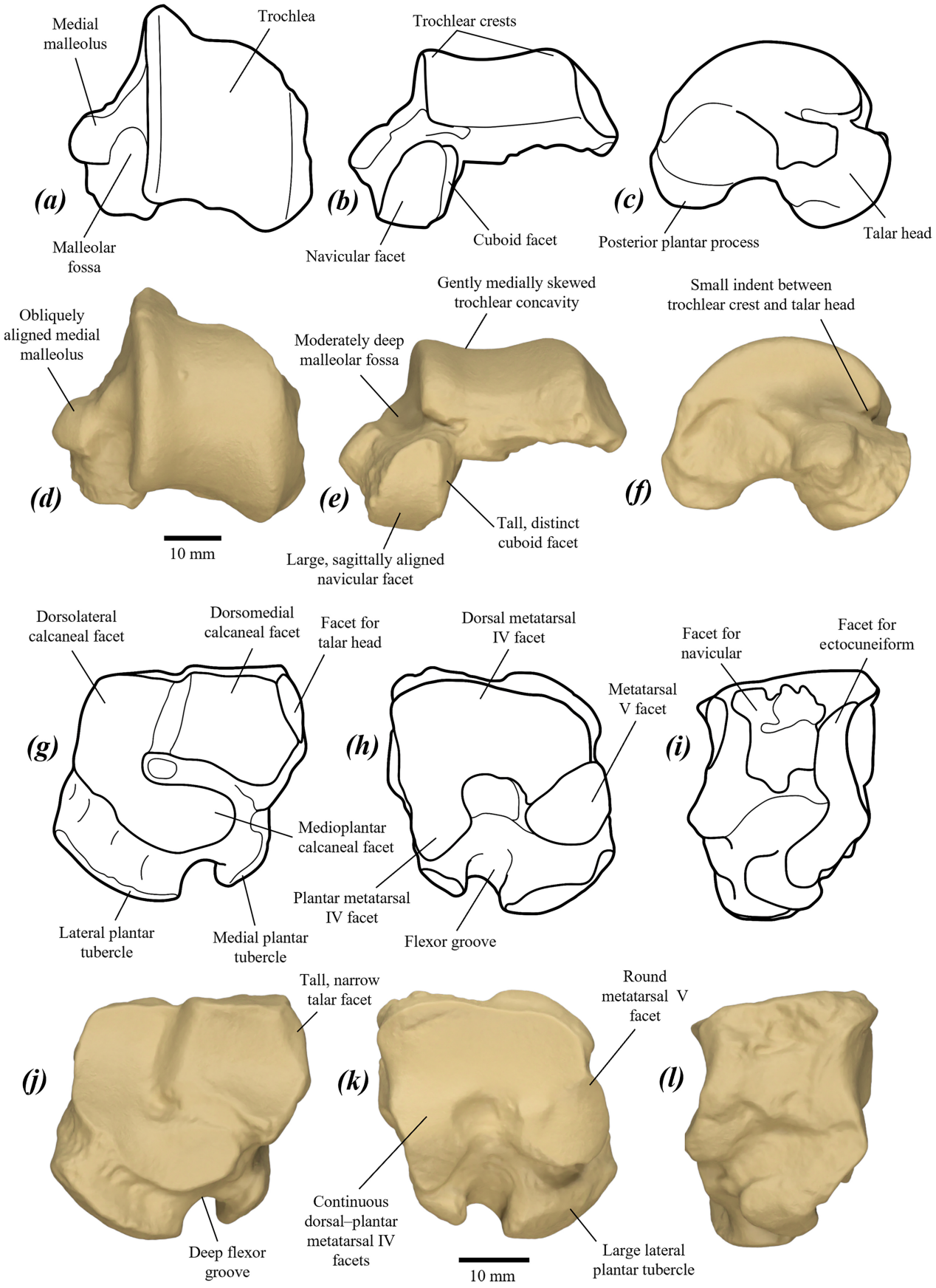

FIGURE 32. left tarsals of *P. anak*: (a–f) talus NMV P39118 in (a, d) dorsal, (b, e) plantar, and (c, f) medial views; (g–l) cuboid P39132 in (g, j) caudal, (h, k) cranial, and (i, l) medial views.

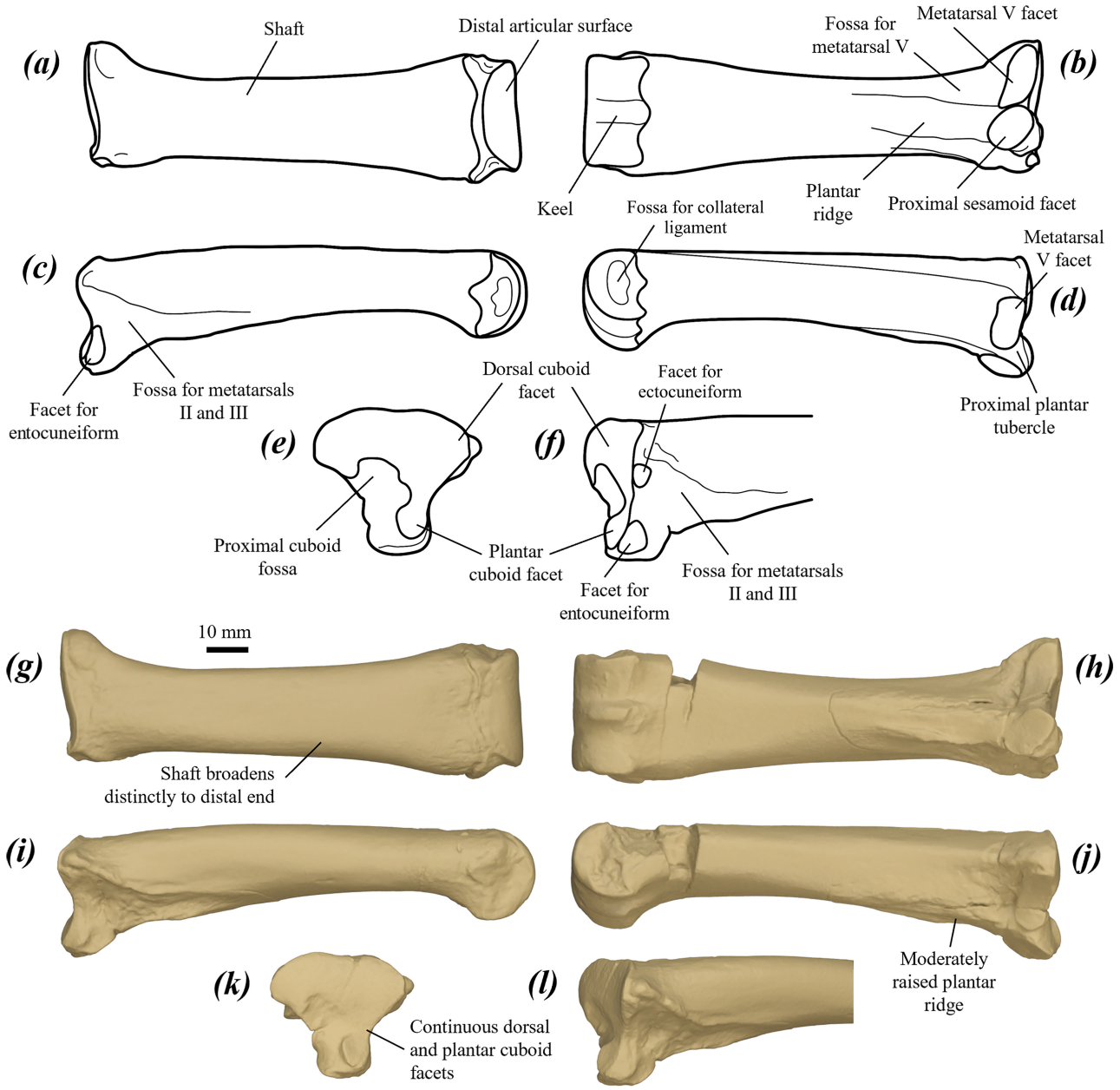

FIGURE 33. left metatarsal IV of *P. anak*: (a–f) line drawings and (g–l) surface scan images in (a, g) dorsal, (b, h) plantar, (c, i) medial, (d, j) lateral, (e, k) proximal/caudal, and (f, l) medioproximal views. Specimens are (a, g) NMV P39118, and (b–f, h–l) NMV P159917b metatarsal IV.

P. otibandus in being larger and taller, with larger plantar tubercles and the dorsal and plantar metatarsal IV facets continuous with one another; from *P. snewini* in being slightly larger and in having the dorsal and plantar metatarsal IV facets continuous with one another, with a larger and more distinct metatarsal V facet; from *C. kitcheneri* in being larger and taller, with the facet for the talar head present medial to the dorsomedial calcaneal facet, a considerably larger plantar tubercle, and a deeper, more elongate flexor groove; from *O. rufus* in being broader, particularly across the plantar section, with a relatively broader dorsolateral calcaneal facet, more medial facing facet for the talar head, more medially situated medial plantar tubercle, broader flexor groove, and a broader, more laterally tilted metatarsal V facet; from *M. fuliginosus* in being larger, squarer in outline in caudal view, and relatively deep and broad, with a less plantarly projected, less elongate, and more dorsolaterally extensive lateral plantar tubercle, a larger and more medially situated medial plantar tubercle, broader flexor groove and a slightly more medially situated plantar cuboid facet; and from *W. bicolor* in being much larger, with a relatively larger, more plantarly projected medial plantar tubercle.

Metatarsal IV (Fig. 33): large and robust, with length divided by minimum shaft width = ~5.5–6.2. Proximal end broad, thickened dorsomedially, with the dorsal component flared laterally, forming a blunt tubercle over the metatarsal V facet; proximal surface roughly

triangular, with a broad dorsal margin. Dorsal cuboid facet broad, gently concave medially, becomes slightly convex and tapers laterally to the rounded dorsolateral margin; medial margin slightly proximally projected; narrows plantarly to be semicontinuous with the much smaller plantar cuboid facet. Plantar cuboid facet small, round, flat, slightly proximally projected, tilted dorsally and slightly medially, situated on the proximal surface of the proximal plantar tubercle. Facet for metatarsal V tall, roughly oblong, concave, not extending plantarly onto the lateral surface of the proximal plantar tubercle; positioned at the proximal end of a deep, elongate ligamental pit. Facet for the entocuneiform very small, slightly craniocaudally compressed, faces proximomedially and abuts the dorsal component of the medial margin of the dorsal cuboid facet. An elongate, shallow fossa extends distally and slightly plantarly from the proximal margin of the medial surface of the shaft for articulation with metatarsals II and II; this fossa is dorsally bounded by a low, thin ridge. Proximal plantar tubercle plantarly projected, rotated slightly laterally and gently caudally deflected. Facet for the entocuneiform very small, situated on the medial surface of the plantar tubercle, abuts the medial margin of the plantar cuboid facet. Proximal sesamoid facet rounded, smooth, and plantarly and slightly laterally tilted, situated on the distal surface of the plantar tubercle.

Shaft broad and gently dorsoplantarly compressed, with a flat to slightly laterally tilted dorsal surface; narrows very slightly to a minimum before the midpoint then broadens steadily to the distal end. Plantar ridge large, broad, rugose, smoothly merges with the shaft around its midpoint. The distal end is broad, with the keel subequally plantarly protrusive to the lateral and medial plantar crests.

The metatarsal IV of *P. anak* differs from that of *P. mamkurra* **sp. nov.** in being generally slightly shorter; from *P. viator* **sp. nov.** in being generally longer; from *P. tumbuna* in being larger; from *P. dawsonae* **sp. nov.** in being more gracile; from *P. otibandus* in being larger and more gracile, with a more raised plantar ridge, dorsal and plantar cuboid facets continuous, and more broadening of the shaft to the distal end; from *P. snewini* in being larger and more elongate, with a relatively longer plantar ridge, dorsal and plantar cuboid facets continuous, and more plantolaterally situated proximal cuboid fossa; from *C. kitcheneri* in being larger and relatively broader, with a more plantarly projected proximal plantar tubercle and a larger facet for the proximal plantar sesamoid; from *O. rufus* and *M. fuliginosus* in being shorter, relatively much broader, much more robust, and less arched in lateral view, with a larger metatarsal V facet, lower plantar ridge, and a larger, more plantarly projected proximal plantar tubercle; and from *W. bicolor* in being much larger and more robust, with a relatively slightly larger proximal plantar tubercle.

Metatarsal V (Fig. 34): fairly robust, with a distinct lateral curve in dorsal view accentuated by the lateral expansion of the distal end. Proximolateral process (for the attachment of the m. abductor metatarsi digiti minimi and m. opponens digiti minimi) large, thick and rugose. Facet for cuboid large and concave, extends from the medial surface of the proximolateral process to the lateral base of the medial plantar tubercle (Fig. 34j); subequal in size to the facet for metatarsal IV; dorsolateral margin raised as a slight lip over the dorsomedial surface of the proximolateral process. Medial plantar tubercle small, rounded, distinct, and proximomedially projected, occasionally with a slight plantar deflection; articular facet for the cuboid extends onto the proximolateral surface. Facet for metatarsal IV quite large, gently convex, and proximodistally short, with depth tapering laterally; extends from the dorsal surface of the shaft onto the cranial surface of the medial plantar tubercle. Lateral plantar tuberosity elongate, broad, rugose, and raised, merges with the shaft around its midpoint; bordered by a deep, narrow plantar groove curving around the medial margin.

Shaft arched slightly in lateral view, with a peak around the midpoint; both shaft and proximal end tall and moderately transversely compressed. Distal end broad and slightly laterally deflected at base. Distal articular surface with a large medial component and a smaller lateral component; medial component broadly convex and bulbous; lateral component small and laterally projected; keel large and plantarly projected. Fossae for collateral ligaments rounded, with the medial fossa particularly deep.

The metatarsal V of *P. anak* differs from that of *P. mamkurra* **sp. nov.** in being generally slightly smaller and more transversely compressed, with a thicker proximolateral process, cuboid facet narrower, more medially tilted in proximal view, less proximally extensive along proximolateral process, and less extensive onto medial plantar tubercle, medial plantar tubercle larger and more proximally projected, and a deeper, straighter plantar groove; from *P. viator* **sp. nov.** in being generally slightly larger, dorsoplantarly shorter, and less transversely compressed, with a broader and more concave cuboid facet, more proximally projected medial plantar tubercle, and a broader, dorsoventrally shorter distal end; from *P. tumbuna* in being longer, more gracile, and more transversely compressed, with the cuboid facet shorter and less extensive along the proximolateral process, more dorsally situated metatarsal IV facet, more elongate lateral plantar tuberosity, and a larger medial plantar tubercle; from *P. dawsonae* **sp. nov.** in having a more raised lateral plantar tuberosity, taller proximolateral process, and a narrower cuboid facet; from *P. otibandus* in being larger, with a larger proximolateral process and a larger, more proximomedially projected medial plantar tubercle; from *C. kitcheneri* in being larger, taller, and more robust, lacking the slight kink of the arch of the shaft immediately proximal to the midpoint in lateral view, with a plantar groove present, a considerably larger plantar tubercle and tuberosity, and a broader cuboid facet; from *O. rufus* and *M. fuliginosus* in being shorter, far broader and more robust, and less arched, with a longer proximolateral process and a larger medial plantar tubercle; and from *W. bicolor* in being much larger, relatively broader, and more robust, with a relatively larger proximolateral process and a more concave cuboid facet.

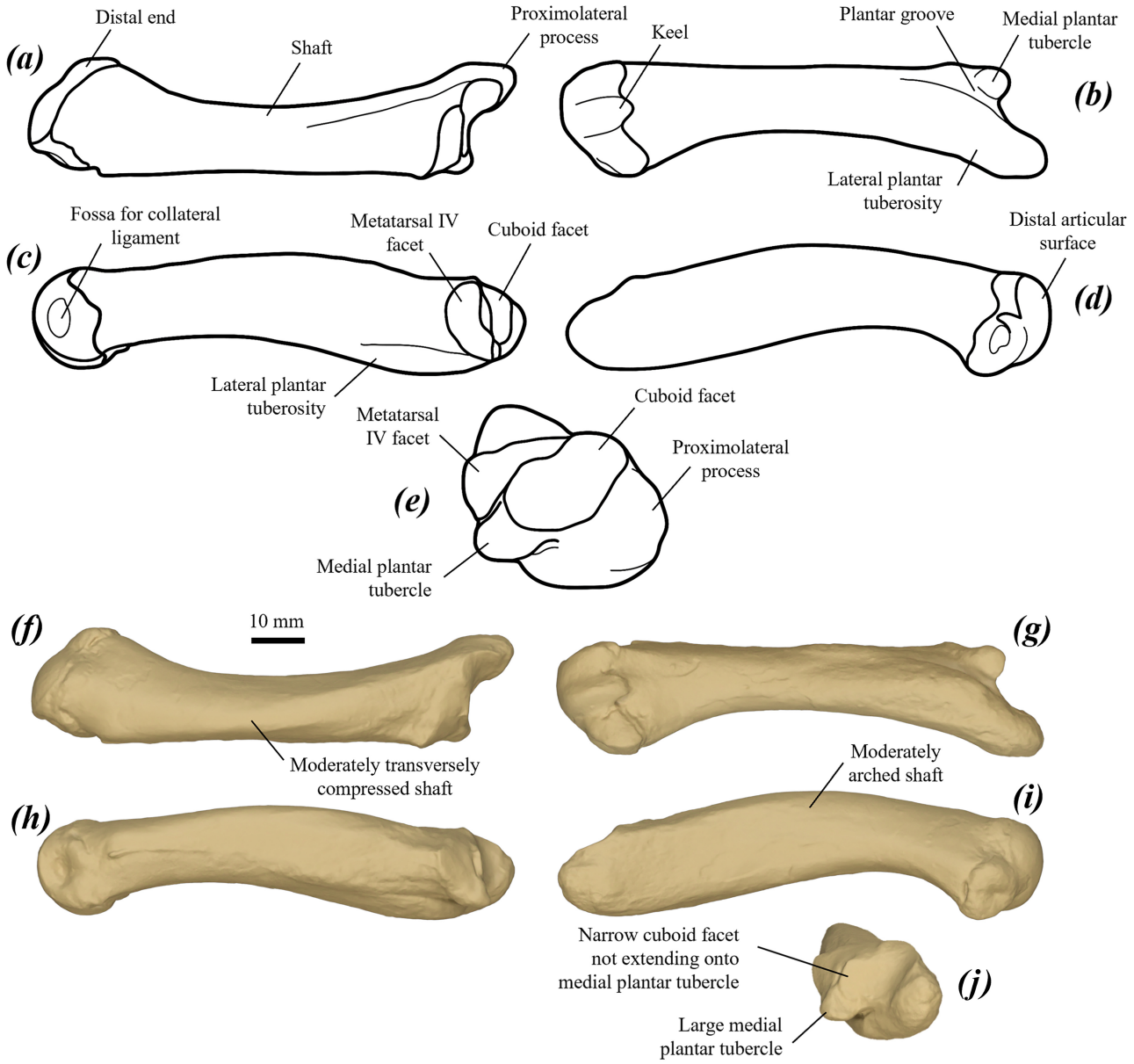

FIGURE 34. left metatarsal V of *P. anak* specimen NMV P39105.91: (a–e) line drawings and (f–k) surface scan images in (a, f) dorsal, (b, g) plantar, (c, h) medial, (d, i) lateral, and (e, k) proximal/caudal views.

Pedal phalanges (Figs 35 & 36): generally short, broad and robust. Proximal phalanx IV: lateral component of proximal end slightly flared laterally. Plantar tubercules distinctly raised and proximodistally elongate, separated by a deep proximodistal valley. Shaft tapers distally in lateral view. Distal end marginally narrower than the proximal end in dorsal view. Trochlea broad and gently concave, particularly plantarly. Middle phalanx IV: very short, robust and particularly dorsoplantarly compressed. Proximal end very wide, flared medially and laterally by large, transversely expanded plantar tubercles (Fig. 35q & r); plantar tubercles projected slightly proximally under the articular surface, tilting the articular surface slightly dorsally. Proximal articular surface broad, smoothly concave, with dorsal margin gently convex in dorsal view. Shaft very short, tapers in lateral view. Distal end distinctly narrower than the proximal end. Distal articular surface gently concave, broadens proximoplantarly. Distal phalanx IV: relatively tall compared to the proximal and middle phalanges. Proximal end tall and domed in proximal view, with the proximal articular surface broad, concave, and slightly dorsoplantarly compressed. Small eminences project laterally and medially over the collateral ligament fossae. Dorsal margin of proximal end becomes more thickened and flared with age; plantar tubercle large and rounded-square in plantar view. Shaft proximodistally short and broad, with dorsal peak rounded-triangular; narrows rapidly in distal half, curves smoothly plantarly in lateral view.

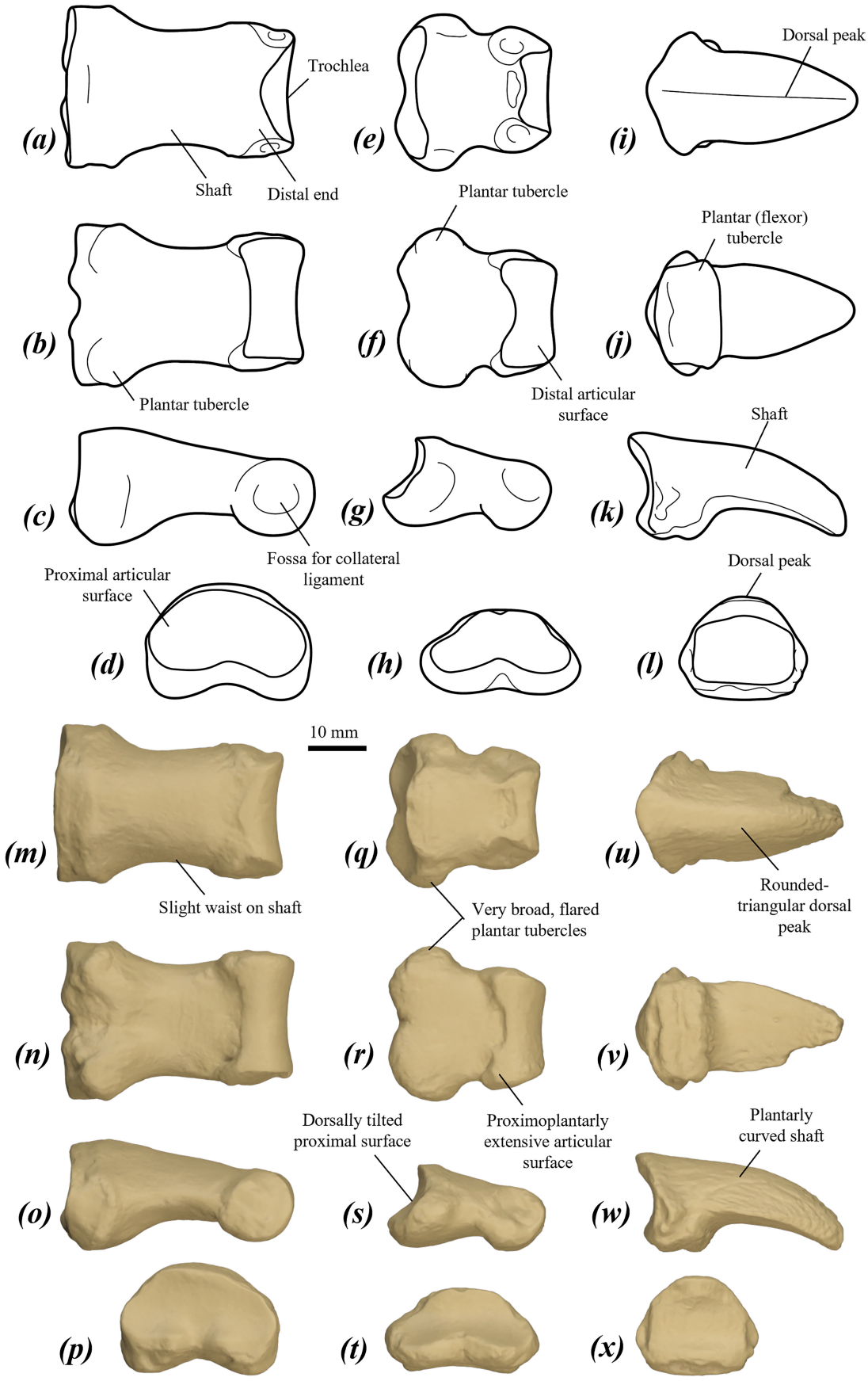

FIGURE 35. right pedal phalanges IV of *P. anak* NMV P39105: (a–l) line drawings and (m–x) surface scan images in (a, e, i, m, q, u) dorsal, (b, f, j, n, r, v) plantar, (c, g, k, o, s, w) lateral, and (d, h, l, p, t, x) proximal views.

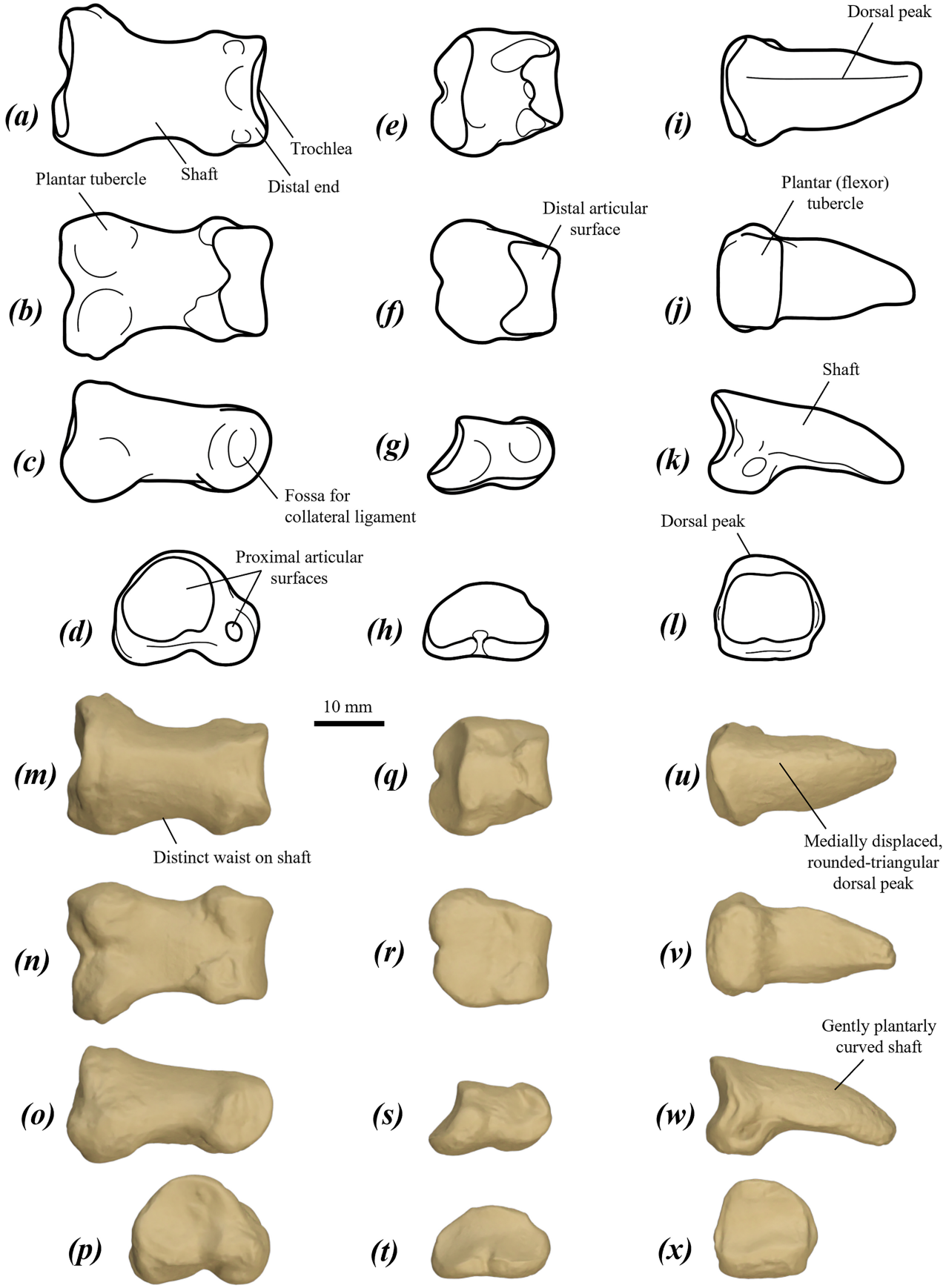

FIGURE 36. right pedal phalanges V of *P. anak* specimen NMV P39105: (a–l) line drawings and (m–x) surface scan images in (a, e, i, m, q, u) dorsal, (b, f, j, n, r, v) plantar, (c, g, k, o, s, w) lateral, and (d, h, l, p, t, x) proximal views.

Proximal phalanx V: not dorsoplantarly compressed, and distinctly asymmetrical transversely. Proximal end domed in proximal view, with the lateral component smaller and laterally and slightly proximally projected. Proximal surface for articulation with the medial component of the distal end of metatarsal V rounded, concave, and tilted slightly medially by the lateral component of the base. A very small second proximal articular surface is present on the lateral component of the base, for articulation with the lateral component of the distal end of metatarsal V. Shaft narrows and tilts slightly plantarly distally. Distal end small, squared and slightly flared laterally, with a small, shallow fossa on the dorsal surface. Distal articular surface gently concave, extends from distal to the plantar surface, absent from dorsal. Middle phalanx V: very short, almost without shaft. Proximal end tilted dorsally by the proximally projected plantar component. Proximal articular surface broad, gently concave, and tilted dorsally and medially. Distal end relatively narrow, with a small, shallow fossa on the dorsal surface. Distal articular surface gently concave and broadens plantarly. Distal phalanx V: quite short and bilaterally asymmetrical, flared laterally. Proximal end tall and rounded, with a rounded dorsal peak. Articular surface rounded-square and gently concave. Shaft very gently dorsoplantarly compressed, narrows rapidly in its distal half, curves slightly plantarly in lateral view, with a rounded-triangular dorsal peak.

The pedal phalanges of *P. anak* differ from those of all compared taxa in having the proximal end of middle phalanx IV relatively far broader due to the broad, flared plantar tubercles. Further differ from those of *P. mamkurra* **sp. nov.** in being relatively shorter and broader, with proximal phalanx IV with a less distinct, more proximally situated waist, middle phalanx IV with the distal articular surface more proximoplantarly extensive, and distal phalanges IV and V lacking V-shaped indentations in the transverse margins of the proximal surface; from *P. viator* **sp. nov.** in being relatively shorter and broader, with proximal phalanx IV with a less distinct waist, middle phalanx IV with a more dorsally tilted proximal end and more proximoplantarly extensive distal articular surface, distal phalanx IV with a more rounded dorsal peak, and distal phalanx V with a more rounded, less distinct, and less medially displaced dorsal peak; from *P. dawsonae* **sp. nov.** in having a longer and more gracile proximal phalanx IV, with more raised plantar tubercles, a slightly narrower waist, more dorsoplantarly compressed shaft, and a less proximodorsally extensive distal articular surface; from *P. otibandus* in being slightly larger, with distal phalanx IV with a more pointed dorsal peak and proximal phalanx V with a more distinct waist; from *P. snewini* in having the middle phalanx IV slightly more dorsoplantarly compressed, with the proximal surface more dorsally tilted, and distal phalanx IV with a more rounded dorsal peak; from *C. kitcheneri* in being relatively broader, more robust, and more dorsoplantarly compressed, particularly the middle phalanges, with broader, shallower trochleae, larger proximal plantar tubercles on proximal and middle phalanges, middle phalanx IV with a less caudoplantarly extensive distal articular surface, and distal phalanges with less angular, more rounded dorsal peaks; from *O. rufus* and *M. fuliginosus* in being relatively broader and more robust, with broader, shallower trochleae, phalanges V larger relative to phalanges IV, proximal phalanx IV with a broader waist, and distal phalanges with a more concave proximal articular surface, a less angular, more rounded dorsal peak, and a more plantarly curved shaft; and from *W. bicolor* in being much larger, relatively broader, and more robust, with middle phalanx IV with a more dorsally tilted proximal surface.

***Protemnodon mamkurra* sp. nov.**

LSID of new species: urn:lsid:zoobank.org:act:1CD200A9-06C2-40FE-B789-AFE64466E2D5

Procoptodon pusio Owen; Owen (1876) pl. 31, figs 1–5. Not *P. pusio* Owen, 1874.

Procoptodon rapha Owen; Owen (1876) pl. 31, figs 6–9. Not *P. rapha* Owen, 1874.

Protemnodon anak Owen; Helgen *et al.* (2006), p. 303, appendix 2; Turney *et al.* (2008), p. 12152; Gillespie *et al.* (2012), p. 40, table 1, fig. 2, ; Gillespie *et al.* (2015), p. 44, table 1; Llamas *et al.* (2015), p. 581; Cascini *et al.* (2019), p. 523. Not *P. anak* Owen, 1874.

Protemnodon brehus (Owen); Tedford (1967), pp. 97–109; Helgen *et al*. (2006), p. 303; Ayliffe *et al.* (2008), p. 1785.

Protemnodon roechus Owen; Helgen *et al*. (2006) p. 303, appendix 2.

Protemnodon sp. cf. *P. roechus*; Jankowski *et al.* (2016), p. 543.

Holotype:

SAMA P59549 (field number FUCN 40 01) partial skeleton: partial LR maxillae, vertebrae T12, L2–4, Ca3 & Ca9?, nine partial ribs; LR humeri, L radius; LR partial pelvis, LR femur, L tibia & R proximal tibial epiphysis, L & partial R fibulae, L calcaneus, & R talus.

Type locality:

Green Waterhole Cave (=Fossil Cave, ASF code 5L81), 37°73'S, 140°5'E, Tantanoola, South Australia. A water-filled karst sinkhole in limestone, located 25 km northwest of Mount Gambier in the Limestone Coast region of far southeastern South Australia (Baird 1985; Horne 1988).

The fossils in the type series of *P. mamkurra* **sp. nov.** were collected in 1979 and 1987–88 by teams from the South Australian Speleological Society Inc. led by Rod Wells (Horne 1988). The faunal composition and relative dating indicate a late Pleistocene age (125–15 ka) (Pledge 1980; Baird 1985; Newton 1988), and five U-series dates taken from cave rafts with no direct association with the *P. mamkurra* **sp. nov.** type material gave an age range of 61.5–59.1 ka (Mather *et al.* 2023).

Paratypes:

Green Waterhole Cave: SAMA P28613 semi-complete juvenile skeleton: R premaxilla fragment, L I1, partial splanchnocranium with maxillae, jugals & palate preserving dP2–M2, with P3 & M3 partially removed from crypt, partial neurocranium, complete mandible

preserving i1a & dp2–m2, with m3 in crypt, vertebrae C1–3 & C5–7, T1, T3, T7 & T12–14, S1–2, & Ca2–?12, eight partial ribs; LR partial scapulae, L humerus, proximal ulna & proximal radius; LR ilia, partial ischia & partial pubes (unfused), L femur & R distal femoral epiphysis, LR tibiae, LR calcanei, LR metatarsals IV; all postcranial epiphyses missing except distal femoral epiphyses. SAMA P27270 partial R maxilla.

Referred specimens:

Western Australia

Kudjal Yolgah Cave, Boranup: WAM 08.8.979 R humeral fragment; WAM 08.8.998 L humeral fragment; WAM 08.8.587 L metacarpals I–V; WAM 08.8.544 R humeral fragments, partial LR ulnae, radial fragment, and ischial fragment.

Tight Entrance Cave, Boranup: WAM 08.1.16 partial R ulna.

Leaena's Breath Cave, Nullarbor: WAM 2020.6.301 R premaxilla fragment; WAM 2020.6.276 partial R maxilla; WAM 2020.6.291 partial juvenile R maxilla; WAM 2020.6.177 neurocranium fragment; WAM 2020.6.182 L I1 and juvenile R I1; WAM 2020.3.535 R DP3 and M1; WAM 2020.6.305 R dentary fragment; WAM 2020.3.221 axis vertebra; WAM 2020.6.384 ulna WAM 2020.3.591 L scaphoid; WAM 2020.6.72 metacarpal V and isolated metacarpal distal epiphysis; WAM 2020.3.211 metacarpal I; WAM 2020.6.199 metacarpal IV; WAM 2020.6.300 L distal manual phalanx ?III; WAM 2020.6.281 proximal manual phalanx ?III; ; WAM 2020.6.377 R tibia; WAM 2020.6.379 L tibia; WAM 2020.6.87 distal tibia fragment; WAM 14.8.5 proximal pedal phalanx IV; WAM 2020.6.180 LR metatarsals V; WAM 2020.6.146 proximal and distal pedal phalanges IV; WAM 2020.6.123 distal pedal phalanx IV; WAM 2020.6.21 middle pedal phalanx V. Numerous unregistered specimens (field code 'LBC') stored in the Western Australian Museum, Perth.

Upper Chamber, Last Tree Cave, Nullarbor: WAM 02.7.11 partial LR dentaries, L I1 and i1; axis vertebra, thoracic, lumbar and caudal vertebrae and fragments, sacrum; partial L clavicle, and L humerus, ulnar fragments, triquetrum, scaphoid, capitatum, hamatum, trapezium, metacarpals II–V and 2x distal phalanges; partial L femur and femoral fragments, partial L tibia, partial LR talus, calcaneus and cuboid, L navicular and ectocuneiform, partial LR metatarsals IV and V, and L and partial R proximal, middle and distal pedal phalanges IV and V; WAM 05.4.71 I1, I3 and i1.

South Australia

Robertson Cave, Naracoorte: SAMA P59547 R dentary; SAMA P59546 R ulna, triquetrum, partial scaphoid, capitatum, hamatum, proximal manual phalanges I–V, middle phalanges II–V, distal phalanges III and V.

Main Fossil Chamber, Victoria Fossil Cave, Naracoorte: SAMA P20819 neurocranium; SAMA P59542 metacarpal III; SAMA P59540 L calcaneus; SAMA P59541 L metatarsal IV; SAMA P59543 juvenile LR metatarsals V.

New entrance, Victoria Fossil Cave: SAMA P20810 proximal manual phalanges II–IV, middle II–III and distal I–V, L calcaneus, R cuboid and metatarsal IV, LR metatarsals V, R proximal, middle and distal pedal phalanges IV and proximal and distal phalanges V.

Curramulka Town Well Cave, Yorke Peninsula: SAMA P59553 R maxilla, neurocranium, LR I1s, L M4, atlas vertebra and R scaphoid; SAMA P13027 partial cranium and mandible.

Queensland

Pearson's Bed, King's Creek, Darling Downs: IS V566 L premaxilla and maxillae.

Darling Downs (site unknown): NHMUK PVOR35942c L metatarsal IV; NHMUK PVOR35946 R metatarsal IV; NHMUK PVOR35948 L metatarsal V.

New South Wales

Site 51, Lake Victoria: NMV P26570 LR femoral and tibial fragments, fibular fragment, partial R calcaneus, partial L metatarsals IV and V, and proximal pedal phalanx IV.

Cathedral Cave, Wellington: AM F161924 partial neurocranium.

Wellington Caves, Wellington (site unknown): AM F104747 partial juvenile R calcaneus.

Wombeyan Caves (site unknown): NMV P54901 partial neurocranium.

Victoria

Site 499, Bacchus Marsh: NMV P187473 partial splanchnocranium.

Hines Quarry, Bacchus Marsh: NMV P160365 & NMV P160366 partial splanchnocranium and partial L dentary (reassociated).

Tasmania

Scotchtown Cave, Smithton: QVM2007 GFV33 partial R metatarsal V.

Bone Aven (CP213), Mt Cripps: QVM2000 GFV10 & QVM2001 GFV11 partial juvenile cranium and R dentary (reassociated); QVM2001 GFV05, QVM2000 GFV13, QVM2000 GFV14, QVM2001 GFV57a/b, QVM2001 GFV57, QVM2001 GFV23 & QVM2001 GFV04 partial cranium R maxilla, two thoracic vertebrae (?T13–14), two lumbar vertebrae (L3 and L5), partial R pelvis, L femur and R fibular fragment (reassociated); QVM2001 GFV06 partial juvenile L dentary; QVM2001 GFV01 R I1; QVM2000 GFV12 R i1; QVM2001 GFV03 R ilium; QVM2001 GFV02 partial L tibia; QVM2001 GFV02b juvenile L tibia; QVM2001 GFV08 L i1; QVM2001 GFV09 partial juvenile R maxilla; QVM2001 GFV10 partial juvenile R dentary; QVM2001 GFV19 L M4; QVM2001 GFV39 partial juvenile R scapula; QVM2001

GFV40 partial juvenile LR femora; QVM2001 GFV58 two caudal vertebrae; QVM2001 GFV72 partial L radius; QVM2002 GFV08 LR premaxilla fragments; QVM2002 GFV21 partial juvenile L ulna; QVM2002 GFV07 caudal vertebra; QVM2003 GFV10 partial juvenile LR humeri; QVM2003 GFV12 partial ischium; QVM2003 GFV28 L fibular fragment.

Specific diagnosis:

Protemnodon mamkurra **sp. nov.** is distinguished from other species of *Protemnodon* by several unique osteological characteristics and by the combination of other dental and postcranial characteristics. The cranium of *P. mamkurra* **sp. nov.** is differentiated from all other members of the genus by possessing: a taller rostrum and broader, more curved, more ventromedially situated occipital condyles relative to the foramen magnum. The axial skeleton differs from all species of *Protemnodon* by having relatively broader, craniocaudally shorter axis vertebra and cervical vertebrae C3–7. The forelimb differs from all other species of *Protemnodon* in having: a more robust ulna and radius; and more dorsopalmarly flattened distal manual phalanges. The pes differs from all other species of *Protemnodon* in having: a calcaneus with large, craniocaudally level and semicontinuous lateral and medial talar facets and a sustentaculum tali with a pointed cranioplantar peak; a cuboid with a broader flexor groove; and distal phalanges IV and V with a V-shaped divot in the lateral and medial margins of the proximal surface.

The species is most similar in aspects of cranial morphology to *P. viator* **sp. nov.** The cranium is further distinguished from that of *P. viator* **sp. nov.** by having a more raised medial ridge on the basioccipital and in having the exoccipital less posteriorly curved over the foramen magnum. The dentary of *P. mamkurra* **sp. nov.** cannot be differentiated from those of *P. viator* **sp. nov.** and *P. dawsonae* **sp. nov.**, and is otherwise most similar to that of *P. anak*, from which it differs in having a more dorsally deflected diastema and i1.

The teeth of *P. mamkurra* **sp. nov.** cannot be differentiated from those of *P. viator* **sp. nov.** The dentition of *P. mamkurra* **sp. nov.** is similar to that of *P. dawsonae* **sp. nov.** and *P. anak,* differing in possessing: a larger I1; uppers molars with a broader, lower and less distinct preparacrista; and in lacking a ventrolingual crest on the i1, instead exhibiting a thick, rounded ventrolingual enamel lip extending smoothly onto the lingual surface. It is further distinguished from *P. dawsonae* **sp. nov.** by having upper molars with no preprotocrista and an unkinked postparacrista. Differs further from *P. anak* in having: a relatively broader DP2 across the anterior cusp; DP3 lacking a distinct, raised preprotocrista (forelink) that forms half of an incomplete protoloph, instead having an absent or very slight preprotocrista and a complete protoloph; P3 with higher, more anteriorly extensive lingual crest that is smoothly curved in lingual view and lower, less distinct and less transversely aligned transverse ridgelets; upper molars with a lower postprotocrista and a stronger postparacrista; M1–M2 with a weaker preparacrista; broader p3 relative to length with fewer, less raised and less distinct ridgelets; and lower molars with a lower, less distinct cristid obliqua and more convex buccal lophid margins in posterior view.

The postcranial skeleton of *P. mamkurra* **sp. nov.** is most similar to that of *P. dawsonae* **sp. nov.** and *P. viator* **sp. nov.** The axial skeleton of *P. mamkurra* **sp. nov.** is further distinguished from that of *P. dawsonae* **sp. nov.** by its lumbar vertebrae with shallower transverse processes and centrum with relatively taller, slightly narrower cranial and caudal extremities, less concave ventrolateral surfaces, less concave ventral margin, and more raised ventral ridge. The hindlimb differs from that of *P. dawsonae* **sp. nov.** by having a pelvis with a larger caudal iliac spine, deeper gluteal fossa, less cranially tilted sacral surface, less laterally projected rectus tubercle, more deeply concave acetabulum and more convex and rugose caudal margin of dorsal part of ischium. The pes differs in having: larger, taller and relatively and absolutely broader calcaneus, with more bulbous lateral talar facet and caudal fibular facet, and fibular facets more plantarly extensive in lateral view; metatarsal IV with larger plantar cuboid facet; and metatarsal V with a less distally extensive lateral plantar tuberosity.

The axial skeleton of *P. mamkurra* **sp. nov.** differs from that of *P. viator* **sp. nov.** in having: the atlas vertebra with lateral vertebral foramina that open laterally instead of caudally, and less caudally projected and extensive wings; taller cervical vertebrae C3–7 with less transversely aligned, more roof-like arches in cranial view, and a less caudoventrally projected caudal extremity of the centrum lacking a slightly bilobed ventral margin. The forelimb differs by its radius having a more distally situated cranial ridge. The manus is differentiated by: a scaphoid with the facets for the hamatum and capitatum less distinct from each other, and a thickened, raised dorsal ridge present on the dorsomedial margin of the radial facet; shorter and more robust metacarpals; and distal manual phalanges lacking a slight dorsal peak.

The hindlimb is differentiated from *P. viator* by: its pelvis having a taller rectus tubercle; a more gracile femur with a lower, less distinct intercondylar crest, a less medially projected lesser trochanter, weaker proximolateral ridge, relatively shorter lesser trochanteric ridge, broader and shallower trochlea, more rounded trochlear crests with relatively broader medial crest; and shorter, broader and much more robust tibia with more laterally curved cnemial crest in cranial view with less angular and distinct distal peak, and thicker proximal section of proximolateral crest. The pes is distinguished from that of *P. viator* **sp. nov.** by: its broader and more robust calcaneus, with a more rounded, less triangular calcaneal tuberosity in cross-section, larger and more bulbous talar facets, a larger and more bulbous fibular facet with a more rounded and caudally projected (rather than laterally projected) caudal component, and a more medially projected sustentaculum tali; a relatively broader cuboid with a less elongate, less plantarly projected lateral plantar tubercle, a less plantarly projected, slightly more

medially situated medial plantar tubercle, a broader, less deeply concave flexor groove, and a broader metatarsal V facet; a broader navicular with a less plantarly extensive ectocuneiform facet; an ectocuneiform with a broader, more oval, and less plantarly extensive navicular facet, and a less deep plantar tubercle which is more rounded in medial view; a longer metatarsal IV with a larger plantar cuboid facet; a longer, less transversely compressed and dorsoplantarly shorter metatarsal V with a more dorsally situated and less plantomedially extensive cuboid facet; a proximal phalanx IV with a weaker waist; a more elongate middle phalanx IV; a distal phalanx IV with a more rounded dorsal peak; and a less transversely asymmetrical distal phalanx V.

Etymology:
Mamkurra ('mahm-KUH-rah') means 'great kangaroo' (*mam* is a prefix meaning 'great', *kurra* is 'kangaroo') in the Bungandidj language of the Boandik people of southeastern South Australia, on whose country the type locality is situated. The name was chosen by Boandik elders and language experts in cooperation with the authors.

Description and comparisons:

Cranium and dentition
Cranium (Fig. 37): *Rostrum*. Rostrum is tall to very tall, and is moderately to strongly ventrally deflected (Fig. 37a). Premaxilla is anteroventrally projected and narrows anteriorly; incisor-bearing part contributes ~50% of the ventral length from the anterior tip to the premaxilla-maxilla suture; lateral surface slightly concave, ventral surface quite planar; dorsal and lateral surfaces of the anterior part are pockmarked with very small foramina. Incisive foramen large and elongate, with a tapering channel extending anterolaterally from the foramen in ventral view, roughly toward I2. Anterior margin of the premaxilla slopes moderately dorsoposteriorly before curving sharply dorsally to the nasal suture; dorsoposterior component ('walls' of nasal cavity) is tall and smoothly convex; ventral premaxilla-maxilla suture is angled posterolaterally; lateral premaxilla-maxilla suture extends straight dorsally before curving smoothly posteriorly toward the posterior of the nasal. Nasal elongate, gently dorsally convex transversely, and projected anteriorly to shared medial point. Buccinator fossa smoothly concave, quite deep and tall, extends dorsally from the ventral margin of the corpus below the diastema to level with the dorsal extremity of the infraorbital foramen, and from immediately anterior to P3/DP2 across the premaxilla-maxilla suture; height and depth smoothly decrease anteriorly. Infraorbital foramen large, opening anteriorly, transversely compressed, positioned dorsal to P3/DP2. Maxillary foramen (posterior to infraorbital canal) large and rounded, with a shallow channel extending posteriorly from the opening along the posterior of the maxilla. Sphenopalatine foramen very small, with a narrow channel that extends posteriorly from it, broadening near the foramen rotundum. The foramen rotundum is large and oval. Frontal has a concave lateral surface, with greatest concavity at the midpoint of the temporal fossa; dorsolateral margin flares increasingly laterally (forming the supraorbital crest) over the anterior of the orbit with age; suture with the parietal is level with or posterior to the posterior margin of the temporal fossa.

Palatal region. Palatine quite broad, with the anterior part of the maxillo-palatine suture adjacent to the masseteric process in young individuals and migrating anteriorly with age to be level with the M1–2 boundary. Palatal fenestrae absent. Anterolateral palatine foramina elongate and situated adjacent to the anterolateral margins of the maxillo-palatine suture. Two small posterolateral foramina are adjacent to M4. Masseteric process large, broad, laterally projected, slightly posteriorly deflected, with ventral tip rotated laterally relative to the base. Mainly contributed by the maxilla, with the posterior component of the base contributed by the jugal. Increases in size, lateral projection and posterior deflection with age.

Lateral cranium. Lacrimal has two foramina on the anterodorsal margin of orbit; one is large, rounded, anteroventrally located, and abuts the midpoint of the anterior margin, the second is smaller and dorsoposteriorly located; both foramina with small crest bounding them dorsoposteriorly. Jugal increases in height posteriorly, before narrowing slightly posteriorly and bifurcating around the anterior tip of the zygomatic process of the squamosal into the postorbital process and an elongate posterior part; the dorsal margins of the suborbital jugal and the postorbital process are flattened and broad. A low, angular ridge extends from immediately posterior to the midpoint of the anterior margin of the jugal across the posterior part. Zygomatic process of the squamosal has a smoothly convex dorsal margin in lateral view, tilted medially to be slightly dorsal facing; lower and less tilted in juveniles. Ventral margin broadens posteriorly toward the glenoid fossa. Medial component of the squamosal is broadly convex and elongate; a low, angular ridge extends from the dorsoposterior base of the zygomatic process, borders the ventral margin of the subsquamosal, and extends dorsoposteriorly to the interparietal. Subsquamosal foramen is rounded, located immediately posterior to the dorsal surface of the base of the zygomatic process. Glenoid fossa broad and flat, abuts the postglenoid process posterolaterally. Postglenoid process moderately well-developed, narrows to a ventral point, and angled anterolaterally in ventral view, with the posteromedial component extending into and semi-fused with the anterior process of the ectotympanic to form a deep, anterior-facing ventral postglenoid foramen. Ectotympanic has a large, rugose anterior process projected ventral to and medial to the postglenoid process. External auditory meatus roughly cylindrical, angled dorsolaterally, not projected laterally beyond the margin of the anterior process of the ectotympanic and subequal in size.

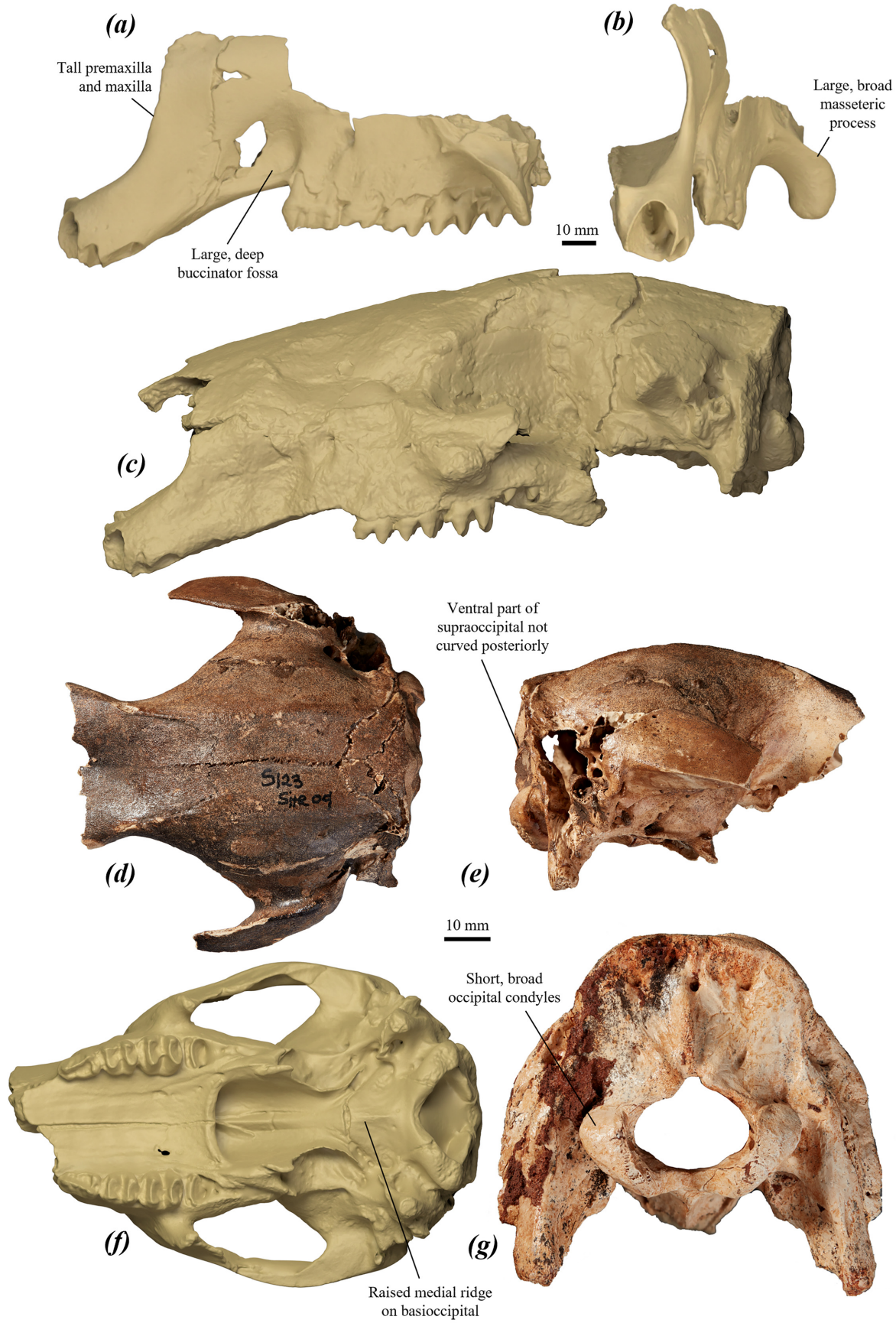

FIGURE 37. partial crania of *Protemnodon mamkurra* **sp. nov.**: (a–b) surface scan images of left premaxilla and partial maxilla of IS V566 in (a) lateral, and (b) anterior views; (c) surface scan image of partial cranium of SAMA P13027 in left lateral view; (d–f) partial juvenile neurocranium of paratype SAMA P28163 in (d) dorsal and (e) right lateral views; (f) surface scan image of partial juvenile cranium of QVM2000 GFV10 in ventral view; and (g) partial neurocranium of SAMA P59553 in posterior view.

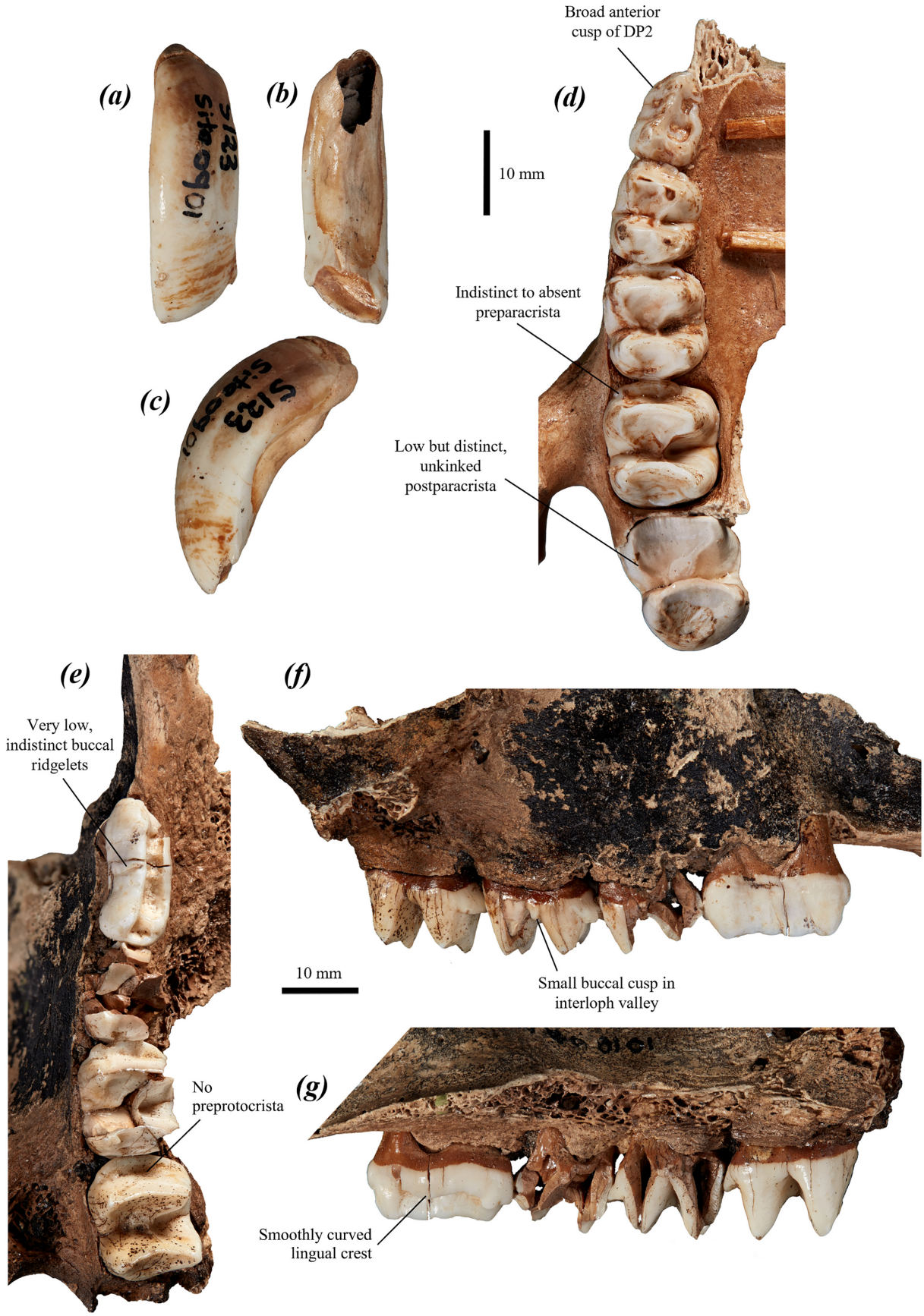

FIGURE 38. upper dentition of *P. mamkurra* **sp. nov.**: (a–c) left I1 of paratype SAMA P28163 in (a) anterior, (b) occlusal/posterior, and (c) lateral views; (d) right DP2–M3 of SAMA P28163 in occlusal view; and (e–g) partial right maxilla and P3, partial M1–2 and M3 in (e) occlusal, (f) buccal, and (g) lingual views.

Neurocranial region. Basioccipital broad, with concave ventrolateral surfaces, and a thin medial ridge that extends from the basisphenoid to immediately anteroventral to the base of the foramen magnum (Fig. 37f); this ridge is very low to absent in juveniles. Alisphenoid posteroventral wing elongate; anterolateral surface of the centrum of the alisphenoid broad and gently convex, extends from the foramen ovale to the petrotympanic fissure. A thin crest projects anteromedially from the base of the paroccipital to merge with the posterior of the pterygoid crest, posteriorly abutted by a deep, rounded, quite large posterior lacerate foramen set into the medial base of the paroccipital process. Pterygoid with medial origin thin and tall, curves anteromedially to continue anteriorly into the pterygoid crest; pterygoid cavity broad, rounded and concave, bordered laterally by a tall, thin and distinct anteroposterior ridge extending from the posterolateral pterygoid crest to abut the medial margin of the foramen ovale.

Dorsal and posterior cranium. Parietal broad and convex. Temporal crest ossification pattern is as in *P. anak*. Nuchal crest low in juveniles, becomes very thickened and raised in adults, particularly laterally; crest extends ventrolaterally from the top of the supraoccipital before bifurcating around the mastoid foramen, with the lateral crest (mastoid-petrosal crest) extending ventrally to form the lateral margin of a short, blunt, slightly laterally flared mastoid process, and the medial (paroccipital) crest continuing ventrolaterally into the lateral margin of the elongate paroccipital process. Occiput is tilted slightly toward the posterior. Foramen magnum broad, oval and slightly compressed dorsoventrally, with a small U-shaped divot into the dorsal margin. Occipital condyles large, broad, gently curved ventromedially, oriented slightly dorsolaterally, extending beneath the foramen magnum, not extending dorsally beyond dorsal margin of the foramen magnum, tapered ventromedially in posterior view and projected posteriorly well beyond the margin of the occiput in lateral view. The dorsolateral margins of the supraoccipital are rounded with a flattened dorsal margin in posterior view; supraoccipital dorsoventrally short in juveniles; height increases relative to width with age, and dorsal margin thickens and flares dorsolaterally; posterior surface is pitted with four or more fossae, particularly the dorsal component, with the depth and the number of fossae increasing with age. A thickened, raised medial ridge runs dorsally from the dorsal margin of the foramen magnum, across the supraoccipital depression, to the centre of the nuchal crest.

The cranium of *P. mamkurra* **sp. nov.** differs from that of *P. anak* in being relatively broader, having a taller rostrum, shorter, broader, more ventrally situated, and more ventromedially curved occipital condyles, less posteriorly curved exoccipital, and in lacking a thin anterior jugal ridge; from *P. viator* **sp. nov.** in having a taller rostrum, shorter, generally broader, more ventromedially curved and generally more ventromedially situated occipital condyles, a more raised, more angular medial ridge on the basioccipital, , and a less posteroventrally curved exoccipital; from *C. kitcheneri* in being larger, relatively broader, more robust, and lacking a bony 'pocket' of the premaxilla within the nasal cavity, with a taller and more robust anterior component of the premaxilla, taller rostrum, larger masseteric process, much thicker and less laterally projected ventral orbital rim, taller zygomatic arch, broader, more curved, more ventromedially situated, and more posteriorly projected occipital condyles, a single anteroposterior ridge meeting medial margin of foramen ovale, and the anterior process of the ectotympanic extending to tip of postglenoid process, rather than wrapping around the posterior surface; and from *W. bicolor* in being much larger and lacking a small, pointed, anteriorly projected eminence on the anterior margin of the jugal, with a more ventrally projected anterior component of the premaxilla, taller rostrum, larger masseteric process, more robust palatine lacking fenestra, broader, more ventromedially situated and more posteriorly projected occipital condyles, a more raised anteroposterior ridge meeting the medial margin of the foramen ovale, relatively larger, more laterally extensive anterior process of the ectotympanic, and a taller, more laterally projected postglenoid process.

Upper dentition (Fig. 38): I1: broad, robust, arcuate, slightly anteroposteriorly compressed, with thick buccal enamel extending around to the edges of the lingual surface, receding from the lingual surface with age. Buccal surface smooth and gently convex. Occlusal surface oval, with buccal enamel forming a slight anterior lip; becomes anteroposteriorly deeper with age. The I2 is not known. I3: elongate, transversely compressed and roughly triangular in buccal view, with the buccal enamel width less than that of I1. A large, buccally gently convex main crest curves anterolingually to sit lingual to the posterior margin of the smaller anterobuccal crest; anterobuccal crest is around half the length of the main crest.

The cheek teeth are high-crowned. DP2: quite short, broad and oblong, broadening posteriorly, with thickened peaks over the anterior and posterior roots linked by a high main crest; morphologically very similar to P3 but anteroposteriorly truncated. Main crest blade-like, anteroposteriorly to slightly posterobuccally orientated, jagged to gently undulating in buccal view with a very low, dorsoventrally aligned ridgelet on the midpoint of the buccal surface. Lingual crest low, extends from the lingual base of the anterior cusp, lingually borders a broad, anteriorly tapering lingual basin, and meets the small, secondary posterolingual peak; a low ridgelet perpendicularly transects the midpoint of the lingual basin. Some specimens have the lingual crest meeting a small, secondary anterolingual peak at the lingual base of the anterior cusp. A small posterior basin abuts the posterior margin, sitting between the main and secondary posterior peaks; removed by a small amount of wear. DP3: broad and molariform, with the protoloph and metaloph markedly narrower than their swollen loph bases; anterior loph longer and narrower than the posterior loph. Precingulum small, narrower than the anterior loph, merges buccally with the thin and low but distinct preparacrista. Preprotocrista absent or very slight. Postparacrista thin and distinct, curves gently lingually into the interloph

valley. Postprotocrista and postmetaconulecrista both thick, curving gently toward the midline of the tooth; postprotocrista continues onto anterior face of metaloph in some specimens. Postmetacrista short and thick.

P3: large and broadly oblong, tapers to a blunted point anteriorly; generally broader posteriorly, with thickened peaks over the anterior and posterior roots linked by a high main crest. In occlusal view, P3 is variably curved buccally toward its posterior, with the posterior part slightly swollen or expanded buccally and slightly rotated buccally, contributing to the variable crescentic shape of the tooth; broad and rounded posteriorly. Main crest high, blade-like, roughly anteroposteriorly orientated with a variable degree of posterobuccal curvature in occlusal view; slightly jagged to gently undulating in buccal view with two or three very low, roughly dorsoventrally aligned ridgelets around the centre of the buccal face, angled slightly toward the midpoint in buccal view. Anterior cusp generally slightly broader than the main crest + lingual crest, with a tall and pointed peak. Anterior peak intersected by a very brief transverse crest, perpendicular to the main crest, which dorsoventrally on the buccal and lingual surfaces, with the lingual ridgelet merging with the anterior margin of the lingual crest. Some specimens with one or two very small, low bumps on the base of the anterior or anterolingual surface of the anterior cusp, very occasionally merging with an unusually anteriorly extensive lingual crest and linking the lingual crest to the anterior cusp. Lingual crest moderately tall, gently undulating in lingual view, extends from the lingual base of the anterior cusp to merge into the secondary posterolingual peak; lingually borders the broad, anteriorly tapering lingual basin; lingual basin V-shaped in cross-section, with one to three indistinct, very low ridgelets perpendicularly transecting the anterior component of the lingual basin. Posterior cusp tall and rounded, continuous with the main crest, which extends and broadens posteriorly to merge with the low, narrow transverse posterior crest. Small posterior basin located between main and posterolingual peaks, posteriorly bordered by the transverse posterior crest; removed by a small amount of wear. Posterolingual peak rounded, lower than the posterior cusp, and linked to the main crest by a thin transverse crest that anteriorly borders the posterior basin.

Molars: rounded-rectangular in occlusal view. Lingual and buccal margins of the lophs are slightly to moderately convex in posterior view, particularly the anterior lophs, with the protoloph and metaloph narrower than their bases; unworn protolophs and metalophs are gently concave posteriorly in occlusal view. Precingulum narrower than the anterior loph, slightly to moderately anteriorly projected, gently medially tilted, generally becoming slightly larger, broader and more projected toward M4; flat, broad and shelf-like when worn; width variable within individuals (see cingula of left and right M2 of paratype SAMA P28163); some specimens (*e.g.* WAM 2020.6.276) with small enamel crenulations on the occlusal surface. Preprotocrista absent or very slight. Preparacrista absent or low and indistinct (Fig. 38d). Postparacrista quite well-developed immediately posterior to the paracone, becomes thinner and less raised toward interloph valley, curves lingually to be adjacent to or merge with the buccal component of the postprotocrista in the interloph valley. Postprotocrista relatively thicker and more raised, particularly in the interloph valley, curves from the protocone to near the midpoint of the interloph valley; continues as a thin and indistinct crest towards metaconule, merging into anterior face of metaloph. Interloph valley slightly narrower than the lophs, occasionally broader in M1 and very rarely in M2. Some specimens with a very small, rounded cusp on the base of the protoloph on the buccal margin of the interloph valley (Fig. 38f), and/or with a very small, rounded cusp on the base of the metaloph in the interloph valley abutting the lingual margin, presence very variable, with either or both cusps variably present in DP3 (*e.g.* QVM2000 GFV10) or on one or more molars, anywhere along the molar row, sometimes present on only one side of the dentition. Premetacrista very slight, extends from the metacone to meet the base of the postparacrista in the interloph valley. Postmetaconulecrista quite thick and raised, arises from the metaconule and curves dorsobuccally to form a small, oblique shelf beneath the posterior basin. Postmetacrista lower, shorter and less distinct, arises from the metacone, deflects lingually to merge into the buccal margin of the posterior basin.

The upper dentition of *P. mamkurra* **sp. nov.** differs from that of *P. anak*, *P. otibandus* and *P. snewini* in having a DP3 lacking a large, distinct preprotocrista forming half of an incomplete protoloph. It further differs from *P. anak* in being generally slightly larger, with broader I1 relative to the length of I3, relatively broader DP2, particularly across the anterior cusp, P3 with a higher, less jagged and more anteriorly extensive lingual crest and lower, less transversely aligned and less distinct transverse ridgelets, generally relatively broader molars with a lower postprotocrista and slightly stronger postparacrista, and M1–2 with a weaker preparacrista; from *P. viator* **sp. nov.** in being generally smaller, with P3 with a slightly narrower anterior relative to length and a relatively narrower anterior loph of M1; from *P. tumbuna* in being larger and higher crowned, with broader, anteroposteriorly shorter I1 lacking a posterobuccal bulge in cross-section, DP2 lacking a small anterolingual crest linking the anterior cusp and lingual crest, relatively narrower P3, and generally less rounded molars in occlusal view with no urocrista present; from *P. dawsonae* **sp. nov.** in having I1 broader relative to I3, P3 with slightly less distinct buccal ridgelets, relatively narrower posterior molars, and molars with a lower and less distinct preparacrista, no preprotocrista, and a gently curved postparacrista; from *P. otibandus* in being larger and higher crowned, with broader, anteroposteriorly shorter I1 lacking a posterobuccal bulge in cross-section, DP2 and P3 with less distinct buccal ridgelets, and molars lacking a urocrista; from *P. snewini* in being larger and higher crowned, with relatively broader P3 across the posterior cuspule; from *C. kitcheneri* in being larger and higher crowned, with larger incisors relative to size of cranium, broader I1 relative to I3, absolutely and more elongate P3 and relatively slightly narrower molars; and

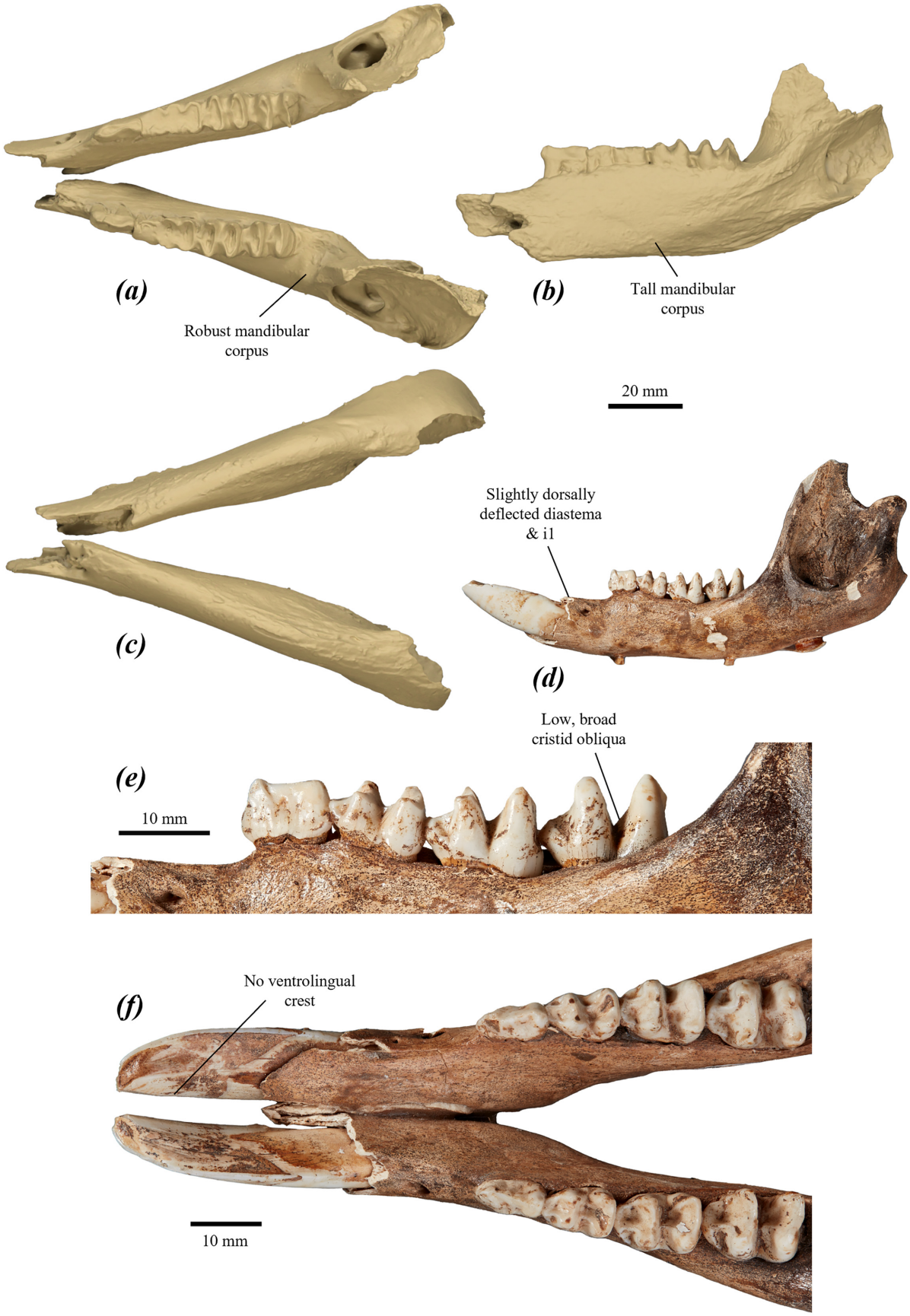

FIGURE 39. mandible and lower dentition of *P. mamkurra* **sp. nov.**: (a–c) surface scan images of left and right dentaries of WAM 02.7.11 in (a) occlusal, (b) lingual, and (c) ventral views; (d) juvenile mandible of paratype SAMA P28163 in left buccal view; (e) left dp2–m2 of P28163 in buccal view; and (f) left and right i1s and dp2–m2 of P28163 in occlusal view.

from *W. bicolor* in being much larger and higher crowned, with relatively broader I1, P3 with a higher lingual crest and a larger posterior basin, and molars with a thicker postprotocrista distinctly extending to the protocone, rather than merging into the centre of the posterior surface of the protoloph.

Dentary (Fig. 39a–d): tall and robust. Dentaries diverge from sagittal plane at ~30° from the axis of the symphysis in dorsal view. Diastema moderately long, increasing in length with age; between half and two-thirds of height of mandibular corpus; dorsal margin level to slightly dorsally deflected, and ventral margin very gently convex, such that first incisor is orientated somewhat dorsally. Mental foramen round to oval, opens laterally, positioned midway between the midpoint and dorsal margin of the lateral surface of the diastema, around one-third of the diastema length from the dp2/p3. Mandibular corpus tall, slightly deeper beneath m1 than m4. Buccinator sulcus distinct but quite shallow, extends along the buccal surface of the mandibular corpus, slightly ventral to and parallel to the three anteriormost cheek teeth. Digastric sulcus generally shallow and broad, situated on the ventral part of the lingual surface of the mandibular corpus, extending roughly from ventral to the base of the coronoid crest to ventral to m2/m3. Ascending ramus tall and quite robust, slightly concave laterally and convex medially. Coronoid crest angled around 70–85° from transverse plane, smoothly convex anteriorly, ascends to rounded, anteroposteriorly short peak; some specimens with slight, rounded corner or elbow at midpoint. Dorsoposterior margin of the coronoid process is deeply concave, curves anteroventrally before levelling out at or slightly ventral to the anterior margin of the mandibular condyle.

Masseteric fossa large and shallow, bounded anteriorly and ventrally by low ridge; margins broadly rounded to U-shaped in lateral view. Masseteric foramen oval and elongate; abuts the anterior margin of the masseteric fossa and shares the anterior part of its lateral lip. Masseteric dental canal deep, separated from the mandibular foramen and the inferior dental canal by a narrow dorsal crest running anteroposteriorly. Medial pterygoid fossa very concave, deep and broad, broadens posteriorly; posteromedial extremity is squared and posterior margin is straight in dorsal view. Mandibular foramen round to oval and transversely compressed; opens posteriorly and slightly medially; located in the anterolateral part of the medial pterygoid fossa at the ventral base of the medial surface of the ascending ramus. Angular process is a thin, elongate crest, quite dorsally and slightly posteriorly projected such that the posterior extremity is level with that of the mandibular condyle. Ventral and posteroventral margin of the dentary similar to that of *P. anak*. The condylar process is not posteriorly projected. Mandibular condyle oval, slightly anteroposteriorly compressed, rotated slightly laterally in dorsal view and tilted medially; occasional a small, rounded eminence extends from the anteromedial margin. Ontogenetic change similar to that of *P. anak*.

The dentary of *P. mamkurra* cannot be differentiated from that of *P. viator* **sp. nov.** nor *P. dawsonae* **sp. nov.** Differs from that of *P. anak* being broader and more robust, with a shorter, more dorsally deflected diastema relative to the tooth row length; from *P. tumbuna* in being generally larger, with a relatively shorter diastema and more anterodorsally situated mental foramen; from *P. otibandus* in being generally slightly more robust, particularly in the diastema; from *P. snewini* in being larger, deeper and more robust, with a more dorsally deflected diastema, slightly more ventrally situated mental foramen, and a less posteriorly projected angular process; from *C. kitcheneri* in being larger and more robust, with a relatively shorter, more dorsally deflected diastema, more posteroventrally situated mental foramen, taller mandibular corpus, deeper buccinator sulcus, anteroposteriorly longer coronoid process, a larger dorsal septum partially separating the masseteric and mandibular foramina, deeper medial pterygoid fossa with higher posterior margin, and a relatively dorsally situated masseteric fossa; and from *W. bicolor* in being much larger, with a more dorsally deflected diastema, deeper buccinator sulcus, broader, more oval mandibular condyle, and a larger dorsal septum partially separating the masseteric and mandibular foramina.

Lower dentition (Fig. 39d–f): i1: large, procumbent and slightly to moderately dorsally deflected, broad and buccally tilted; acuminate when unworn, becoming shorter and rounder in cross-section with wear; enamel completely covers the buccal surface; dorsobuccal margin with thin, raised enamel crest; enamel thick and rounded around the ventrolingual margin, lacking ventrolingual crest (Fig. 39f), covers the ventral half of the lingual surface when unworn, with the lingual enamel layer tapering posteriorly such that well-worn i1s lack lingual enamel.

Tooth row roughly straight and parallel in occlusal view, very slightly convex in juveniles; in lateral view, tooth row slopes slightly ventrally toward the posterior, with the rate of wear along tooth row highly variable as a result of the variable degree of the tooth row angle. dp2: morphologically very similar to p3 but anteroposteriorly truncated; tall and triangular in cross-section, roughly oblong to mucronate in occlusal view, broadens gently to its posterior. Main crest thin, aligned anteroposteriorly, extends from over the anterior root to over the posterior root and twists lingually to end over the posterolingual extremity; an indistinct dorsoventrally aligned ridgelet is located around the midpoints of the buccal and lingual surfaces. Anterior cuspid semi-distinct from the main crest, being slightly broader, with very slight dorsoventrally aligned posterior ridgelets. dp3: molariform, very similar to the morphology of m1 but relatively narrower. Both lophids crests significantly narrower than bases, protolophid narrows slightly more; both lophid crests slightly convex posteriorly in occlusal view when unworn to moderately worn. The lophid bases are slightly bulged buccally. Precingulid moderately developed, narrower than the trigonid, and tapers anteriorly. Paracristid thin and raised; lingual component anteroposteriorly aligned, curves smoothly posterobuccally to the protoconid; wears quickly. Premetacristid narrow and moderately anteriorly

projected, contributing to quite deep and rounded trigonid basin. Postprotocristid thin and indistinct, lingually deflected to midpoint of the base of interlophid valley and merges with lingual component of cristid obliqua; wears quickly. Cristid obliqua quite tall and slightly thickened, curves posterobuccally to hypoconid. Preentocristid distinct, slightly thickened, anteriorly projected from entoconid. Postcingulid small, shelf-like, slightly narrower than posterior of talonid base.

p3: elongate and oblong in occlusal view, typically with slight waist, occasionally with parallel margins or slight transverse bulge around the midpoint; typically broader across posterior root than anterior root but occasionally subequal; tall and triangular in cross-section. Main crest; blade-like, straight, anteroposteriorly linking pointed anterior cuspid and blunt, posteriorly rounded posterior cuspid; twists slightly to moderately lingually past posterior cuspid; buccal and lingual surfaces have one to three indistinct, roughly dorsoventrally aligned ridgelets that extend to peak of crest, such that unworn and slightly worn crest appears slightly jagged in buccal view. When unworn, a very brief transverse crest intersects the main crest and anterior cusp perpendicularly, extending down from peak to form slight posterior-facing ridgelet. The anterior base of the anterior cuspid occasionally has a small, irregular bump projected slightly anteriorly or anterolaterally.

Molars: high-crowned, quite broad and rounded in occlusal view, with the interlophid valley narrower than the lophid bases; when unworn or slightly worn, the protolophid and hypolophid crests are posteriorly convex or have an oblique mesial kink toward the posterior; lingual component of the hypolophid is slightly posteriorly tilted, becomes straight and perpendicular to tooth row centreline with moderate wear. The buccal margins of the lophids are slightly more convex than the lingual margins in posterior view. Precingulid moderately developed, typically narrows to a rounded point. Paracristid with lingual component large and square; buccal component thick and raised, extends straight posteriorly before curving dorsobuccally to the protoconid. Protolophid and protoconid enamel 'folding' is similar to that of *P. anak*. Premetacristid very low, often indistinct or absent, extends from the lingual margin of the trigonid basin to the metaconid. Cristid obliqua thick and generally low, arises from slightly buccal to the midpoint of the interlophid valley, curves very slightly buccally and extends to the hypoconid (Fig. 39e–f). Preentocristid very low, broad and indistinct, arises midway between the base of the cristid obliqua and the lingual extremity of the interlophid valley and deflects slightly lingually as it rises to the entoconid. When little worn, the hypoconid is distinctly taller than the entoconid and is slightly lingually displaced. Postcingulid narrow and slight on m1 and 2, typically becoming more broader and shelf-like in m3 and particularly m4; occasionally present as a wrinkled bulge on the posterior lophid base.

The lower dentition of *P. mamkurra* **sp. nov.** differs from that of all other species of *Protemnodon* except *P. viator* **sp. nov.** in having a broader posterior of the p3 relative to length. It further differs from *P. anak* in having a broader i1 with a lower dorsobuccal crest and no ventrolingual crest, slightly broader dp2, p3 with fewer, lower and less distinct ridgelets on the main crest, generally slightly larger molars with a smaller precingulid, more convex buccal lophid margins when slightly worn, and a lower, less distinct cristid obliqua when unworn or slightly worn; from *P. viator* **sp. nov.** in being generally smaller; from *P. tumbuna* in being larger and higher crowned, with a relatively larger, broader i1 with no ventrolingual crest, and m3 and m4 with less convex buccal lophid margins and a lower premetacristid; from *P. dawsonae* **sp. nov.** in being generally larger and higher crowned, with the i1 lacking a low, thick ventrolingual crest; from *P. otibandus* in being larger and higher crowned, with relatively larger, broader i1 lacking a ventrolingual crest, and m3 and 4 with less convex buccal lophid margins; from *P. snewini* in being larger and higher crowned, with relatively larger, broader and more dorsally deflected i1 lacking ventrolingual crest and with enamel more extensive across ventral component of lingual surface, p3 with fewer, less distinct ridgelets on main crest, and molars with larger premetacristid and smaller precingulid; from *C. kitcheneri* in being larger and higher crowned, with a broader and more spatulate i1 lacking a ventrolingual crest, relatively broader deciduous premolars, larger and more elongate p3, and molars with narrower lophid crests and a postcingulid; and from *W. bicolor* in being much larger, with a broader and more spatulate i1 lacking a ventrolingual crest, p3 with less raised and less distinct ridgelets on the main crest, and molars with a generally more anteriorly prominent precingulid and a thicker, lower cristid obliqua.

Axial skeleton

Atlas (C1) (Fig. 40): large and broad. Arch slightly cranially inclined, craniocaudally short, with dorsal tubercule situated cranially between two shallow fossae containing small foramina. Wings weakly developed in juveniles, relatively larger in adults; dorsoventrally compressed and slightly caudally deflected, with the cranial and caudal margins not extending past those of the cranial or caudal articular foveae. Cranial articular surfaces deep and strongly concave, dorsal margins are rounded, ventral margins come to a ventromedial rounded point; shallow fossa at the midpoint of the medial margin in juveniles, absent to very slight in adults. Caudal articular surfaces broad, flat to very slightly concave and angled roughly 40° medially from the sagittal plane, with the dorsal margin rounded; ventral section comes to a rounded ventromedial point; ventral margins relatively separate in juveniles, converging with age. Lateral vertebral foramen situated in a small, deep fossa on the dorsal surface of the arch at the cranial base of the wing, opening laterally (Fig. 40e).

The atlas vertebra of *P. mamkurra* **sp. nov.** differs from that of *P. anak* in being craniocaudally shorter and more dorsoventrally compressed; from *P. viator* **sp. nov.** in having lateral vertebral foramina that open laterally instead of caudally, and less caudally projected and extensive wings; from *C. kitcheneri* in being broader and

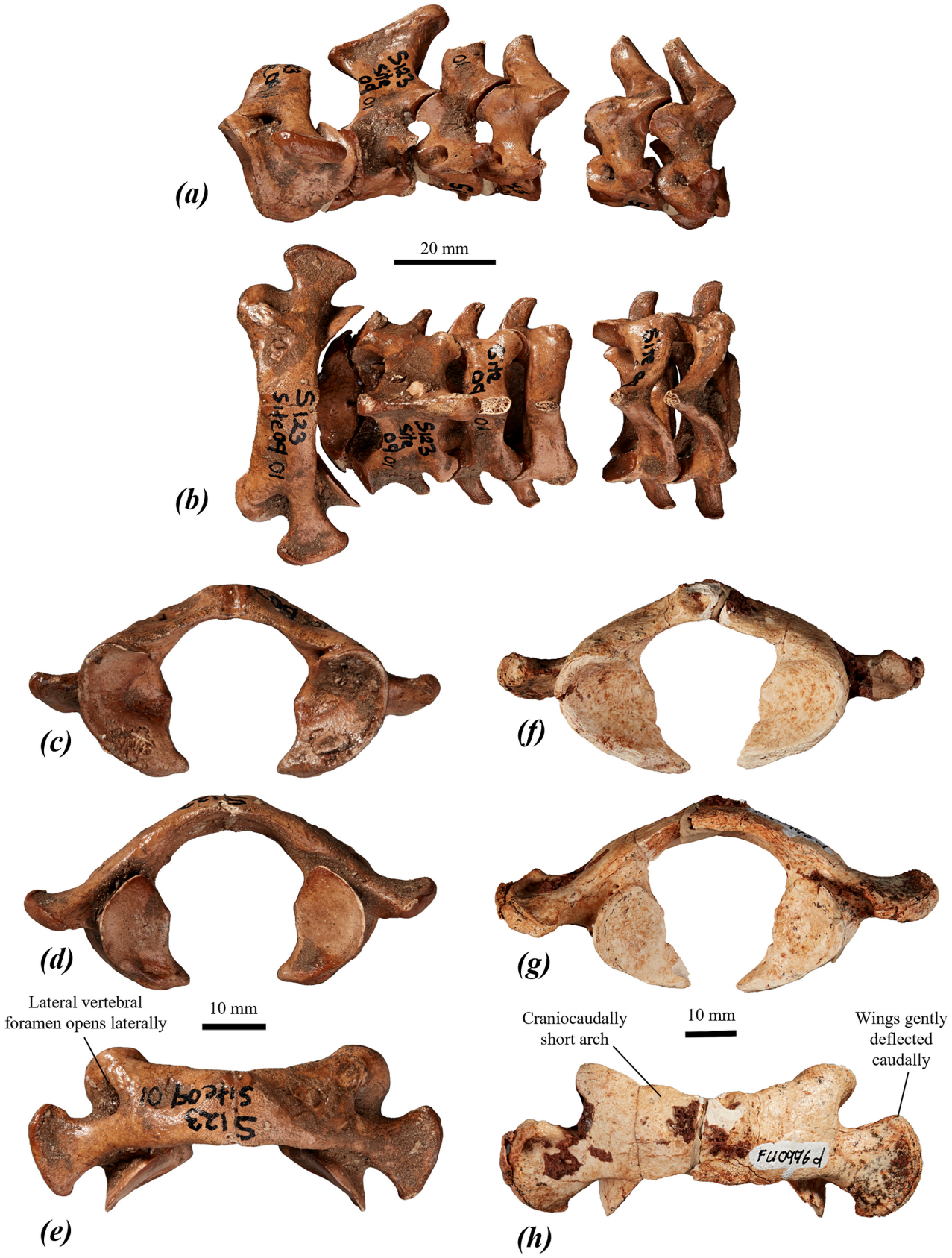

FIGURE 40. cervical vertebrae of *P. mamkurra* **sp. nov.**: (a–b) re-articulated cervical vertebrae C1–4 and C6–7 of paratype SAMA P28163 in (a) left lateral, and (b) dorsal views; (c–e) atlas vertebra C1 of SAMA P28163 in (c) cranial, (d) caudal, and (e) dorsal views; and (f–h) atlas vertebra of SAMA P59553 in (f) cranial, (g) caudal, and (h) dorsal views.

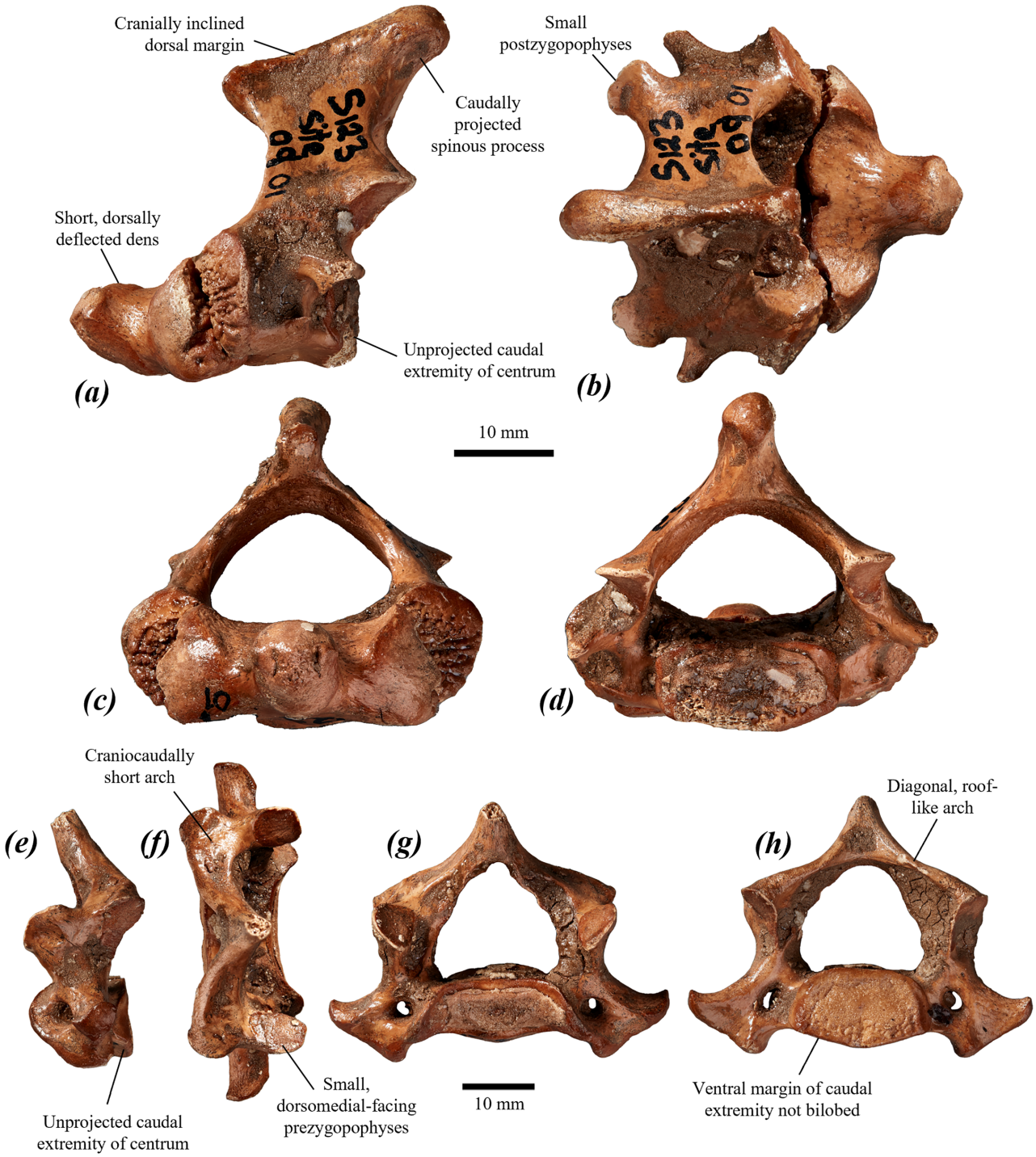

FIGURE 41. cervical vertebrae of *P. mamkurra* **sp. nov.**: (a–d) axis vertebra C2 of paratype SAMA P28163 in (a) left lateral, (b) dorsal, (c) cranial, (d) and caudal views; and (e–h) cervical vertebra C7 of SAMA P28163 in (e) left lateral, (f) dorsal, (g) cranial, and (h) caudal views.

craniocaudally shorter relative to height, with less cranially projected, less dorsally concave cranial articular surfaces and less medially tilted caudal articular surfaces; from *O. rufus* in being generally larger, with more caudally deflected wings, larger dorsal tubercle, less dorsally concave and less cranially projected cranial articular surfaces, and more ventrally situated caudal articular surfaces; from *M. fuliginosus* in being larger, and broader relative to height, with a larger dorsal tubercle, more caudoventrally situated lateral vertebral foramina, less dorsally concave cranial articular surfaces, and more caudally deflected wings; and from *W. bicolor* in being larger, with a larger dorsal tubercle, more dorsoventrally aligned cranial articular surfaces, more dorsoventrally aligned and less medially tilted caudal articular surfaces, and shorter ventromedial processes.

Axis (C2) (Figs 40a–b & 41a–d): craniocaudally short and broad; centrum broader than its depth, with height subequal to depth. The dens is robust and slightly dorsally deflected (Fig. 41a). Cranial articular surfaces gently convex, with the articular surfaces angled roughly 40–45° from the sagittal plane; lateral halves not preserved. Spinous process elongate, with the lateral surfaces gently concave in cranial view; dorsal margin straight in lateral view, gently inclined cranially, thickened and projected cranially beyond the margin of the arch (Fig. 41a), not extending cranially past the margin of the centrum and the cranial articular surfaces, bulging at the caudal end, projected caudally beyond the margin of the postzygopophyses. The vertebral canal is oval and dorsoventrally flattened. The width of the centrum tapers caudally. Transverse foramina round, positioned at the caudal end of the centrum in lateral view, bounded ventrolaterally by a thin, delicate ridge. Transverse processes small, not extending laterally beyond the margin of the postzygopophyses. Postzygopophyses small, with tear-drop shaped articular surfaces. Caudal extremity of the centrum very slightly projected caudally, not extending past the margins of the transverse processes, postzygopophyses and spinous process; the lateral margins are level with the medial margins of the postzygopophyses in caudal view.

The axis vertebra of *P. mamkurra* **sp. nov.** differs from that of *P. anak* in being much shallower relative to width, with a shorter and more dorsally deflected dens, more convex and dorsolaterally tilted cranial articular surfaces, smaller, more rounded postzygopophyses, a more caudally projected spinous process with a more cranially tilted dorsal margin, and a much less caudally projected caudal extremity of the centrum; from *P. viator* **sp. nov.** and *P. dawsonae* **sp. nov.** in being shallower relative to width, with a less caudally projected caudal extremity of the centrum; from *C. kitcheneri* in being larger, and shallower relative to width, with a lower, more cranially tilted and caudally extensive spinous process, smaller, less elongate postzygopophyses, and relatively larger, broader and less caudally projected caudal extremity of the centrum; from *O. rufus* in being shallower relative to width, with the caudal extremity of the centrum less caudally projected; from *M. fuliginosus* in being larger, and shallower relative to width, with a more caudally projected spinous process; and from *W. bicolor* in being larger and relatively broader, with a more rounded dens, less laterally tilted cranial articular surfaces, a relatively smaller spinous process with a straight (rather than convex) dorsal margin and a broader, slightly less caudally projected caudal extremity of the centrum.

Cervical vertebrae (C3–7) (Figs 40a–b & 41e–h): C5 is not known. The articulated neck is distinctly short relative to the width of the cervical vertebrae. The cervical vertebrae are roughly pentagonal in cranial view, with arches tilted cranially; centrum and arches very short relative to width; increasingly short toward C7. Cranial extremity of the centrum very broad relative to height, and slightly concave, particularly at the lateral margins, which are slightly cranially projected. Prezygopophyses small, not extending cranially past cranial extremity, with articular surfaces rounded in C3, becoming more elongate and oval toward C7, narrower than length and angled slightly to moderately medially; no ridge separates the articular surface from the dorsal surface of the arch. Spinous processes not preserved in entirety; bases narrow, becoming broader and slightly more cranially tilted towards C7. Vertebral canal low and rounded in C3, becoming taller toward C7 and approaching rounded-triangular in shape. Transverse processes mostly abraded; poorly developed in juveniles, becoming relatively broad and thickened with age; caudally deflected and craniocaudally short in C3, becoming decreasingly caudally deflected and slightly deeper toward C7; tubercle on the ventral base of the transverse processes is elongate, transversely thickened and ventrally projected in C6 such that the ventral margin of the centrum is concave in cranial view, with the tubercle broader, shorter, slightly pointed, more cranially situated and tilted cranially in C7. Postzygopophyses small, typically not extending beyond the caudal extremity of the centrum, with the articular surfaces slightly to moderately laterally tilted, roughly circular in C3, becoming slightly elongate and oval toward C6–7. Caudal extremity unprojected, very broad relative to height, flat in dorsal view, and very slightly convex around the lateral margins in caudal view.

The cervical vertebrae of *P. mamkurra* **sp. nov.** differ from those of *P. anak* in being craniocaudally much shorter, with a lower, broader cranial extremity of the centrum, smaller, less cranially projected and less cranially tilted prezygopophyses, a less horizontal, more roof-like arch (Fig. 41h), smaller postzygopophyses and a lower, broader, much less caudoventrally projected caudal extremity of the centrum; from *P. viator* **sp. nov.** in being craniocaudally shorter relative to width, with a less horizontal, more roof-like arch, slightly smaller pre- and postzygopophyses, and a less caudoventrally projected caudal extremity of the centrum that lacks a slightly bilobed ventral margin (Fig. 41h); from *P. tumbuna* in having a considerably taller C3, with relatively broader cranial and caudal articular surfaces and a much more dorsally deflected, less horizontal arch in cranial view; from *C. kitcheneri* in being relatively taller and craniocaudally shorter, with a shorter, broader cranial extremity of the centrum, smaller, less craniolaterally projected prezygopophyses, a more dorsally projected, roof-like arch, smaller, less caudolaterally projected postzygopophyses, and a shorter, broader and less caudally projected caudal extremity of the centrum; from *O. rufus* and *M. fuliginosus* in being broader and less elongate, with smaller and less laterally projected pre- and postzygopophyses, a deeper, more transversely compressed spinous process, a less concave cranial extremity of the centrum and less convex, less caudally projected caudal extremities; and from *W. bicolor* in being larger and relatively slightly taller, with the vertebral canal taller and more rounded-triangular in C6–7, and with the ventral tubercles of the transverse processes present as small, pointed, cranially tilted eminences on C7.

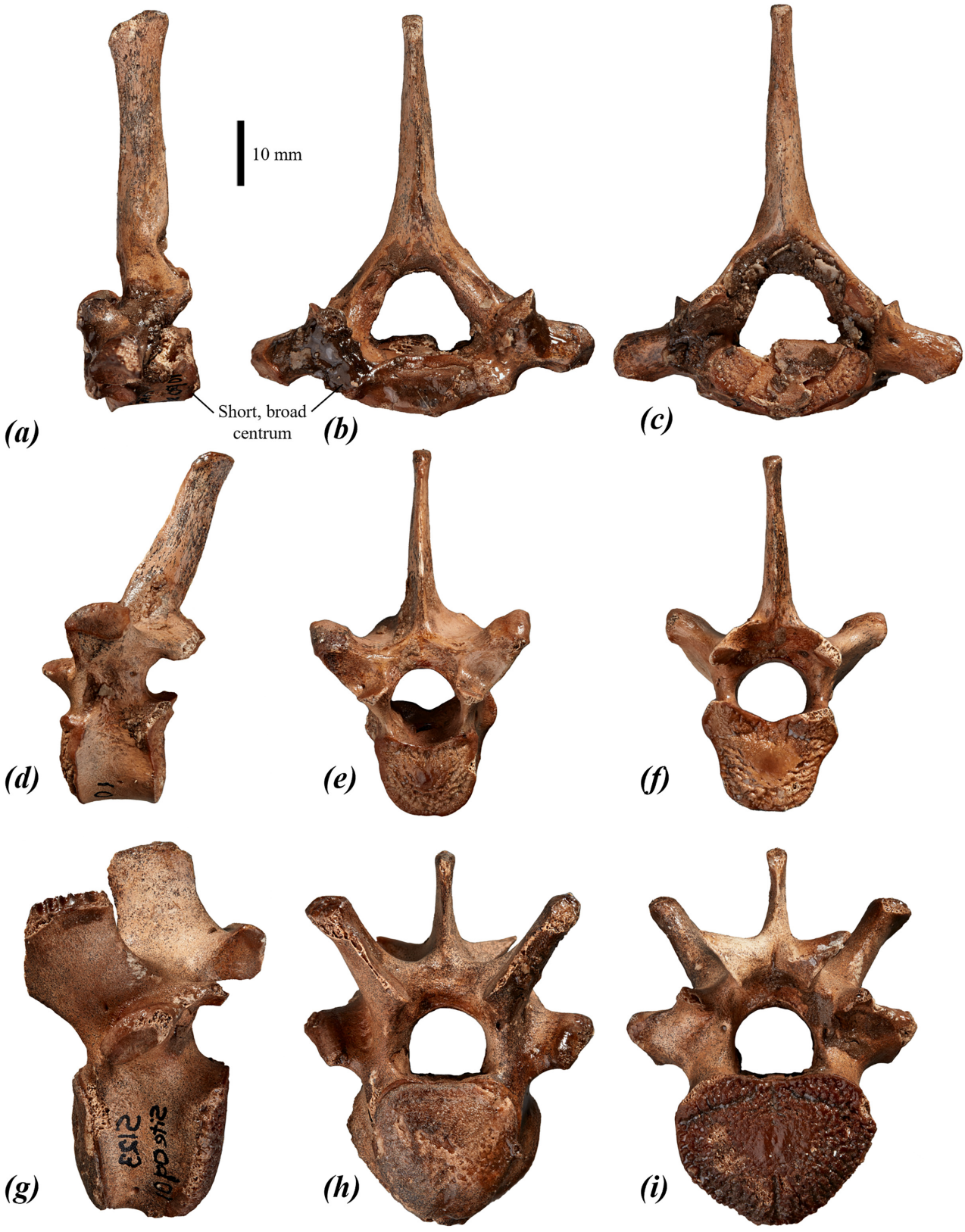

FIGURE 42. juvenile thoracic vertebrae T3 (a–c), T7 (d–f), and T13 (g–i) of *P. mamkurra* **sp. nov.** paratype SAMA P28163 in: (a, d, g) left lateral, (b, e, h) cranial, and (c, f, i) caudal views.

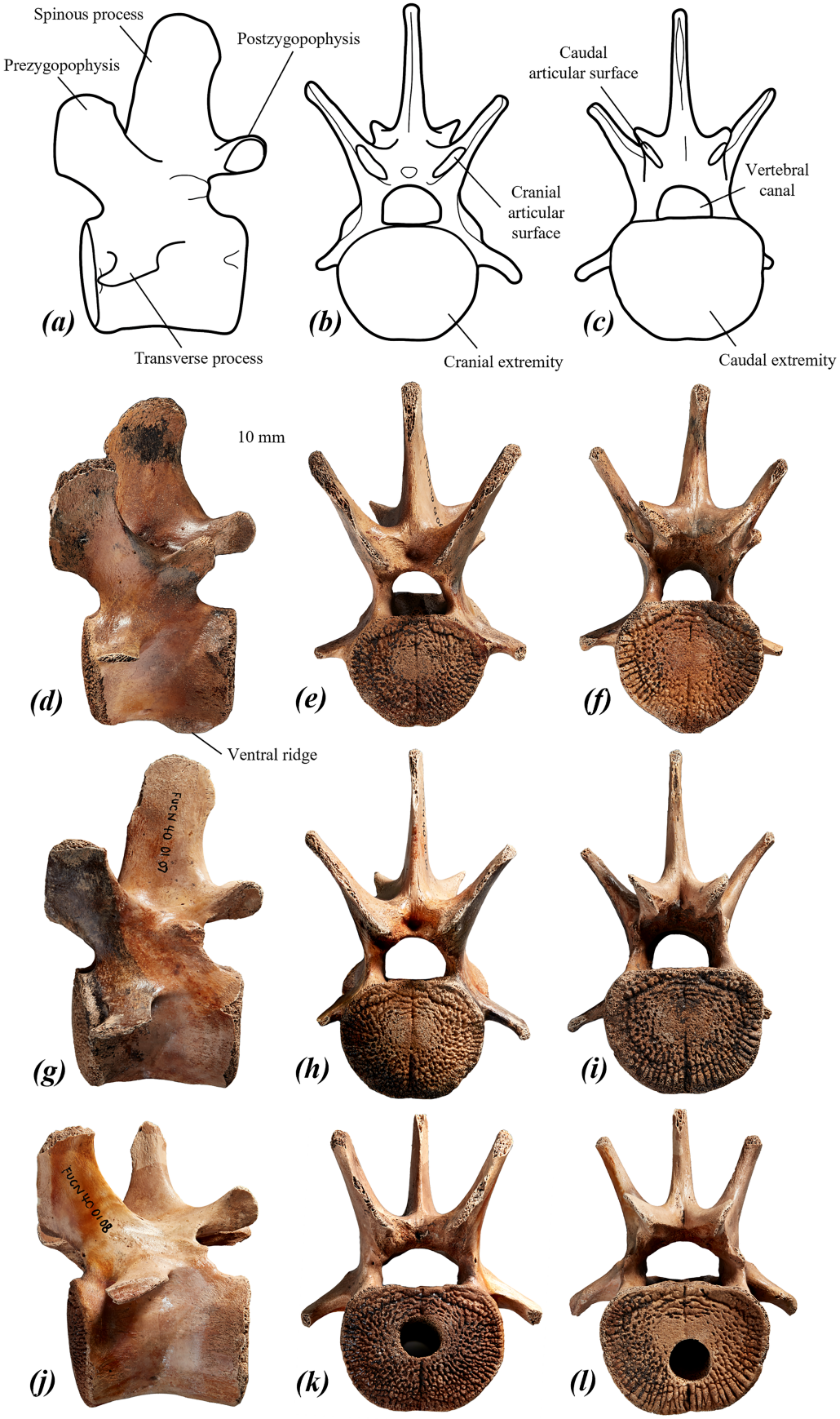

FIGURE 43. lumbar vertebrae of *P. mamkurra* **sp. nov.** holotype SAMA P59549: (a–c) line drawing of lumbar vertebra L3 in (a) left lateral, (b) cranial, and (c) caudal views; and lumbar vertebrae L2 (d–f), L3 (g–i), and L4 (j–l) in (d, g, j) left lateral, (e, h, k) cranial, and (f, i, l) caudal views.

Thoracic vertebrae (T1, 3, 7, 12–14) (Fig. 42): vertebrae craniocaudally short relative to width, with centra increasing in height and depth toward T14; diapophyses (fovea costales processus transversi) are short and robust in T1–3, migrating dorsally onto arch and becoming dorsally deflected by T7, becoming shorter and more robust in T12–14 (situated dorsal to cranial articular facets in T12 only); caudal foveae large and dorsolaterally flared such that the caudal extremity appears heart-shaped in caudal view. T1: cranial extremity of the centrum unprojected, dorsoventrally very short relative to width, and very slightly concave; caudal extremity of the centrum unprojected, badly abraded in available specimens. Prezygopophyses small and short, with the articular facets circular to oval and tilted medially. The arch is low and robust. Spinous process tall, straight in lateral view, with parallel cranial and caudal margins, relatively thick at base and narrowing gently dorsally. The cranial margin of the ventral surface has deep, semicircular costal foveae (demifacets) for articulation with rib 1. Diapophyses slightly ventrally tilted.

T3: cranial extremity of the centrum slightly ventrally tilted, with concave dorsal margin and broadly rounded ventral and lateral margins in cranial view. Prezygopophyses small and short, articular facets circular to oval and laterally tilted. The arch is fairly low and robust. Spinous process tall, thick at the base and narrowing dorsally, with a small caudal eminence on the tip. T7: cranial extremity has gently concave dorsal margin. Prezygopophyses small and short, with articular facets circular to oval and tilted laterally. The arch is robust, and taller than in T3. Spinous process tall, thickened at the base, narrows dorsally, with a small caudal eminence on tip; caudally deflected in lateral view; slightly lower than in T3.

T12 is the 'transitional' thoracic vertebra, the last vertebra possessing smaller, dorsal facing, cranially projected prezygopophyses but with differentiated postzygopophyses which articulate with enlarged, dorsomedial facing, strongly dorsally projected prezygopophyses is. T12 is also the anticlinal vertebra within the thoracic spine, with cranial extremities of T13–14 slightly dorsally inclined. T12: cranial extremity has concave dorsal margin. Prezygopophyses small and short, with articular facets circular to oval and tilted laterally. Only the caudal foveae are present on T12–14, with size decreasing toward T13, present in T13 and 14 as a slight outward rotation of the lateral margins of the caudal extremity. Spinous process less tall than in T1–7, narrow, deep and caudally deflected, with straight cranial margin and gently concave caudal margin. T13 and 14: prezygopophyses are greatly enlarged, taller, cranially projected and laterally deflected with articular facets medially inclined. Caudal accessory processes, ancillary to postzygopophyses, are present on T13 as small tubercles on caudal surfaces of diapophyses and on T14 as marked triangular eminences arising on caudal surface midway between arch and diapophyses. Spinous process straight, deeper than in T12, and with very slightly concave to straight caudal margin.

The position of the transitional thoracic vertebra is T12 in *P. mamkurra* **sp. nov.** and *P. viator* **sp. nov.**, while all compared non–*Protemnodon* taxa except *C. kitcheneri* have this transitional vertebra at T11. The thoracic vertebrae of *P. mamkurra* **sp. nov.** are not differentiated from those of *P. viator* **sp. nov.** They differ from those of *P. anak* in having the centra of the cranial thoracic vertebrae (T1–3) relatively shorter and broader; from *C. kitcheneri* in being larger, with T1, 3 and 7 craniocaudally shorter relative to width, the spinous processes of T1 and 3 less transversely compressed, and the diapophyses of T7 more dorsally deflected; differ further from those of *O. rufus* in being craniocaudally shorter relative to width, with spinous process of T7 less caudally deflected, and taller, more craniodorsally situated cranial articular surfaces and more dorsally situated postzygopophyses on T12 and 13; from *M. fuliginosus* in being generally larger, and longer relative to width, with more dorsally situated postzygopophyses on T12 and 13; and from *W. bicolor* in being larger with a relatively taller centrum, and in T12 and 13 having less cranially deflected prezygopophyses and more dorsally situated diapophyses.

Lumbar vertebrae (L1–5) (Fig. 43): large and robust; width and depth of centra subequal, increasing in absolute size towards L5; ventrolateral surfaces of centra strongly concave. Prezygopophyses large, projected cranially well beyond the margin of the centrum and angled craniodorsally from base before deflecting dorsally around the midpoint, with the cranial articular surfaces small, slightly rugose and oval. Spinous processes quite tall and robust in L1–2, becoming less deep and more gracile toward L5. Postzygopophyses quite small and rounded with the articular surfaces oval and tilted laterally and slightly ventrally. A short, broad, ventral ridge is present on L1 and 2, thickens caudally along the centrum. Caudal accessory processes of L1 and 2 are lobe-shaped, dorsocaudally projected processes that arise cranioventral to the bases of the postzygopophyses.

L1: cranial and caudal extremities of the centrum rounded with gently flattened dorsal margins. The vertebral canal is narrow and domed. Spinous process deep, and thickened at the base. L2: cranial extremity rounded, and caudal extremity distinctly oval with broadly flattened dorsal margin. The vertebral canal is broad and oval. Transverse processes small, planar, cranially deflected, situated slightly dorsal to midpoint of craniolateral margin of cranial extremity of the centrum. Small anapophyses are present on the lateral margin of the caudal extremity in L2 and 3, very reduced in L4–5. L3–5: cranial and caudal extremities of the centrum oval with broadly flattened dorsal margins. The vertebral canal is semicircular in L3 and 4, broader and more domed in L5. Caudal accessory processes present only as small rugose tubercles in L3 and as very small, pointed, caudally projected eminences on L4–5. Transverse processes shift dorsally and caudally towards L5 to be positioned on the pedicle, becoming longer, deeper and more planar in profile.

The lumbar vertebrae of *P. mamkurra* **sp. nov.** are not confidently differentiated from *P. viator* **sp. nov.** differ from *P. dawsonae* **sp. nov.** in being larger, with shallower

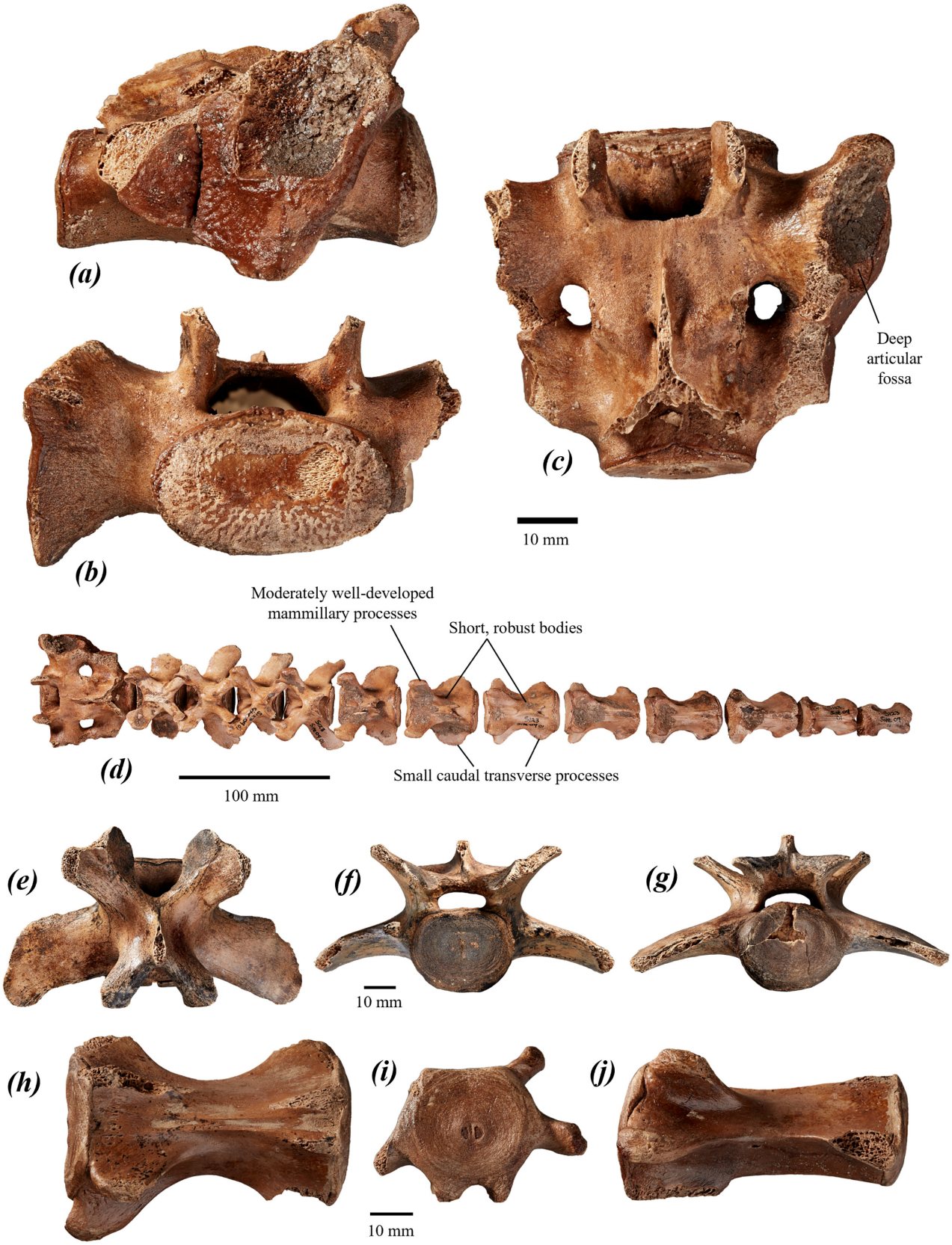

FIGURE 44. sacral and caudal vertebrae of *P. mamkurra* **sp. nov.**: (a–c) juvenile sacrum S1–2 of paratype SAMA P28163 in (a) right lateral, (b) cranial, and (c) dorsal views; (d) re-articulated juvenile sacrum and caudal vertebrae Ca1–12 of P28163 in dorsal view; (e–g) Ca3 of holotype SAMA P59549 in (e) dorsal, (f) cranial, and (g) caudal views; and (h–j) Ca9 of SAMA P59549 (h) dorsal, (i) cranial, and (j) left lateral views.

transverse processes and centrum, relatively taller, slightly narrower cranial and caudal extremities, less concave ventrolateral faces, a less concave ventral margin, and a more raised ventral ridge; from *C. kitcheneri* in being larger and more elongate; from *M. fuliginosus* and *O. rufus* in being larger and more robust, with five (rather than six) lumbar vertebrae, taller centra more circular in cranial view, and lacking distinct twinned dorsal canals; and from *W. bicolor* in being larger and in numbering five. *Sacrum (S1–2, 3) (Fig. 44a–d)*: large to very large, made up of two or three robust, fused vertebrae; roughly triangular in dorsal view. Cranial extremity of the centrum is oval. The vertebral canal is roughly crescentic to reniform. Prezygopophyses fairly small, cranially projected with slight dorsal deflection; articular surfaces small, slightly craniocaudally elongate and facing dorsomedially; dorsal margins not preserved. Wings well-developed, sub-triangular in lateral view, expand toward lateral edges, particularly ventrally, and taper caudally; auricular surfaces tilted dorsally; a broad, rugose, deeply concave fossa is present on the dorsolateral surface of each wing. The median sacral crest (fused spinous processes) is not preserved. Transverse processes thicker in the cranial component, become more dorsoventrally compressed and flare laterally in the caudal component. Two large, round sacral foramina pass dorsoventrally through the sacrum at the synostoses of the fused S1 and S2 vertebrae. Postzygopophyses short, quite robust, projected caudolaterally, with the articular surfaces flat and rounded, angled ventrolaterally. The caudal extremity of the centrum is taller and more rounded than the cranial extremity.

The sacrum of *P. mamkurra* differs from that of *P. anak* in having a larger, more deeply concave fossa on dorsolateral surface of the wings; from *O. rufus* in being larger and more robust, with a broader vertebral canal, more dorsally tilted auricular surfaces, and a broader caudal component; and from *M. fuliginosus* in being larger, with the centrum relatively taller in cranial view and lacking small, shallow fossae either side of the craniodorsal midline, the vertebral canal relatively broader, lower and roughly crescentic (rather than an inverted 'heart' shape), the auricular surface relatively more extensive craniodorsally and caudally, S2 in ventral view relatively broader, more robust, and having only two sacral foramina between S1 and S2 (whereas in *M. fuliginosus* there is an extra pair around the midpoint of the dorsal surface of S1).

Caudal vertebrae (Ca1?–12) (Fig. 44d–j): short, broad and robust. Centra: of Ca1–4 are broader than they are long; of Ca1–5 (proximal caudal vertebrae) are craniocaudally short, with slightly ventrally inclined cranial and caudal extremities; of Ca6 onward are straighter and more elongate; Ca9–12 (mid-distal caudal vertebrae) are quite short and robust, narrow to a waist. The vertebral canal is very low and broad in Ca2, becoming increasingly low toward Ca5, extremely small in Ca6–8 and absent in mid-distal vertebrae. Prezygopophyses: in Ca1–4 are large, laterally projected, dorsally deflected and distally flared, with articular surfaces angled dorsomedially and projected craniomedially; in Ca5, are large, dorsally deflected, and extend beyond the cranial extremity of the centrum; in Ca6–12, are increasingly reduced, as mammillary processes, without articular surfaces. Postzygopophyses: in Ca1–4, are relatively small and unflared distally with small, rounded articular surfaces; in Ca5, are very reduced, narrow, non-articular, that do not extend caudally beyond the caudal extremity; in Ca6–12, are increasingly reduced that shift caudally to abut the caudal margin as low, thin, parallel ridges in the distal vertebrae. Transverse processes: those of the proximal vertebrae are fractured and incomplete; on Ca1, are deep; on Ca2, very elongate laterally; become increasingly shorter craniocaudally and more caudally deflected towards Ca5; in Ca6–7, depth greater than width; in Ca8, very reduced cranial transverse processes; in Ca9–12, small, thick, and blunt, cranial processes relatively larger than caudal. Spinous processes: in Ca1–4 are rounded, increasingly small; very reduced or absent in Ca5 onward. Cranioventral processes: small, blunt, ventrally projected, first present on Ca6, are positioned close to the midline and curve gently mesially; become more mesially curved and taller, thicker, and more elongate relative to vertebrae distally.

The caudal vertebrae of *P. mamkurra* differ from those of *P. anak* being generally slightly more robust and in having smaller mammillary and caudal transverse processes on Ca7; from *P. viator* in being shorter and more robust, with the Ca7 caudal transverse processes and Ca8 cranial processes narrower and more caudally curved; from *P. tumbuna* in being larger; from *C. kitcheneri* in having the proximal vertebrae with slightly more ventrally deflected transverse processes and less ventrally facing cranial extremities, and the distal vertebrae with relatively thick cranial transverse processes; from *O. rufus* in being craniocaudally shorter relative to width, with the caudal transverse processes on Ca4–7 longer relative to the length of the centrum; from *M. fuliginosus* in having a smaller spinous process in Ca1–4, shallower, broader and distally more rounded transverse processes in the proximal vertebrae, and relatively more robust distal vertebrae; and from *W. bicolor* in being larger and more robust, with generally more transversely compressed tips of the mammillary processes, and the caudal transverse processes on Ca4–7 longer relative to the length of the centrum.

Forelimb and pectoral girdle

Clavicle (Fig. 45a–f): craniocaudally compressed along the shaft and at acromial articular end. Clavicle curves gently posteriorly towards the acromial end in cranial view, gently convex along the anterior margin. Sternal articular end not preserved. Laterally, it expands in depth steadily to a large, slightly thickened, distinctly caudally curved acromial end and comes to a blunted point.

The clavicle of *P. mamkurra* differs from that of *P. otibandus* in being slightly more robust and less craniocaudally compressed, with a slightly larger acromial articular end relative to the size of the clavicle; from *C. kitcheneri* in being larger, deeper and more craniocaudally

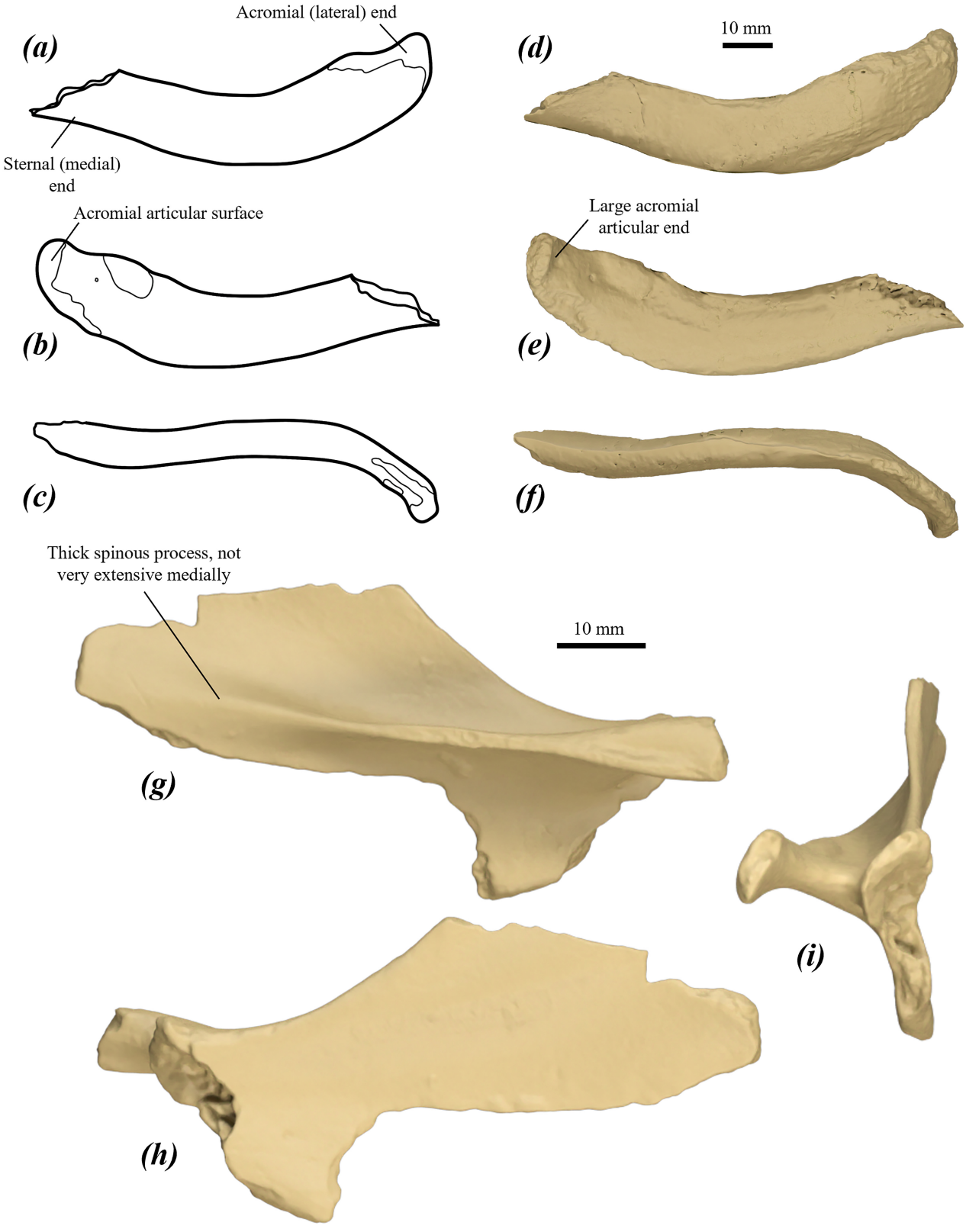

FIGURE 45. upper forelimb elements of *P. mamkurra* **sp. nov.**: (a–c) line drawings and (d–f) surface scan images of partial left clavicle of WAM 02.7.11 in (a, d) cranial, (b, e) caudal, and (c, f) anterior views; and (g–i) surface scan images of juvenile right scapular fragment of QVM2001 GFV39 in (g) dorsolateral, (h) ventromedial, and (i) proximal/anterolateral.

compressed, with a relatively larger acromial end; from *O. rufus* and *M. fuliginosus* in being slightly more robust, with a slightly more caudally curved and less posteriorly curved acromial end; and from *W. bicolor* in being much larger and deeper, with a more caudally curved acromial end with more pointed tip.

Scapula (Fig. 45g–i): only the juvenile scapula is known, which is gracile and delicate. Lateral (humeral) component of the cranial border is very slightly concave. Infraspinous fossa partially preserved; appears significantly larger than the supraspinous fossa. Glenoid cavity oval and gently concave, with slight anteroposterior compression. Infraglenoid tubercule unprojected and slightly rugose, with a small, broad fossa present on the medial component. Scapular spine slightly cranially deflected in lateral view. Acromion incompletely preserved; interpreted as being quite elongate, broadening distally, with dorsolateral surface flat and broad. Scapular notch gently concave, with an angle of ~120°. Lateral component of the subscapular fossa planar to gently concave caudally, moderately concave beneath the scapular spine and becoming gently convex toward the cranial border.

The scapula of *P. mamkurra* **sp. nov.** cannot be differentiated from that of *P. viator*. It differs from that of *P. anak* in a having thicker, less medially extensive scapular spine; from *C. kitcheneri* in having a less anteroposteriorly compressed glenoid cavity with a less anterolaterally projected glenoid tubercle and coracoid process, a small, broad fossa on the infraglenoid tubercule, and a slightly concave (rather than straight) lateral component of the caudal border; from *O. rufus* in having craniocaudally shallower scapular neck, less cranially tilted spine and broader scapular notch; from *M. fuliginosus* in having a slightly less elongate glenoid cavity, a small, broad fossa on the infraglenoid tubercule, and a slightly less cranially deflected scapular spine; and from *W. bicolor* in being larger, with a craniocaudally shallower neck, thicker, less medially extensive spine, more robust acromion, and a broader scapular notch.

Humerus (Fig. 46a–d): broad and robust, with thick, well-developed proximal muscle attachments. Head roughly hemispherical, rounded and moderately projected caudally. Greater tubercule broad, projected marginally dorsal to articular surface of head. Lesser tubercule not preserved, base appears broad and rounded. Proximal shaft deep, deepening proximally; in cranial view, shaft possesses slight to moderate medial deflection, with axis situated across shaft at pectoral crest. Bicipital groove broad and shallow in juveniles, becomes deeper, slightly narrower and more distally extensive in adults. Pectoral crest thick, raised and slightly laterally tilted, situated at or just past the midpoint of the humeral shaft; becomes higher and more pronounced proximally with age. Deltoid tuberosity low in juveniles, becomes thicker, more rugose and slightly pointed in adults, situated on the lateral surface of the shaft, level with the proximal half of the pectoral crest. Insertion of m. latissimus dorsi located on the medial surface of the shaft opposite the deltoid tuberosity, marked by a small rugose area in juveniles and by a broad, shallow, irregularly shaped fossa in adults.

Distal end short, broad, and roughly triangular in cranial view. Lateral supracondylar ridge quite narrow, extends around one-third of the humeral length, with the proximal margin coming to a small, rounded point two-thirds of the distance from the trochlea to the pectoral crest (Fig. 46a). Capitulum and ulnar facet large, robust, laterally situated, abutting the lateral epicondyle, width roughly two-thirds of total distal width; capitulum smoothly and strongly convex, with lateral margin rounded and gently tapering; ulnar facet with the medial margin relatively straight and slightly bevelled. The trochlea is wide and quite shallow. The olecranon fossa is moderately deep and slightly medially displaced. Radial fossa quite small, variable in depth; deep relative to smaller, shallower coronoid fossa positioned immediately proximal to trochlea. Medial supracondylar bridge broad, thin craniocaudally; supracondylar foramen elongate and strongly flattened craniocaudally.

The humerus of *P. mamkurra* **sp. nov.** differs from that of *P. anak* in being shorter, with a shorter bicipital groove, shorter pectoral crest, less distinctly straight and raised medial margin of ulnar facet, and a relatively shorter lateral supracondylar ridge with a more pointed proximal peak; from *P. viator* in having the proximal peak of the lateral supracondylar ridge more pointed and relatively further from the distal extent of the pectoral crest; from *P. tumbuna* in being more robust, with a shorter, broader distal end, and in lacking a low, broadly rounded ridge linking the pectoral crest and the medial supracondylar bridge; from *C. kitcheneri* in being relatively shorter and more robust, with a more medially projected head, taller and deeper greater tubercle, more deeply concave bicipital groove, much deeper proximal shaft, generally lower and less elongate deltoid tuberosity, much lower, less elongate, less distally extensive and straighter pectoral crest, and broader medial and lateral supracondylar ridges, and in lacking a crest on the distal margin of the attachment site for m. latissimus dorsi; from *O. rufus* in being more robust, with a deeper greater tubercle and proximal shaft, more deeply concave bicipital groove, more distally situated pectoral crest relative to the deltoid tuberosity, broader and relatively shorter distal end, and more pointed proximal peak of lateral supracondylar ridge; from *M. fuliginosus* being more robust, with a deeper and taller greater tubercle, deeper proximal shaft, more deeply concave bicipital groove, much broader capitulum, ulnar facet and distal end, broader, shallower and less concave olecranon fossa, and a shorter, thicker deltoid tuberosity and pectoral crest; and from *W. bicolor* in being larger, with a more medially projected head, taller and deeper greater tubercle, deeper, less raised and less elongate deltoid tuberosity, less raised, straighter, less extensive pectoral crest, broader distal end, and a broader medial supracondylar bridge.

Ulna (Fig. 46e–g): quite short, robust and gently transversely compressed, much more gracile in juveniles. Olecranon quite long relative to the ulnar length; robust, tapering to the distal end, very gently caudally deflected. Proximomedial flexor fossa moderately concave. Facet for

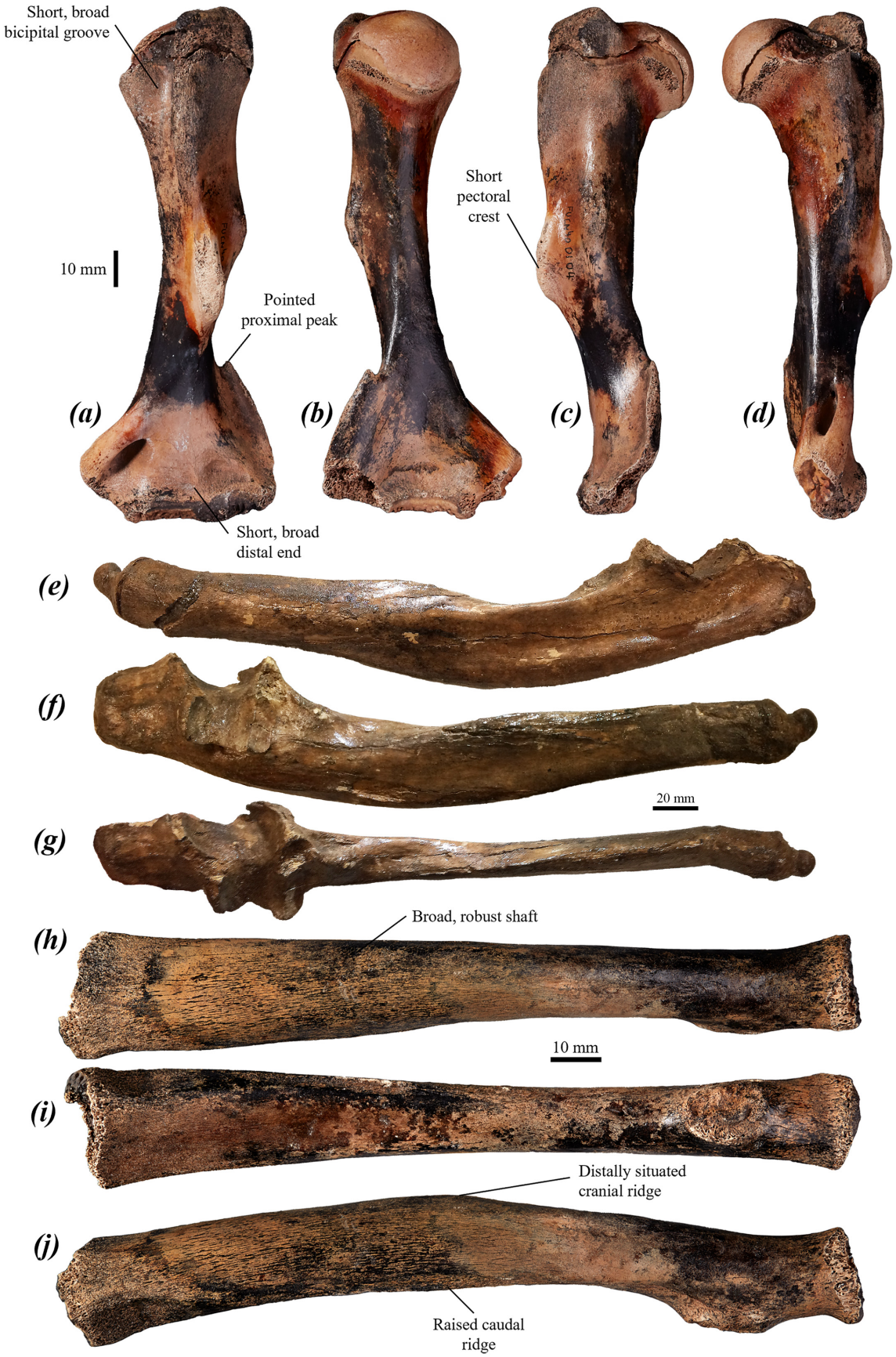

FIGURE 46. forelimb elements of *P. mamkurra* **sp. nov.**: (a–d) partial left humerus of holotype SAMA P59549 in (a) cranial, (b) caudal, (c) lateral, and (d) medial views; (e–g) right ulna of SAMA P59546 in (e) lateral, (f) medial, and (g) cranial views; and (h–j) partial left radius of holotype in (h) cranial, (i) caudal, and (j) medial views.

humeral articulation large, quite shallow, with the trochlear notch present as a gently rounded medial ridge; medial component particularly large; anconeal process with a deeply obtuse angle, narrower than the combined coronoid process and radial facet; coronoid process large, rounded in proximal view, projected cranially and slightly laterally. Radial facet crescentic in juveniles to semicircular in adults, proximodistally short, broad. Ulnar tuberosity small, narrow and rugose. Shaft curves gently cranially in its proximal component, straightens distally; height tapers slightly distally in lateral view; cranial margin of the midpoint to the distal component marked by a ridge that arises on the dorsolateral margin (interosseous border with the radius, and the cranial margin of the origin of m. flexor digitorum profundus ulnaris) and extends distally and slightly medially to the medial margin of the distal epiphysis; a low ridge extends from the medial margin of the ulnar tuberosity, along the dorsomedial margin of the shaft and onto the medial surface of the distal component. Distal epiphysis robust, circular in distal view; styloid process robust, rounded and cranially deflected.

The ulna of *P. mamkurra* **sp. nov.** differs from all compared taxa in its greater robustness when adult, particularly of the distal shaft. It further differs *P. anak* in being shorter, with a lesser degree of recurve in lateral view, and a more transversely compressed distal shaft in cross-section; from *P. viator* **sp. nov.** in being generally shorter; from *P. tumbuna* in being larger; from *P. otibandus* in its broader olecranon; from *C. kitcheneri* in being deeper, straighter in cranial view, with a less cranially deflected olecranon, more medially flared coronoid process, less rounded radial facet, and the distal shaft less cranially curved; from *O. rufus* in being deeper, with a less cranially deflected olecranon, broader and less laterally tilted lateral component of humeral facet, less bilobed lateral margin of humeral facet, more anteriorly situated, less laterally tilted radial facet, and much less tapering of the distal shaft; from *M. fuliginosus* in being larger and deeper, with a less medially flared coronoid process, less bilobed lateral margin of humeral facet and more distally projected styloid process; and from *W. bicolor* in being larger and deeper, with a less cranially deflected and projected olecranon, less medially flared coronoid and anconeal processes, and a shallower humeral facet.

Radius (Fig. 46h–j): robust with slight to strong curvature. Radial head circular to slightly oval. Radial neck slightly flattened proximal to the radial tubercule. Radial tubercule rugose, oval and smoothly, gently projected. Shaft cross-section circular to rounded-triangular immediately distal to the radial tubercle; very craniocaudally compressed in the middle to distal shaft. Cranial ridge thick and low or absent, arises closer to the midpoint of the shaft than to the radial tubercle. Caudal ridge thin, extends across the midpoint of the shaft (Fig. 46j); more raised, elongate and distinct in larger specimens. Distal end teardrop-shaped to roughly triangular in distal view; scaphoidal facet broad and slightly concave; styloid process quite robust, caudomedially situated and slightly curved caudolaterally. Ulnar notch broad, quite shallow and elongate; deeper and more elongate in older individuals.

The radius of *P. mamkurra* **sp. nov.** differs from that of *P. anak* in being shorter, more robust, and generally more curved, with greater craniocaudal compression of the distal shaft and a more flattened caudomedial surface of the distal shaft; from *P. viator* **sp. nov.** in being shorter, more robust, and generally more curved, with a more distally situated cranial ridge, more raised and distinct caudal ridge, and a more craniocaudally compressed distal shaft; from *P. tumbuna* in having a more craniocaudally compressed distal shaft and a more caudolaterally curved and caudally situated styloid process; from *P. otibandus* in being more robust, with a lower cranial ridge, shallower proximal shaft, and a more craniocaudally compressed distal shaft; from *C. kitcheneri* in being generally larger, typically with a lower, less proximally extensive caudal ridge and the scaphoidal facet not tilted cranially; from *O. rufus* in being shorter and more robust, with a slightly greater degree of the shaft curvature and a more raised caudal ridge; from *M. fuliginosus* in being larger and more robust, with greater craniocaudal compression of the distal shaft and a deeper, broader and more distinct ulnar notch; and from *W. bicolor* in being larger and more robust, with a lower caudal ridge and a more triangular distal shaft in cross-section.

Manus

Scaphoid (Fig. 47a–h): broad and robust, roughly semicircular in dorsal view. Palmar process dorsopalmarly compressed and medially projected. Radial facet broad, rounded and smoothly convex, extends from the posteropalmar margin over most of the dorsoposterior surface of the body of the scaphoid; ridge for articulation with the styloid process of the radius is thick and dorsally raised (Fig. 47g). Facet for the hamatum gently convex, continuous medially with the large, concave facet for the capitatum. Facet for the trapezoid small, dorsopalmarly compressed, situated mesially on the anterodorsal margin. Facet for the trapezium broad, strongly convex, situated on the anterior surface of a rounded and highly dorsopalmarly compressed medial projection. A broad, shallow fossa is present on the palmar surface of the base of the palmar process, anteropalmar to the medial margin of the radial facet.

The scaphoid of *P. mamkurra* **sp. nov.** differs from that of *P. viator* **sp. nov.** in having a narrower palmar process and the facets for the hamatum and the capitatum less distinct from each other, with a thickened, raised dorsal ridge present for the styloid process of the radius and a broader facet for the trapezoid; from *P. otibandus* in having the palmar process less palmarly drooped and more anteriorly deflected; from *C. kitcheneri* in being broader, with a broader and more anteropalmarly deflected palmar process, the hamatal and trapezoidal facets more distinct, and the hamatal facet convex instead of concave; from *O. rufus* in being broader, with a larger palmomedial fossa; from *M. fuliginosus* in being larger, with a shorter, rounder and less craniocaudally compressed medial component and a deeper palmomedial fossa; and from *W. bicolor* in being much larger, with a deeper, more transversely compressed and much less palmarly curved palmar process.

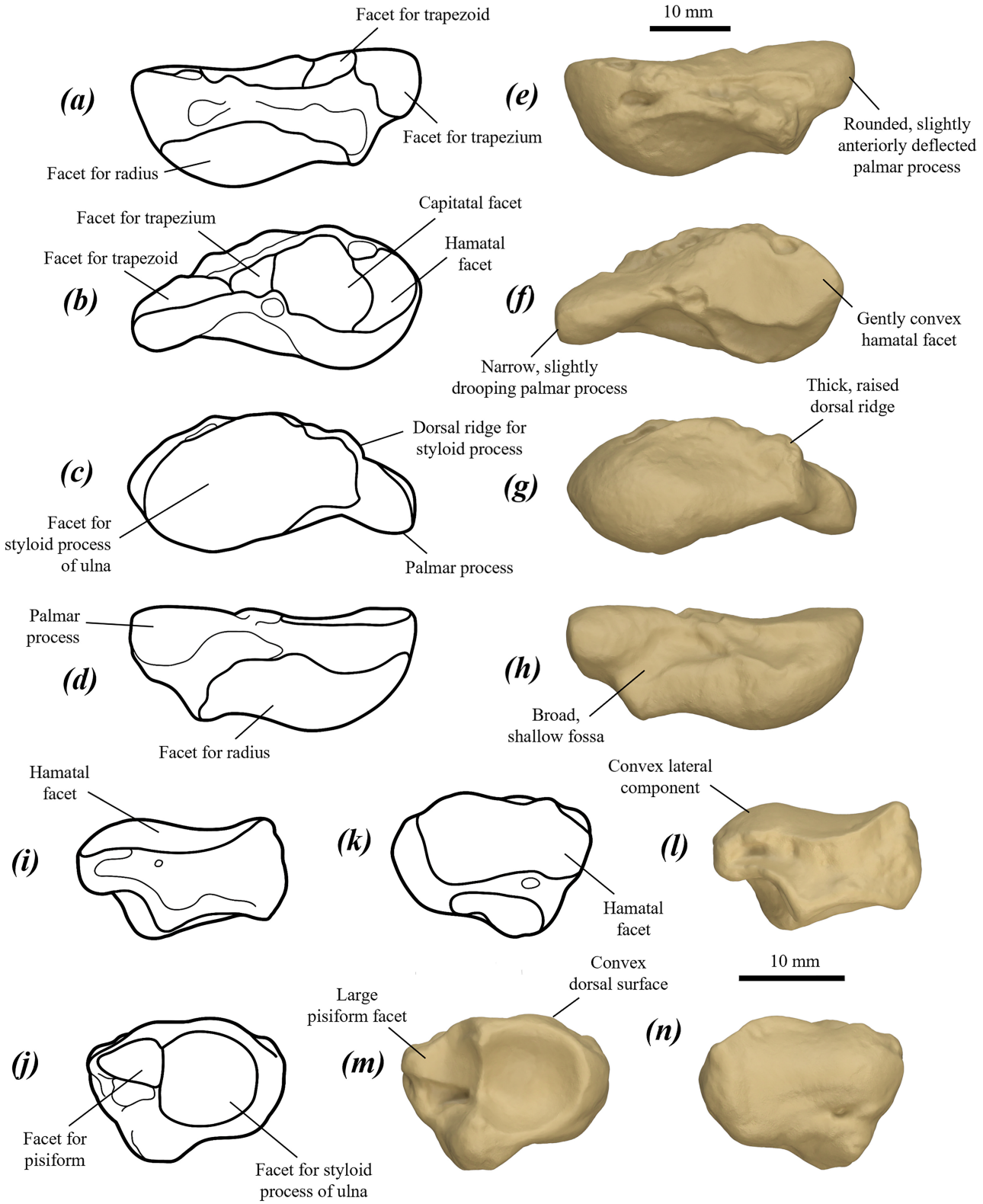

FIGURE 47. left carpals of *P. mamkurra* **sp. nov.** WAM 02.7.11: (a–d) line drawings and (e–h) surface scan images of scaphoid in (a, e) dorsal, (b, f) anterior (distal), (c, g) posterior (proximal), and (d, h) palmar views; and (i–k) line drawings and (l–n) surface scan images of triquetrum in (i, l) dorsal, (j, m) posterior, and (k, n) anterior views.

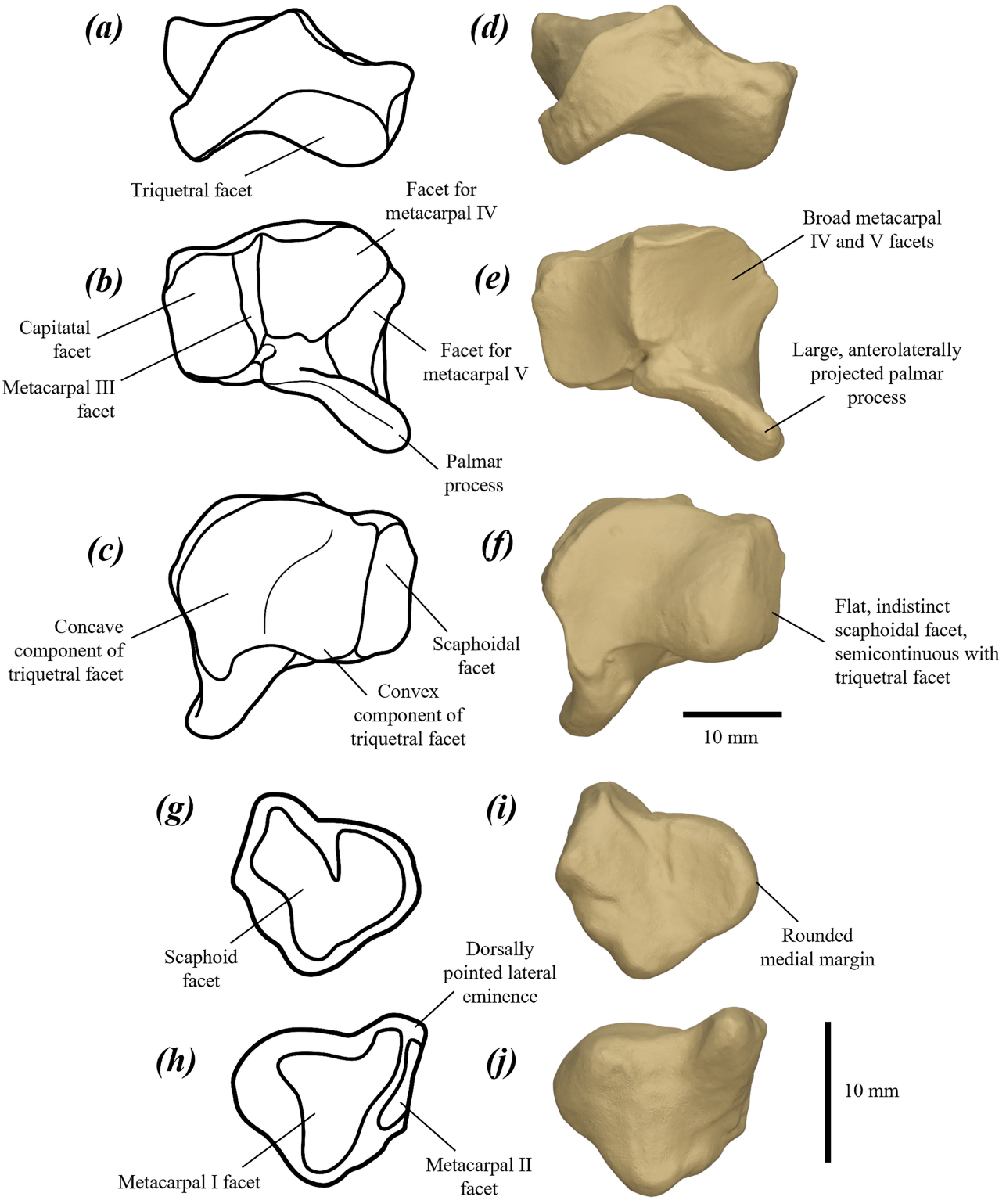

FIGURE 48. left carpals of *P. mamkurra* **sp. nov.** WAM 02.7.11: (a–c) line drawings and (d–f) surface scan images of the hamatum in (a, d) dorsal, (b, e) anterior, and (c, f) posterior views; and (g–h) line drawings and (i–j) surface scan images of trapezium in (g, i) palmar, and (h, j) anterodorsal views.

Triquetrum (cuneiform) (Fig. 47i–n): roughly two-thirds the size of the hamatum, anteroposteriorly compressed, roughly oval in posterior view, with a convex dorsal surface (Fig. 47m). Facet for the ulnar styloid process round, and smoothly, moderately concave. Facet for the pisiform half the size of the styloid facet, roughly triangular in posterior view, and gently concave, with a small, shallow lateral fossa. A tubercle on the posteropalmar surface projects posteriorly beneath the styloid facet and the pisiform facet. Facet for the hamatum broader than it

is tall, with a smoothly convex lateral component, a gently concave medial component, and a slightly convex centre. A small foramen is present beneath the lateral component of the hamatal facet. The posterior and anterior margins of the dorsal surface are dorsally flared, increasingly so laterally.

The triquetrum of *P. mamkurra* **sp. nov.** differs from that of *P. otibandus* in having a more convex dorsal surface and a slightly larger pisiform facet; from *C. kitcheneri* in being larger and relatively slightly broader, with a larger pisiform facet and a more convex lateral component of the hamatal facet; from *O. rufus* in being larger, with a taller, more deeply concave pisiform facet, a larger posteropalmar tubercle, and a broader hamatal facet; from *M. fuliginosus* in being larger, taller, relatively narrower, and lacking a pointed medial projection; and from *W. bicolor* in being much larger, with the pisiform facet more deeply concave, more posterior facing and less laterally rotated, and the hamatal facet broader and more smoothly convex on the lateral component.

Hamatum (Fig. 48a–f): tall, broad, and anteroposteriorly quite short. The posteromedial component is tall, narrow, squarish, and projected. Facet for the triquetrum large, broad, gently dorsally tilted, and occupying the posterior surface with a slight extension onto the base of the posterior of the palmar process; anterior component tall, transversely concave, and posterior facing, with a convex dorsal margin; posterior component of triquetral facet shorter, gently convex and posterolaterally facing, situated on the posteromedial projection of the hamatum. Facet for the scaphoid flat and indistinct, situated on the posteromedial surface and abutting the medial margin of the triquetral facet and the lateral margin of the capitatal facet. Facet for the capitatum continuous with the facet for the lateral surface of the posterior end of metacarpal III; gently and smoothly concave, curving over a very small, shallow foramen; semicontinuous posteriorly with the scaphoidal facet, meeting at a sharp corner. Facet for metacarpal IV squared and smoothly concave; almost indistinct from the facet for metacarpal V. Facet for metacarpal V concave, covering the craniodorsal surface of the palmar process. Palmar process large, tall, anteroposteriorly flattened, projecting palmarly and tilted strongly anterolaterally with a slight lateral rotation (Fig. 48e).

The hamatum of *P. mamkurra* **sp. nov.** differs from that of *P. viator* **sp. nov.** in being shallower, with a less concave scaphoidal facet, broader combined metacarpal IV and V facets relative to the capitatal and metacarpal III facets, a larger, taller and anterolaterally projected (rather than posteropalmarly projected) palmar process, and a concave (rather than convex) metacarpal V facet; from *P. otibandus* in being larger and shallower, with the facet for the triquetrum more extensive medially to be semicontinuous with (rather than distinctly separate from) the facet for the scaphoid, and the palmar process larger, taller and anterolaterally projected (rather than posteropalmarly projected); from *C. kitcheneri* in being larger, taller and more robust, with a more dorsally curved triquetral facet for metacarpal IV, a smaller facet for metacarpal V, and the palmar process anteroposteriorly deeper, less projected and less anteriorly deflected; from *O. rufus* in being larger and deeper, with a taller posteromedial component, less concave scaphoidal facet, and a broader and smoother metacarpal IV facet; from *M. fuliginosus* in being larger, with a relatively much taller anterior component of the triquetral facet, semicontinuous (rather than distinct) hamatal and metacarpal III facets, and a larger, narrower palmar process; and from *W. bicolor* in being much larger, with a flatter scaphoidal facet, semicontinuous hamatal and metacarpal III facets, and a relatively larger facet for metacarpal III.

Capitatum (Fig. 49): triangular to roughly oblong in dorsal view, with the palmar surface roughly triangular due to narrowing of the process on the posteropalmar margin. Facet for the hamatum rounded-triangular, smoothly and gently convex, pointed posteriorly, occupies the posterolateral surface, with a small, rounded fossa against the dorsoposterior margin. Facet for the scaphoid posteriorly flat, becomes taller and slightly concave anteriorly; covers posteromedial surface, posteriorly semicontinuous with hamatal facet. Facet for metacarpal III large, covers the anterior surface, subdivided into a semicontinuous smaller medial component and a larger lateral component for the medial and lateral processes of the posterior end of metacarpal III; both gently concave with a narrow, gently convex medial margin. A shallow, broad, oblong fossa is present beneath the metacarpal III facet on the anterior surface. The anteromedial surface is anteroposteriorly short, with a tall, concave facet for the medial component of the posterior facet of metacarpal II occupying the anterior component. Facet for the trapezium narrow and flat, on posteropalmar component of medial surface. Two fairly large, rounded, linked tubercles are situated against the anterior margin of palmar surface.

The capitatum of *P. mamkurra* **sp. nov.** differs from that of *P. viator* **sp. nov.** in being anteroposteriorly shorter with a smaller palmar process, and in having a small fossa present on the dorsoposterior surface (Fig. 49f) and a larger fossa present on the anterior surface beneath the metacarpal III facet (Fig. 49g); from *P. otibandus* in being larger with a blunt palmar process; from *C. kitcheneri* in being larger and less deep, with a taller medial component of the metacarpal III facet and a taller, narrower and more medially situated facet for metacarpal II; from *O. rufus* in being larger, with a taller facet for the trapezoid and a small dorsoposterior fossa; from *M. fuliginosus* in being larger and broader, with a taller facet for the trapezoid and a flatter metacarpal III facet; and from *W. bicolor* in being much larger, with a larger, more convex facet for the hamatum.

Trapezium (Fig. 48g–j): articulates with the dorsoanterior surface of the palmar process of the scaphoid. Broad and roughly rounded in anterior view, with a large, pointed eminence against the lateral margin on the anterodorsal surface for articulation with the anteromedial surface of the trapezoid and with the dorsal component of the posterior surface of metacarpal I. The anteromedial component is broadly rounded. Facet for the scaphoid broad, and smoothly, deeply concave. Facet for metacarpal I has a larger, rounded medial component that continues laterally into a smaller, gently convex dorsolateral component on the pointed anterolateral eminence.

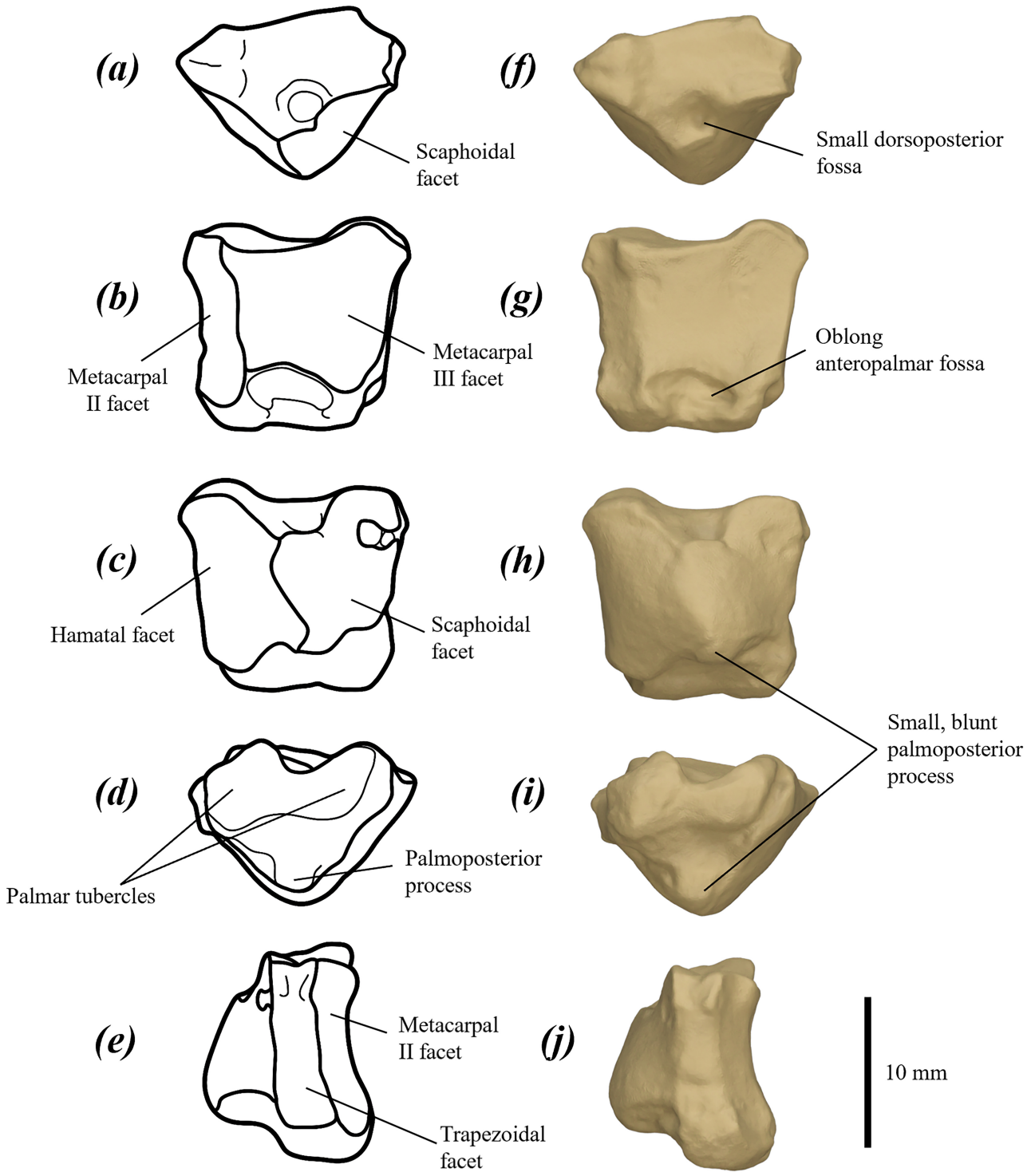

FIGURE 49. line drawings (a–e) and surface scan images (f–j) of left capitatum of *P. mamkurra* **sp. nov.** WAM 02.7.11 in: (a, f) dorsal, (b, g) anterior, (c, h) posterior, (d, i) palmar, and (e, j) medial views.

The trapezium of *P. mamkurra* **sp. nov.** differs from that of *P. viator* **sp. nov.** in being slightly broader, with a more rounded medial margin; from *C. kitcheneri* in having a more concave facet for the palmar process of the scaphoid; from *O. rufus* and *M. fuliginosus* in being larger relative to the trapezoid, with a more pointed anterolateral eminence, and a more distinct facet for metacarpal I with more distinct medial and lateral components; and from *W. bicolor* in being both absolutely larger and larger relative to trapezoid, with a more deeply and smoothly concave facet for the palmar process, and a broader, more distinct facet for metacarpal I.

Metacarpals I–IV (Fig. 50a–d): short and robust, with the shaft and distal end slightly dorsopalmarly compressed and the proximal surfaces dorsally tilted, particularly metacarpals III and IV (Fig. 50a). Metacarpal I: extremely

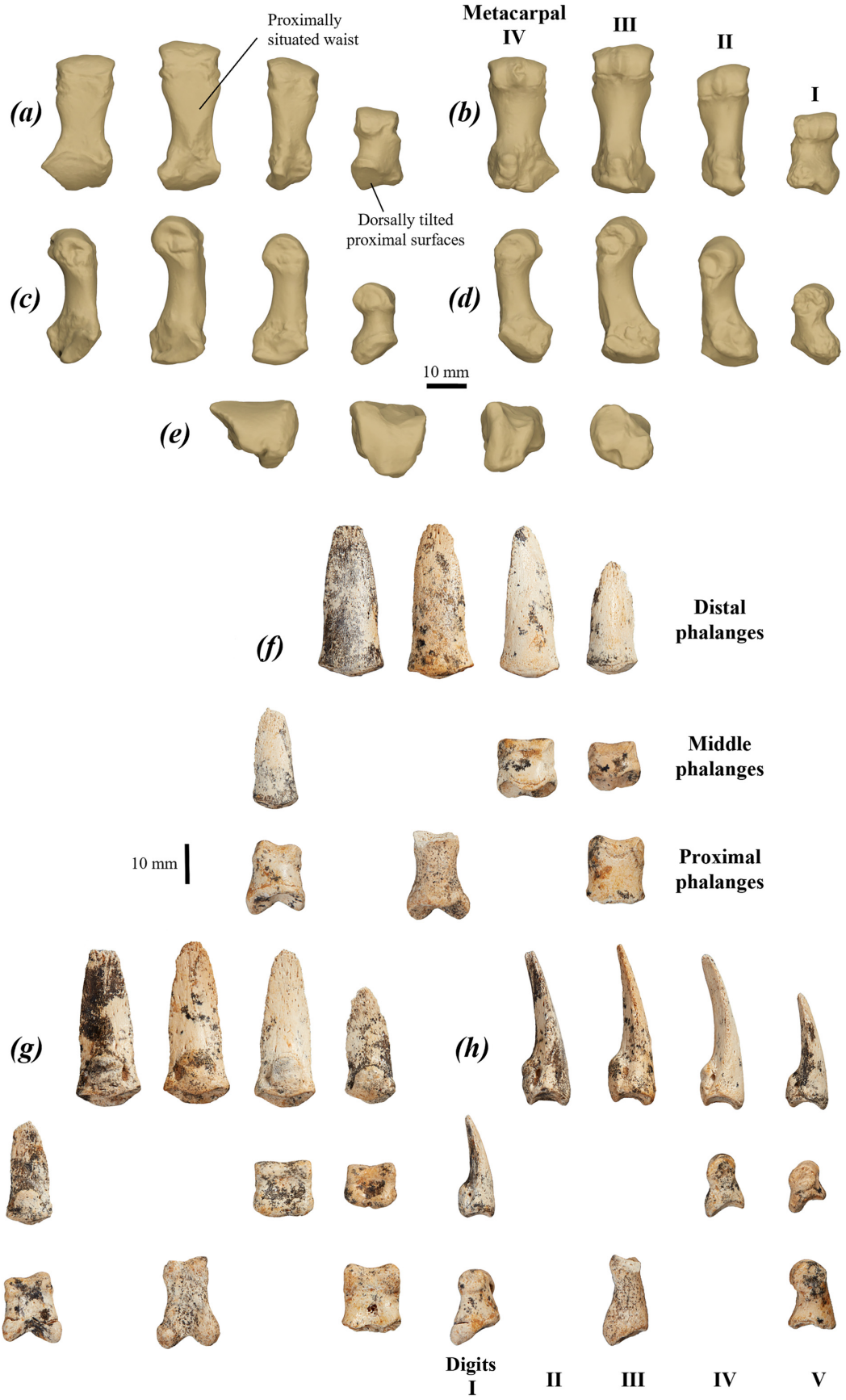

FIGURE 50. metacarpals and manual phalanges of *P. mamkurra* **sp. nov.**: (a–e) surface scan images of left metacarpals I–IV of WAM 02.7.11 in (a) dorsal, (b) palmar, (c) lateral, (d) medial, and (e) proximal views; and (f–h) right distal phalanges I–V, middle phalanges IV–V, and proximal phalanges I, III, and V of SAMA P20810 in (f) dorsal, (g) palmar, and (h) medial views.

short and robust, with a broad, thickened proximal end and an asymmetrical distal end. Metacarpal II: elongate relative to the other metacarpals; proximal end narrow, with a tall, narrow facet for the capitatum abutting the lateral margin of the smaller, broader facet for the trapezium and trapezoid. Distal end strongly asymmetrical, with the lateral component enlarged. Metacarpal III: proximal end broad and dorsopalmarly quite tall with the palmar component abraded. Shaft proximally narrow, steadily broadens to a broad distal end. Distal end with an enlarged keel. Metacarpal IV: proximal end enlarged, with the proximal facet for the hamatum large, flat, tilted slightly dorsally, roughly triangular in proximal view, and laterally projected in dorsal view. Medial facet for metacarpal III tall and narrow. Lateral facet for metacarpal V relatively broader, gently concave and angled anteriorly. Shaft narrows to a waist quite close to the proximal end, broadens and deepens steadily distally. Distal end broad.

The metacarpals of *P. mamkurra* **sp. nov.** do not differ from those of *P. anak*. They differ from those of *P. viator* in being shorter and more robust, with the narrowest point of the shaft closer to the proximal end; from *P. otibandus* in being larger and more robust; from *C. kitcheneri* in being slightly more gracile, with a narrower proximal shaft, squarer and less convex distal end, and a squarer and more projected proximolateral process of metacarpal III; from *O. rufus* in being larger; from *M. fuliginosus* in being larger and much more robust; and from *W. bicolor* in being larger and much more robust, with more dorsally tilted proximal surfaces.

Manual phalanges (Fig. 50f–h): proximal phalanges: short, broad, robust and dorsopalmarly compressed, with the proximal articular facet tilted distinctly dorsally. Distal end with a moderately shallow, slightly V-shaped trochlea. Middle phalanges: very short, broad and dorsopalmarly compressed, with a slightly dorsally tilted proximal articular surface. Distal end broad with a very shallowly concave trochlea. Distal phalanges: elongate, with a smoothly concave proximal articular surface. Palmar tubercles small and weakly palmarly projected. Shaft spatulate, straight to slightly palmarly curved, and extremely dorsopalmarly compressed, with a gently convex dorsal surface.

The manual phalanges of *P. mamkurra* **sp. nov.** differ from those of *P. anak* in having proximal phalanges with a slightly shallower trochlea and distal phalanges with a longer, more dorsopalmarly compressed shaft; from *P. viator* **sp. nov.** in being generally slightly longer, particularly the distal phalanges, which have a flatter palmar surface and lack a slight dorsal peak; from *P. otibandus* in having much shorter, broader shafts, greater degree of dorsopalmar compression and palmarly uncurved distal shafts; from *C. kitcheneri* in being smaller relative to metacarpals, relatively broader and far more dorsopalmarly compressed, particularly middle and distal phalanges, with the proximal surface of the proximal phalanges more dorsally tilted, trochleae broader and less V-shaped, and the distal phalanges dorsally rounded and un-peaked with less palmar curvature of the shaft; from *O. rufus* in being relatively broader, with the distal phalanges longer, more dorsopalmarly compressed and more palmarly curved; from *M. fuliginosus* in being larger, much broader and more robust, with proximal phalanges with shallower trochlea and less projected, more gently rounded proximal flexor tubercules, and distal phalanges with the shaft far less curved palmarly and very slightly rounded dorsally (rather than sharply peaked); and from *W. bicolor* in being larger, more dorsopalmarly compressed and more robust, with slightly more dorsally tilted proximal surfaces on the proximal and middle phalanges.

Hindlimb

Pelvis (Fig. 51): ilium: robust, well-developed and roughly L-shaped in cross-section. Epiphysis of iliac crest not known; iliac crest thick and broad, aligned transversely; width gently increases to maximum at the iliac crest. Iliac fossa shallow, extends one-third of the length of the ischium in juveniles; deeper, more concave and extends distally three-quarters of the length of the ilium in adults. Gluteal fossa broad, deeply concave, narrows distally, extends to the iliac crest. Caudal iliac spine (tuber sacrale) arises rapidly on the caudal surface of the base of the ilium, opposite the rectus tubercule; thick and tall proximally for origin of a large mm. gluteus, becomes thinner and slightly lower distally, extends to the iliac crest. Sacral surface (articular surface for wings of sacrum) deep, thickened and craniocaudally aligned with a slight cranial tilt, surrounded by a rugose surface, abuts the caudoventral margin of the medial surface of the caudal iliac spine, projects cranially as a low ridge with a thin crest that forms the cranial iliac spine and contributes to depth of iliac fossa; extends to the cranioventral margin in older specimens. Lateral iliac spine broad, slightly thinner than the caudal spine, with the lateral margin gently concave and curved slightly laterally to the projected dorsolateral extremity of the iliac crest. Rectus tubercule large, rugose, roughly triangular, and gently narrowing cranially onto the lateral iliac spine; increases in relative size with age. Acetabulum large, tall and deeply concave, deepest in the ventral component; taller than craniocaudal depth; acetabular fossa deep, partially covered cranially and caudally by a lip that projects from the acetabular surface, and with the angle, width and curvature variable within individuals.

Ischium: very deep, transversely compressed, gently concave medially and convex laterally; caudal margin rugose and gently undulating from the origin of mm. gemelli; deflected slightly caudally relative to the axis of the ilium; caudal component thickens toward the ventral margin and curves slightly caudolaterally to the large, laterally projected ischiatic tuberosity. Iliopubic (iliopectineal) eminence slightly projected, rounded, broad and rugose. Caudomedial surface of the ischium with a broad, smoothly concave coccygeal fossa for the origin of a large m. coccygeus. The craniodorsal angle of the obturator foramen is acute and rounded.

Pubis: narrows ventral to the iliopubic eminence, broadens ventromedially and becomes transversely thinner toward the pubic tubercle; pubis thickening at the ilial junction with age; planar at the pubic symphysis, thins caudoventrally

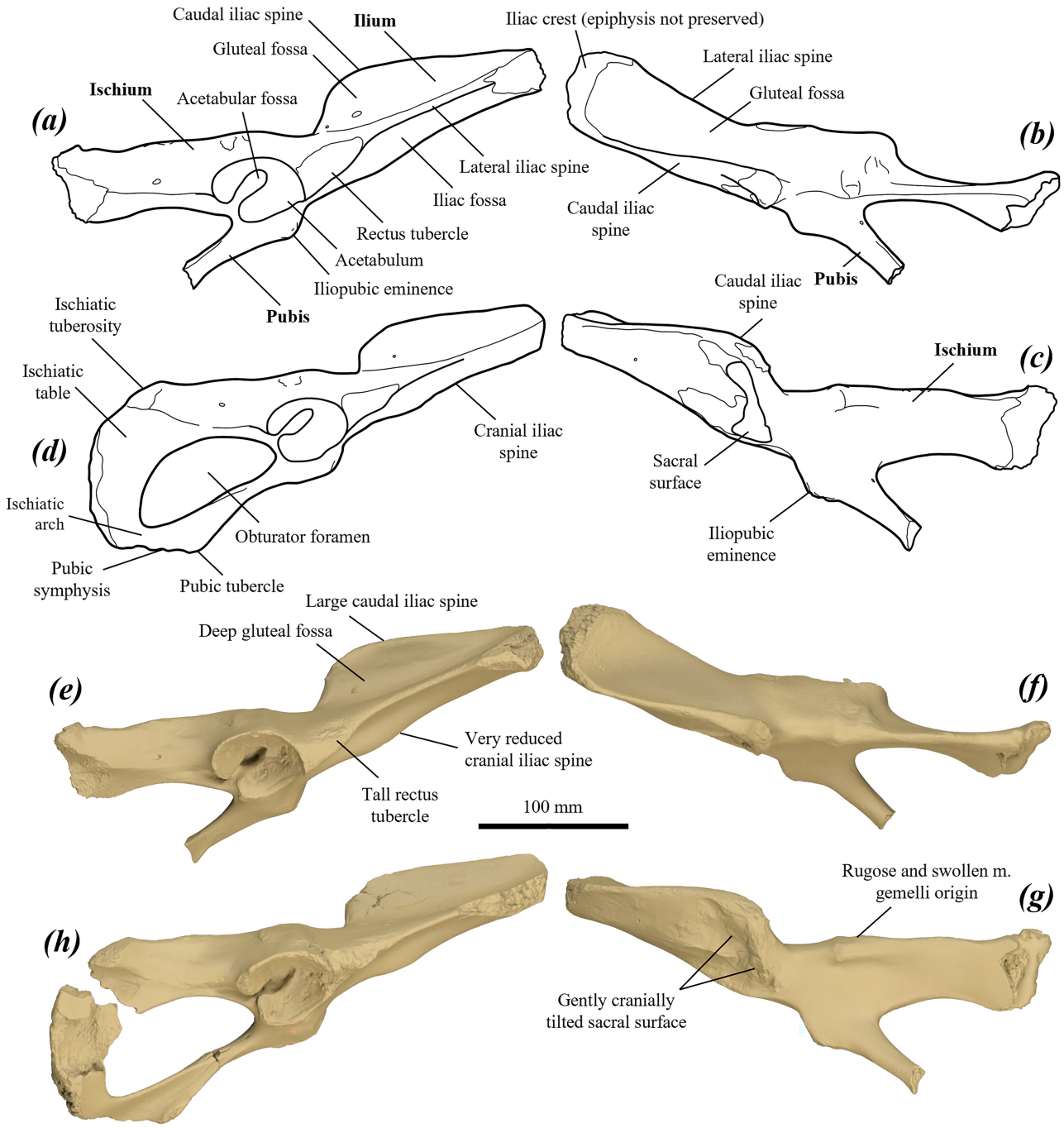

FIGURE 51. line drawings (a–d) and surface scan images (e–g) of partial right pelves of *P. mamkurra* **sp. nov.**: (a–c, e–g) partial pelvis of holotype SAMA P59549 in (a, e) lateral, (b, f) caudodorsal, and (c, g) medial views; and (d, h) partial pelvis of QVM2001 GFV23 in lateral view.

before thickening to the ischiatic symphysis. Pubic tubercle (area of articulation for the epipubic) is abraded, interpreted as being raised and slightly rugose. Ischiatic table tall and planar, thickens toward the robust ischiatic arch.

The pelvis of *P. mamkurra* **sp. nov.** differs from that of *P. viator* **sp. nov.** in having a slightly less broad lateral iliac spine and a more elongate rectus tubercle; from *P. tumbuna* in having its acetabulum opening more laterally and less cranioventrally, with a more deeply concave ventral component, larger iliopubic eminence, and a narrower, more planar ischium that is slightly longer relative to the ilium and is more caudally deflected relative to the axis of the ilium in lateral view; from *P. dawsonae* **sp. nov.** in being generally larger, with a larger caudal iliac spine, deeper gluteal fossa, less cranially tilted articular surface for the wings of the sacrum, less laterally projected rectus tubercle, more deeply concave acetabulum, and a more convex and rugose caudal margin of the craniodorsal component of the ischium; from *C.*

kitcheneri in being larger, with a far

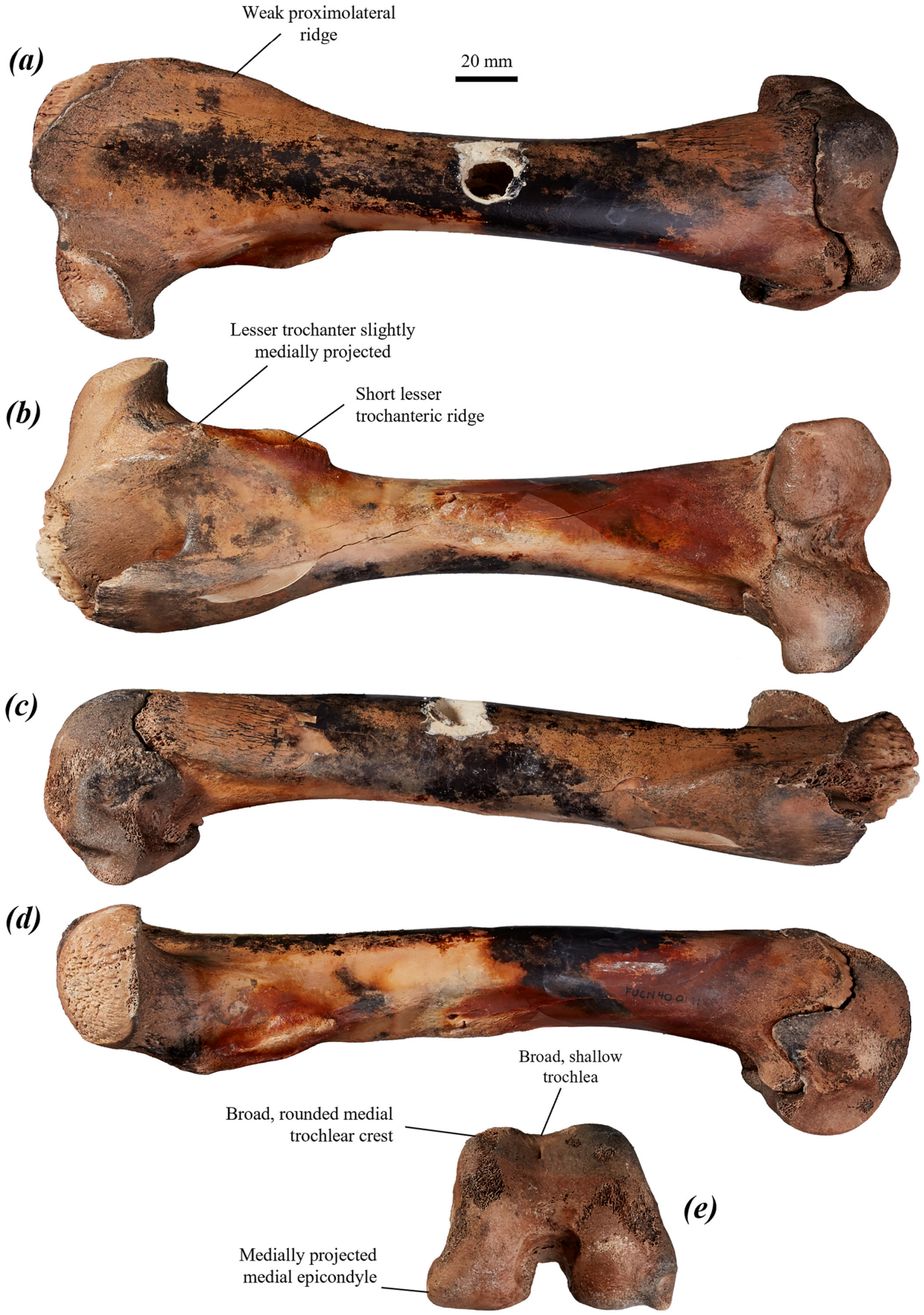

FIGURE 52. left femur of holotype SAMA P59549 for *P. mamkurra* **sp. nov.** in: (a) dorsal, (b) ventral, (c) lateral, (d) medial, and (e) distal views.

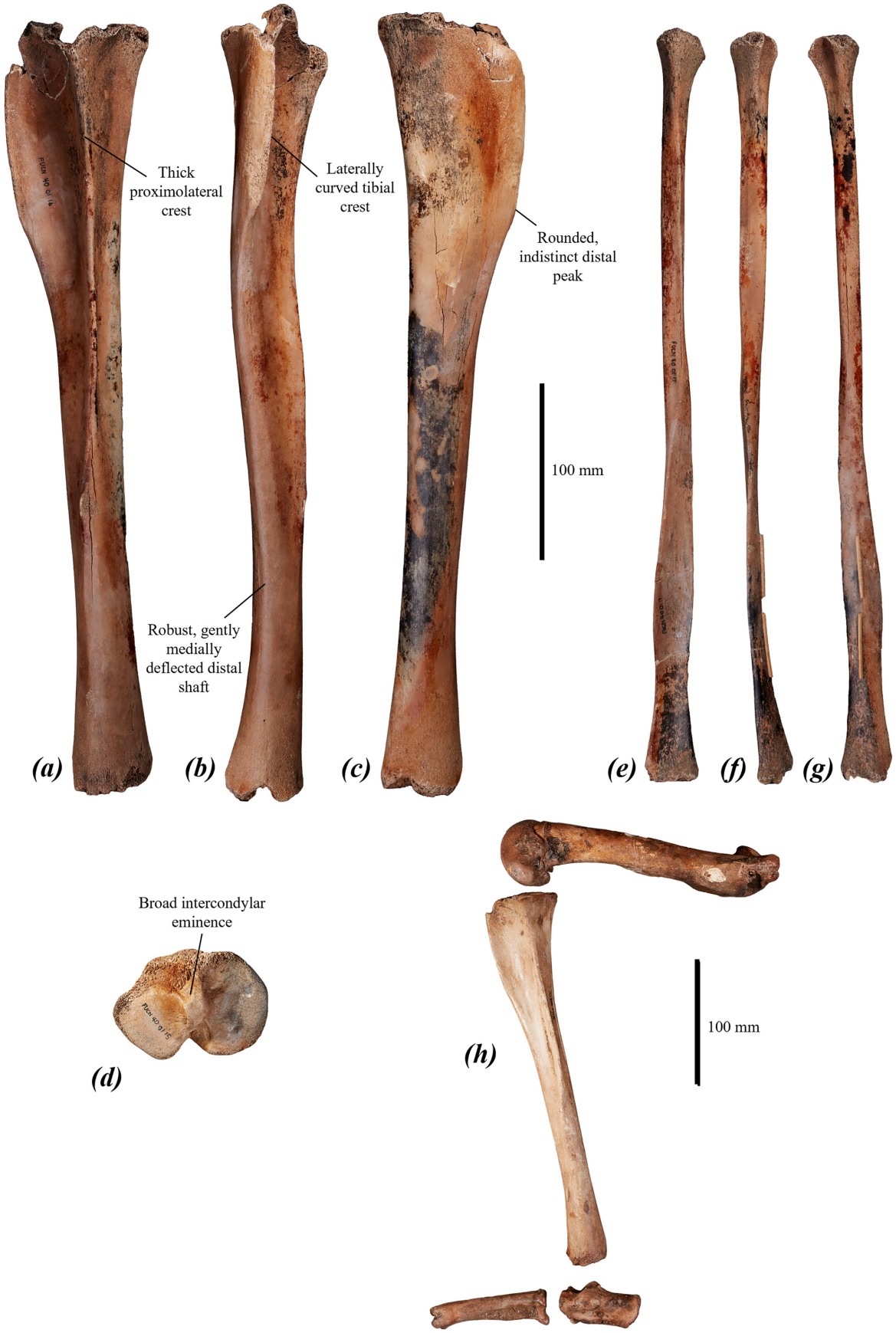

FIGURE 53. hindlimb elements of *P. mamkurra* **sp. nov.**: (a–c) partial left tibia of holotype SAMA P59549 in (a) lateral, (b) cranial, and (c) medial views; (d) left proximal tibial epiphysis of holotype in proximal view; (e–g) right fibula of holotype in (e) medial, (f) cranial, and (g) lateral views; and (h) re-articulated partial juvenile left hindlimb of paratype SAMA P28163 in lateral view, showing femur, tibia, calcaneus and metatarsal IV.

broader and deeper gluteal fossa, narrower and less distally extensive iliac fossa, more caudally and dorsally situated sacral surface relative to the acetabulum, and a rounder and shallower acetabulum; from *O. rufus* and *M. fuliginosus* in being larger and more robust, with a far broader and deeper gluteal fossa, less distally extensive iliac fossa, broader lateral iliac spine, and greater maximum acetabulum diameter relative to the ilial length; and from *W. bicolor* in being far larger, with the iliac crest aligned more transversely and less craniocaudally, a broader and deeper gluteal fossa, a narrower and less distally extensive iliac fossa, a broader lateral iliac spine, particularly dorsally, the caudal iliac spine lacking a small, pointed eminence on the caudoventral shoulder, the rectus tubercle with a smaller, shallower fossa on the lateral surface, more deeply concave ventral component of the acetabulum, a more robust pubis where it abuts the acetabulum, and a higher, more distinct dorsoventral ridge that leads to the lateral surface of the ischiatic tubercle.

Femur (Figs 52 & 53h): large and elongate, with the shaft straight in dorsal and lateral views. Head large, hemispherical, dorsomedially projected, and gently flared dorsally. Proximal end very broad, with a smoothly, distinctly convex dorsal surface. Intertrochanteric crest low, curving from the ventromedial base of the greater trochanter to the lesser trochanter. The greater trochanter is not known. Greater trochanteric ridge broad, thick, slightly ventrally arched, and slightly laterally projected to form a low, rugose proximolateral ridge on the dorsolateral margin of the proximal end (Fig. 52a); proximolateral ridge is slightly more raised and distally extensive in older specimens. Trochanteric fossa extends distally to level with the lesser trochanter. Lesser trochanter is present as a moderately medially projected rugose eminence, remains an unfused epiphysis until well into adulthood; merges distally into the thick, raised, medially orientated lesser trochanteric ridge (point of insertion for an enlarged m. iliopsoas) on the ventromedial surface of the shaft, which becomes more medially projected distally.

Quadratus tubercule raised, oval and situated on the proximodistal midpoint of the ventral surface of the shaft, narrows and extends proximally to level with lesser trochanter. Shaft broadens from midpoint toward the distal end, becomes flatter on the ventral surface. An elongate fossa is present on the caudolateral shaft adjacent to the ventrolateral margin of the distal epiphysis, roughly triangular in ventral view and narrows proximally; the partial origin of the m. flexor digitorum superficialis.

Femur distal epiphysis broad and robust. Lateral trochlear crest broad and rounded, taller than the slightly narrower medial crest. Intercondylar fossa broad, rounded; broadest at midpoint, narrows dorsally. Lateral condyle broad, with the ventral surface gently convex. Trochlea shallow and broad. Fibular facet on the lateral condyle slightly ventrally deflected and distinctly laterally projected. Medial condyle with the distal and ventral surfaces convex in juveniles, roughly planar with rounded margins in adults. Lateral epicondyle has the ventral component projected ventrolaterally such that the lateral surface is distinctly sloped; a shallow and rugose fossa is present around the midpoint of the lateral surface, and a moderately deep fossa is present on the ventral margin and is angled slightly distally, both points of origin of the m. gastrocnemius lateralis. Medial epicondyle gently dorsally tilted, with the ventral component moderately projected and bulged; medial gastrocnemial fossa shallow, rounded, rugose, situated on the centre of the medial surface.

The femur of *P. mamkurra* **sp. nov.** differs from that of *P. anak* in being slightly more robust, with a less dorsally deflected head, weaker proximolateral ridge and deeper trochlea, and the trochlear crests subequally raised (rather than the lateral crest being more raised); from *P. viator* in being longer and more gracile, with a lower, less distinct intertrochanteric crest, less medially projected lesser trochanter, weaker proximolateral ridge, relatively shorter lesser trochanteric ridge, broader and shallower trochlea, more rounded trochlear crests with a relatively broader medial trochlear crest, and a more medially projected ventral component of the medial epicondyle; from *P. tumbuna* in being larger and more robust, with a less elongate and more proximally situated quadratus tubercle; from *P. otibandus* in being larger, with the trochlea broader and shallower, and the medial condyle relatively broader; from *C. kitcheneri* in having a narrower shaft relative to length, a relatively large femoral head, more distally extensive trochanteric ridge and ventromedial ridge, straighter shaft in dorsal view, lack of distinct anti-clockwise rotation of the distal epiphysis in distal view, less reduced medial trochlear crest relative to lateral crest in distal view, broader intercondylar fossa, and a smaller, less ventrally projected lateral epicondyle; from *O. rufus* and *M. fuliginosus* in being generally larger and more robust, with a relatively larger proximal end, more laterally displaced trochanteric ridge and trochanteric fossa such that the ventral face of the proximal end is relatively broader, a more distally extensive lesser trochanteric ridge, more elongate and more distally situated quadratus tubercle, relatively broad distal end, less raised lateral trochlear crest, less pointed medial trochlear crest, shallower trochlea, and a more proximally situated lateral gastrocnemial fossa; and from *W. bicolor* in being larger and more robust, with a relatively larger and more dorsally deflected head, less distally extensive trochanteric fossa relative to the head, more distally extensive lesser trochanteric ridge, less proximally situated quadratus tubercle, less dorsoventrally compressed distal shaft, relatively lower, broader distal condyles, shallower trochlea, larger fibular facet on the lateral condyle, and a more proximally situated lateral gastrocnemial fossa.

Tibia (Fig. 53a–d, h): short and robust, with the proximal shaft bowed gently medially and the distal shaft bowed gently laterally in cranial view. Proximal epiphysis width subequal to its depth (cranial component of the epiphysis not preserved in available specimens; size based on the depth of the proximal tibia of holotype). Medial condyle medially and caudally rounded, deeper and slightly narrower than the lateral condyle. Lateral condyle comes to rounded points at the lateral and caudal margins, with a moderately deep groove in the craniolateral margin.

Intercondylar eminence low and broad. Proximal fibular facet narrow, deep, shelf-like, and orientated ~40° laterally from the sagittal plane. Cnemial crest deep, thickened and elongate, extends ~25% of the total tibial length, with the lateral surface moderately concave and the medial surface moderately convex. Proximolateral crest thin and raised, becomes thinner and more raised distally before merging smoothly with the shaft distal to the midpoint of the tibia. Distal component of the shaft briefly narrows to a minimum before expanding smoothly to the distal end in all axes, but particularly craniomedially, with a slight medial deflection; minimum shaft circumference is at ~three-quarters of length. Distal fibular facet extends for the distal two-fifths of the lateral surface of the tibial shaft. Distal epiphysis large and broad; medial tuberosity thick and robust, with a blunt medial malleolus; talar trochlea broadly concave with rounded cranial and caudal ventral eminences.

The tibia of *P. mamkurra* **sp. nov.** differs from that of *P. anak* in being shorter and more robust, with a thicker proximal component of the proximolateral crest; from *P. viator* **sp. nov.** in being shorter and much more robust, and in having a more laterally curved cnemial crest in cranial view with less angular and distinct distal peak, a thicker proximal component of proximolateral crest, and a slightly more medially deflected distal component of the shaft; from *P. tumbuna* in being longer and more gracile, with a less elongate cnemial crest relative to the total length, thinner proximolateral crest, and a narrower and less flattened distal fibular facet; from *P. otibandus* in being larger, with a smaller and narrower proximal fibular facet and a deeper, more elongate cnemial crest; from *P. snewini* in being shorter and much more robust, with a less angular and distinct distal peak of the cnemial crest, thicker proximal component of proximolateral crest, and a far shorter distal shaft relative to the proximal component; from *C. kitcheneri* in being larger and more robust, with a lower, broader intercondylar eminence, less deeply concave muscular groove on the proximal epiphysis, more distally extensive proximolateral crest, and a relatively deeper distal component of the shaft with greater expansion to the distal epiphysis; from *M. fuliginosus* and *O. rufus* in being far shorter and more robust, with a lower, broader intercondylar eminence, broader proximal epiphysis with a deeper muscular groove, a more concave cnemial crest on the lateral surface, and a greater degree of expansion of the distal shaft toward the epiphysis; and from *W. bicolor* in being larger and more robust, with a broader proximal fibular facet, thicker proximolateral crest, less angular cnemial crest peak, and a more rounded talar trochlea.

Fibula (Fig. 53e–g): proximal epiphysis large, with a broad facet for tibia, and a tall, thickened caudal process for articulation with the fibular facet on the lateral epicondyle of the femur. Shaft with the proximal component thick and roughly triangular in cross-section, with a broad, rounded groove on the craniolateral surface for the major origin of a large m. extensor digitalis IV; shaft transitions to tear-drop shaped in cross-section before flattening around its midpoint; distal component is crescentic in cross-section and very deep in the craniocaudal plane, with the lateral surface convex and the medial surface concave; deepens briefly distally, shallows to a waist and deepens to maximum at distal end; shallow proximodistally aligned groove on lateral surface of distal end. The distal epiphysis is not known.

The fibula of *P. mamkurra* **sp. nov.** differs from that of *P. anak* in being more robust; from *P. viator* **sp. nov.** in being shorter, with less broadening and shallowing of the section of the shaft immediately proximal to the distal epiphysis; from *C. kitcheneri* in its relatively larger proximal epiphysis and relatively deeper distal shaft; from *O. rufus* in being shorter and much more robust, with broader proximal end, deeper groove for m. extensor digitalis IV and deeper distal component of the shaft; from *M. fuliginosus* in its much greater robustness, more thickened, raised proximomedial ridge, and more triangular proximal shaft in cross-section; and from *W. bicolor* in being larger and more robust, with relatively larger proximal epiphysis.

Pes

Calcaneus (Figs 53h & 54a–f): large, broad and very robust. Calcaneal tuberosity tall and domed, narrowing only slightly cranially in dorsal view, and dorsally rounded in cross-section. Caudal surface tall and domed in caudal view; two small, semicontinuous transverse valleys, occasionally continuous as single broad valley, extend across the bottom half. Plantar surface rugose, subrectangular in plantar view, becomes thicker, broader and more rugose with age; cranial section narrows slightly cranially and extends to level with the cranial margin of the sustentaculum tali; caudal component slightly thicker, consists of the caudal epiphysis wrapping cranioplantarly under the tuberosity. Cranial plantar tubercule distinct, rounded, immediately craniomedial to the craniomedial margin of the plantar surface. Sustentaculum tali large, tall, deep, medially projected beyond medial margin of talar facet; tapers to a pointed, cranioplantar peak (Fig. 54c); caudal margin gently convex in medial view; becomes more projected, more rugose and slightly more extensive caudally with age. Flexor groove very broad and deep.

Fibular facet very large, bulbous, tapers medially; caudal part large, roughly oval, and dorsolaterally projected, with an indistinct medial margin (Fig. 54a & f); cranial part low, and elongated toward the lateral margin of the dorsolateral cuboid facet. Lateral talar facet large, strongly convex and semi-cylindrical, semi-fused with the medial talar facet but with contours distinct; a small, rounded fossa, for articulation with the plantar process of the craniolateral margin of the talus, abuts the craniolateral margin of this facet. Medial talar facet large, oval, flat to slightly concave and cranially inclined, craniocaudally level with the lateral talar facet; articular surface extends onto the caudal face to form a convex, rounded lip. A small, rounded, variably deep, caudal-facing fossa extends beneath the lateral component of the caudal margin of the medial facet.

A small facet abuts the medial margin of the dorsomedial facet on the medial surface of the calcaneal

head for articulation with the talar head. Dorsomedial cuboid facet broad, roughly pentagonal in cranial view, and gently convex; lateral margin 'stepped' to dorsolateral facet, as in *P. anak*; a deep, subrectangular to oval fossa is situated immediately plantarly. Dorsolateral cuboid facet tall, cranially projected, tilted plantarly and slightly medially, convex in lateral view, tapers plantarly and curves medially to be continuous with the plantomedial facet; dorsal margin angled plantolaterally or with a distinct step on the medial component of the dorsal margin; the rounded lateral margin curves plantomedially to the plantomedial facet. Plantomedial cuboid facet quite small, oval, short and broad.

The calcaneus of *P. mamkurra* **sp. nov.** differs from all compared taxa in having a sustentaculum tali with a pointed cranioplantar peak, and craniocaudally level and semicontinuous medial and lateral talar facets (Fig. 54a). It further differs from that of *P. anak* in being generally more robust, with a less rounded caudal fibular facet with less distinct margins, and more bulbous, dorsally projected medial talar and fibular facets; from *P. viator* **sp. nov.** in being lower, considerably broader, and more robust, with larger, more bulbous talar facets, a larger, more bulbous fibular facet with a more rounded and caudally projected (rather than laterally projected) caudal part, and a more medially projected sustentaculum tali; from *P. tumbuna* in being larger and taller, with a larger medial talar facet, relatively narrower and more convex medial cuboid facet, and a planar, less medially flared plantar surface; from *P. dawsonae* **sp. nov.** in being larger, taller and more robust, with more bulbous lateral talar and caudal fibular facets, and fibular facet with a more plantarly extensive lateral part in lateral view; from *P. otibandus* in being larger, with a relatively taller calcaneal tuberosity, less medially displaced calcaneal head, and a relatively larger, more caudally projected caudal part of the fibular facet; from *C. kitcheneri* in being larger, taller and more robust, with a larger, more rounded caudal part of fibular facet that lacks a thin, laterally flared lateral margin, larger and more bulbous talar facets, more cranially extensive and less laterally tilted plantar surface, and a broader plantomedial cuboid facet; from *O. rufus* and *M. fuliginosus* in being larger, much broader and more robust, with a broadly rounded, domed calcaneal tuberosity in cross-section (rather than narrow and peaked), more medially projected sustentaculum tali, a larger, more convex, more dorsally swollen and more caudally extensive fibular facet, a more bevelled 'step' between the dorsal cuboid facets, a broader dorsolateral cuboid facet, and a narrower dorsomedial cuboid facet; and from *W. bicolor* in being much larger, relatively broader and more robust, with a larger, more bulbous fibular facet and lateral talar facet, and a larger, relatively broader, and less cranially tilted medial talar facet with a rounded caudal lip.

Talus (Fig. 54g–i): robust and considerably width greater than length. Trochlear crests rounded, subequal in height and breadth, orientated in the sagittal plane. Trochlea quite deep and smoothly concave. Medial malleolus extends medially and slightly cranially, bounded craniolaterally by a broad, very shallow malleolar fossa. Talar head broad, tall in lateral view, projected craniolaterally, and plantarly deflected. Facet for the cuboid distinct, flat, roughly triangular, facing craniolaterally on the lateral surface of the head. Navicular facet large and tall, extends medially and caudoplantarly from the cranial surface of the talar head to its caudoplantar extent, plantar to the medial malleolus (Fig. 54h–i). Posterior plantar process large, thick, rugose, and plantarly projected; comes to a rounded point in medial view. In plantar aspect, the medial calcaneal facet is broad and rounded, with a large, planar, caudal-facing cranial part curving to meet a smaller, concave caudal part; lateral calcaneal facet is broad, deeply concave, roughly cylindrical, and tapers medially.

The talus of *P. mamkurra* **sp. nov.** differs from that of *P. anak* and *P. viator* **sp. nov.** in being relatively broader, and having a deeper trochlea with a less medially skewed concavity, more plantarly projected talar head, more medially aligned and projected medial malleolus, and a larger, more medially extensive navicular facet; from *P. otibandus* in being larger, with a broader, shallower malleolar fossa, slightly more plantomedially extensive navicular facet, and a deeper plantar concavity that separates the talar head from the posterior plantar process; from *P. snewini* in being larger and relatively broader, with a more deeply concave trochlea, more medially projected medial malleolus and talar head, larger cuboid facet on talar head, broader and more caudoplantarly extensive navicular facet, and a larger notch between the cranial margin of medial trochlear crest and the talar head; from *C. kitcheneri* in being larger, with a cuboid facet present on the talar head and a broader, medially deflected, and more caudoplantarly extensive navicular facet; from *O. rufus* and *M. fuliginosus* in being larger and relatively broader, with the trochlear crests more even in height, the trochlea deeper and a broader, more plantar facing, medially deflected and caudoplantarly extensive navicular facet; and from *W. bicolor* in being much larger and relatively broader, with a less medially skewed trochlear concavity, larger cuboid facet, more plantomedially extensive navicular facet, shallower malleolar facet, more transversely aligned medial malleolus, and a more rounded posterior plantar process in medial view.

Cuboid (Fig. 55a–c): large, broad and roughly rectangular in dorsal view except for 'stepped' calcaneal facet. Dorsomedial calcaneal facet caudally projected, slightly broader and dorsoplantarly shorter than dorsolateral facet. Dorsolateral calcaneal facet tall and plantomedially continuous, with a short, rounded plantomedial calcaneal facet. Facet for articulation with the talar head quite small, roughly triangular, and slightly concave, abuts the dorsomedial calcaneal facet on the craniodorsal margin of the medial surface. Metatarsal IV facet very large, slightly concave, with the medial part of the dorsal margin gently convex. Metatarsal V facet large, very broad and oval (Fig. 55b), dorsoplantarly short, laterally projected, slightly concave and slightly laterally tilted; incompletely separated from the metatarsal IV facet. Lateral plantar tubercle very broad, craniocaudally

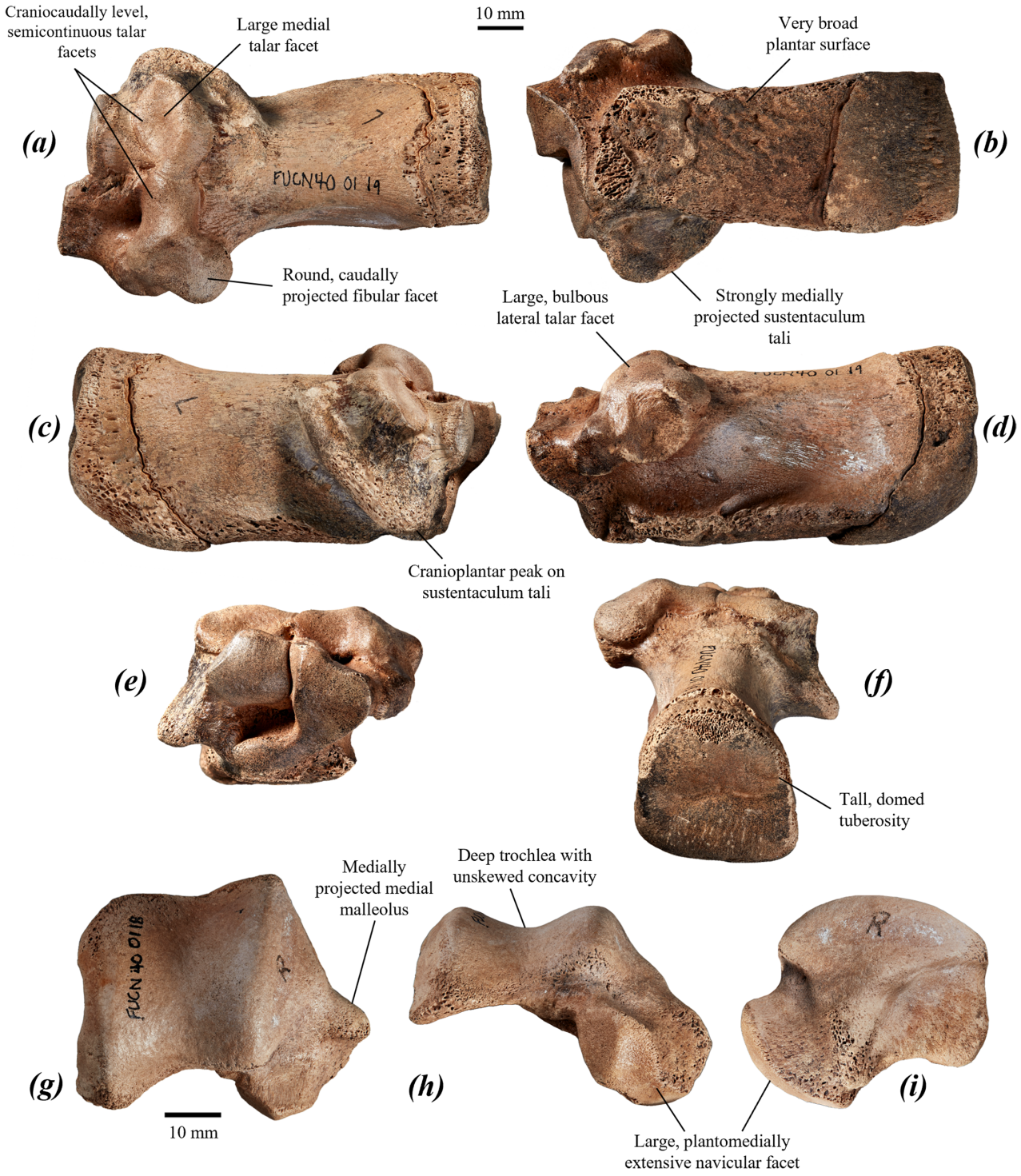

FIGURE 54. left calcaneus and talus of *P. mamkurra* **sp. nov.** holotype SAMA P59549: (a–f) calcaneus in (a) dorsal, (b) plantar, (c) medial, (d) lateral, (e) cranial, and (f) caudodorsal views; and (g–i) talus in (g) dorsal, (h) cranial, and (i) medial views.

compressed (Fig. 55a); extends laterally and slightly caudally over caudoplantar part of the lateral surface. Medial plantar tubercle partially abraded in available specimens; small, plantomedially projected and quite elongate; small relative to lateral plantar tubercle, separated by a broad, moderately shallow flexor groove. The area of articulation with the navicular on the dorsocaudal part of the medial surface is rugose, and wraps cranially around the facet for the talar head. Facet for the ectocuneiform indistinct, tall, craniocaudally very short, with semicontinuous dorsal and plantar sections; dorsal component abuts the medial margin of the metatarsal IV facet on the cranial margin of the medial surface; plantar component extends plantarly, along the medial margin of the plantar cuboid facet, onto the base of the medial surface of the medial plantar tubercle.

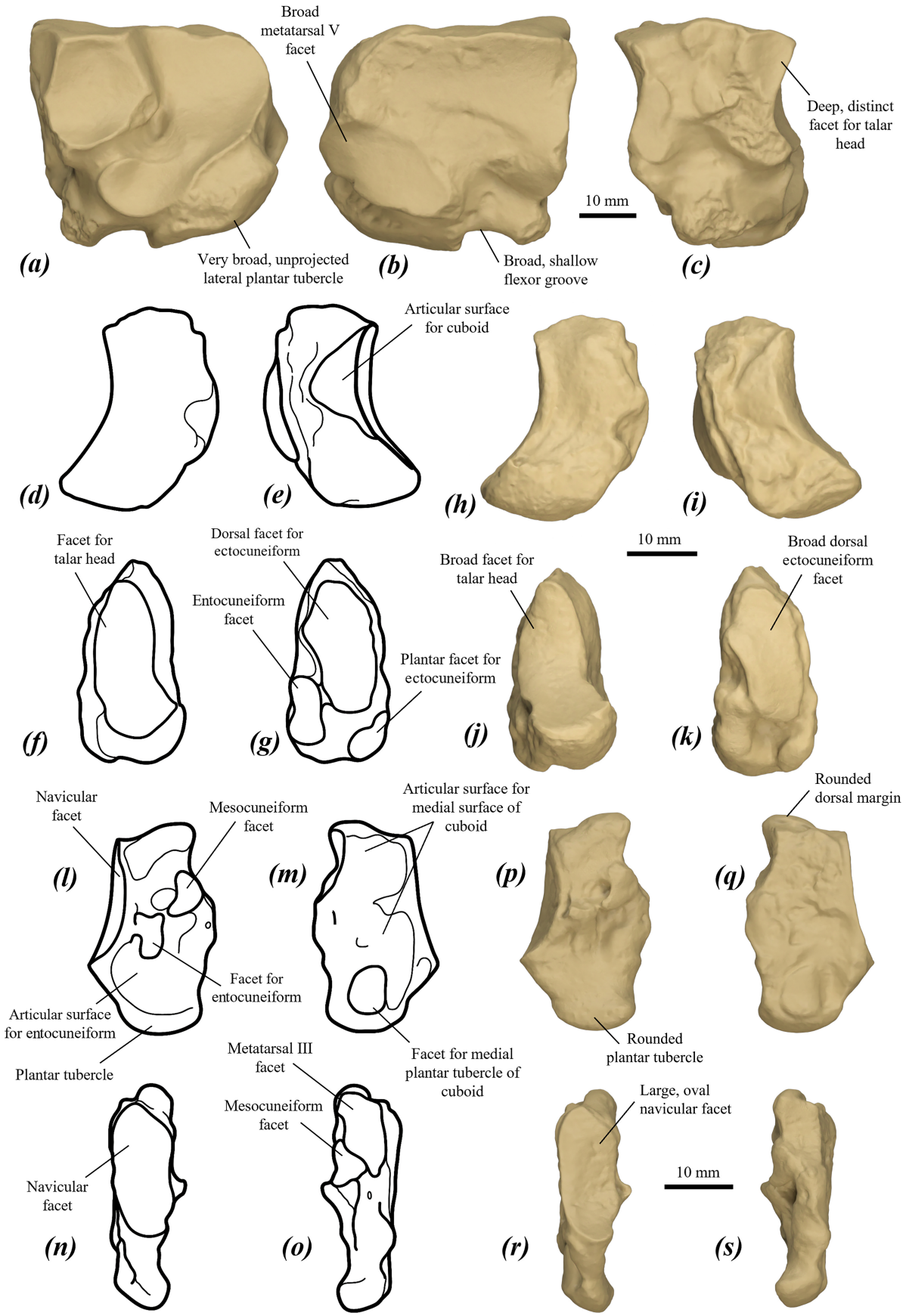

FIGURE 55. tarsal elements of *P. mamkurra* **sp. nov.**: (a–c) surface scan images of right cuboid of specimen SAMA P20810 in (a) caudal/proximal, (b) cranial/distal, and (c) medial views; (d–g) line drawings and (h–k) surface scan images of left navicular of WAM 02.7.11 in (d, h) medial, (e, i) lateral, (f, j) caudal, and (g, k) cranial views; and (l–o) line drawings and (p–s) surface scan images of right ectocuneiform of WAM 02.7.11 in (l, p) medial, (m, q) lateral, (n, r) caudal, and (o, s) cranial views.

The cuboid of *P. mamkurra* **sp. nov.** differs from that of all compared taxa in having a broader metatarsal V facet and from all taxa except *W. bicolor* in having a broader flexor groove. It further differs from *P. anak* in having a deeper, more distinct talar facet, less plantarly projected lateral plantar tubercle, and a shallower flexor groove; from *P. viator* **sp. nov.** in being broader relative to height, with a shallower, less plantarly projected lateral plantar tubercle, less plantarly projected, slightly more medially situated medial plantar tubercle, and a shallower flexor groove; from *P. otibandus* in being larger, with a less dorsally flared dorsomedial margin, more distinct step between dorsal calcaneal facets, broader dorsolateral calcaneal facet, larger and more distinct talar facet, shallower medial fossa for navicular and ectocuneiform, less plantarly projected lateral plantar tubercle, dorsal metatarsal IV facet continuous with the plantar facet, and a less concave metatarsal V facet; from *P. snewini* in being larger and broader, with a less dorsally flared dorsomedial margin, relatively broader dorsolateral calcaneal facet, shallower medial fossa for the navicular and ectocuneiform, and a larger, more plantarly projected and more medially situated medial plantar tubercle; from *C. kitcheneri* in being larger, taller and broader relative to depth, with a facet for the talar head present, a larger and more caudally extensive medial plantar tubercle, and a deeper flexor groove; from *O. rufus* in being larger, broader and relatively dorsoplantarly shorter, with a broader, less inset dorsolateral calcaneal facet, more medial facing facet for the talar head, broader and less plantarly projected lateral plantar tubercle, larger, more medially situated projected medial plantar tubercle, and a more medially situated plantar metatarsal IV facet; from *M. fuliginosus* in being larger, relatively broader, and squarer in outline in caudal view, with a much less plantarly projected, more dorsolaterally extensive lateral plantar tubercle, larger, more projected medial plantar tubercle, and a more medially extensive plantomedial calcaneal facet; and from *W. bicolor* in being much larger and relatively broader, with a broader dorsolateral calcaneal facet relative to the dorsomedial facet, larger step between dorsomedial and dorsolateral calcaneal facets, broader and less plantarly projected lateral plantar tubercle, and a larger medial plantar tubercle.

Navicular (Fig. 55d–k): tall, narrow and quite deep, tapering slightly in width dorsally; cranial margin slightly taller than the caudal margin. Facet for the talar head smoothly concave, with the plantar part broad, rounded and tilted dorsally. Facet for the cuboid situated on the lateral surface, semicontinuous with the dorsal component of the lateral margin of the talar facet. Facet for the entocuneiform small, oval, transversely compressed and tilted slightly plantarly; situated against the plantomedial margin of the cranial surface. Dorsal facet for the ectocuneiform large, tall, fairly narrow and gently convex, extends from the dorsal margin of the cranial surface to level with the facet for the entocuneiform; plantar facet for the ectocuneiform is very small, rounded, convex and situated on the cranioplantar surface against the medial margin; lateral and slightly plantar to the entocuneiform facet, completely separate from the dorsal facet.

The navicular of *P. mamkurra* **sp. nov.** differs from that of *P. viator* **sp. nov.** in being broader, with a less plantarly extensive dorsal ectocuneiform facet; from *P. otibandus* in being larger, and deeper relative to height, with a less laterally flared dorsal ectocuneiform facet and a more medially tilted facet for the entocuneiform; from *C. kitcheneri* in being larger and taller; from *O. rufus* in being less deep relative to height, with a less deeply concave talar head facet, separate dorsal and plantar sections of the ectocuneiform facet, more dorsally situated facet for the entocuneiform relative to the plantar margin of the ectocuneiform facet, and in lacking an eminence on the medial margin of the cranial surface between the dorsal ectocuneiform facet and the entocuneiform facet; from *M. fuliginosus* in being larger, and shallower relative to height, with separate dorsal and plantar sections of ectocuneiform facet, and in lacking an eminence on the medial margin of the cranial surface; and from *W. bicolor* in being much larger, with a taller plantar ectocuneiform facet and a slightly more plantarly situated entocuneiform facet.

Ectocuneiform (Fig. 55l–s): tall, transversely compressed, and tapering slightly dorsally in medial view, with a rounded dorsal margin (Fig. 55q). Facet for the navicular oval, gently concave and slightly laterally tilted, occupies the dorsal part of the caudal surface. Articular surface for the entocuneiform large and slightly concave, occupies the plantar part of the medial surface, with a small, irregular facet on the dorsal edge of the articular area. Facet for metatarsal III fairly narrow and concave, situated against the dorsal margin of the cranial surface; sits dorsal to a small, narrow, irregular eminence. Facet for the mesocuneiform small and rounded, immediately plantomedial to the metatarsal III facet. Plantar tubercle rounded in medial view, rugose and thickened at the plantar margin, with a slight medial deflection; lateral surface articulates with the medial plantar tubercle of the cuboid.

The ectocuneiform of *P. mamkurra* **sp. nov.** differs from that of *P. viator* **sp. nov.** in being slightly broader, with a broader, more oval and less plantarly extensive navicular facet and a shallower plantar tubercle that is more rounded in medial view; from *P. otibandus* in being larger and relatively slightly taller, with a gently rounded dorsal margin (rather than distinctly rounded-triangular); from *C. kitcheneri* in being larger, with a larger, less cranially deflected plantar tubercle and a broader, less plantarly extensive navicular facet; from *O. rufus* in being larger, with a more oval navicular facet, smaller cranial eminence, narrower, deeper, less plantarly projected and less cranially deflected plantar tubercle, and a relatively larger metatarsal III facet; from *M. fuliginosus* in being larger and broader, with a more oval navicular facet, smaller cranial eminence, and a deeper, less cranially deflected plantar tubercle; and from *W. bicolor* in being much larger, with a more oval navicular facet, smaller cranial eminence, and a larger, more rounded plantar tubercle.

Metatarsal IV (Fig. 56a–f): large and robust, shaft robustness index ~5.3–6. Dorsal cuboid facet has the medial part flat to gently concave and the lateral part flat

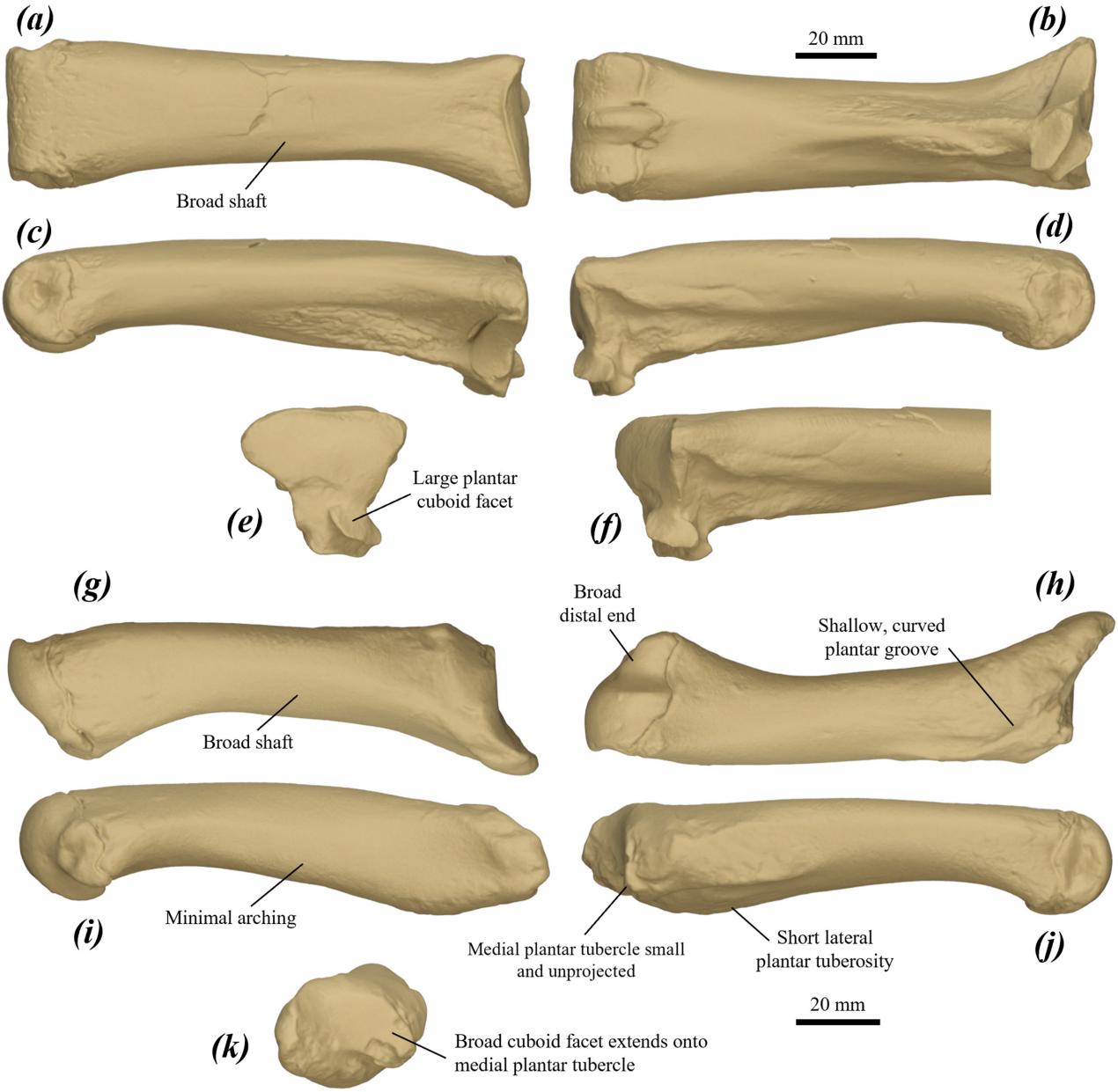

FIGURE 56. surface scan images of left metatarsals IV (a–f) and V (g–k) of *P. mamkurra* **sp. nov.** SAMA P20810 in: (a, g) dorsal, (b, h) plantar, (c, i) lateral, (d, j) medial, (e, k) proximal, and (f) proximomedial views.

to gently convex, such that the dorsal margin is slightly S-shaped in dorsal view; lateral component is laterally projected with its plantar margin tapering dorsally to a rounded point in proximal view; continuous plantomedially with the plantar cuboid facet. Proximal fossa shallow, abuts the proximal margin of the metatarsal V facet and the lateral margin of plantar cuboid facet. Plantar cuboid facet round to oval, slightly convex to concave, tilted slightly to sharply dorsomedially; situated opposite the proximal plantar sesamoid facet on the proximal surface of a thick, plantarly projected plantar tubercle. Facet for articulation with the plantolateral component of the ectocuneiform small, rounded, and medially tilted, situated on the proximal surface of the plantar tubercle, medial to and occasionally semicontinuous with the plantar cuboid facet. Proximal plantar sesamoid facet round to oval, flat to gently concave, facing plantolaterally to cranioplantarly. Articular surface for metatarsal III indistinct; situated in an elongate, rugose shallow fossa on the medial surface of the proximal end, bordered dorsally by a thin ridge extending distoplantarly from the dorsomedial corner of the dorsal cuboid facet. Dorsal facet for the ectocuneiform very small, on the medial surface of the proximal end, abuts the medial margin of the dorsal component of the dorsal cuboid facet. Facet for metatarsal V tall, proximodistally short; shape variable but generally oblong with rounded dorsal and plantar components; extending plantarly onto the lateral surface of the plantar tubercle.

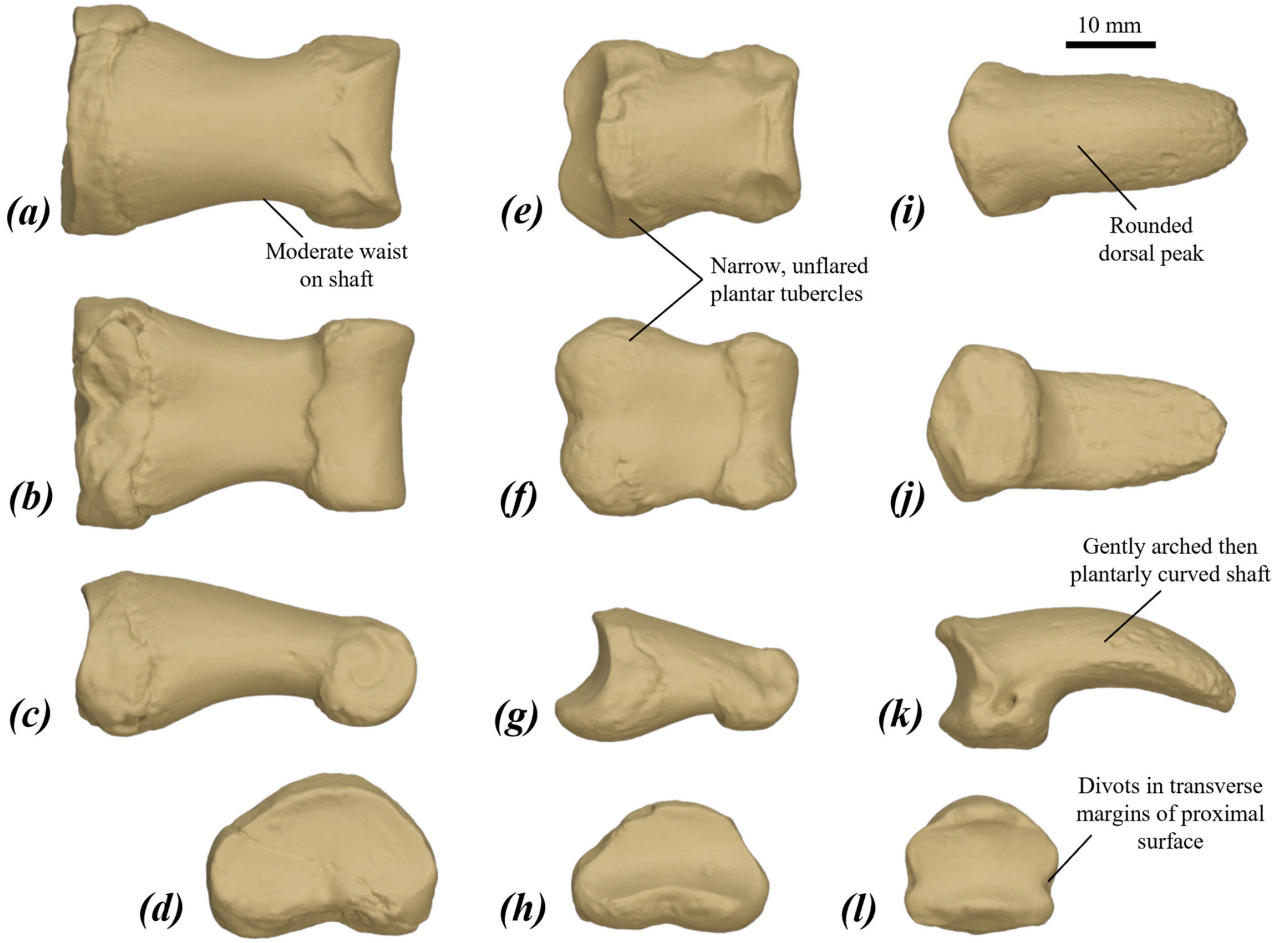

FIGURE 57. surface scan images of left (a–d) proximal, (e–h) middle, and (i–l) distal pedal phalanges IV of *P. mamkurra* **sp. nov.** SAMA P20810 in: (a, e, i) dorsal, (b, f, j) plantar, (c, g, k) medial, and (d, h, l) proximal views.

Plantar ridge broad, rugose, extends distally from the base of the plantar tubercle with a very slight lateral deflection, gently merges into the plantar surface of the shaft around the midpoint. Shaft minimum width situated at around one-third of length from the proximal end, then expands gently, particularly on the lateral margin, to the broad distal end; shaft quite low in lateral view, becomes lower distally; dorsal surface of the shaft flat proximally, becoming gently rounded distally. Distal end broad; fossae for collateral ligaments circular and quite deep; keel slightly subequally to slightly more projected than lateral and medial ridges.

The metatarsal IV of *P. mamkurra* **sp. nov.** differs from that of *P. anak* in being slightly longer; from *P. viator* **sp. nov.** in being longer, with a larger plantar cuboid facet; from *P. tumbuna* in being larger; from *P. dawsonae* **sp. nov.** in having a larger plantar cuboid facet; from *P. otibandus* in being larger and more gracile, with dorsal and plantar cuboid facets continuous, and the plantar ridge more raised; from *P. snewini* in being larger and longer, with the dorsal and plantar cuboid facets continuous, the proximal cuboid fossa more plantolaterally situated, and a relatively longer plantar ridge; from *C. kitcheneri* in being larger, broader and more robust, with a larger, more plantarly projected proximal plantar tubercle and a more raised plantar ridge; from *O. rufus* and *M. fuliginosus* in being much shorter, less arched in lateral view and much more robust, with a larger facet for metatarsal V, less plantarly projected proximoplantar ridge and a broader, more planar proximal dorsal surface; and from *W. bicolor* in being much larger and more robust, with a relatively slightly larger proximal plantar tubercle.

Metatarsal V (Fig. 56g–k): broad and very robust, with length to distal facet width index ~4.1–4.8. Proximolateral process quite large, blunt, rugose, transversely compressed and slightly laterally deflected, contributing to the curved shape of the element in dorsal view. Facet for the cuboid broad and concave, covers most of the medial surface of the proximolateral process and continues plantomedially onto the proximal surface of the medial plantar tubercle (Fig. 56k). Facet for metatarsal IV oval to semicircular in dorsomedial view, extends over the dorsal part of the proximomedial surface; articular surface semicontinuous with the facet for the cuboid. Lateral plantar tuberosity broad, moderately elongate and rugose, for the partial insertion of the m. opponens digiti minimi; bounded on the medial margin by a narrow, shallow, curved plantar groove. Medial plantar tubercle small, rounded and

plantomedially projected. Shaft broad; slightly arched in lateral view; cross-section oval and slightly compressed in an oblique plantolateral–dorsomedial plane; narrows toward the midpoint then broadens and increases slightly in height towards the distal end. Distal end very broad, with articular facets similar to those of *P. anak*.

The metatarsal V of *P. mamkurra* **sp. nov.** differs from that of *P. anak* in being generally slightly larger, and broader, with a thinner proximolateral process, cuboid facet less medially tilted in proximal view, broader, smaller and less proximally projected medial plantar tubercle, and a shallower, more curved plantar groove; from *P. viator* **sp. nov.** in being slightly longer, broader, and lower, particularly proximally, with a more dorsally situated and less plantomedially extensive facet for the cuboid; from *P. tumbuna* in being longer, more gracile and more obliquely compressed across shaft, with a more dorsally situated metatarsal IV facet, more elongate lateral plantar tuberosity, and a narrower distal end; from *P. dawsonae* in having a less distally extensive lateral plantar tuberosity; from *P. otibandus* in being larger and broader, with a thinner proximolateral process, larger, broader cuboid facet, and shallower plantar groove; from *C. kitcheneri* in being larger, broader and more robust, lacking the slight kink of the arch of the shaft immediately proximal to the midpoint in lateral view, with a larger lateral plantar tuberosity, larger medial plantar tubercle, and a larger, more caudally extensive facet for the cuboid; from *O. rufus* and *M. fuliginosus* in being relatively much broader and much more robust, with a longer, more laterally projected proximolateral process, broader, more plantomedially projected and more concave cuboid facet, and a broader distal end; and from *W. bicolor* in being much larger, relatively broader and more robust, with a larger proximolateral process.

Pedal phalanges (Figs 57 & 58): proximal phalanx IV: short, broad and dorsoplantarly compressed; proximal articular surface broad and domed, slightly flared laterally. Proximal plantar tubercles low and rugose, separated by a shallow groove. Shaft narrows slightly to a waist, then broadens to a broad distal end; trochlea broad and shallow; fossae for the collateral ligaments fairly shallow and semicircular. Middle phalanx IV: fairly short, broad and dorsoplantarly compressed. Proximal articular surface moderately concave, angled moderately dorsally; dorsal margin convex in dorsal view. Proximal plantar tubercles low and broad. Shaft fairly short with slight waist, broadens gently to distal end; trochlea broad and shallow; fossae for the collateral ligaments fairly shallow and semicircular. Distal phalanx IV: short and robust. Proximal end quite broad, with articular surface concave, and roughly pentagonal in proximal view; transverse margins with V-shaped indentation at midpoints (Fig. 57l). Plantar tubercle large and subrectangular. Shaft arches upward slightly before smoothly curving plantarly (Fig. 57k), with the dorsal peak rounded to very gently rounded-triangular; in dorsal view the medial and lateral margins are very slightly convex and taper slightly beyond the midpoint; tip rounded.

Proximal phalanx V: robust, with the proximal end slightly broader than tall, and large, rounded and rugose plantar tubercles. Proximal articular surface round, concave and medially displaced in proximal view. Shaft with a very slight waist; distal end with the collateral fossae very shallow and large. Middle phalanx V: very short, broad, dorsoplantarly compressed, and decreases in height distally; distinctly asymmetrical, with the proximal and distal surfaces medially and laterally tilted, respectively. Plantar tubercles low and rounded. Proximal articular surface gently concave, domed, tilted dorsally and slightly medially. Shaft extremely short and typically with no waist. Distal end with the fossae for the collateral ligaments tall, shallow and dorsally displaced; trochlea gently concave and the articular surface dorsoplantarly quite short. Distal phalanx V: short, broad and robust, bilaterally asymmetrical, with the dorsal peak medially displaced and the lateral part substantially broadened; proximal end roughly pentagonal in proximal view, medial and lateral margins with slight concavities at midpoints in proximal view; articular surface concave with a very slight medial ridge; plantar tubercle small and rounded in plantar view. Shaft arches upward gently before smoothly curving plantarly, with a slight, rounded dorsal peak; medial and lateral margins very gently convex in dorsal view.

The pedal phalanges of *P. mamkurra* **sp. nov.** differ from those of all compared taxa in their distal phalanges IV and V having a V-shaped divot in the medial and lateral margins of proximal end, and in the having the shafts of distal phalanges IV and V gently arched. They further differ from *P. anak* in being more elongate, with proximal phalanx IV having a more distinct waist that is situated more distally, middle phalanx IV with a relatively far narrower proximal end and a less proximoplantarly extensive distal articular surface; from *P. viator* **sp. nov.** in being generally slightly longer, with deeper collateral fossae on the proximal and middle phalanges, proximal phalanx IV with a broader waist, more elongate middle phalanx IV with relatively smaller, less distally extensive plantar tubercles, distal phalanx IV with a more rounded dorsal peak, and distal phalanx V less asymmetrical; from *P. dawsonae* **sp. nov.** in having proximal phalanx IV with a slightly broader distal end and a slightly narrower waist; from *P. otibandus* in being larger and more elongate, with proximal phalanx IV having a broader distal end and middle phalanx IV having a broader trochlea; from *P. snewini* in being larger, having more elongate middle phalanx IV with a broader distal articular surface and smaller fossae for the collateral ligaments, and a broader distal phalanx IV with a more rounded dorsal peak; from *C. kitcheneri* in being larger, broader and more dorsoplantarly compressed, with broader, shallower trochleae, middle phalanx IV with more a dorsally tilted proximal surface and less caudoplantarly extensive distal articular surface, and distal phalanges with a rounded, almost peak-less dorsal surface; from *O. rufus* and *M. fuliginosus* in being relatively shorter, broader, more dorsoplantarly compressed and much more robust, with distal phalanx IV having a more rounded, less pointed dorsal peak; and from *W. bicolor* in being larger and more robust, with middle phalanx IV having a more dorsally tilted proximal surface.

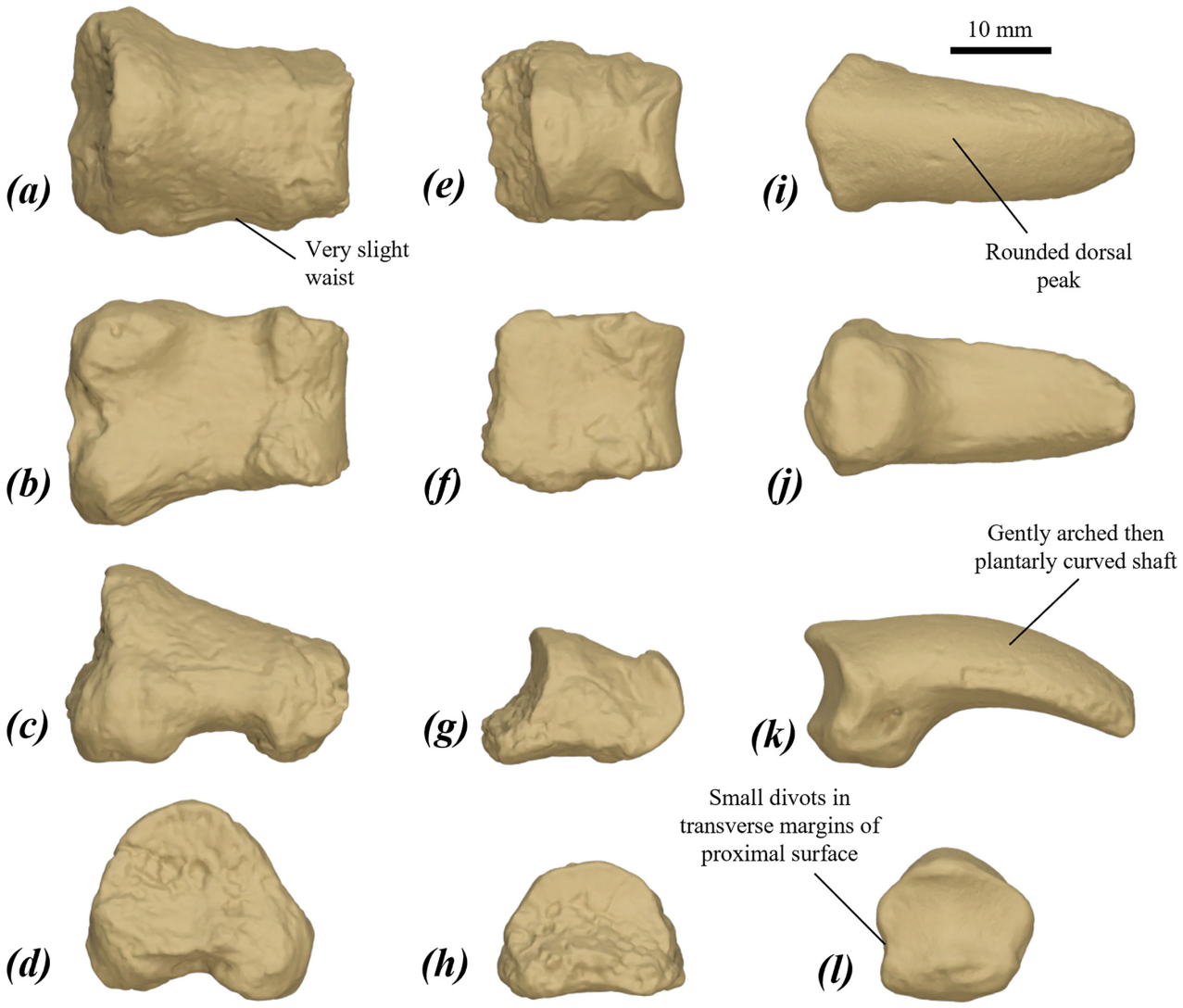

FIGURE 58. surface scan images of (a–d) right proximal, (e–h) left middle, and (i–l) right distal pedal phalanges V of *P. mamkurra* **sp. nov.** in: (a, e, i) dorsal, (b, f, j) plantar, (c, g, k) medial, and (d, h, l) proximal views. Proximal and middle phalanges (a–h) are of WAM 02.7.11; distal phalanx (i–l) is of SAMA P20810.

Remarks:
For a discussion of the taxa *P. roechus* Owen, 1874 and *P. brehus* (Owen, 1874) and their relationship to *P. mamkurra* **sp. nov.** and *P. viator* **sp. nov.**, see the segment at the end of the 'Systematic palaeontology' section titled, 'Status of other species previously referred to *Protemnodon*'.

***Protemnodon viator* sp. nov.**
LSID of new species: urn:lsid:zoobank.org:act:A3A47C56-B6B7-4C0A-853F-B57FEC5A6983

Protemnodon brehus (Owen); Helgen *et al.* (2006), p. 303, appendix 2. See also Janis *et al.* (2020), table 1; Jones *et al.* (2021), table 1; Wagstaffe *et al.* (2022), figs 6 & 7, table 1; Janis *et al.* (2023), SI table 1.

Protemnodon sp. cf. *brehus*; Flannery & Gott (1984), pp. 405, 407 & 408, figs 11 & 12.

Protemnodon sp. cf. *roechus*; Flannery (1984), p. 125, table 1.

Holotype:
SAMA P59552; near complete skeleton, lacking sacrum, caudal vertebrae Ca3, 4 and 15+, L pisiform, hamatum, capitatum, trapezoid, trapezium and four manual phalanges, and L middle pedal phalanx V (Fig. 59). Found wholly articulated and collected by A. B. Camens in 2019.

Type locality:
SIAM Site 5, 29.7832°S, 140.1164°E, Lake Callabonna Fossil Reserve, northeastern South Australia. Lacustrine late Pleistocene fossil deposits (deposited during a drought phase commencing about 48 ka in sediments 54.2–50.4 ka) (McInerney *et al.* 2022). Worthy and Camens *et al*. in 2013, 2014, 2018 and 2019 led joint Flinders University–University of Adelaide expeditions to the lake, recovering a wealth of fossil material including all the type material listed for this species. Lake Callabonna is an ephemeral salt-lake in the far southeast of the Lake Eyre Basin that

FIGURE 59. left lateral view of the semi-complete skeleton of SAMA P59552, the holotype specimen for *Protemnodon viator* **sp. nov.**

forms part of a chain from Lake Gregory to Lake Frome, curving southeasterly around the northern margins of the Gammon Ranges.

Paratypes:

SAMA P53835a (SIAM Site 4, Lake Callabonna, 29.7879°S, 140.1161°E) partial articulated skeleton (preserved with SAMA P53835b); lacking atlas vertebra, sacrum, caudal vertebrae, R forelimb distal to the radial facet on the ulna, and the entire L side except a partial L pes.

SAMA P53835b partial articulated juvenile skeleton *in situ* with SAMA P53835a; cranium with I1–3 and DP2–M1, mandible with i1 and dp2–m1; lacking thoracic vertebrae T4–14 and lumbar, sacral and caudal vertebrae, L ilium, L distal tibia and L pes, and entire R side except the pelvis and manual phalanges.

SAMA P53836 (SIAM Site 5, Lake Callabonna 29.7338°S, 140.1305°E) partial skeleton; cranium, L dentary, R i1; partial L humerus, partial L ulna and distal epiphysis, proximal radius, partial L pisiform, proximal manual phalanx V; R distal fibular epiphysis, L calcaneal fragment, and L middle pedal phalanx V.

SAMA P59550 (Tedford Site, Lake Callabonna, 29.7820°S, 140.1348°E) partial skeleton; cranium with partial L I1 and P3–M4, L and partial R dentaries preserving i1 and p3–m4; vertebrae C1 and partial C2, partial Ca1–4 and 6–9; L scapula, L humerus,

proximal L ulnar fragment and R ulna, partial R radius, R metacarpal III, articulated L metacarpals I–III and proximal–distal manual phalanges I–III; partial LR pelvis, proximal LR femoral fragments, partial R femur, partial LR fabellae, articulated L tibia and fibula, distal R tibial fragments, distal R fibular fragments, LR calcanei, LR tali, partial R cuboid and L cuboid fragment, partial LR naviculars, R and partial L ectocuneiforms, LR proximal metatarsals IV, L and proximal R metatarsals V, proximal plantar sesamoid for metatarsals IV and V, partial LR proximal–distal pedal phalanges IV and V.

SAMA P59548 (SIAM Site 5, 29.7780°S, 140.1403°E) partial cranium with I1–3 and P3–M4, L dentary with i1 and p3–m4.

Referred specimens:

Western Australia

Christmas Creek, Mueller Ranges: WAM 68.10.77 L metatarsal IV; WAM 68.10.78 L metatarsal V; WAM 68.10.80 proximal pedal phalanx V; WAM 68.10.82 proximal pedal phalanx IV.

Quanbun Station, Fitzroy Crossing: WAM 66.7.9 R upper molar; WAM 63.11.8 R i1; WAM 82.7.36 middle pedal phalanx IV.

South Australia

Lake Callabonna Fossil Reserve: SAMA P59551 partial skeleton. SIAM77 'A01' partial cranium; SIAM37 'A07' partial cranium and R dentary; SIAM43 'A08' R dentary; SIAM77 'A02' partial L dentary; SIAM37 'A10' L i1, R humerus and L femur; SIAM37 'A09' L I1, R i1, and L radius; SIAM37 'A11' L radius; SIAM37 'A03/A05' R calcaneus, cuboid, and metatarsals IV and V; SIAM37 'A04/A06' R calcaneus, cuboid, and metatarsal IV; AMNH FM145501 L calcaneus, talus, metatarsals IV and V, and pedal phalanges IV and V. NMNH PAL498886 R calcaneus, cuboid, talus, metatarsal IV, partial metatarsal V, and middle and distal pedal phalanges IV and V.

Cooper's Last, Cooper Creek: SAMA P46824 partial R ulna.

Malkuni Waterhole, Cooper Creek: SAMA P54629 axis vertebra; SAMA P25074 L ilium; SAMA P25098 articulated partial L pes; SAMA P50549 R calcaneus.

Waralamanko Waterhole, Cooper Creek: SAMA P25187 partial L ulna; SAMA P25203 partial L femur.

Site '075' (-28.5609°S, 138.0394°E), Cooper Creek: SAMA P54425 R calcaneus.

Lookout Locality, Warburton River: SAMA P52601 partial juvenile L dentary; SAMA P25290 L metatarsal V.

Mulyanna Site, Warburton River: SAMA P25455 L tibia.

Main Fossil Chamber, Victoria Fossil Cave, Naracoorte: SAMA P59545 R metatarsal V.

New South Wales

Wellington Caves, Wellington (site unknown): AM F16490 neurocranium; AM F104147 R metatarsal IV.

Victoria

Site 1534, Level 2, Lancefield Swamp: NMV P40385 L metatarsal V.

Spring Creek Locality: NMV P42526 partial cranium and L dentary; NMV P173087 L femur and proximal tibial epiphysis.

Specific diagnosis:

Protemnodon viator **sp. nov.** is differentiated from other species of *Protemnodon* by multiple autapomorphies and a unique combination of cranial and postcranial characteristics. The cranium of the species is separated from both *P. mamkurra* **sp. nov.** and *P. anak*, the two species of *Protemnodon* for which the orbit is known, by having a more anteroventrally slanted orbit in lateral view. The forelimb differs from all other species of *Protemnodon* in having: a radius with a more proximally situated cranial ridge; and more gracile metacarpals. The hindlimb differs from all other species of *Protemnodon* in having: a more robust femur, with a more raised, more distinct intercondylar crest and a more medially projected lesser trochanter that form a large, medially projected triangular crest ventral to the femoral head. The pes is distinguished from that of all other species of *Protemnodon* by: its taller, relatively narrower calcaneus with a less medially projected sustentaculum tali; and taller, more transversely compressed metatarsal V.

Protemnodon viator **sp. nov.** is most similar in aspects of cranial morphology to *P. mamkurra* **sp. nov.** It further differs from the cranium of *P. mamkurra* **sp. nov.** by its dorsoventrally shorter rostrum, lower medial ridge on the basioccipital, and more posteroventrally curved exoccipital over the foramen magnum. The dentary of *P. viator* **sp. nov.** cannot be differentiated from that of *P. mamkurra* **sp. nov.**, and is otherwise morphologically closest to *P. dawsonae* **sp. nov.** and *P. anak*, from which it differs in having a taller mandibular corpus when fully grown. The dentition of *P. viator* **sp. nov.** cannot be differentiated from that of *P. mamkurra* **sp. nov.**

Protemnodon viator **sp. nov.** is most similar in aspects of postcranial skeletal morphology to *P. dawsonae* **sp. nov.** and *P. mamkurra* **sp. nov.** The axial skeleton of *P. viator* differs from both *P. mamkurra* **sp. nov.** and *P. dawsonae* **sp. nov.** in having more elongate caudal vertebrae. It is further separated from *P. dawsonae* **sp. nov.** by having a broader axis vertebra with a thicker spinous process, less laterally tilted postzygopophyses with more concave articular surfaces, and a bilobed, rather than rounded, ventral margin of the caudal extremity of the body. Additionally differs from *P. mamkurra* **sp. nov.** in having: an atlas vertebra with lateral vertebral foramina that open caudally, instead of laterally, and broader, more caudally projected wings; a more elongate axis vertebra, with a more caudally projected caudal extremity of the centrum; more elongate cervical vertebrae (C3–7), with a more

horizontal, less roof-like arch, slightly larger pre- and postzygopophyses, and a more caudoventrally projected caudal extremity of the body with a slightly bilobed ventral margin; broader, straighter caudal transverse processes on caudal vertebra Ca7 and broader, straighter cranial processes on Ca8.

The forelimb of *P. viator* **sp. nov.** additionally differs from that of *P. mamkurra* **sp. nov.** in having: a humerus with the peak of the lateral supracondylar ridge less pointed and closer to the distal margin of the pectoral crest; a more gracile ulna; and a more elongate radius with a lower, less distinct caudal ridge and a less craniocaudally compressed distal shaft. The manus differs in having: a scaphoid with a broader palmar process, the facets for the hamatum and capitatum more distinct from each other, and the entire mesial section thickened instead of having a distinct, raised, transverse dorsal ridge for articulation with the styloid process of the radius; proximal phalanges with slightly less proximally projected palmar tubercles; and narrower, less dorsopalmarly compressed distal phalanges with larger, more palmarly projected palmar (flexor) tubercles.

The hindlimb of *P. viator* **sp. nov.** can be differentiated further from that of *P. mamkurra* **sp. nov.** in having: an ilium with a slightly broader lateral iliac spine and a shorter rectus tubercle; a femur with a more raised proximolateral ridge, narrower, deeper trochlea, narrower trochlear crests, the peak of the medial trochlear crest more pointed, and a less medially projected ventral section of the medial epicondyle; and a much more elongate tibia, which is longer relative to femoral length, with a thinner proximal section of the proximolateral crest, the cnemial crest less laterally curved with a more angular and distinct distal peak, and a straighter distal shaft in cranial view. The hindlimb of *P. viator* **sp. nov.** differs from that of *P. dawsonae* **sp. nov.** in having a pelvis with a more deeply concave gluteal fossa and acetabulum.

The pes of *P. viator* **sp. nov.** further differs from that of *P. mamkurra* **sp. nov.** and *P. dawsonae* **sp. nov.** in having: a calcaneus with a more triangular, less rounded calcaneal tuberosity in cross-section; shorter metatarsal IV; metatarsal V with a narrower, more dorsally situated facet for the cuboid; and a proximal pedal phalanx IV with a narrower waist. The pes further differs from *P. dawsonae* **sp. nov.** in having: a calcaneus with a deeper lateral talar facet and a narrower, more rotated medial talar facet; metatarsal V with a taller, less elongate proximolateral process and a less proximally projected medial plantar tubercle; and a proximal phalanx IV with a broader distal end relative to the proximal end. The pes additionally differs from *P. mamkurra* **sp. nov.** in having: a calcaneus with a smaller, more caudally displaced medial talar facet, less convex lateral talar facet, and a smaller, less dorsally bulbous fibular facet; a talus with a less cranially projected talar head and with its navicular facet aligned in the sagittal plane, rather than curving plantomedially; a taller, narrower cuboid with a longer, more plantarly projected lateral plantar tubercle, more plantarly projected medial plantar tubercle, and a deeper, narrower flexor groove; a narrower navicular with a more plantarly extensive ectocuneiform facet; ectocuneiform with a narrower, more plantarly extensive navicular facet and a deeper plantar tubercle that is squarer in medial view; relatively shorter, broader middle phalanx IV; distal phalanx IV having a more triangular dorsal peak and lacking distinct triangular divots on the medial and lateral margins of the proximal surface; and proximal phalanx V with a narrower waist.

Etymology:

Latin; nominative singular noun, meaning 'traveller' or 'wayfarer', in reference to the inferred greater vagility of this species compared to other species of *Protemnodon*.

Description and comparisons:

Cranium and dentition

Cranium (Figs 60 & 61): large and robust, with an elongate neurocranium. *Rostrum*. Rostrum moderately tall and elongate;; slightly ventrally deflected in juveniles, becomes more so with age. Diastema elongate, extends for roughly 70% of rostrum, and consists of slightly more maxilla than premaxilla. Premaxilla elongate, anteroventrally projected; ventral surface broad and flat, ventral width subequal to slightly less than the width across the nasal cavity; incisor-bearing component contributes ~50% of the ventral length from the anterior tip to the premaxilla-maxilla suture; anterodorsal margin slopes dorsoposteriorly (around the anterior margin of the nasal cavity) before curving steadily dorsally to the nasal suture; dorsoposterior part ('walls' of the nasal cavity) gently convex; ventral premaxilla-maxilla suture is angled distinctly posterolaterally, lateral premaxilla-maxilla suture extends straight dorsally before curving smoothly posteriorly toward the posterior of the nasal. The anterolateral surface of the anterior part of the premaxilla is pockmarked with very small foramina. Incisive foramen large and elongate, with a tapering channel extending anterolaterally from the foramen in ventral view, roughly toward I2; more posteriorly positioned relative to the incisors in mature individuals. Buccinator fossa large, smoothly concave, and quite deep, becoming shallower anteriorly; extends dorsally from ventral margin of diastema to midpoint of maxilla, and anteriorly from immediately anterior to P3/DP2 to between premaxilla-maxilla suture and base of I3. Infraorbital foramen large, narrow, opens anteriorly and positioned dorsal to P3/DP2. Nasal narrow, elongate and very slightly convex dorsally, forms slight concavity along mesial suture, with a linear lateral suture; projects anteriorly past the premaxilla and tapers to a mesial point. Frontal strongly concave at midpoint of temporal fossa, broadens toward anterior and flares over orbit; anterior suture with nasal and maxilla sinusoidal.

Lateral cranium. Temporal fossa elongate, with orbit slanted distinctly anteroventrally in lateral view (Fig. 60a). Lacrimal quite large and laterally projected, with small dorsoposterior foramen and larger anteroventral foramen, both with rounded tubercle situated immediately dorsoposteriorly, particularly large in some specimens. Masseteric process similar to that of *P. mamkurra* **sp. nov.**

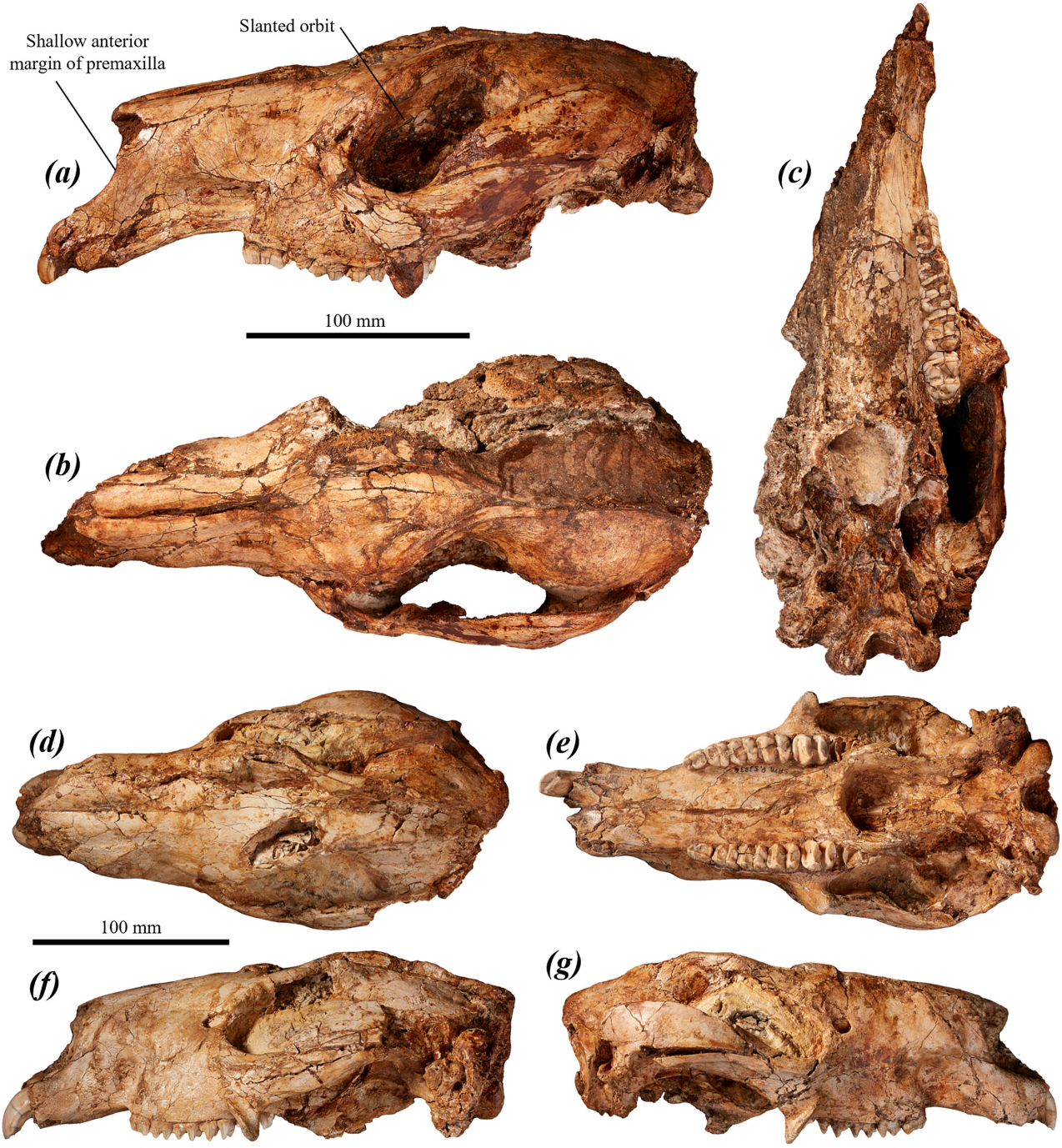

FIGURE 60. crania of *P. viator* **sp. nov.**: (a–c) partial cranium of paratype SAMA P59550 in (a) left lateral, (b) dorsal, and (c) ventral views; and (d–g) young adult cranium of paratype SAMA P53836 in (d) dorsal, (e) ventral, (f) left lateral, and (g) right lateral views.

Jugal dorsal surface flattened and slightly flared; curves dorsally posteriorly and bifurcates into a short, broad postorbital process and an elongate, narrow, ventrolaterally situated posterior part reaching almost to the glenoid fossa; posterolateral surface with low, angular ridge, merging anteriorly into laterally projected lip from ventral margin of orbit. The zygomatic arch is orientated dorsoposteriorly at 40–45° relative to axis of cheek tooth row. Zygomatic process of squamosal tilted slightly dorsally, posteriorly tall, smoothly convex laterally and with dorsal margin smoothly convex, particularly in older individuals; tapers anteriorly to elongate point between the postorbital process and the posterior part of the jugal.

Palatal region. Maxilla ventrally broad, and flat to very gently concave. Maxillary foramen quite large, round and opens posteriorly, with a broad, rounded valley extending posteriorly from the opening; sphenopalatine foramen round and slightly smaller. Palatine thick, broad and lacking fenestrae, with a narrow, elongate anterolateral foramen level with the anterior of M3, and a small,

rounded posterolateral foramen adjacent to the posterior of M4; lateral margin tapers gently anteriorly before forming a linear transverse maxilla-palatine suture level with the abutment of M2–M3; posterior margin concave to slightly V-shaped, situated posterior to M4. Pterygoid crest thin and elongate, with the anterior peak tall and slightly posteriorly deflected. Pterygoid (anteromedial) wing of the alisphenoid relatively low and thick, abuts the pterygoid crest laterally, flares posterolaterally and lowers to merge into the body of the alisphenoid.

Dorsal and posterior cranium. Parietals broad and smoothly convex. Supraoccipital broad and quite tall, smoothly curves posteriorly toward the foramen magnum, such that the exoccipital projects beyond the posterior margin of the parietal and the supraoccipital is slightly concave; dorsolateral margin is rounded and dorsal margin is flattened; a very low, broad medial ridge is occasionally present; supraoccipital is low in juveniles, height increases relative to width with age though height typically does not exceed occipital width. Foramen magnum broad, oval and slightly to moderately dorsoventrally compressed. Occipital condyles large and quite tall; situated lateral to and angled obliquely beneath the foramen magnum, not extending dorsally beyond the dorsal margin of the foramen magnum (Fig. 61b); taper ventromedially in posterior view and project posteriorly well beyond the margin of the occipitals in lateral view; in young individuals, the dorsolateral margin of each condyle is ventral to a rounded and variably shallow foramen on the exoccipital, becoming obscured by larger, more elongate condyles in older individuals.

Neurocranial region. Temporal crest morphology and ossification are as in *P. anak*. Basioccipital broad and smoothly convex, with a low medial ridge that becomes more raised and angular with age (Fig. 61a); condyloid foramen is rounded, partially to completely covered by the anteroventral margin of the occipital condyles in ventral view. Medial pterygoid origin thin and tall; curves anteromedially to continue anteriorly into the pterygoid crest. Pterygoid fossa very deep and elongate, bordered by a low, narrow, rounded anteroposterior ridge extending from the base of the pterygoid wing of the alisphenoid to abut the medial margin of the foramen ovale. Anterolateral surface of the body of the alisphenoid is broad, and flat to gently convex; extends from the foramen ovale to the petrotympanic fissure, with a very small, rugose eminence abutting the medial margin of the anterior process of the ectotympanic. Glenoid fossa broad, flat and abutting the postglenoid process posteriorly. Postglenoid process moderately well-developed, tapering to a pointed or squared ventral margin; angled anterolaterally in ventral view, with the posteromedial component extending ventrally into, and semi-fused with, the anterior process of the ectotympanic, forming a deep, anterior-facing ventral postglenoid foramen. Ectotympanic has a large, rugose anterior process projected ventral to and medial to the postglenoid process. External auditory meatus roughly cylindrical, angled dorsolaterally; not projected laterally beyond the margin of the anterior process of the ectotympanic.

The cranium of *P. viator* **sp. nov.** differs from all compared taxa in possessing a more anteroventrally slanted orbit; from *P. anak* in being relatively broader, with a slightly shorter diastema relative to cranial length, generally broader, slightly more curved, more ventrally situated occipital condyles, and in lacking a thin anterior jugal ridge; from *P. mamkurra* **sp. nov.** in having a dorsoventrally shorter rostrum, taller, straighter, generally more dorsally situated occipital condyles, a more posteroventrally curved exoccipital, and a lower, more rounded medial ridge on the basioccipital; from *C. kitcheneri* in being larger, relatively broader and more robust, lacking a bony nasal cavity 'pocket', and having a less domed, less anteriorly projecting nasal, a taller, more robust anterior part of the premaxilla, larger masseteric process, a much thicker and less laterally projected ventral orbital rim, taller zygomatic arch, more posteriorly projected occipital condyles, a single anteroposterior ridge meeting the medial margin of the foramen ovale, and the anterior process of the ectotympanic extending to the ventral or ventromedial tip of the postglenoid process (rather than wrapping around posterior surface); and from *W. bicolor* in being much larger, lacking a small, pointed, anteriorly projected eminence on the anterior margin of the jugal, and having a more ventrally projected anterior part of the premaxilla, larger masseteric process, more robust palatine lacking fenestra, more posteriorly projected occipital condyles, more raised anteroposterior ridge meeting the medial margin of the foramen ovale, relatively larger, more laterally extensive anterior process of the ectotympanic, and a taller, more laterally projected postglenoid process.

Upper dentition (Fig. 62): I1: broad, robust and arcuate, with thick buccal enamel extending around to the edges of the lingual surface; buccal surface smooth and gently convex, with a very shallow vertical groove in juveniles; occlusal surface oval; with wear, the enamel recedes from the lingual surface and the occlusal surface narrows and deepens, occasionally develops a distinct angle between the top of the buccal enamel and the dentine (Fig. 62b). I2: small and narrow, with gently convex buccal enamel extending onto the lingual margins; posterolingual crest small, with an associated mesial groove on the buccal enamel, lost when tooth is slightly worn; enamel recedes from the lingual surface and the occlusal surface shortens and broadens with wear. I3: elongate, transversely compressed and trapezoidal to roughly triangular in buccal view; buccal enamel convex, buccal length less than the width of I1 (Fig. 62a). Main curves anterolingually to sit lingual to the posterior margin of the similarly shaped anterobuccal crest. Anterobuccal crest is around half the length of the main crest.

The cheek teeth are high-crowned. DP2: morphologically very similar to P3 but anteroposteriorly truncated; quite short, broad and oblong, broadens posteriorly, with thickened peaks over the anterior and posterior roots linked by the high main crest. Main crest blade-like, anteroposteriorly to slightly posterobuccally orientated, and jagged to gently undulating in lateral view, with a very low, dorsoventrally aligned ridgelet on the

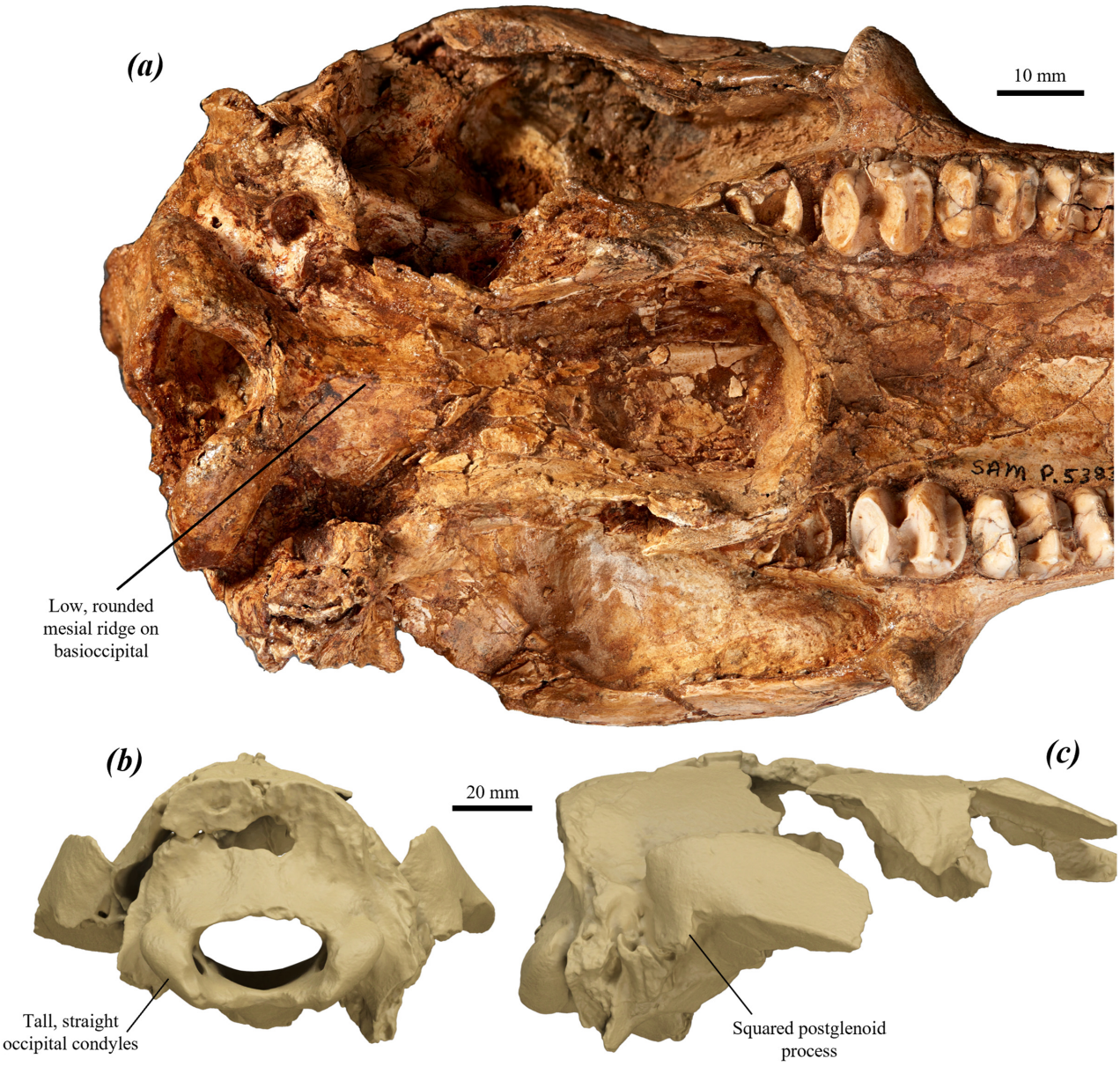

FIGURE 61. neurocrania of *P. viator* **sp. nov.**: (a) ventral view of partial cranium of paratype SAMA P59550 showing the basicranium; and (b–c) surface scan images of partial neurocranium of NMV P42526 in (b) posterior, and (c) right lateral views.

midpoint of the buccal face. Lingual crest low and gently undulating in lingual view, extends from the lingual base of the anterior cusp to the small, secondary posterolingual peak; lingually borders a broad, anteriorly tapering lingual basin, perpendicularly transected by a low ridgelet anterior to the midpoint. A small posterior basin with moderately high anterior and posterior margins sits at the posterior margin of the DP2, between the posterior and posterolingual peaks, removed by a small amount of wear. DP3: molariform, short and broad, with the protoloph and metaloph markedly narrower than the swollen loph bases; anterior loph longer and narrower than the posterior loph. Precingulum small, narrower than the anterior loph, merges buccally with the thin, low but distinct preparacrista. Postparacrista thin and distinct, extends straight from the paracone to the buccal margin of the interloph valley. Postprotocrista and postmetaconulecrista curve gently toward the midline of the tooth; in some specimens, postprotocrista extends onto anterior face of metaloph as a low but distinct crest.

P3: large, elongate and oblong, tapers to a small, blunted cusp at the anterior base; generally slightly broader posteriorly, with posterior margin rounded; in occlusal view, P3 varies from straight to slightly buccally curved toward the posterior, with the posterior component very slightly rotated buccally, contributing to the occasional slightly crescentic shape of the tooth. Thickened peaks over the anterior and posterior roots are linked by the tall main crest. Main crest high, blade-like and roughly anteroposteriorly orientated with occasional very slight posterobuccal curvature in occlusal view, slightly jagged to gently undulating in lateral view with two or three low

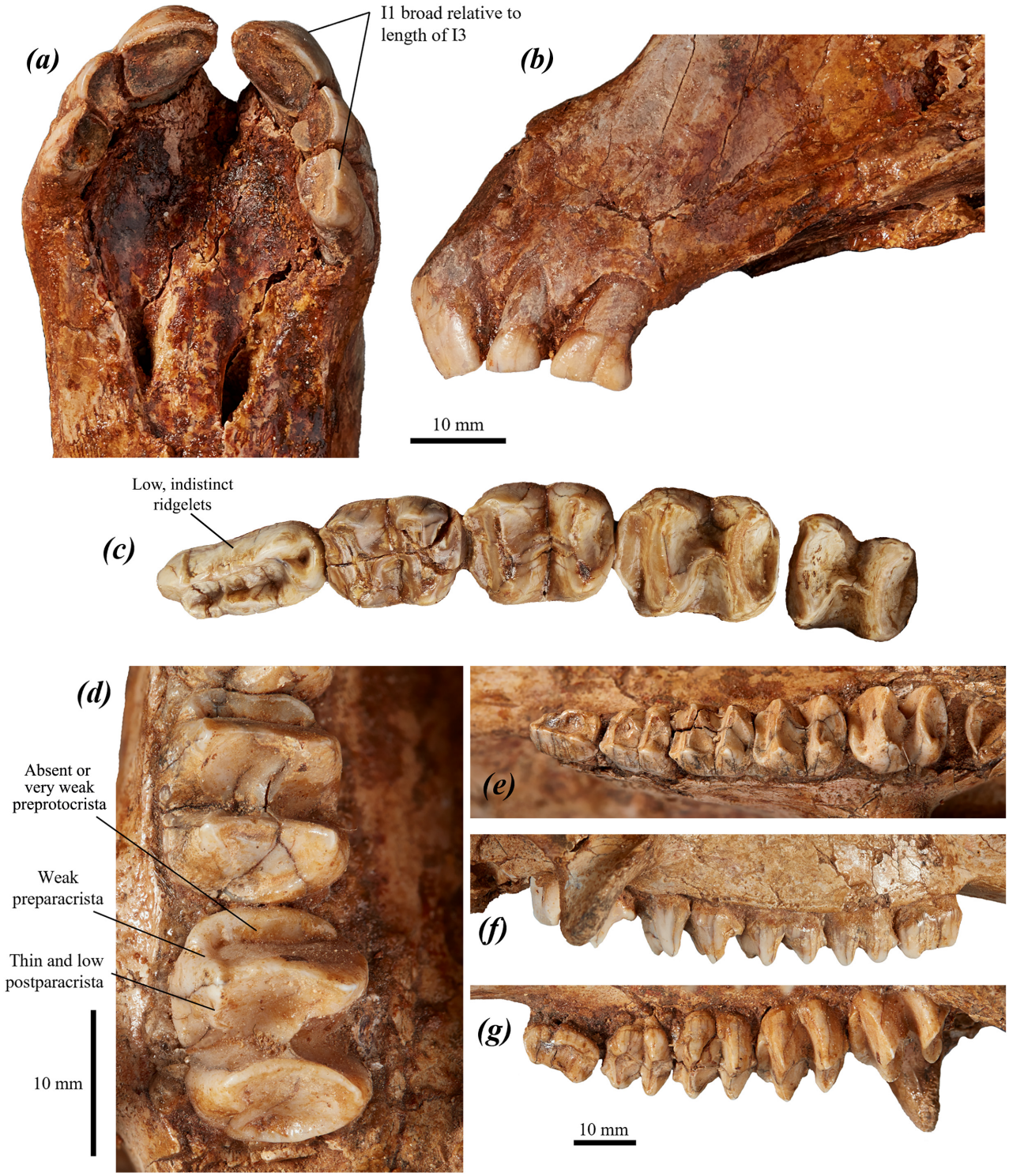

FIGURE 62. upper dentition of *P. viator* **sp. nov.**: (a–b) premaxillae, with heavily worn left and right I1–3, of holotype SAMA P59552 in (a) occlusal, (b) left lateral/buccal views; (c) heavily worn P3–M4 of paratype SAMA P59550 in occlusal view; (d) M2–3 of paratype SAMA P53836 in occlusal view; and (e–g) DP2–M3 of paratype SAMA P53836 in (e) occlusal, (f) buccal, and (g) lingual views.

to very low, dorsoventrally aligned ridgelets on the midpoint of the buccal face. Anterior cusp generally slightly narrower than the posterior, with the peak tall and coming to a rounded point; peak intersected by very brief transverse crest. Lingual crest moderately high, extends from the lingual base of the anterior cusp to merge into the posterolingual peak, with two or three gentle, rounded peaks. Lingual crest borders broad lingual basin, which is perpendicularly transected by one to three very low, indistinct ridgelets. Main posterior peak quite tall and

rounded, continuous with the main crest, which extends and broadens posteriorly to merge with a low, narrow transverse posterior crest. Posterolingual peak rounded, lower than the main peak and linked to the main crest by a thin transverse crest, anteriorly bordering the posterior basin. A small posterior basin sits between the main and posterolingual peaks, posteriorly bordered by the transverse posterior crest, removed by a small amount of wear.

Molars: rounded-rectangular; interloph valley generally slightly narrower than the lophs; occasionally the M1, and more rarely M2, are rounded, with a broad interloph valley. Lingual and buccal margins of the lophs slightly to moderately convex in posterior view, particularly the anterior lophs, with the protoloph and metaloph narrower than the corresponding loph base; unworn protolophs and metalophs are gently concave posteriorly in occlusal view. Precingulum variably broad, narrower than the anterior loph, extends from the anterobuccal margin to adjacent to the anterolingual margin, gently medially tilted; flat, broad and shelf-like when worn; generally becoming slightly larger, broader and more projected toward M4; some specimens with small enamel crenulations on occlusal surface; preprotocrista absent or very slight. Preparacrista usually absent, sometimes present but very low and indistinct. Postparacrista thin and low but distinct; initially straight before curving lingually to be adjacent to or merging with the buccal component of the postprotocrista in the interloph valley. Postprotocrista relatively thicker, straighter and more raised, extends from the protocone to around the midpoint of the interloph valley; in most specimens, the postprotocrista extends to or near to the metaconule as a low, thin crest. A very small, rounded cusp is variably present (on one or more molars, sometimes on only one side of the dentition) on the base of the protoloph on the buccal margin of the interloph valley (Fig. 62d), and/or on the base of the metaloph in the interloph valley abutting the lingual margin (see SAMA P53836), with either or both cusps occasionally present in DP3. Premetacrista very slight, extends from the metacone to meet the base of the postparacrista in the interloph valley Postmetaconulecrista quite thick and raised, arises from the metaconule and curves dorsobuccally to form an oblique shelf beneath the posterior basin. Postmetacrista lower, shorter and less distinct; arises from the metacone and deflects lingually to merge into the buccal margin of the posterior basin.

The upper dentition of *P. viator* **sp. nov.** differs from that of *P. anak* in being generally larger, with a broader I1 relative to the length of I3, a relatively broader DP2–3, a DP3 with a very slight to absent preprotocrista and a complete protoloph, a more robust and relatively broader P3 across the anterior cusp with lower, less distinct transverse ridgelets on the main crest and a higher, less jagged and relatively more elongate (more anteriorly extensive) lingual crest, and generally relatively broader molars with lower, less distinct preparacrista; from *P. mamkurra* **sp. nov.** in being generally larger, with P3 with a slightly broader anterior relative to length and relatively narrower anterior loph of M1; from *P. tumbuna* in being larger and higher crowned, with the molars generally less rounded in occlusal view, precingulum more anteriorly projected, and the postprotocrista higher and more distinct; from *P. dawsonae* **sp. nov.** in being larger, with a broader I1 relative to I3, relatively slightly narrower posterior molars, and molars with a less distinct and gently curved (rather than kinked) postparacrista; from *P. otibandus* in being larger and higher crowned, with broader I1, less raised and less distinct transverse ridgelets on P3, relatively broader DP2 and 3, DP2 with fewer and lower transverse ridgelets, and molars always lacking a urocrista and having the postprotocrista, postmetacrista and postmetaconulecrista higher and more distinct; from *P. snewini* in being much larger and higher crowned, with P3 relatively broader, and molars relatively narrower, with higher and more distinct postprotocrista, postmetacrista and postmetaconulecrista; from *C. kitcheneri* in being much larger and higher crowned, with P3 broader anteriorly, longer relative to the molars and with a higher, relatively longer lingual crest, and molars with a higher postprotocrista; and from *W. bicolor* in being much larger and higher crowned, with a relatively broader I1, P3 with a higher lingual crest and a larger posterior basin, and molars with a thicker postprotocrista distinctly extending to the protocone, rather than merging into the centre of the posterior surface of the protoloph.

Dentary (Fig. 63a–f): robust, tall and transversely compressed, with a moderately elongate and gently tapering diastema projected straight or slightly deflected dorsally. Mandibular symphyseal plate elongate, extends along the entirety of the diastema to abut the posterior margin of i1. Mental foramen round to oval, opens laterally to anterolaterally, located roughly one-quarter of the distance from dp2/p3 to i1 and between one-quarter and one-third of the distance from the dorsal margin of the diastema to the ventral margin. Depth of the mandibular corpus decreases slightly from below p3 to m4. Digastric sulcus broad, varies from shallow to very shallow, extends from beneath the posterior of the molar row toward the anteroventral margin of the medial pterygoid fossa. Buccinator sulcus distinct but quite shallow, extends along the buccal surface of the mandibular corpus with a slight ventral tilt posteriorly, slightly ventral to the three–four anteriormost cheek teeth.

Ascending ramus tall and slightly convex medially. Coronoid crest angled 70–90° from the plane of the tooth row; straight to slightly convex; coronoid process becomes anteroposteriorly shorter dorsally and curves to a rounded, posteriorly projected crest; crest smaller and more pointed in juveniles. Masseteric fossa tall, shallow, broadly U-shaped in lateral view; bounded anteriorly and ventrally by a low ridge; posterior part is shallower than the anterior component, with a posterolateral lip from the laterally projected 'shoulder' present on the base of the condylar process. Masseteric foramen deep, oval, elongate and transversely compressed; situated in the anteroventral part of the masseteric fossa, abutting the anterior margin and sharing the anterior part of the lateral lip. Masseteric dental canal very deep, separated from the mandibular foramen and the inferior dental canal by a narrow dorsal

crest running anteroposteriorly. Medial pterygoid fossa large, broad and very deeply concave, broadened and deepened by the tall, medially projected angular process. Mandibular foramen moderately sized, round to oval, and transversely compressed. Angular process present as a thin anteroposterior crest, extends dorsoposteriorly along the posterior component of medial margin of medial pterygoid fossa, unprojected posteriorly. Posteroventral margin of dentary rounded and smoothly convex in lateral view, straightens dorsally to meet the posteroventral margin of the mandibular condyle. Condylar process tall, not posteriorly projected; occasional very slight dorsal projection. Mandibular condyle flat and smooth, oval with a small indent in the posterior margin, slightly anteroposteriorly compressed and tilted medially and slightly anteriorly.

The dentary of *P. viator* **sp. nov.** cannot be differentiated from that of *P. mamkurra* **sp. nov.** It differs from that of *P. anak* in being generally larger, broader and more robust, with a shorter, more dorsally deflected diastema relative to tooth row length; from *P. tumbuna* in being larger, with a more anterodorsally situated mental foramen and a straighter, slightly more posteriorly deflected coronoid crest; from *P. dawsonae* in being generally larger; from *P. otibandus* in being larger and more robust, with a more robust diastema, taller mandibular corpus, shallower posterior part of the masseteric fossa, and a less anteriorly tilted mandibular condyle; from *P. snewini* in being larger and more robust, with a much taller mandibular corpus, particularly posteriorly, a less elongate and taller diastema relative to the mandibular corpus, and a squarer, less posteriorly projected angular process; from *C. kitcheneri* in being larger and more robust, with a relatively shorter, more dorsally deflected diastema, more posteroventrally situated mental foramen, taller mandibular corpus, deeper buccinator sulcus, anteroposteriorly longer coronoid process, deeper medial pterygoid fossa with a higher posterior margin, larger dorsal septum partially separating the masseteric and mandibular foramina, and a relatively dorsally situated masseteric fossa; and from *W. bicolor* in being much larger, with a more dorsally deflected diastema, a deeper buccinator sulcus, a broader, more oval mandibular condyle, and a larger dorsal septum partially separating masseteric and mandibular foramina.

Lower dentition (Fig. 63d–g): i1: procumbent, broad and robust; acuminate and ventrobuccally-dorsolingually compressed when unworn, cross-section becomes shorter and rounder with wear. Thick enamel completely covers the buccal surface. Dorsobuccal margin has a thin, raised enamel crest. The enamel is thick and rounded around the ventrolingual margin and covers the ventral half of the lingual surface when unworn, with the lingual enamel layer tapering posteriorly such that well-worn i1s lack lingual enamel.

The cheek teeth are high-crowned. Tooth rows are roughly straight and parallel in occlusal view, occasionally very slightly convex in juveniles; in lateral view, tooth row is sloped slightly ventrally toward the posterior; the proportional rate of wear along the tooth row is highly variable as a result of the variability of the tooth row angle. dp2: morphologically very similar to p3 but anteroposteriorly about half as long; blade-like, tall and triangular in cross-section, roughly oblong to mucronate in occlusal view, broadens gently to the posterior. Main crest thin, gently undulating, aligned anteroposteriorly, extends from over the anterior root to over the posterior root and twists lingually to the posterolingual extremity; buccal and lingual surfaces have a very low, indistinct ridgelet or undulations aligned dorsoventrally. Anterior cuspid semi-distinct from the main crest, being slightly broader with slightly raised posterior margins. dp3: molariform, very similar to the morphology of m1 but relatively narrow; both the lophids crests are significantly narrower than the bases, and are slightly convex posteriorly in occlusal view when unworn to moderately worn; lophid bases bulge slightly buccally. Precingulid fairly small, variably narrow, width tapers anteriorly. Paracristid thin, encircles the base of the premetacristid and curves around the anterior margin of the precingulid, creating a distinct, deep trigonid basin, then turns posteriorly, climbs rapidly and twists buccally to the protoconid; when worn, it extends posteriorly as a low ridge and curves buccally to the protoconid. Premetacristid low and thin, climbs posterolingually from the trigonid basin with a slight buccal curve to the metaconid; removed by a small amount of wear. Postprotocristid very slight to absent, anteroposteriorly aligned, merges with the cristid obliqua in the interlophid valley. Cristid obliqua slightly buccally displaced, thin and moderately high when unworn; mostly part of the trigonid, with a low talonid contribution extending to the hypoconid. Preentocristid low and broad, extends lingually from adjacent to the cristid obliqua to the entoconid. Postcingulid small, shelf-like to slight and lipped, slightly narrower than the posterior of the talonid base.

p3: blade-like, tall and triangular in cross-section with 'bulging' buccal and lingual bases, elongate and oblong in occlusal view; typically with a slight waist, occasionally with parallel or posteriorly diverging margins or a slight bulge around the centre; typically broader across the posterior root than the anterior root. Anterior cuspid has its posterior margins marked by posterior facing ridgelets that occasionally extend dorsally to form a short transverse crest that intersects main crest; anterior cuspid occasionally has a slight anterior eminence at its base. Main crest linear, anteroposteriorly aligned, twists distinctly lingually over the posterior root; lingual and buccal surfaces with one to three low, rounded, indistinct, roughly dorsoventrally aligned ridgelets on crest, such that unworn and slightly worn crest appears slightly jagged in buccal view.

Molars: rounded-rectangular in occlusal view, with the interlophid valley slightly broader to narrower than the lophid bases; when unworn or slightly worn, the protolophid and hypolophid are posteriorly convex or have a mesial kink toward the posterior in occlusal view; lingual component of the hypolophid is slightly posteriorly tilted, becoming straight and perpendicular to the tooth row centreline with moderate wear; buccal margins of the

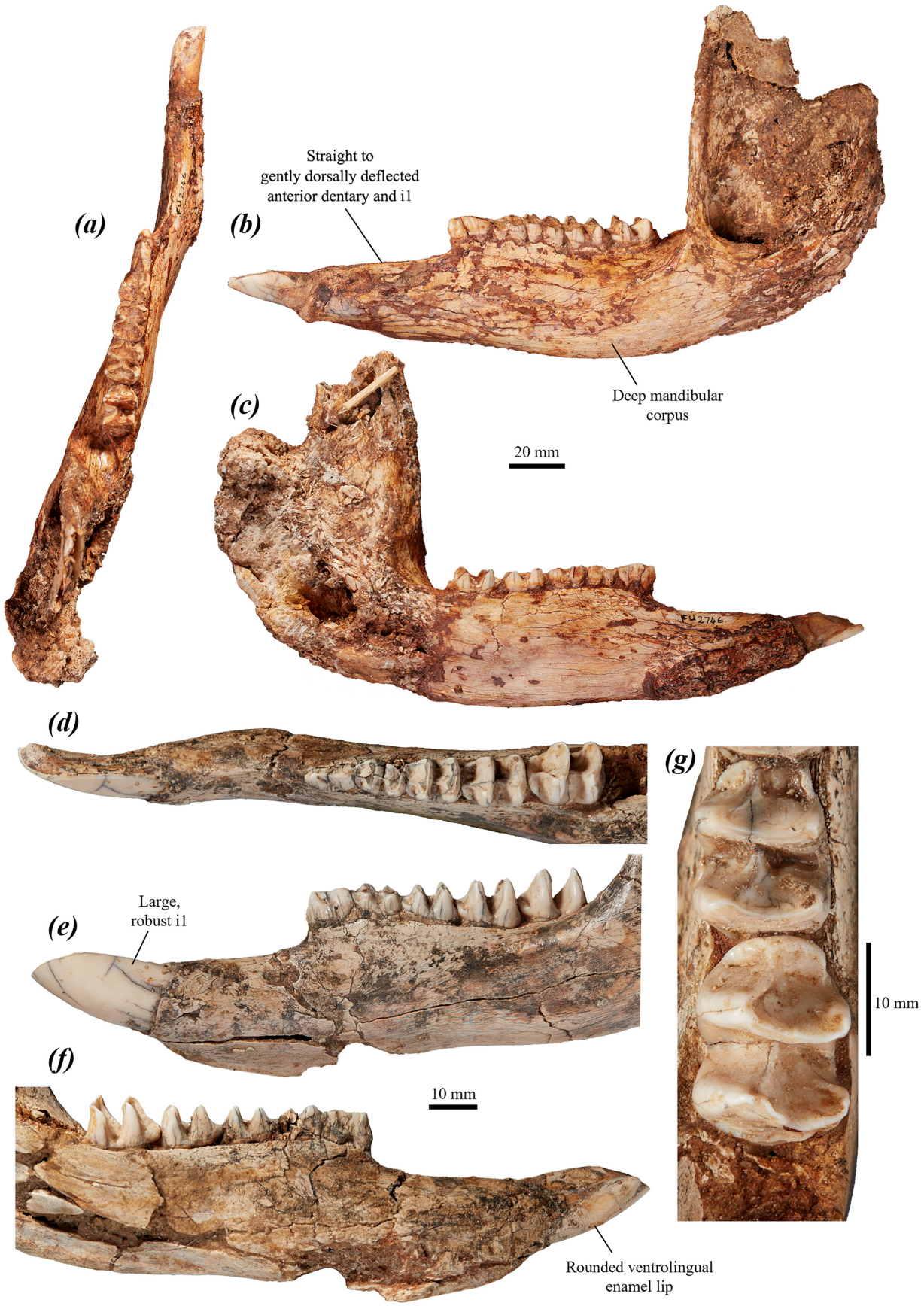

FIGURE 63. lower dentition of *P. viator* **sp. nov.**: (a–c) left dentary of paratype SAMA P59550 in (a) occlusal, (b) buccal, and (c) lingual views; (d–f) left dentary, with i1 and dp2–m3, of paratype SAMA P53836 in (d) occlusal, (e) buccal, and (f) lingual views; and (g) m2–3 of SAMA P53836 in occlusal view.

lophids slightly more convex than the lingual margins in posterior view. Precingulid fairly large, typically comes to a rounded point but is sometimes rounded. Paracristid thick and raised; lingual component anterolingually projected, bounds anterobuccal margin of trigonid basin then ascends posteriorly and curves gently buccally to the protoconid; the degree of buccal curve increases with molar wear. When unworn, the protoconid is higher than the metaconid; 'folding' of protoconid enamel is as in *P. anak* and *P. mamkurra* **sp. nov.** Cristid obliqua thick and quite low, mostly part of the talonid, arises from the midpoint or slightly buccal to the midpoint of the interlophid valley, curves very slightly buccally and extends to the hypoconid. Preentocristid very low, broad and indistinct, arises midway between the base of the cristid obliqua and the lingual extremity of the interlophid valley and deflects slightly lingually to meet the entoconid. When little worn, the hypoconid is distinctly taller than the entoconid and slightly lingually displaced. Postcingulid narrow and slight on m1–m2, becomes broader and shelf-like in m3 and particularly in m4.

The lower dentition of *P. viator* **sp. nov.** differs from that of all other species of *Protemnodon* except *P. mamkurra* **sp. nov.** in having a broader posterior of the p3 relative to length. It further differs from *P. anak* in having broader i1 with less raised dorsobuccal crest and lacking ventrolingual crest, dp2 slightly broader, p3 with fewer, less raised and less distinct ridgelets on main crest, and larger, generally relatively broader molars with a smaller precingulid and more convex buccal lophid margins; from *P. mamkurra* **sp. nov.** in being generally larger; from *P. tumbuna* in being larger and higher crowned, with relatively larger, broader i1 lacking a ventrolingual crest, relatively broader p3, and m3–4 with less convex buccal lophid margins and a less raised premetacristid; from *P. dawsonae* **sp. nov.** in being generally larger and higher crowned, with i1 lacking a low, thick ventrolingual crest; from *P. otibandus* in being larger and higher crowned, with relatively larger, broader i1 lacking a ventrolingual crest, relatively broader p3 and m3–4 with less convex buccal lophid margins; from *P. snewini* in being larger and higher crowned, with relatively larger, broader and more dorsally deflected i1 lacking a ventrolingual crest and having enamel more extensive across the ventral component of the lingual surface, p3 with fewer, less distinct ridgelets on the main crest, and molars with a smaller precingulid and larger premetacristid; from *C. kitcheneri* in being larger and higher crowned, with broader, more spatulate i1 lacking a ventrolingual crest, relatively broader dp2 and 3, larger and absolutely more elongate p3 that is longer relative to molar lengths, and molars with narrower lophid crests, a stronger premetacristid, higher cristid obliqua, and a postcingulid present; and from *W. bicolor* in being much larger, with a broader, more spatulate i1 lacking a ventrolingual crest, p3 with less raised, less distinct ridgelets on the main crest, and molars with narrower lophid crests, generally more anteriorly projected precingulid, and a thicker, lower cristid obliqua.

Axial skeleton

Atlas (C1) (Fig. 64a–d): large, broad and quite robust. Arch thick and deep, with a raised, rugose, cranially situated dorsal tubercle. Cranial articular surfaces very broad, deeply concave, particularly in dorsoventral plane, and angled strongly medially; ventromedial components narrow to rounded points. Ventromedial processes elongate, rounded in ventral view, and close medially but not touching. Caudal articular surfaces rounded, gently concave, and very slightly extending down the ventromedial processes. Wings large, broad, and flaring from a craniocaudally deep base; extend caudally to or beyond caudal extent of caudal articular surfaces (Fig. 64c). Lateral vertebral foramina large, quite broad, craniocaudally shallow and opening dorsocaudally (Fig. 64d); extend from immediately cranial to base of wings onto dorsolateral surface of arch.

The atlas vertebra of *P. viator* **sp. nov.** differs from that of *P. anak* in having a slightly less deep arch and more rounded caudal articular surfaces; from *P. mamkurra* **sp. nov.** in having lateral vertebral foramina that open caudally instead of laterally, with broader, caudally projected wings; from *C. kitcheneri* in being larger and relatively broader, with a deeper arch, larger dorsal tubercle, lateral vertebral foramina opening caudally, and less caudally projected caudal articular surfaces, and lacking a broad groove that extends ventrally from the lateral ventral foramina; from *O. rufus* in being larger, with a deeper arch, dorsal tubercle present and broader and more caudally deflected wings; from *M. fuliginosus* in being larger, with a dorsal tubercle present, and broader, more caudally deflected wings; and from *W. bicolor* in being larger, relatively slightly taller and more solidly built, with a rounder, less pointed dens, rounded and slightly taller cranial articular surfaces, a less convex dorsal margin of the spinous process, and a broader caudal extremity of the centrum.

Axis (C2) (Fig. 64e–h): moderately craniocaudally short, quite broad and robust. Dens elongate and gently dorsally deflected. Cranial articular surfaces broad, tall and gently convex; angled laterally and very slightly dorsally. Arch quite thick, tall and roof-like. Vertebral canal rounded to domed. Spinous process tall, very elongate and tilted strongly cranially, with the dorsal margin linear (Fig. 64e); cranial component thickened, rugose and projected slightly beyond cranial margin of arch, narrows caudally before thickening to very elongate, projected caudal extremity, extending caudally beyond margin of postzygopophyses and caudal extremity of the centrum. Postzygopophyses quite small, caudally projected and flared laterally; articular surfaces concave and face ventrally, with a very slight caudal and lateral tilt. Transverse processes abraded; bases preserved interpreted as suggesting quite short and thin morphology. Ventral surface of the centrum broad and rugose, with low, elongate, rugose tubercle on mesial midline of cranial component and broad, shallow fossae either side of the base of the caudal extremity of the centrum. Caudal extremity of the centrum very slightly caudally projected, gently dorsoventrally compressed and slightly dorsally tilted, with gently bilobed ventral margin (Fig. 64h) projecting very slightly caudally.

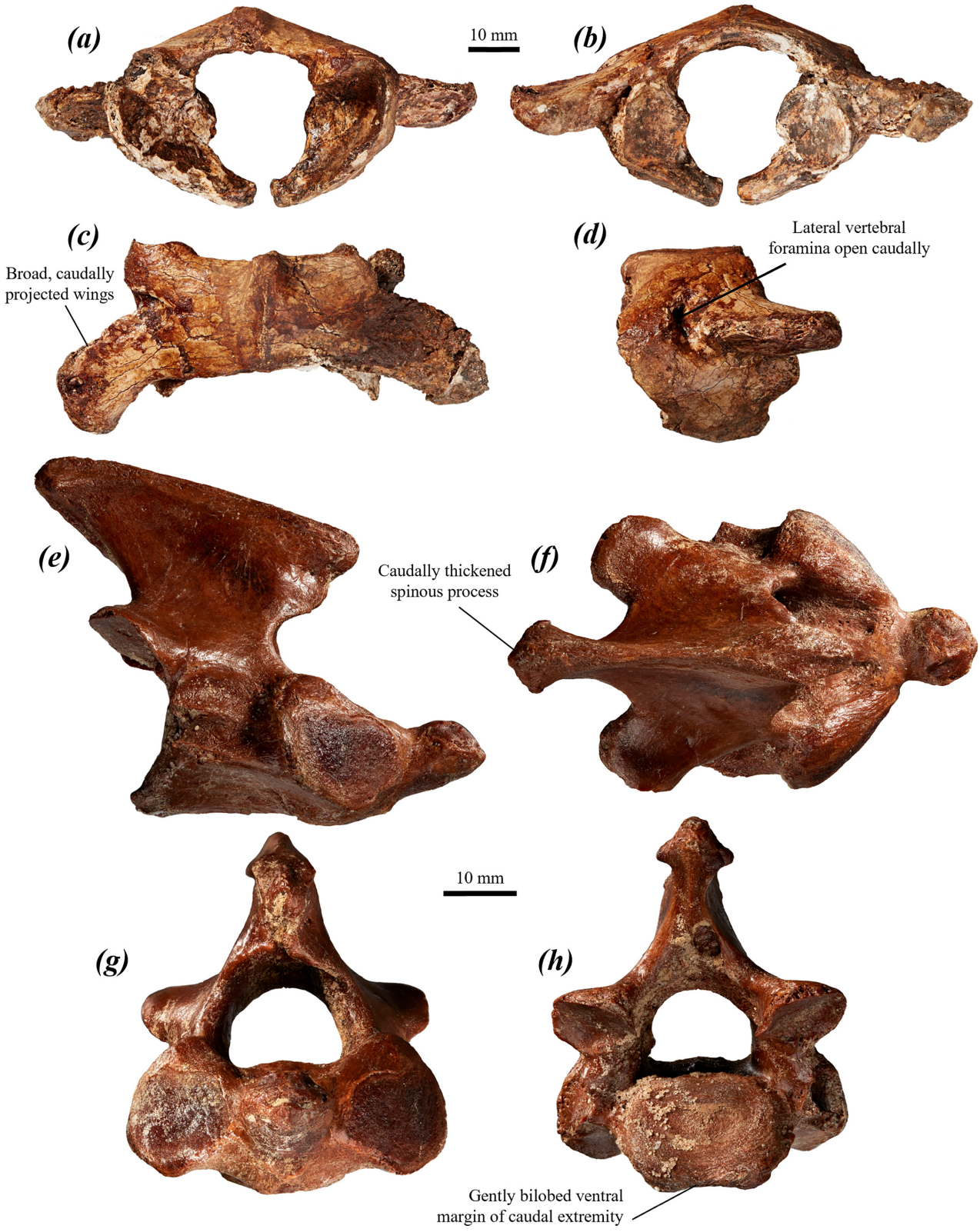

FIGURE 64. cervical vertebrae of *P. viator* **sp. nov.**: (a–d) partial atlas vertebra of paratype SAMA P59550 in (a) cranial, (b) caudal, (c) dorsal, and (d) left lateral views; (e–h) axis vertebra of SAMA P54629 in (e) right lateral, (f) dorsal, (g) cranial, and (h) caudal views.

The axis of *P. viator* **sp. nov.** differs from that of *P. anak* in being much less elongate, with more convex and dorsolaterally tilted cranial articular surfaces, a shorter and more dorsally deflected dens, smaller, more rounded postzygopophyses, a more caudally projected spinous process with a more cranially tilted dorsal margin and a less elongate base, and a much less caudally projected caudal extremity of the centrum; from *P. mamkurra* **sp. nov.** in being longer relative to width, with caudal extremity of the centrum more caudally projected; from *P. dawsonae* **sp. nov.** in being larger and broader, with a broader spinous process, less laterally tilted postzygopophyses with more concave articular surfaces, and a bilobed, rather than rounded, ventral margin of the caudal extremity of the centrum; from *C. kitcheneri* in being larger, and broader relative to depth, with a broader, more cranially slanted and more caudally extensive spinous process, and a relatively larger, broader and less caudally projected caudal extremity of the centrum with a bilobed ventral margin; from *O. rufus* and *M. fuliginosus* in being larger, and in having a thicker spinous process with a cranially slanted dorsal margin and thickened, caudally projected caudal tip, and caudal extremity of the centrum with bilobed ventral margin; and from *W. bicolor* in being larger, with a deeper arch, larger dorsal tubercle, more caudally deflected wings and less caudally projected caudal articular surfaces.

Cervical vertebrae (C3–C7) (Fig. 65a): quite short and broad; the articulated neck exhibits distinct dorsal curvature through C4–7, centred around C6. Cranial extremity of the centrum broad and concave, particularly at the lateral margins, with slight ventral tilt. Prezygopophyses moderately well-developed and broad, not extending cranially past cranial extremity; articular surfaces dorsal facing and slightly craniomedially tilted; no ridge separates articular surface from dorsal surface of arch. Vertebral canal not known. Arch broad and approaching horizontal. Spinous process mostly abraded; bases narrow, becoming shallower and broader towards C7. The ventral surface of is centrum gently convex. Transverse processes poorly developed in juveniles, becoming relatively broad and thickened with age; quite thickened, broad and caudally deflected, most caudally deflected in C3, broadest in C4, becoming decreasingly caudally deflected and increasingly thicker and narrower towards C7; tubercle on ventral base of transverse processes very low, narrow and slightly elongate in C5, distinctly more elongate craniocaudally, thickened and ventrally projected in C6, and shorter, broader, slightly cranially deflected and more cranially situated in C7. Postzygopophyses moderately well-developed and broad, extending marginally beyond caudal extremity of the centrum; articular surfaces slightly to moderately laterally tilted. Caudal extremity of the centrum broad and slightly caudoventrally projected, with a slightly bilobed ventral margin.

The cervical vertebrae of *P. viator* **sp. nov.** differ from those of from *P. anak* in being lower, broader and less deep, with smaller pre- and postzygopophyses, lower, broader cranial extremity of the centrum and lower, broader, less caudoventrally projected caudal extremity of the centrum with a slightly bilobed ventral margin; from *P. mamkurra* **sp. nov.** in being deeper, with more horizontal, less roof-like arch, slightly larger pre- and postzygopophyses and more caudoventrally projected caudal extremity of the centrum with a slightly bilobed ventral margin; from *P. tumbuna* in being larger and slightly more elongate, with more robust transverse processes; from *C. kitcheneri* in being less elongate, with a less caudally projected caudal extremity of the centrum; from *O. rufus* in having more robust transverse processes and less cranially projected arches; and from *M. fuliginosus* and *W. bicolor* in being larger, with smaller, less cranially projected ventral tubercles of the transverse processes on C3–5 and smaller, less elongate ventral transverse tubercles on C6 and 7.

Thoracic vertebrae (T1–T14) (Fig. 65a): only preserved *in situ* in articulated specimens paratype SAMA P53835 and holotype SAMA P59552. Thoracic vertebrae total 14; vertebrae craniocaudally short relative to width. Rib length increases rapidly to maximum at ribs 6 and 7 (rib 7 length = ~215 mm), decreases steadily to rib 14. T1–3: entirely obscured by scapulae in both available specimens, which also obscure all but tip of spinous process of T4 and obscure majority of T5 and 6; heads of ribs hide area ventral to pedicles in T7–13; all vertebrae tightly articulated, obscuring view of cranial and caudal extremities of the centra. Spinous process long, slightly caudally curved and strongly caudally deflected in T4–8, with that of T4 most transversely compressed; in T5 and 6 relatively thick and robust; in T7 and 8 increasing in depth and transverse compression; in T9 quite deep and lacking caudal deflection; in T10–14 undeflected, with thickened tips and increasingly short and deep. Pre- and postzygopophyses mostly abraded or obscured in T1–10, appear quite small, undeflected laterally or dorsally, situated on arch, with position beginning to migrate slightly dorsally from T9; in T11 relatively larger, with postzygopophyses situated on caudolateral base of the spinous process; T12 is a transitional vertebra, with smaller, dorsal facing, cranially projected prezygopophyses and robust, ventrolateral facing, dorsolaterally projected postzygopophyses; T13 and 14 with very large, deep, transversely compressed, dorsomedial facing, dorsolaterally projected prezygopophyses and quite short, robust and ventrolateral facing postzygopophyses. Diapophyses short but quite deep and robust; gently dorsally deflected in T7–10; become shorter, more robust and less dorsally deflected in T11–14 (extend dorsally above cranial articular surfaces in T12 only). Caudal accessory processes ancillary to postzygopophyses; present on T13 as small triangular eminences on caudal surface of the base of diapophyses; in T14 elongate, lobe-shaped processes extending from caudal surface between arch and diapophysis to articulate with lateral surface of prezygopophyses of L1.

The thoracic vertebrae of *P. viator* **sp. nov.** cannot be differentiated from those of *P. mamkurra* **sp. nov.** They differ from *P. anak* in having generally relatively larger, more robust diapophyses; from *C. kitcheneri* in being larger with relatively larger, more robust diapophyses and

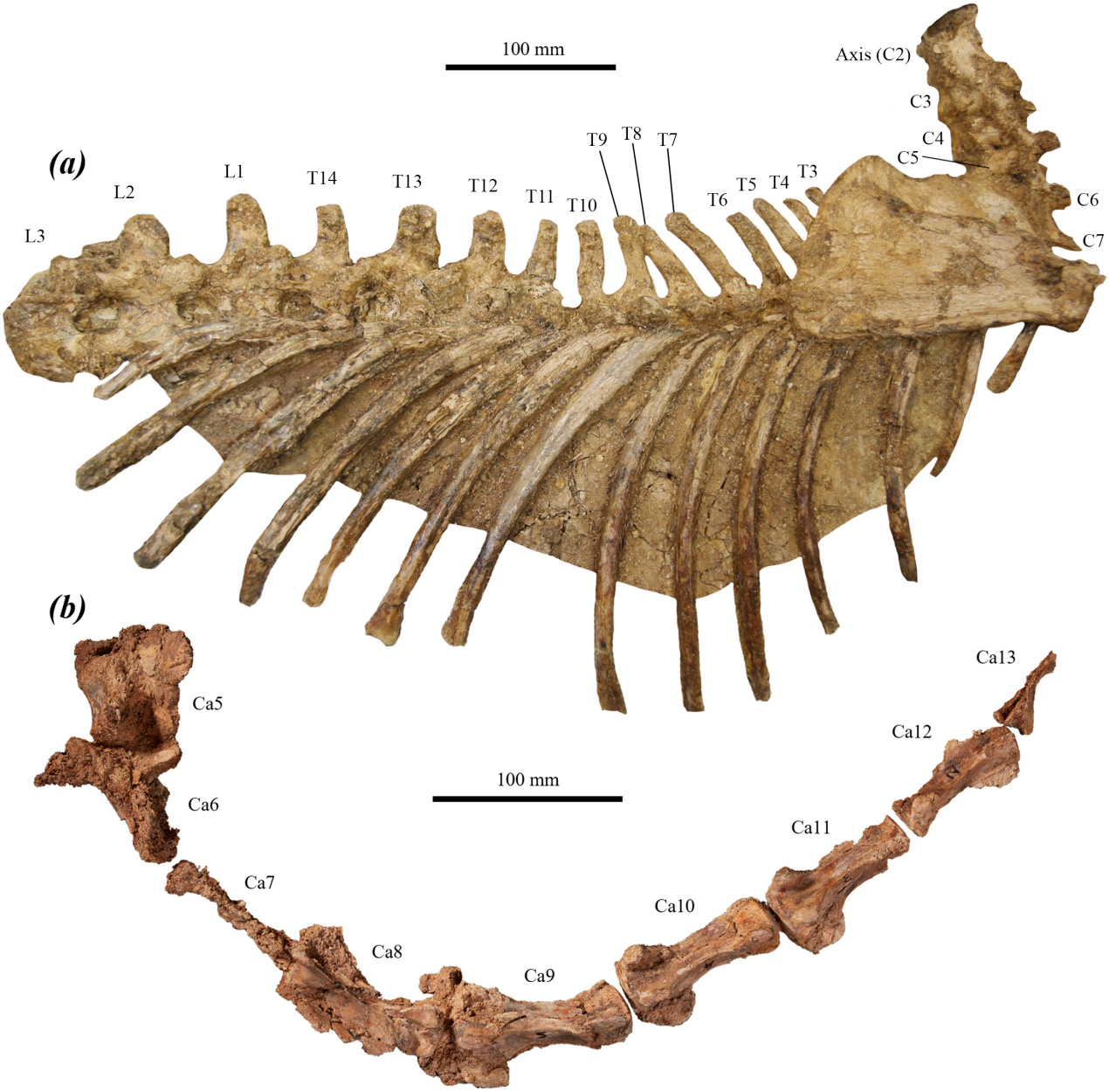

FIGURE 65. (a) partial articulated cervical, thoracic and lumbar spine, right scapula, clavicle and ribs of *P. viator* **sp. nov.** holotype SAMA P59552 in right lateral view; and (b) partial caudal spine of articulated and re-articulated Ca5–13 in left lateral view.

possibly, based on comparison of the articulated thoracolumbar column, lesser thoracic lordosis (ventral curvature) and thoracolumbar kyphosis (dorsal curvature); from *O. rufus*, *M. fuliginosus*, and *W. bicolor*, in numbering 14, with the transitional vertebra situated at T12 rather than T11; further from *O. rufus* in having the spinous processes of T5–8 relatively shorter and more caudally curved, and the diapophyses of T6–8 slightly more cranially deflected; further from *M. fuliginosus* in having relatively shorter spinous processes on T5–8; and further from *W. bicolor* in being much larger, with less dorsally deflected diapophyses in T7–10 and relatively taller spinous processes on T10–13.

Lumbar vertebrae (L1–5) (Fig. 65a): lumbar vertebrae total five; vertebrae quite large and robust; in most complete available specimen, ventral component of L1–3 partially obscured or abraded and dorsal components of L4 and 5 abraded; vertebral canals, caudal extremities of the centra, and cranial and caudal articular surfaces not visible due to articulation. Centrum length slightly greater than width; gently increase in size and length toward L5; ventral and lateral surfaces bowed strongly inwards, creating a distinct waist at the midpoint. Cranial extremities of the centrum not visible in L1, 2 and 5 and abraded in L3; large and rounded in L4. Prezygopophyses large, projected cranially well beyond the margin of the centrum and angled craniodorsally from the base before curving dorsally toward the tip; cranial articular surfaces interpreted as strongly medially tilted. Spinous processes quite tall and robust, very deep and transversely

compressed in L1–2; slightly cranially deflected in L1; undeflected in L2; abraded in L3–5. Postzygopophyses quite small, rounded and gently laterally deflected. Caudal accessory processes present on L1 and 2 as lobe-shaped, dorsocaudally projected processes arising on lateral surface of arch, cranioventral to bases of postzygopophyses; abraded in L3–5. Transverse processes mostly obscured on L1, arise on lateral surface of the centrum immediately caudal to cranial margin; on L2 arise on lateral surface of the centrum midway between cranial margin and midpoint, dorsoventrally planar and projected ventrolaterally before curving strongly cranially; become slightly deeper and situated more dorsally in L3–5.

The lumbar vertebrae of *P. viator* **sp. nov.** cannot be differentiated from those of *P. mamkurra* **sp. nov.** They differ from those of *P. dawsonae* **sp. nov.** in being generally larger, with less deep transverse processes, centrum with relatively taller, narrower cranial and caudal extremities, less deeply concave ventrolateral surfaces, and a less deeply concave ventral margin in lateral view; from *C. kitcheneri* in being larger, with a relatively slightly longer centrum; from *O. rufus* and *M. fuliginosus* in numbering five, with a deeper, more robust spinous process; and from *W. bicolor* in being much larger and in numbering five.

Caudal vertebrae (Ca1–13, 18–20) (Fig. 65b): numerical position of distal vertebrae not certain; large and moderately robust. Prezygopophyses: in Ca1–4, large, flattened, flared and rounded across distal margins with articular surfaces angled dorsomedially and projected craniomedially, becoming deeper and more flared toward Ca5; Ca6 has tall, less laterally projected non-articular mammillary processes (prezygopophyses); Ca7 onwards have increasingly smaller, blunter and thicker mammillary processes lacking articular surfaces. Postzygopophyses: in Ca1–4, relatively taller and narrower than prezygopophyses, with small, rounded articular surfaces; Ca7 and distal vertebrae have increasingly reduced postzygopophyses that migrate caudally to abut the caudal margin as low, thin, parallel ridges in the distal vertebrae. Centra: Ca1–5, craniocaudally short with slightly ventrally inclined cranial and caudal extremities; Ca6 onward, centra become straighter and more elongate, before decreasing in size and length around Ca10; Ca12–14, increasingly short, robust centra that narrow to a strong waist; Ca18–20 very short and robust; cranial and caudal extremities of the centrum remain rounded with slight dorsoventral compression throughout the caudal vertebrae. Vertebral canal: low and broad in Ca1, becoming increasingly low toward Ca4, extremely small in Ca6–9 and absent in distal vertebrae. Transverse processes: poorly preserved in the available proximal vertebrae; Ca1, flattened and deep; Ca2, very deep and broad; Ca3 and 4, broader, shorter, more caudally situated and more caudally deflected; large and flattened in Ca5; Ca6 lacks cranial transverse processes and Ca7 has extremely small, thin cranial transverse processes, Ca6 and 7 have short, broad caudal transverse processes adjacent to the caudal margin with curved cranial margins extending cranially as thin ridges, processes less curved and broader in Ca7; distal vertebrae possess small, blunt, dorsoventrally compressed and ventrally deflected cranial and caudal transverse processes linked by a thin, low ridge that lowers to minimum around the midpoint of the centrum, with the cranial processes relatively larger than the caudal; cranial and caudal transverse processes slightly cranially and caudally deflected respectively. Spinous process: increasingly small and rounded in Ca1–4; very reduced or absent in Ca5 onward. Cranioventral processes: small, blunt, ventrally projected on Ca6, positioned close to the midline and curving gently mesially toward the tip; become larger, thicker, more mesially curved, and more elongate relative to vertebra distally.

The caudal vertebrae of *P. viator* **sp. nov.** differ from those of *P. anak* in being generally more elongate, with the caudal transverse processes of Ca7 shorter and slightly broader; from *P. mamkurra* **sp. nov.** in being more elongate and in having broader, straighter caudal transverse processes on Ca7 and cranial processes on Ca8; from *P. tumbuna* and *P. dawsonae* **sp. nov.** in being larger and more elongate; from *C. kitcheneri* in being larger, with broader, more laterally flared prezygopophyses in Ca2–4, broader caudal transverse processes on Ca7, and more elongate distal caudal vertebrae; from *O. rufus* in having broader, more laterally flared prezygopophyses in Ca1–5, broader caudal transverse processes on Ca7, and in having Ca7 (rather than Ca6) as the first vertebra to bear cranial transverse processes; from *M. fuliginosus* in being larger and more robust, with the prezygopophyses of the proximal caudal vertebrae more rounded around the distal margins, subequally broad cranial and caudal extremities of the centra of Ca4–6 (rather than cranial extremity being narrower), and in having Ca7 (rather than Ca6) as the first vertebra to bear cranial transverse processes; and from *W. bicolor* in being much larger and more elongate, with larger caudal transverse processes on Ca7–11.

Pectoral girdle and forelimb

Scapula (Fig. 66a–c): large, slightly broader than depth. Acromion well-developed, thickened and lobed in dorsal view, deepens to a rounded lateral end, projects laterally beyond margin of the supraglenoid tubercle. Spine cranially inclined in lateral view; lateral component tall and thickened, becomes lower medially to merge with the scapular body well short of the cranial angle (Fig. 66a). Scapular notch moderately deep and obtuse, around 110°. The cranial border is thickened. Cranial angle thickened, rounded and obtuse. The medial border between the cranial and caudal angles is not preserved. Caudal angle roughly right-angled. Caudal border linear to very slightly convex with a slight caudal eminence close to the caudal angle; distinctly thickened relative to the infraspinous fossa and other borders, becoming thicker, rounded and swollen laterally. Supraspinous fossa very gently concave, roughly half the size of the infraspinous fossa. Infraspinous fossa large and gently convex. Subscapular fossa slightly concave, with a very slight convexity bounding a slight, shallow mesial channel that extends transversely, ventral to the scapular spine. Glenoid cavity large, concave, oval and transversely compressed, with the cranial component gently projected laterally. Supraglenoid tubercle thin, blunt

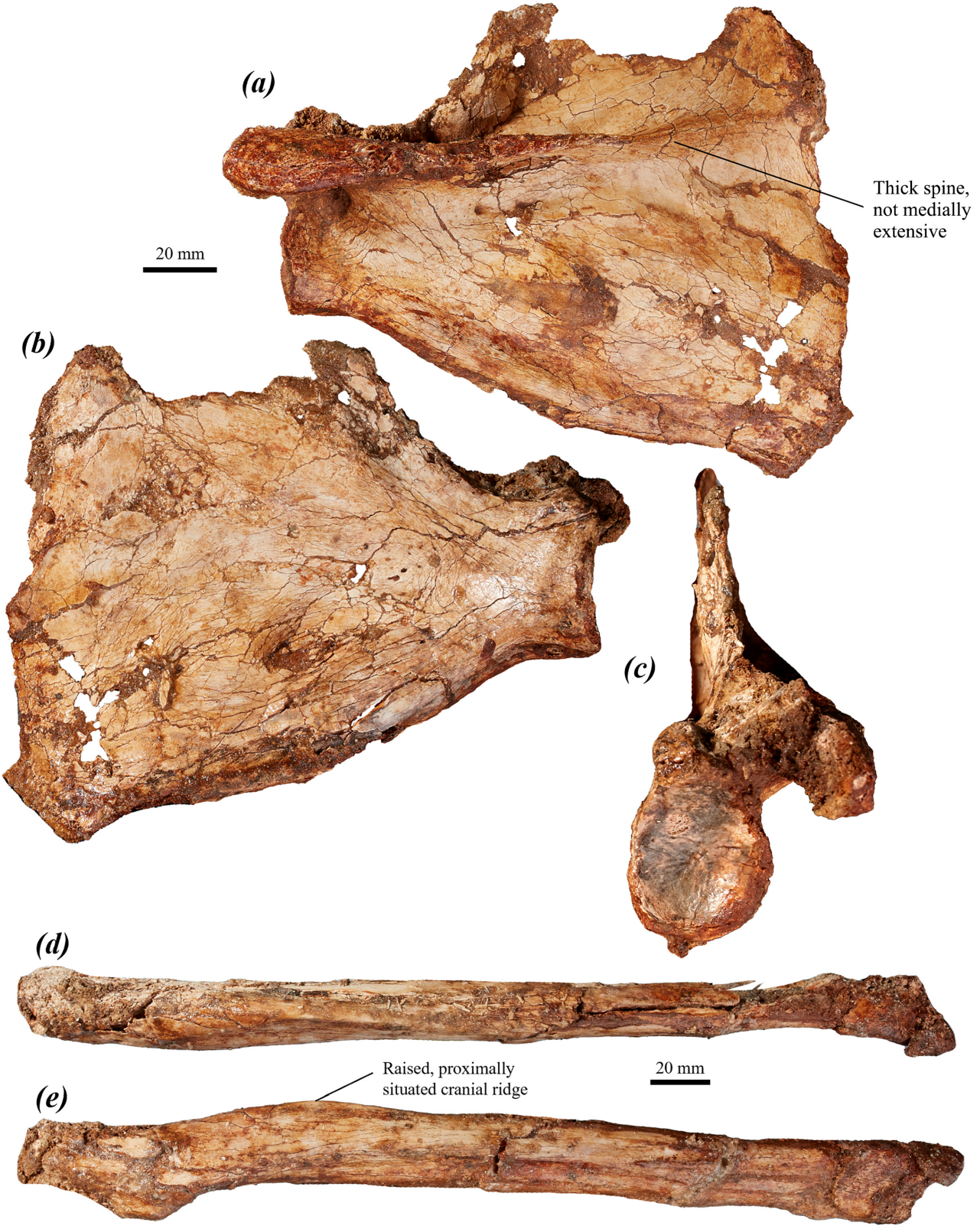

FIGURE 66. left upper forelimb elements of *P. viator* **sp. nov.** paratype SAMA P59550: (a–c) partial scapula in (a) dorsolateral, (b) ventromedial, and (c) proximal/humeral views; and (d–e) partial radius in (d) cranial, and (e) medial views.

and slightly projected laterally. Coracoid process blunt and tubercular, slightly larger than, and situated slightly ventromedial to, the supraglenoid tubercle. Infraglenoid tubercle present as a short, broad, shallow and rugose fossa that abuts the caudal margin of the glenoid.

The scapula of *P. viator* **sp. nov.** cannot be confidently differentiated from that of *P. mamkurra* **sp. nov.** due to the fragmentary and juvenile nature of the material of the latter. It differs from that of *P. anak* in being less broad, with a thicker and less medially extensive spine; from *C. kitcheneri* in being larger, with a relatively slightly larger supraspinous fossa, a thicker, lower and less medially extensive scapular spine, a less anteroposteriorly compressed glenoid fossa, and a less anterolaterally projected supraglenoid tubercle and coracoid process; from *O. rufus* in being relatively slightly broader, with a slightly less medially extensive spine and a less anteroposteriorly compressed glenoid fossa; from *M. fuliginosus* in being larger, with slightly less medially extensive spine and a more lobe-shaped, less laterally extensive acromion; and from *W. bicolor* in being larger, with a less medially extensive caudal component and a thicker, less medially extensive and more cranially tilted spine.

Humerus (Fig. 67a–d): sexually dimorphic, with humeral length greater in males than in females. Humerus quite short and robust with thick, well-developed ridges for muscle attachment, becoming considerably more robust and muscle-scarred in older individuals (*e.g.* SAMA P59550). Humeral head roughly hemispherical, rounded and moderately caudomedially projected. Greater tubercule large to very large, broad and craniocaudally compressed, ranges from level with humeral head dorsally to markedly taller. Lesser tubercule quite tall, subequal with or slightly taller than head; blunt and rounded in lateral view, deep and oval in dorsal view; very small in juveniles. Proximal shaft robust and deep; in cranial view, the proximal component of the shaft has a slight medial deflection, with the axis situated across the shaft at the pectoral crest (*e.g.* SAMA P53836). Bicipital groove broad and very shallow in juveniles, becomes deeper, slightly narrower and distally more extensive in adults. Pectoral crest thick, high, elongate, rugose and slightly laterally tilted, extends distally to two-thirds of humeral length; becomes higher and more pronounced proximally with age. Deltoid tuberosity situated on the lateral surface of the shaft, level with the proximal part of the pectoral crest; low and gently rugose in juveniles, becoming thicker, more rugose and rounded to slightly pointed in adults. Insertion of m. latissimus dorsi marked by a small rugose area in juveniles and a broad, shallow, irregular fossa in adults.

Distal end broad and quite short. Lateral supracondylar ridge quite broad, extends slightly more than one-third of humeral length to adjacent to the distal margin of the pectoral crest, comes to a small, rounded point proximally. Capitulum and ulnar facet large, robust, laterally situated, abutting the lateral epicondyle; combined width roughly two-thirds of the epicondylar width; capitulum smoothly and strongly convex with a rounded, tapering lateral margin; ulnar facet with a relatively straighter medial margin with a gently bevelled edge; trochlea wide and quite shallow. Olecranon fossa large, extensive proximally, and moderately deep, becoming deeper with age. Radial fossa and coronoid fossa small and fairly shallow. Medial supracondylar bridge broad, quite thin craniocaudally; very thin to absent in juveniles. Supracondylar foramen oval, elongate and moderately flattened craniocaudally. Medial epicondyle comes to a rounded, medially projected point.

The humerus of *P. viator* **sp. nov.** differs from that of *P. anak* in being shorter, with a shorter pectoral crest, relatively slightly broader distal end, and a more convex lateral margin of the lateral supracondylar ridge; from *P. mamkurra* **sp. nov.** in having the peak of the lateral supracondylar ridge less pointed and closer to the distal margin of the pectoral crest; from *P. tumbuna* in being more robust, in lacking a low, rounded ridge linking the medial supracondylar bridge with the distal end of the pectoral crest, and in having a relatively shorter distal end; from *P. otibandus* in being larger; from *C. kitcheneri* in lacking a crest on the distal margin of the attachment site for the m. latissimus dorsi, and in having a more medially projected head, deeper, taller greater tubercle, taller lesser tubercle, more deeply concave bicipital groove, deeper proximal shaft, less elongate, generally less raised deltoid tuberosity, straighter, less raised pectoral crest, more elongate distal end, broader lateral supracondylar ridge with a more pointed proximal peak, and a broader medial supracondylar bridge; from *O. rufus* in being more robust, lacking a shallow fossa immediately distal to the supracondylar foramen, and in having a larger lesser tubercle, deeper proximal shaft, smaller, blunter deltoid tuberosity, thicker, more raised pectoral crest, and a relatively broader distal end; from *M. fuliginosus* in being generally larger and more robust, with a deeper, taller greater tubercle, deeper proximal shaft, less raised deltoid tuberosity, straighter pectoral crest, relatively broader distal end, broader capitulum and ulnar facet, ulnar facet with a less squared medial margin, and a shallower trochlea; and from *W. bicolor* in being larger, with a more medially projected head, taller, deeper greater tubercle, deeper, less raised and less elongate deltoid tuberosity, straighter, less raised pectoral crest, broader distal end, and a broader medial supracondylar bridge.

Ulna (Fig. 67e–g): large, elongate, quite deep and moderately transversely compressed. Olecranon quite short relative to ulnar length, and transversely compressed, tapering in lateral view to a blunt, squared distal end; a small, triangular process projects medially from the ventral component of the epiphysis; robustness, height, degree of transverse compression and relative length of olecranon are much less in juveniles than in adults. Facet for humeral articulation broad, with the trochlear notch broadly rounded and indistinct; medial component deeply concave, more elongate and situated more cranially than the lateral component, with the medial margin having a slight concavity between the convex margins of the anconeal and coronoid processes; lateral component relatively shallow, smoothly concave, and tilted and projected laterally. Anconeal process low relative to the coronoid process, with a rounded, reflex mesial angle;

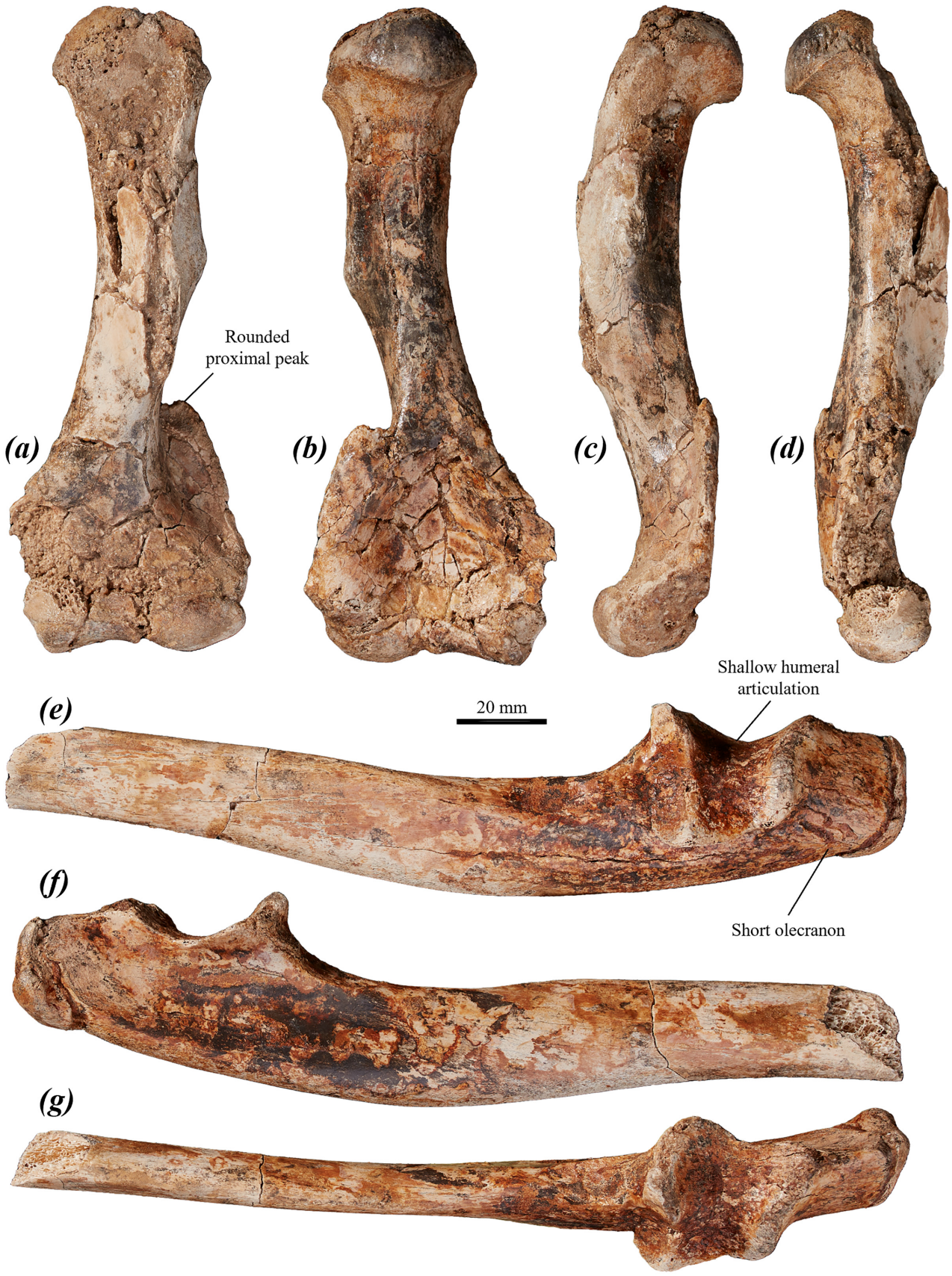

FIGURE 67. left forelimb elements of *P. viator* **sp. nov.** paratype SAMA P53836: (a–d) partial humerus in (a) cranial, (b) caudal, (c) lateral, and (d) medial views; and (e–g) partial ulna in (e) lateral, (f) medial, and (g) cranial views.

coronoid process tall, quite broad, and smoothly rounded in posterior view, meets the shaft at abrupt angle on cranial margin. Radial facet broad and roughly semicircular. Ulnar tuberosity narrow, quite elongate, slightly rugose and flat to gently concave. Lateral surface of ulna convex proximally, becoming flat toward the midpoint of the shaft; proximomedial flexor fossa gently concave. Shaft gently medially curved in cranial view; proximal component deep and highly transversely compressed, curved gently cranially, straightens distally; ventral surface broadest beneath the olecranon, tapers slowly anteriorly; broad, low ridge arises on the lateral margin of the cranial surface of the shaft midway between the ulnar tuberosity and the midpoint of the shaft; distal component of the shaft slightly broader and less tall than proximally, but remains transversely compressed. Distal epiphysis with a broad, rounded base, abruptly narrows to a short, medially hooked styloid process with a globular tip; a small, squared projection is on the caudolateral face of the base of the epiphysis for articulation with the pisiform.

The ulna of *P. viator* **sp. nov.** differs from that of *P. anak* in being generally broader and less elongate, with a longer olecranon and the distal shaft more transversely compressed and less cylindrical; from *P. mamkurra* **sp. nov.** in being more gracile, with a longer olecranon relative to total length; from *P. tumbuna* in being larger; from *P. otibandus* in being lower and less dorsoventrally compressed, with a relatively shorter olecranon, less deeply concave humeral facet, taller, broader coronoid process, and a shallower proximomedial flexor fossa; from *C. kitcheneri* in being larger, deeper and more robust, with a relatively longer olecranon, less raised trochlear notch, broader humeral facet, less rounded radial facet, and the shaft height tapering more distally; from *O. rufus* in being deeper and more robust, with a less dorsally deflected, longer olecranon relative to ulnar length, taller, more medially flared coronoid process, less laterally tilted lateral component of the humeral facet, less bilobed lateral margin of the humeral facet, broader, less laterally tilted radial facet, and a more transversely compressed shaft; from *M. fuliginosus* in being larger and more robust, with shallower and more elongate humeral facet, lower anconeal process, lower, more medially flared coronoid process, and a less bilobed lateral margin of the humeral facet; and from *W. bicolor* in being larger, with a less dorsally projected, less cranially deflected olecranon, much less medially flared anconeal process, lower coronoid process, broader radial facet, and a lower cranial ridge on the shaft.

Radius (Fig. 66d–e): elongate and straight to slightly curved. Radial head circular to slightly oval and smoothly concave. Radial neck tapers slightly to the radial tubercule. Radial tubercule rugose, round to oval and smoothly projected. Shaft cross-section is oval to tear-drop shaped immediately distal to the radial tubercle, becomes a gently craniocaudally compressed oval in the middle to distal shaft; shaft gently broadens distally from the midpoint. Cranial ridge broad, distinct, situated proximally, on the cranial surface midway between the radial tubercle and the midpoint of the shaft (Fig. 66e). Caudal ridge very low, indistinct and slightly rugose, located on the caudolateral surface of the middle of the shaft. Ulnar notch broad, quite shallow and elongate. The distal epiphysis is quite large; scaphoidal facet broad, gently caudally tilted and concave; cranial component of the distal surface gently convex; a small, blunt tubercle is on the caudolateral margin; styloid process quite large, slightly transversely compressed, medially situated and slightly curved caudally.

The radius of *P. viator* **sp. nov.** differs from that of all compared taxa in having a more proximally situated cranial ridge (bar *P. tumbuna*, for which no proximal radius is known), for the origin of the m. extensor carpi radialis. It further differs from *P. anak* in having the caudal ridge lower and less distinct; from *P. mamkurra* **sp. nov.** in being more elongate and generally less curved, with a lower, less distinct caudal ridge and a less craniocaudally compressed distal shaft; from *P. tumbuna* in being larger, with a lower, less distally extensive caudal ridge, more craniocaudally compressed distal shaft, and a smaller styloid process relative to the scaphoidal facet; from *P. otibandus* in being generally larger, with a less raised caudal ridge; from *C. kitcheneri* in being larger, with a thicker, more raised cranial ridge, less raised caudal ridge, and a caudally tilted (rather than slightly cranially) scaphoidal facet; from *O. rufus* in being more robust; from *M. fuliginosus* in being larger, with a more transversely compressed proximal shaft and a larger medial part of the distal epiphysis; and from *W. bicolor* in being larger, lacking a short caudomedial ridge on the distal shaft, and in having a thicker raised cranial ridge, less raised, less elongate caudal ridge, and a longer, less transversely compressed styloid process.

Manus

Scaphoid (Figs 68a–c & 69a–d): broad and robust, roughly semicircular in dorsal view; dorsopalmarly short and slightly arched in anterior view. Radial facet broad, tilted slightly dorsally, extends from the posteromedial margin, across the proximal surface, to the posterior margin of the palmar process; rounded and smoothly convex laterally, gently concave medially. Palmar process broad, lobe-shaped, highly dorsopalmarly compressed and anteropalmarly projected. Facet for the hamatum quite broad and convex, covers the lateral component of the anterior surface. Facet for the capitatum large, quite tall and concave. Facet for the trapezoid small and oval, abutting the capitatal facet on the anterodorsal margin of the palmar process. Facet for the trapezium broad and strongly convex with indistinct margins, wraps around the anterior surface of the palmar process.

The scaphoid of *P. viator* **sp. nov.** differs from that of *P. mamkurra* **sp. nov.** in having a broader palmar process, and hamatal and capitatal facets more distinct from each other, with the mesial component thickened instead of having a distinct, raised transverse dorsal ridge for articulation with the styloid process of the radius; from *P. otibandus* in being larger, lacking a raised dorsal ridge, and in having a more flattened radial facet and a more

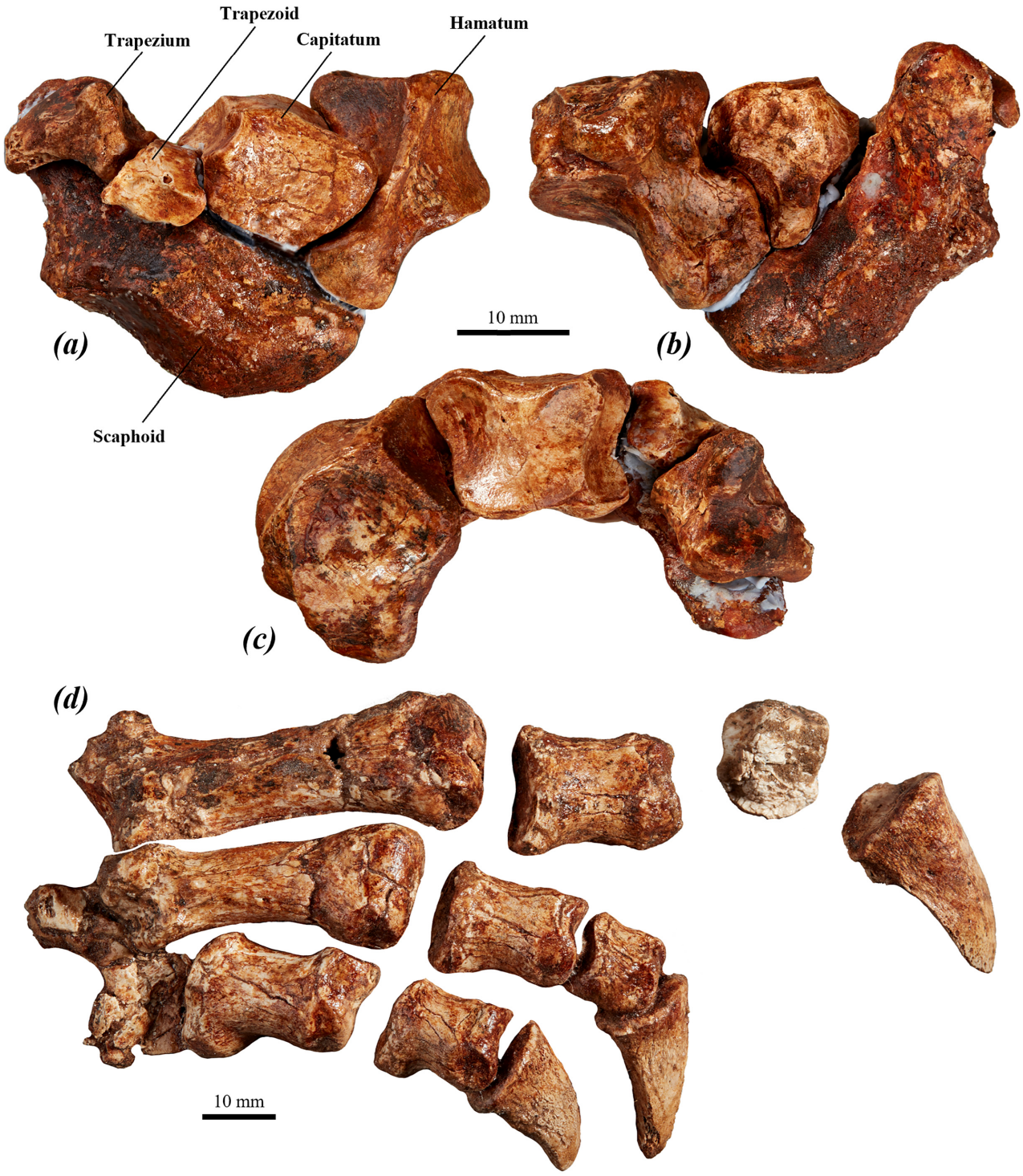

FIGURE 68. re-articulated sections of the manus of *P. viator* **sp. nov.**: (a–c) right scaphoid, hamatum, capitatum, trapezoid and trapezium of holotype SAMA P59552 in (a) dorsal, (b) palmar, and (c) distal/anterior views; and (d) left manual digits I–III of paratype SAMA P59550 in dorsomedial view.

dorsopalmarly compressed palmar process; from *C. kitcheneri* in being broader, with a concavity present on the medial component of the radial facet, a broader, more anteropalmarly deflected palmar process, hamatal and trapezoidal facets more discrete, and the hamatal facet strongly convex (instead of concave and palmarly tilted); from *O. rufus* and *M. fuliginosus* in being larger, lacking a raised dorsal ridge, and in having the radial facet positioned more on the posterior surface and less dorsally; and from *W. bicolor* in being much larger, with a more concave capitatal facet and a larger hamatal facet.

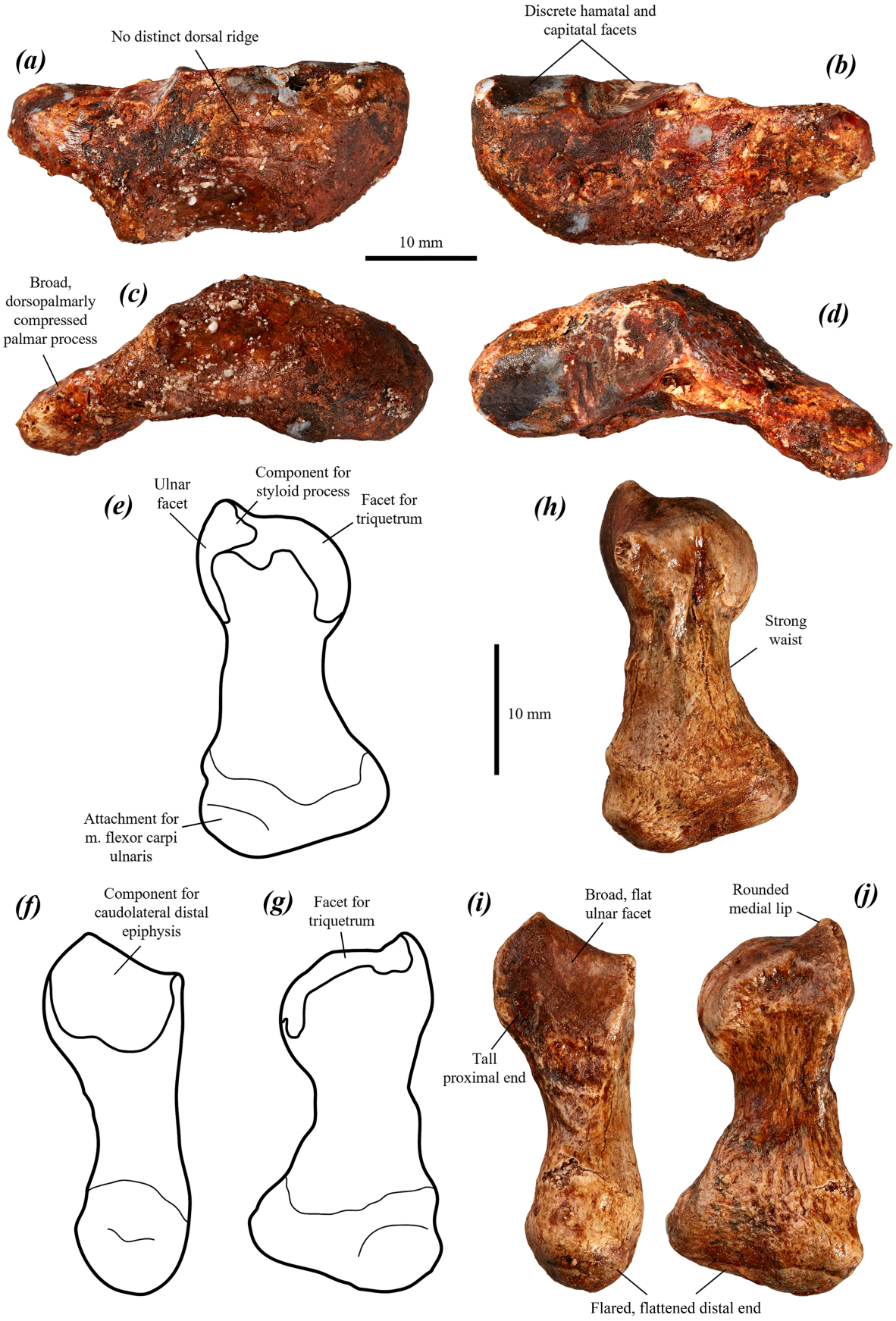

FIGURE 69. right carpals of *P. viator* **sp. nov.** holotype SAMA P59552: (a–d) scaphoid in (a) dorsal, (b) palmar, (c) proximal/posterior, and (d) distal/anterior views; and (e–g) line drawings and (h–j) stacked photos of pisiform in (e, h) dorsal, (f, i) palmar, and (g, j) posterior views.

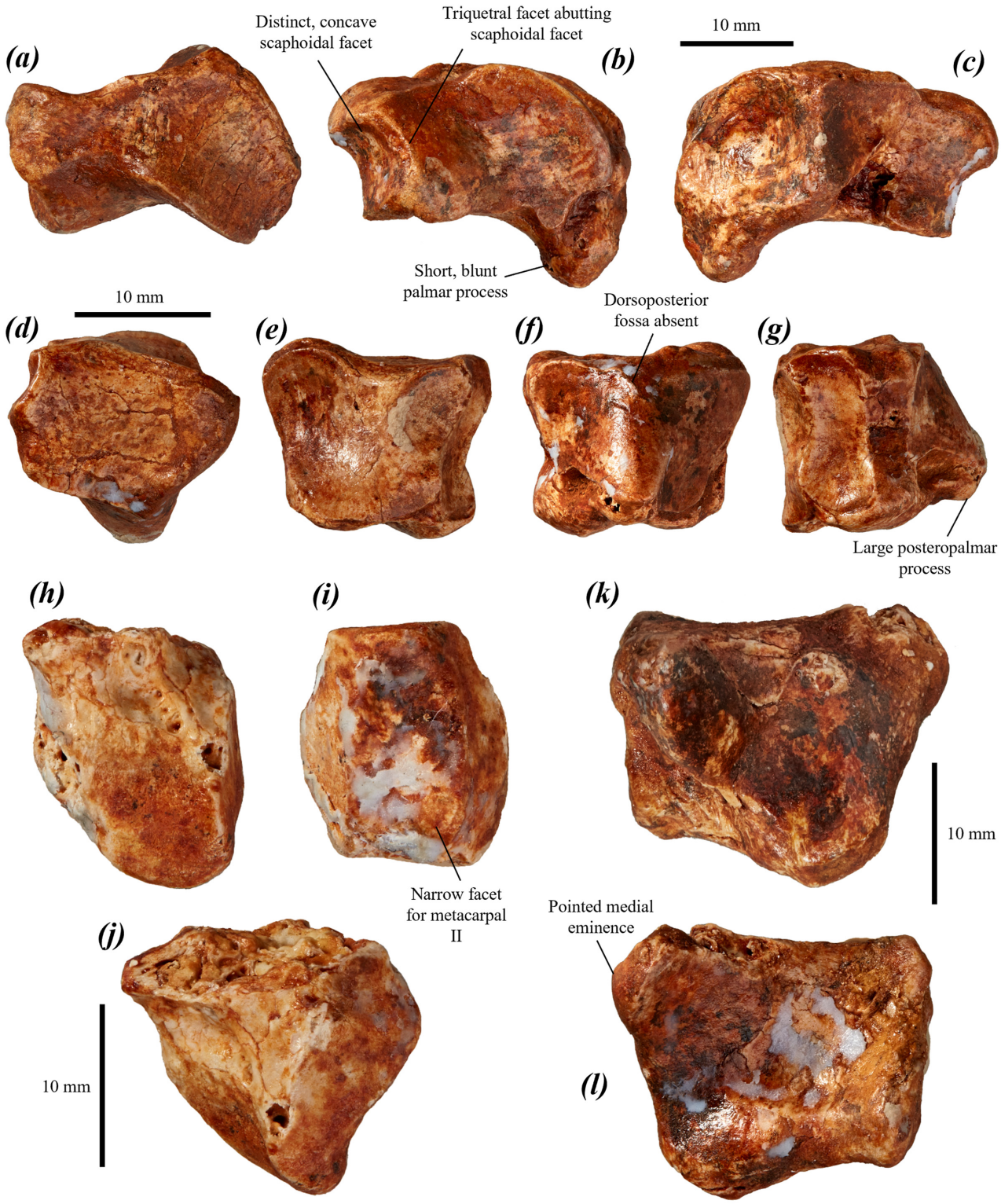

FIGURE 70. right carpals of *P. viator* **sp. nov.** holotype SAMA P59552: (a–c) hamatum in (a) dorsal, (b) proximal/posterior, and (c) distal/anterior views; (d–g) capitatum in (d) dorsal, (e) distal, (f) proximal, and (g) medial views; (h–j) trapezoid in (h) proximal, (i) distal, and (j) dorsal views; and (k–l) trapezium in (k) dorsal, and (l) palmar views.

Pisiform (Fig. 69e–j): quite broad, with an anteroposteriorly flared, flattened distal (lateral) end, a narrow waist and a large, posteriorly squared proximal end. Facet for the ulna has a large and flat posterior component, with a rounded medial lip; facet extends onto the medial surface and narrows to a slightly concave area of articulation for the styloid process of the ulna. Facet for the triquetrum rounded, convex and situated on the anteromedial surface; continuous posteriorly with the facet for the styloid process.

The pisiform of *P. viator* **sp. nov.** differs from that of *P. otibandus* in being larger, with a taller proximal end and a much larger, flatter posterior ulnar facet (Fig. 69j); from *C. kitcheneri* in being larger and less dorsopalmarly compressed, with narrower waist, more flared distal end and more distinct facets; from *O. rufus* in being larger and broader, with more distinct waist; from *M. fuliginosus* in being larger, with smaller anterodorsal eminence on proximal end; and from *W. bicolor* in being much larger, more robust and less dorsopalmarly compressed, particularly proximal end, with deeper distal end and taller, flatter facet for the styloid process.

Hamatum (Figs 68a–c & 70a–c): broad, robust and roughly boot-shaped in dorsal view. Posteromedial component large, squarish and projected. Facet for the triquetrum large, broad, occupies posterior surface except for posterior of palmar process; anterior component tall, slightly concave and faces directly posteriorly, with flared, convex dorsal margin in posterior view; posterior component lower, slightly dorsally tilted, gently convex and faces posterolaterally, situated on posteromedial process of the hamatum. Facet for the scaphoid small and dorsopalmarly concave, abuts medial margin of triquetral facet on posteromedial surface. Facet for the capitatum gently concave, roughly arch-shaped on anteromedial surface, curves over small, deep foramen; continuous with facet for lateral surface of proximal end of metacarpal III, semicontinuous posteriorly with scaphoidal facet, meeting at sharp corner. Facet for metacarpal IV rounded and smoothly concave, with convex lateral lip extending palmolaterally onto anterior surface of palmar process; indistinct from facet for metacarpal V. Palmar process thick and blunt, projects palmarly and slightly laterally from lateral component.

The hamatum of *P. viator* **sp. nov.** differs from that of *P. mamkurra* **sp. nov.** in being deeper, with a more concave scaphoidal facet, narrower combined metacarpal IV and V facets relative to the capitatal and metacarpal III facets, shorter, blunter, posteropalmarly projected palmar process (Fig. 70b), and a convex metacarpal V facet; from *P. otibandus* in being larger, with triquetral facet more extensive medially to be semicontinuous with, rather than distinctly separate from, the scaphoidal facet; from *C. kitcheneri* in being slightly larger and more robust, with the posteromedial component more squared, more dorsally flared, more concave triquetral facet that is semicontinuous medially with the scaphoidal facet, more concave facet for metacarpal IV, smaller, less concave and less laterally rotated facet for metacarpal V, and an anteroposteriorly deeper, less projected and less anteriorly deflected palmar process; from *O. rufus* in being larger, with the triquetral and scaphoidal facets semicontinuous and the palmar process relatively smaller, blunter and lacking anterior deflection for articulation with the palmar surface of metacarpal V; from *M. fuliginosus* in being larger, with a relatively smaller medial component and a dorsopalmarly shorter dorsolateral margin of the triquetral facet; and from *W. bicolor* in being much larger, with a less deeply concave triquetral facet, relatively larger facet for metacarpal III, and a much less palmarly extensive palmar process.

Capitatum (Figs 68a–c & 70d–g): quite small, and rectangular to roughly oblong in dorsal view, with the palmar surface roughly triangular due to narrowing of the posteropalmar margin into a short, cone-like point. Facet for the hamatum squarish and slightly concave to slightly convex, with a posterior tilt; occupies majority of lateral surface; a small, rounded fossa sits against the anteropalmar margin. Facet for the scaphoid concave medially, becoming gently convex laterally; covers the posteromedial surface and extends laterally, with a slight palmar curve, to wrap around the posterior edge where it is continuous with the hamatal facet. Facet for metacarpal III large, covers the anterior surface and subdivides into a semicontinuous smaller medial component and a larger lateral component for the medial and lateral processes of the posterior end of metacarpal III. Medial surface anteroposteriorly short, with a tall, concave facet for the medial part of the posterior facet of metacarpal II occupying the anterior section. Facet for the trapezium very narrow and indistinct, on the posteropalmar section of the medial surface.

The capitatum of *P. viator* **sp. nov.** differs from that of *P. mamkurra* **sp. nov.** in being deeper, having a larger posteropalmar process, and lacking a small, rounded dorsoposterior fossa; from *P. otibandus* in being larger; from *C. kitcheneri* in being squarer in dorsal view, with a larger posteropalmar process, taller medial section of metacarpal III facet, and a taller, narrower and more medially situated facet for metacarpal II; from *O. rufus* in being larger and deeper; from *M. fuliginosus* in being larger, generally squarer and deeper, with a larger and more pointed posteropalmar process; and from *W. bicolor* in being much larger, and slightly deeper in dorsal view, with larger, deeper hamatal facet.

Trapezoid (Figs 68a–c & 70h–j): considerably smaller than the trapezium; very small and palmomedially abraded; positioned between the capitatum and trapezium with a slight dorsal displacement. Facet for the capitatum tall, narrow and gently convex. Facet for the scaphoid fairly narrow and gently concave. Facet for the trapezium mostly abraded in available specimen; preserved is a small, pointed anteromedial eminence for articulation with the posterolateral surface of the dorsolateral eminence of the trapezium. A very small, roughly triangular facet is on the anterior surface for articulation with metacarpal II.

The trapezoid of *P. viator* **sp. nov.** differs from that of all compared taxa in having a smaller articulation with metacarpal II. It further differs from *C. kitcheneri* in being smaller relative to the capitatum; from *O. rufus*

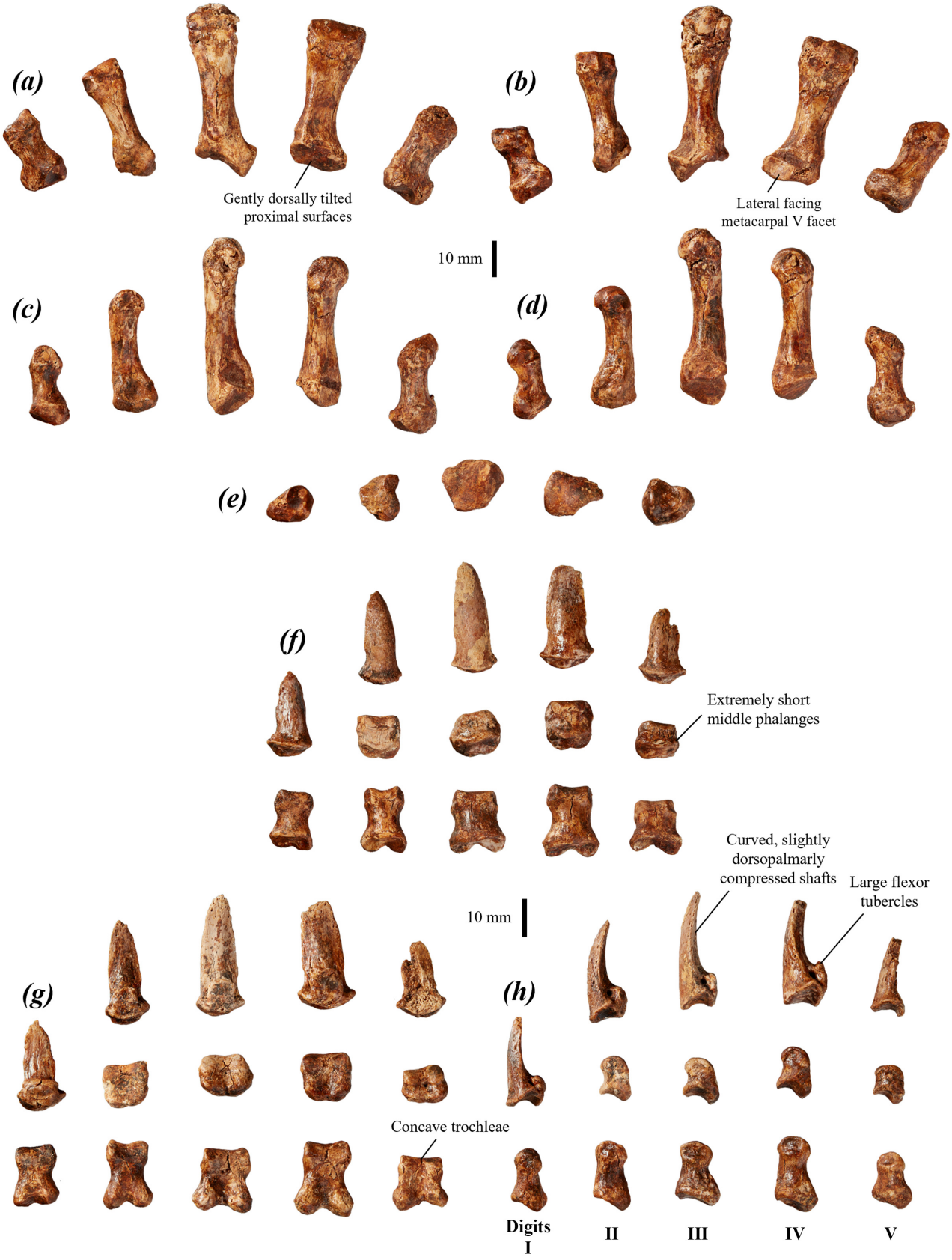

FIGURE 71. right metacarpals and manual phalanges of *P. viator* **sp. nov.** holotype SAMA P59552: (a–e) metacarpals I–V in (a) dorsal, (b) palmar, (c) lateral, (d) medial, and (e) proximal views; and (f–h) proximal, middle and distal manual phalanges I–V in (f) dorsal, (g) palmar, and (h) lateral views.

and *M. fuliginosus* in being smaller relative to the trapezium; and from that of *W. bicolor* in being absolutely larger, and smaller relative to the trapezium.

Trapezium (Figs 68a–c & 70k–l): considerably larger than the trapezoid; broad and trapezoidal in anterior view, with a large, pointed eminence against the lateral margin on the anterodorsal surface for articulation with the anteromedial surface of the trapezoid and with the dorsal component of the posterior surface of metacarpal I; articulates with the dorsoanterior surface of the palmar process of the scaphoid, such that the broad, dorsally tapering and dorsally concave facet for metacarpal I faces anteriorly. Facet for the scaphoid broad and deeply, smoothly concave. Facet for metacarpal I has a larger, rounded medial section that continues laterally into a smaller, gently convex dorsolateral section on the pointed anterolateral eminence.

The trapezium of *P. viator* **sp. nov.** differs from that of *P. mamkurra* **sp. nov.** in being slightly narrower, with a more pointed medial margin; from *C. kitcheneri* in having a more concave facet for the palmar process of the scaphoid; from *O. rufus* and *M. fuliginosus* in being larger relative to the trapezoid, with a more pointed anterolateral eminence and a more distinct facet for metacarpal I with more discrete medial and lateral sections; and from *W. bicolor* in being absolutely larger and larger relative to the trapezoid, with a more deeply, smoothly concave facet for the palmar process of the scaphoid and a broader, more distinct facet for metacarpal I.

Metacarpals (Figs 68 & 71a–e): sexually dimorphic, with males exhibiting significantly greater robustness and greater length of metacarpals than females; metacarpals II–IV most elongate; each narrows to a distinct waist. Metacarpals I and V: proximal ends have a large, blunt tubercle on the medial and lateral surfaces respectively; both with distal ends distinctly asymmetrical, skewed mesially. Metacarpal IV: broad proximal facet for articulation with the capitatum, tilted dorsally and slightly medially; facet for metacarpal V faces laterally, abuts the lateral margin of the capitatal facet on the lateral surface of the proximal end. Metacarpal III: longest, with the proximal end separated into a longer, medially deflected medial process and a very short, laterally deflected lateral eminence; distal end has a particularly large, palmodistally prominent keel. Metacarpal II: slightly shorter than III and IV and considerably more gracile; lateral margin of the proximal end wraps slightly around the proximomedial margin of metacarpal III. Metacarpal I: shortest, with the tall, narrow proximal facet for the trapezium slightly laterally situated and tilted dorsally.

The metacarpals of *P. viator* **sp. nov.** differ from those of *P. anak* in being more gracile, with metacarpal V facet on metacarpal IV distinctly lateral facing (rather than anterior facing) (Fig. 71b); from *P. mamkurra* **sp. nov.** in being more gracile, with a relatively narrow distal end of metacarpal III and a less dorsally tilted proximal articular surface on metacarpals IV and V; from *P. otibandus* in being larger and more gracile, with a lateral facing metacarpal V facet on metacarpal IV; from *C. kitcheneri* in being more elongate, with generally broader proximal articular surfaces, more pronounced waists, and less convex distal articular surfaces; from *O. rufus* in being larger and more gracile, with much larger proximomedial and proximolateral tubercles on metacarpals I and V respectively; from *M. fuliginosus* in being larger, with metacarpals I and V more gracile and with much larger proximomedial and proximolateral tubercles; and from *W. bicolor* in being much larger and slightly less dorsopalmarly compressed, with a larger proximolateral process on metacarpal III.

Manual phalanges (Figs 68d & 71f–h): short and robust relative to metacarpals, excluding distal phalanges III and IV, which are quite elongate; proximal and middle phalanges are increasingly symmetrical mesially. Proximal phalanges: broad; proximal and distal articular surfaces gently concave; proximal articular surfaces slightly dorsally tilted, with low, rounded palmar tubercles slightly proximally projected beneath. Middle phalanges: extremely short, broad and dorsopalmarly compressed, with gently dorsally tilted proximal articular surfaces, and shafts lacking a waist. Distal phalanges: quite long, with a large palmar tubercle, and shafts gently palmarly curved and highly dorsopalmarly compressed; broader in males than in females.

The manual phalanges of *P. viator* **sp. nov.** differ from those of *P. anak* in having proximal phalanges with slightly less dorsally tilted proximal surfaces and shallower, very gently concave (rather than broadly V-shaped) trochleae, and distal phalanges with more palmarly curved shafts; from *P. mamkurra* **sp. nov.** in being generally shorter, with proximal phalanges with slightly less dorsally tilted proximal surfaces, and distal phalanges slightly more palmarly curved, narrower, less dorsopalmarly compressed (less spatulate) with larger and more palmarly projected palmar tubercles; from *P. otibandus* in being larger and relatively short and robust, with more dorsopalmarly compressed distal phalanges with smaller palmar tubercles; from *C. kitcheneri* in being significantly shorter relative to the metacarpals, relatively broader and far more dorsopalmarly compressed (particularly the middle phalanges), with broader and less V-shaped trochleae, and dorsally rounded (un-peaked) distal phalanges with less palmar curvature of the shaft; from *O. rufus* in being larger, more robust and more dorsopalmarly compressed, with relatively shorter proximal phalanges, and relatively longer distal phalanges with more palmarly curved shafts; from *M. fuliginosus* in being larger and relatively short and robust, with much more dorsopalmarly compressed and spatulate distal phalanges; and from *W. bicolor* in being much larger, relatively broader and more robust, with less dorsally tilted proximal surfaces on the proximal phalanges.

Hindlimb

Pelvis (Fig. 72): ilium, ischium and pubis unfused in juveniles. Ilium: robust, well-developed and roughly L-shaped in cross-section. Iliac crest thick, broad, gently rounded along the dorsal margin, aligned transversely and projected slightly laterally; extends onto the dorsal end of the caudal iliac spine; ilium gently increases to maximum

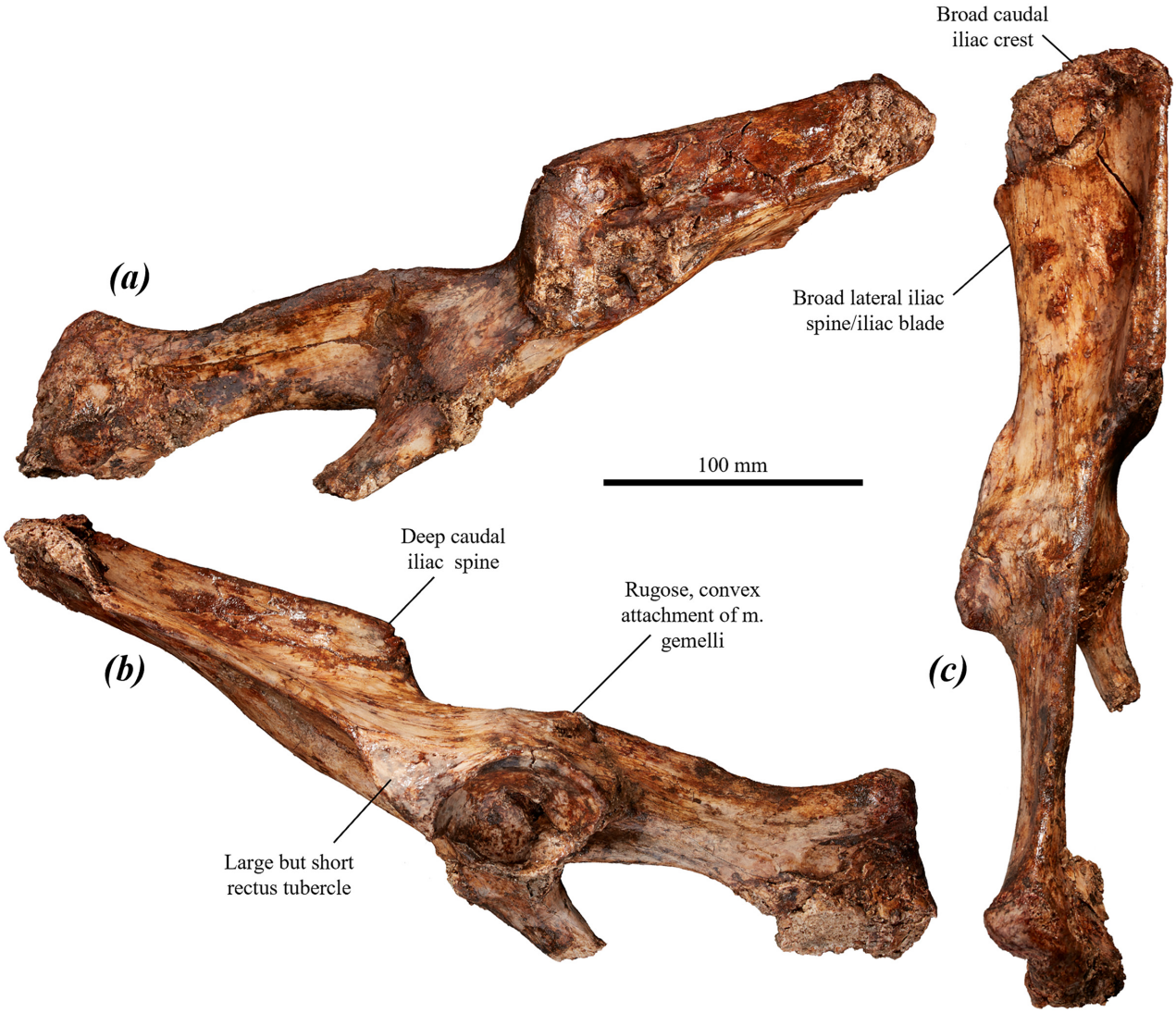

FIGURE 72. partial left pelvis of *P. viator* **sp. nov.** paratype SAMA P59550 in: (a) medial, (b) lateral, and c) caudodorsal views.

width at the iliac crest. Iliac fossa extends around three-quarters of the length of the ilium in adults, shorter and shallower in juveniles; extends from craniodorsal to the acetabulum and curves along the lateral surface of the cranial iliac spine; quite deeply concave proximally, becomes shallower distally. Gluteal fossa broad and deeply concave, extends to the iliac crest. Caudal iliac spine arises on the caudomedial surface of the base of the ilium opposite the rectus tubercule and projects caudally; thick and deep in proximal component for the origin of a large mm. gluteus, becomes steadily thinner and lower distally, extends to the iliac crest. Sacral surface large, very rugose and concave; articular surface for the wings of the sacrum deep and aligned craniocaudally with a slight cranial tilt; sacral surface deeper in older specimens such that the cranial margin projects cranially as a broad, low ridge with a thin crest (the cranial iliac spine) to contribute to the depth of the iliac fossa. Lateral iliac spine very broad, thin relative to the caudal spine; margin slightly and irregularly concave, curves laterally to projected dorsolateral extremity at the iliac crest. Rectus tubercule quite large, rugose, roughly triangular, narrows rapidly onto the lateral spine; increases in relative size with age.

Acetabulum large, tall and deeply concave; taller than depth, deepest in the proximal section; acetabular fossa deep, with the angle, width and curvature variable within individuals; partially covered cranially and caudally by a lip projecting from the acetabular surface; poorly developed in juveniles, with the cranial and caudal margins relatively very low. Ischium: very deep ventral to the acetabulum, transversely compressed, gently concave on medial surface and convex on lateral surface; caudal margin gently rugose and undulating from the origin of the mm. gemelli; deflected slightly caudally relative to the axis of the ilium; caudal component broadens toward the broad, laterally projected ischiatic tuberosity; caudal surface of the dorsal section of the ischium (caudally adjacent to the acetabulum) very broad, convex and rugose; caudomedial surface of the ischium has a broad, smoothly concave fossa. The iliopubic eminence is a slightly projected rounded point, broad and rugose. Craniodorsal angle of the obturator foramen is acute and

rounded, with the ventral angle broadly rounded and obtuse. Pubis: narrows ventral to the iliopubic eminence, broadens and craniocaudally flattens toward the pubic tubercle; becomes significantly more robust and broader at the dorsal base with age. Ischiatic table tall, deep and transversely compressed.

The pelvis of *P. viator* **sp. nov.** differs from that of *P. mamkurra* **sp. nov.** in having a slightly broader lateral iliac spine and a shorter rectus tubercle; from *P. tumbuna* in having a more curved caudally ilium in lateral view, a less laterally projected rectus tubercle, acetabulum opening laterally and less cranioventrally, larger iliopubic eminence, and a narrower, more planar ischium that is slightly longer relative to ilium length and slightly caudally deflected relative to the axis of the ilium in lateral view; from *P. dawsonae* **sp. nov.** in being larger, with a slightly deeper caudal iliac spine, more deeply concave gluteal fossa, broader, more rugose and more convex caudal surface of the dorsal section of the ischium, and a more deeply concave acetabulum; from *C. kitcheneri* in being larger, with a far broader, deeper gluteal fossa, narrower, less distally extensive iliac fossa, more rounded cranial iliac spine, more caudally and dorsally situated sacral surface relative to the acetabulum, and a rounder, shallower acetabulum; from *O. rufus* and *M. fuliginosus* in being generally larger and more robust, with a far broader and deeper gluteal fossa, a less distally extensive iliac fossa, more rounded cranial iliac spine, broader lateral iliac spine, and a greater maximum acetabulum diameter relative to ilium length; and from *W. bicolor* in being far larger, having the caudal iliac spine lack a small, pointed eminence on the caudoventral shoulder, and in having the iliac crest aligned more transversely and less craniocaudally, a broader, deeper gluteal fossa, a narrower, less distally extensive iliac fossa, broader lateral iliac spine (particularly dorsally), rectus tubercle with a smaller, shallower fossa on lateral surface, and a higher, more distinct dorsoventral ridge leading to the lateral surface of the ischiatic tubercle.

Epipubic (Fig. 59): thin, straight and flattened; broadens and thickens to the proximal articulation with the pubis.

The epipubic of *P. viator* **sp. nov.** differs from that of *C. kitcheneri* in being larger and more gracile; from *O. rufus* and *M. fuliginosus* in being more robust at the pubic articulation; and from *W. bicolor* in being much larger.

Femur (Fig. 73): large, short and robust, with the shaft straight in dorsal view and very slightly bowed dorsally in lateral view. Head large, hemispherical, dorsomedially projected and flared dorsally. The greater trochanter is not known; greater trochanteric ridge very broad, thick, slightly ventrally arched and laterally projected to form a raised, rugose proximolateral ridge on the dorsolateral margin of the proximal end (Fig. 73a); proximolateral ridge more raised and distally longer in more mature specimens; probable origin point for an enlarged m. vastus lateralis. Trochanteric fossa extends distally to level with the lesser trochanter. The proximal end is very broad, with a smoothly, distinctly convex dorsal surface. Intertrochanteric crest raised, ventromedially projected and very distinct, extends distomedially from the ventromedial base of the greater trochanter to the lesser trochanter. Lesser trochanter is a large, rugose eminence, projected medially from the proximal end and slightly ventrodistal to the head, situated at medial peak of a broadly obtuse (110–120°), medially projected conjunction of the intertrochanteric crest and the lesser trochanteric ridge; lesser trochanteric ridge thick, very raised and strongly medially projected, particularly in older individuals, extends distolaterally with slight dorsal deflection to merge into the femoral shaft between one-third and half of femoral length.

Femur shaft round to very slightly transversely compressed in cross-section; width tapers to a minimum around the midpoint and broadens to the distal end; ventral surface gently convex, becomes planar and gently medially tilted distally; in some specimens (see NMV P173087), lesser trochanteric ridge extends as a very low, rounded ridge to merge into the shaft near to the quadratus tubercle. Quadratus tubercle situated between one-third and midpoint of the length of the shaft, on the ventral surface of the shaft with a slight medial displacement; large, raised, rugose, elongate and oval, with a tapering rugose patch extending proximally to adjacent to or onto the proximal end. A small, deep fossa sits on the proximoventral margin of the lateral condyle on the ventrolateral surface of the shaft, continuing into a broad, shallow fossa on the proximal surface of the lateral condyle; lateral fabellae preserved between these fossae and the caudolateral margin of proximal tibial epiphysis in SAMA P53835a and SAMA P59550 indicate the partial origin of the m. flexor digitorum superficialis from a thick tendon in these two fossae.

Femur distal epiphysis large, robust and quite tall. Trochlea quite wide, deep and with the concavity approaching V-shaped, distinctly medially skewed and displaced (Fig. 73e). Trochlear crests tall, with the medial crest considerably lower and narrower than the lateral crest. Intercondylar fossa variably narrow (see SAMA P25203 versus SAMA P59550) and very deep, broadest at the midpoint before narrowing to the slightly laterally displaced ventrodistal component. Condyles broadest across the ventral surfaces, with the lateral condyle slightly broader and quite concave laterally, due to the lateral projection and ventral deflection of the lateral epicondyle for the well-developed fibular facet; lateral condyle larger and broader in distal view. Both epicondyles increase in size with age, with an associated increase in the size and depth of the fossae. Lateral epicondyle very large, tall and strongly laterally projected, particularly the ventral part, with a slight ventral deflection in distal view; a small, deep, rounded fossa on the distal margin of the ventral part and a broad, shallow, rounded fossa on midpoint of lateral surface are for the origins of the m. gastrocnemius lateralis. Medial epicondyle relatively flat and unprojected, with a small, deep, rounded mesial fossa for the attachment of the m. gastrocnemius medialis.

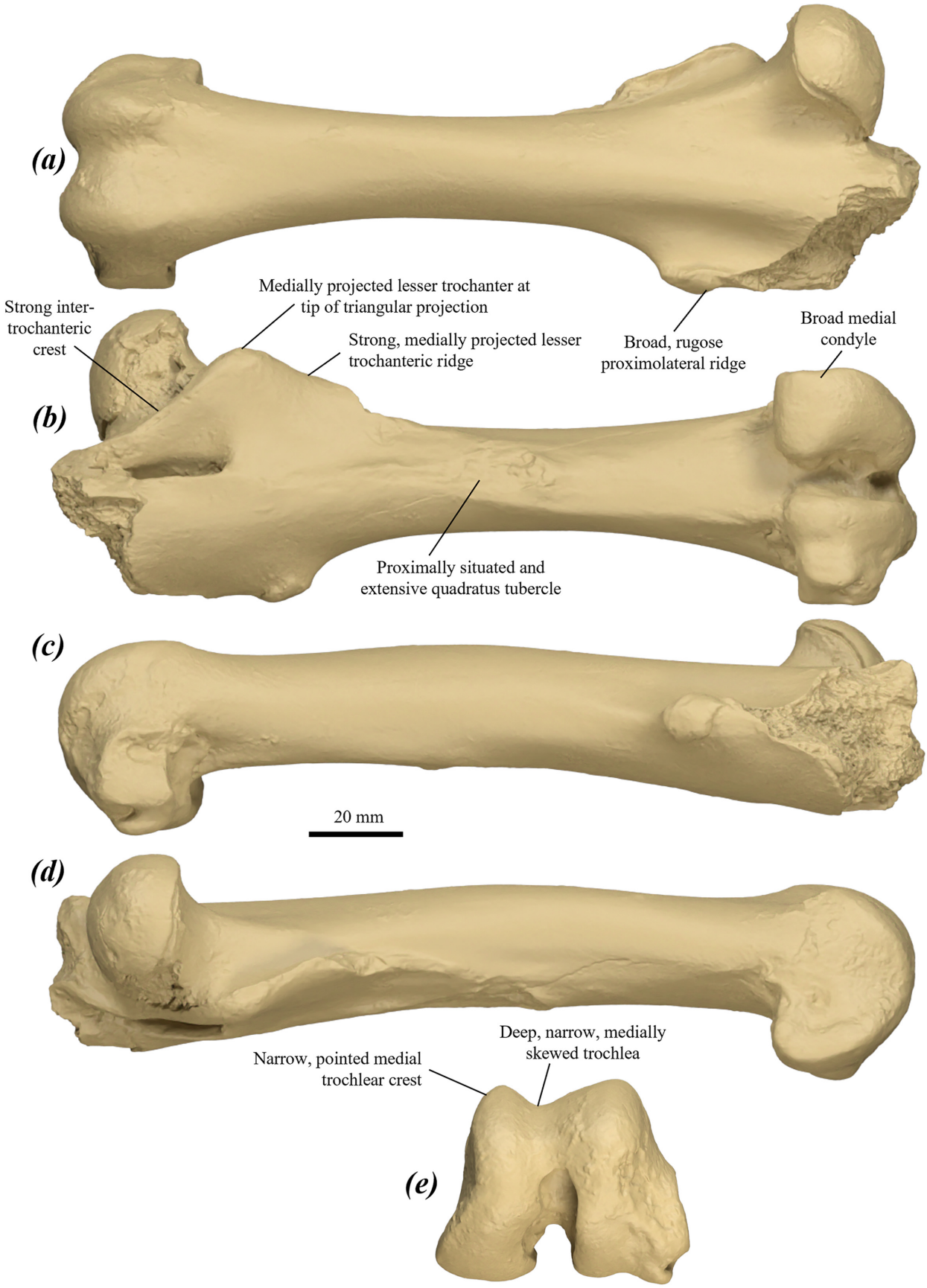

FIGURE 73. surface scan images of left femur of *P. viator* **sp. nov.** NMV P173087 in: (a) dorsal, (b) ventral, (c) lateral, (d) medial, and (e) distal view.

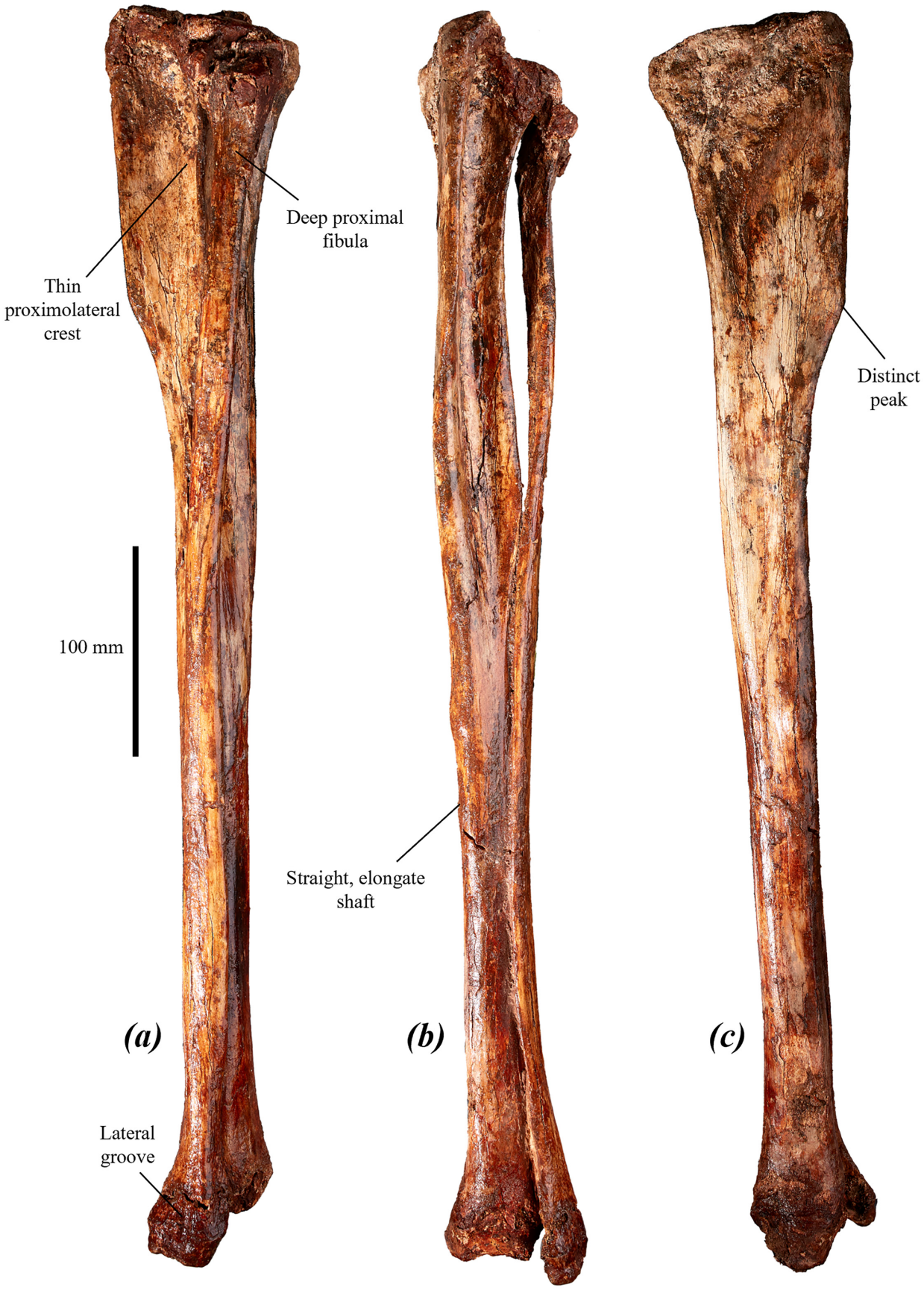

FIGURE 74. articulated left tibia and fibula of *P. viator* **sp. nov.** paratype SAMA P59550 in: (a) lateral, (b) cranial, and (c) medial views.

The femur of *P. viator* **sp. nov.** differs from other species of *Protemnodon* in being relatively shorter and more robust, with a more raised and more distinct intercondylar crest, and a more medially projected lesser trochanter and lesser trochanteric ridge forming a large, medially projected triangular crest ventral to the femoral head. Further differs from that of *P. mamkurra* **sp. nov.** in having a more raised proximolateral ridge, a narrower, deeper trochlea, narrower trochlear crests, medial trochlear crest coming to a more pointed peak, and a less medially projected ventral part of the medial epicondyle; from *P. anak* in having a narrower medial trochlear crest and a deeper, narrower trochlea; from *P. tumbuna* in being larger, with a relatively less elongate and more proximally situated quadratus tubercle and the lateral trochlear crest coming to a narrower peak; from *P. otibandus* in being larger, with a more medially projected lesser trochanter and a broader ventral surface of the medial condyle; from *C. kitcheneri* in being larger and more robust, with higher intertrochanteric and proximolateral ridges, a more medially projected lesser trochanter, straighter and more distally extensive lesser trochanteric ridge, less medially displaced quadratus tubercle, deeper trochlea, more pointed medial trochlear crest, and a less distally situated lateral gastrocnemial fossa; from *O. rufus* in being larger and more robust, with relatively broader proximal and distal ends, a relatively larger head, more raised proximolateral ridge and intercondylar crest, more medially projected lesser trochanter, straighter and more distally extensive lesser trochanteric ridge, more elongate quadratus tubercle, shallower fossa for the partial origin of the m. flexor digitorum superficialis, less raised trochlear crests, more laterally projected lateral epicondyle, and a more proximally situated lateral gastrocnemial fossa; from *M. fuliginosus* in being larger and more robust, with a less distally extensive trochanteric fossa, a more raised, distinct intercondylar crest, more medially projected lesser trochanter, more raised proximolateral ridge, longer lesser trochanteric ridge, longer, more proximally extensive quadratus tubercle, shorter distolateral fossa for the origin of the m. flexor digitorum superficialis, relatively slightly more raised dorsal section of the medial condyle, more dorsodistally extensive intercondylar fossa, and a more proximally situated lateral gastrocnemial fossa; and from *W. bicolor* in being larger and considerably more robust, with a relatively larger, more dorsally deflected head, a more medially projected lesser trochanter, less distally extensive trochanteric fossa relative to head, much more distally extensive lesser trochanteric ridge, more raised proximolateral crest, less dorsoventrally compressed distal shaft, broader, less raised trochlear crests, shallower trochlea, larger fibular facet on lateral condyle, and a more laterally projected lateral epicondyle.

Tibia (Fig. 74): large and elongate. In cranial view, the proximal component is bowed very slightly medially, but the distal shaft is quite straight. Proximal epiphysis deeper than width; medial condyle narrow, deep and slightly projected caudally; lateral condyle much less deep, smaller and more extended laterally with a large, concave muscular groove in the craniolateral margin. Proximal fibular facet elongate, narrow and shelf-like, orientated ~40° from the sagittal plane. Cnemial crest deep and elongate, with an indistinct, rugose, curved distal peak, below which it slowly thickens and merges with into the midpoint of the shaft; lateral surface gently concave and medial surface very slightly convex. Proximolateral crest thin and very raised, extends and thickens distally to merge into the distal fibular facet on the distolateral surface of the shaft. Shaft elongate; minimum shaft diameter is in the distal quarter, with the diameter increasing gently to the distal epiphysis. Distal fibular facet extends on the lateral surface from slightly proximal to the midpoint of the shaft to immediately proximal to the distal epiphysis. Distal epiphysis robust; talar trochlea roughly square, gently concave and with the cranial part projected to face the articular surface caudally; medial tuberosity narrow and very deep with a blunt medial malleolus.

The tibia of *P. viator* **sp. nov.** differs from that of all species of *Protemnodon* except *P. snewini* in being more gracile. It further differs from *P. anak* in having a straighter distal shaft in cranial and lateral views; from *P. mamkurra* **sp. nov.** in being longer and in having a less laterally curved cnemial crest with a more angular and distinct distal peak, a thinner proximal section of the proximolateral crest, and a straighter distal shaft in cranial view; from *P. tumbuna* in being larger, much longer, and straighter in cranial view, with a more angular and distinct peak of the cnemial crest; from *P. otibandus* in being larger, with a shallower proximal fibular facet, narrower intercondylar eminence, narrower and less rounded cranial section of the proximal epiphysis, and a more angular, distinct peak of the cnemial crest; from *P. snewini* in being more robust, with a deeper, narrower proximal epiphysis; from *C. kitcheneri* in being larger and more gracile, with a relatively narrower proximal epiphysis, taller intercondylar eminence, more raised proximal part of proximolateral crest and relatively deeper shaft with greater expansion to distal epiphysis; from *O. rufus* in being more robust, with a more laterally deflected cranial section of the proximal epiphysis, more elongate cnemial crest, slightly thicker and weaker proximolateral crest, and a shorter distal shaft relative to the proximal shaft; from *M. fuliginosus* in being larger and more robust, with a more laterally curved cnemial crest and a straighter shaft in lateral view; and from *W. bicolor* in being larger, having the proximal epiphysis with a deeper intercondylar eminence and a narrower, less cranially tilted cranial component, and in its more raised proximolateral crest and larger talar trochlea.

Fibula (Fig. 74): elongate and curved very slightly caudally toward the proximal end. Proximal epiphysis large and deep; caudal process for articulation with the fibular facet on the lateral condyle of femur is proximally projected, tall, deep and narrow; a large, blunt tubercle is present on the lateral surface of the base of the epiphysis, probably for the origin of the m. flexor digitorum profundus; a small, deep concavity for the tibiofibular ligament sits at the craniolateral base of the process for femoral articulation. Proximal shaft initially roughly triangular in cross-section, narrows to flattened distally,

then broadens slightly and tapers craniocaudally before flaring craniocaudally to the distal epiphysis; a broad, deep groove extends down the caudomedial surface of the shaft from the proximal epiphysis; fibula first articulates with the tibial shaft two-fifths of the distance to the distal end, after which the fibular shaft narrows and deepens, becoming thin and slightly crescentic in cross-section. Some specimens (see SAMA P59550) have a narrow lateral groove extending from the distal shaft onto the lateral surface of the epiphysis. Distal epiphysis large and deep, narrows cranially. Calcaneal facet has a narrow, flat caudal section that is tilted strongly medially to be almost blade-like, then broadens and rotates to face ventrally in its smoothly rounded, gently convex cranial section.

The fibula of *P. viator* **sp. nov.** differs from that of *P. anak* in having a relatively narrower distal epiphysis with a shallower lateral groove and a broader, less medially slanted caudal calcaneal facet; from *P. mamkurra* **sp. nov.** in being longer, with a deeper, narrower proximal shaft, and stronger broadening and craniocaudal tapering of the distalmost shaft before the epiphysis; from *C. kitcheneri* in being larger, with relatively larger proximal and distal epiphyses and a deeper distal shaft; from *O. rufus* in being much more robust, with a relatively larger, deeper proximal epiphysis and a deeper distal shaft; from *M. fuliginosus* in being larger and more robust, with a larger lateral tubercle on the proximal epiphysis, a relatively taller process for articulation with the fibular facet of the femur, a much deeper distal shaft, and a more medially tilted caudal part of the calcaneal facet; and from *W. bicolor* in being larger and more robust, with a relatively larger proximal end and the distal shaft with a more distinct craniocaudal taper.

Pes (Fig. 75a–d)

Calcaneus (Fig. 76a–f): tall, fairly narrow and elongate. Calcaneal tuberosity tall, narrow and roughly triangular in cross-section; broadens caudally to a thickened caudal epiphysis; medial surface flat to gently concave and lateral surface gently concave, becomes deeply concave beneath the fibular facet. Caudal surface for the gastrocnemial tendon very tall and domed, with a narrow transverse groove across the midline, occasionally mesially kinked. Plantar surface rugose, triangular in plantar view, narrows to a rounded point cranially and extends to the level with the cranial margin of the sustentaculum tali; becomes thicker, broader and more rugose with age; a thickened caudal component arises from the caudal epiphysis. Cranial plantar tubercule small but distinct and plantomedially projected; sits immediately caudal to the plantar margin of the plantomedial cuboid facet.

The calcaneal head is large, tall and fairly narrow. Sustentaculum tali large and quite elongate caudally and plantarly, moderately medially projected, subequal to or slightly more than medial talar facet, with caudoplantar margin rounded and coming to blunted peak on the cranioplantar margin; thickens medially with age; flexor groove broad and deep. Fibular facet large and laterally projected, with cranial and caudal sections separated on lateral edge by a short, broad transverse groove and linked medially by a narrow section of facet semicontinuous with the lateral talar facet; caudal component small, caudal-facing, oval to smoothly triangular, slightly convex and with margins indistinct except for a crest-like, laterally projected lateral margin (Fig. 76a); cranial section larger and dorsally flat to concave with a convex, rounded lateral face. Lateral talar facet broad, convex and tapering very slightly medially, approaches square in dorsal view; a rounded, gently concave fossa of moderate depth sits immediately cranial to the lateral talar facet for articulation with the craniolateral end of the talus, with a small, blunt tubercle, more raised with age, on the medial margin of the fossa. Medial talar facet small, concave, cranially tilted, rounded to slightly craniocaudally compressed, caudally displaced relative to the lateral talar facet, with the cranial component inset into the dorsal surface of the calcaneal head; articular surface extends slightly onto the caudal surface to create a slight rounded lip.

Facet for the talar head small, abuts the medial margin of the dorsomedial facet on the medial surface of the calcaneal head. Dorsomedial cuboid facet broad, gently convex, rounded or oval to smoothly rectangular with rounded dorsomedial margin, generally broader than dorsolateral facet; occasionally dorsally displaced relative to dorsolateral facet; moderately deep, dorsoplantarly compressed fossa immediately plantar to dorsomedial cuboid facet. Dorsolateral cuboid facet tall, quite narrow, slightly concave to slightly convex and cranially projected; extends plantarly and slightly medially, narrowing to become the plantomedial facet. Plantomedial cuboid facet variable, but generally small, slightly convex, rounded in cranial view and not extending medially beyond the midpoint of the dorsomedial facet; slightly dorsoplantarly compressed in some specimens (see SAMA P50549); curves distinctly dorsomedially in some specimens.

The calcaneus of *P. viator* **sp. nov.** differs from that of other species of *Protemnodon* and of *C. kitcheneri* in being relatively taller, narrower and more gracile, and in having a less medially projected sustentaculum tali. It further differs from that of *P. anak* in having a less distinct, less rounded and more laterally projected caudal component of the fibular facet; from *P. mamkurra* in having a narrower plantar surface, a smaller, more caudally displaced medial talar facet, less convex lateral talar facet, smaller, less dorsally bulbous fibular facet, and a more rounded sustentaculum tali; from *P. tumbuna* in being larger, with a relatively broader dorsomedial cuboid facet, less medially displaced calcaneal head, and a planar, less medially flared plantar surface that is less rounded in plantar view; from *P. dawsonae* **sp. nov.** in being larger, with a more triangular, less rounded calcaneal tuberosity in cross-section, deeper lateral talar facet, and a narrower and more sagittally aligned medial talar facet; from *P. otibandus* in being larger, with a more triangular calcaneal tuberosity in cross-section, relatively broader dorsomedial cuboid facet, and the lateral surface of the calcaneal head beneath the fibular facet much taller and more concave; from *C. kitcheneri* in being larger, with a flatter, less laterally tilted and more cranially extensive plantar surface, a deeper, flatter lateral talar facet, and a

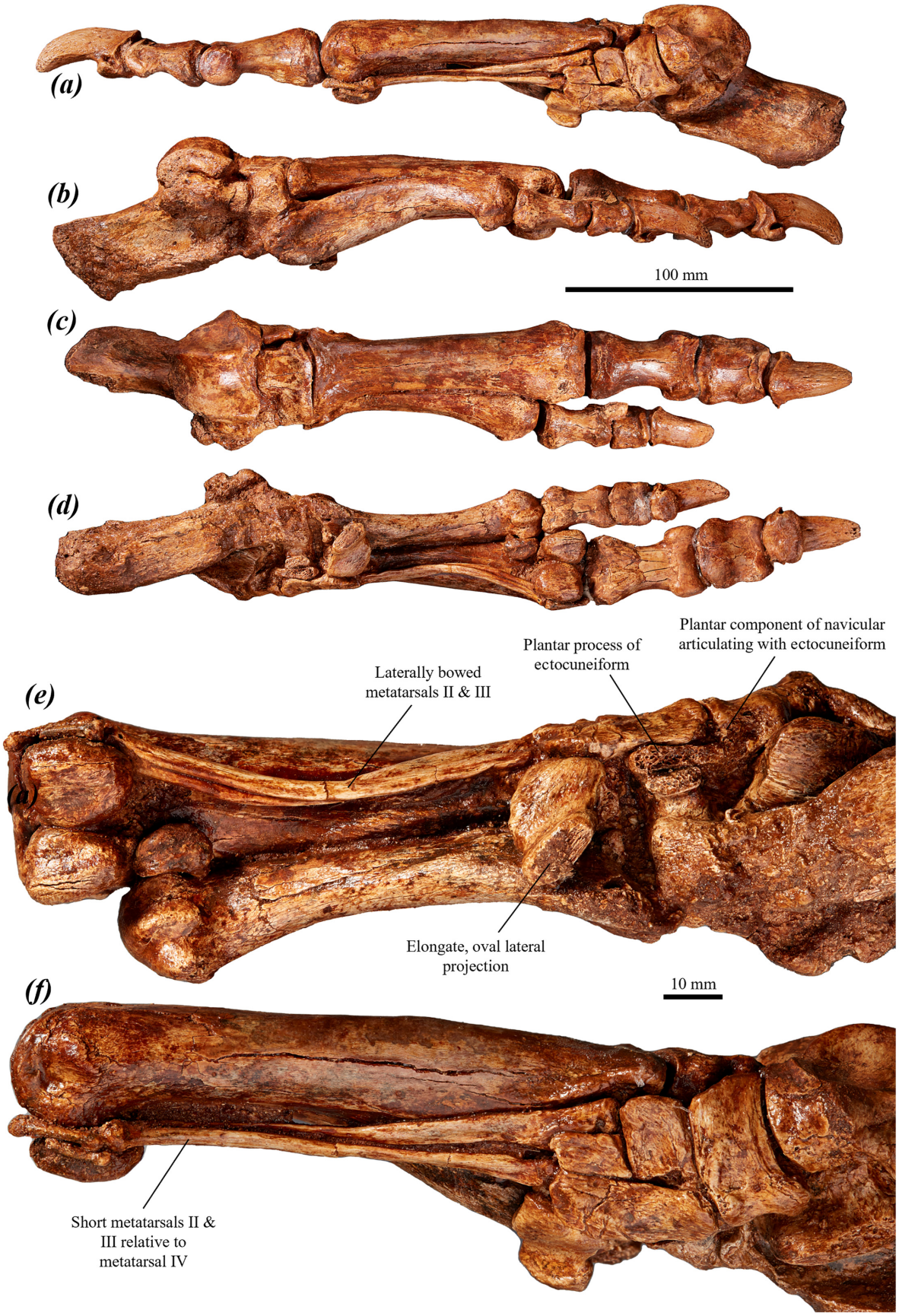

FIGURE 75. right pes of *P. viator* **sp. nov.** holotype SAMA P59552: (a–d) articulated pes in (a) medial (b) lateral, (c) dorsal, (d) plantar views; and (e–f) articulated metatarsals II–V, proximal phalanges II and III, plantar sesamoids, and tarsals in (e) plantar, and (f) medial views.

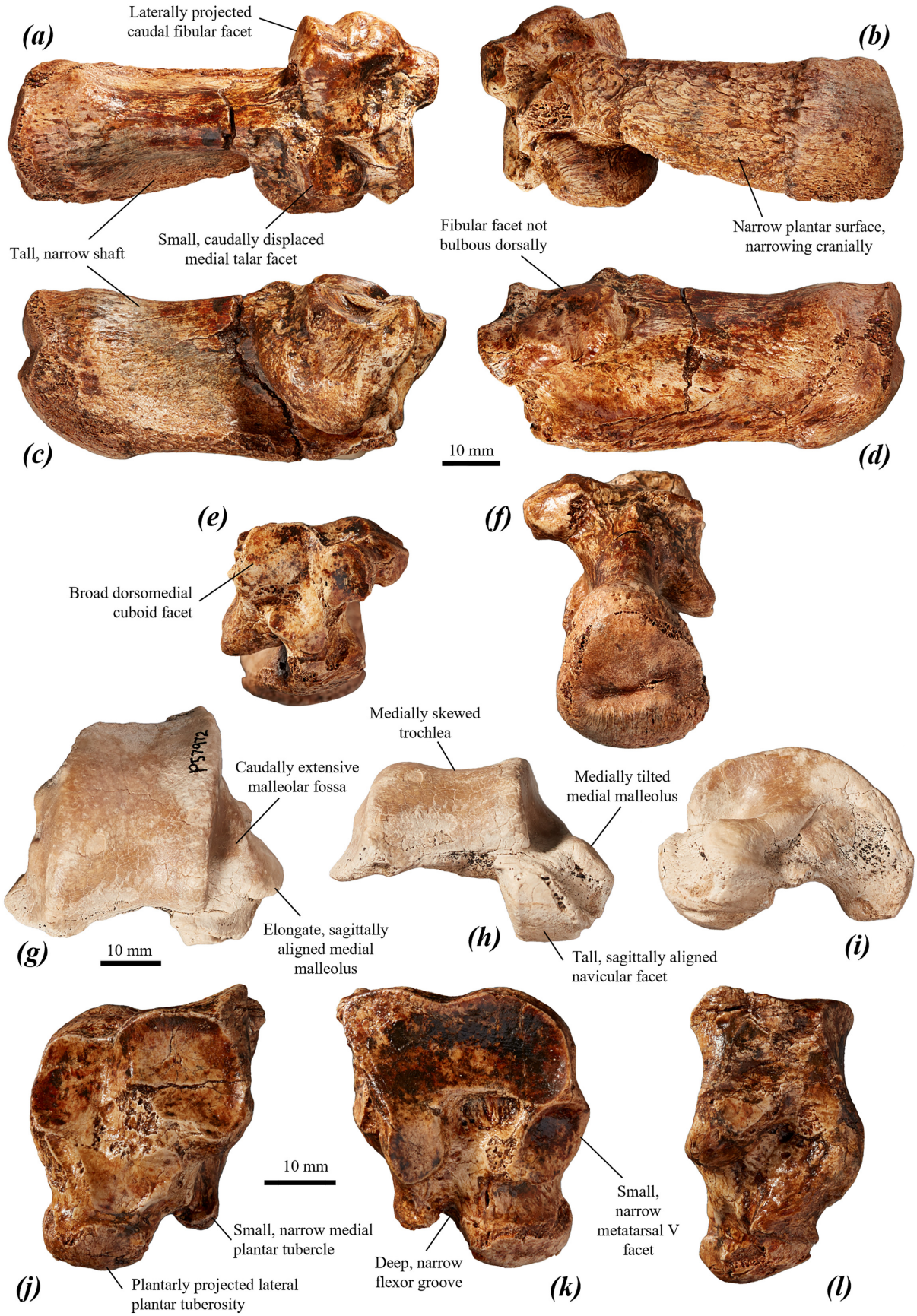

FIGURE 76. tarsal elements of *P. viator* **sp. nov.**: (a–f) left calcaneus of holotype SAMA P59552 in (a) dorsal, (b) plantar, (c) medial, (d) lateral, (e) cranial, and (f) caudodorsal views; (g–i) right talus of SAMA P57972 in (g) dorsal, (h) cranial, and (i) medial views; and (j–l) right cuboid of SAMA P59552 in (j) caudal, (k) cranial, and (l) medial views.

less laterally tilted dorsomedial cuboid facet; from *O. rufus* in being larger and slightly broader, with a less laterally displaced head, more medially projected sustentaculum tali, no articular surface for the posterior plantar process of the talus, flatter and deeper lateral talar facet with a shallower cranial fossa, less cranially tilted medial talar facet, more dorsally projected fibular facets, plantar surface that broadens caudally, and a smaller cranial plantar tubercle; from *M. fuliginosus* in being larger and relatively taller, with a more medially projected sustentaculum tali, more caudally projected caudal fibular facet, and less laterally and more dorsally projected fibular facets; and from *W. bicolor* in being larger and relatively taller, with a more triangular tuberosity in cross-section, broader medial talar facet with rounded caudal lip, and a broader dorsomedial cuboid facet relative to dorsolateral facet.

Talus (Fig. 76g–i): large and robust, width greater than craniocaudal length. Trochlear crests equal in height, come to rounded points with the medial crest slightly more pointed; trochlea moderately shallow, with the concavity slightly medially skewed. Medial malleolus elongate, extends cranially and slightly medially, and mediocaudally tilted; malleolar fossa shallow, elongate and smoothly concave, with a slight ridge at the cranial margin that distinctly separates the fossa from the dorsal surface of the talar head. Talar head craniomedially projected and plantarly deflected. Articular facet for the navicular large and tall, extends caudoplantarly to beneath medial malleolus. Articular facet for the cuboid smaller and lateral facing, with a very slight cranioplantar tilt. Posterior plantar process short, thick and rounded. On the plantar surface, the medial calcaneal facet is craniocaudally short and deeply concave, with the cranial lip plantarly projected, and lateral calcaneal facet broad and smoothly concave.

The talus of *P. viator* **sp. nov.** differs from that of *P. anak* in lacking small indent between cranial margin of medial trochlear crest and talar head, and in having a less cranially projected talar head, medial malleolus more aligned in the sagittal plane, and the concavity of the trochlea more medially skewed; from *P. mamkurra* **sp. nov.** in having a less cranially projected talar head, with the malleolar fossa slightly more caudally situated and the navicular facet aligned in the sagittal plane (rather than curving plantomedially); from *P. otibandus* in being larger, with a shallower, more elongate and more caudally situated malleolar fossa and a more elongate and medially tilted medial malleolus; from *C. kitcheneri* in being larger and relatively slightly more elongate, with a less medially skewed trochlear concavity, a facet for the cuboid present on the talar head, and a more caudoplantarly extensive navicular facet; from *O. rufus* in being larger and relatively broader, with deeper trochlea, shallower malleolar fossa, less medially projected medial malleolus, less medially projected, more plantarly deflected talar head, more lateral facing cuboid facet, and a deeper, less projected posterior plantar process; from *M. fuliginosus* in being larger and relatively broader, with deeper trochlea, shallower malleolar fossa, less medially projected medial malleolus, less medially projected, more plantarly deflected talar head and larger cuboid facet; and from *W. bicolor* in being much larger, with a less medially skewed trochlear concavity, more caudoplantarly extensive navicular facet, and a more rounded posterior plantar process in medial view.

Cuboid (Fig. 76j–l): tall, robust, quite broad and roughly rectangular in dorsal view, with a step in the caudal margin for the calcaneal facets. Dorsolateral calcaneal facet quite tall, narrow and concave, continuous plantarly with the thin, elongate plantomedial facet. Dorsomedial calcaneal facet broad, squarish, concave and posteriorly projected, separated from the dorsolateral facet by a bevelled step. Facet for the talar head tall, thin, situated on the dorsal part of mediocaudal margin; slightly dorsally flares the caudal part of dorsomedial margin. Facet for the navicular small and rounded, occasionally indistinct, situated caudal to a tall fossa on the cranial part of the medial surface. Facet for the ectocuneiform tall and craniocaudally shallow, extends down the cranial margin of the medial surface onto the medial surface of the medial plantar tubercle. Dorsal metatarsal IV facet broad and slightly concave, covers the entire dorsal section of the cranial surface; medial component smoothly continuous with the slightly plantarly tilted plantomedial metatarsal IV facet; dorsal margin straight, becomes sinusoidal in cranial view in older individuals. Facet for metatarsal V quite large, broad, concave, rounded to oval and slightly laterally tilted, semicontinuous with the mediolateral margin of the dorsal metatarsal IV facet; separated from the plantomedial metatarsal IV facet by a moderately shallow, rugose fossa. Lateral plantar tubercle very large and plantarly projected, rounded to slightly elongate and oval in plantar view; caudal section occasionally extends dorsolaterally (see SAMA P25098). Medial plantar tubercle small, narrow, plantarly projected and quite elongate, separated from the lateral tubercle by the deep, narrow flexor groove.

The cuboid of *P. viator* **sp. nov.** differs from those of all species of *Protemnodon* in being taller and relatively narrower, with larger, more plantarly projected lateral and medial plantar tubercles and a deeper flexor groove (Fig. 76j–k). Further differs from that of *P. anak* and *P. mamkurra* **sp. nov.** in having a slightly more laterally situated medial plantar tubercle and a narrower flexor groove; from *P. otibandus* in being larger, with a more dorsally situated navicular facet and more elongate plantar tubercles; from *P. snewini* in being larger, with a more bevelled step between the dorsal calcaneal facets, more caudally tilted facet for the talar head, more medially situated medial plantar tubercle and broader flexor groove; from *C. kitcheneri* in being larger and taller, with a relatively narrower dorsomedial calcaneal facet, a facet for the talar head present, a larger, more plantarly projected lateral plantar tubercle, larger, more plantarly projected and more medially situated medial plantar tubercle, and a broader, deeper flexor groove; from *O. rufus* in being generally larger and relatively broader, with relatively broader dorsomedial calcaneal facet, more medially tilted facet for the talar head, more medially situated medial plantar tubercle, broader flexor groove and more medially situated plantar metatarsal IV facet; from *M. fuliginosus*

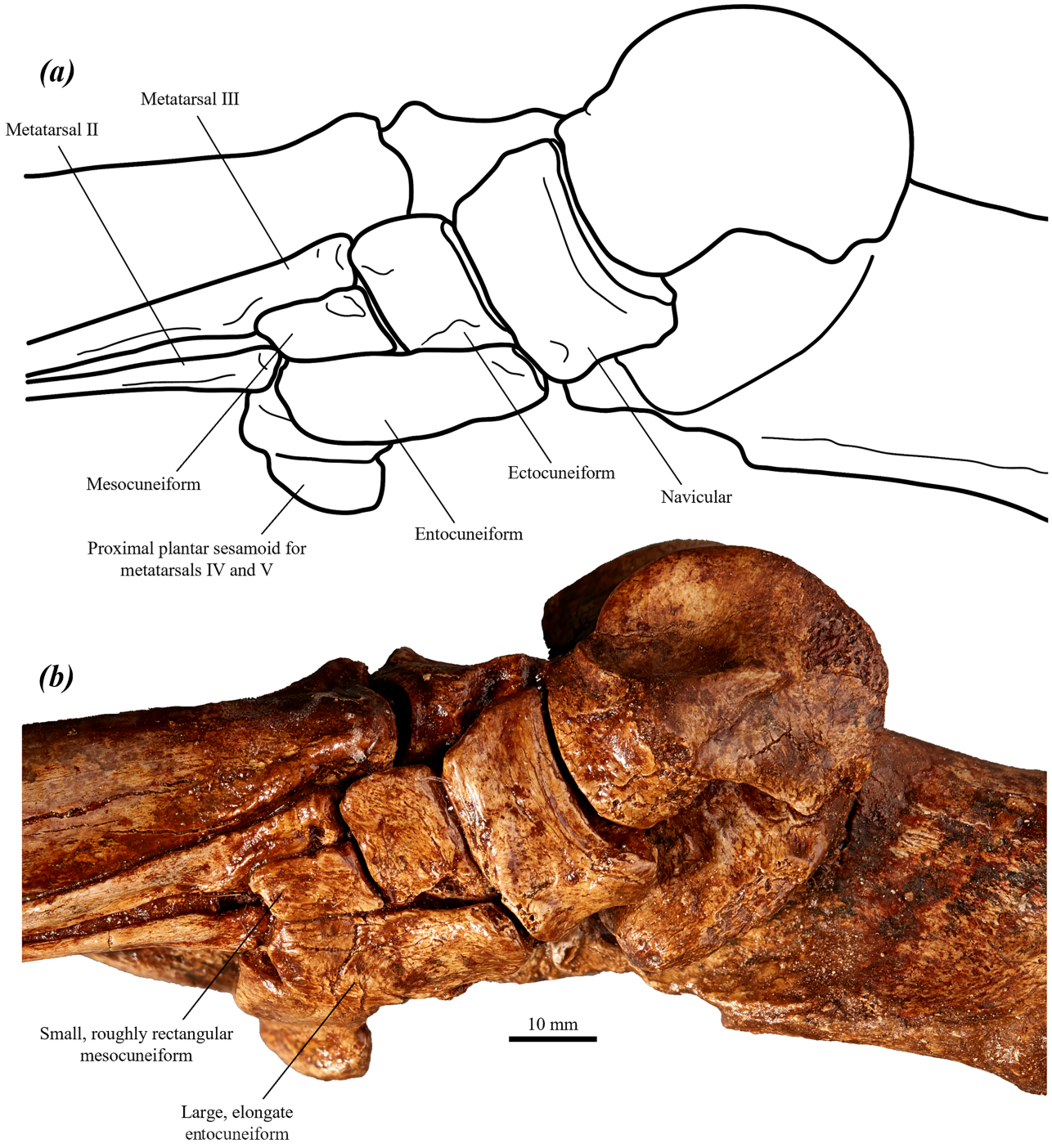

FIGURE 77. (a) line drawing and (b) photo of articulated tarsals of right pes of *P. viator* **sp. nov.** holotype SAMA P59552 in medial view.

in being larger and relatively deeper, with deeper navicular/ectocuneiform fossa on plantar component of medial surface, more medially situated medial plantar tubercle and broader flexor groove; and from *W. bicolor* in being larger and relatively taller, with more plantarly projected plantar tubercles and a deeper, narrower flexor groove.

Navicular (Figs 75e–f & 77): tall, very narrow and quite deep, with the width tapering slightly dorsally; caudal margin slightly taller than the cranial margin. Facet for the talar head gently concave, with the plantar section thickened and slightly caudally projected. Facet for the entocuneiform small and rounded, situated against the plantomedial margins of the cranial surface. Facet for the ectocuneiform tall and narrow, extends the entirety cranial surface, with plantar section lateral to the entocuneiform facet.

The navicular of *P. viator* **sp. nov.** differs from that of *P. mamkurra* **sp. nov.** in being broader, with a more plantarly extensive facet for the ectocuneiform; from

P. otibandus in being larger and broader, and deeper relative to height, with a less laterally flared facet for the ectocuneiform and a more medially tilted facet for the entocuneiform; from *C. kitcheneri* in being larger, taller and narrower; from *O. rufus* in being larger, narrower and less deep relative to height, with less deeply concave facet for the talar head, narrower, slightly more laterally situated and less smoothly convex facet for the ectocuneiform, and lacking an eminence on the medial margin of the cranial surface between the ectocuneiform facet and entocuneiform facet; from *M. fuliginosus* in being larger, taller and narrower, with a slightly more laterally situated facet for the ectocuneiform and lacking an eminence on the medial margin of the cranial surface; and from *W. bicolor* in being much larger and relatively narrower.

Ectocuneiform (Figs 75e–f & 77): tall, highly transversely compressed, slightly tapered dorsally in medial view and very slightly convex medially in caudal view. Facet for the navicular tall, narrow and gently concave, occupies almost all of the caudal surface. Facet for the entocuneiform large and moderately to deeply concave, occupies plantar component of medial surface. Facet for metatarsal IV small and rounded, situated against craniodorsal margin of lateral surface. Facet for the cuboid tall, craniocaudally thin and tapers plantarly, covers majority of caudal component of lateral surface. Facet for metatarsal III tall, narrow and gently concave, against dorsal margin of cranial surface; sits dorsal to small, narrow triangular eminence. Facet for the mesocuneiform small to very small and narrow, immediately plantar and occasionally slightly medial to metatarsal III facet. Plantar tubercle squarish in medial view, rugose and thickened at the plantar margin with a slight medial deflection; articulates on its lateral surface with the medial plantar tubercle of the cuboid.

The ectocuneiform of *P. viator* **sp. nov.** differs from that of *P. mamkurra* in being slightly narrower, with a narrower, less concave, more plantarly extensive navicular facet and a deeper plantar tubercle; from *P. otibandus* in being slightly more transversely compressed and relatively taller, with the dorsal margin level (rather than rounded-triangular) and a more deeply concave entocuneiform facet; from *C. kitcheneri* in being larger, with a larger, less cranially deflected plantar tubercle, larger facet for the mesocuneiform, and the facet for the cuboid not abutting the facet for metatarsal III; from *O. rufus* in being larger, with the navicular facet extending much further plantarly, a smaller cranial eminence, narrower, deeper, less plantarly projected and less cranially deflected plantar tubercle, and a relatively larger metatarsal III facet; from *M. fuliginosus* in being larger, with a more plantarly extensive navicular facet, larger facet for the mesocuneiform, and a less medially deflected plantar tubercle; and from *W. bicolor* in being larger, with a less concave, more plantarly extensive navicular facet.

Mesocuneiform (Figs 75f & 77): small to very small, rectangular to oblong in medial view, quite elongate, transversely compressed and dorsoplantarly short; articulates with the mediocaudal surface of the proximal base of metatarsal III; entire caudal surface articulates with the cranial component of the dorsal surface of the entocuneiform. An extremely small cranial facet for metatarsal II is sometimes present beneath the facet for metatarsal III.

The mesocuneiform of *P. viator* **sp. nov.** differs from that of *O. rufus* and *M. fuliginosus* in being larger and more robust.

Entocuneiform (Figs 75e–f & 77): very elongate, transversely compressed and quite dorsoplantarly short; broadens and shortens caudally to a small, rounded and slightly dorsally tilted facet for the navicular; cranial section of the dorsal margin articulates with mesocuneiform. Facet for metatarsal II small, rounded and strongly dorsolaterally tilted; situated on dorsal component of cranial surface. The cranioplantar section of the lateral surface articulates with the lateral surface of the proximal plantar tubercle of metatarsal IV and with the medial margin of the proximal plantar sesamoid for metatarsals IV and V.

The entocuneiform of *P. viator* **sp. nov.** differs from that of *O. rufus* in being larger and more rectangular in medial view, with a taller caudal end and a slightly more laterally situated facet for metatarsal II; from *M. fuliginosus* in being larger and more rectangular in medial view, with a taller, less pointed cranial end and a slightly more laterally situated facet for metatarsal II; and from *W. bicolor* in being larger and more rectangular in medial view with a less pointed cranial end.

Proximal plantar sesamoid for metatarsals IV and V (Figs 75e–f & 77): broad and dorsoplantarly compressed, with a larger, rounded to oval medial section for articulation with the proximal plantar tubercle of metatarsal IV and a smaller, elongate, oval lateral projection for articulation with the plantomedial surface of the lateral plantar tuberosity of metatarsal V; dorsal surface of the proximomedial section articulates with the proximal plantar ridge on metatarsal IV. Lateral projection slightly plantarly deflected, creating a broad, shallow plantar groove across the medial section toward the entocuneiform for the m. flexor digitorum profundus IV + V.

The proximal plantar sesamoid of *P. viator* **sp. nov.** differs from that of *O. rufus* in being broader, with a larger facet for the plantar tubercle of metatarsal IV; from *M. fuliginosus* in being much larger and much broader, with the medial section more elongate, and the lateral projection relatively enlarged and projected to articulate with the plantar surface of the metatarsal V lateral plantar tuberosity, rather than abutting the medial surface of the shaft; and from *W. bicolor* in being larger and relatively slightly deeper.

Metatarsals II, III and phalanges (Figs 75e–f & 77): extremely gracile; III slightly longer than II, both shorter than metatarsal IV; both with shafts bowed distinctly laterally toward midpoint. Metatarsal III: proximal end tall and narrow, rapidly decreases in height to shaft; articulates proximally with mesocuneiform, ectocuneiform and metatarsals II and metatarsal IV. Metatarsal II: proximal end relatively small and very slightly plantarly deflected; articulates proximally with metatarsal III, entocuneiform

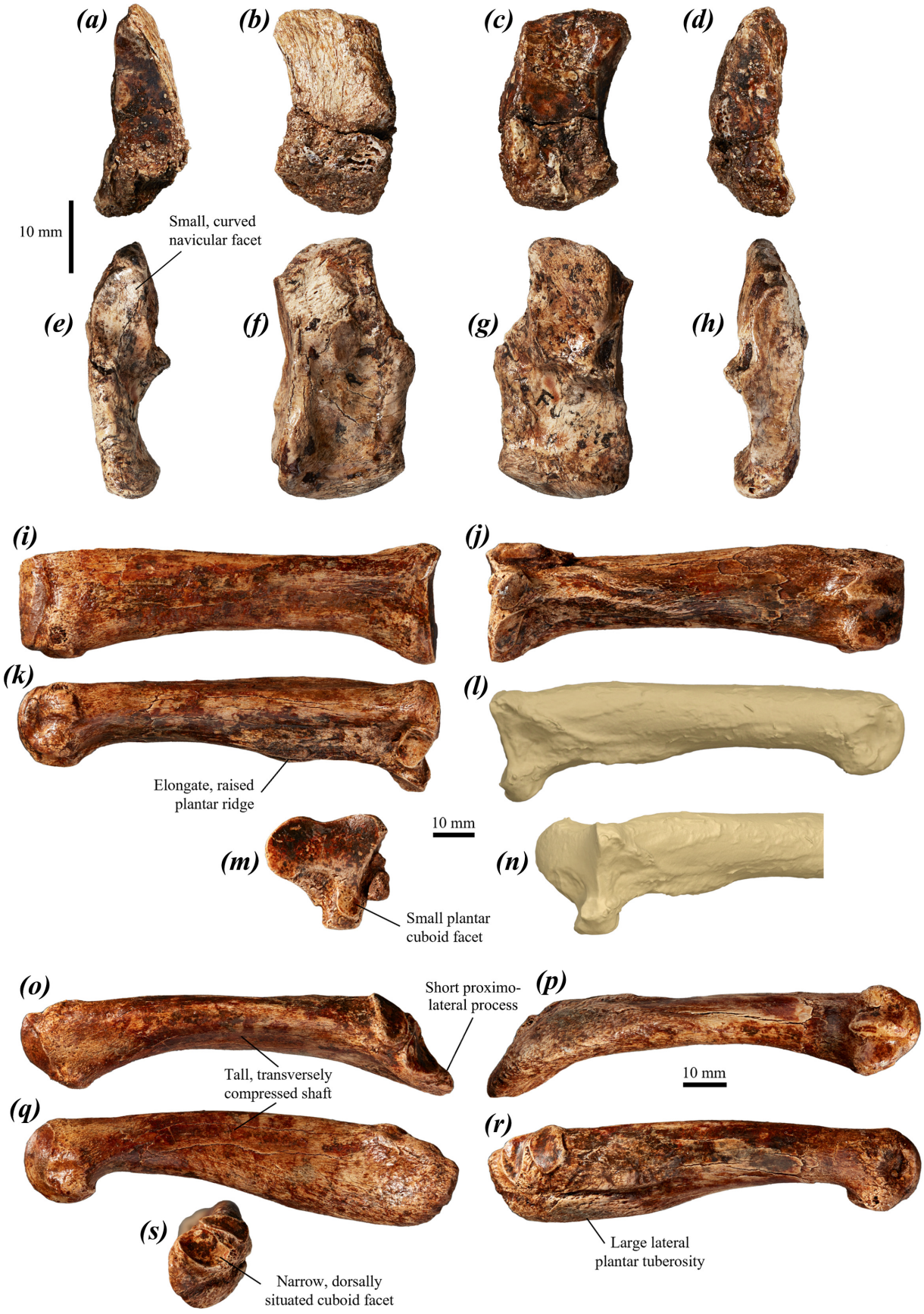

FIGURE 78. tarsal elements of *P. viator* **sp. nov.**: (a–d) left navicular of holotype SAMA P59552 and (e–f) right ectocuneiform of paratype SAMA P59550 in (a, e) caudal, (b, f) medial, (c, g) lateral, and (d, h) cranial views; left metatarsals IV (i–k, m) and V (o–s) of SAMA P59552 in (i, o) dorsal, (j, p) plantar, (k, q) lateral, (r) medial, and (m, s) proximal views; and (l, n) surface scan images of left metatarsal IV of NMNH 498886 in (l) medial, and (n) proximomedial views.

and very slightly with mesocuneiform. Shafts transversely compressed proximally, become rounded in cross-section and gently taper distally. Distal ends small, bulbous and rounded.

Proximal phalanges for metatarsals II and III: very small and short; proximal ends thickened; shafts narrow to a waist before thickening to rounded, slightly bulbous distal ends. The distal end of phalanx for metatarsal II is not preserved.

The metatarsals II, II and phalanges of *P. viator* **sp. nov.** differ from those of *P. otibandus* in having metatarsals II and III slightly more gracile and shorter relative to length of metatarsal IV, with the shafts much more laterally bowed; from *O. rufus* and *M. fuliginosus* in having much shorter and more robust metatarsals, with a taller proximal end of metatarsal III, metatarsal II with a more laterally situated entocuneiform articulation, and a slightly longer proximalphalanx of metatarsal II; and from *W. bicolor* in being larger and slightly more robust, with the phalanges much shorter relative to the length of metatarsal IV.

Metatarsal IV (Figs 75e–f & 78a–f): short and fairly robust. Dorsal cuboid facet large and broad, with the lateral part flat to gently convex and the medial part flat to gently concave; dorsal margin flat to gently sinusoidal; medial part of dorsal facet continuous plantarly with the plantar cuboid facet, which abuts medial margin; plantar cuboid facet small, round to oval, generally flat and angled slightly to sharply dorsomedially, situated on the proximal surface of the thick, plantarly projected plantar tubercle, opposite the proximal plantar sesamoid facet; proximal cuboid fossa shallow and laterally situated; very small, occasionally indistinct facet for articulation with the plantolateral part of the ectocuneiform on the medial surface of the plantar tubercle, sometimes semicontinuous with the plantar cuboid facet. Proximal plantar sesamoid facet round to oval, flat to gently concave. Facet for metatarsal III indistinct, situated in elongate, shallow, rugose metatarsal III fossa on medial surface of proximal end, bordered dorsally by a thin ridge extending plantodistally from dorsomedial corner of dorsal cuboid facet. Dorsal facet for the ectocuneiform small and rounded to absent, abuts the dorsal section of the medial margin of dorsal cuboid facet. Facet for metatarsal V concave, tall and craniocaudally quite shallow; shape variable, but generally oblong with rounded dorsal and plantar parts; not extending plantarly onto the lateral surface of the plantar tubercle.

Plantar ridge broad, rounded and rugose, extends distally with a slight lateral deflection from the base of the plantar tubercle, merges into the plantar surface of the shaft at its midpoint; bordered medially by the fossa for metatarsal III and laterally by the fossa for metatarsal V. Shaft broadens gently, particularly on the lateral margin, to a broad distal end; lateral margin appears more concave proximally due to the projected lateral part of the base; taller proximally and quite low distally; proximal part of the dorsal surface of the shaft generally slightly laterally tilted, becoming flat to gently rounded distally. Distal end broad; fossae for the collateral ligaments circular and quite deep; keel narrow and subequally to slightly more plantarly projected than the lateral and medial crests.

The metatarsal IV of *P. viator* **sp. nov.** differs from that of *P. anak* in being generally slightly shorter; from *P. mamkurra* **sp. nov.** in being shorter, generally with a smaller plantar cuboid facet; from *P. tumbuna* in being larger; from *P. dawsonae* **sp. nov.** in being shorter and more gracile; from *P. otibandus* in being larger and more gracile, with a more raised plantar ridge and continuous dorsal and plantar cuboid facets; from *P. snewini* in being slightly larger and more elongate, with a relatively longer plantar ridge, continuous dorsal and plantar cuboid facets, and a more plantolaterally situated proximal cuboid fossa; from *C. kitcheneri* in being larger and broader, with a more plantarly projected proximal plantar tubercle and a larger facet for the proximal plantar sesamoid; from *O. rufus* and *M. fuliginosus* in being shorter, broader, much more robust and less arched in lateral view, with a larger facet for metatarsal V, lower plantar ridge, and a larger, more plantarly projected proximal plantar tubercle; and from *W. bicolor* in being larger, relatively broader and more robust, with a more plantarly projected proximal plantar tubercle.

Metatarsal V (Fig. 78g–k): quite robust and curved slightly laterally toward distal end; tall and highly transversely compressed, particularly proximally, giving the proximal end a distinct bulged appearance in lateral view; length to distal end width index ~4.4–5.4; slightly arched in lateral view. Proximolateral process quite proximodistally short and blunt, quite tall, slightly laterally deflected, transversely compressed, and rugose. Cuboid facet oval to rounded, gently concave, extends from the dorsal surface and medial surface of the base of the proximolateral process onto the proximal base of the medial plantar tubercle. Facet for metatarsal IV quite large, convex, variably oval, proximodorsally adjacent to or abutting the cuboid facet and extending medially from dorsal surface to above midpoint of medial surface. Lateral plantar tuberosity very elongate and rugose, distinctly plantarly projected, merges distally into the plantar shaft; bounded on the medial margin by a narrow channel separating it from the medial plantar tubercle. Medial plantar tubercle small, rounded and plantomedially projected; considerably less plantarly projected than lateral tuberosity. Shaft decreases in height and broadens to the distal end. Distal end quite tall; medial and lateral facets subequal in width.

The metatarsal V of *P. viator* **sp. nov.** differs from those of other species of *Protemnodon* in being more transversely compressed. It further differs from that of *P. anak* in being generally slightly taller and less elongate, with a narrower, less concave cuboid facet (Fig. 78k), less proximally projected medial plantar tubercle, and a narrower and taller distal end; from *P. mamkurra* **sp. nov.** in being taller, particularly proximally, and generally less elongate, with a narrower, more dorsally situated cuboid facet; from *P. tumbuna* in being more elongate and gracile, with a larger, more elongate lateral plantar tuberosity, more dorsally situated metatarsal IV facet, and a taller, narrower distal end with a more pointed keel; from *P. dawsonae* **sp. nov.** in being taller, particularly

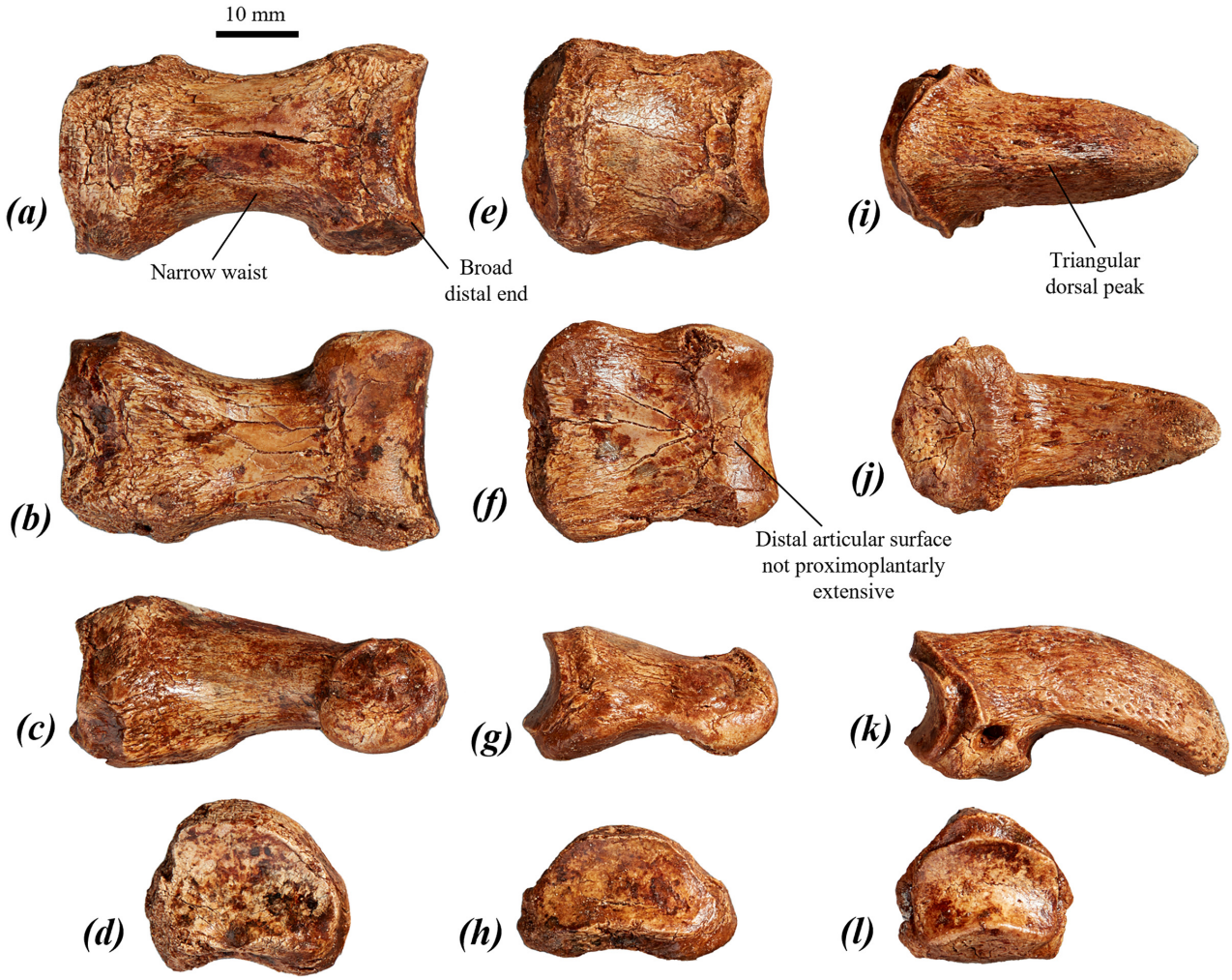

FIGURE 79. right (a–d) partial proximal, (e–h) middle, and (i–l) distal pedal phalanges IV of *P. viator* **sp. nov.** holotype SAMA P59552 in: (a, e, i) dorsal, (b, f, j) plantar, (c, g, k) medial, and (d, h, l) proximal views.

proximally due to the more raised lateral plantar tuberosity, and less elongate, with a narrower, more dorsally situated cuboid facet, a taller, less elongate proximolateral process, and a less proximally projected medial plantar tubercle; from *P. otibandus* in being larger and more elongate, with a narrower and more dorsally situated cuboid facet and the metatarsal IV facet less extensive medially and more distinct from the cuboid facet; from *C. kitcheneri* in being slightly larger, more robust and taller, particularly proximally, due to the larger lateral plantar tuberosity, and lacking the slight kink of the arch of the shaft immediately proximal to the midpoint in lateral view, with a taller, more rounded proximolateral process and a more rounded, slightly more dorsally tilted facet for the cuboid; from *O. rufus* and *M. fuliginosus* in being far shorter, broader, less arched and less transversely compressed, with a longer proximolateral process and a larger medial plantar tubercle; and from *W. bicolor* in being larger, more robust and taller, particularly proximally, with a larger proximolateral process and narrower, rounder and more concave cuboid facet and metatarsal IV facet.

Pedal phalanges (Figs 79 & 80): proximal phalanx IV: dorsoplantarly compressed and quite elongate, with a narrow waist, and broad proximal and distal ends. Proximal end low and domed, with the proximal plantar tubercles very low, elongate and rugose; proximal articular facet broad and concave with rounded dorsal margin. The height of the shaft gently decreases to the distal end. Distal end trapezoidal in distal view, with the fossae for the collateral ligaments extremely shallow to absent. Trochlea very gently concave. Middle phalanx IV: short, broad and very dorsoplantarly compressed, with a very slight waist. Proximal end broad, with the lateral and plantar margins thickened and rugose. Proximal plantar tubercles low and gently rugose, with rugose surface extending onto the lateral and medial surfaces of the proximal shaft and extending further distally in older individuals. Proximal articular surface broad, very low and concave. Distal end with very shallow fossae for the collateral ligaments. Trochlea very slightly concave dorsally and deepens plantarly; articular facet is not extensive proximoplantarly. Distal phalanx IV: quite tall and robust. Proximal articular facet concave and roughly

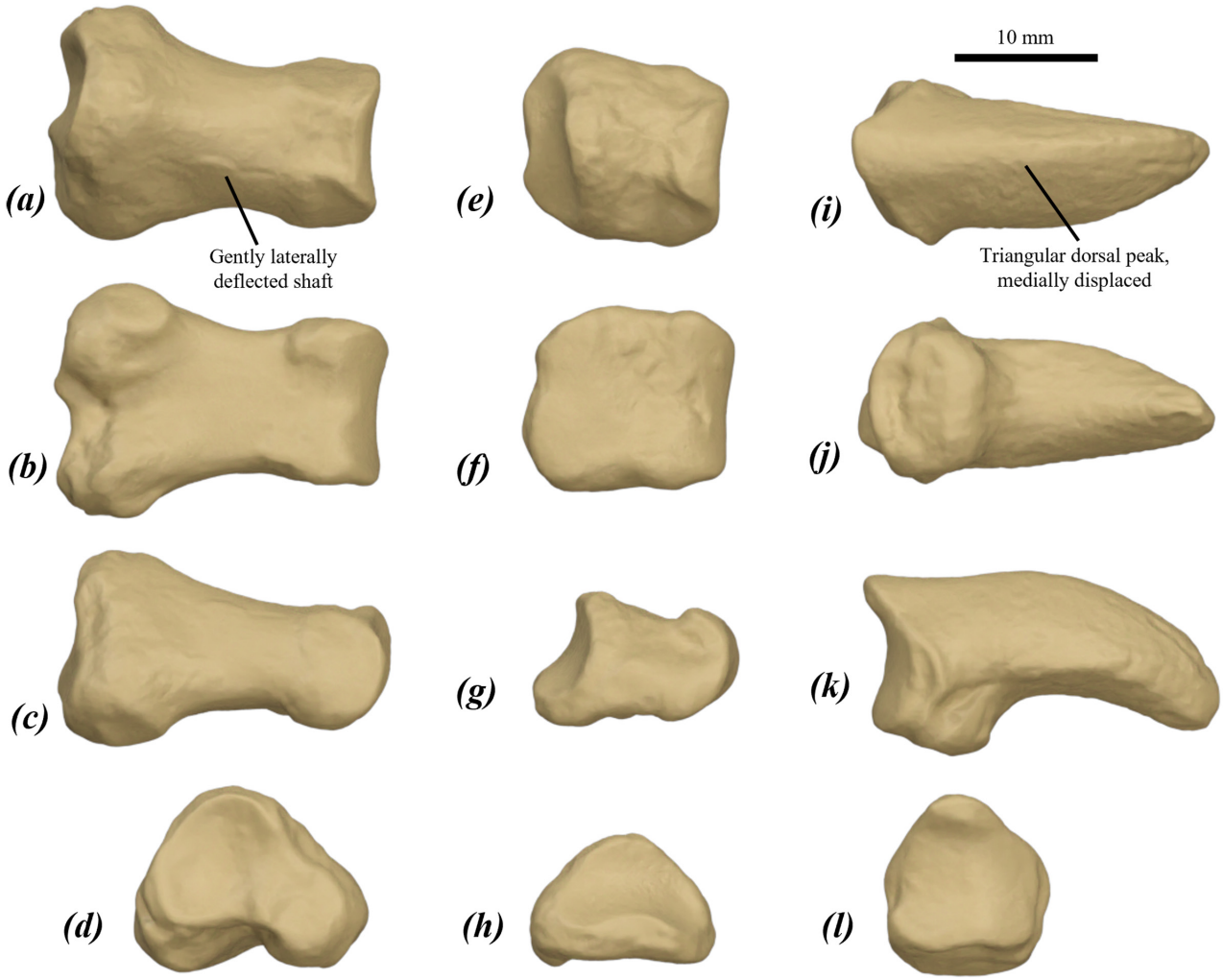

FIGURE 80. surface scan images of (a–d) right proximal, (e–h) left middle, and (i–l) right distal pedal phalanges IV of *P. viator* **sp. nov.** NMNH 498886 in: (a, e, i) dorsal, (b, f, j) plantar, (c, g, k) right transverse, and (d, h, l) proximal views.

pentagonal; proximal plantar tubercle large, rugose and oval in plantar view. Shaft with a slightly rounded triangular peak in cross-section, curves distinctly plantarly in lateral view and narrows steadily to a rounded point in dorsal view.

Proximal phalanx V: proximal end slightly broader than tall, with large, rounded and rugose plantar tubercles; proximal articular surface round, concave and medially displaced in proximal view. Height decreases distally, with a slight waist on the shaft in dorsal view. Distal end with fossae for the collateral ligaments absent; trochlea gently concave; articular surface not very extensive dorsally. Middle phalanx V: very short, broad, dorsoplantarly compressed and decreasing in height distally; distinctly asymmetrical, with the proximal and distal surfaces medially and laterally tilted respectively. Proximal end with low, rounded plantar tubercles; proximal articular surface gently concave, dorsally domed and tilted dorsomedially. Shaft extremely short with no waist. Distal end with the fossae for the collateral ligaments very shallow and dorsally displaced; trochlea gently concave and articular surface dorsoplantarly quite short. Distal phalanx V: elongate and distinctly asymmetrical; dorsal peak of the shaft and proximal end medially displaced (Fig. 80i) and shaft very slightly medially curved. Proximal end with a small, rounded projection on the medial and lateral margins; fossae for the collateral ligaments small and deep; plantar tubercle small and rounded in plantar view; proximal articular surface concave and rounded-rectangular. Shaft with a rounded triangular dorsal peak and a convex plantar margin in cross-section, smoothly plantarly curved distally, narrows rapidly at the distal end to a rounded point.

The pedal phalanges of *P. viator* **sp. nov.** differ from those of *P. anak* in being more elongate, with proximal phalanx IV having a more distinct waist, middle phalanx IV having a relatively narrower, less dorsally tilted proximal end and a less proximoplantarly extensive distal articular surface, distal phalanx IV having a more pointed dorsal peak, and distal phalanx V having a more pointed, more medially displaced dorsal peak; from *P. mamkurra* **sp. nov.** in being generally slightly shorter, with shallower collateral fossae on the proximal and middle phalanges, proximal phalanges with a narrower waist, a relatively

broader middle phalanx IV with relatively larger, more distally extensive plantar tubercles, distal phalanx IV with a more triangular dorsal peak and lacking distinct triangular divots on the medial and lateral margins of the proximal articular surface, and distal phalanx V with a more pointed, more medially displaced dorsal peak; from *P. dawsonae* **sp. nov.** in having more gracile proximal phalanx IV with a narrower waist and broader distal end relative to the proximal end; from *P. otibandus* in being larger, with a more elongate proximal phalanx IV having a narrower waist, distal phalanx IV with a more triangular proximal surface, more pointed dorsal peak, and a less dorsoplantarly compressed, more plantarly curved shaft, proximal phalanx V with a more concave proximal articular surface, less laterally deflected shaft, and a broader trochlea, a more elongate middle phalanx V with a more medially tilted proximal surface, and distal phalanx V with a more pointed dorsal peak; from *P. snewini* in being larger, with middle phalanx IV having a narrower distal articular surface relative to the distal width and a smaller distal end relative to proximal end in lateral view, and distal phalanx IV having a longer and less plantarly projected plantar tubercle; from *C. kitcheneri* in being broader, more robust and more dorsoplantarly compressed, particularly the middle phalanges, with a broader, slightly shallower trochleae, middle phalanx IV with a less caudoplantarly extensive distal articular surface and distal phalanges with more rounded dorsal peaks; from *O. rufus* and *M. fuliginosus* in being broader and more robust, with the phalanges V slightly larger relative to the phalanges IV and the distal phalanges having a slightly less angular, more rounded dorsal peak and a more plantarly curved shaft; and from *W. bicolor* in being larger and more robust, with a narrower waist on proximal phalanx IV.

Protemnodon tumbuna Flannery *et al.*, 1983

Protemnodon tumbuna Flannery *et al.*, 1983: *Proc. Lin. Soc. N.S.W.*, 107, pp. 84–91, figs 4 & 5. Menzies & Ballard (1994), pp. 123–131, figs 6–9. Prideaux *et al.* (2022), pp. 11–13, 15, figs 7 & 8, table 3.

Protemnodon hopei Flannery, 1992a: *Alcheringa*, 16, pp. 326–329, fig. 2. See also Helgen *et al.* (2006), p. 303, Appendix 2.

Holotype:
PNG 83-40-8, a partial R maxilla preserving DP2–M1, with P3 removed from crypt; infraorbital foramen preserved; specimen fractured dorsal to infraorbital foramen, immediately lingual to molar row and posterior to M1. Figured in Flannery (1992a), fig. 4a–d.

Type locality:
Stratum C, Nombe Rockshelter, late Pleistocene Chimbu Province, Papua New Guinea (Flannery *et al.* 1983). This rockshelter is situated in mid-Eocene to early Oligocene Chimbu Limestone, on the northeastern face of Mt Elimbari ridge. Altitude is ~1720 m above sea level (Flannery *et al.* 1983).

Paratype:
PNG 82-40-20, a semi-complete L dentary preserving i1, partial p3 and m1–m4. Anterior of diastema abraded; fractured ascending ramus, coronoid process and ventral masseteric fossa missing fragments; mandibular condyle and angular process absent. Collected during archaeological excavations led by M-J. Mountain from 1978–1980.

Referred specimens:

Papua New Guinea

Nombe Rockshelter, Chimbu Province: NCA X2-13-241 partial R ulna; NCA A1-18 partial ilium and L metatarsal V; NCA M71-9 partial R ulna; NCA H71-9 partial R calcaneus; NCA 071 R metatarsal V.

LOG site, Haeapugua Basin, Tari Province: PM25622 semi-complete skeleton (specimen missing).

LOK site, Haeapugua Basin, Tari Province: PM25623 partial L dentary.

Central Papua

Kelangurr Cave, West Baliem Valley: AM F83613 maxillae; AM F83413 partial L dentary; AM F83612 R dentary; AM F83614 partial juvenile L dentary; AM F113144 cervical vertebra C3; AM F88917 caudal vertebra (Ca8?); AM F113142 juvenile R humerus; AM F88914 partial L ulna; AM F88925 partial L radius; AM F113140 partial ilium; AM F113143 juvenile ilium; AM F113141 partial L tibia; AM F88922 partial fibula; AM F88921 partial L calcaneus; AM F88929 partial L calcaneus; AM F88927 partial L metatarsal IV; AM F88930 partial R metatarsal IV; AM F113146 L metatarsal V.

West Baliem River, near Ambowak village, West Baliem Valley: AM F83611 L I1; AM F88923, AM F88924 L femur and tibia.

Revised specific diagnosis:
Protemnodon tumbuna is separated from the other species of *Protemnodon* by several skeletal autapomorphies and by a unique combination of craniodental and postcranial characteristics. The hindlimb of *P. tumbuna* differs from all species of *Protemnodon* in having: a more gracile femur with a more elongate, more distally situated quadratus tubercle; a more robust tibia with a particularly low proximolateral crest, especially distally, and a more elongate cnemial crest; a calcaneus with a distinctly convex, caudomedially flared plantar surface that extends dorsolaterally onto the lateral surface of the calcaneal tuberosity; and a shorter, more robust metatarsal V with a relatively shorter lateral plantar tuberosity.

The dentary of *P. tumbuna* most closely resembles that of *P. otibandus*, but differs in its more posteroventrally situated mental foramen. The dentition of *P. tumbuna* is most similar to that of *P. otibandus*, but differs in having: P3 with three (rather than four or five) less raised and less distinct buccal ridgelets; more rounded molars in occlusal view; and i1 with a less raised, less distinct ventrolingual crest.

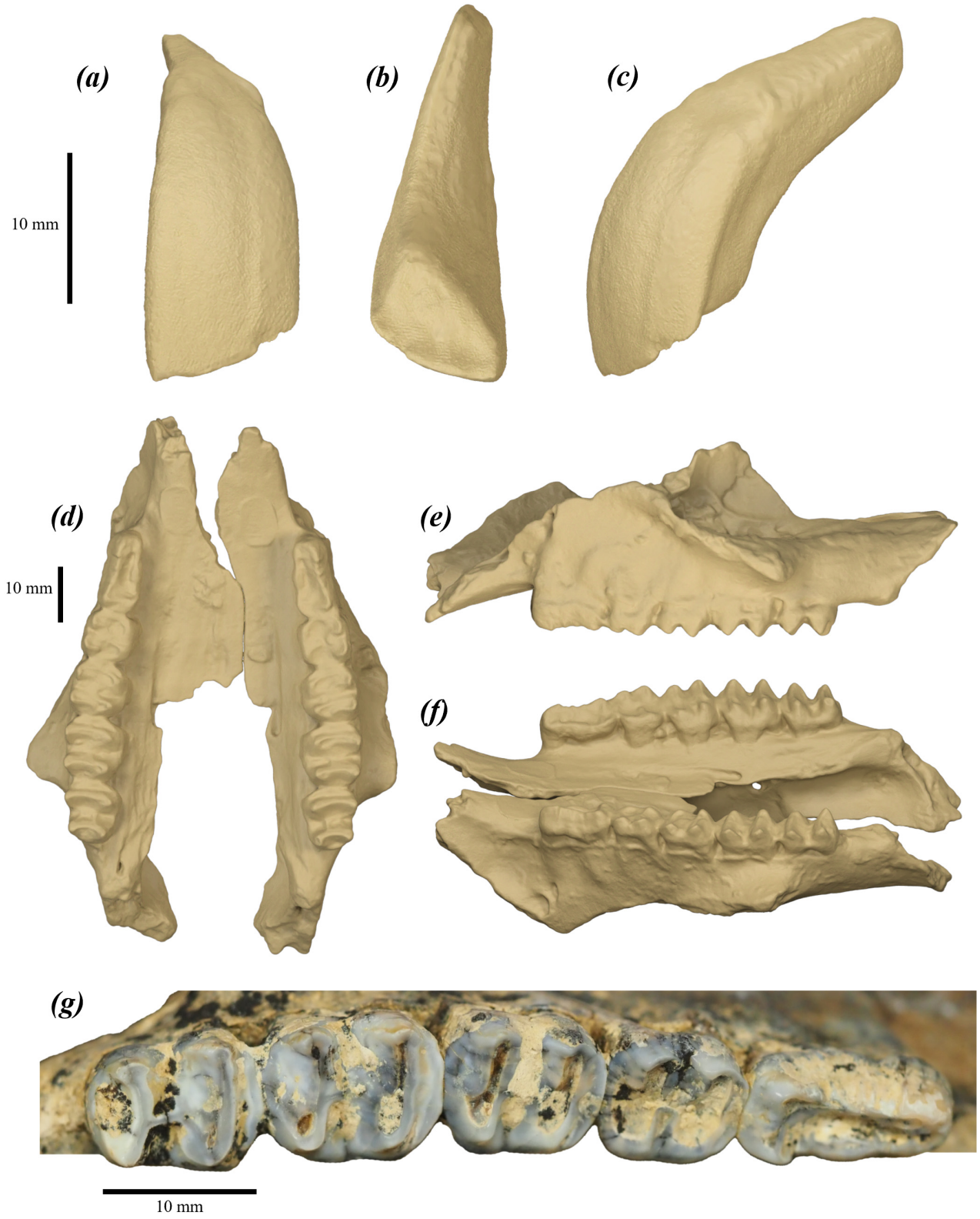

FIGURE 81. upper dentition and maxillae of *P. tumbuna*: (a–c) surface scan images of left I1 of AM F83611 in (a) anterior, (b) occlusal, and (c) buccal views; (d–f) surface scan images of partial maxillae of AM F83613 in (d) ventral/occlusal, (e) left lateral/buccal, and (f) right ventrolateral/occlusobuccal views; and (g) right P3–M4 of AM F83613 in occlusal view.

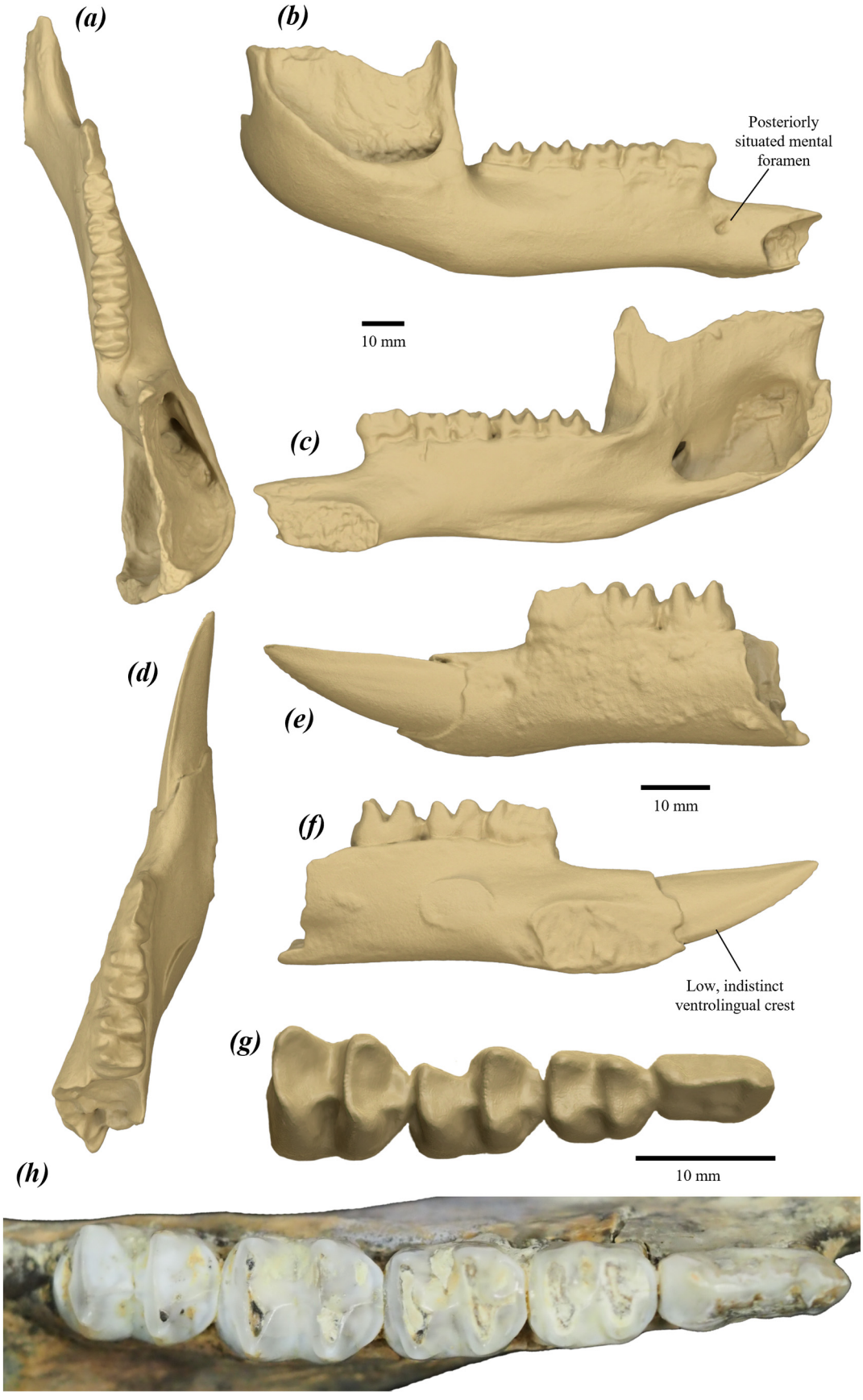

FIGURE 82. dentary and lower dentition of *P. tumbuna*: (a–c) surface scan images of partial right dentary of AM F83612 in (a) occlusal, (b) buccal, and (c) lingual views; (d–f) surface scan images of partial left juvenile dentary, with i1 and dp2–m1, of AM F83614 in (d) occlusal, (e) buccal, and (f) lingual views; (g) right dp2–m2 of PNG 82-40-9 in occlusal view; and (h) right p3–m4 of AM F83612 in occlusal view.

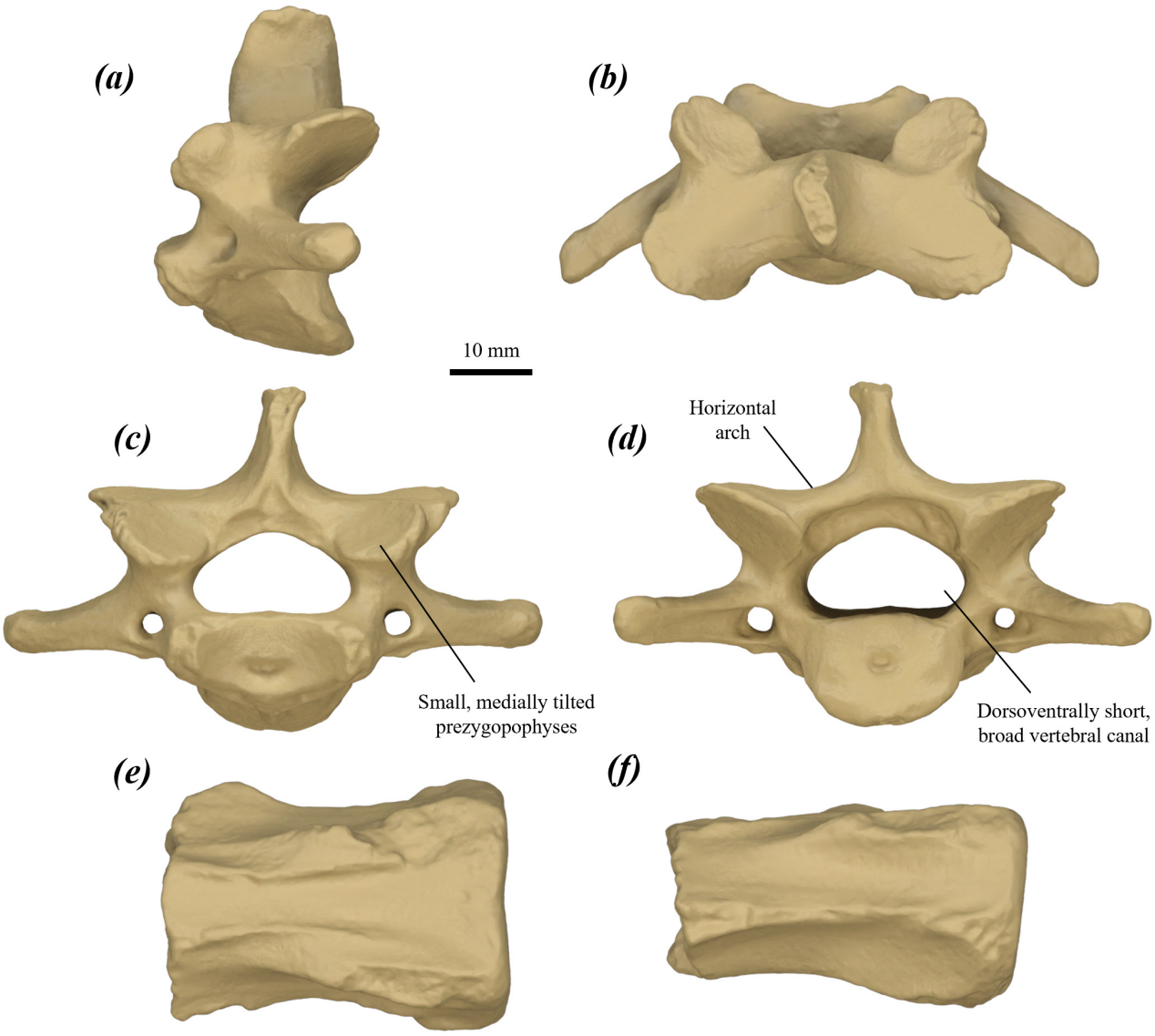

FIGURE 83. surface scan images of vertebrae of *P. tumbuna*: (a–d) cervical vertebra C3 of AM F113144 in (a) left lateral, (b) dorsal, (c) cranial, and (d) caudal views; and (e–f) partial caudal vertebra Ca8 of AM F88917 in (e) dorsal, and (f) lateral views. Not preserved in AM F88917 are the cranial extremity of the centrum, the mammillary processes and both sets of transverse processes.

The hindlimb of *P. tumbuna* is morphologically closest to that of *P. otibandus*. It further differs from that of *P. otibandus* by having: a tibia with a thicker proximolateral crest; calcaneus with a larger, deeper fossa cranial to the lateral talar facet; and metatarsal V with a taller proximolateral process, a proximodistally shorter metatarsal IV facet, and a smaller medial plantar tubercle.

Etymology:
The name *tumbuna* means 'ancestor' or 'of the ancestors' in Tok Pisin (Neo-Melanesian Pidgin). It is used in double-allusion, first in reference to the primitive morphology of some aspects of the dentition the species, and second, to its association with the Pleistocene human inhabitants of highland Papua New Guinea (Flannery *et al.* 1983, p. 84).

Description and comparisons:
For craniodental description, see original description by Flannery *et al.* (1983, pp. 87–90). For purposes of comparison, cranium and dentition are figured below (Figs 81 & 82). The semi-complete skeleton of *P. tumbuna* (PM25622) figured and described by Menzies & Ballard (1994) is currently missing and could not be included in this description.

Axial skeleton
Cervical vertebra (C3?) (Fig. 83a–d): craniocaudally quite short, dorsoventrally compressed and broad. Cranial extremity of the centrum gently and smoothly concave with a ventral tilt; broad, dorsoventrally compressed oval in cranial view. Prezygopophyses small and projected cranially subequal to the cranial extremity

of the centrum; cranial articular surfaces round, flat and facing dorsally with medial and cranial tilt. Vertebral canal small, quite broad, dorsoventrally low and oval to reniform. Arch thick and low, approaches horizontal in cranial view. Spinous process subequal in depth to the arch, and transversely very compressed; dorsal margin abraded in available specimen. Transverse processes broad and quite gracile, with no ventral deflection, and caudal deflection of ~40° from the transverse plane. Transverse foramina small and round, extends along the caudal surface of the transverse processes as shallow channels facing very slightly ventrally. Postzygopophyses quite small, projected caudally subequal to caudal extremity of the centrum; caudal articular surfaces round, flat and facing ventrally with a lateral and caudal tilt. Caudal extremity of the centrum oval, smoothly convex and slightly caudally projected with a gentle dorsal tilt.

The C3 of *P. tumbuna* differs from that of *P. anak* in being much shallower, with smaller, more medially tilted prezygopophyses, smaller, more laterally tilted postzygopophyses, a lower, broader vertebral canal, lower cranial extremity of the centrum and much less caudoventrally projected caudal extremity of the centrum; from *P. mamkurra* **sp. nov.** in being less tall relative to width, with relatively narrower cranial and caudal articular surfaces, and the arch much less dorsally deflected and more horizontal in cranial view; from *P. viator* **sp. nov.** in being smaller and craniocaudally slightly shorter, with more robust transverse processes; from *C. kitcheneri* in being shallower, relatively shorter and broader, with longer transverse processes, less elongate, less cranially projected prezygopophyses, lower, broader vertebral canal, broader cranial extremity of the centrum, and a broader, relatively larger, and less caudoventrally projected caudal extremity of the centrum; from *O. rufus* in being craniocaudally shorter and relatively broader, with smaller, less elongate pre- and postzygopophyses, a broader vertebral canal, and more dorsally situated, less caudoventrally deflected transverse processes; from *M. fuliginosus* in being craniocaudally shorter and relatively broader, with a more horizontal arch in cranial view, broader, less gracile and less caudally deflected transverse processes, and a broader vertebral canal; and from *W. bicolor* in being larger, craniocaudally shorter and more robust, with less elongate prezygopophyses, less caudally deflected transverse processes, a broader, oval (rather than reniform) vertebral canal, and the ventral margin of the caudal extremity of the centrum not bilobed.

Caudal vertebra (Ca8?) (Fig. 83e–f): single available vertebra is fragmentary; numerical position is not certain. Centrum craniocaudally short and quite broad; cranial extremity oval with small, rounded dorsolateral corners; caudal extremity abraded. Cranial transverse processes extremely small and slightly ventrally situated. Prezygopophyses abraded, appear large, quite elongate at the base and dorsolaterally situated. Caudal transverse processes mostly abraded in the available specimen; they arise from thin craniocaudal ridges along the transverse surfaces, broaden and thicken adjacent to the caudal extremity.

Forelimb

Humerus (Fig. 84): elongate, narrow and quite deep with well-developed ridges for muscle attachments. Head roughly hemispherical, round in dorsal view and moderately caudomedially projected. Greater tubercle mostly abraded; appears broad, quite low and rounded. Lesser tubercule quite low and blunt; oval and deep in dorsal view. Proximal shaft quite broad and deep. Pectoral crest elongate, raised and situated distinctly proximally, such that the distal peak sits just past the midpoint of the shaft. Deltoid tuberosity in joey (Fig. 84h–k) elongate, very low and indistinct, situated on lateral surface of the shaft, level with the proximal part of the pectoral crest. The area of insertion of the m. latissimus dorsi is a quite proximally situated, distinct and elongate fossa on the joey, positioned midway between the lesser tubercle and the distal peak of the pectoral crest on the medial surface of the shaft. Shaft narrow and very deep. Distal end narrow, elongate and rotated slightly medially. Lateral supracondylar ridge quite narrow and elongate, extends ~two-fifths of humeral length in joey, with the proximal peak coming to a small point. Capitulum and ulnar facet moderately distally projected, and slightly laterally displaced; combined width is roughly four-fifths of the epicondylar width; capitulum smoothly gently convex; trochlea wide and deep. Olecranon fossa large, broad and deep; radial fossa rounded and shallow; coronoid fossa smaller, shallower and quite broad. Medial supracondylar bridge broad, quite thick craniocaudally and elongate, aligned distinctly proximodistally such that the section over the supracondylar foramen projects medially; continues proximally and slightly laterally as a very low, broad ridge that merges with the distal end of the pectoral crest (Fig. 84d). Supracondylar foramen large, oval and moderately flattened craniocaudally; very elongate in the joey.

The humerus of *P. tumbuna* is not confidently differentiated from that of *P. otibandus*. It differs from that of *P. anak* in being smaller, with relatively more proximally situated pectoral crest, more proximally situated insertion of m. latissimus dorsi, more transversely compressed shaft, and relatively narrower and more elongate distal end; from *P. mamkurra* **sp. nov.** and *P. viator* **sp. nov.** in being more gracile, and in having a more proximally situated insertion of the m. latissimus dorsi, a relatively narrower, more elongate distal end, and a low, broadly rounded ridge linking the pectoral crest and the medial supracondylar bridge; from *C. kitcheneri* in having a more dorsally raised lesser tubercle, deeper proximal shaft, straighter, less raised pectoral crest, more transversely compressed shaft, relatively more elongate distal end, broader lateral supracondylar ridge, and a broader medial supracondylar bridge; from *O. rufus* in being more robust, with a deeper proximal shaft, more transversely compressed shaft, a more raised crest of the greater tubercle, and a broader capitulum and ulnar facet relative to the distal width; from *M. fuliginosus* in being more robust, with a relatively larger head, relatively more elongate distal end, and a broader capitulum and ulnar facet relative to distal width; and from *W. bicolor* in being

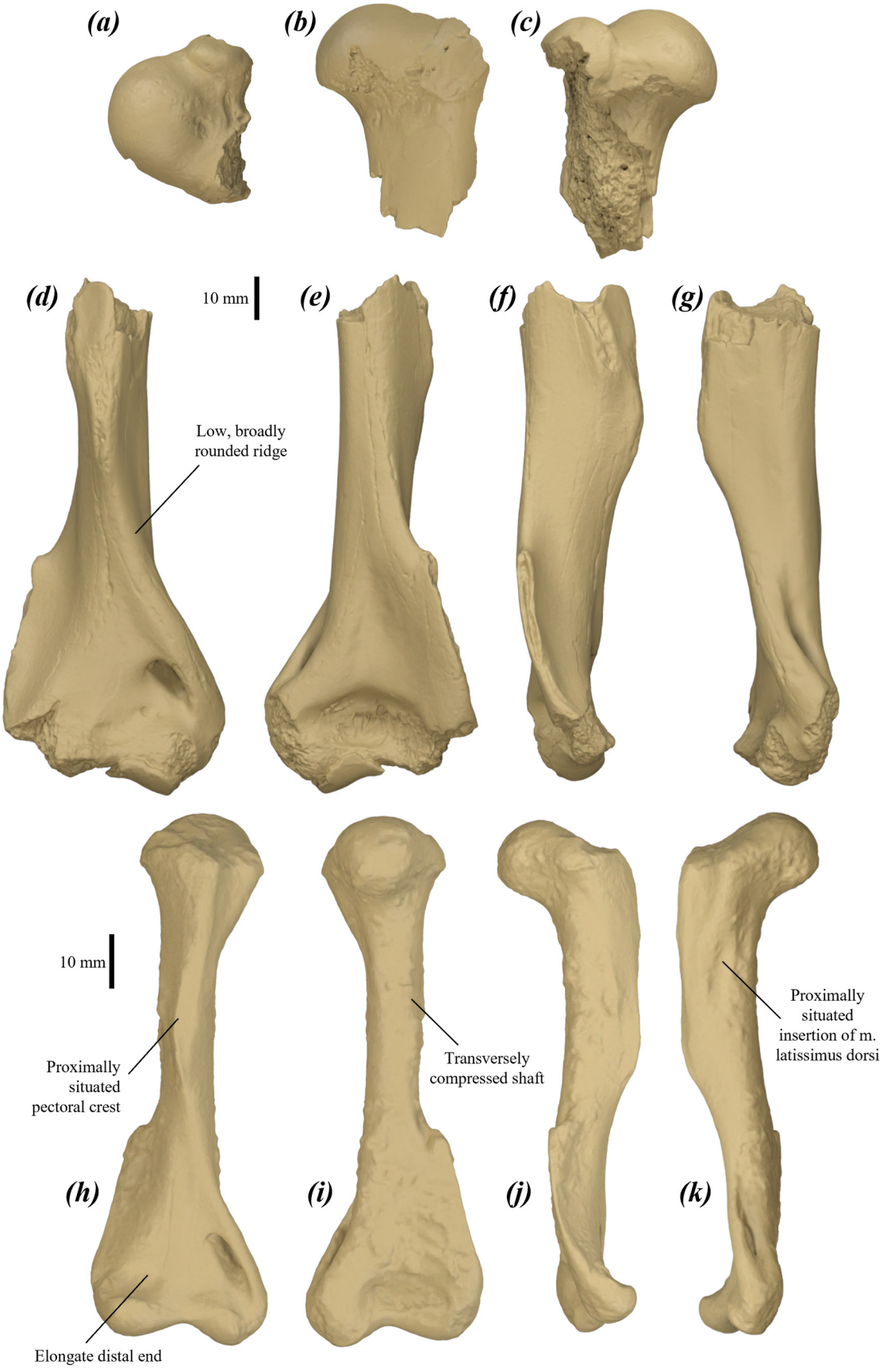

FIGURE 84. surface scan images of right humeri of *P. tumbuna*: (a–c) proximal humeral fragment of AM F83612 in (a) dorsal, (b) lateral, and (c) medial views; (d–g) distal humerus of AM F83614 in (d) cranial, (e) caudal, (f) lateral, and (g) medial views; and (h–k) juvenile humerus of AM F113142 in (h) cranial, (i) caudal, (j) lateral, and (k) medial views.

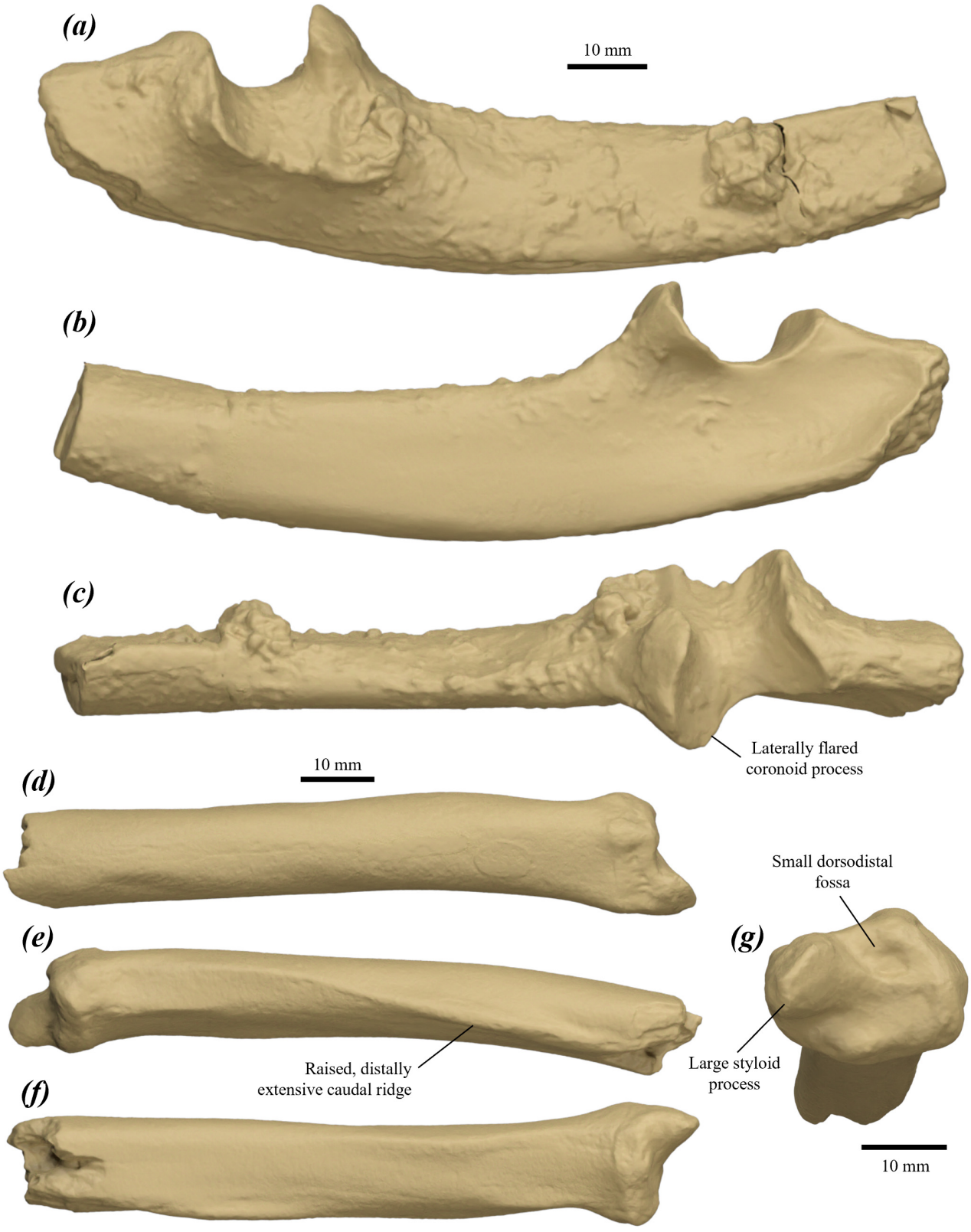

FIGURE 85. surface scan images of partial forelimb elements of *P. tumbuna*: (a–c) proximal right ulna of specimen NCA-M71-9 in (a) lateral, (b) medial, and (c) cranial views; and (d–g) distal radius of AM F83612 in (d) cranial, (e) lateral), (f) caudal, and (g) distal views.

larger and less laterally bowed in cranial view, lacking a narrow dorsoventral groove on the medial face of the lesser tubercle, and in having a less medially projected lesser tubercle, more proximally situated insertion of the m. latissimus dorsi, straighter pectoral crest, and a broader capitulum and ulnar facet relative to the distal width.

Ulna (Fig. 85a–c): olecranon quite large and broad, tapers in height distally; a small eminence is present on the caudomedial margin, extends slightly anteriorly; lateral surface very gently convex. The proximomedial flexor fossa is strongly concave. Humeral facet large, with a smoothly rounded trochlear notch; medial section deeply concave; lateral section broad, very shallow and laterally tilted, with a sinusoidal lateral margin projected slightly laterally; anconeal process low and quite narrow relative to the coronoid process and the radial notch; coronoid process tall, rounded and distinctly medially deflected, with variable breadth. Radial facet broad and gently concave. Ulnar tuberosity indistinct and rugose. Proximal shaft deep and quite transversely compressed, with a slight medial deflection to the cranial section in cross-section; caudal margin very gently convex, approaches straight beneath the olecranon and humeral facet; curvature of the cranial margin increases smoothly distal to the radial facet.

The ulna of *P. tumbuna* is not confidently differentiated from that of *P. otibandus*. It differs from that of *P. anak* in being smaller, with a shallower, less transversely compressed shaft; from *P. mamkurra* **sp. nov.** in being smaller; from *P. viator* **sp. nov.** in being smaller, with a lower, more laterally flared coronoid process; from *C. kitcheneri* in being larger and deeper, with a slightly taller, more posteriorly tilted coronoid process and a less laterally tilted lateral section of the humeral facet; from *O. rufus* in being deeper and more transversely compressed, with a less cranially deflected olecranon, less medially flared anconeal process, taller coronoid process, and a less laterally tilted lateral section of the humeral facet; from *M. fuliginosus* in having a less tall olecranon, taller anconeal process, a posteriorly deflected coronoid process, and an anteroposteriorly shorter, less laterally tilted lateral section of the humeral facet; and from *W. bicolor* in being larger, with a relatively longer, cranially undeflected olecranon and a lower, narrower anconeal process.

Radius (Fig. 85d–g): quite robust and gently curving caudomedially toward the distal end. Distal shaft moderately compressed obliquely (craniolaterally to caudomedially). Caudal ridge distinct, quite tall, thin and elongate, extends along the caudal then caudolateral surface of the shaft to merge into the caudal margin of the ulnar notch. Distal end broad, rounded and craniocaudally compressed, with a small tubercle on the cranial surface; scaphoidal facet distal facing, broad and gently concave with a craniocaudally short, small, rounded fossa centred in the slightly cranially swollen cranial part of the facet; styloid process quite large and slightly transversely compressed, forms a flattened, rounded tip; ulnar notch extends and tapers proximally along the caudolateral surface as a very shallow, elongate fossa.

The radius of *P. tumbuna* is not confidently differentiated from that of *P. otibandus*. It differs from that of *P. anak* in having a less craniocaudally compressed distal shaft, larger styloid process relative to the scaphoidal facet, more oval distal end in distal view, and the cranial component of distal surface with a small fossa (Fig. 85g); from *P. mamkurra* **sp. nov.** in having a less craniocaudally compressed distal shaft and a less caudally situated styloid process; from *P. viator* **sp. nov.** in being smaller, with a less craniocaudally compressed distal shaft, more raised and more distally extensive caudal ridge, and a larger styloid process relative to the scaphoidal facet; from *C. kitcheneri* in a having more cranially situated styloid process and a less cranially situated scaphoidal facet; from *O. rufus* in having a broader distal shaft and more raised caudal ridge; from *M. fuliginosus* in having a broader, more craniocaudally compressed distal shaft and a more raised caudal ridge; and from *W. bicolor* in being larger, with a lower caudomedial ridge on the distal shaft and a relatively longer, more cranially situated styloid process.

Hindlimb

Pelvis (Fig. 86): ilium: elongate, quite straight in ventrolateral view, roughly L-shaped in cross-section and curves gently laterally toward the dorsal end. The epiphysis of the iliac crest is not known; iliac crest deep in dorsal view; ilium increases in depth to maximum at the iliac crest. Iliac fossa narrow and shallow. Gluteal fossa broad, moderately concave, becomes shallower dorsally, extends to the iliac crest. Caudal iliac spine arises abruptly on the caudomedial surface of the base of the ilium opposite the rectus tubercule; thick and tall ventrally for the origin of a large mm. gluteus, becomes thinner and lower dorsally, extends to the iliac crest; in some specimens, a small, pointed eminence is present on the caudoventral shoulder (see NCA-A1-18). Sacral surface very rugose, concave and roughly rounded. Cranial iliac spine present as a very low, short crest, briefly arising opposite the base of the caudal iliac spine and merging into the body of the ilium. Lateral iliac spine tall and slightly thinner than the caudal spine; lateral margin gently concave, extends straight in lateral view to the iliac crest. Rectus tubercule short, protuberant, rugose, roughly triangular, narrows onto the base of the lateral spine.

Acetabulum large and deeply concave, opens laterally and slightly cranioventrally, becomes shallower ventrally, with the height greater than the craniocaudal depth; acetabular fossa not known. Ischium: dorsal part robust, deep, quite transversely compressed, and gently concave medially, with the lateral surface strongly convex; undeflected, aligned with the axis of the ilium in lateral view. Ventral ischium incompletely preserved in available specimens. Iliopubic eminence very low, rounded in outline, quite elongate and rugose. The pubis is not known.

The pelvis of *P. tumbuna* differs from that of compared species of *Protemnodon* in having a straighter ilium in lateral view (rather than curving caudally), the acetabulum opening less laterally and more cranioventrally (Fig. 86b), and a broader (less transversely compressed) ischium. It further differs from that of *P. mamkurra* **sp. nov.** in being

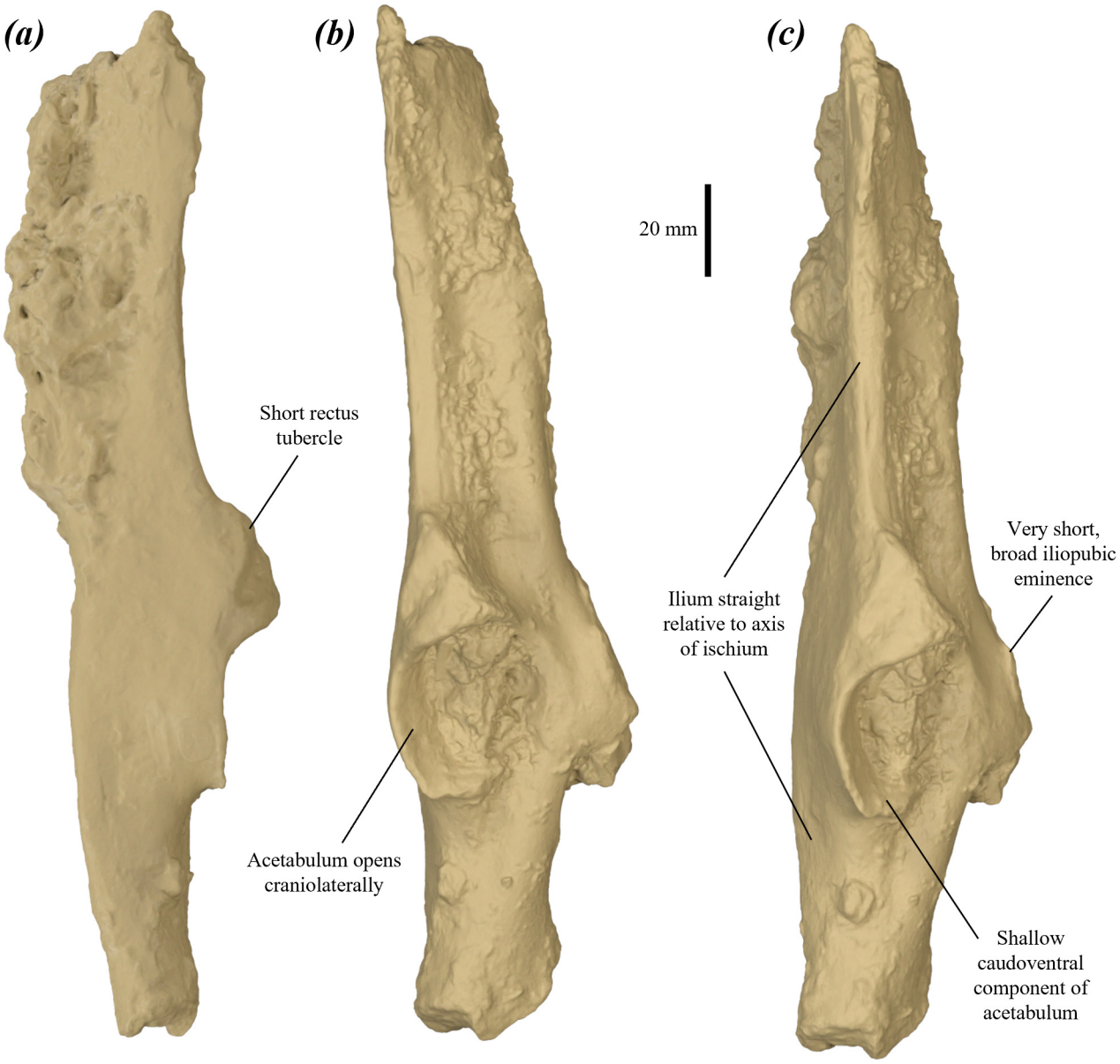

FIGURE 86. surface scan images of partial pelvis, mainly ilium and proximal ischium, of *P. tumbuna* AM F113140 in: (a) caudal, (b) craniolateral, and (c) lateral views.

generally smaller, with a shorter rectus tubercle, acetabulum with a more deeply concave ventral section, and a smaller iliopubic eminence; from *P. viator* **sp. nov.** in having a smaller iliopubic eminence; from *P. dawsonae* **sp. nov.** in having a more laterally projected rectus tubercle; from *C. kitcheneri*, *O. rufus*, *M. fuliginosus* and *W. bicolor* in being more robust, with a broader lateral iliac spine, deeper gluteal fossa, much shallower, less distally extensive iliac fossa, and a less tall, more laterally projected rectus tubercle; and additionally from *O. rufus*, *M. fuliginosus* and *W. bicolor* in having a more ventrally opening acetabulum.

Femur (Fig. 87): long, gracile, although most of the proximal end is not preserved in the available specimen. Lesser trochanteric crest distal margin intact; projects medially from the ventromedial surface of the base of the proximal end; thickened, raised, and interpreted as being quite elongate distally. Shaft straight, broadens slightly and deepens substantially toward the distal end (Fig. 87c); ventral surface flattens distally. Quadratus tubercule very elongate, rugose and very raised, extends distally from slightly proximal of the midpoint of the ventral surface of the shaft to just over three-quarters of the femoral length (Fig. 87b). The ventrolateral fossa for the partial origin of the m. flexor digitorum superficialis is small, rounded, and situated on the proximal surface of the lateral condyle; extends briefly along the shaft.

Distal end tall. Lateral trochlear crest tall and fairly broad; medial crest not preserved. Trochlea deep, narrow and V-shaped. Intercondylar fossa deep and quite short, such that fossa opening is more distal than ventral. Condyles with the ventral and distal surfaces and the distolateral part

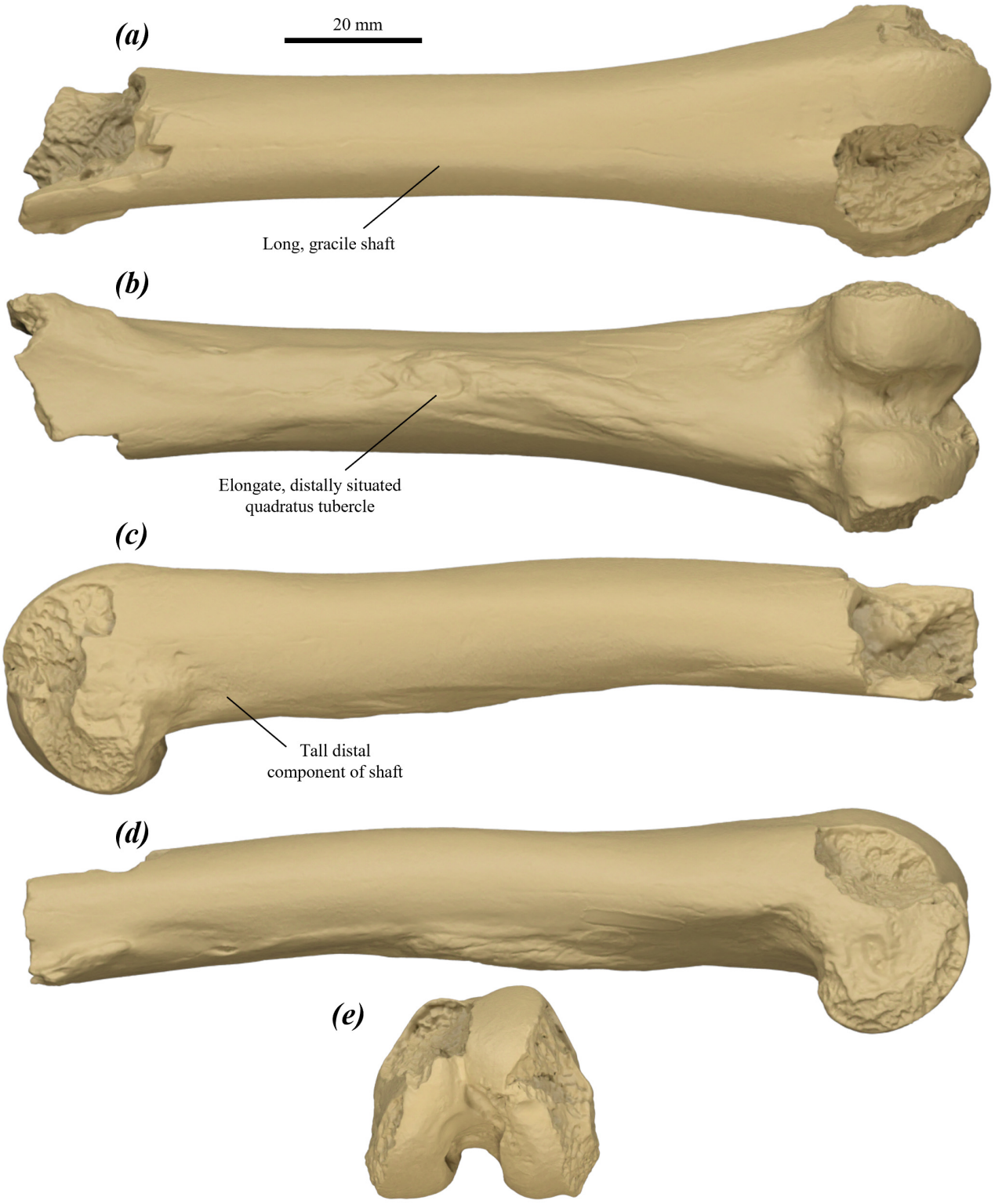

FIGURE 87. surface scan images of partial left femur of *P. tumbuna* AM F88924 in: (a) dorsal, (b) ventral, (c) lateral, (d) medial, and (e) distal views. Not preserved in specimen are the entire proximal end and the lateral and medial surfaces of the distal epiphysis.

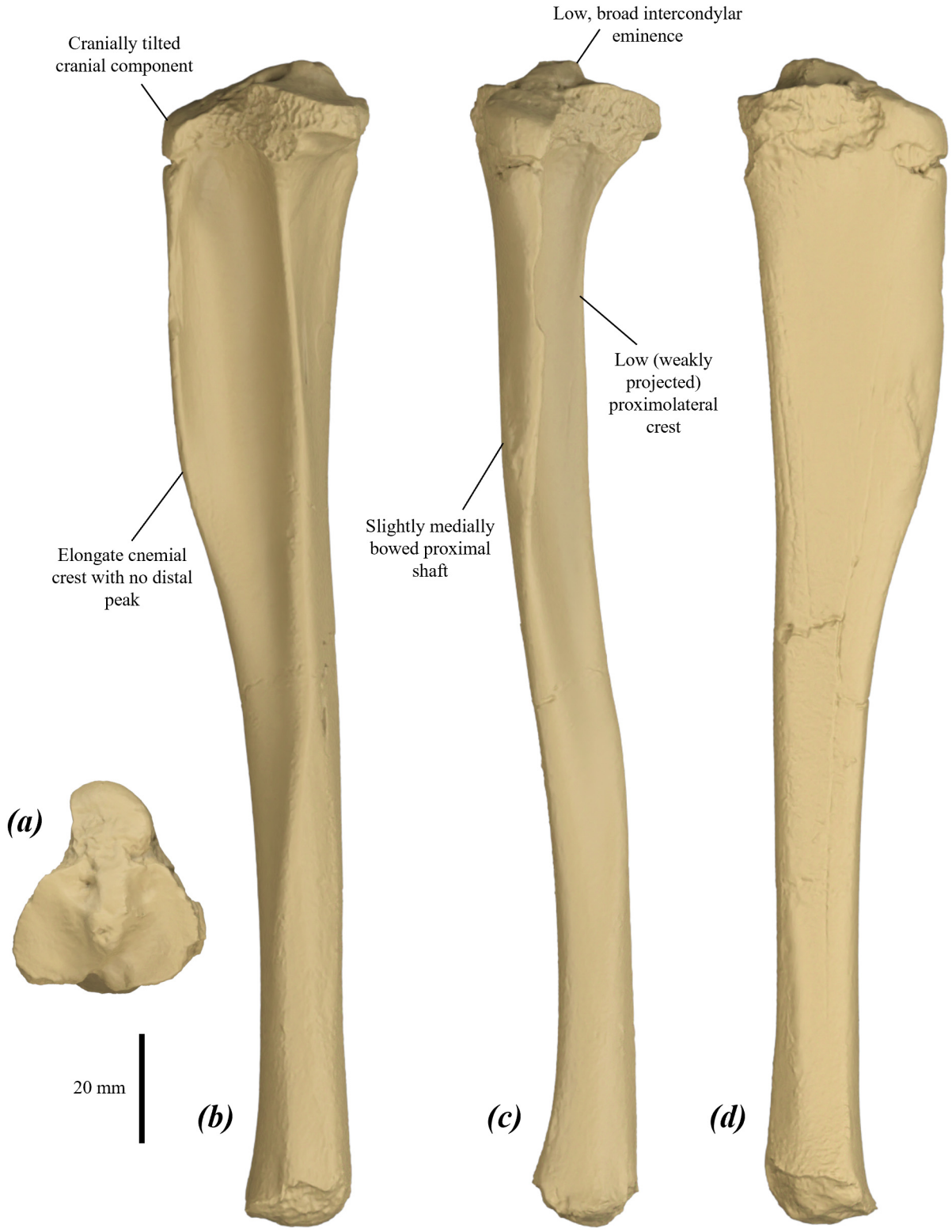

FIGURE 88. surface scan images of left tibia of *P. tumbuna* AM F88923 in: (a) proximal, (b) lateral, (c) cranial, and (d) medial views. Specimen is missing distal epiphysis.

of the lateral condyle not preserved; fibular facet abraded. Medial gastrocnemial fossa large, shallow and rounded; lateral gastrocnemial fossa small, shallow and rounded.

The femur of *P. tumbuna* cannot be differentiated from that of *P. otibandus*. It differs from all other compared species of *Protemnodon* in being more gracile, and from all compared taxa in having a taller distal shaft and a more elongate and distally situated quadratus tubercle. Further differs from that of *P. anak*, *P. mamkurra* **sp. nov.** and *P. viator* **sp. nov.** in being smaller; from *C. kitcheneri* in being more elongate, with a less medially displaced quadratus tubercle and a rounder, more proximally situated lateral gastrocnemial fossa; from *O. rufus* and from *M. fuliginosus* in having a relatively broader shaft, broader distal epiphysis, lower trochlear crests, and a more proximally situated lateral gastrocnemial fossa; and from *W. bicolor* in being larger and more robust, with less raised trochlear crests and relatively broader distal condyles.

Tibia (Fig. 88): short and robust. Proximal epiphysis width subequal to depth; cranial section slightly convex and distinctly cranially tilted; medial condyle elongate, slightly greater in surface area than lateral condyle; lateral condyle broad and rounded; intercondylar eminence low and broad. Proximal fibular facet mostly abraded. transversely quite broad.

Proximal shaft bowed very slightly medially and distal shaft bowed slightly laterally in cranial view. Cnemial crest deep, thickened and relatively elongate, extending just over one-third of the tibial length (Fig. 88b); lateral surface moderately concave and medial surface moderately convex; variably large muscle-scarred area on the craniodistal margin of medial surface for the partial origin of the m. gastrocnemius medialis or for the attachment of the medial superficial fascia. Proximolateral crest thick and quite low (Fig. 88c), particularly distally; merges smoothly with the shaft around the midpoint of the tibia. Distal shaft narrows very slightly before expanding slightly to the distal end, rounded to squarish in cross-section, becomes more rounded distally. Distal fibular facet deep, flattened, extends down the distal one-third of the lateral surface of the shaft. The distal epiphysis is not known.

The tibia of *P. tumbuna* differs from all compared taxa in being more robust, with a particularly low proximolateral crest, especially distally, and a relatively more elongate cnemial crest, and differs from all species except some specimens of *P. mamkurra* **sp. nov.** in having no distinct distal peak on the cnemial crest. It further differs from that of *P. anak* in being shorter, with lower, broader intercondylar eminence, cranially tilted cranial section of the proximal epiphysis, and a thicker proximolateral crest; from *P. mamkurra* **sp. nov.** in being shorter, with a thicker proximolateral crest and deeper, more flattened distal fibular facet; from *P. viator* in being smaller, shorter, and more bowed in cranial view, with a broader intercondylar eminence and cranially tilted cranial section of the proximal epiphysis; from *P. otibandus* in having thicker proximolateral crest; from *P. snewini* in being shorter; from *C. kitcheneri* in being shorter, with a less straight shaft in cranial view, a lower, broader intercondylar eminence, thicker cnemial crest that is slightly more laterally curved in cross-section, thicker proximolateral crest, deeper, more distinct distal fibular facet, and the distal shaft expanding more to the distal end; from *O. rufus* and *M. fuliginosus* in being shorter and much more robust, with a less straight shaft in cranial view, lower, broader intercondylar eminence, cranially tilted cranial section of the proximal epiphysis, thicker cnemial crest that is slightly more laterally curved in cross-section, thicker proximolateral crest, and deeper and more distinct distal fibular facet; and from *W. bicolor* in being larger and more robust, with a larger, broader intercondylar eminence, a more cranially tilted cranial section of the proximal epiphysis, relatively thicker cnemial crest, thicker proximolateral crest, particularly distally, and a deeper, more distinct distal fibular facet.

Pes

Calcaneus (Fig. 89): available specimens are fragmentary and badly abraded; small, low and robust. Calcaneal tuberosity quite broad, low and rounded-triangular in cross-section; broadens caudally, with the caudoplantar part flaring medially (Fig. 89a). Caudal epiphysis rounded and robust, with a narrow transverse valley across the centre of the caudal surface. Plantar surface broad, rugose, oblong in plantar view and distinctly convex, with the medial margin increasingly medially flared toward the caudal end, and the lateral component wrapping around the plantolateral margin of tuberosity onto a convex lateral surface. Calcaneal head broad; the midline of the head in the sagittal plane is medially offset relative to that of the calcaneal tuberosity, particularly visible in the relatively medial placement of the medial margin of the lateral talar facet. Sustentaculum tali broad, thick and medially projected; flexor groove very broad and deep. Fibular facet mostly abraded, appears small, slightly laterally projected, rounded and bulbous dorsally. Lateral talar facet broad, with slight medial tapering; smoothly convex in the sagittal plane; a large, rounded, shallow fossa is present immediately cranial to lateral talar facet; medial talar facet small, oval, orientated caudomedially to craniolaterally and strongly cranially tilted; caudally displaced relative to the lateral facet.

Facet for the talar head; very small, rounded, abuts the dorsomedial margin of the dorsomedial facet on the medial surface of the calcaneal head. Dorsomedial cuboid facet gently convex with a slightly rounded dorsomedial margin, separated from the dorsolateral facet by a deep, bevelled step, plantar section not preserved in available specimens; dorsolateral cuboid facet subequal in width to the dorsomedial facet, very cranially projected and gently plantarly tilted, with a slightly rounded dorsal margin; tapers slightly and curves plantomedially into the broad, dorsoplantarly short, medially situated and slightly medially tilted plantomedial cuboid facet.

The calcaneus of *P. tumbuna* differs from that of all compared taxa in having a caudomedially flared, distinctly convex plantar surface, extending dorsolaterally onto the lateral surface of the tuberosity, and a more medially displaced calcaneal head. It further differs from that of

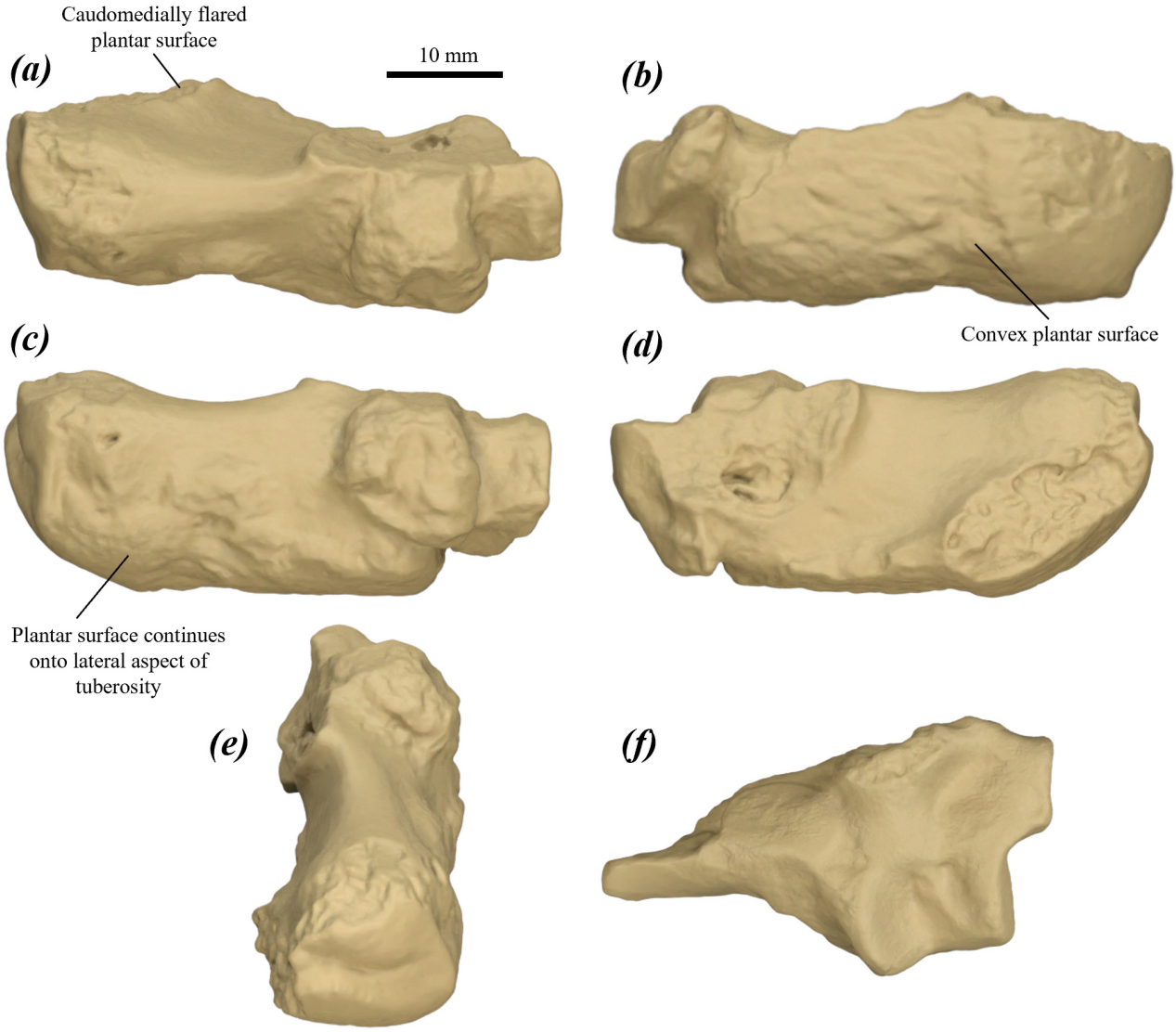

FIGURE 89. surface scan images of partial calcanei of *P. tumbuna*: (a–e) partial right calcaneus of specimen NCA-H71-9 in (a) dorsal, (b) plantar, (c) lateral, (d) medial, and (e) caudodorsal views; and (f) craniodorsal left calcaneal fragment of AM F88929 in dorsal view. Not preserved in NCA-H71-9 are the medial margin of the plantar surface/tuberosity and the medial component of the head; not preserved in AM F88929 are the caudal and plantar components of the calcaneus and the fibular facet.

P. anak in being smaller and lower; from *P. mamkurra* **sp. nov.** in being smaller and lower, with a smaller, more caudally displaced medial talar facet and a relatively broader, less convex medial cuboid facet; from *P. viator* **sp. nov.** in being smaller and more robust, with a relatively narrower dorsomedial cuboid facet and a more medially displaced calcaneal head; from *P. dawsonae* **sp. nov.** in being smaller; from *P. otibandus* in having a larger, deeper fossa cranial to the lateral talar facet; from *C. kitcheneri* in having a more medially rotated head; from *O. rufus* in being much shorter, lower and relatively broader, lacking an articular surface for the posterior plantar process of talus, and in having a larger, more medially projected sustentaculum tali, more medially rotated head, less triangular, more rounded calcaneal tuberosity in cross-section, more transversely aligned, less cranially tilted medial talar facet, the lateral talar facet with a shallower cranial fossa, and a relatively broader dorsomedial cuboid facet; from *M. fuliginosus* in being slightly larger, much shorter, lower and relatively broader, and in having a larger, more medially projected sustentaculum tali, more medially rotated head, less triangular, more rounded calcaneal tuberosity in cross-section, more transversely aligned, less cranially tilted medial talar facet, and the lateral talar facet with a shallower cranial fossa; and from *W. bicolor* in being larger, broader and more robust, with broader medial talar facet.

Metatarsal IV (Fig. 90a–g): two available specimens fragmentary and extremely abraded. Proximal surface medially tilted; dorsal cuboid facet mostly abraded, interpreted as broad; plantar cuboid facet mostly abraded, situated on the proximal surface of the plantar tubercle. Plantar tubercle quite large, plantarly projected and slightly proximally deflected. Metatarsal III fossa tall, elongate,

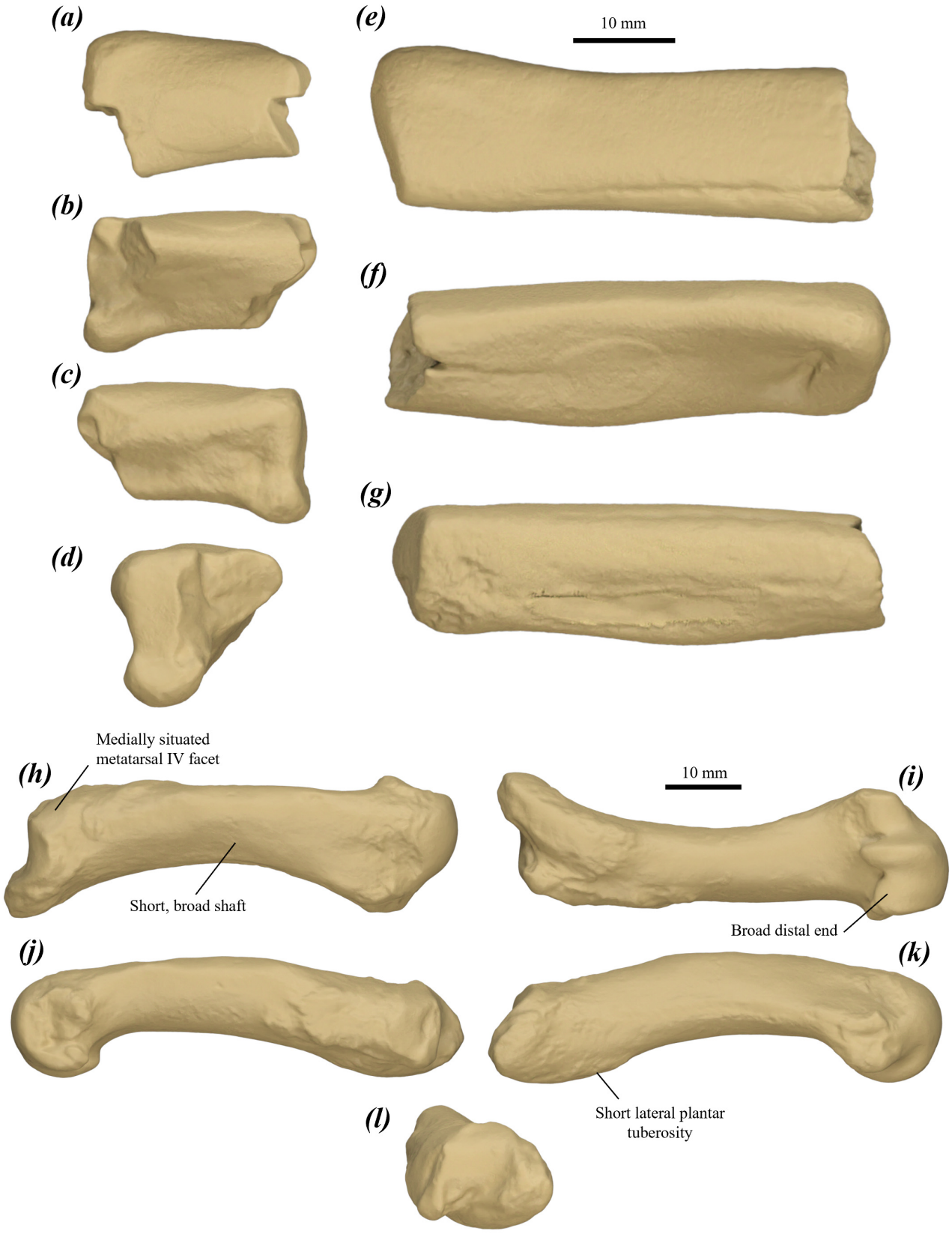

FIGURE 90. surface scan images of metatarsals IV and V of *P. tumbuna*: (a–d) proximal right metatarsal IV fragment of AM F88930 in (a) dorsal, (b) lateral, (c) medial, and (d) proximal views; (e–g) proximal left metatarsal IV fragment of AM F88927 in (e) dorsal, (f) lateral, and (g) medial views; and (h–l) right metatarsal V of NCA-071 in (h) dorsal, (i) plantar, (j) medial, (k) lateral, and (l) proximal views. Both AM F88927 and AM F88930 show evidence of rolling and severe abrasion.

shallow, and slightly rugose. Facet for metatarsal V partially abraded; tall, quite deep, gently concave and oblong. Plantar ridge large, rugose, rounded in cross-section, extends distally from the base of the plantar tubercle to slowly merge with the plantar shaft; bordered medially by the fossa for metatarsal III and laterally by the fossa for metatarsal V. Shaft very slightly rounded dorsally; height tapers to the midpoint.

The metatarsal IV of *P. tumbuna* cannot be differentiated from that of *P. otibandus*. It differs from that of *P. anak*, *P. mamkurra* **sp. nov.**, *P. viator* **sp. nov.**, *P. dawsonae* **sp. nov.** and *P. snewini* in being smaller; from *C. kitcheneri* in having a larger proximal plantar tubercle and a more raised plantar ridge; from *O. rufus* and *M. fuliginosus* in being relatively broader and more robust, and a having less plantarly raised plantar ridge relative to the proximal plantar tubercle; and from *W. bicolor* in being larger and more robust.

Metatarsal V (Fig. 90h–l): very short and robust; curves slightly laterally distally; variably arched in lateral view. Proximolateral process tall, blunt, rugose, curves slightly medially, proximodistally quite short, and transversely compressed. Cuboid facet large, quite tall, rounded and smoothly concave, with the dorsal margin slightly raised; extends from the medial margin of the posterior surface across the majority of the medial surface of the proximolateral process. Metatarsal IV facet quite small, broad, gently convex, slightly raised and oblong; situated on the medial and dorsomedial surfaces of the shaft, abuts the posterior margin of the shaft. Lateral plantar tuberosity short, low, broad and rugose (Fig. 90k), separated from the medial plantar tubercle by a narrow, very shallow channel. Medial plantar tubercle small, smoothly rounded and plantarly and proximomedially projected. Shaft rounded in cross-section; broadens significantly from the midpoint to the distal end, particularly on the lateral margin. Distal end very broad; fossae for collateral ligament large, rugose and shallow.

The metatarsal V of *P. tumbuna* differs from all species of *Protemnodon* in being more robust, with a shorter lateral plantar tuberosity. It further differs from that of *P. anak* in being shorter and not transversely compressed, with a taller cuboid facet that is more extensive along the proximolateral process, a more medially situated metatarsal IV facet, and a smaller medial plantar tubercle; from *P. mamkurra* **sp. nov.** in being shorter and more robust, with a more medially situated metatarsal IV facet and a broader distal end; from *P. viator* **sp. nov.** in being shorter and not transversely compressed, with a lower lateral plantar tuberosity, more medially situated metatarsal IV facet, and a lower, broader distal end with a more rounded keel; from *P. dawsonae* **sp. nov.** in being smaller, with a shorter, broader proximolateral process and a smaller medial plantar tubercle; from *P. otibandus* in not being transversely compressed, and in having a taller proximolateral process, proximodistally shorter metatarsal IV facet, and a smaller medial plantar tubercle; from *C. kitcheneri* in being shorter and relatively much broader, lacking a slight kink in the arch of the shaft immediately proximal to the midpoint in lateral view, with a larger, more rounded cuboid facet, a plantar groove present, and a larger medial plantar tubercle and lateral plantar tuberosity; from *O. rufus* and *M. fuliginosus* in being much shorter, much more robust, and not transversely compressed, with larger medial plantar tubercle and deeper, more distinct plantar groove; and from *W. bicolor* in being larger, much more robust, and not transversely compressed, and in having a larger proximolateral process and a more convex cuboid facet.

Remarks:

Protemnodon hopei Flannery, 1992a, was described from craniodental material of four or five individuals from Kelangurr Cave and from sediments in the nearby West Baliem River, West Papua. The taxon was described as having most in common morphologically with *P. otibandus* and *P. tumbuna*. Some of the purportedly diagnostic features (Flannery 1992a), however, vary significantly within species (see Figs 113–115 & Figs 121–125). The following is an extract from the specific diagnosis, where the morphology of *P. hopei* is contrasted with that of other species of *Protemnodon*: 'differing from *P. tumbuna* in being larger, with proportionately longer premolars, P3 with a straight rather than concave [buccal face of main] crest, and in having relatively narrower molars' (Flannery 1992a, p. 326). Although it was stated (Flannery 1992a) that *P. hopei* possesses relatively narrower molars than topotypic specimens of *P. tumbuna*, they are actually slightly broader relative to length (Flannery *et al.* 1983, table 3; Flannery 1992a, table 2; SI Measurement Dataset). *Protemnodon hopei* has also been described as differing from *P. tumbuna* by having 'better developed anteroposterior links on the molars, indicating adaptation to a more abrasive diet' (Hope *et al.* 1993, p. 124). However, we do not find that the taxa can be diagnosed on the basis of these characteristics.

The differences between relative and absolute dental dimensions of specimens referred to *P. hopei* and *P. tumbuna* are not sufficient to support these representing two species (see Figs 113–115 & Figs 121–125). The larger sample sizes of other species of *Protemnodon*, for example *P. anak*, illustrate the degree of variation that may be manifested within species of the genus. Thus, although the holotype palate of *P. hopei*, the only specimen preserving the upper dentition of this taxon, does possess relatively and absolutely wider molars than are seen in the holotype of *P. tumbuna*, the only upper dental material known at the time that *P. hopei* was described, the difference is considerably less than that seen within the sample of *P. anak*. The same is true of the premolar length relative to the molars. Although this does cluster specimens into loose taxonomic groups (see Fig. 121) it varies to such an extent in the better-sampled *P. anak* and other Australian Pleistocene species as to render the difference seen between the two samples in question here insignificant. The concavity of the buccal crest of the P3 is highly variable within *Protemnodon* species, for example within *P. mamkurra* **sp. nov.** (see Fig. 109). The crown height of the lower molars of *P. tumbuna* is lower than that of *P. hopei* when allowing for differing wear

stage. However, given the greater range of relative molar crown heights within the better-sampled *P. anak*, this feature is insufficient to separate the two taxonomically (see Figs 121–123).

Comparison of the postcranial material of *P. hopei* with that of *P. tumbuna* from Nombe Rockshelter and that figured in Menzies & Ballard (1994, pp. 130–131, figs 8 & 9) shows strong similarities. Both samples show an elongate ilium, an acetabulum rotated cranioventrally, a long, gracile femur paired with a short, robust tibia, and a very short, broad, arched metatarsal V. It is noted that the three dentary specimens of *P. hopei* do possess a deeper digastric sulcus than that seen in *P. tumbuna*, but again, this character varies greatly within the better-sampled material from the Australian Pleistocene. In the absence of reliable characters to separate the two holotypes, and since no features were found in the postcranial elements that served to differentiate between the two taxa, *P. hopei* is here considered to be a junior synonym of *P. tumbuna*.

***Protemnodon dawsonae* sp. nov.**

LSID of new species: urn:lsid:zoobank.org:act:231A7C0D-FF39-458E-8703-1AF7B6FBCE77

Protemnodon devisi Bartholomai; Bartholomai (1973) pl. 22, fig. 3. Not *P. devisi*, Bartholomai, 1973.

Protemnodon sp. cf. *devisi*; Dawson *et al.* (1999) pp. 276–278, fig. 7.

Holotype:

AM F161915 R partial cranium, preserving M1–4, maxilla, and partial lacrimal, frontal, palatine, and jugal. Collected on an excavation at Big Sink by Prideaux and Fusco *et al.* in 2016.

Type locality:

Big Sink doline, Bone Cave–Phosphate Mine system, Wellington Caves (32°36' S, 148°55' E), central eastern New South Wales. The Big Sink unit is made up of pale red-orange, consolidated sediments on the southern wall of the Big Sink doline (Osborne 1997). Though the deposit has not been dated directly, biochronology and biocorrelation with dated assemblages suggest a Pliocene age for the Big Sink LF (Dawson *et al.* 1999).

Paratypes:

Big Sink doline: AM F69835 partial L premaxilla, with I1–I3; AM F69836 L premaxilla fragment; AM F69838 L I1; AM F69839 R I1; AM F69840b partial L maxilla; AM F69841 partial L maxilla; AM F69845 partial R maxilla; AM F69842 L P3; AM F69844 L P3; AM F161923 L P3; AM F69858 & AM F65859 partial LR dentaries (reassociated); AM F69860 partial L dentary; AM F69868 L i1; AM F69869 R i1; AM F161921 R dentary fragment; AM F161920 partial axis vertebra; AM F161914 partial axis vertebra; AM F161918 partial lumbar vertebra L2?; AM F161911 caudal vertebra Ca2?; AM F161912 caudal vertebra Ca3?; AM F161919 ilial fragment; AM F161913 partial R calcaneus; AM F161917 partial L metatarsal IV; AM F109039 R metatarsal IV; AM F106040 L metatarsal V; AM F161916 proximal pedal phalanx IV.

Referred specimens:

South Australia

Stirton Quarry, Lake Kanunka: SAMA P50399 partial juvenile R maxilla with P3 from crypt; UCMP 322655 R P3.

Site 4 (V77015), Lake Kanunka: UCMP 170678 m4; UCMP 156881 R ilium, partial pubis and ischium.

Queensland

Sand Scree Locality, Chinchilla: QM F7071 partial L dentary.

Chinchilla, Darling Downs (site unknown): QM F4712 partial juvenile L maxilla.

Specific diagnosis:

Protemnodon dawsonae **sp. nov.** is differentiated from all other species of *Protemnodon* by one dental autapomorphy and a unique combination of dental and postcranial attributes. The upper dentition of *P. dawsonae* **sp. nov.** differs from that of all species of *Protemnodon* in having upper molars with the postparacrista distinctly inflected lingually then buccally ('kinked') in the interloph valley. The i1 of *P. dawsonae* **sp. nov.** differs from all species of *Protemnodon* except *P. tumbuna* in having a thick, low ventrolingual crest on the i1.

The dentary and dentition of *P. dawsonae* **sp. nov.** are most similar to those of *P. otibandus*, *P. mamkurra* **sp. nov.** and *P. viator* **sp. nov.** The dentary of *P. dawsonae* **sp. nov.** cannot be differentiated from that of *P. mamkurra* **sp. nov.** or *P. viator* **sp. nov.**, but it differs from *P. otibandus* in having a taller, more robust anterior dentary, particularly around the i1. The dentition further differs from that of *P. otibandus* in having: a broader, anteroposteriorly shorter I1; relatively larger, broader and more robust i1; and a broader p3 relative to length. It further differs from that of *P. mamkurra* **sp. nov.** and *P. viator* **sp. nov.** in being lower crowned, with: I1 absolutely narrower and narrower relative to I3; and upper molars with a narrower protoloph relative to the loph base when unworn, and a thinner, more raised preparacrista.

The upper dentition of *P. dawsonae* **sp. nov.** differs from that of *P. snewini* in having: relatively broader P3; and molars with a higher, more distinct preparacrista. The dentary differs from that of *P. snewini* in being larger and more robust, with: a more robust and more dorsally deflected diastema, and a taller mandibular corpus. The lower dentition differs from that of *P. snewini* in being larger and higher crowned, with: broader, more robust i1; relatively broader p3; and relatively broader molars with a smaller precingulid.

The postcranial skeleton of *P. dawsonae* **sp. nov.** is most similar to that of *P. mamkurra* and *P. viator*. The proximal phalanx IV of *P. dawsonae* differs from those of all species of *Protemnodon* except *P. viator* **sp. nov.** in having a more proximodorsally extensive distal articular surface. Its axial skeleton is differentiated from

P. mamkurra **sp. nov.** by having: a relatively narrower, deeper axis vertebra; lumbar vertebrae with deeper transverse processes and a centrum with relatively slightly broader cranial and caudal extremities, more deeply concave ventrolateral surfaces, a more deeply concave ventral margin in lateral view, and a less raised ventral ridge. The hindlimb differs from that of *P. mamkurra* **sp. nov.** in having a pelvis with a relatively smaller caudal iliac spine, less deeply concave gluteal fossa, and a less convex, less rugose caudal margin of the dorsal section of the ischium. The pes differs in having: a relatively taller, narrower calcaneus with a caudally displaced medial talar facet relative to the lateral talar facet and a sustentaculum tali with a rounded (rather than pointed) cranioplantar peak; metatarsal IV with a smaller plantar cuboid facet; and narrower metatarsal V with a more distally extensive lateral plantar tuberosity.

The axial skeleton of *P. dawsonae* **sp. nov.** is distinguished from that of *P. viator* **sp. nov.** in having: a narrower axis vertebra with a thinner spinous process, more laterally tilted postzygopophyses with less concave articular surfaces, and a rounded (rather than bilobed) ventral margin of the caudal extremity of the centrum; and shorter, more robust caudal vertebrae. The hindlimb differs from *P. viator* **sp. nov.** in having a pelvis with a less deeply concave gluteal fossa. The pes of *P. dawsonae* **sp. nov.** differs from that of *P. viator* **sp. nov.** in having: a broader, dorsoplantarly shorter calcaneus with a more rounded calcaneal tuberosity in cross-section, less deep lateral talar facet, broader medial talar facet, and a more medially projected sustentaculum tali; relatively broader, dorsoplantarly shorter metatarsal V with a more elongate proximolateral process and a more proximally projected medial plantar tubercle; and a more robust proximal phalanx IV with a weaker waist.

The pes of *P. dawsonae* is distinguished from that of *P. otibandus* in having: a calcaneus with a less medially displaced head and a narrower calcaneal tuberosity; metatarsal IV with continuous dorsal and plantar cuboid facets, a more concave, less laterally projected metatarsal V facet, larger plantar tubercle, more raised plantar ridge, and a relatively more plantarly projected keel; a more elongate metatarsal V, with a narrower, less dorsally projected cuboid facet; and a more elongate proximal pedal phalanx IV.

Etymology:

Named for Dr Lyndall Dawson, for her contributions to the study of macropodid systematics and the Big Sink assemblage.

Description and comparisons:

Cranium and dentition

Cranium (Fig. 91d): jugal has a quite large, slightly posteriorly deflected and laterally projected masseteric process, with morphology very similar to that of *P. mamkurra* **sp. nov.** Ventral margin of the orbit is dorsally displaced relative to the maxillary shelf. Maxillary foramen small and round, opens posteriorly. Pterygoid is elongate. No vacuities are present on the preserved section of the palate.

The known portion of the cranium of *P. dawsonae* **sp. nov.** differs from that of *C. kitcheneri* and *W. bicolor* in having a higher maxillary shelf relative to the position of the base of the masseteric process, and a higher ventral margin of the orbit with a less laterally projected lip.

Upper dentition (Figs 91 & 92): I1: robust, broad and arcuate. Enamel covers the anterior, buccal, and lingual surfaces, and is removed from the sides of the posterior surface by a small amount of wear. Occlusal surface broad and roughly rectangular in slightly worn specimens, becomes longer and rounder with increased wear. I2: arcuate, relatively small and narrow. Enamel covers the buccal and lingual surfaces, with the lingual enamel removed only by very extensive wear. Small posterobuccal crest is removed by a small amount of wear, leaving a slight concavity on buccal surface. I3: elongate, transversely compressed and trapezoidal to roughly triangular in buccal view; buccal enamel convex, buccal length greater than the width of I1 (Fig. 91a). Main crest curves anterolingually to sit lingual to the posterior margin of the similarly shaped anterobuccal crest. Anterobuccal crest is around half the length of the main crest.

Cheek tooth row is straight to very slightly curved in adults. DP2: morphologically very similar to P3 but anteroposteriorly truncated; oblong, quite short and broad, broadens posteriorly, with thickened peaks over the anterior and posterior roots linked by the main crest. Main crest high, blade-like, anteroposteriorly to slightly posterobuccally orientated, jagged to gently undulating in buccal view, with a low, dorsoventrally aligned ridgelet on the midpoint of the buccal surface. Lingual crest low, extends from the lingual base of the anterior cusp to the small, secondary posterolingual peak; lingually borders a broad, anteriorly tapering lingual basin with a low transecting ridgelet. Posterior basin small, abuts the posterior margin, sits between the main and secondary posterior peaks; removed by a small amount of wear. DP3: molariform, fairly broad; anterior loph longer and narrower than the posterior loph; lingual bases of lophs swollen; interloph valley width subequal to that of lophs. Precingulum and cristae worn to absence in sole available specimen.

P3: large, oblong and quite elongate, generally slightly broader posteriorly, with thickened peaks over the anterior and posterior roots linked by the main crest; straight to curving very slightly buccally toward the posterior, with posterior section very slightly rotated and swollen buccally, contributing to occasional slightly crescentic shape of the tooth. Main crest high, blade-like and roughly anteroposteriorly orientated with occasional very slight posterobuccal curvature in occlusal view; slightly jagged to gently undulating in buccal view; three dorsoventrally aligned ridgelets on the buccal surface, posterior ridgelets lower, with anteriormost ridgelet typically more raised and angular; in some specimens, small buccal ridgelets form enamel crenulations at the buccal base of the main crest (Fig. 92g). Anterior peak quite tall, forms a rounded point; peak intersected by a very brief transverse crest,

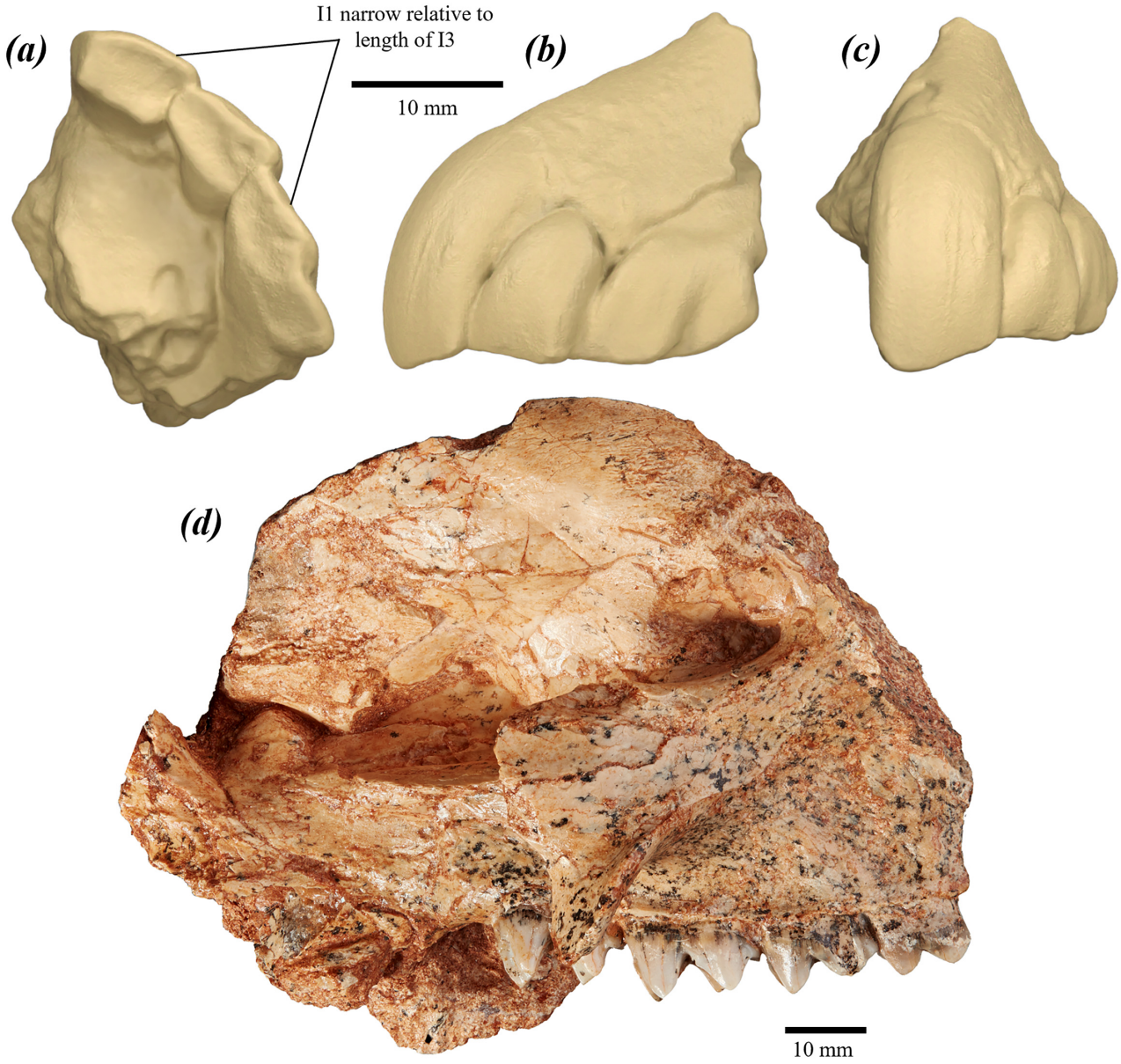

FIGURE 91. (a–c) surface scan images of left I1–3 of *P. dawsonae* **sp. nov.** AM F69835 in (a) occlusal, (b) buccal/lateral, and (c) anterior views; and (d) partial right cranium of *P. dawsonae* **sp. nov.** holotype AM F161915 in right lateral view, showing M1–4, maxilla, and partial lacrimal, frontal, palatine, and jugal.

perpendicular to main crest, extends down buccal and lingual faces as a low ridgelet on posterior margins of anterior cusp, with lingual ridgelet merging into the anterior margin of the lingual crest; small, blunted cusp present at the anterior base, often lingually situated. Lingual crest low, undulating in lingual view, with a single low, smoothly rounded peak near the anterior margin; crest extends posteriorly, from or slightly posterior to the lingual base of the anterior cusp, to merge into the posterolingual peak; lingually borders a broad lingual basin, which is perpendicularly transected by three very low, indistinct ridgelets, roughly opposing the buccal ridgelets. Posterior cuspule broad and posteriorly rounded. Main posterior peak quite tall and rounded, continuous with the main crest, which extends and broadens posteriorly to merge with the low transverse posterior crest. Posterolingual peak rounded, lower than the main peak, linked to the main crest by a thin transverse crest that anteriorly borders the posterior basin. A small posterior basin sits between the main and posterolingual peaks, posteriorly bordered by the transverse posterior crest; removed by a small amount of wear.

Molars: rounded-rectangular in occlusal view, with M1 and usually M2 more rounded than the posterior molars. Precingulum quite broad, slightly narrower than the anterior loph, gently medially tilted, extends from the anterior base of the preparacrista to adjacent to the anterolingual margin; generally becomes slightly larger, broader and more projected toward M4; flat, broad and shelf-like when worn; some specimens (see SAMA P50399) have a small

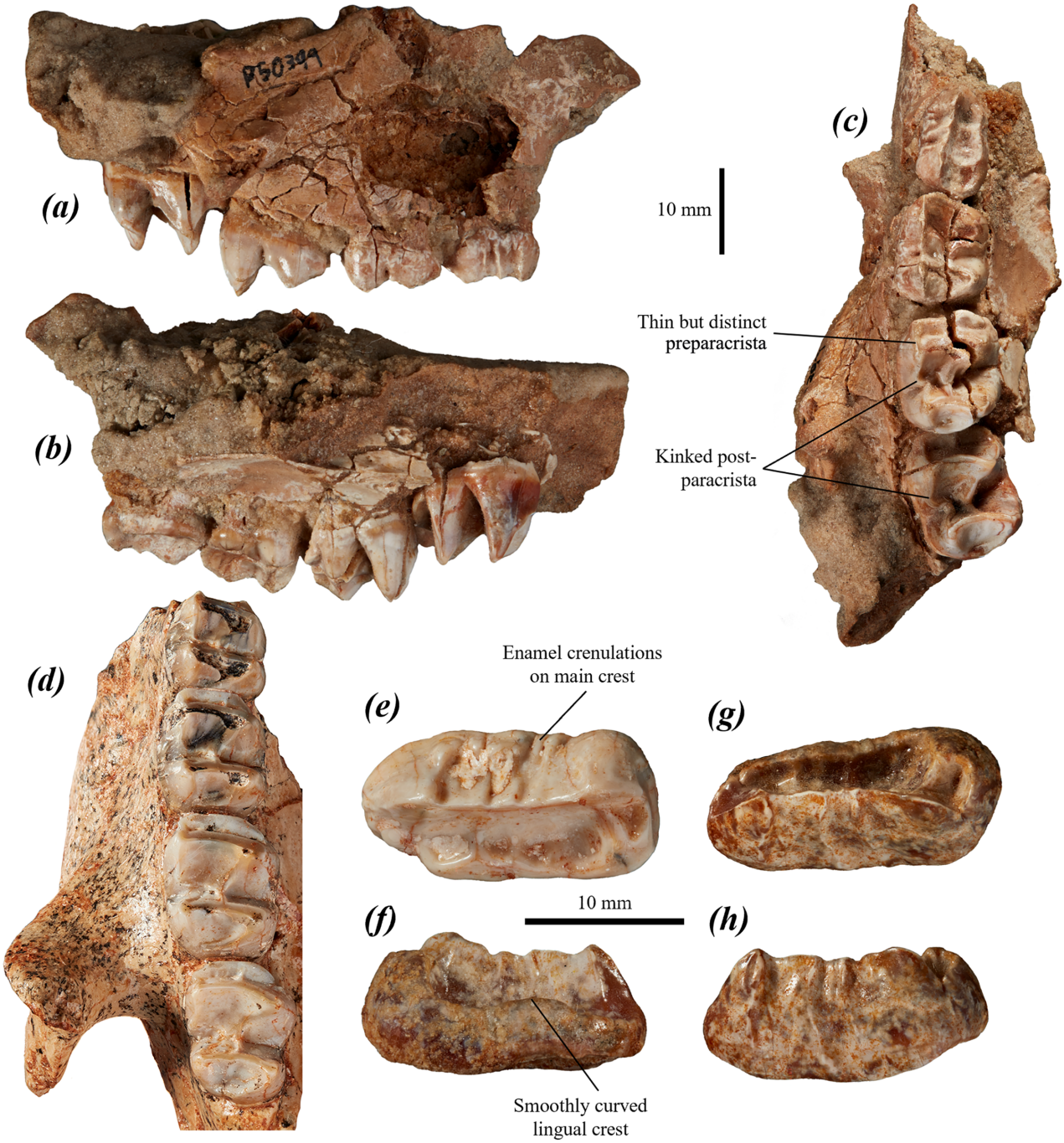

FIGURE 92. upper dentition of *P. dawsonae* **sp. nov.**: right DP2–M2 of SAMA P50399 in (a) buccal, (b) lingual, and (c) occlusal views; (d) right M1–4 of holotype AM F161915 in occlusal view; (e) left P3 of AM F161923 in occlusal view; and right P3 (removed from crypt) of SAMA P50399 in (f) lingual, (g) occlusal, and (h) buccal views.

preprotocrista extending very briefly up the anterior of the protoloph from around the midpoint of the precingulum. Preparacrista quite thin but distinct and straight, continuous with the buccal margin of the precingulum and extending to the paracone. Postparacrista thin, raised and distinctly kinked, extends straight posteriorly from the paracone before twisting strongly lingually near the base of the interloph valley and proceeding nearly to the end of the postprotocrista in the lingual valley (Fig. 92c–d). Postprotocrista broad and quite straight, extends from protocone to around the midpoint of interloph valley; in most specimens, the postprotocrista extends onto the anterior face of the metaloph. Premetacrista slight, extends from metacone to meet base of postparacrista in interloph valley Postmetaconulecrista quite thick and raised, arises from metaconule and curves dorsobuccally to almost beneath metacone to form moderate oblique shelf beneath posterior basin. Postmetacrista lower, shorter and less distinct, extends straight from metacone to buccal margin of postmetaconulecrista or deflects slightly lingually to merge into buccal margin of posterior basin.

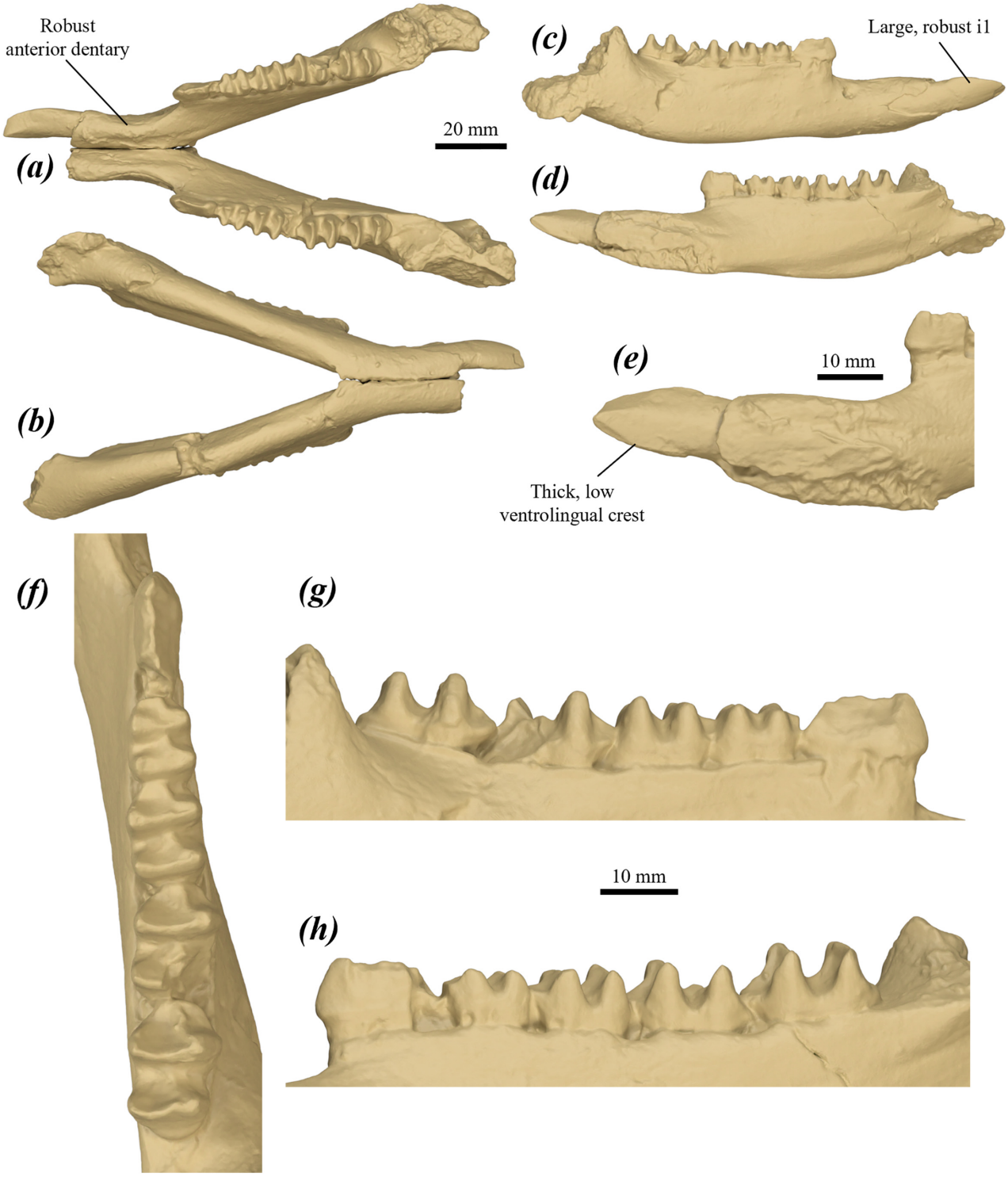

FIGURE 93. dentaries and right lower dentition of *P. dawsonae* **sp. nov.**: mandible (re-associated dentaries) AM F69858 (right dentary) and AM F69859 (left dentary) in (a) occlusal, and (b) ventral views; right dentary AM F69858 in (c) buccal, and (d) lingual views, and (e) lingual view of i1; and p3–m4 of AM F69858 in (f) occlusal, (g) buccal, and (h) lingual views.

The upper dentition of *P. dawsonae* **sp. nov.** differs from that of all other species of *Protemnodon* in having the postparacrista distinctly inflected lingually then buccally in the interloph valley. It further differs from *P. anak* in having larger P3 with lower, less distinct buccal and lingual ridgelets and a less jagged, more smoothly undulating and more anteriorly extensive lingual crest, and relatively broader molars with a narrower protoloph relative to the protoloph base when unworn; from *P. mamkurra* **sp. nov.** and *P. viator* **sp. nov.** in having I1 narrower relative to I3, P3 with slightly more raised and distinct buccal ridgelets, and molars with a thinner, more raised and more

distinct preparacrista and a narrower protoloph relative to the loph base when unworn; additionally differs from *P. mamkurra* **sp. nov.** in having relatively narrower posterior molars; from *P. tumbuna* in being larger and slightly higher crowned, with I1 lacking posterobuccal bulge, and generally less rounded molars in occlusal view with a more raised, more distinct preparacrista and lacking a urocrista; from *P. otibandus* in being generally larger, with broader, anteroposteriorly shorter I1 lacking a posterobuccal bulge and molars lacking a urocrista; from *P. snewini* in being larger, with relatively broader P3 and molars with a higher, more distinct preparacrista; from *C. kitcheneri* in being larger and higher crowned, with larger incisors relative to size of cranium and an absolutely and relatively more elongate P3; and from *W. bicolor* in being much larger, and higher crowned, with P3 with a higher lingual crest and a larger posterior basin, and molars with a thicker postprotocrista distinctly extending to the protocone (rather than merging into the centre of the posterior surface of the protoloph).

Dentary (Fig. 93a–d): robust, moderately tall, and gently transversely compressed, with a long, robust and gently tapering anterior dentary ventral to the diastema, projected straight anteriorly or slightly deflected dorsally (Fig. 93a). Angle between the dentaries at the mandibular symphysis is ~35–40°. Mandibular symphyseal plate large and elongate, extends along the entirety of the anterior dentary to abut the posterior margin of i1. Mental foramen round to oval, opens dorsolaterally to anterodorsolaterally, located roughly one-fifth of distance from dp2/p3 to i1 and around one-quarter of distance from the diastema to the ventral margin. Mandibular corpus height generally subequal below p3 and m4, with the width at a minimum ventral to m1 and increasing gently posteriorly. Digastric sulcus shallow and broad, extends from beneath the posterior of the molar row to adjacent to the anteroventral margin of the medial pterygoid fossa. Buccinator sulcus distinct but quite shallow, extends along the buccal surface of the mandibular corpus with a slight ventral tilt posteriorly, slightly ventral to the three–four anteriormost cheek teeth.

The dentary of *P. dawsonae* **sp. nov.** cannot be differentiated from that of *P. mamkurra* **sp. nov.** It differs from that of *P. anak* in being slightly broader and more robust, with a more dorsally deflected diastema; from *P. viator* **sp. nov.** in being generally slightly smaller; from *P. tumbuna* in being larger, with a more dorsally situated mental foramen; from *P. otibandus* in being slightly more robust, particularly in the diastema; from *P. snewini* in being larger and more robust, with a more robust and more dorsally deflected diastema and a taller mandibular corpus; from *C. kitcheneri* in being larger and more robust, with a relatively shorter, more dorsally deflected diastema, more posteroventrally situated mental foramen, and a taller mandibular corpus; and from *W. bicolor* in being much larger, with a more dorsally deflected diastema.

Lower dentition (Fig. 93c–h): i1: procumbent and slightly dorsally deflected; broad, tilted dorsally and transversely compressed; acuminate when unworn, becomes shorter and rounder in cross-section with wear. Thick enamel completely covers the buccal surface. Dorsobuccal and ventrolingual crests low and thick (Fig. 93e). Enamel covers the ventral third of the lingual surface and tapers posteriorly.

p3: very similar in morphology to that of *P. mamkurra* **sp. nov.** and *P. viator* **sp. nov.**; oblong and elongate in occlusal view, typically with a slight waist; typically subequally broad across posterior and anterior moieties; tall and triangular in cross-section with bulging buccal and lingual bases. Anterior cuspid has a dorsoventrally aligned buccal and lingual ridgelet on posterior margin. Main crest linear, anteroposteriorly aligned and twists slightly lingually over the posterior root. Both surfaces of the main crest with two or three low, rounded, indistinct, roughly dorsoventrally aligned ridgelets extending to the peak of the crest, such that the crest appears slightly undulating in buccal view.

Molars: high-crowned, broad and rounded in occlusal view, with interlophid valley varying from slightly broader to slightly narrower than the lophid bases; when unworn or slightly worn, protolophid and hypolophid are posteriorly convex or have an oblique mesial kink toward the posterior in occlusal view; buccal margins of the lophids are slightly more convex than the lingual margins in posterior view. Precingulid narrow, anteriorly projected, usually forms a rounded corner; a slight raised lip is present around the anterior margin when unworn. Paracristid quite thick and raised; lingual component arises from the anterolingual edge of the trigonid basin, extends buccally then straight posteriorly before the buccal component ascends, curving gently buccally, to the protoconid; the degree of buccal curve and thickness increases with molar wear. Protoconid higher than the metaconid and slightly lingually displaced. Cristid obliqua thick and low, mostly contributed by the talonid; arises slightly buccal to the midpoint of the interlophid valley, curves very slightly buccally and extends to the hypoconid. Preentocristid absent to very low, broad and indistinct, arises midway between the base of the cristid obliqua and the lingual extremity of the interlophid valley and deflects slightly lingually to meet the entoconid. When unworn, the hypoconid is distinctly taller than the entoconid and sits slightly buccal of the midline of the tooth. Postcingulid narrow and slight on m1–m2, becomes broader and occasionally shelf-like in m3 and particularly in m4.

The lower dentition of *P. dawsonae* **sp. nov.** differs from that of all compared taxa except *P. mamkurra* **sp. nov.** and *P. viator* **sp. nov.** in having a lower, thicker ventrolingual crest on i1. It further differs from *P. anak* in being slightly larger, with a more robust i1, and p3 with lower, less distinct ridgelets on the main crest and generally relatively broader molars; from *P. mamkurra* **sp. nov.** and *P. viator* **sp. nov.** in being generally smaller and slightly lower crowned, with a ventrolingual crest present on i1; from *P. tumbuna* **sp. nov.** in being larger and higher crowned, with relatively broader p3, and narrower molars with less convex buccal margins of lophids; from *P. otibandus* in being generally larger, with larger, broader and more robust i1 and relatively broader p3; from *P. snewini* in being larger and higher crowned, with broader,

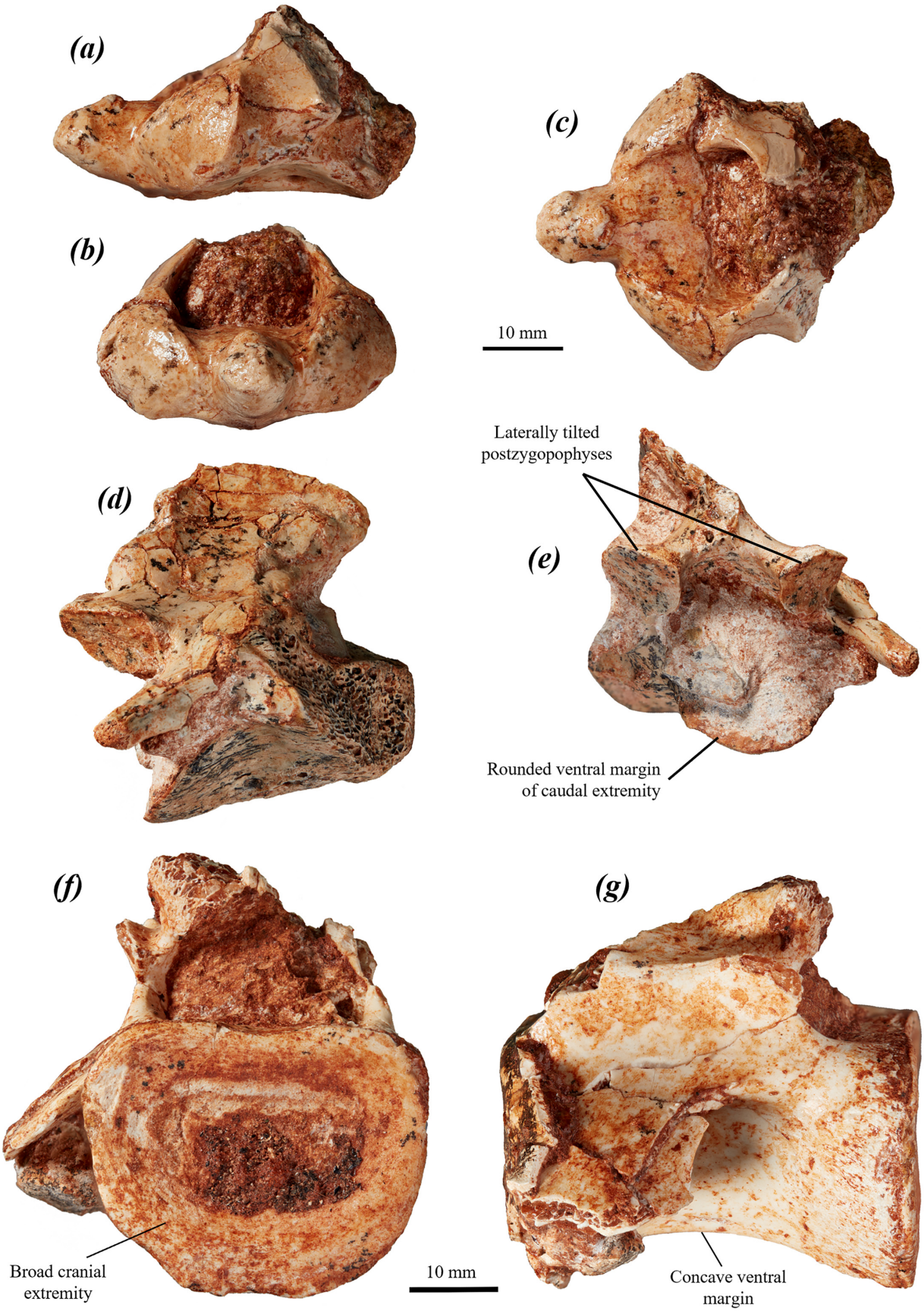

FIGURE 94. vertebrae of *P. dawsonae* **sp. nov.**: partial axis vertebra AM F161920 in (a) left lateral, (b) cranial, and (c) dorsal views; partial axis vertebra AM F161914 in (d) right lateral, and (e) caudal views; and (f–g) lumbar vertebra L2? AM F161918 in (f) cranial, and (g) lateral views.

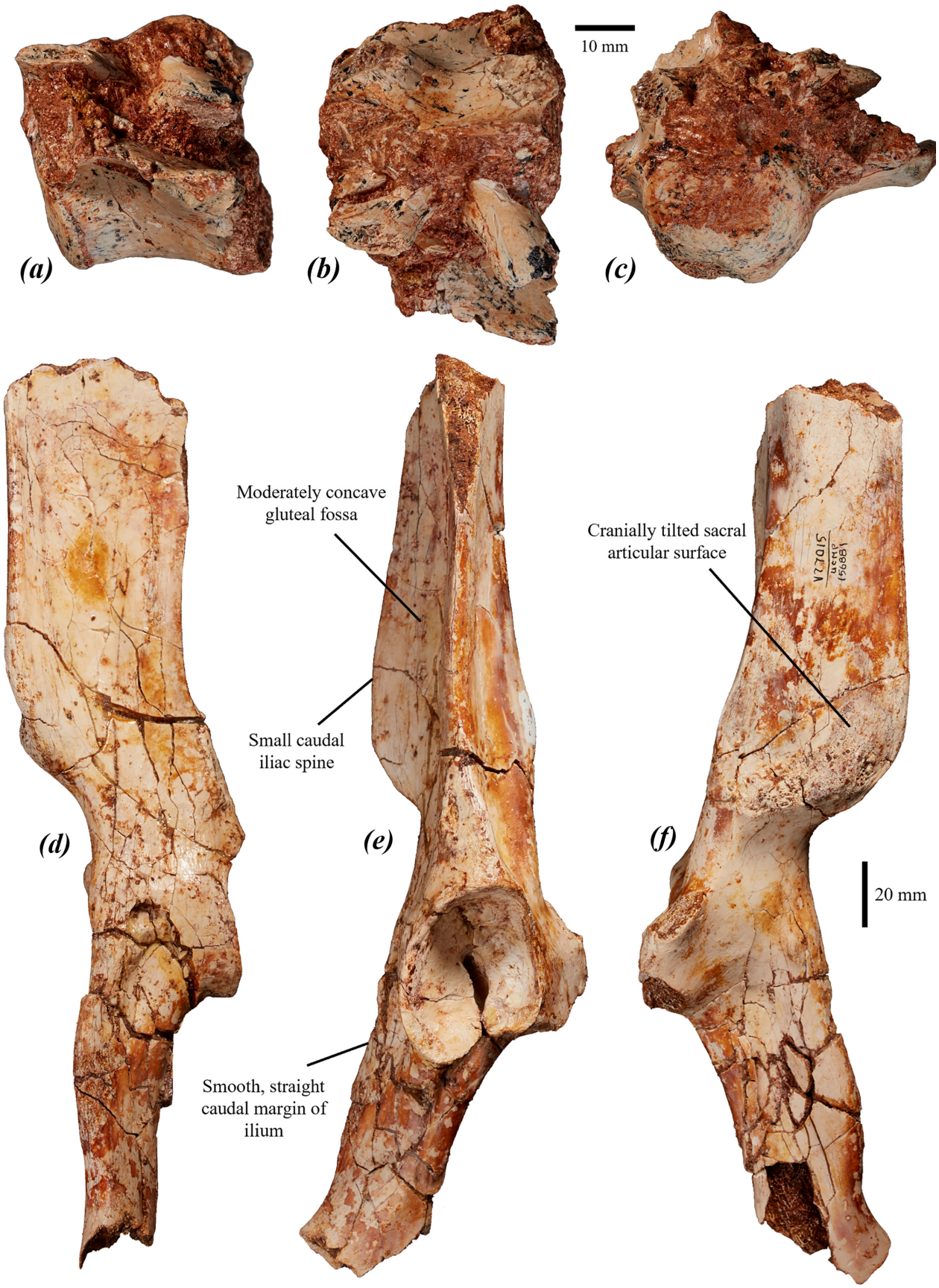

FIGURE 95. caudal vertebra Ca2? of *P. dawsonae* **sp. nov.** AM F161911 in (a) lateral, (b) dorsal, and (c) cranial views.(d–f) partial pelvis, predominantly ilium and caudal component of ischium, of *P. dawsonae* **sp. nov.** UCMP 156881 in: (d) caudal, (e) lateral, and (f) medial views.

more robust i1, relatively broader p3, and relatively broader molars with a smaller precingulid; from *C. kitcheneri* in being larger and higher crowned, with broader and more spatulate i1, relatively broader deciduous premolars, absolutely more elongate p3 that is longer relative to molar length, and molars with narrower lophid crests, higher cristid obliqua and a postcingulid present; and from *W. bicolor* in being much larger, with broader, more spatulate i1, p3 with less raised and distinct ridgelets on the main crest, and molars with narrower lophid crests and a generally more anteriorly prominent precingulid.

Axial skeleton

Axis (C2) (Fig. 94a–e): moderately craniocaudally short, quite broad and robust. Dens short, blunt and gently dorsally deflected. Cranial articular surfaces broad and convex; angled laterally and slightly dorsally. Arch mostly crushed or absent in available specimens; appears thick and quite low. Vertebral canal roughly oval and gently domed. Spinous process crushed and caudally abraded, appears quite tall, thin and tilted slightly cranially, with gently convex dorsal margin and cranial extremity projecting past cranial margin of arch. Postzygopophyses fairly small and flared slightly laterally, caudally projected beyond caudal extremity of the centrum and subequally to the caudal extremity of the transverse processes; articular surfaces very slightly concave and facing caudoventrally, with a moderate lateral tilt. Transverse processes quite thick and long, with a strong caudal and slight ventral deflection. Ventral surface of the centrum broad, with a slightly raised medial ridge. Caudal extremity of the centrum incompletely preserved; gently caudally and ventrally projected and slightly dorsally tilted, with a rounded ventral margin.

The axis vertebra of *P. dawsonae* **sp. nov.** differs from that of *P. anak* in being relatively and absolutely much less elongate, with a less elongate, slightly more dorsally deflected dens, dorsoventrally shorter, slightly more convex cranial articular surfaces, much less caudally projected caudal extremity of the centrum, and smaller, less elongate postzygopophyses; from *P. mamkurra* **sp. nov.** in being deeper relative to width, with the caudal extremity of the centrum more caudally projected; from *P. viator* **sp. nov.** in being smaller and narrower, with a thinner spinous process, more laterally tilted postzygopophyses with less concave articular surfaces and a rounded (rather than bilobed) ventral margin of the caudal extremity of the centrum; from *C. kitcheneri* in being broader relative to length, with a lower mesial ventral ridge, more laterally tilted caudal articular surfaces, and a relatively larger, broader caudal extremity of the centrum; from *O. rufus* in being relatively slightly shorter and broader, with a less dorsally deflected dens and the dorsal margin of the spinous process rounded and convex (rather than level); from *M. fuliginosus* in being larger, with a slightly more convex dorsal margin of the spinous process, longer, more ventrally deflected transverse processes, less laterally flared, slightly more caudally projected postzygopophyses, and a more ventrally projected caudal extremity of the centrum; and from *W. bicolor* in being larger, with a more rounded dens and more lateral facing cranial articular surfaces.

Lumbar vertebrae (L2?) (Fig. 94f–g): robust; centrum short and broad, narrows to a waist; ventrolateral surfaces concave and laterally tilted, with the ventral margin concave in lateral view. Cranial extremity of the centrum gently convex and rounded with a flattened dorsal margin, slightly taller than the caudal extremity. Caudal extremity of the centrum gently concave and broadly rounded with a flattened dorsal margin. Vertebral canal quite low, broad and domed in cranial view. The prezygopophyses and spinous process are completely abraded. Transverse processes mostly abraded; bases highly dorsoventrally compressed, ventrally deflected and situated on the cranial part of the lateral surfaces. Postzygopophyses almost entirely abraded, bases appear thickened and robust. The base of a small anapophysis is present on the arch ventrolateral to the base of the postzygopophysis; transversely compressed and slightly caudally deflected, with a low ridge extending cranially from the base.

The L2? of *P. dawsonae* **sp. nov.** differs from that of *P. mamkurra* **sp. nov.** and *P. viator* **sp. nov.** in being smaller, with deeper transverse processes and a centrum with relatively lower, broader cranial and caudal extremities, more concave ventrolateral surfaces, more concave ventral margin in lateral view and a less raised ventral ridge; from *C. kitcheneri* in being relatively slightly longer; from *O. rufus* in being slightly larger, with a broader centrum relative to height and relatively deeper transverse processes; from *M. fuliginosus* in being larger, with less dorsoventrally compressed cranial and caudal extremities of the centrum and a more concave ventral margin in lateral view; and from *W. bicolor* in being much larger, with a centrum having a less distinct waist in ventral view and a less ventrolaterally swollen caudal section.

Caudal vertebrae (Ca2 & 3?) (Fig. 95a–c): numerical position of the vertebrae is not certain; vertebrae short and robust. Pre- and postzygopophyses heavily abraded in available specimens; prezygopophyses have a thick proximal section that is slightly dorsoventrally compressed and dorsally deflected; postzygopophyses short, robust and caudolaterally projected, with articular surfaces small, flat and round; bases of pre- and postzygopophyses merge at the centre of the arch around the base of the spinous process. Centrum shallow, slightly arched in lateral view, with ventrally tilted cranial and caudal extremities; cranial extremity rounded; caudal extremity slightly dorsoventrally compressed and oval, with that of Ca2 slightly ventrally projected relative to the cranial extremity. Vertebral canal low and broad in Ca2; very low in Ca3. Transverse processes very deep in C2, extend from adjacent to the cranial margin of the centrum to adjacent to the caudal margin, dorsoventrally very thin, particularly cranially, caudally deflected, quite broad cranially and steadily broaden caudally; very abraded in Ca3, extend from slightly cranial of the midpoint of the centrum to abut the caudal margin with some caudal deflection.

The Ca2? and 3? of *P. dawsonae* **sp. nov.** differ from those of *P. mamkurra* **sp. nov.** and *P. viator* **sp. nov.** in

being smaller; from *C. kitcheneri* in being more elongate, with more laterally deflected prezygopophyses; from *O. rufus* in having Ca2 broader and taller relative to length; from *M. fuliginosus* in being larger, more robust and in having Ca3 slightly taller relative to length; and from *W. bicolor* in being larger, with more laterally deflected prezygopophyses.

Hindlimb

Pelvis (Fig. 95d–f): ilium robust, quite well-developed and roughly L-shaped in cross-section. Iliac crest epiphysis is not known; ilium gently increases to its maximum width at the iliac crest. Iliac fossa shallow craniomedial to the rectus tubercle, becomes shallower dorsally along the cranioventral surface of the ilium; extends around three-quarters of the length of the ilium. Gluteal fossa broad and moderately concave, particularly around the midpoint; extends to the iliac crest. Caudal iliac spine arises on the medial surface of the base of the ilium, opposite the rectus tubercule, thickens and rises rapidly, extends to the iliac crest; thick and deep ventrally for the origin of a large mm. gluteus, steadily becomes thinner and slightly shallower distally. Sacral surface large, very rugose and concave; articular surface for the wings of the sacrum deep and shelf-like with a strong cranial tilt; cranial margin of the sacral surface projects cranially in a broad, low ridge with a slight crest (cranial iliac spine) and contributes to the depth of the iliac fossa. Lateral iliac spine very broad, thin relative to the caudal spine; lateral margin slightly concave and curving laterally. Rectus tubercule quite rugose, roughly triangular, narrows strongly onto the lateral spine.

Acetabulum quite large, dorsoventrally tall and concave, taller than the craniocaudal depth, due chiefly to an enlarged caudoventral section; acetabular fossa deep, with the angle, width and curvature variable within individuals, partially covered cranially and caudally by lip projecting from the acetabular surface. Caudal surface of the dorsal section of the ischium (caudally adjacent to the acetabulum) broad and gently convex. Ischium badly crushed ventral to the acetabulum in the available specimen; craniocaudally deep and transversely compressed; caudal margin gently rugose and slightly convex from the origin of the mm. gemelli; deflected slightly caudally relative to the axis of the ilium; caudal section broadens toward the ventral margin.

The pelvis of *P. dawsonae* **sp. nov.** differs from that of *P. mamkurra* and *P. viator* in being smaller, with a smaller caudal iliac spine, shallower gluteal fossa, narrower, less rugose and less convex caudal surface of the dorsal section of the ischium (Fig. 95e), and a less deeply concave acetabulum; from *P. tumbuna* in having a more curved ilium in lateral view, less laterally projected rectus tubercle, acetabulum opening more laterally and less cranioventrally, and a more transversely compressed ischium; from *C. kitcheneri*, *O. rufus* and *M. fuliginosus* in being more robust, with a more dorsally situated sacral surface relative to the position of the acetabulum, shallower, less distally extensive iliac fossa, broader, deeper gluteal fossa, and a smaller, less projected iliopubic eminence; and from *W. bicolor* in being much larger, with the iliac crest aligned more transversely and less craniocaudally, broader, deeper gluteal fossa, narrower, less distally extensive iliac fossa, broader lateral iliac spine, particularly dorsally, caudal iliac spine lacking a small, pointed eminence on the caudoventral shoulder, and the rectus tubercle having a much smaller, shallower fossa on the lateral surface.

Pes

Calcaneus (Fig. 96): moderately sized, robust and quite low. Calcaneal tuberosity short, broad and low, broadens plantarly and caudally, increases slightly in height caudally; domed in cross-section; lateral surface becomes deeply concave plantar to the fibular facets. Caudal epiphysis broad, thickened and rugose, oval to domed in posterior view; a shallow transverse groove extends across the caudal surface. Plantar surface thickened, rugose and quite broad, tapers gently cranially in plantar view and extends cranially to level with the cranial fibular facet, with the craniomedial margin deflected laterally around the cranial plantar tubercle. Cranial plantar tubercle generally small, rounded to oval, abuts or is caudally adjacent to the plantar margin of the plantomedial facet for the cuboid.

The calcaneal head is large and broad, with a very slight medial rotation in dorsal view. Sustentaculum tali large, medially projected beyond the margin of the medial talar facet, not extensive caudally, caudal margin is rounded with a flat cranioplantar margin; flexor groove quite deep and broad. Medial talar facet slightly caudally displaced relative to lateral talar facet, broad and oval, craniocaudally compressed, slightly projected dorsally, tilted strongly cranially in medial view; caudal margin with a distinct rounded lip, particularly over the lateral part. A small, variable ridge extends caudally from the caudolateral margin of the medial talar facet, tapers and lowers caudally; occasionally present only as a slight swelling. Lateral talar facet broad, craniocaudally short, smoothly convex, roughly semicylindrical and tapering from the lateral margin to the midpoint. Fibular facets large relative to the lateral talar facet, bulbous and projected laterally; cranial component low, elongate, more laterally projected than the caudal component of the facet, and tilted cranially in lateral view; caudal component roughly rounded, gently convex, and facing caudally, with distinct plantar and medial margins.

Facet for the talar head small; abuts the medial margin of the dorsomedial cuboid facet on the medial surface of the calcaneal head. Dorsomedial cuboid facet roughly oval in cranial view, gently convex, slightly broader than the dorsolateral facet, from which it is separated by a tall, quite bevelled step. Dorsolateral cuboid facet tall, cranially projected, very slightly concave and tilted plantarly and slightly medially, curves plantomedially to be continuous with the plantomedial facet. Plantomedial cuboid facet much smaller than the dorsal facets, dorsoplantarly compressed and broad, occasionally rounded. A shallow, oblong fossa is present between the dorsomedial and plantomedial cuboid facets.

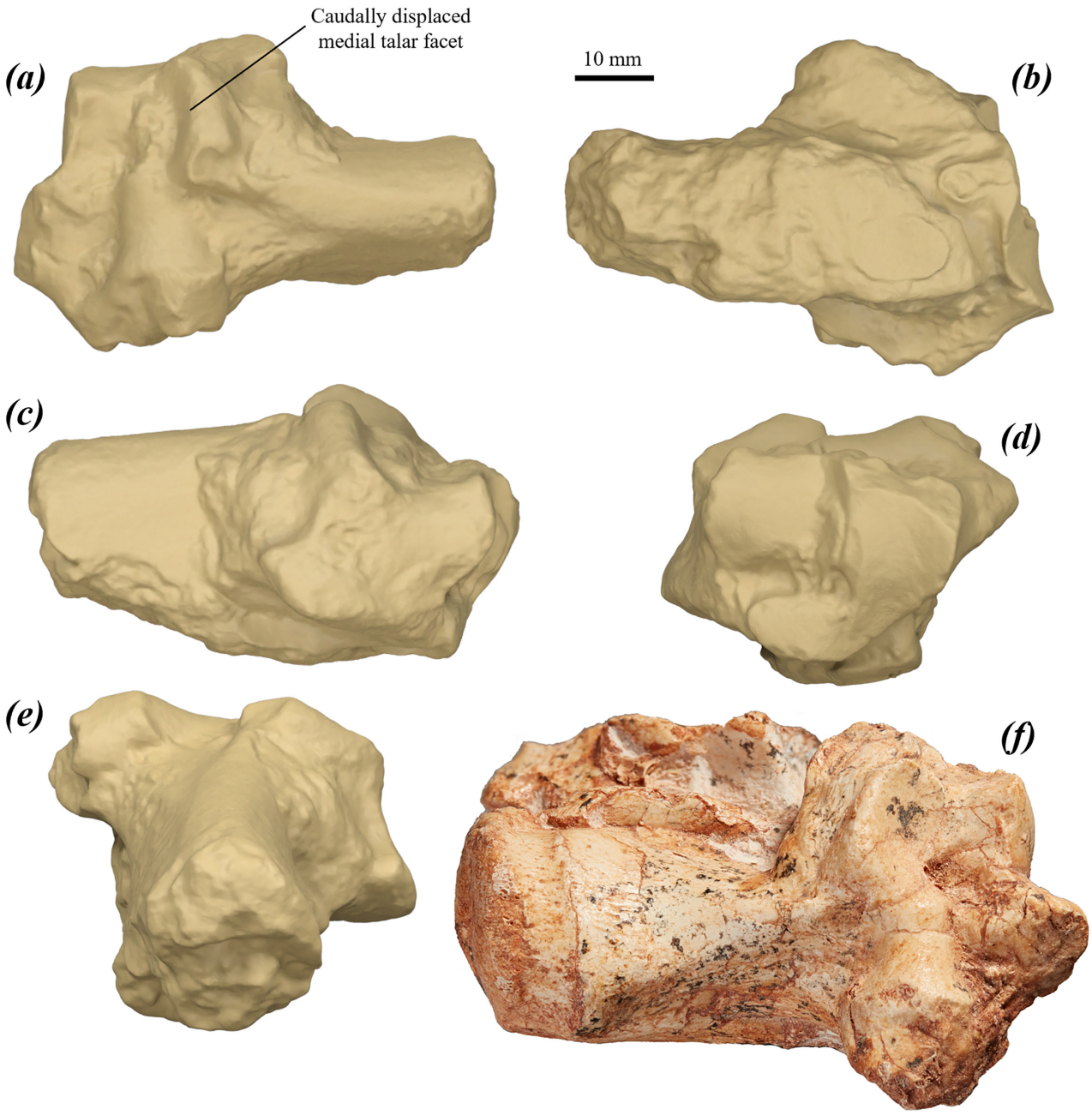

FIGURE 96. partial calcanei of *P. dawsonae* **sp. nov.**: (a–e) surface scan images of partial left calcaneus AM F106042 in (a) dorsal, (b) plantar, (c) medial, (d) cranial, and (e) caudodorsal views; and (f) right calcaneus AM F161913 in dorsal view. AM F161913 is dorsoplantarly crushed, the tuberosity is warped medially, and it remains partially embedded in matrix and bone fragments, visible on the medial margin of the tuberosity.

The calcaneus of *P. dawsonae* **sp. nov.** differs from that of *P. anak* in being dorsoplantarly shorter, with a narrower plantar surface, slightly shallower lateral talar facet, less rounded, less distinct caudal fibular facet, and a shallower flexor groove; from *P. mamkurra* **sp. nov.** in being smaller, lower and narrower, with a more caudally displaced medial talar facet, less bulbous lateral talar and caudal fibular facets, fibular facets less plantarly extensive laterally, and a more rounded sustentaculum tali; from *P. viator* **sp. nov.** in being smaller, lower and broader, with a more rounded, less dorsally pointed calcaneal tuberosity in cross-section, craniocaudally shorter lateral talar facet, broader, more transversely aligned medial talar facet, and more medially projected sustentaculum tali; from *P. tumbuna* in having the head less medially displaced, a flatter, less convex plantar surface, and less medial flaring of the caudoplantar margin of the calcaneal tuberosity; from *P. otibandus* in having the head less medially displaced, with a narrower calcaneal tuberosity; from *C. kitcheneri* in being larger and relatively taller, with a less concave, less medially tilted plantar surface; from *O. rufus* in being broader and relatively lower, with a less

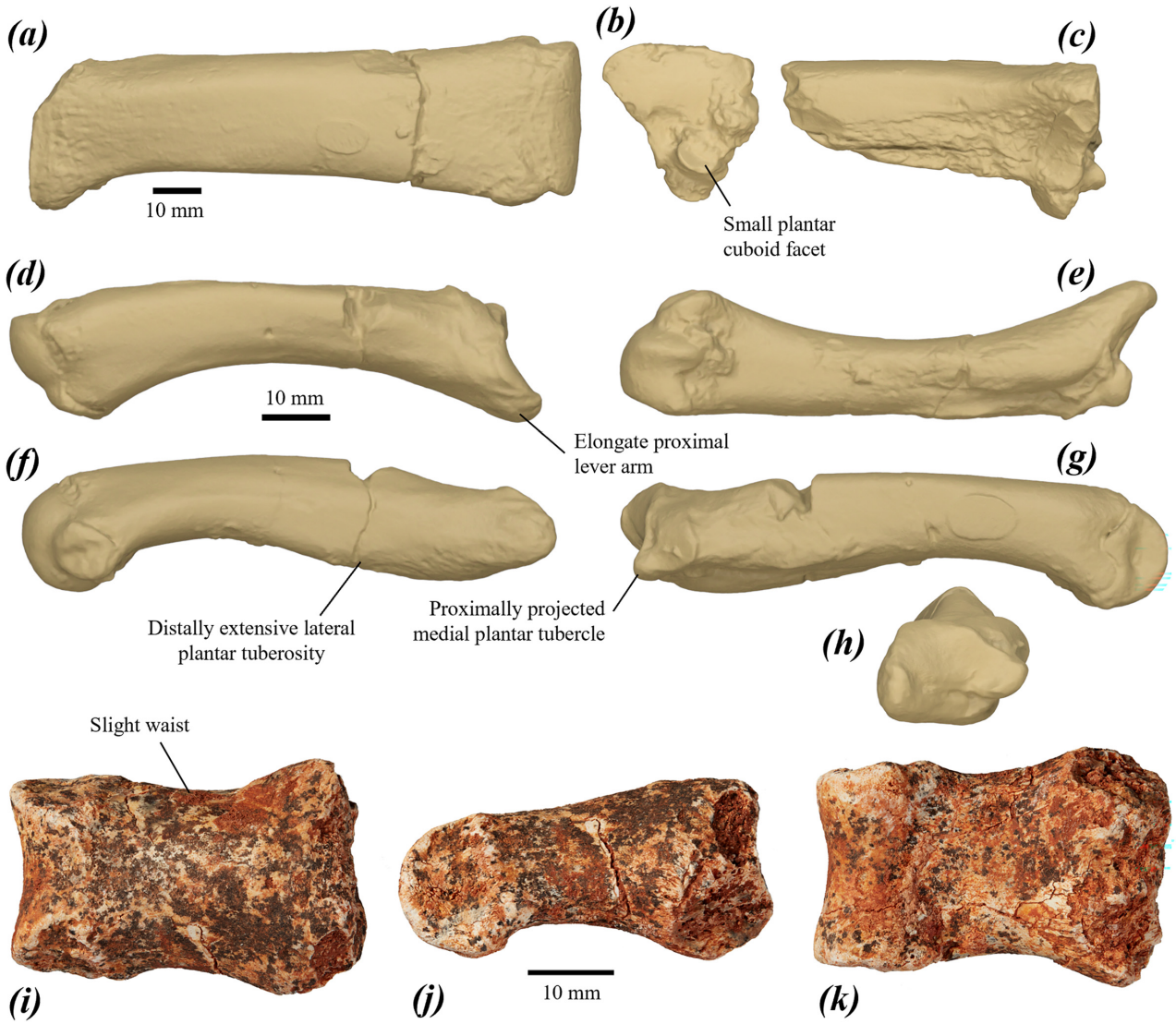

FIGURE 97. pedal elements of *P. dawsonae* **sp. nov.**: (a) surface scan image of partial right metatarsal IV AM F106039 in dorsal view; (b–c) surface scan images of partial left metatarsal IV of AM F106041 in (b) proximal, and (c) lateral views; (d–h) surface scan images of left metatarsal V of AM F106040 in (d) dorsal, (e) plantar, (f) lateral, (g) medial, and (h) proximal views; and (i–k) partial right proximal pedal phalanx IV of AM F161916 in (i) dorsal, (j) medial, and (k) plantar views.

elongate tuberosity, no caudomedial facet for the posterior plantar process of the talus, less cranially tilted medial talar facet, shallower fossa cranial to the lateral talar facet, relatively narrower dorsolateral cuboid facet, more bevelled step between the dorsal cuboid facets, more medially projected sustentaculum tali, and a deeper flexor groove; from *M. fuliginosus* in being larger, broader and relatively lower, with a less elongate tuberosity, shallower fossa cranial to the lateral talar facet, relatively narrower dorsolateral cuboid facet, more bevelled step between the dorsal cuboid facets, more medially projected sustentaculum tali, and a deeper flexor groove; and from *W. bicolor* in being larger, relatively broader and more robust, with broader medial talar facet and more medially projected sustentaculum tali.

Metatarsal IV (Fig. 97a–c): large, long and quite robust. Dorsal cuboid facet very similar to that of *P. mamkurra* **sp. nov.**; proximal cuboid fossa small, shallow and plantolaterally situated; plantar cuboid facet quite small, round, very gently concave and tilted distinctly dorsally and slightly medially, extends plantarly partially onto proximal surface of deep, plantarly projected plantar tubercle. Proximal plantar sesamoid facet quite large, broad, flat, round to oval, faces distoplantarly and is tilted laterally. Articular surface for metatarsal III indistinct, situated in an elongate, shallow, rugose metatarsal III fossa on the medial surface of the proximal end, bordered dorsally by an indistinct, low ridge extending plantodistally from the dorsomedial corner of the dorsal cuboid facet. Dorsal facet for the ectocuneiform small and tapering plantarly, facing proximomedially, adjacent to the dorsal section of medial margin of dorsal cuboid facet; small facet for the plantolateral component of ectocuneiform situated on the proximomedial surface of the plantar

tubercle, semicontinuous with the plantar cuboid facet. Facet for metatarsal V large, concave, slightly cranially tilted, moderately tall and proximodistally short; shape variable but generally oblong with rounded dorsal and plantar parts; extends plantarly onto the base of the lateral surface of the plantar tubercle.

Plantar ridge quite broad, rugose, squarish to rounded in cross-section, extends distally with a very slight lateral deflection from the base of the plantar tubercle, merges into the plantar surface of the shaft before the midpoint; bordered medially by the fossa for metatarsal III and laterally by the fossa for metatarsal V. Shaft morphology very similar to that of *P. mamkurra* **sp. nov.** Distal end broad; fossae for the collateral ligaments circular and quite deep; keel slightly more plantarly projected than the lateral and medial crests.

The metatarsal IV of *P. dawsonae* **sp. nov.** does not differ from those of *P. anak* and *P. mamkurra* **sp. nov.** It differs from that of *P. viator* **sp. nov.** in being larger, with a relatively broader proximal plantar sesamoid facet and a larger plantar facet for the ectocuneiform; from *P. tumbuna* in being larger; from *P. otibandus* in being larger, with continuous dorsal and plantar cuboid facets, a more concave, less laterally projected metatarsal V facet, larger plantar tubercle, more raised plantar ridge, and a relatively more plantarly projected keel; from *P. snewini* in being larger, with a smaller, more plantolaterally situated cuboid fossa; from *C. kitcheneri* in being larger and broader, with a larger, more plantarly projected proximal plantar tubercle and a more raised plantar ridge; from *O. rufus* and *M. fuliginosus* in being shorter, much broader and more robust, with a larger facet for metatarsal V, the shaft more dorsoplantarly compressed and broadening more to the distal end, a less plantarly projected proximoplantar ridge, and a broader, more planar proximal dorsal surface; and from *W. bicolor* in being much larger, relatively broader and more robust, with a relatively slightly larger proximal plantar tubercle.

Metatarsal V (Fig. 97d–h): quite elongate and gently transversely compressed proximally, with a distinct lateral curve to the distal component in dorsal view accentuated by the lateral expansion of the distal end. Proximolateral process blunt, thick and rugose. Cuboid facet broad, broader than the facet for metatarsal IV, concave, particularly medially, extends across the medial surface of the proximolateral process onto the lateral base of the medial plantar tubercle; dorsolateral margin raised to slight lip over dorsomedial surface of proximolateral process. Facet for metatarsal IV proximodistally deep but tapering laterally, and gently convex; extends from the dorsal surface of the shaft onto the medial plantar tubercle. Lateral plantar tuberosity large, broad, rugose and quite raised, merges with the shaft just past the midpoint; separated from the medial plantar tubercle by a broad, shallow plantar groove curving distally along the medial margin. Medial plantar tubercle small, distinct, rounded, and proximomedially projected. Shaft gently and smoothly arched in lateral view with the highest point around the midpoint. Distal end broad, laterally flared and slightly laterally deflected at base. Distal articular surface very similar to that of *P. mamkurra* **sp. nov.** Fossae for collateral ligaments large, rounded and quite deep.

The metatarsal V of *P. dawsonae* **sp. nov.** differs from that of *P. anak* in having less raised lateral plantar tuberosity, less tall proximolateral process and broader cuboid facet; from *P. mamkurra* **sp. nov.** in having a narrower cuboid facet and a more distally extensive lateral plantar tuberosity; from *P. viator* **sp. nov.** in being longer and slightly less transversely compressed, with a lower, more elongate proximolateral process, narrower cuboid facet, more proximally projected medial plantar tubercle, and a less raised lateral plantar tuberosity; from *P. tumbuna* in being larger and more elongate, with a longer, narrower proximolateral process, larger medial plantar tubercle, and a narrower cuboid facet; from *P. otibandus* in being more elongate, with a narrower, less dorsally projected cuboid facet and a slightly narrower distal end; from *C. kitcheneri* in being larger, broader and more robust, lacking the slight kink of the arch of the shaft immediately proximal to the midpoint in lateral view, with a larger medial plantar tubercle, more medially situated facet for metatarsal IV, and a more raised lateral plantar tuberosity; from *O. rufus* and *M. fuliginosus* in being far shorter and broader, less arched and much less transversely compressed, with a longer proximolateral process and a larger medial plantar tubercle; and from *W. bicolor* in being larger, relatively broader and more robust, with a larger proximolateral process and a more concave cuboid facet.

Proximal pedal phalanx IV (Fig. 97i–k): fairly short, robust, and dorsoplantarly compressed. Proximal articular surface mostly abraded in available specimen, appears domed and gently concave. Proximal plantar tubercles partially abraded, appear low and rugose, separated by a shallow valley. Shaft narrows slightly to a waist, broadens very slightly to the distal end. Distal articular surface proximodorsally quite extensive; trochlea broad and quite shallow. Fossae for the collateral ligaments shallow and semicircular.

The proximal phalanx IV of *P. dawsonae* **sp. nov.** differs from those of *O. rufus* and all compared species of *Protemnodon* except *P. viator* **sp. nov.** in having a more proximodorsally extensive distal articular surface. It further differs from *P. anak* in being shorter and more robust, with less projected plantar tubercles, a slightly broader waist, and a less dorsoplantarly compressed shaft; from *P. mamkurra* **sp. nov.** in being shorter, with a slightly broader waist, and a slightly narrower distal end; from *P. viator* **sp. nov.** in being more robust, with a broader waist and a narrower distal end; from *P. otibandus* in being more elongate; from *C. kitcheneri* in being much broader and more robust, and lacking a small fossa immediately proximal to the dorsal margin of the distal articular surface; from *O. rufus* in being slightly shorter, much broader and more robust, with a broader waist and a less dorsoplantarly compressed distal shaft; from *M. fuliginosus* in being larger, far broader and more robust; and from *W. bicolor* in being larger, relatively broader and more robust.

Remarks:
For discussion of the taxon *Protemnodon devisi* Bartholomai, 1973 and its relationship to *P. dawsonae* **sp. nov.**, see the segment below titled, 'Status of other species previously referred to *Protemnodon*'.

The material from Big Sink LF provides evidence for only one species of *Protemnodon* (Dawson *et al.* 1999), all of which is allocated here to *P. dawsonae* **sp. nov.** These fossils are of a large kangaroo, similar in size to *P. anak*, separated from all other species of *Protemnodon* by its upper molars with a kinked postparacrista and from other Pliocene species by its large, robust i1 with a low, thick ventrolingual crest. Craniodental fossils from Stirton Quarry, Lake Kanunka, and Sand Scree Locality, Chinchilla that match this morphotype are also allocated to *P. dawsonae* **sp. nov.** As the m4 from Site 4, Lake Kanunka, falls within the dental dimensions of and is most similar in morphology to *P. dawsonae* **sp. nov.**, and as it was found in association with the partial pelvis, we allocate both to that species, albeit with less confidence than the other referred specimens.

Protemnodon otibandus Plane, 1967

Protemnodon otibandus Plane, 1967: *Bull. Bur. Min. Res., Geo. & Geophys., Aus.*, 86, pp. 26–44, figs 5–10. See also: Mahoney& Ride (1975), p. 23.

Protemnodon chinchillaensis Bartholomai, 1973: *Mem. Qld. Mus.*, 16, pp. 347–354, pl. 20, 21, 23. See also Flannery & Archer (1984), pp. 375–376, figs A & B.

Protemnodon anak Owen; De Vis (1895) (*partim*), pp. 104–109. Not *P. anak*, Owen, 1874.

Protemnodon devisi Bartholomai: Tedford *et al.* (1992), p. 187. Not *P. devisi*, Bartholomai, 1973.

Protemnodon Owen sp. indet.; Tedford *et al.* (1992), pp. 186–187.

Holotype:
CPC 6771: near-complete R dentary preserving i1 & p3–m4; posteromedial fracture along margin of pterygoid fossa with pterygoid process not preserved. Figured Plane (1967), figs 5 & 6.

Reassociated here are the holotype, CPC 6771, and specimen UCMP 69895, a semi-complete L dentary preserving the base of the i1 and p3–m4, based on extreme similarity in dimensions, degree of molar wear, morphology, shape of mandibular symphyseal plates and preservation. UCMP 69895 was collected by the same expedition from the same locality as the holotype.

Type locality:
'Watut 1', UCMP V6234, west bank of Upper Watut River (7°13' S, 146°32' E), Otibanda Fm., Morobe Province, Papua New Guinea. The type section contains fossiliferous sandstone and mudstone with conglomerate and intercalated pyroclastic rocks. Potassium–Argon dating of a pyroclastic rock sample, taken from an outcrop of the Otibanda Fm. approximately 250 m downstream from the type locality, gave an age of 2.9 ± 0.4 Ma (Hoch & Holm 1986), placing it in the late Pliocene.

Paratype(s):
Premaxilla fragments: UCMP 69832. Partial maxilla: UCMP 69851–69854, UCMP 69857. I1: UCMP 69790–69800, UCMP 69877, UCMP 69859. I2: UCMP 63631, UCMP 69803, UCMP 69804, UCMP 69806, UCMP 69825, UCMP 69826. I3: UCMP 69827–69831. DP2: UCMP 69833. P3: UCMP 69834–69839, UCMP 69863, UCMP 69864. M1: UCMP 69840–69842. M3: UCMP 69843, UCMP 69844. M4: UCMP 69847–69849. Dentary fragments: UCMP 69896, UCMP 69897, UCMP 69981, UCMP 69986, UCMP 69987, UCMP 69991, UCMP 69899, UCMP 69900. Juvenile dentary: CPC 6772. i1: UCMP 69860, UCMP 69871–69878. p3: UCMP 69861, UCMP 69863, UCMP 69864, UCMP 69879. m1: UCMP 69865. m3: UCMP 69870. m4: UCMP 69898.

Referred specimens:

Papua New Guinea

Site 2, Watut River: UCMP 45345 vertebral fragment, R calcaneus, talar fragment, metatarsals IV and V, distal pedal phalanx IV, and proximal & middle pedal phalanges V.

Sunshine 3, Watut River: UCMP 71414 partial R talus and metatarsal IV, partial LR metatarsals V and proximal pedal phalanges IV, and middle pedal phalanx IV.

Sunshine General, Watut River: UCMP 45344 LR femoral fragments.

Watut 1, Watut River: UCMP 70036 R i1; UCMP 70045 clavicle; UCMP 70059 partial R humerus, ulna, radius and articulated manus; UCMP 70054 partial R radius; UCMP 70065 partial L femur; UCMP 70066 partial L femur; UCMP 70038, 70039, 70584 and 70585 femoral fragments, partial LR tibiae, L and partial R calcaneus, L cuboid, LR metatarsals IV and V, and proximal and distal pedal phalanges IV; UCMP 70078 L cuboid; UCMP 70006 partial R metatarsal IV; UCMP 70007 partial R metatarsal IV.

Woodard 2, Watut River: UCMP 45246 partial juvenile R premaxilla, partial L maxilla, partial R maxilla, R P3, and partial mandible; UCMP 45248 partial R maxilla; UCMP 45250 R talus; UCMP 45253 L cuboid.

Woodard 3/Site 3, Watut River: UCMP 45247 L calcaneus, R talus, articulated R cuboid, ectocuneiform and metatarsals II, III and IV, R metatarsal V, proximal, middle and distal pedal phalanges IV, and middle and distal pedal phalanges V.

Woodard 4, Watut River: UCMP 45244 partial premaxilla, maxillae and L dentary, and tibial fragments.

Northwest bank of Kikori River, Gulf Province: AM F134486 pelvic fragment with acetabulum.

South Australia

Stirton Quarry (V5772), Lake Kanunka: UCMP 56894 L dentary; UCMP 156893 R calcaneus.

Site 6 (27° 51.327' S, 137° 53.385' E), Toolapinna Waterhole, Warburton River: SAMA P50566 R dentary.

Toolapinna Waterhole, Warburton River: SAMA P25504 partial L maxilla.
Lawson–Daily Quarry, Lake Palankarinna: UCMP 57195 L tibia.

Queensland
Chinchilla, Darling Downs (site unknown): QM F4719 L maxilla; QM F5239 partial juvenile L maxilla; QM F5246 partial R dentary.

New South Wales
Bow LF, Hunter Valley: AM F59530 partial L maxilla; AM F59533 partial L maxilla.

Victoria
Nowa Nowa Arm, Lake Tyers: NMV P26893 partial R maxilla.

Revised specific diagnosis:
Protemnodon otibandus is distinguished from all other species of *Protemnodon* by one unique skeletal characteristic and by a combination of other dental and skeletal characteristics. The pes of *P. otibandus* differs from all other species of *Protemnodon* in having a calcaneus with a slightly medially offset head relative to the calcaneal tuberosity. In *P. tumbuna* this condition is more extreme, with the head more strongly medially displaced; in all other species of *Protemnodon* the head of the calcaneus is not medially displaced.

Protemnodon otibandus is most similar in dentary morphology to *P. anak*, *P. dawsonae* **sp. nov.** and *P. tumbuna*. It differs from that of *P. anak* and *P. dawsonae* **sp. nov.** in its less robust anterior dentary, particularly around the i1. It differs further from *P. anak* in its more dorsally deflected diastema; and from *P. tumbuna* in having a more anterodorsally situated mental foramen.

Protemnodon otibandus is most similar in dental morphology to *P. snewini* and *P. tumbuna*. The dentition differs from *P. snewini* in having: P3 with a broader posterior relative to the anterior cusp and a higher lingual crest; relatively broader upper molars with a less anteriorly prominent precingulum, a more raised, more distinct postparacrista, and a urocrista; and more robust, less lanceolate i1. The dentition differs from that of *P. tumbuna* in having: P3 with more raised, more distinct buccal ridgelets; less rounded molars; and i1 with a thinner, more raised ventrolingual crest.

Protemnodon otibandus is most similar in aspects of skeletal morphology to *P. tumbuna* and *P. snewini*. The hindlimb differs from *P. tumbuna* in having: a femur with a less elongate and more proximally situated quadratus tubercle; and a narrower tibia with a thinner, more raised proximolateral crest and a less distally extensive cnemial crest with a more defined peak. The pes further differs from that of *P. tumbuna* in having: a calcaneus with a more planar plantar surface with less flaring of the medial margin and a smaller, shallower fossa cranial to the lateral talar facet; and more transversely compressed metatarsal V with dorsoplantarly shorter proximolateral process, longer metatarsal IV facet and larger medial plantar tubercle. The hindlimb differs from that of *P. snewini* in having a tibia with a larger, broader proximal fibular facet. The pes differs from that of *P. snewini* in having: talus with a deeper trochlea and a deeper concavity between the posterior plantar tubercle and the talar head; cuboid with a less dorsomedially flared dorsomedial section, a much smaller talar facet, and a larger, more plantomedially projected medial plantar tubercle; metatarsal IV with a dorsoplantarly shorter, more plantarly situated proximal cuboid fossa; and distal phalanx IV with a more rounded dorsal peak.

Etymology:
In reference to the geological formation of the type locality, the Otibanda Formation.

Description and comparisons:
For craniodental description, see the original description by Plane (1967, pp. 28–39). For comparative purposes, the cranium, dentary and dentition are figured below (Figs 98 & 99).

Pectoral girdle and forelimb
Clavicle (Fig. 100a–c): craniocaudally compressed in the middle section and at the acromial articular end, becomes rounded in cross-section toward the sternal articular end; curves gently posteriorly towards both ends in caudal view, to be gently convex anteriorly; steadily increases in depth medially to the slightly thickened, smoothly ventrally curved acromial articular end, and forms a blunted point. Sternal articular end thickened, rounded in medial view; epiphysis not preserved, but the medial surface has a convex posterior part and a small, deep fossa in its centre.

The clavicle of *P. otibandus* differs from that of all compared species in being more craniocaudally compressed. It further differs from that of *P. mamkurra* **sp. nov.** in being slightly less robust, with a relatively slightly smaller acromial articular end; from *C. kitcheneri* in being more curved, with a relatively larger acromial articular end; from *O. rufus* and *M. fuliginosus* in having a slightly more caudally curved and less posteriorly curved acromial end, and a much less anteroposteriorly concave sternal articular surface; and from *W. bicolor* in being larger and deeper, with a more ventrally curved acromial end with a more pointed tip, and the sternal end not strongly anteroposteriorly compressed.

Humerus (Fig. 100d–e): only one distal fragment known; distal end broad. Lateral supracondylar ridge quite thick and convex cranially at distal end; lateral epicondyle not preserved. Capitulum and ulnar facet broad, weakly projected and laterally situated, close to the lateral epicondyle; combined width is roughly three-quarters of the epicondylar width; capitulum smoothly convex; ulnar facet with the medial margin relatively straight and unbevelled; trochlea wide and quite shallow. Olecranon fossa broad and deep; radial fossa quite large and deep compared to the coronoid fossa; coronoid fossa partially preserved, appears shallow, broad and proximodistally short. Medial supracondylar bridge partially preserved,

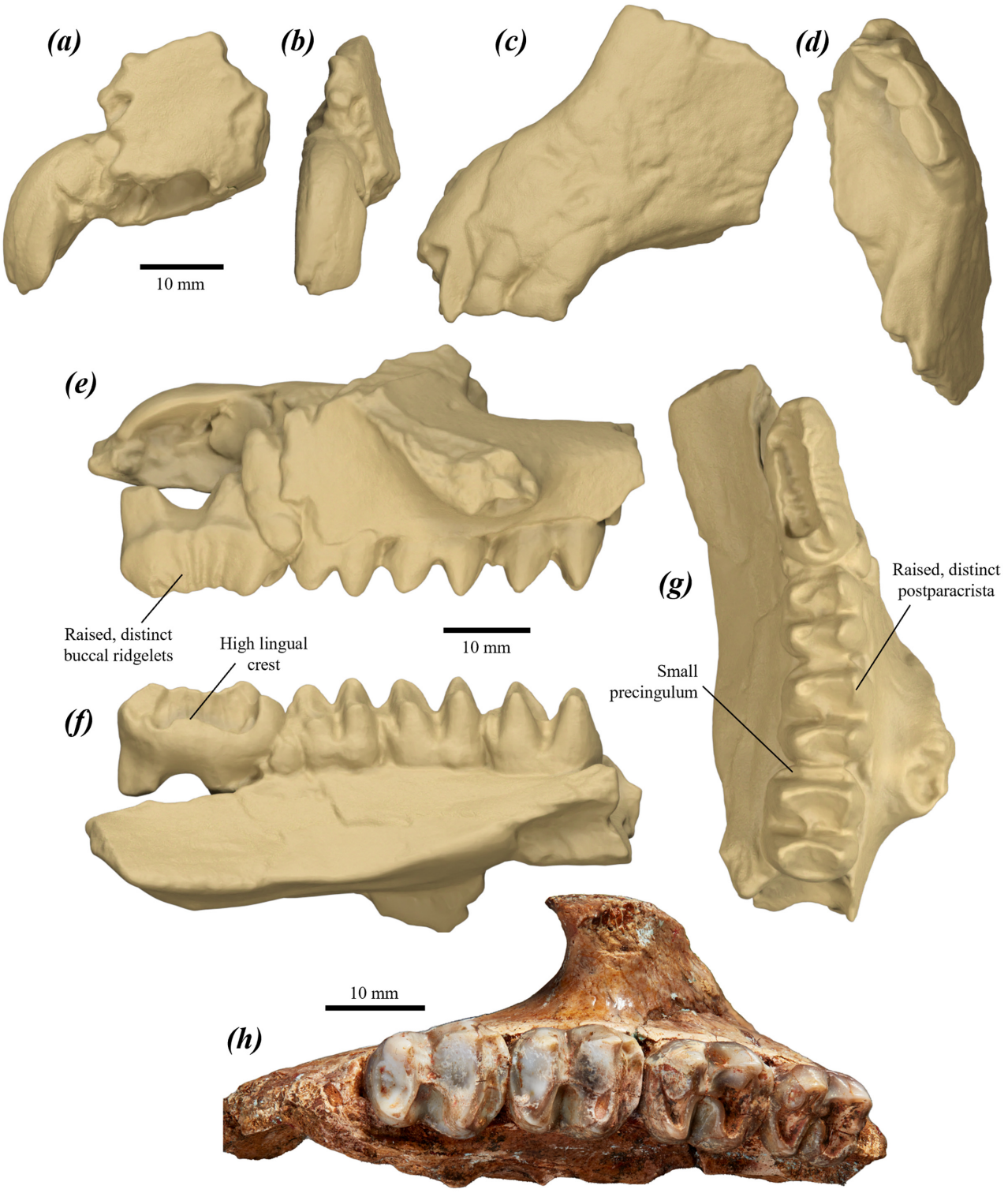

FIGURE 98. upper dentition of *P. otibandus*: (a–b) surface scan images of left I1 of UCMP 45246 in (a) lateral/buccal, and (b) anterior views; (c–d) surface scan images of left premaxilla fragment with partial I1 and I2–3 of paratype UCMP 69832 in (c) lateral/buccal, and (d) occlusal views; (e–g) surface scan images of partial left maxilla with P3–M3 of paratype UCMP 69857 in (e) buccal, (f) lingual, and (g) occlusal views; and (h) partial right maxilla of NMV P22650 from Jemmy's Point, Lake Tyers, in occlusal view.

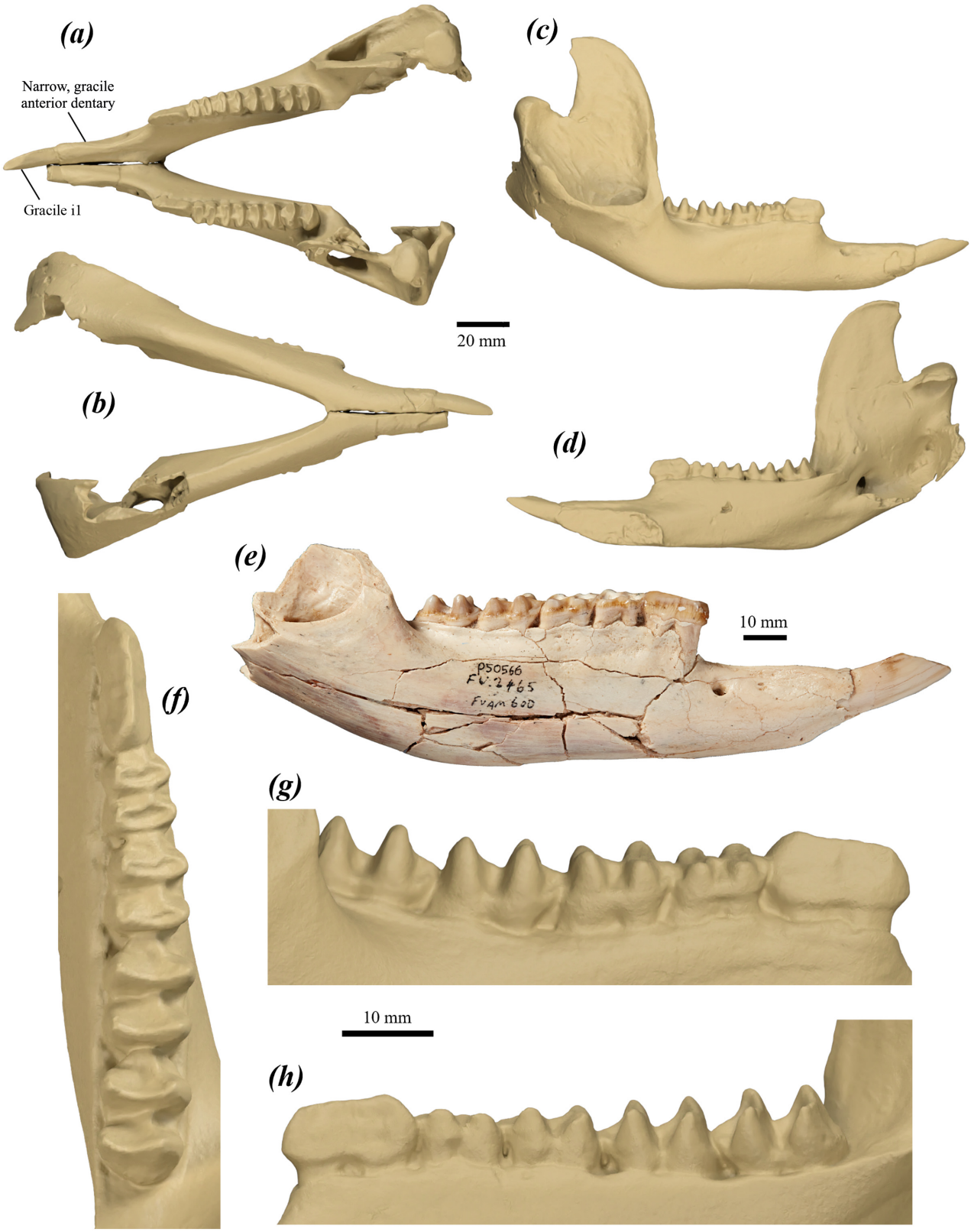

FIGURE 99. dentaries and lower dentition of *P. otibandus*: (a–b) surface scan images of re-articulated right dentary of holotype CPC 6771 and left dentary of UCMP 69895 in (a) occlusal, and (b) ventral views; (c–d) surface scan images of right dentary of CPC 6771 in (c) buccal, and (d) lingual views; (e) partial right dentary of SAMA P50566 from Toolapinna Waterhole, Lake Eyre Basin, in buccal view; and (f–h) surface scan images of right p3–m4 of CPC 6771 in (f) occlusal, (g) buccal, and (h) lingual views.

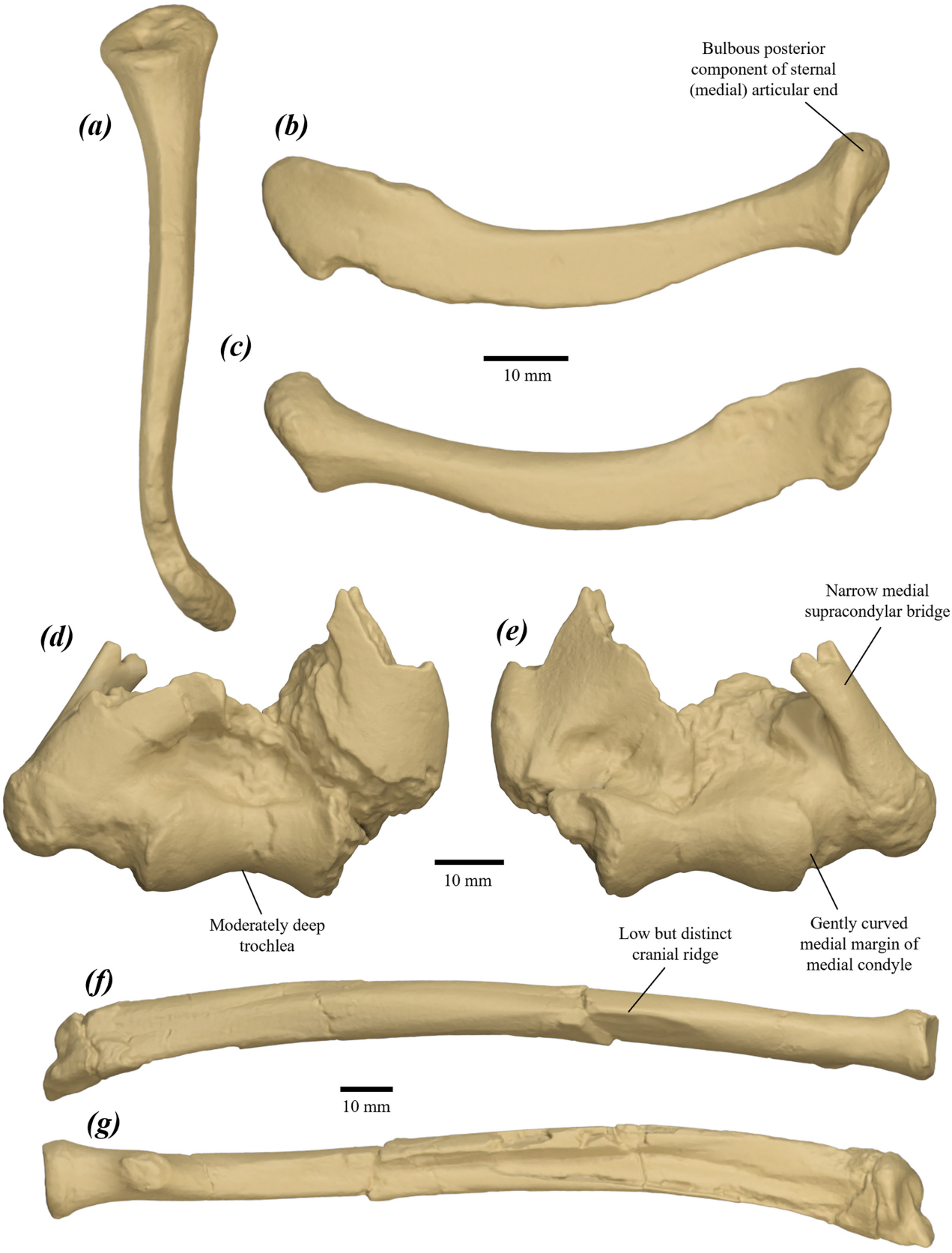

FIGURE 100. surface scan images of right upper forelimb elements of *P. otibandus*: (a–c) clavicle of UCMP 70045 in (a) anterior, (b) dorsal, and (c) ventral views; (d–e) distal humeral fragment of UCMP 70059 in (d) caudal, and (e) cranial views; and (f–g) radius of UCMP 70059 in (f) cranial, and (g) caudal views.

appears broad, and thin craniocaudally; supracondylar foramen appears large and quite flattened craniocaudally. Medial epicondyle large, rounded, rugose and very slightly distally projected.

The humerus of *P. otibandus* does not differ from that of *P. tumbuna*. It differs from *P. anak* in being smaller, with a smaller capitulum and ulnar facet, a narrower medial supracondylar bridge, shallower trochlea, and a more curved, less distinct and less distally projected medial margin of the ulnar facet; from *P. mamkurra* **sp. nov.** and *P. viator* **sp. nov.** in being smaller, with a less projected capitulum and ulnar facet, and less bevelled medial margin of the ulnar facet; from *C. kitcheneri* in having a broader medial supracondylar bridge; from *O. rufus* in having a broader distal end, broader distal part of the lateral supracondylar ridge, and a relatively larger ulnar facet; from *M. fuliginosus* and *W. bicolor* in having a broader distal end, broader distal part of the lateral supracondylar ridge, and a shallower trochlea; and additionally differs from *W. bicolor* in being larger.

Ulna (Fig. 101a–i): moderately large, deep, transversely compressed, curved cranially in lateral view and gently medially curved in cranial view. Olecranon quite elongate, transversely compressed and tapers in height to a blunt, slightly caudally deflected in lateral view, with a squared distal end. Proximal section of the lateral surface of the ulna is flat; proximomedial flexor fossa smoothly, deeply concave. Facet for the humeral articulation is quite broad, with no visible trochlear notch; medial part deeply concave, more elongate and situated more cranially than the lateral part; lateral part relatively shallow, smoothly concave and tilted and projected laterally, with the lateral margin abraded in the sole known specimen; anconeal process low relative to the coronoid process, with an obtuse, slightly rounded mesial angle; coronoid process tall, quite narrow, and smoothly rounded in posterior view; merges gently into the shaft distally (Fig. 101a). Radial facet mostly abraded, but appears roughly semicircular and abuts the lateral three-quarters of the anterior margin of the lateral part of anconeal facet. Ulnar tuberosity low, narrow, quite elongate, slightly thickened and rugose. Proximal part of the shaft is slightly crushed; interpreted as having been transversely compressed and deep; caudal margin straight beneath the olecranon and the humeral facet, curves gently cranially past the humeral facet, and straightens distally; midpoint of the cranial surface of the shaft has thin ridge tilted laterally. Distal end has a cone-shaped base, smoothly narrows to a projected, globular styloid process.

The ulna of *P. otibandus* does not differ from that of *P. tumbuna*. It differs from *P. anak* in being smaller and lacking a large caudomedial eminence on the olecranon, with a less deep proximal shaft and a more concave medial surface beneath the humeral facet; from *P. mamkurra* **sp. nov.** in being more gracile and more transversely compressed, with a relatively longer olecranon; from *P. viator* **sp. nov.** in being generally smaller, deeper and more dorsoventrally compressed, with relatively longer olecranon, more deeply concave humeral facet, narrower coronoid process with a gentler slope anteriorly into the shaft (rather than meeting the shaft at almost a right angle), and a shallower proximomedial flexor fossa; from *C. kitcheneri* in being generally larger, and deeper and more transversely compressed proximally, with a less cranially deflected olecranon, taller, less medially flared coronoid process, and a lower, more proximally situated cranial ridge on the shaft; from *O. rufus* in being more robust, and deeper and more transversely compressed proximally, with a less cranially deflected olecranon, less medially flared anconeal process, and a taller coronoid process; from *M. fuliginosus* in being larger and more robust, and deeper and more transversely compressed proximally, with a less tall olecranon, less medially flared anconeal process, and a taller coronoid process; and from *W. bicolor* in being larger, with a relatively longer, cranially undeflected and unprojected olecranon, lower, narrower anconeal process, and a lower, less medially flared coronoid process.

Radius (Fig. 100f–g): elongate, with a gently arched shaft curving mediocaudally past the radial tubercle. Radial head broad, oval and smoothly concave. Radial neck narrows to the radial tubercule. Radial tubercule rugose, oval and smoothly projected. Shaft cross-section oval immediately distal to the radial tubercle, quickly transitions to strongly craniomedially-caudolaterally compressed by the midpoint; gently broadens distally. Cranial ridge short, quite thin and located immediately proximal to the midpoint of the shaft; caudal ridge relatively thinner and more raised on the caudomedial to caudal surface. Distal end large and craniocaudally compressed with a small tubercle on the cranial surface; scaphoidal facet broad, slightly caudally tilted and gently concave, located caudal to a low, shallow fossa across the cranial section; styloid process broad, craniocaudally compressed and tapering to a rounded tip. Ulnar notch broad, very shallowly concave and elongate, slowly tapers proximally along the caudolateral surface.

The radius of *P. otibandus* cannot be not differentiated from that of *P. tumbuna*. It differs from *P. anak* in being generally smaller, with the distal end more craniocaudally compressed; from *P. mamkurra* **sp. nov.** in having a less raised cranial ridge and a shallower proximal shaft; from *P. viator* in being shorter, with a more raised caudal ridge and a less proximally situated cranial ridge; from *C. kitcheneri* in having a more raised cranial ridge, less elongate caudal ridge, and a caudally (rather than cranially) tilted scaphoidal facet; from *O. rufus* in being more robust, with a larger radial tubercle, and more raised caudal ridge; from *M. fuliginosus* in being more robust, with a relatively larger proximal epiphysis and a more raised caudal ridge; and from *W. bicolor* in being larger.

Manus

Scaphoid (Fig. 101e–g, i): broad, roughly semicircular in dorsal view with a broadly convex proximal surface; dorsopalmarly shortens medial to the midpoint. Radial facet broad and strongly, smoothly convex, extends from posteriorly adjacent to the triquetral facet, across the posterior surface, to the posterior margin of the palmar process; becomes gently concave medially due to a low, rounded eminence on the medial margin and a broad,

raised, anteroposteriorly short crest located slightly medial of the centre of the dorsal surface, for articulation with the styloid process of radius. Palmar process broad, tapers in dorsal view to a rounded tip, slightly anteroposteriorly compressed and curves distinctly palmarly toward the tip. Facet for the hamatum large, covers anterolateral surface. Facet for the capitatum slightly broader than the hamatal facet; covers the centre of the anterior surface. Facet for the trapezoid palmarly convex and dorsally concave beneath anterior of dorsal crest, abuts capitatum facet on anterodorsal surface of palmar process. Facet for the trapezium tall, rounded and convex, wraps around the anteromedial surface of the palmar process.

The scaphoid of *P. otibandus* differs from that of *P. mamkurra* **sp. nov.** in having a slightly more palmarly curved and anteriorly deflected palmar process, with a shallower fossa on the medial part of the palmar surface; from *P. viator* **sp. nov.** in being smaller, with a raised dorsal ridge, a taller, more convex radial facet, larger medial eminence, and a less dorsopalmarly compressed palmar process; from *C. kitcheneri* in being broader, with a raised dorsal ridge and a broader, more anteropalmarly deflected palmar process; from *O. rufus* in being broader, with a larger palmomedial fossa and a more dorsopalmarly compressed palmar process; from *M. fuliginosus* in being relatively broader, with a broader, more smoothly convex radial facet and a less deep, more palmarly curved palmar process; and from *W. bicolor* in being much larger, with a low, rounded eminence present on the medial margin of the radial facet.

Pisiform (Fig. 101e–i): quite elongate and distinctly dorsopalmarly flattened; large, squared proximal end constricts to a narrow waist and flares anteroposteriorly to the thickened, rounded distal end. The posteromedial facet for the styloid process of the ulna is small, located on the posteromedial margin.

The pisiform of *P. otibandus* differs from that of *P. viator* in being smaller, with a more dorsopalmarly compressed proximal end and a much smaller proximal ulnar facet; from *C. kitcheneri* in being larger relative to the other carpals and more elongate, with a narrower waist and a more dorsopalmarly compressed distal end; from *O. rufus* and *M. fuliginosus* in being more elongate, with a narrower waist and a more dorsopalmarly compressed base lacking an anterodorsal tubercle; and from *W. bicolor* in being larger and more robust, with a relatively larger, deeper distal end.

Triquetrum (Fig. 101e–i): broad and blocky; dorsal surface gently convex with small ridges along the anterior and posterior margins. The palmar surface forms a rounded point at the posterior margin. Facet for the styloid process of the ulna rounded and concave. Facet for the pisiform long and dorsopalmarly short. Facet for the hamatum large, occupying most of the anterior surface.

The triquetrum of *P. otibandus* differs from that of *P. mamkurra* **sp. nov.** in having a flatter dorsal surface and a slightly smaller pisiform facet; from *C. kitcheneri* in being larger relative to the other carpals, with a broader and flatter dorsal surface and a slightly more laterally and less palmarly situated facet for the pisiform; from *O. rufus* in having flatter dorsal surface, with a smaller and more palmarly situated facet for the pisiform; from *M. fuliginosus* in being deeper, with a flatter dorsal surface; and from *W. bicolor* in being absolutely larger, larger relative to the size of the pisiform, and more robust.

Hamatum (Fig. 101e–h): quite deep and blocky, with a narrow, blunted palmar process projecting palmomedially from the posteromedial edge; dorsal surface is gently convex; a small, rounded eminence projects posteromedially. Facet for the triquetrum quite broad and mostly posterior facing, occupies the lateral part of the posterior surface except for on the palmar process; a small posterior part of the facet extends onto the posteromedial process of the hamatum, with the medial margin distinct and separate from the facet for the scaphoid. Facet for the scaphoid small and concave, on posteromedial surface. Facet for the capitatum small, narrow and facing anteromedially, with slight dorsal lip. Facet for metacarpal III narrow and faces anteromedially. Facet for metacarpal IV broad, narrows palmarly onto the medial base of the palmar process. Facet for metacarpal V quite large and anterolaterally facing, covers the majority of the anterior surface of the palmar process, with a rounded palmar lip.

The hamatum of *P. otibandus* differs from that of *P. mamkurra* **sp. nov.** in being smaller and deeper, with the triquetral facet distinctly separate from the scaphoidal facet, and a smaller, posteropalmarly projected palmar process; from *P. viator* **sp. nov.** in being smaller, with a smaller triquetral facet that is less deeply inset, less extensive medially, and distinctly separate from the scaphoidal facet; from *C. kitcheneri* in having a broader triquetral facet and larger facets for the capitatum and metacarpal III; from *O. rufus* in having a slightly more palmarly situated triquetral facet and a less anteriorly deflected and extensive palmar process; from *M. fuliginosus* in being slightly deeper, with a more laterally situated triquetral facet relative to the scaphoidal facet, and a less palmarly projected, much less anteriorly curved palmar process; and from *W. bicolor* in being larger and deeper, with the scaphoidal and triquetral facets distinct rather than abutting, and a broader, less palmarly projected palmar process.

Capitatum (Fig. 101e–g): tall and blocky, with a flat dorsal surface and a rugose, slightly concave, roughly triangular palmar surface. Posteropalmar process very slight to absent. Facet for the scaphoid located on the medial component of the posterior surface. Facet for the triquetrum slightly larger than the scaphoidal facet, situated on the posterolateral surface. Facet for metacarpal III broad, with semi-distinct anterior and anterolateral components; a small, dorsally opening mesial fossa on a slight corner separates the slightly broader anterolateral facet from the smaller anterior facet. Facet for the posterolateral articulation of metacarpal II small, quite tall and narrow, medially abuts the anterior section of the facet for metacarpal III. Facet for the trapezoid tall, narrow and gently concave, anteromedially abuts the scaphoidal facet.

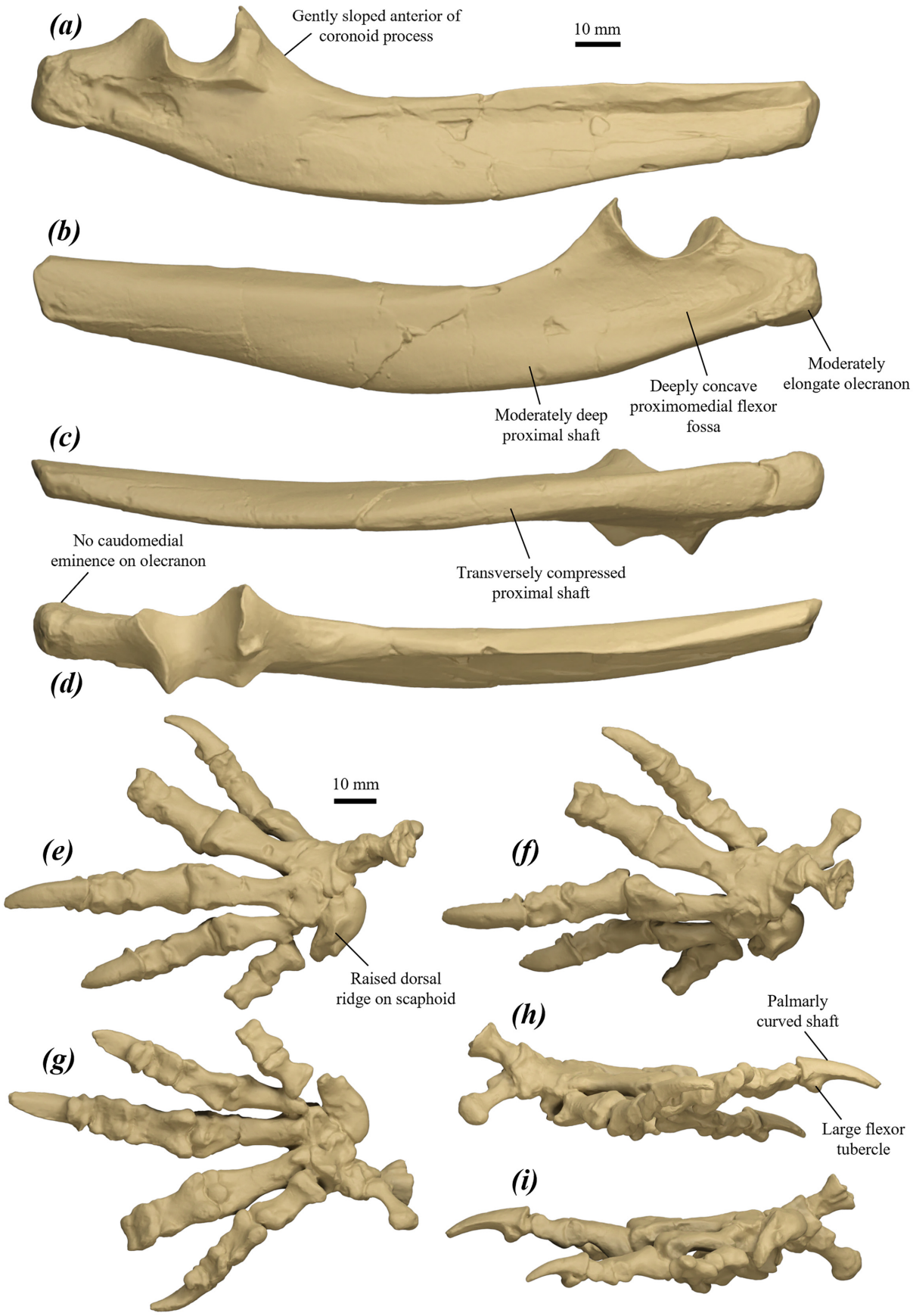

FIGURE 101. surface scan images of right lower forelimb elements of *P. otibandus* UCMP 70059: (a–d) partial ulna in (a) lateral, (b) medial, (c) caudal, and (d) cranial views; and (e–i) partial articulated manus, with ulnar styloid process attached, in (e) dorsal, (f) dorsolateral, (g) palmar, (h) lateral, and (i) medial views. Elements not preserved in the manus are the trapezoid, trapezium, and distal phalanges I and IV.

The capitatum of *P. otibandus* differs from that of *P. mamkurra* **sp. nov.** and *P. viator* **sp. nov.** in being smaller and lacking a blunt posteropalmar process; from *C. kitcheneri* in being generally squarer and less rounded, lacking a posteropalmar process and in having the dorsal surface flat instead of convex; from *O. rufus* in being slightly anteroposteriorly deeper; from *M. fuliginosus* in being squarer in dorsal view, with a more medially and less anteriorly facing facet for metacarpal II and a less medially projected facet for the trapezoid; and from *W. bicolor* in being larger, deeper, and squarer in dorsal view, with a larger, deeper hamatal facet.

Metacarpals (Fig. 101e–i): short and quite robust, with metacarpals II–IV relatively more elongate; each shaft narrows to a distinct waist; tall proximally, becoming dorsopalmarly compressed distally, particularly II–IV; all with large, broad and rounded distal keels. Metacarpal I: shortest, with a tall, narrow facet for the trapezium laterally situated on the proximal surface; a large, blunt tubercle on the palmomedial surface of the proximal end projects medially; metacarpals I and V have distinctly asymmetrical distal ends, skewed mesially. Metacarpal II: substantially shorter than III and IV, with the lateral surface of the proximal end articulating against the anterolateral surface of the capitatum and the lateral surface of the proximal end of metacarpal III; distal end has a distinctly enlarged lateral section. Metacarpal III: longest, with the proximal end separated into a longer, medially deflected medial process and a short, laterally deflected lateral process. Metacarpal IV: has a broad proximal facet for articulation with the capitatum, tilted dorsally and slightly medially, with the dorsal margin distinctly concave in dorsal view. Metacarpal V: proximal end has a large, blunt tubercle on the palmolateral surface that is strongly projected laterally; shaft curves slightly palmarly.

The metacarpals of *P. otibandus* differ from those of *P. anak* in being slightly smaller; from *P. mamkurra* **sp. nov.** in being smaller and slightly more gracile; from *P. viator* **sp. nov.** in being smaller and more robust; from *C. kitcheneri* in being more elongate, with shafts with more pronounced waists, generally broader proximal articular surfaces, flatter and less convex distal articular surfaces and generally squarer distal ends; from *O. rufus* in being relatively slightly broader; from *M. fuliginosus* in being slightly more elongate; and from *W. bicolor* in being much larger.

Manual phalanges (Fig. 101e–i): short, broad, dorsopalmarly compressed and quite symmetrical, particularly proximal and middle phalanges; proximal phalanx II more gracile than other proximal phalanges; proximal phalanges slightly shorter than the corresponding distal phalanges. Proximal phalanges: palmar tubercles raised, rounded and proximally projected; trochlea moderately shallow and quite narrow. Middle phalanges: very short, broad and dorsopalmarly compressed; shafts have very slight waists. Distal phalanges: quite long, with the palmar tubercle large and palmodistally projected (Fig. 101h), and the shaft palmarly curved, slightly dorsopalmarly compressed and smoothly rounded on the dorsal surface.

The manual phalanges of *P. otibandus* differ from those of *P. anak* in being smaller, with more palmarly curved distal phalanges; from *P. mamkurra* **sp. nov.** in having less dorsopalmar compression, longer, narrower proximal and middle shafts, and more palmarly curved distal phalangeal shafts; from *P. viator* **sp. nov.** in being smaller and more gracile, with less dorsopalmarly compressed distal phalanges with more projected palmar tubercles; from *C. kitcheneri* in being broader, far more dorsopalmarly compressed, particularly the middle and distal phalanges, and significantly shorter relative to the metacarpals, with broader, less V-shaped trochleae, more dorsally tilted proximal surfaces of proximal phalanges, and dorsally rounded distal phalanges with less palmar curvature of the shaft; from *O. rufus* in being slightly broader, with proximal phalanges having a broader distal end relative to the proximal end, and distal phalanges having longer, more dorsopalmarly compressed and palmarly curved shafts; from *M. fuliginosus* in having the proximal and middle phalanges with slightly more dorsally tilted proximal surfaces and less V-shaped trochleae, and more dorsopalmarly compressed distal phalanges with palmarly curved shafts; and from *W. bicolor* in being larger.

Hindlimb

Femur (Fig. 102a–e): mid-sized and gracile. Head large, very broad, rounded, hemispherical, dorsomedially projected and situated quite close to the medial base of the greater trochanter with the thick epiphyseal surface continuous between the two; rotated distally such that the articular surface faces slightly medially; the base of the trochanter is deep. Proximal end fairly broad, with the dorsal surface convex in the mesial third. Greater trochanter large, blunt, transversely compressed and slightly medially deflected; thickened on the dorsal surface of the base. Greater trochanteric ridge and trochanteric fossa poorly preserved in available specimens; appear elongate in UCMP 45344, with a deep fossa in UCMP 70065. Intertrochanteric crest quite thick, moderately raised and curves distally with slight medial deflection; ventromedially orientated in cross-section; abuts the small, rugose lesser trochanter. Lesser trochanteric ridge thick, raised, distally elongate and ventromedially projected.

Shaft straight, round in cross-section, with the caudal surface flattened and broadened distally for the insertion of the ischiatic portion of the mm. adductores. The quadratus tubercule is situated around the midpoint of the ventral surface of the shaft; raised and oval. Distolateral fossa for the m. flexor digitorum superficialis elongate, shallow and lateral-facing. Distal end tall and robust. Lateral trochlear crest broad and rounded relative to the medial crest, but subequal in height. Trochlea deep and approaches V-shaped (Fig. 102d). Intercondylar fossa large and deep, extends dorsodistally to just past the midpoint of the distal surface. Condyles broad, subequal in width and gently convex ventrally. Lateral epicondyle tall, rounded and laterally very projected; lateral gastrocnemial fossa deep and rounded. Fibular facet quite broad, laterally projected and slightly caudally deflected. Medial epicondyle has a slight lateral projection of the ventral component; medial gastrocnemial fossa broad and very slightly concave.

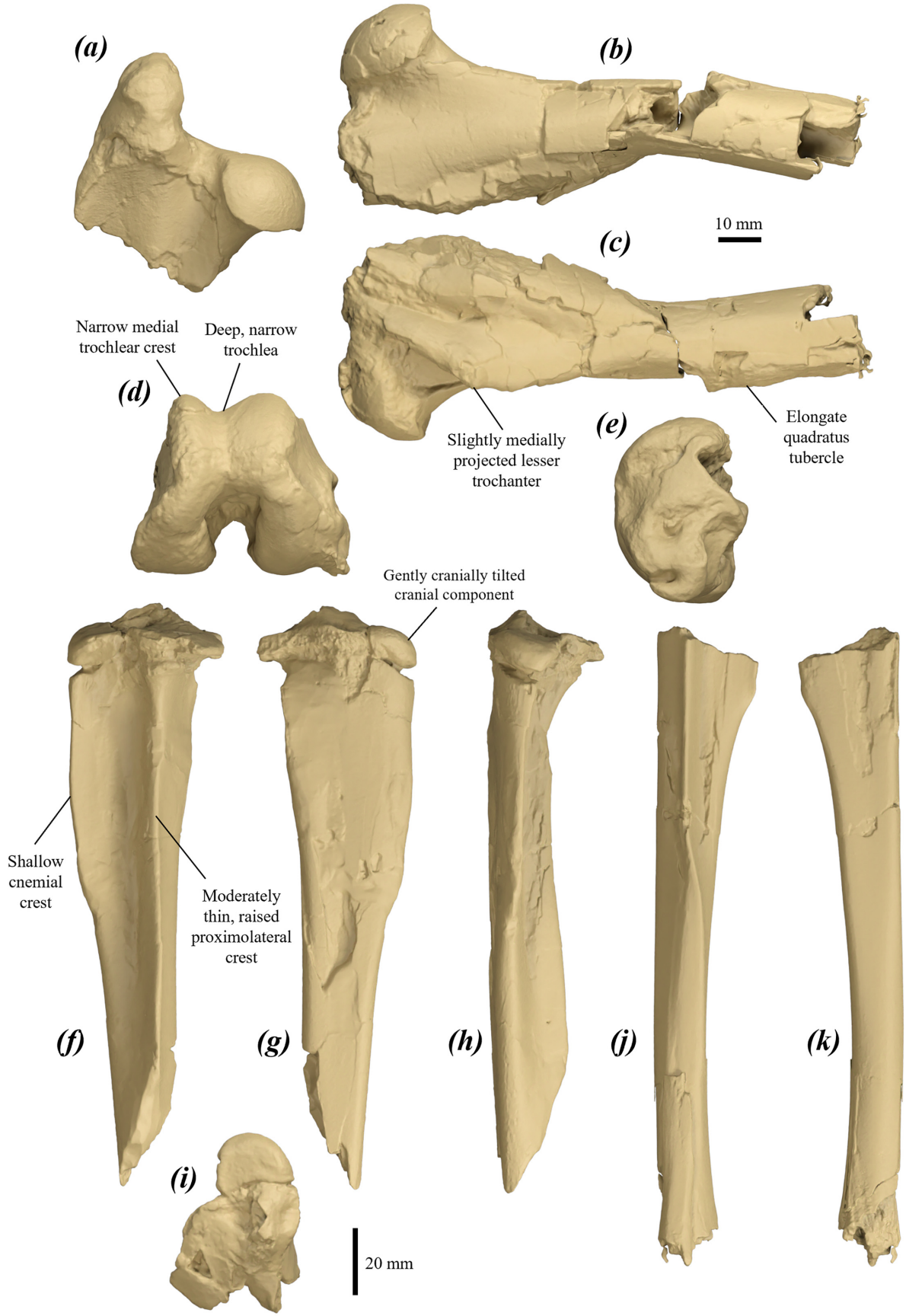

FIGURE 102. surface scan images of partial hindlimb elements of *P. otibandus*: (a) proximal right femoral fragment of UCMP 70665 in dorsal view; (b–c) partial proximal right femur of UCMP 45344 in (b) dorsal, and (c) ventral views; (d–e) left distal femoral epiphysis of UCMP 45344 in (d) distal, and (e) lateral views; (f–i) partial proximal left tibia of UCMP 70584 in (f) lateral, (g) medial, (h) cranial, and (i) proximal views; and (j–k) partial right tibial shaft in (j) lateral, and (k) medial views.

The femur of *P. otibandus* differs from that of *P. anak* in being smaller, with a deeper, narrower trochlea and a narrower, more raised medial trochlear crest; from *P. mamkurra* **sp. nov.** in being smaller, with a narrower, deeper trochlea, and a narrower medial trochlear crest and medial condyle; from *P. viator* **sp. nov.** in being smaller, with a less medially projected lesser trochanter, and a narrower medial trochlear crest and medial condyle; from *P. tumbuna* in having a less elongate, more proximally situated quadratus tubercle; from *C. kitcheneri* in having a more elongate, medially deflected and transversely compressed greater trochanter, deeper trochlea, trochlear crests subequal in height, and a less elongate and more proximally situated lateral gastrocnemial fossa; from *O. rufus* in having a more medially deflected greater trochanter, head positioned closer to the base of the greater trochanter, more distally extensive lesser trochanteric ridge, relatively broader distal condyles, trochlear crests subequal in height, more laterally projected lateral epicondyle, and a more proximally situated lateral gastrocnemial fossa; from *M. fuliginosus* in being generally larger, with a more elongate, more transversely compressed greater trochanter, more distally extensive lesser trochanteric ridge, relatively broader distal condyles, deeper trochlea, more laterally projected lateral epicondyle, and a more proximally situated lateral gastrocnemial fossa; and from *W. bicolor* in being larger, with a relatively larger, more dorsally projected and more medially tilted head, more rounded greater trochanter, more distally extensive lesser trochanteric crest, more distally situated quadratus tubercle, broader, less raised trochlear crests, slightly deeper trochlea, larger fibular facet on the lateral condyle, and a more laterally projected lateral epicondyle.

Tibia (Fig. 102f–k): quite small, short and robust. Proximal epiphysis partially preserved; cranial component narrow and moderately cranially tilted; lateral condyle caudolaterally rounded and projected; intercondylar eminence tall, thick and elongate; medial condyle not known. Proximal fibular facet large, deep, broad and caudolaterally projected, with a slight distal deflection. Cnemial crest thick and shallow (Fig. 102f); peak quite distinct and rugose, crest broadens distally, gently lowers, becomes rounder and merges gently into the shaft. Proximolateral crest raised and rounded proximally, rapidly narrowing and steadily becoming very raised before merging into the distal fibular facet at the midpoint of the shaft. Distal fibular facet extends from the midpoint of the shaft to the distal epiphysis; deep, distinct, slightly convex and slightly craniolaterally projected, particularly proximally. Distal shaft broad, particularly distally. Distal end very broad, with a gently convex trochlear articular surface, roughly rectangular and slightly caudally tilted; medial tuberosity large and elongate, and medial malleolus elongate and ventrally projected with caudal part curving caudomedially.

The tibia of *P. otibandus* differs from that of *P. anak* in being shorter, with a relatively slightly broader distal epiphysis; from *P. mamkurra* **sp. nov.** in being smaller, with larger, broader proximal fibular facet and a shallower, relatively less distally extensive cnemial crest; from *P. viator* **sp. nov.** and *P. snewini* in being smaller and more robust, with a larger, broader proximal fibular facet, gently cranially tilted cranial section of the proximal epiphysis, and a slightly more curved cnemial crest in cranial view; from *P. tumbuna* in being more gracile, with a thinner, more raised proximolateral crest, and a less distally extensive cnemial crest with a more defined peak; from *C. kitcheneri* in having broader proximal fibular facet, thicker proximal part of the proximolateral crest, and a deeper, more distinct distal fibular facet; from *O. rufus* and *M. fuliginosus* in being more robust, with a cranially tilted cranial section of the proximal epiphysis, broader proximal fibular facet, relatively longer cnemial crest with less distinct distal peak, thicker proximolateral crest, deeper, more distinct distal fibular facet and more craniocaudally compressed distal epiphysis; and from *W. bicolor* in being larger, with a deeper proximal fibular facet, thicker proximolateral crest, relatively more elongate cnemial crest with a less angular, less distinct distal peak, and a broader talar trochlea.

Fibula: only known specimen is a fragmentary distal shaft; articulates with the lateral surface of the distal half of the tibia. Proximal end interpreted as being large and broad based on the size of the proximal fibular facet on the tibia. Distal shaft quite deep and gently crescentic in cross-section, thickens distally.

Pes

Calcaneus (Fig. 103a–f): short, low and robust. Calcaneal tuberosity broad, low and domed in cross-section, almost squared immediately caudal to the calcaneal head. Caudal epiphysis low and rounded in caudal view with a thin, shallow, transverse channel on the caudal surface. Plantar surface thick, rugose, quite broad and gently narrowing cranially, and curving slightly laterally to a rounded point lateral to the cranial plantar tubercle; a thicker and more plantarly projected caudal section is formed from the caudal epiphysis. Cranial plantar tubercule small, rounded, plantarly projected and immediately caudoplantarly adjacent to the plantar margin of the plantomedial cuboid facet.

Calcaneal head large and broad; midline in the sagittal plane is slightly medially offset relative to that of the calcaneal tuberosity (Fig. 103a). Sustentaculum tali broad, thick and rounded with no distinct peak in medial view; projected medially slightly beyond the medial margin of the medial talar facet, extends caudally well past the caudal margins of the talar facets; flexor groove very broad and deep, accentuated by the medial projection of the plantar surface. Fibular facet small, with semi-distinct cranial and caudal components, separated by a broad groove; caudal component quite small, roughly oval, unprojected caudally, slightly projected laterally, and medially semicontinuous with lateral talar facet; cranial component lower than the caudal component, broad, laterally projected and slightly laterally tilted, with the dorsal surface gently concave. Lateral talar facet broad, quite tall, smoothly convex with distinct medial tapering; a rounded, very shallow fossa is immediately cranial to the lateral talar facet, with a small, low, rounded tubercle on the medial margin of the fossa; medial talar facet caudally

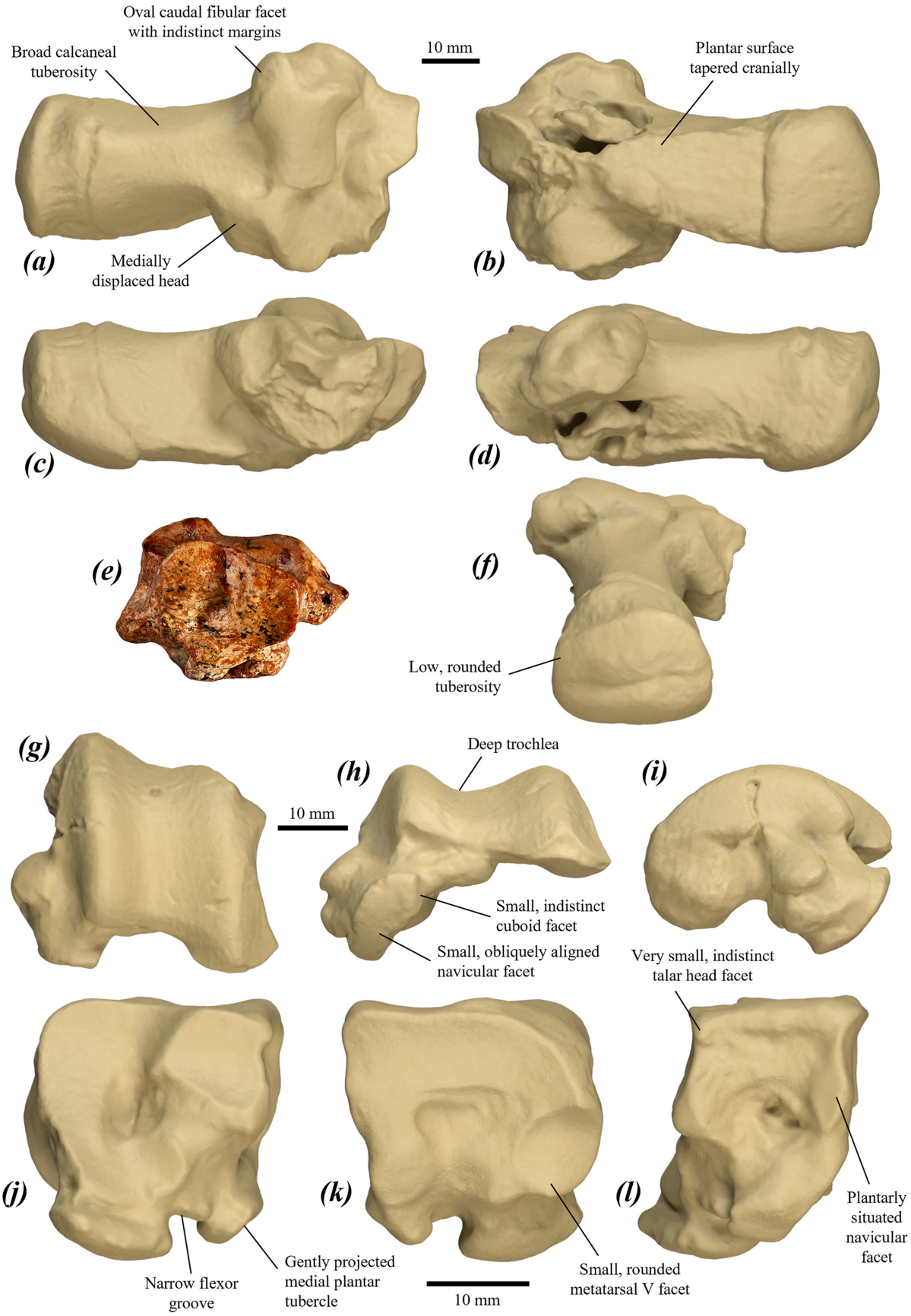

FIGURE 103. left tarsal elements of *P. otibandus*: (a–d, f) surface scan images of partial calcaneus of UCMP 70584 in (a) dorsal, (b) plantar, (c) medial, (d) lateral, and (f) caudodorsal views; (e) calcaneus of UCMP 45247 in cranial view; (g–i) surface scan images of talus of UCMP 70584 in (g) dorsal, (h) cranial, and (i) medial views; and (j–l) surface scan images of cuboid of UCMP 70078 in (j) caudal, (k) cranial, and (l) medial views.

displaced relative to the lateral facet; small, oval, dorsally slightly projected, orientated caudomedially to craniolaterally and strongly cranially tilted, with a rounded lip along the caudomedial margin; smoothly continues caudally into a very low, rounded tubercle or ridge merging caudally into the dorsolateral margin of the tuberosity.

Talar head facet very small, rounded, abuts the dorsomedial margin of the dorsomedial facet on the medial surface of the calcaneal head. Dorsomedial cuboid facet squarish with a rounded dorsomedial margin, gently convex and slightly dorsally projected; separated from the dorsolateral facet by a deep, bevelled step; small, shallow fossa sits immediately plantarly. Dorsolateral cuboid facet tall, subequal in width to the dorsomedial facet, cranially projected and roughly semicircular, with curved dorsal and lateral margins; extends plantarly and curving medially to be continuous with the plantomedial facet. Plantomedial cuboid facet small, broad, dorsoplantarly short and oblong; extends medially past the midpoint of the dorsomedial facet.

The calcaneus of *P. otibandus* differs from all compared species in having the calcaneal head slightly medially offset relative to the calcaneal tuberosity. It further differs from *P. anak* in being smaller and lower, with a relatively shorter, slightly broader tuberosity that is more rounded dorsally in cross-section, less straight, more cranially tapered plantar surface, less rounded, less distinct and less caudolaterally projected caudal component of the fibular facet, less concave plantolateral margin of the dorsolateral-plantomedial facet, and a more laterally tilted dorsomedial cuboid facet; from *P. mamkurra* **sp. nov.** in being smaller and lower, with a slightly narrower, more cranially tapered plantar surface, more rounded sustentaculum tali, less bulbous lateral talar facet, relatively smaller medial talar facet that is more cranially tilted and more caudally displaced relative to the lateral facet, more laterally tilted dorsomedial cuboid facet, and a less medially tilted dorsolateral cuboid facet; from *P. viator* **sp. nov.** in being smaller, lower, shorter and much more robust, with a lower, more rounded tuberosity in cross-section, relatively narrower dorsomedial cuboid facet, and in having the lateral surface of the calcaneal head beneath the fibular facet dorsoplantarly much shorter and less concave; from *P. tumbuna* in having a less medially displaced head relative to the tuberosity, more planar plantar surface with less flaring of the medial margin, and a smaller, shallower fossa cranial to the lateral talar facet; from *P. dawsonae* **sp. nov.** in having a broader calcaneal tuberosity; from *C. kitcheneri* in being larger and taller, with a more planar, more cranially extensive and less laterally tilted plantar surface, more dorsally projected medial talar facet, and a less caudally projected, less distinct caudal component of the fibular facet; from *O. rufus* and *M. fuliginosus* in being much broader and more robust, with a broadly rounded, domed calcaneal tuberosity in cross-section, more pointed, more medially projected sustentaculum tali, less cranially extensive cranial component of the fibular facet, more bevelled step between the dorsal cuboid facets, and a more curved, less cranially extensive plantar surface that broadens caudally; and from *W. bicolor* in being larger and relatively broader, with a relatively larger fibular facet and a broader medial talar facet.

Talus (Fig. 103g–i): slightly width greater than craniocaudal length. Trochlear crests equal in height, with the medial peak thinner and less rounded. Trochlea is fairly deep and medially skewed (Fig. 103h). Medial malleolus large, rounded, smoothly convex, dorsal facing, extends medially and slightly cranially, bounded laterally by a deep, rounded malleolar fossa; rounded, plantomedially projected tubercle situated plantar to the medial malleolus on the medial surface of the talar neck. Talar head broad and distinctly plantarly deflected, creating a concave divot between the head and cranial margin of medial trochlear crest. Facet for the navicular broad dorsally and extending caudoplantarly to beneath anterior margin of medial malleolus. Facet for the cuboid very small, slightly convex and lateral facing, with a very slight cranioplantar tilt. Posterior plantar process rugose, very broad and thickened, deep, plantarly projected and rounded. On the plantar surface, the medial calcaneal facet is rounded and concave, abuts a small, deep, rounded mesial fossa, and the lateral calcaneal facet is very large, broad, deeply concave, becomes deeper laterally.

The talus of *P. otibandus* differs from that of *P. anak* in being smaller, with a broader navicular facet that is more obliquely angled in cranial view, larger, more obliquely aligned medial malleolus, and a small tubercle plantar to the medial malleolus on the medial surface; from *P. mamkurra* **sp. nov.** in being smaller, with a deeper malleolar fossa, smaller cuboid facet, less medially projected talar head, and a deeper plantar groove between the navicular facet and the posterior plantar tubercle; from *P. viator* **sp. nov.** in being smaller, with a shorter, more concave, and more cranially situated malleolar fossa, a dorsal facing medial malleolus, and a deeper plantar groove between the navicular facet and the posterior plantar tubercle; from *P. snewini* in having a deeper trochlea and a deeper concavity between the posterior plantar tubercle and the talar head; from *C. kitcheneri* in having a more medially projected medial malleolus, more caudoplantarly extensive navicular facet, a facet for the cuboid present on the navicular head, and a deeper lateral calcaneal facet; from *O. rufus* in being relatively broader and more caudolaterally extensive, with a deeper trochlea and a larger, more rounded posterior plantar process; from *M. fuliginosus* in being generally larger, relatively broader and more caudolaterally extensive, with a deeper trochlea and a deeper, broader and more rounded posterior plantar process; and from *W. bicolor* in being larger and relatively broader, with a more caudoplantarly extensive navicular facet and a broader, more rounded posterior plantar process.

Cuboid (Figs 103j–l, 104a–d): square and robust. Dorsomedial calcaneal facet squarish, caudally projected, smoothly concave and subequal to the dorsolateral calcaneal facet, separated by a bevelled step; dorsolateral calcaneal facet tall, gently concave and extending plantarly and slightly medially to be continuous with

the plantar calcaneal facet; plantar calcaneal facet broad, dorsoplantarly short, oblong and gently concave, with the medial margin situated lateral to the transverse midpoint of the dorsomedial facet, situated on the caudal base of the lateral plantar tubercle. Dorsal margin of the medial surface marked by a low, rounded ridge projecting medially over a tall, broad fossa for articulation with the caudodorsal part of the ectocuneiform and the craniodorsal part of the navicular.

Facet for the talar head narrow and indistinct. Facet for the navicular small and narrow on the caudal margin of dorsal part of the medial surface, adjacent to the medial margin of the dorsomedial calcaneal facet. Facet for the ectocuneiform very tall and thin, extends from near the dorsal margin of the medial surface past the midpoint of the cranial margin, with a distinct, rounded second facet on the plantomedial surface of the medial plantar tubercle. Lateral plantar tubercle large, broad and quite plantarly projected, oval to round in plantar view; occasionally deflected caudally (see UCMP 70078). Medial plantar tubercle moderately small, rounded, less plantarly projected than the lateral tubercle and slightly medially deflected; separated from the lateral tubercle by a variably deep, narrow flexor groove. Facet for metatarsal IV broad and very gently concave, with the dorsomedial margin medially projected; not continuous plantarly with the small, rounded, plantarly tilted plantar facet for metatarsal IV. Facet for metatarsal V fairly small, rounded, gently concave, slightly plantolaterally tilted and laterally projected.

The cuboid of *P. otibandus* differs from that of *P. anak* in being smaller and lower, with less plantarly projected plantar tubercles, and the dorsal and plantar metatarsal IV facets distinct from one another; from *P. mamkurra* **sp. nov.** in being smaller, with less distinct step between the dorsal calcaneal facets, slightly narrower dorsolateral calcaneal facet, smaller, less distinct talar head facet, deeper medial fossa for the navicular and ectocuneiform, more plantarly projected lateral plantar tubercle, narrower flexor groove, more laterally tapered metatarsal IV facet that is distinct from the plantar metatarsal IV facet, and a smaller, narrower, more concave metatarsal V facet; from *P. viator* **sp. nov.** in being smaller, shorter and relatively broader, with a more plantarly situated navicular facet, less elongate, less plantarly projected plantar tubercles, and a shallower flexor groove; from *P. snewini* in having less dorsomedially flared dorsomedial section, more level dorsal calcaneal facets in caudal view, more plantarly extensive plantomedial calcaneal facet, much smaller talar facet, and a much larger, more plantomedially projected medial plantar tubercle; from *C. kitcheneri* in being slightly larger and taller, with a facet for the talar head present, more plantarly projected lateral plantar tubercle, larger, more elongate and more medially situated medial plantar tubercle, and separate dorsal and plantar metatarsal IV facets; from *O. rufus* in being relatively broader, particularly across the plantar section, with a relatively broader dorsolateral calcaneal facet, a smaller, less distinct facet for the talar head, less plantarly projected lateral plantar tubercle, more medially situated medial plantar tubercle, broader flexor groove, and a more medially situated plantar metatarsal IV facet; from *M. fuliginosus* in being generally larger and relatively broader, particularly across plantar section, with a smaller, less distinct facet for the talar head, more deeply concave medial fossa for the navicular and ectocuneiform, broader and less plantarly projected lateral plantar tubercle, larger and more medially situated medial plantar tubercle, broader flexor groove, and separate dorsal and plantar metatarsal IV facets; and from *W. bicolor* in being larger and relatively broader, with a less plantarly projected lateral plantar tubercle and a larger, more plantarly projected medial plantar tuberosity.

Navicular (Fig. 104a–b, d): tall, roughly crescentic in medial view and transversely compressed dorsally, broadens gently plantarly, particularly around the laterally flared facet for the ectocuneiform; medial surface rugose. Talar facet smoothly concave and dorsally tilted. Facet for the ectocuneiform tall, gently convex and quite narrow, extends from the dorsal margin of the cranial surface just past the midpoint; plantar component broadens and flares laterally. Facet for the entocuneiform quite small and narrow, oval and situated slightly plantar of the midpoint of the cranial surface, level with the plantar margin of the ectocuneiform facet.

The navicular of *P. otibandus* differs from that of *P. mamkurra* **sp. nov.** in being smaller, and shallower relative to height, with a more laterally flared dorsal ectocuneiform facet and a less medially tilted facet for the entocuneiform; from *P. viator* **sp. nov.** in being smaller and slightly shallower, with a more medially deflected plantar section and a dorsoplantarly shorter facet for the ectocuneiform; from *C. kitcheneri* in being taller and relatively shallower; from *O. rufus* in being taller and relatively shallower, with a more expanded plantar section, and a slightly more plantarly situated facet for the entocuneiform; from *M. fuliginosus* in being larger and much taller; and from *W. bicolor* in being larger, with a more medially flared plantar section.

Ectocuneiform (Fig. 104a–b, d): tall and quite transversely compressed; dorsal margin forms a thick, rounded-triangular mesial point, accommodating the articulation of the dorsolateral surface with metatarsal IV. Facet for the navicular tall and quite narrow transversely, broadens plantarly, occupies the entire caudal surface. Facet for metatarsal III concave, quite tall and narrow, occupies the dorsal section of the cranial surface. Facet for the mesocuneiform very small and roughly oval, on the cranial section around the midpoint of the medial surface, plantar to the metatarsal III facet. Medial surface has the dorsal section smooth and gently convex, plantar section pitted and rugose. A small, thin eminence is present on the caudal part of the midpoint of the medial surface, probably for articulation with the entocuneiform.

The ectocuneiform of *P. otibandus* differs from all compared species in its rounded-triangular dorsal margin. It further differs from *P. mamkurra* **sp. nov.** in being smaller and relatively slightly dorsoventrally shorter; from *P. viator* **sp. nov.** in being slightly less transversely compressed and relatively taller, with a less deeply concave entocuneiform

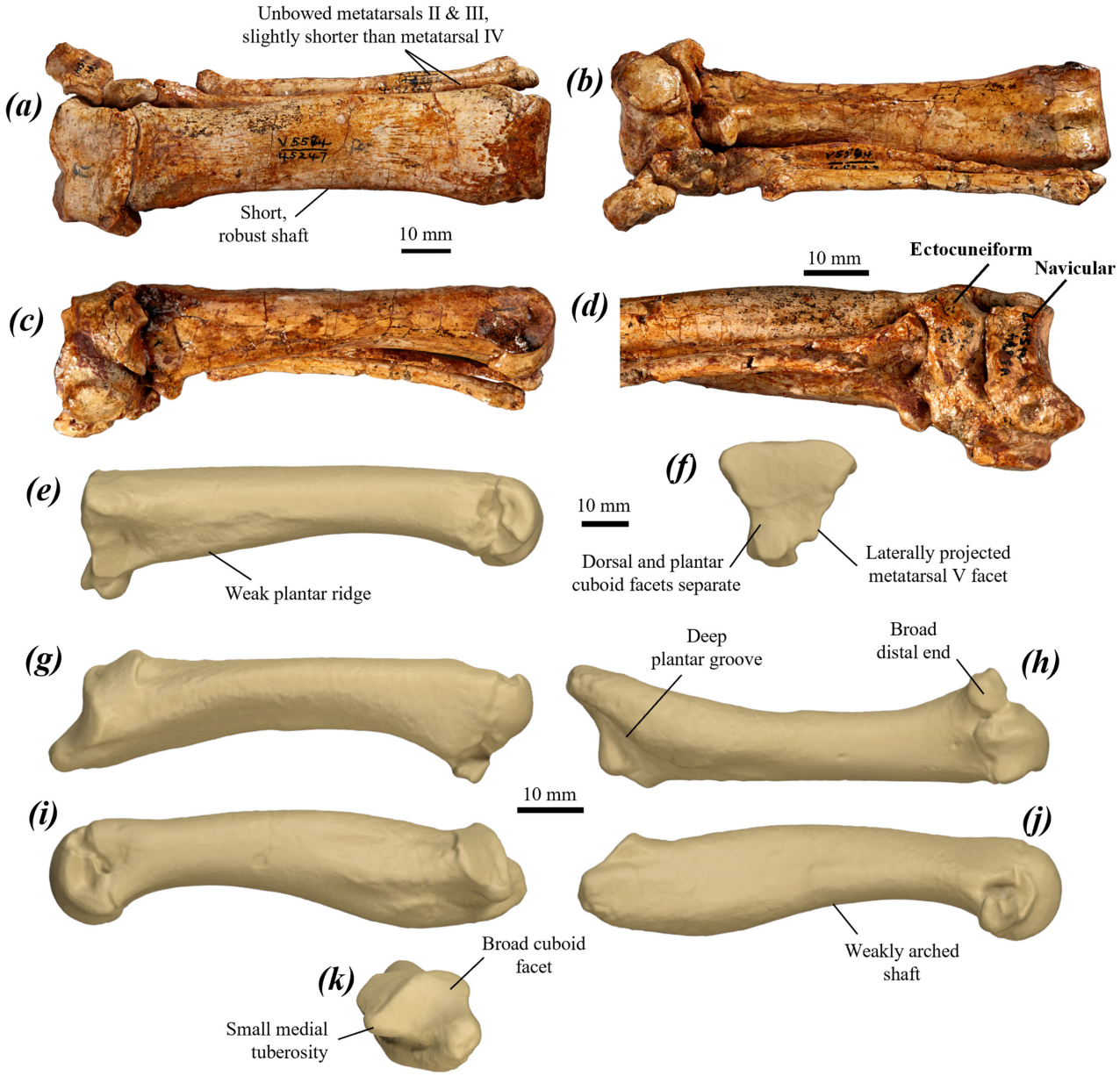

FIGURE 104. right tarsal elements of *P. otibandus*: (a–d) articulated cuboid, navicular, ectocuneiform, and metatarsals II–IV of UCMP 45247 in (a) dorsal, (b) plantar, (c) lateral, and (d) medial views; (e–f) surface scan images of metatarsal IV of UCMP 70584 in (e) lateral, and (f) proximal views; and (g–k) surface scan images of metatarsal V of UCMP 70585 in (g) dorsal, (h) plantar, (i) medial, (j) lateral, and (k) proximal views.

facet; from *C. kitcheneri* in having a slightly larger and more cranial facing facet for the mesocuneiform; from *O. rufus* in having a smaller cranial eminence, more plantarly extensive articulation with the navicular, and a less cranially deflected plantar process; from *M. fuliginosus* in being larger and taller, with a more plantarly extensive facet for the navicular; and from *W. bicolor* in being larger and slightly less transversely compressed, with a less concave, slightly more plantarly extensive navicular facet.

Metatarsals II and III (Fig. 104a–d): both very gracile; III longer than II, both slightly shorter than metatarsal IV; II straight, III very slightly bowed laterally. Proximal end of metatarsal III: articulates with the mesocuneiform, ectocuneiform and metatarsals II and IV; tall and narrow with a smoothly convex ectocuneiform facet; entocuneiform facet small, rounded and situated on the plantar part of the medial surface. Proximal end of metatarsal II: articulates with metatarsal III and possibly with both the entocuneiform and mesocuneiform; relatively small and unflared compared to the metatarsal III proximal end. Shafts transversely compressed proximally; metatarsal III shaft rapidly decreases in height from the proximal end, becomes rounded in cross-section and gently tapers distally; metatarsal II broadens slightly and is un-tapered. Distal ends small, bulbous and rounded. The phalanges are not known.

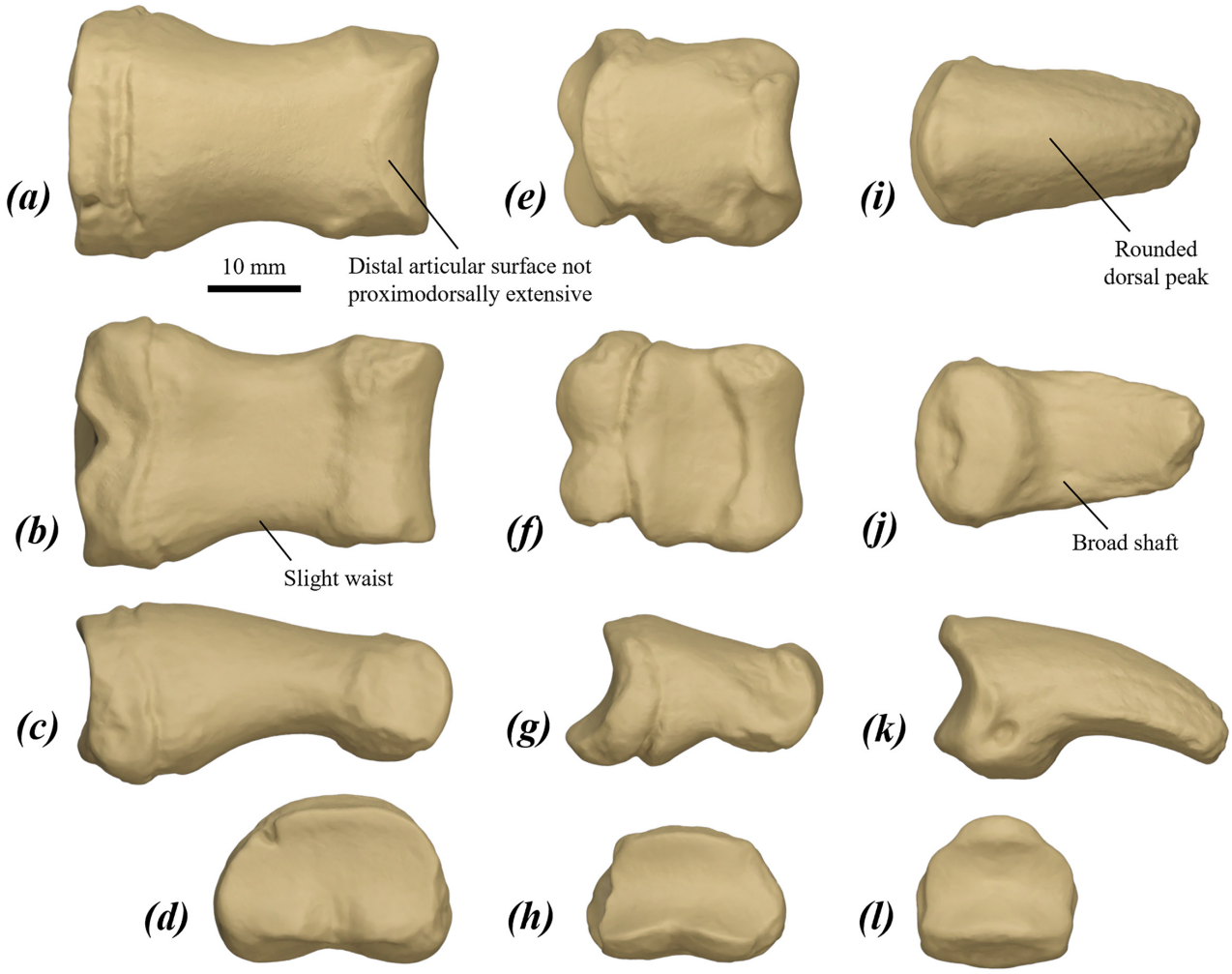

FIGURE 105. surface scan images of left (a–d) proximal, (e–h) middle, and (i–l) distal pedal phalanges IV of *P. otibandus* specimen UCMP 70584 in: (a, e, i) dorsal, (b, f, j) plantar, (c, g, k) medial, and (d, h, l) proximal views.

Metatarsals II and III of *P. otibandus* differ from those of all compared taxa in having shafts that are less laterally bowed. They further differ from those of *P. viator* **sp. nov.** in being slightly more robust and longer relative to the length of metatarsal IV; from *M. fuliginosus* and *O. rufus* in being much shorter, more robust and longer relative to length of metatarsal IV, with a taller proximal end for articulation with metatarsal III; and from *W. bicolor* in being larger and more robust.

Metatarsal IV (Fig. 104a–f): short and robust. Proximal end dorsal margin flat to gently rounded; dorsal cuboid facet broad, with the lateral section flat to gently convex and the medial section flat to gently concave; dorsal facet separate from the plantar cuboid facet, separated by a broad, very shallow transverse proximal fossa; plantar cuboid facet small, rounded, slightly proximally projected and tilted dorsally and slightly medially, extends plantarly onto the proximal surface of the plantar tubercle. Facet for the dorsolateral section of the ectocuneiform small, semicircular and distinct, situated against the dorsal margin of the medial surface of the proximal end, facing medially. Plantar tubercle quite small, plantarly projected and slightly proximally deflected. Proximal plantar sesamoid facet small, rounded to squarish and laterally tilted. Facet for metatarsal III indistinct, situated in the shallow, rugose metatarsal III fossa, bordered dorsally by a thin ridge extending plantodistally from the dorsomedial corner of the dorsal cuboid facet. Facet for the ectocuneiform very small, tall and thin, abuts the midpoint of the proximal margin of the medial surface of the shaft; smaller facet for articulation with the plantolateral section of the ectocuneiform occasionally present on the proximal section of the medial surface of the plantar tubercle (see UCMP 70584, L metatarsal IV). Facet for metatarsal V tall, quite deep, distally tilted, gently concave and oblong, projects proximally or proximoplantarly to create one or two small, rounded eminences on the lateral margin of proximal fossa in proximal surface.

Plantar ridge broad, weakly raised (Fig. 104e), rugose, rounded to square in cross-section, extends distally from the distal base of plantar tubercle to slowly merge with plantar shaft. Shaft flat to very slightly rounded dorsally; height tapers distally, broadens gently to distal end. Distal

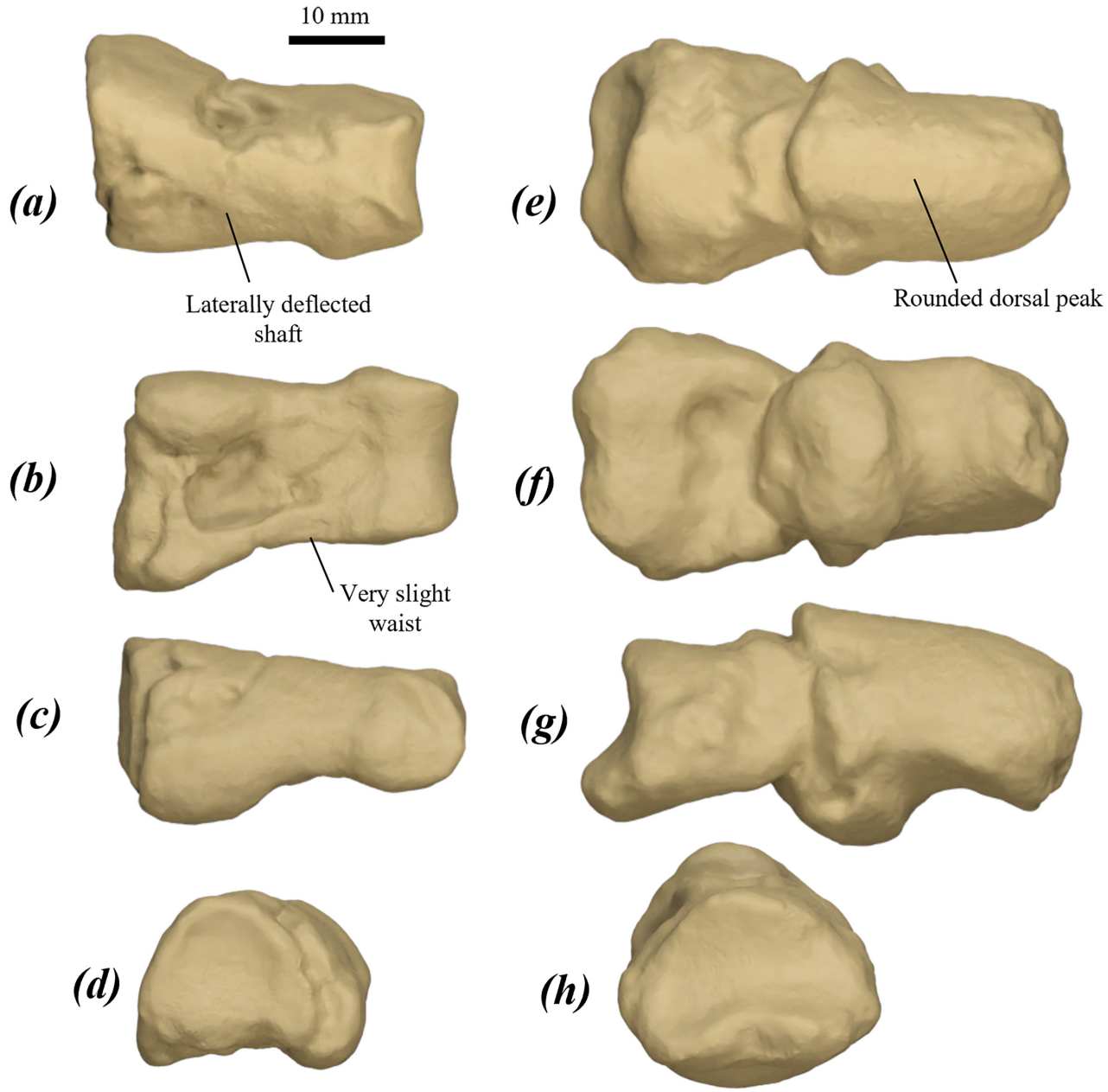

FIGURE 106. surface scan images of right (a–d) proximal pedal phalanges V, and (e–h) articulated middle and partial distal pedal phalanges V of *P. otibandus* specimen UCMP 45247 in: (a, e) dorsal, (b, f) plantar, (c, g) medial, and (d, h) proximal views.

end large with fossae for collateral ligaments deep and rounded; keel rounded and more plantarly projected than medial and lateral eminences.

The metatarsal IV of *P. otibandus* cannot be differentiated from that of *P. tumbuna*. It differs from that of *P. anak*, *P. mamkurra* **sp. nov.** and *P. dawsonae* **sp. nov.** in being smaller and more robust, with separate dorsal and plantar cuboid facets (Fig. 104f) and a less raised plantar ridge; from *P. viator* **sp. nov.** in being smaller and more robust, with separate dorsal and plantar cuboid facets, a less raised plantar ridge and a shaft with a weaker proximal waist; from *P. snewini* in being slightly shorter and more robust, with a smaller proximal cuboid fossa; from *C. kitcheneri* in being broader, with separate dorsal and plantar cuboid facets, less narrowing of the proximal shaft, and a more raised plantar ridge; from *O. rufus* and *M. fuliginosus* in being much shorter, broader and more robust, with separate dorsal and plantar cuboid facets, a lower plantar ridge, and a more plantarly projected proximal plantar tubercle; and from *W. bicolor* in being much larger, relatively broader and more robust, with a relatively slightly larger plantar tubercle.

Metatarsal V (Fig. 104g–k): very short, robust and transversely compressed with a slight medial tilt; curves slightly laterally distally; slightly arched in lateral view; length to distal facet width index ~4–4.7. Proximolateral process blunt, rugose, proximodistally quite short and transversely compressed. Facet for the cuboid very broad,

gently concave and slightly raised at distal margin, mostly proximal facing; extends from proximal surface of the medial plantar tubercle across proximal surface of the shaft onto base of dorsomedial surface of proximolateral process and dorsolaterally over dorsal surface of the base of proximolateral process. Facet for metatarsal IV broad, gently convex, slightly raised and rounded to square; proximally abuts facet for the cuboid, extends medially onto dorsomedial surface of the medial plantar tubercle. Lateral plantar tuberosity broad, long and rugose, separated from medial plantar tubercle by narrow, shallow channel. Medial plantar tubercle very small, sometimes indistinct, gently medially projected. Distal end broad; medial fossa for the collateral ligaments larger and deeper than the lateral fossa.

The metatarsal V of *P. otibandus* differs from that of *P. anak* in being smaller, with a relatively smaller proximolateral process and a relatively smaller, less proximomedially projected medial plantar tubercle; from *P. mamkurra* **sp. nov.** in being smaller and narrower, with a smaller, slightly narrower cuboid facet, deeper plantar groove, and a larger lateral plantar tuberosity; from *P. viator* **sp. nov.** in being smaller, shorter and less transversely compressed, with a broader, more medially situated cuboid facet and a more medially extensive metatarsal IV facet that is less distinct from the cuboid facet; from *P. tumbuna* in being slightly more gracile and more transversely compressed, with dorsoplantarly shorter proximolateral process, proximodistally longer metatarsal IV facet and larger medial plantar tubercle; from *P. dawsonae* **sp. nov.** in being shorter, with more dorsally projected cuboid facet and slightly broader distal end; from *C. kitcheneri* in being shorter and broader, lacking slight kink of arch of the shaft immediately proximal to midpoint in lateral view, with a larger medial plantar tubercle and lateral plantar tuberosity, and a deeper, more distinct plantar groove; from *O. rufus* and *M. fuliginosus* in being much shorter, broader, less transversely compressed, and less arched in lateral view, with a larger medial plantar tubercle and a deeper, more distinct plantar groove; and from *W. bicolor* in being larger, relatively broader and more robust.

Pedal phalanges (Fig. 105 & 106): Proximal phalanx IV: short, robust and slightly dorsoplantarly compressed, with a slight waist on the shaft. Proximal end domed, with the proximal plantar tubercles low and rounded; proximal articular facet broad and gently concave with a rounded dorsal margin. Distal end with large, very shallow fossae for the collateral ligaments; trochlea gently concave. Middle phalanx IV: short and broad; proximal end broad, with the proximal plantar tubercles very low and projected slightly proximally. Proximal articular surface dorsally rounded, concave and tilted slightly dorsally. Shaft height decreases distally, with a very slight waist. Distal end with quite deep fossae for the collateral ligaments; trochlea narrow and very slightly concave dorsally, deepens and broadens plantarly. Distal phalanx IV: quite short, broad and robust; proximal articular facet concave and roughly pentagonal, forms a rounded, slightly proximodorsally projected dorsal peak. Flexor tubercle large and plantarly projected, oval in plantar view. Shaft with a rounded dorsal peak (Fig. 105i), curves gently downward in lateral view.

Proximal phalanx V: quite tall, robust and asymmetrical; shaft laterally deflected relative to the proximal surface. Proximal end slightly broader than tall; plantar tubercles large, rounded and rugose, lateral tubercle projected plantolaterally past the articular surface; proximal articular surface round, gently concave and medially displaced in proximal view. Shaft rounded and triangular in cross-section. Distal end with very shallow fossae for the collateral ligaments; trochlea broad and shallow, and articular surface not extensive dorsally. Middle phalanx V: very short, broad and very dorsoplantarly compressed. Proximal end with very low plantar tubercles; proximal articular surface gently concave and tilted strongly dorsally. Shaft very short, decreases in height distally, with no waist. Distal end with fossae for collateral ligaments very shallow and tall. Distal phalanx V: tall, robust and asymmetrical, with the dorsal peak of the shaft and the proximal end medially displaced; small, deep fossae for the collateral ligaments. Plantar tubercle large and rounded in plantar view. Shaft with a rounded dorsal peak and a strongly convex plantar margin in cross-section. Distal end abraded in available specimens.

The pedal phalanges of *P. otibandus* differ from those of *P. anak* in being slightly smaller, with middle phalanx IV less dorsoplantarly compressed (Fig. 105h) and lacking large, transversely flared plantar tubercles, distal phalanx IV with a more rounded dorsal peak, and proximal phalanx V with a less distinct waist; from *P. mamkurra* **sp. nov.** in being smaller and shorter, with proximal phalanx IV with a narrower distal end, and middle phalanx IV with a narrower trochlea; from *P. viator* **sp. nov.** in being slightly smaller, with proximal phalanx IV shorter with a broader waist, distal phalanx IV more dorsoplantarly compressed with a more rounded dorsal peak and a less plantarly curved shaft, proximal phalanx V with a less concave proximal articular surface, a more laterally deflected shaft, and a narrower trochlea, middle phalanx V shorter with a less medially tilted proximal surface, and distal phalanx V with a more rounded dorsal peak; from *P. snewini* in having relatively narrower middle phalanx IV across the proximal end and a slightly broader distal phalanx IV with a more rounded dorsal peak; from *P. dawsonae* **sp. nov.** in having proximal phalanx IV with a less proximodorsally extensive distal articular surface; from *C. kitcheneri* in being shorter, lower, broader and more robust, with broader, shallower trochleae, middle phalanges with more dorsally tilted proximal surfaces, and distal phalanges with much more rounded, less pointed dorsal peaks; from *O. rufus* and *M. fuliginosus* in being shorter, lower, broader and much more robust, particularly the middle phalanges, with proximal phalanx IV having a broader waist, the middle phalanges with a more dorsally tilted proximal surface, and distal phalanges with a more rounded, less pointed dorsal peak in cross-section and a more plantarly curved shaft in lateral view; and from *W. bicolor* in being larger, relatively broader and more robust.

Remarks:

***Holotypes of* P. chinchillaensis *and* P. devisi**

During the printing of Bartholomai (1973), an error occurred wherein the images of the holotypes of *P. chinchillaensis* and *P. devisi* and their respective captions were inadvertently switched. This resulted in the image of the holotype for *P. chinchillaensis* (Bartholomai 1973, pl. 23, figs 3 & 4) being labelled as the holotype for *P. devisi*, and the image of the holotype for *P. devisi* (Bartholomai 1973, pl. 21, figs 3 & 4), being labelled as the holotype for *P. chinchillaensis*. Bartholomai (1975) included an erratum correcting this mistake. During I.A.R.K.'s visit to the palaeontological collection of the Queensland Museum in late 2018, the curator, Dr Scott Hocknull, and I.A.R.K. noted that the registration numbers of each holotype reflected those assigned to them incorrectly in plates 21 & 23 of Bartholomai (1973). Dr Hocknull reviewed the situation, and, informed by the apparent intent of Bartholomai (1973) and by the descriptions of the specimens in the fossil register of the Queensland Museum, altered the number of each type to its original designation in the species diagnosis of Bartholomai (1973). The official stance of the museum is that the holotype of *P. chinchillaensis* has the registration number QM F5246 and that the holotype of *P. devisi* has the registration number QM F4710.

***Identities of* P. otibandus *and* P. chinchillaensis**

Prior to this study, there was some cause to doubt the separate taxonomic identities of *P. otibandus* and *P. chinchillaensis*. *Protemnodon otibandus* was the first species of *Protemnodon* of undoubted Pliocene age to be described, and the first from New Guinea (Plane 1967). Later, Plane (1972) tentatively allocated a partial maxilla from Lake Tyers, southeastern Victoria, to *P. otibandus*. Despite this, when *P. chinchillaensis* was described from the Pliocene material of the Chinchilla Sand, Bartholomai (1973) made comparisons with all species of *Protemnodon* recognised at the time with the exception of *P. otibandus,* the species with which it was most similar. Flannery & Archer (1984) noted the lack of a urocrista on the anterior upper molars of *P. chinchillaensis*, the presence of which was implied therein to be autapomorphic in *P. otibandus*, though Flannery (1994) stated '*Protemnodon otibandus* is extremely similar in morphology to *P. chinchillaensis*. They may even be conspecific' (p. 45).

The New Guinean material of *P. otibandus* is very restricted in geographic area and time, contrasting with other species of *Protemnodon*, which are sampled over longer time intervals across wider geographic areas. With the exception of a single maxilla of probable Pliocene age preserving P3–M3, from near Koroba in the Hela Province of montane central PNG (Flannery 1990a), all New Guinean material of *P. otibandus* comes from the Awe LF of the Otibanda Fm. in Morobe Province, eastern PNG (Fig. 1) (Plane 1967; Flannery 1994). This sample, by the standards of the better-sampled *P. anak*, shows tightly clustered dental dimensions and a more uniform craniodental and postcranial morphology, insofar as both are known. That said, various features that have been described as diagnostic of *P. otibandus* are in fact variable within the type series. Plane (1967) described *P. otibandus* as having a distinct buccal cuspid in the talonid basin of the m1. However, this cuspid is variable within the paratypes of *P. otibandus*—for *e.g.*, extremely reduced in UCMP 69896 and absent from UCMP 45246—and thus its absence from the holotype of *P. chinchillaensis* is not considered taxonomically significant. The dental morphology of *P. chinchillaensis* was described by Bartholomai (1973) in the species diagnosis as differing from other members of the genus in having relatively curved molar links, a shallow mandibular ramus and swollen anterolingual protolophid bases. It is not clear whether the phrase 'molar links' refers to the upper or lower dentition, or which crista(e) and/or cristid(s) in particular are more curved in this taxon. The paracristid and cristid obliqua on the lower molars were described as curved in the species description, but this is a feature of all species of *Protemnodon*, and neither the paracristid nor cristid obliqua in any specimens referred to *P. chinchillaensis* by Bartholomai (1973) appear especially curved. The postprotocrista in the upper molars was described as curved in the species description, but this does not appear to be especially the case in any specimens of *P. chinchillaensis* examined, including the two figured partial maxillae (QM F5239 and QM F4719; Bartholomai 1973, pl. 20). The curvature of the postparacrista was not mentioned, though this was observed to regularly vary even within individuals of species of *Protemnodon*, including a specimen figured by Bartholomai (1973; QM F4719, pl. 20).

Dentary height is quite variable within species of *Protemnodon* (Fig. 110). Within the sample of *P. anak*, the spread in the measurements of this feature encompasses that of all Pliocene species of *Protemnodon*, so the relatively small differences in dentary height between the small samples of *P. chinchillaensis* and *P. otibandus* can be effectively discounted.

It is unclear what Bartholomai (1973) meant by 'swollen anterolingual protolophid base' (p. 352), as no swelling in this part of the lower molars of the holotype and referred specimens of *P. chinchillaensis* was identified in this study. Unpublished research suggests that this trait was not evident in any specimen (Lyndall Dawson, pers. comm. 2001). It is possible that the use of the term protolophid by Bartholomai (1973) was the result of a *lapsus calami* and that the author instead intended to refer to the anterolingual base of the protoloph of the upper molars, as this area of the upper molar is indeed distinctly convex, with the degree of swelling decreasing toward the posterior of the molar row. Regardless, this trait is shared by specimens of *P. otibandus*. Therefore, as the holotype of *P. chinchillaensis*, a dentary, has no features to confidently distinguish it from the type material of *P. otibandus*, and nor indeed does any other referred element, we find *P. chinchillaensis* Bartholomai, 1973 to be a junior synonym of *P. otibandus* Plane, 1967.

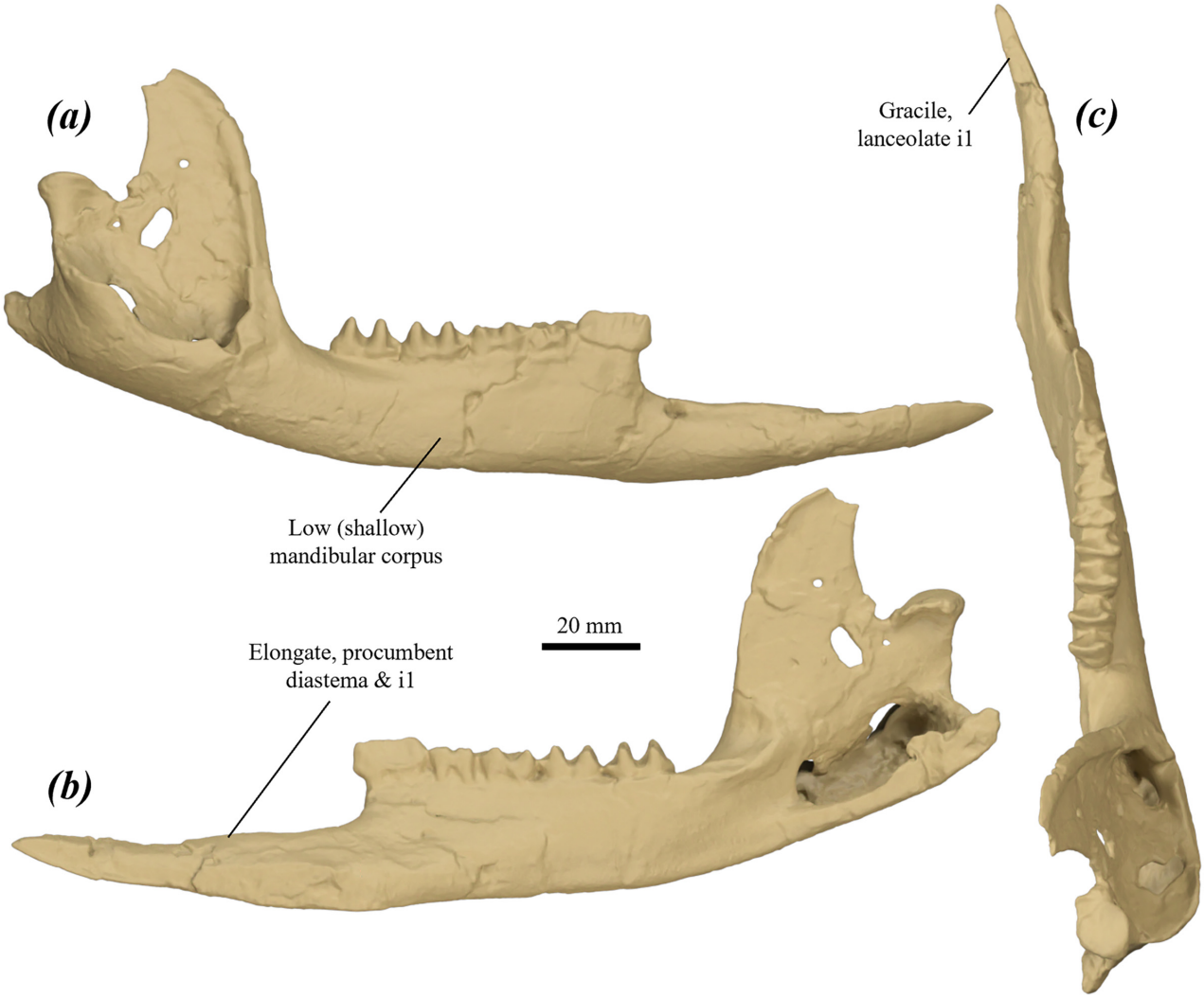

FIGURE 107. rendered image of the holotype of *Protemnodon snewini* QM F9061, a right dentary in: (a) buccal, (b) lingual, and (c) occlusal views, with certain diagnostic features labelled.

Protemnodon snewini Bartholomai, 1978

Protemnodon snewini Bartholomai, 1978: *Mem. Qld. Mus*. 18(2): pp. 131–136, figs 2 & 3, pl. 24, figs 1–4, pl. 25, fig. 1.

Protemnodon Owen *Protemnodon* sp.; Archer & Wade (1976) (*partim*), pp. 390–391, pl. 57a.

Holotype:
QM F9061 (Fig. 107), complete R dentary preserving i1, p3–m4. Figured in Bartholomai (1978) pl. 24, fig. 4, pl. 25, figs 1a & b.

Type locality:
Bluff Downs LF, Bluff Downs Station, Allingham Fm., north Queensland, Australia. The Allingham Fm. is considered early Pliocene, with a minimum radiometric date of 3.62 ± 0.5 Ma from overlying basalt and a maximum age of 5.2 Ma inferred from the known period of volcanic activity producing the underlying layer containing basalt (Mackness *et al.* 2000).

Paratype(s):
None.

Referred specimens:

Queensland
Bluff Downs LF, Allingham: AM F9074 maxillae; AM F7810 partial R maxilla; AM F9072 L DP3; AM F7788 L DP3; AM F9073 R DP3; AM F7786 R P3; AM F9062 R P3; AM F9069 R M1; AM F7809 L M3; AM F9071 L M3; AM F9066 partial L M3; AM F7811 R M4; AM F7824 R dp3; AM F9070 partial L p3; AM F9064 R m1; AM F9068 R m3; AM F9065 L m3; AM F9063 partial R m4; AM F9067 partial R m4; AM F9075 L tibia, fibula, metatarsal IV and middle and distal pedal phalanges IV; AM F9076 L talus, cuboid and partial metatarsal V.

Revised specific diagnosis:
Protemnodon snewini is separated from other species of *Protemnodon* by several autapomorphic characteristics of

the dentition and dentary, and by a combination of other osteological features. The dentary of *P. snewini* differs from all other species of *Protemnodon* in being more gracile. The dentition of *P. snewini* is distinguished from all species of the genus by: its P3 with a lower lingual crest and a narrower posterior width relative to the anterior; and more elongate, lanceolate i1.

The dentary of *P. snewini* is most like that of *P. anak* and *P. otibandus*. It further differs from those of *P. anak* and *P. otibandus* in having a more ventrally situated masseteric fossa relative to the cheek tooth row. It is additionally distinguished from that of *P. otibandus* in having a less dorsally deflected diastema and a more anterodorsally situated mental foramen.

The dentition of *P. snewini* most closely resembles that of *P. anak* and *P. otibandus*. The dentition further differs from that of *P. anak* in being lower crowned, with a broader P3 relative to length, particularly across the anterior cusp, lower, less distinct and less dorsoventrally aligned buccal ridgelets, and a lower, less jagged and more anteriorly extensive lingual crest. Additionally differs from *P. otibandus* in its relatively narrower upper molars with a more anteriorly prominent precingulum and a less raised, less distinct postparacrista.

The hindlimb of *P. snewini* most closely resembles that of *P. anak* and *P. otibandus*, but differs from both in having a distal phalanx IV with a more pointed dorsal peak. The hindlimb is differentiated from that of *P. anak* in having a more gracile tibia, with a relatively less elongate cnemial crest with a less distinct distal peak and a more elongate proximolateral crest relative to total length. The pes further differs from that of *P. anak* by: talus lacking the small indent present between the cranial margin of the medial trochlear crest and the talar head; cuboid with separate dorsal and plantar metatarsal IV facets and a smaller, less distinct metatarsal V facet; more robust metatarsal IV with a relatively shorter plantar ridge, separate dorsal and plantar cuboid facets, and a more dorsomedially situated proximal cuboid fossa; and middle pedal phalanx IV with much less lateral and medial flaring of the proximal plantar tubercles.

The hindlimb differs from that of *P. otibandus* in having a tibia with smaller, narrower proximal fibular facet. The pes differs from that of *P. otibandus* in: talus with a shallower trochlea and a shallower concavity between the posterior plantar tubercle and the talar head; cuboid with a more dorsomedially flared dorsomedial section, much larger talar facet, and a smaller and less plantomedially projected medial plantar tubercle; and metatarsal IV with a taller, more dorsally situated proximal cuboid fossa.

Etymology:
Named for Mr W. Snewin, who discovered the Allingham site with Mr J. Barrett.

Remarks:
Protemnodon snewini was described from a complete right dentary, a maxilla and palatal fragment and a partial hindlimb, all found near to each other in the same stratigraphic unit of the mid-Pliocene Allingham Fm., northern central Queensland. They were deemed likely to belong to the same individual, but were registered separately. The partial hindlimb consists of a left tibia, fibula, metatarsal IV, and medial and partial distal phalanges IV (Bartholomai 1978, fig. 2). Bartholomai (1978) also described and figured several other disassociated hindlimb elements—a talus, calcaneus, cuboid, partial metatarsal V and proximal pedal phalanx IV—tentatively allocating them to this species. These were all registered as a single specimen (QM F9076), although they represent multiple individuals. Of these elements, only the cuboid, talus and the distal metatarsal V fragment (Bartholomai 1978, fig. 2) have a morphology that would be consistent with belonging to a single species of *Protemnodon*. The element referred to as a proximal pedal phalanx IV, in fact, represents the middle phalanx IV of a larger species of macropodid and is thus not allocated herein to *P. snewini*. The calcaneus is considered to be more akin to that of a species of *Macropus*, and likewise is not referred to this species.

Protemnodon snewini shares some features with *Congruus kitcheneri*, such as a gracile i1, procumbent diastema and shallow, elongate dentary. However, the similarities of its cheek dentition to other species of *Protemnodon* and possession of the characteristic form of the middle pedal phalanx IV—short, very broad and dorsoplantarly compressed—are the chief drivers of its inclusion in the genus *Protemnodon*.

The material allocated to *Protemnodon* sp. from Corra-Lynn Cave (Pledge 1992) on Yorke Peninsula, South Australia, which consists of various partial, isolated craniodental specimens, is here considered morphologically more similar to *P. snewini* than to any other species of *Protemnodon*. For the following reasons we refrain from allocating it to a species of *Protemnodon*. Firstly, due to the presence of various plesiomorphic features in that material, such as a particularly low lingual crest on the P3, which suggest the Corra-Lynn material may be of an unknown, more plesiomorphic species. Secondly, while the deposit has previously been considered early Pliocene in age, recent but unpublished dates suggest an earlier age for the material. Lastly, expeditions are planned to extract further material from the Corra-Lynn deposit, and we do not wish to pre-emptively describe and allocate the material when more may be about to be found that could greatly aid more accurate taxonomic description and placement.

Status of other species previously referred to *Protemnodon*

Australian Pleistocene species

Protemnodon brehus (Owen, 1874): *Phil. Trans. Roy. Soc*. 164, p. 272—*nomen dubium*.

Protemnodon mimas Owen, 1874: *Phil. Trans. Roy. Soc*. 164, p. 278—*nomen dubium*.

Protemnodon roechus Owen, 1874: *Phil. Trans. Roy. Soc.* 164, p. 281—*nomen dubium*.

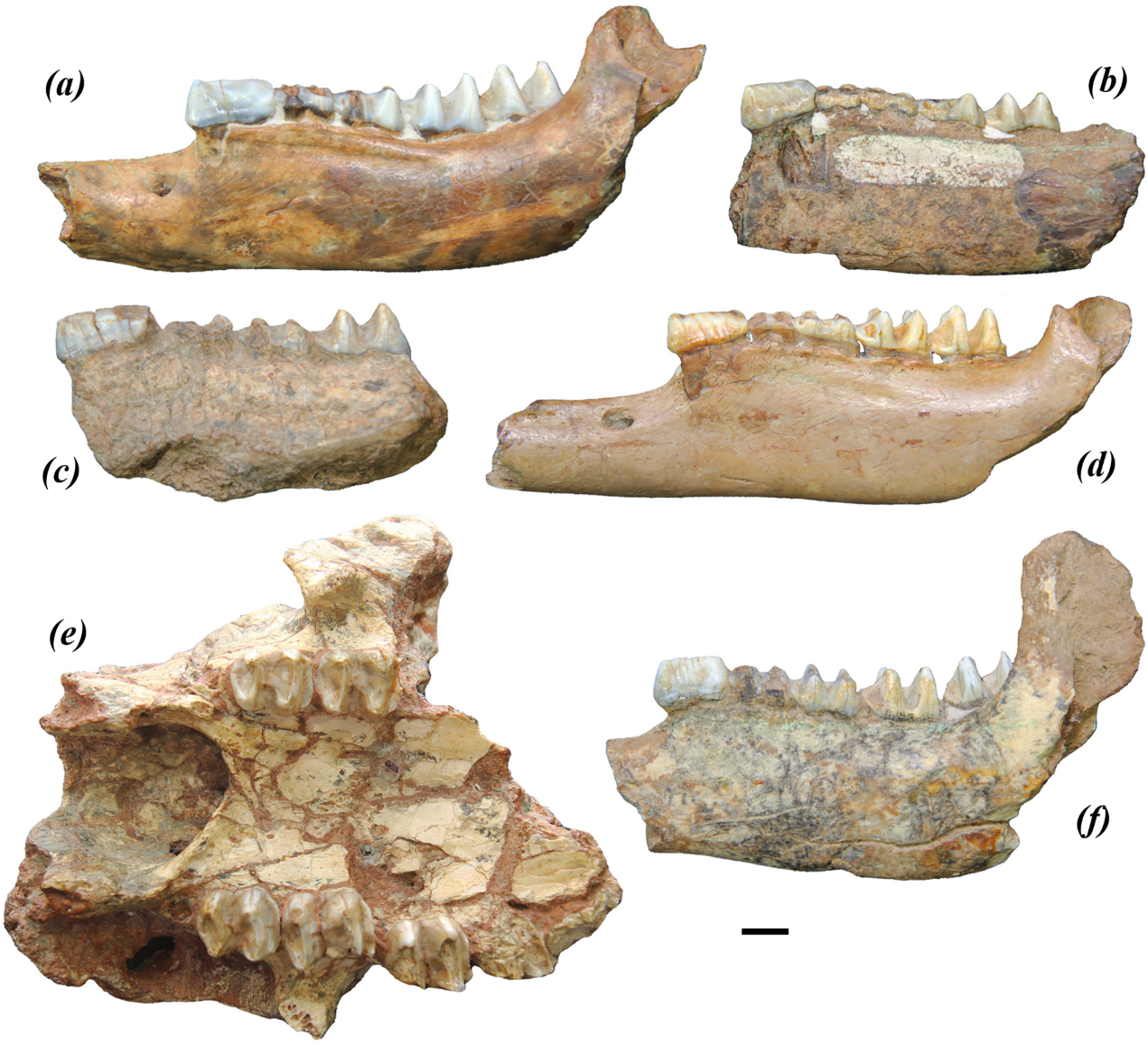

FIGURE 108. Owen's (1874, 1877) type specimens for species of *Protemnodon*: (a–d, f) all partial left dentaries in buccal view, the holotypes of (a) *P. antaeus*, NHMUK PVM2258; (b) *P. anak*, NHMUK PVM1895; (c) *P. roechus*, NHMUK PVOR35968; (d) *P. og*, NHMUK PVOR35963; (f) *P. mimas*, NHMUK PVOR43351; and (e) the lectotype of *P. brehus*, NHMUK PVOR43303a, partial maxillae and palate in occlusal view.

Protemnodon antaeus Owen, 1877: *Researches on the fossil remains of the extinct mammals of Australia; with a notice of the extinct marsupials of England*. 1, p. 448—*nomen dubium*.

This section discusses the taxonomic history and status of the remaining species of *Protemnodon* described by Owen (1874, 1877), including justification for the designation of *Protemnodon roechus* and *P. brehus* as *nomina dubia* and for the erection of two *species novae* from the Australian Pleistocene. For reference, all of the holotypes and lectotypes for Owen's (1874, 1877) six species of *Protemnodon* are figured here (Fig. 108). Note that, as per ICZN Article 61, the holotype specimen (*i.e.* the name-bearing type) is the sole specimen that provides the diagnostic features of the *nomen*—the type (not the type series, *i.e.* paratypes, nor referred specimens) provides the objective standard of reference for the application of the name it bears (ICZN 1999). A loss of the utility of a *nomen* is the criterion for status as *nomen dubium*, although the *nomen* remains valid and available.

The following is an extract from the redescription of *P. roechus* from Bartholomai (1973), where the dental morphology of the species was contrasted with that of *P. anak* and *P. brehus*: '[*Protemnodon*] *roechus* is distinguished from other known species of *Protemnodon* by both its extreme size and generally distinct morphology. In particular, the relatively less ornamented nature of its permanent lower premolar, the broadly rounded, swollen condition of the posterior crown bases of the lower molars, the non-vertical transecting ridges of the permanent upper premolars, the crescentic shape of this tooth in occlusal view and the generally marked tuberculation of

the lingual extremity of the median valley in the upper molars are all useful in the morphological separation of the species. Overlap in size does occur with *P. brehus*, but by applying a combination of the characters available separation of the species is achieved' (Bartholomai 1973, p. 346).

Nevertheless, the distinction as made by Bartholomai (1973) is in fact not so clear. For a variety of reasons, *P. brehus* and *P. roechus* have never been clearly delimited. The lectotype specimen for *P. brehus*, NHMUK PVOR43303a, is a partial palate containing left M3–M4 and right M2–M4. However, the holotype specimen for *P. roechus*, NHMUK PVOR35968, is a left dentary fragment containing heavily worn p3–m3, and as such the holotypes have no shared features for direct comparison. Three of the five characteristics stated by Bartholomai (1973) as distinguishing *P. roechus* from other species of *Protemnodon* are in the upper cheek teeth, which are not preserved in the holotype of *P. roechus*, and the holotype of neither species preserves a P3. The results of our analyses and the morphological comparisons of the material of *Protemnodon* from across Australia indicate that the characteristics described above do not distinguish two distinct morphotypes, but instead describe features that vary continuously within the sample.

The statement by Bartholomai (1973, p. 346) that specimens of *P. roechus* are characterised by "extreme size" that differentiates them from those of *P. brehus* is not well-supported by the data presented in that paper (Bartholomai 1973, fig. 9), which show almost identical mean dimensions for the lower dentition, nor by the data presented here (See Figs 116–122). The 'crescentic shape' of the P3 varies greatly within the sample of Pleistocene P3s not attributable to *P. anak* (Fig. 109). The description of the 'relatively less-ornamented nature of its [p3]' most probably refers to the narrow, roughly dorsoventrally orientated ridgelets on the lingual and buccal faces of the p3. These ridgelets, when numerous and thin but distinct, are diagnostic of *P. anak*, and are less numerous and less distinct in other Pleistocene Australian material of species of *Protemnodon*. No discrete difference in the number or size of these ridgelets is discernible in the sample of Pleistocene Australian material when excluding that of *P. anak*. These ridgelets disappear almost completely with a moderate degree of wear, and so in older and thus often skeletally larger individuals with a greater degree of dental wear, the premolar appears increasingly less ornamented. It is possible that this biased Bartholomai's (1973) morphological analysis by causing larger individuals, *i.e.* those more likely to be assigned to *P. roechus*, to seemingly possess p3s with fewer, less raised vertical ridgelets.

The condition of rounded, swollen posterior lophid bases is present in various lower molar specimens of *Protemnodon* from the Pleistocene, including individuals of *P. anak*, rather than solely individuals allocated to *P. roechus*. This condition is seen in molars with residual postcingulids and very occasionally in large molars with fully developed postcingulids (as in the holotype of *P. mimas*, NHMUKPV OR43351).

Our extensive survey of fossils of species of *Protemnodon* from the Australian Pleistocene has revealed that there are indeed two Australian Pleistocene morphotypes of *Protemnodon* aside from *P. anak* (*P. mamkurra* **sp. nov.** and *P. viator* **sp. nov.**); however, they are primarily distinguishable on postcranial features. Neither can be delimited based on either the upper or lower cheek dentition and they have similar size ranges. As illustrated in Figs 116–120, any divide in terms of dental dimensions between the type material of *P. mamkurra* **sp. nov.** and *P. viator* **sp. nov.** is filled by isolated dental or craniodental specimens allocated to *P. mamkurra* **sp. nov.** or *viator* **sp. nov.** These specimens do not cluster in any distinct groups, but rather are spread between and around the groupings of *P. mamkurra* **sp. nov.** and *P. viator* **sp. nov.** specimens. This demonstrates the inefficacy of diagnosing these two taxa based on the few small differences in dental dimension groupings, as these do not serve to delimit with any confidence the many remaining fragmentary specimens.

Because the holotypes of neither *P. brehus* nor *P. roechus* can be unambiguously associated with either one of the two Pleistocene forms identifiable on the basis of partial and complete skeletons, neither nomina can be used to describe the taxa observed. We therefore recognise *P. brehus* (Owen, 1874) and *P. roechus* Owen, 1874 as *nomina dubia*.

This leaves *P. mimas* Owen, 1874, previously synonymised with *P. brehus*, and *P. antaeus* Owen, 1877, previously synonymised with *P. roechus*. Owen (1874) observed that *P. antaeus* differed from *P. mimas* in its lack of a postcingulid and in having a larger p3 relative to its molars, and from *P. roechus* in being smaller. However, because these traits and proportions vary within species (Fig. 121) (see also Bartholomai 1973, p. 346) to a much greater degree than separates the holotypes of *P. antaeus*, *P. mimas* and *P. roechus*, and because the holotypes of *P. mimas* and *P. antaeus*, both partial left dentaries with p3–m4 with moderate wear (NHMUK PVOR43351 and NHMUK PVM2258, respectively), cannot be unambiguously associated with either *P. mamkurra* **sp. nov.** or *P. viator* **sp. nov.**, *P. mimas* Owen, 1874 and *P. antaeus* Owen, 1877 are also considered *nomina dubia*.

Nombe nombe

Protemnodon nombe Flannery, Mountain & Aplin 1983: *Proc. Linn. Soc. N.S.W.* 107(2), p. 91.

Nombe nombe (Flannery, Mountain & Aplin 1983); Kerr & Prideaux 2022, *Trans. Roy. Soc. S.A.* 146(2), pp. 295–318.

Nombe nombe (Flannery *et al.*, 1983) possesses various characteristics of the dentary and the lower molars that show it does not belong in the genus *Protemnodon* (see Kerr & Prideaux 2022). The m3 and m4 in the holotype and the referred specimen, which are the least worn molars, possess a distinct postprotocristid and a strongly developed premetacristid, with the lophid crest gently S-shaped in occlusal view. These molars also lack the folding of the enamel around the protoconid and paracristid seen

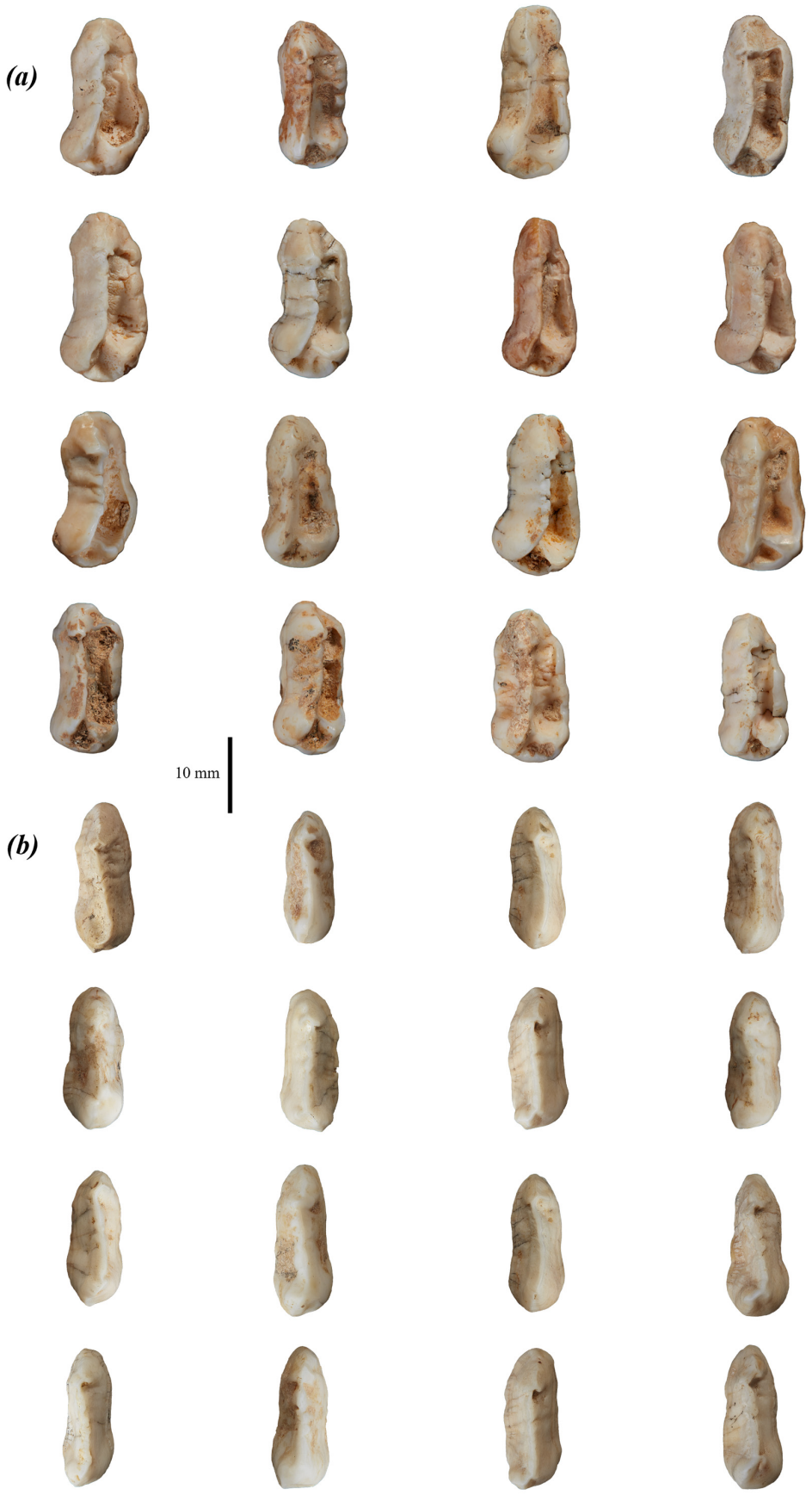

FIGURE 109. occlusal view of 16 unworn to lightly worn right (a) upper and (b) lower third premolars of SAMA P24098 (single specimen number for multiple individuals) of *Protemnodon mamkurra* **sp. nov.** or *P. viator* **sp. nov.** from Goulden's Hole, southeastern South Australia, showing the morphological and size variation visible in permanent premolars within a sample of one or possibly two species from a single locality.

in the molars of most macropodins. The buccal and lingual margins of the lophids are strongly convex in posterior view, giving the molar crowns a distinctly rounded look. The medial pterygoid and masseteric fossae of the posterior mandible are more enlarged in the referred specimen, relative to the dimensions of the dentition, than is seen in any species of *Protemnodon*. The mandibular foramen and pterygoid fossa are not preserved in the holotype and the masseteric fossa is only partially preserved but, based on the wide angle of the medial margin of the anterior of the masseteric fossa, this muscular insertion area was similarly enlarged in both specimens of *N. nombe*. The digastric sulcus is deep and narrow, indicating an increased capacity for abduction of the mandible. Both specimens possess a long, quite deep buccinator sulcus, in common with species of *Protemnodon*, but the groove is angled more posteroventrally and is less parallel with the cheek tooth row. As this combination of characteristics does not closely align *N. nombe* with any macropodid genus, it was classified as a member of the new monospecific genus *Nombe*, probably with affiliations to more basal macropodines (Kerr & Prideaux 2022).

Pliocene species

Protemnodon devisi

Protemnodon devisi Bartholomai, 1973: *Mem. Qld. Mus*. 16(3), p. 354—*nomen dubium*.

Protemnodon devisi was described by Bartholomai (1973) as being distinguishable from *P. otibandus* '… by its smaller permanent premolars and generally larger molars. The trigonid basin in lower molars is broader in *P. devisi* while the [pre]cingulum in upper molars also appears broader. The upper molars are less ovate in occlusal view, and usually have a moderately well-defined lingual swelling at the margin of the [interloph] valley. The distinct cuspid at the [buccal] end of the [interlophid valley] in m1, regarded by Plane (1967) as diagnostic in *P. otibandus,* is not developed in any specimen of *P. devisi*' (p. 359).

The holotype of *P. devisi* (QM F4710, a partial L dentary) preserves only p3 and partial m2–4 with a high level of wear, preventing some molar comparisons with *P. otibandus*. As is the case with *P. chinchillaensis*, reference to the variation seen within the better-sampled species *P. anak* shows that the predicted range of premolar length relative to molar length for a larger sample of *P. otibandus* would include the sampled range of *P. devisi* (Fig. 121). The relative width of the trigonid basin is quite variable in the molars of species of *Protemnodon*, possibly because it is affected by the angle and development of both the premetacristid and the paracristid, as well as the width of the lophid itself, but the feature is certainly too worn in the holotype of *P. devisi* to be diagnostic in any case. The presence of the cuspid on the buccal margin of the m1 interlophid valley in *P. otibandus* is variable and not diagnostic (see absence in the unworn m1 of UCMP 45246, paratype). Regardless, the m1 is not preserved in the holotype of *P. devisi* and so the condition of its talonid basin is not known. As these differences constitute the whole of the specific diagnosis with respect to features of the dentary, there are no grounds for placing the holotype outside of *P. otibandus*. There is good evidence for a generally larger (though size is not of diagnostic use) species of *Protemnodon* in Pliocene Australian deposits (*P. dawsonae* **sp. nov.**). This species is supported by characters of the upper molars and i1, which are not preserved in the holotype of *P. devisi*. As the holotype of *P. devisi* cannot be unambiguously associated with either *P. otibandus* or *P. dawsonae* **sp. nov.**, *P. devisi* is considered a *nomen dubium* rather than a junior synonym.

'Protemnodon n. sp. A'

Several specimens were referred to '*Protemnodon* n. sp. A' by Piper (2016), who described but did not formally name a taxon from mostly isolated upper cheek teeth from the early Pliocene Hamilton LF (4.46 ± 0.1 Ma) (Turnbull *et al.* 2003), early mid Pleistocene Nelson Bay LF (0.78–1.77 Ma) (Aziz-ur-Rahman & McDougall 1972; MacFadden *et al.* 1987), and the early Pleistocene Dog Rocks LF (2.06–2.58 Ma) (Whitelaw 1991), southwestern Victoria. Piper (2016) included a complete description and diagnosis but refrained from assigning a formal name or type specimen due to the need for more complete material and for a taxonomic review of the genus. All specimens listed under *Protemnodon* n. sp. A are isolated upper cheek teeth with the exception of NMV P216005, an associated DP2, unerupted P3 and M1 from Nelson Bay and NMV P201862b, an associated M1 and M3 from Dog Rocks.

The following is an extract from the specific diagnosis: '…differs from all other known species of *Protemnodon*, except *P. otibandus* and *P. chinchillaensis*, in possessing a P3 that is relatively more elongate compared to upper molars (see table 2), and from all species in having upper molars that are more rounded in occlusal outline (*i.e.* unconstricted across the [interloph] valley—base of lophs expanded lingually and swollen in the [buccal] moiety of the [interloph] valley, forming a convex [buccal] margin in occlusal view). Differs from all species except *P. otibandus* and *P. tumbuna* in having gently sloping lingual loph margins and a variably developed postlink on anterior molars in some individuals' (Piper 2016, p. 243). Our morphological comparisons suggest that the dental material allocated by Piper (2016) to *Protemnodon* n. sp. A most likely represents two or three species of *Protemnodon* from the Pliocene and Pleistocene, as discussed below.

Piper (2016) identified the mean ratio of M1 length to P3 length in *Protemnodon* n. sp. A as 0.54, in contrast to the more similar lengths in all taxa except *P. otibandus* and *P. chinchillaensis*. However, the teeth identified as M1s have narrow protoloph bases relative to the metalophs, very narrow anterior cingula, anterior moieties rotated distinctly toward the lingual side and overall anteroposterior constriction, consistent with the morphology of the DP3 in species of *Protemnodon*, particularly that of *P. viator* **sp. nov.** (*e.g.* SAMA P53836)

and *P. mamkurra* **sp. nov.** (*e.g.* SAMA P21863). Therefore, the apparent great difference in relative size between the P3 and M1 in this taxon is a result of the accidental comparison of the dimensions of the P3 with those of the DP3 rather than the larger and more elongate M1.

Two DP2s from Nelson Bay LF with distinct morphologies were allocated to this taxon; one was included due to its association with diagnostic material, the other by morphological association (Piper 2016, fig. 8, a–c and d–f respectively). The former of the DP2s, NMV P216005, is associated with an unerupted P3 and what was listed as an M3 (Piper 2016, fig. 8m–o, fig. 9p–r respectively). This DP2, which is broad and rounded in occlusal view, falls within the morphological definitions of *P. mamkurra* **sp. nov.** and *P. viator* **sp. nov.** Based on its relative loph widths and the slight rotation of its anterior moiety towards the lingual side, the 'M3' of this specimen is in fact an M1. The associated unerupted P3 and the DP2 are within the morphological bounds of both *P. mamkurra* **sp. nov.** and *P. viator* **sp. nov.** The second DP2 is attributable to *P.* sp. cf. *P. anak* due to its small size, narrow posterior relative to total length, and anteroposteriorly short lingual valley. Thus, although the material used to describe this species is definitely of the genus *Protemnodon*, the isolated nature of all but five of the teeth has been a factor in its misidentification as a new species. We conclude that none of the material listed under '*Protemnodon* n. sp. A' reflects a hitherto unrecognised species of *Protemnodon*.

Protemnodon *sp. from Lachitu Cave*

An upper cheek tooth specimen (PM 26591) was referred to *Protemnodon* sp. by Koungoulos *et al.* (2024), wherein it was considered to be a dp3 and to probably represent an undescribed species. The specimen comes from a Pleistocene deposit in Lachitu Cave on the far northwestern coast of Papua New Guinea, and represents both the first lowland occurrence of a Pleistocene species of *Protemnodon* in New Guinea and the northernmost record of any megafaunal marsupial (Koungoulos *et al.* 2024). PM 26591 was considered a dp3 rather than an m1 on the basis of: its slightly narrower anterior region relative to the posterior, with a rounded, more pointed anterior cingulid; a strongly sloping and relatively straight buccal margin of the protoconid and hypoconid; a prominent premetacristid; distinctly anteriorly concave lophid crests; a lingually positioned point of greatest curvature in the protolophid and hypolophid; and a high and convex dorsal edge of the lingual portion of the anterior cingulid with a concave and low buccal portion (Koungoulos *et al.* 2024, p. 4). While these differences do demonstrate that PM 26591 may represent a dp3, we believe that this is far from certain and note many features that link the tooth with the m1 and m2 of *P. tumbuna*.

We consider it likely, or at least possible, that the tooth is an m1 based on its morphology and proportions. The differences then cited by Koungoulos *et al.* (2024) to illustrate how PM 26591 differs from specimens of *P. tumbuna* may then be equally well or better explained by the specimen representing an m1 rather than it representing an undescribed species. PM 26591 was described as differing from the dp3 of *P. tumbuna* specimen PNG 82-40-13 as follows: '...the protoloph[id] and hypoloph[id] are subequal in width rather than the latter being considerably wider; the lophid ridges appear somewhat higher and noticeably narrower relative to the base, and the buccal profile protoconid/hypoconid to the crown base is more strongly sloped with the dorsal-most portion presenting mildly convex whilst the ventral-most appears mildly concave (this pattern being more pronounced for the hypoconid),' (Koungoulos *et al.* 2024, p. 4).

There are certain features of PM 26591 that suggest it to be an m1. Firstly, PM 26591 is large (11.36 mm long), more similar in size to the m1 and m2 of *P. tumbuna* than to the dp3. If it is an m1 or m2, then the difference in size between PM 26591 and the teeth of the comparative specimens becomes negligible, or at least much less significant. The protolophid and hypolophid (or trigonid and talonid) are subequal in width, which is typical of the m1 and m2 of most macropodines, as in *P. tumbuna* referred specimen PNG 82-40-9 (Fig. 82g). In *P. tumbuna* the paracristid is more lingually situated relative to the protoconid in the m1 and m2 than in the dp3. The paracristid of PM 26591 is centrally rather than buccally situated, very similar to that in the m1 and m2 of PNG 82-40-9, suggesting that it is not a dp3. PM 26591 is described as differing from the dp3 of *P. tumbuna* in having a narrower protolophid and hypolophid relative to the lophid bases. However, as is visible in the dp3 and molars of *P. tumbuna* specimen PNG 82-40-9, the protolophid and hypolophid are narrower relative to the lophid bases in the m1 and more so in the m2. This may explain the perceived difference in PM 26591. The anterolingual margin is rounded and convex in the m1 and m2 of *P. tumbuna*, and is straighter and flatter in the dp3. The anterolingual margin of PM 26591 is slightly convex in the manner of the m1 of PNG 82-40-9, not flattened and narrowed, leading to a central and anteriorly protruding rounded point at the anterior tip of the paracristid, in the manner of the dp3.

We agree that the buccal margin of the lophids is unusually sloped, but note that the buccal margins of the lophids of the molars are slightly more sloped in the m1 and m2, as the protoconid and hypoconid are more lingually situated. So, the degree to which PM 26591 differs from the compared specimens in this regard would likely be reduced if it is indeed an m1 or m2. It is possible that this is the unusual dp3 of an undescribed species, but there is perhaps better reason to believe that it is an m1 or m2. If it is the latter, the case for it as evidence of an undescribed species of *Protemnodon* is considerably weakened, without repeating the comparative analysis. We consider the specimen to probably represent an m1, and allocate it to *P.* sp. cf. *P. tumbuna*.

Results

Skeletal dimensions and proportions

The following plots show those dimensions that are directly referred to in the 'Systematic palaeontology' section above.

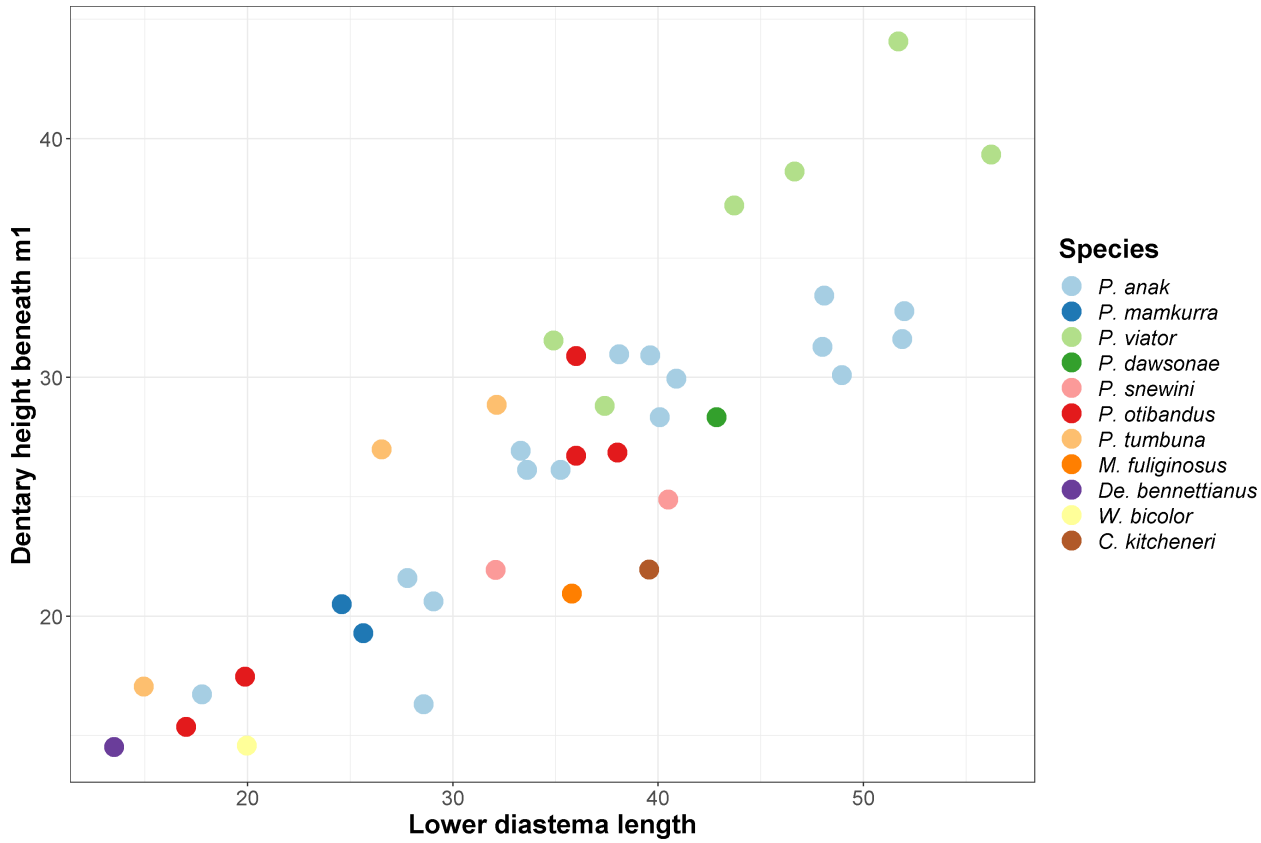

FIGURE 110. scatterplot of lower (mandibular) diastema length versus height of the mandibular corpus beneath m1 in specimens of *P. anak*, *P. mamkurra* **sp. nov.**, *P. viator* **sp. nov.**, *P. dawsonae* **sp. nov.**, *P. snewini*, *P. otibandus*, *P. tumbuna*, and four extrageneric taxa.

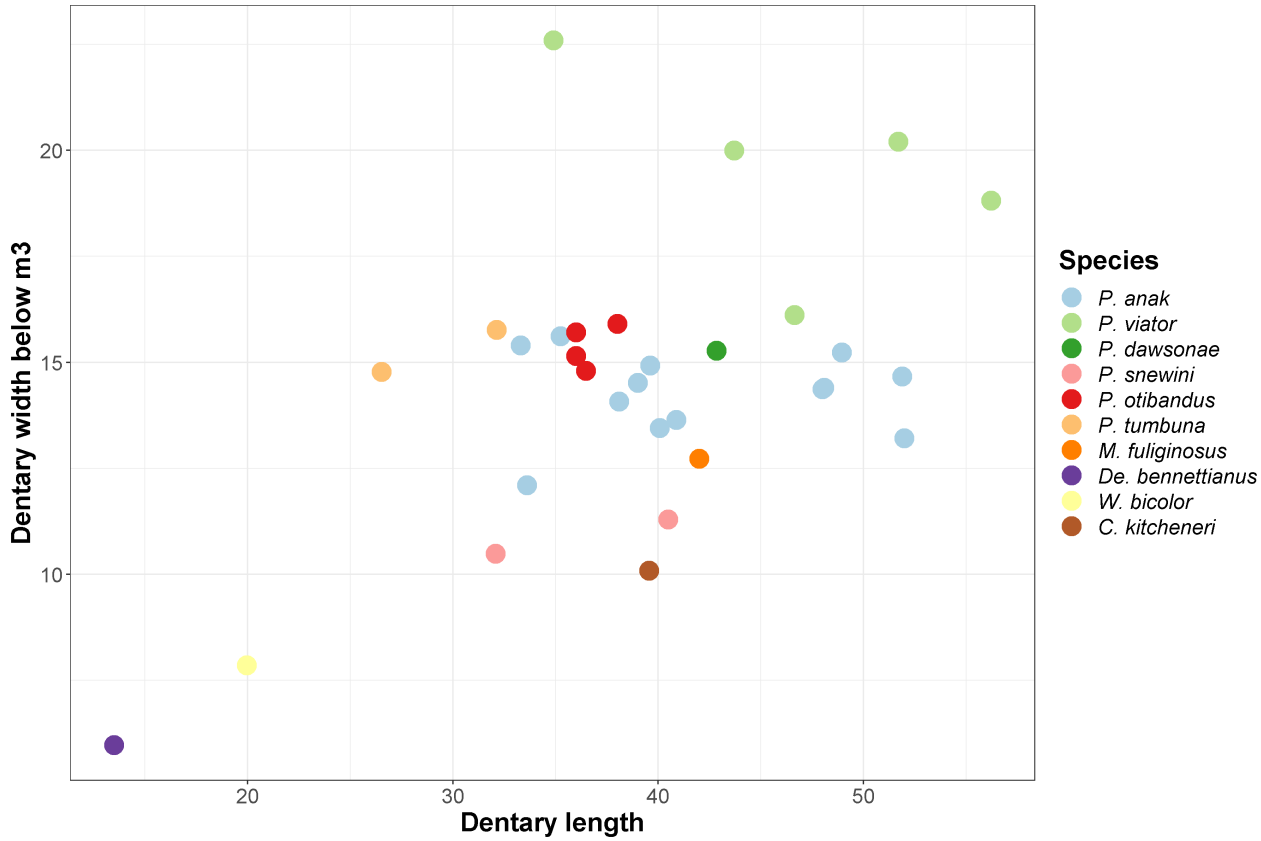

FIGURE 111. scatterplot of anterior dentary length (distance from the anterior margin of the masseteric fossa to the base of the crown of i1) versus width of the mandibular corpus beneath m3 in specimens of *P. anak*, *P. viator* **sp. nov.**, *P. dawsonae* **sp. nov.**, *P. snewini*, *P. otibandus*, *P. tumbuna*, and four extrageneric taxa.

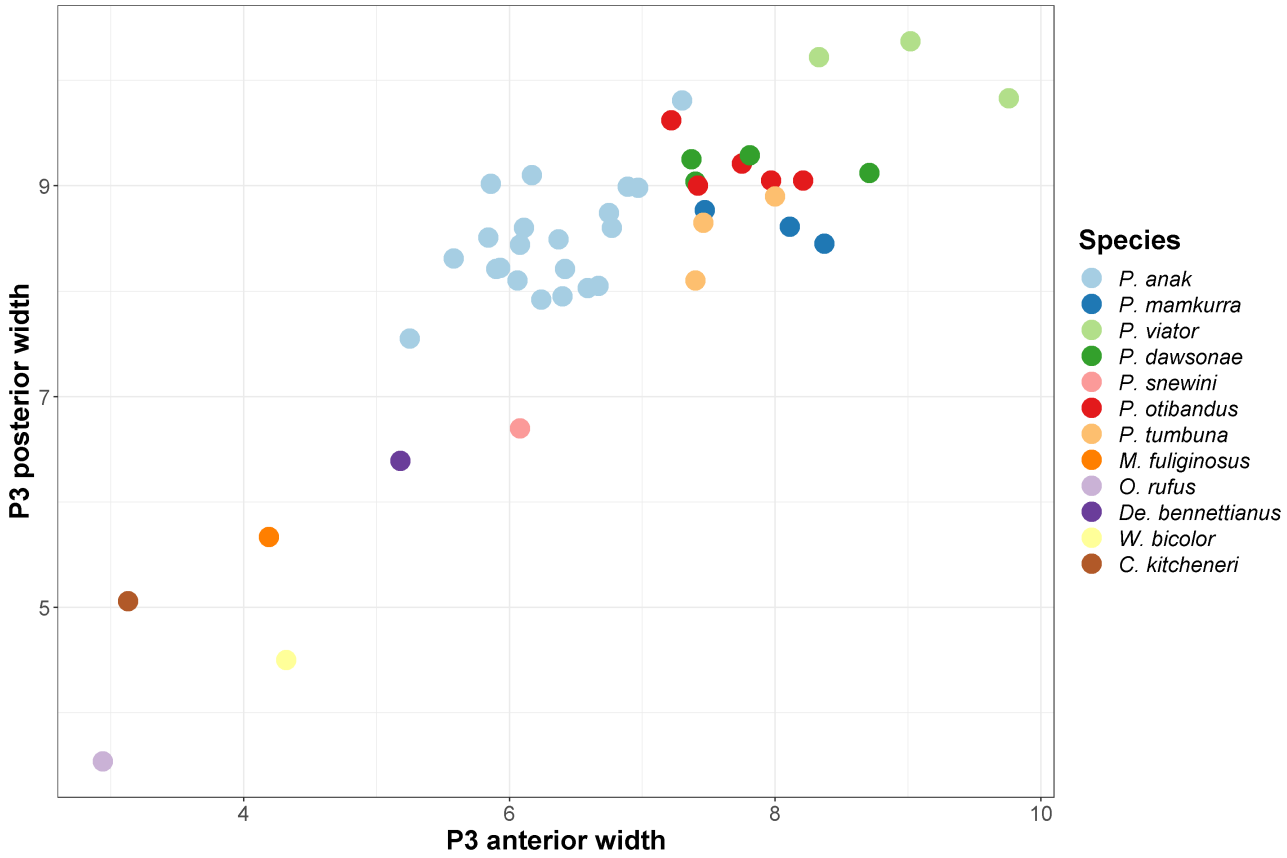

FIGURE 112. scatterplot of P3 anterior width versus P3 posterior width of P3 in specimens of *P. anak*, *P. mamkurra* **sp. nov.**, *P. viator* **sp. nov.**, *P. dawsonae* **sp. nov.**, *P. otibandus*, *P. tumbuna*, *P. snewini*, and five extrageneric taxa.

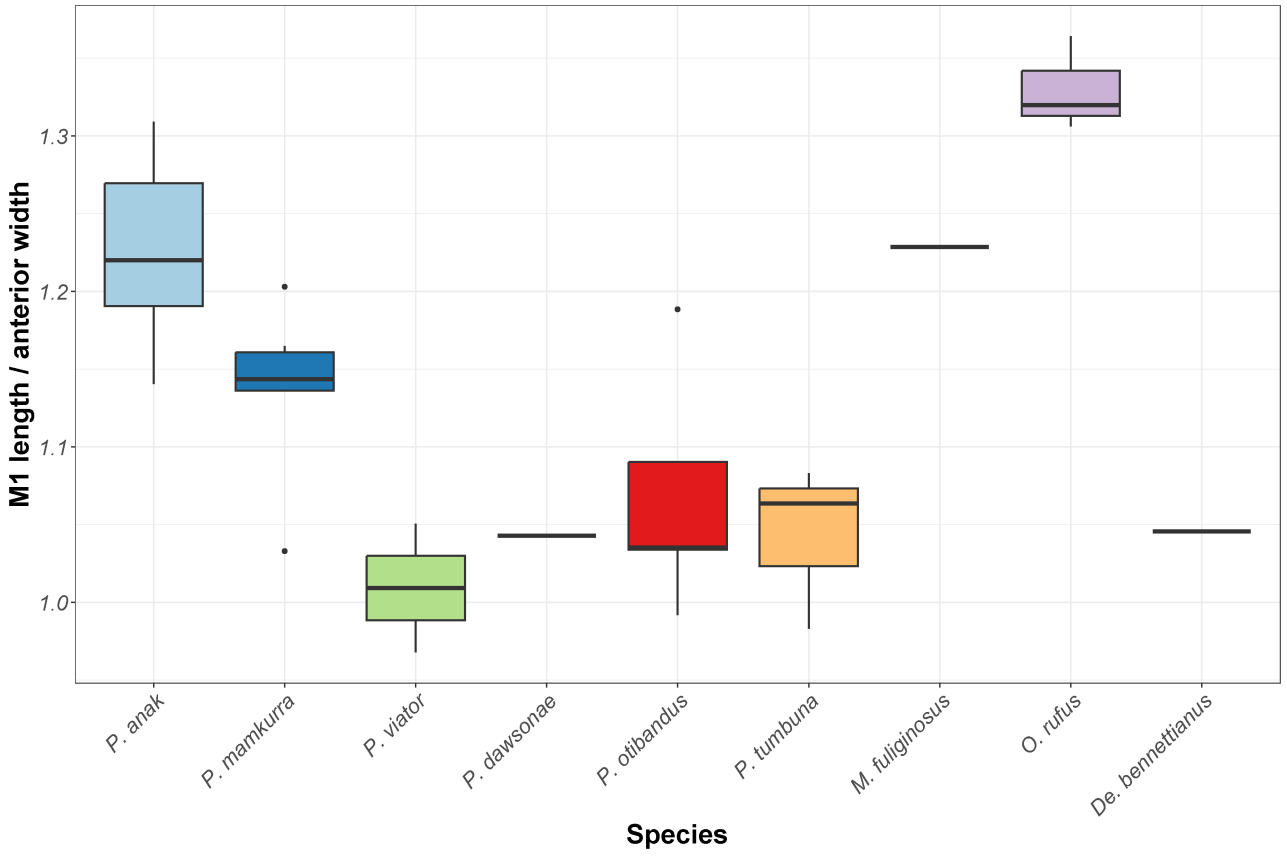

FIGURE 113. boxplot of M1 length divided by anterior width in specimens of *P. anak*, *P. mamkurra* **sp. nov.**, *P. viator* **sp. nov.**, *P. dawsonae* **sp. nov.**, *P. otibandus*, *P. tumbuna*, and three extrageneric taxa.

the larger specimens of *P. snewini*, *M. fuliginosus* and *C. kitcheneri*. *Protemnodon anak* shows a wide range of values across the centre of the spread of species of *Protemnodon*, with the shorter, broader specimens having similar values to *P. otibandus*. *Protemnodon tumbuna* shows the smallest dentary length values of the genus, but similar widths to *P. otibandus*, *P. dawsonae* **sp. nov.** and the widest specimens of *P. anak*. *Protemnodon snewini* shows smaller dentary widths beneath the m3 than other species of *Protemnodon* with similar dentary lengths, more similar to *M. fuliginosus* and *C. kitcheneri*.

Dentary

Figure 110: of the species of *Protemnodon*, the height of the mandibular corpus beneath the m1 is greatest in *P. viator* **sp. nov.**, which has greater absolute values for lower diastema length and mandibular corpus height than *P. tumbuna* but show a similarly high mandibular corpus to diastema ratio. The largest specimens of *P. anak* have similar lower diastema lengths to those of *P. viator* **sp. nov.**, but with lower dentary height values; *P. anak* has a wide spread of values, encompassing the graphed range of *P. otibandus* and *P. dawsonae* **sp. nov.** The two specimens of *P. mamkurra* **sp. nov.** are juvenile, and place at the lower end of the range of *P. anak*; *P. snewini* shows fairly low dentary heights relative to diastema length, slightly higher than *C. kitcheneri* and *M. fuliginosus*.

Figure 111: *Protemnodon viator* **sp. nov.** shows the greatest values for the width of the mandibular corpus beneath the m3, with a maximum value considerably greater than that of the other species of *Protemnodon*; the length of the dentary of *P. viator* **sp. nov.** is similar to *P. anak*, *P. dawsonae* **sp. nov.** and

Dentition

Upper (all species)

Figure 112: The species of *Protemnodon* have absolutely greater P3 anterior and posterior widths than *M. fuliginosus*, *O. rufus*, *De. bennettianus*, *W. bicolor* and *C. kitcheneri*. With the exception of *P. snewini*, they also have relatively larger anterior widths than those of the listed extrageneric taxa. *Protemnodon anak* has generally narrower anterior widths than other species of *Protemnodon* except *P. snewini,* which has a similar anterior width but a relatively narrower posterior width. *Protemnodon mamkurra* **sp. nov.**, *P. tumbuna*, *P. dawsonae* **sp. nov.** and *P. otibandus* group close together, with slightly greater anterior widths than *P. anak*. *Protemnodon viator* **sp. nov.** has the largest anterior and posterior widths for the P3.

Figure 113: *Protemnodon anak* has the proportionally narrowest M1 anterior loph of any species of the genus, with similar values to *M. fuliginosus* and slightly lower than *O. rufus*. The M1 anterior loph of *P. mamkurra* **sp. nov.** is relatively broader than *P. anak* and narrower than *P. viator* **sp. nov.**, *P. dawsonae* **sp. nov.**, *P. otibandus* and *P. tumbuna*, all of which are similarly broad, comparable with that of *De. bennettianus*.

Figure 114: The M2 of *P. anak* shows generally relatively narrower anterior lophs than those of *P. mamkurra* **sp. nov.**, *P. viator* **sp. nov.**, and *P. dawsonae* **sp. nov.**, which all have similar values; the M2s of *P. snewini*, *P. otibandus* and *P. tumbuna* are the proportionally broadest of the species of *Protemnodon*, with similar values to that of *De. bennettianus* and slightly broader than those of *W. bicolor* and *C. kitcheneri*.

Figure 115:In the widths of the M3 anterior loph relative to the length, *P. anak* and *P. mamkurra* **sp. nov.** are the narrowest of the species of *Protemnodon*, similar to *W. bicolor* and the broader specimens of *M. fuliginosus*; that of *P. snewini* is slightly broader, similar to the narrowest specimens of *P. otibandus*; those of *P. viator* **sp. nov.**, *P. dawsonae* **sp. nov.**, *P. otibandus* and *P. tumbuna* are broadest of the genus, occupying similar space, slightly narrower than that of *De. bennettianus*.

*Upper (*P. mamkurra **sp. nov.**, P. viator **sp. nov.** *and* P. mamkurra **sp. nov.** *or* viator **sp. nov.***)*

Figures 116 & 117: the anterior width of the P3 is similar in the specimens of *P. mamkurra* **sp. nov.** to those of *P. viator* **sp. nov.**, with three specimens each spread in a similar area to each other and to the specimens of *P. mamkurra* **sp. nov.** or *viator* **sp. nov.** The posterior width of the P3 is greater in the three specimens of *P. viator* **sp. nov.** than in the two of *P. mamkurra* **sp. nov.**, with the specimens of *P. mamkurra* **sp. nov.** or *viator* **sp. nov.** spread around both groupings and across the area between the two.

Figures 118–120: the six specimens of *P. mamkurra* have narrower m1 anterior widths than the two of *P. viator*, with the specimens of *P. mamkurra* **sp. nov.** or *viator* **sp. nov.** showing a similar spread to those of *P. mamkurra* **sp. nov.** *Protemnodon mamkurra* **sp. nov.** and *P. viator* **sp. nov.** show similar lengths and anterior widths in the M2 and M3, with the specimens of *P. mamkurra* **sp. nov.** or *viator* **sp. nov.** spread in a similar range.

Lower (all)

Figure 121: The species of *Protemnodon* possess a considerably shorter p3 relative to m3 length than *De. bennettianus*, and a longer p3 relative to m3 length than *W. bicolor* and *C. kitcheneri*. *Protemnodon anak* exhibits a wide range, including within their range that shown by most of the other species; *P. dawsonae* **sp. nov.**, *P. snewini*, *P. otibandus* and *P. tumbuna* have similar dimensions to each other, in the upper half of the range of *P. anak*; *P mamkurra* **sp. nov.** values are similar to the lower specimens of *P. anak*. The range of *P. viator* **sp. nov.** extends to having the relatively shortest p3 of the species of *Protemnodon*.

Figure 122: The species of *Protemnodon* have larger m2 lengths and anterior widths than those of *De. bennettianus*, *W. bicolor* and *C. kitcheneri*, with m2s generally relatively wider than those of *M. fuliginosus* and *O. rufus*. *Protemnodon snewini* has the smallest m2 dimensions of the sample of the species of *Protemnodon*, slightly smaller than *P. tumbuna*. *Protemnodon anak*, *P. dawsonae* **sp. nov.** and *P. otibandus* have similar values, while *P. mamkurra* and *P. dawsonae* **sp. nov.** are in the top end of the range of *P. anak*. *Protemnodon viator* **sp. nov.** has the largest values.

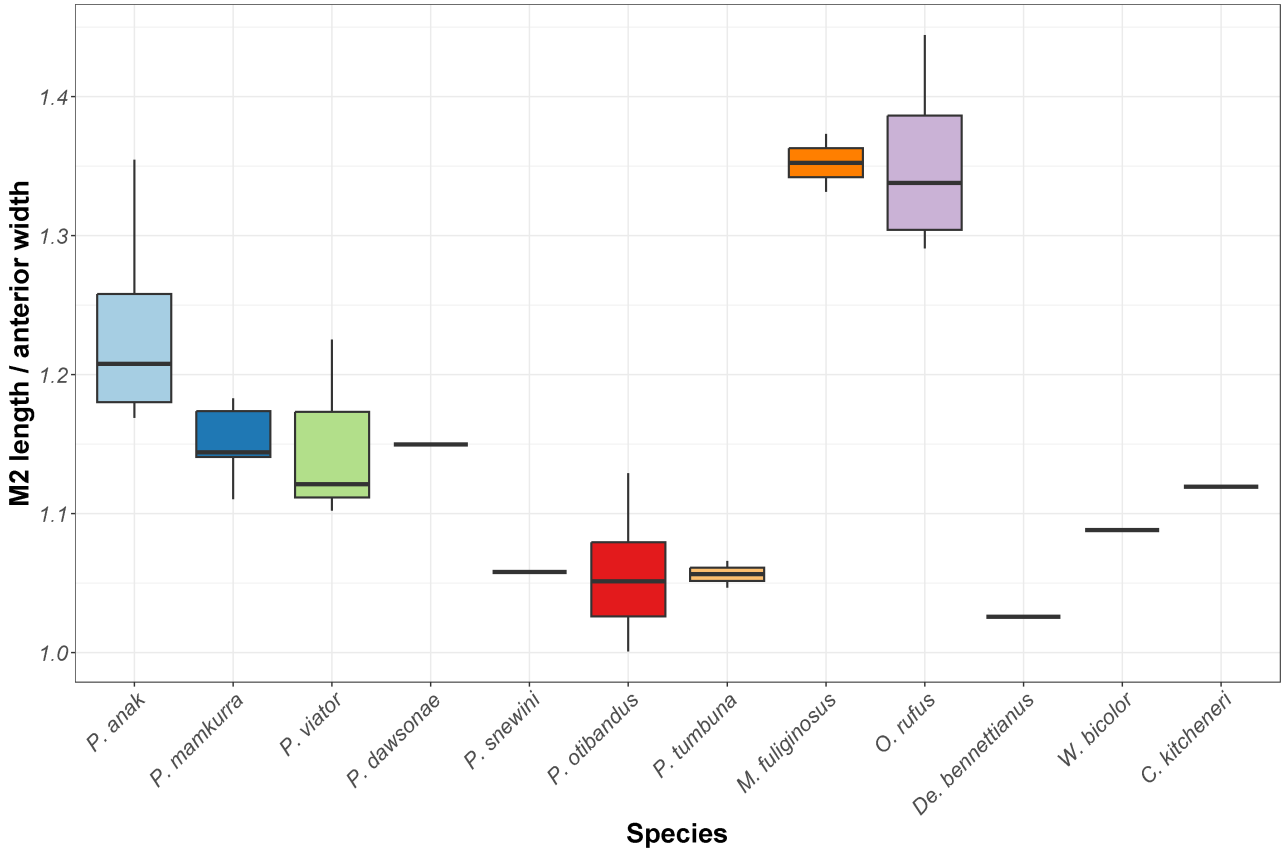

FIGURE 114. boxplot of M2 length divided by anterior width in specimens of *P. anak*, *P. mamkurra* **sp. nov.**, *P. viator* **sp. nov.**, *P. dawsonae* **sp. nov.**, *P. snewini*, *P. otibandus*, *P. tumbuna*, and five extrageneric taxa.

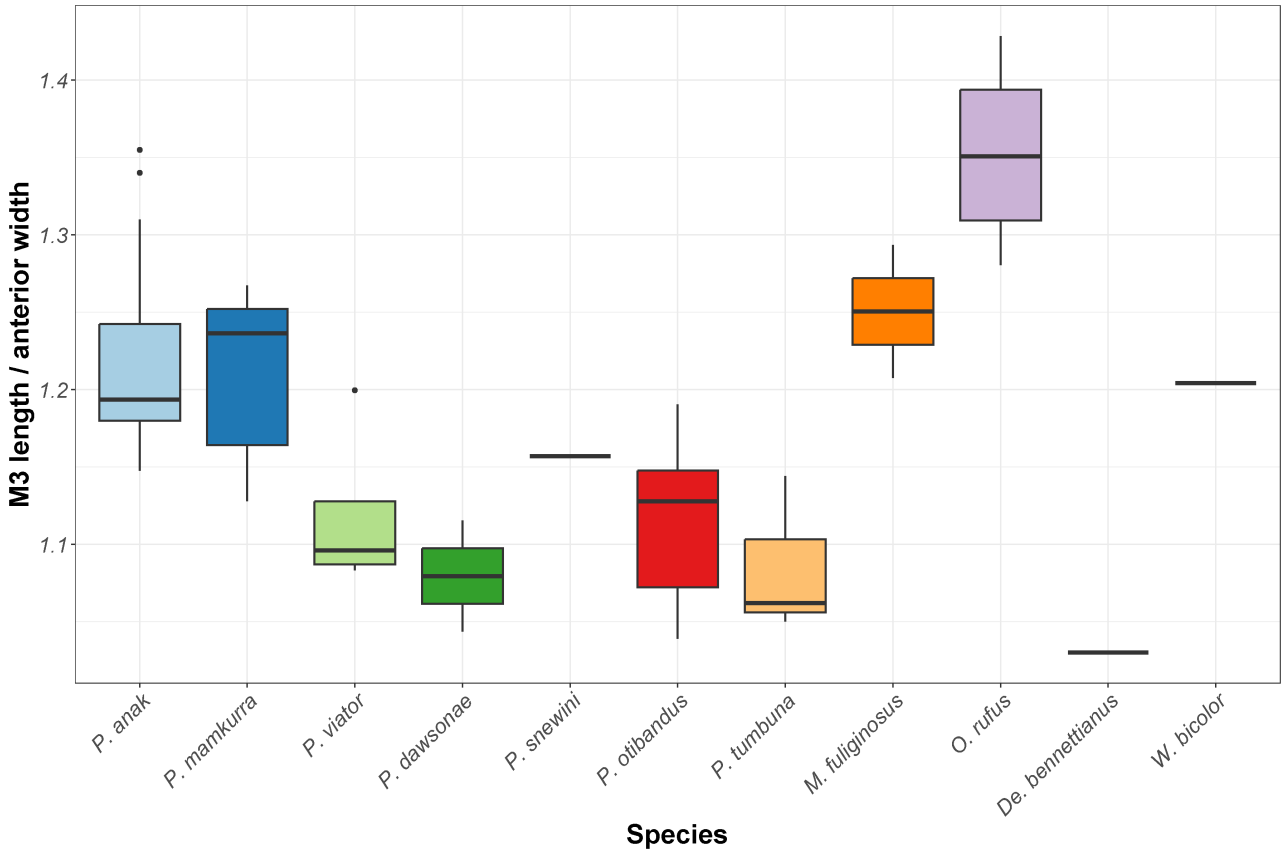

FIGURE 115. boxplot of M3 length divided by anterior width in specimens of *P. anak*, *P. mamkurra* **sp. nov.**, *P. viator* **sp. nov.**, *P. dawsonae* **sp. nov.**, *P. snewini*, *P. otibandus*, *P. tumbuna*, and four extrageneric taxa.

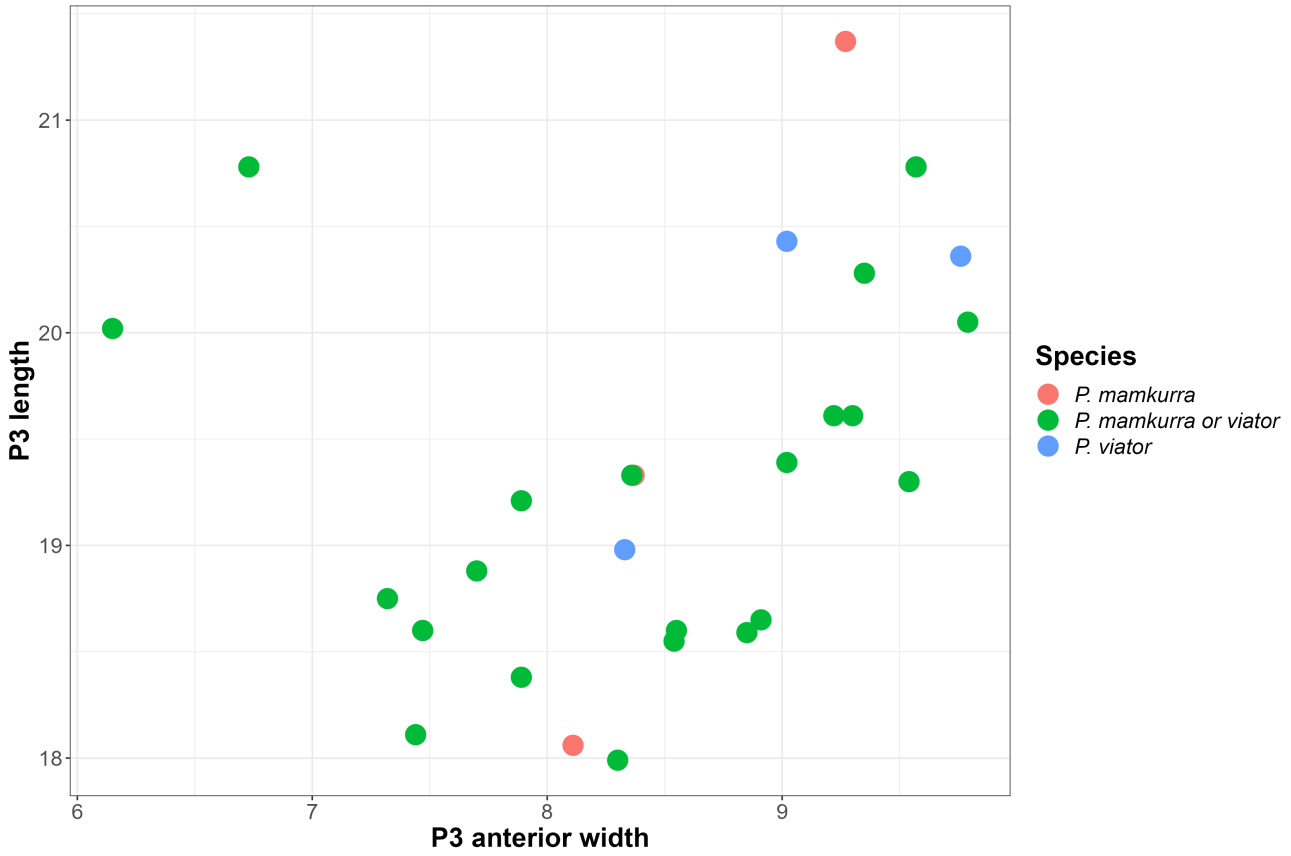

FIGURE 116. scatterplot of P3 anterior width versus length in specimens of *P. mamkurra* **sp. nov.**, *P. viator* **sp. nov.**, and specimens allocated to *P. mamkurra* **sp. nov.** or *viator* **sp. nov.**

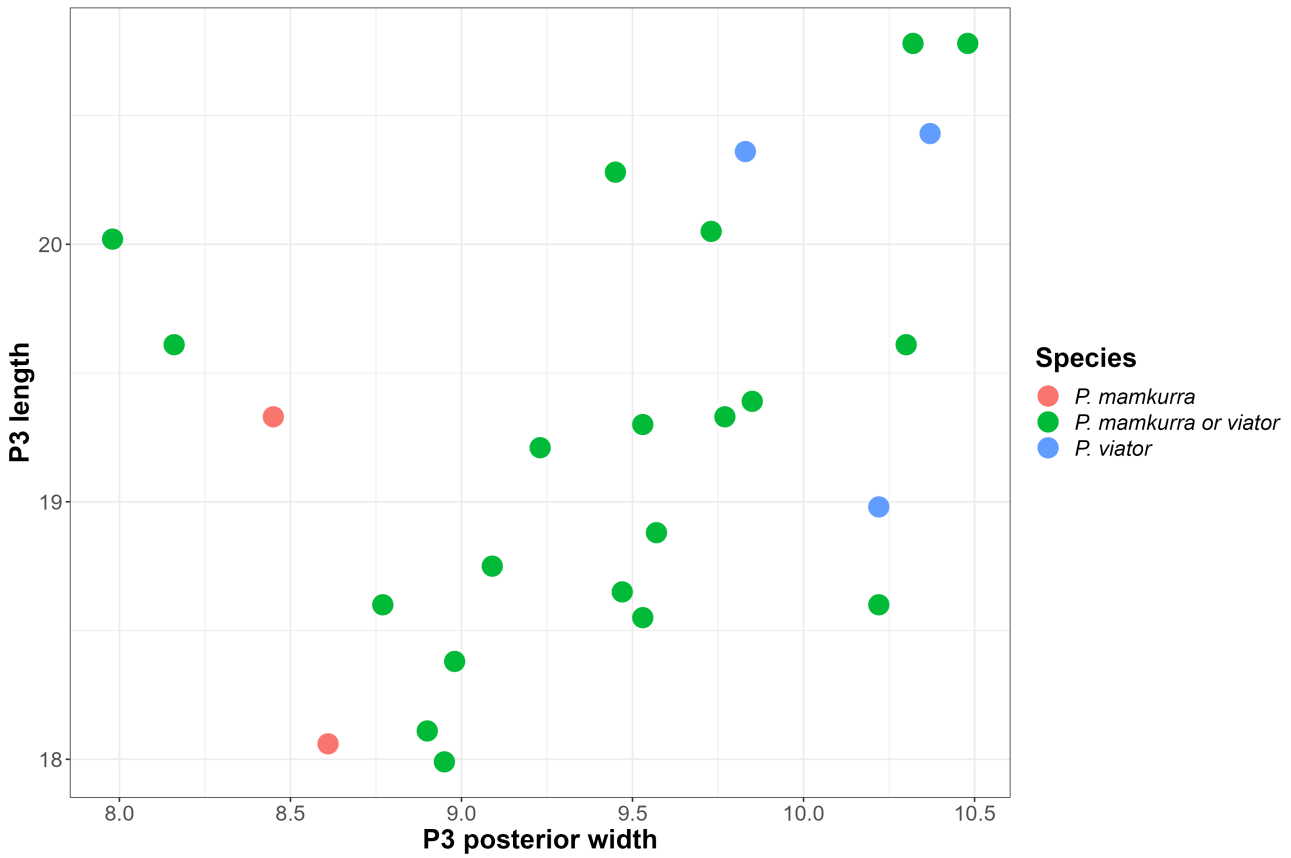

FIGURE 117. scatterplot of P3 posterior width versus length in specimens of *P. mamkurra* **sp. nov.**, *P. viator* **sp. nov.**, and specimens allocated to *P. mamkurra* **sp. nov.** or *viator* **sp. nov.**

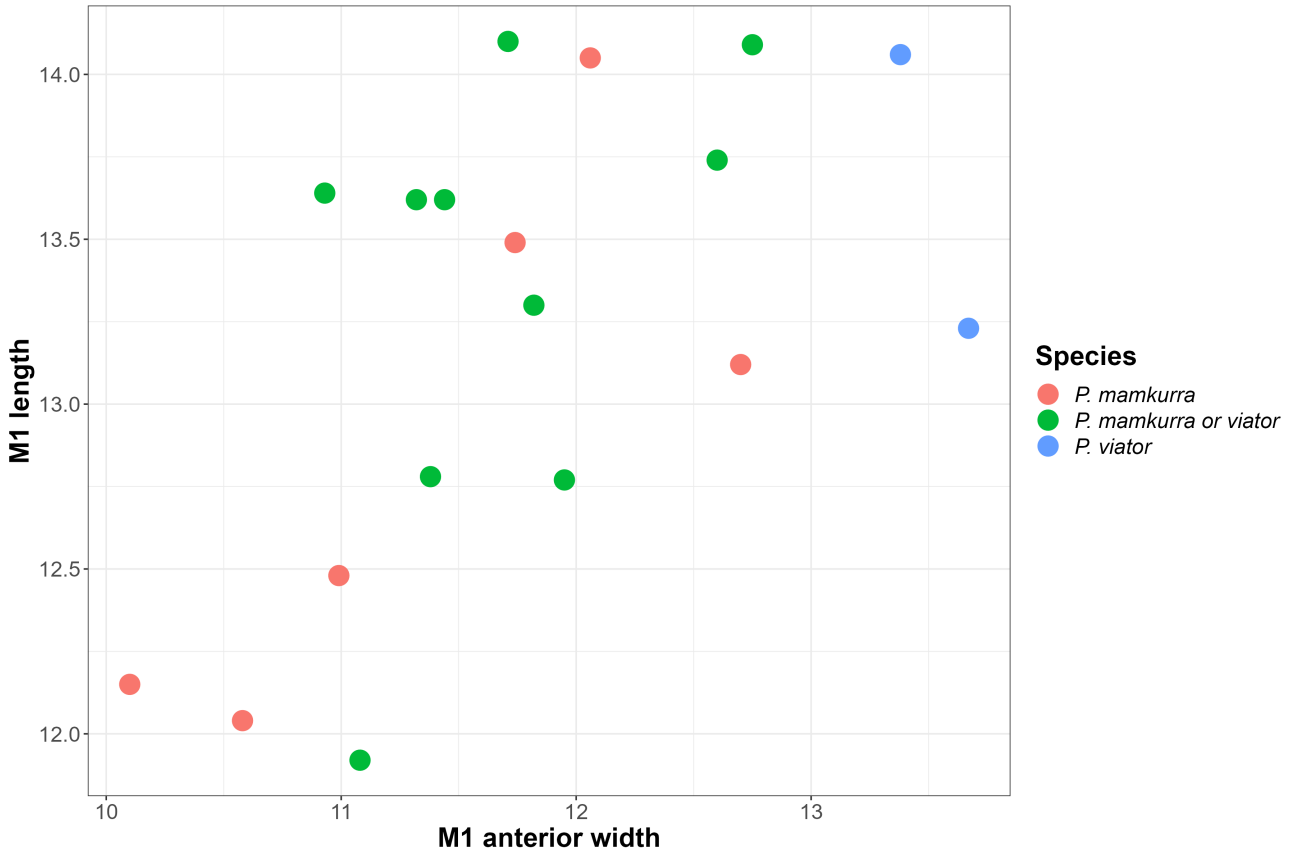

FIGURE 118. scatterplot of M1 anterior width versus length in specimens of *P. mamkurra* **sp. nov.**, *P. viator* **sp. nov.**, and specimens allocated to *P. mamkurra* **sp. nov.** or *viator* **sp. nov.**

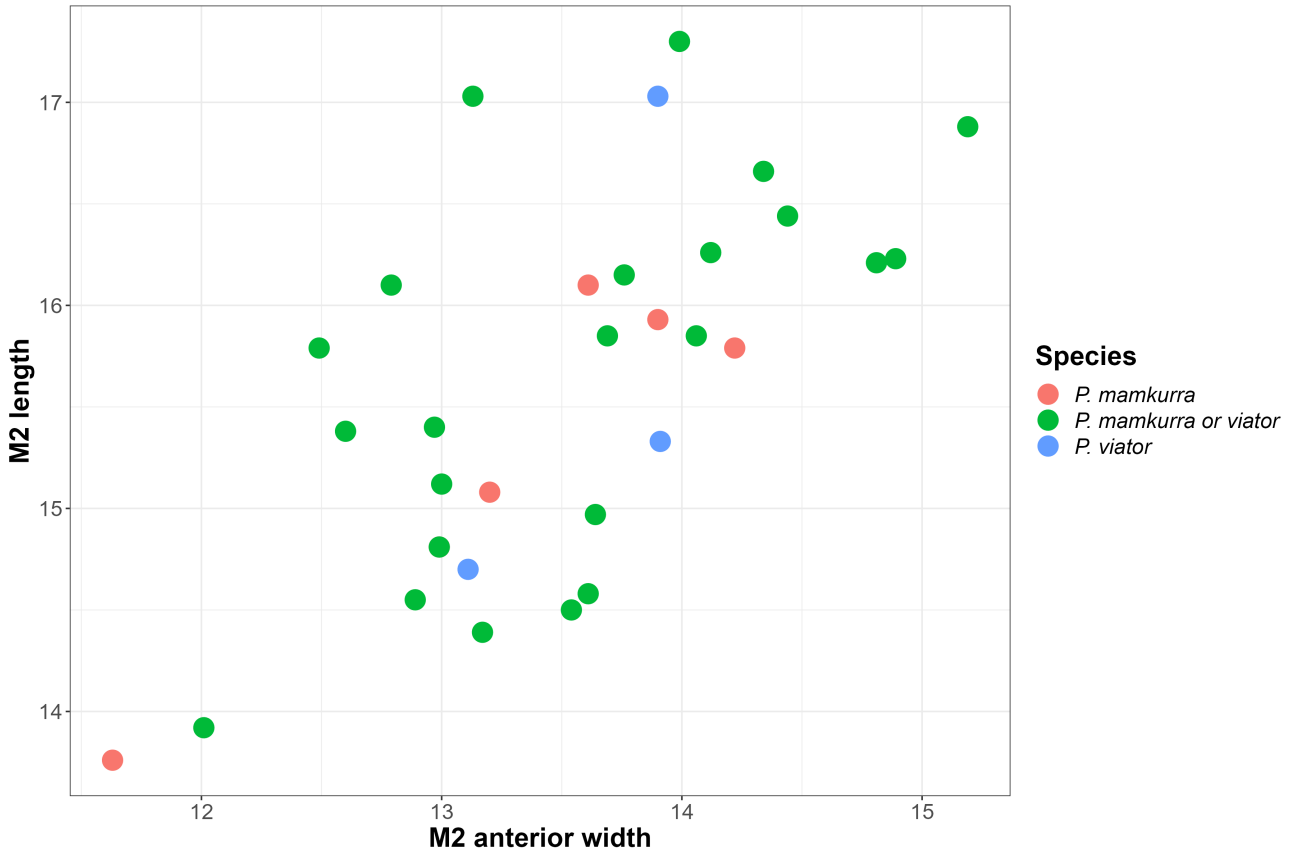

FIGURE 119. scatterplot of M2 anterior width versus length in specimens of *P. mamkurra* **sp. nov.**, *P. viator* **sp. nov.**, and specimens allocated to *P. mamkurra* **sp. nov.** or *viator* **sp. nov.**

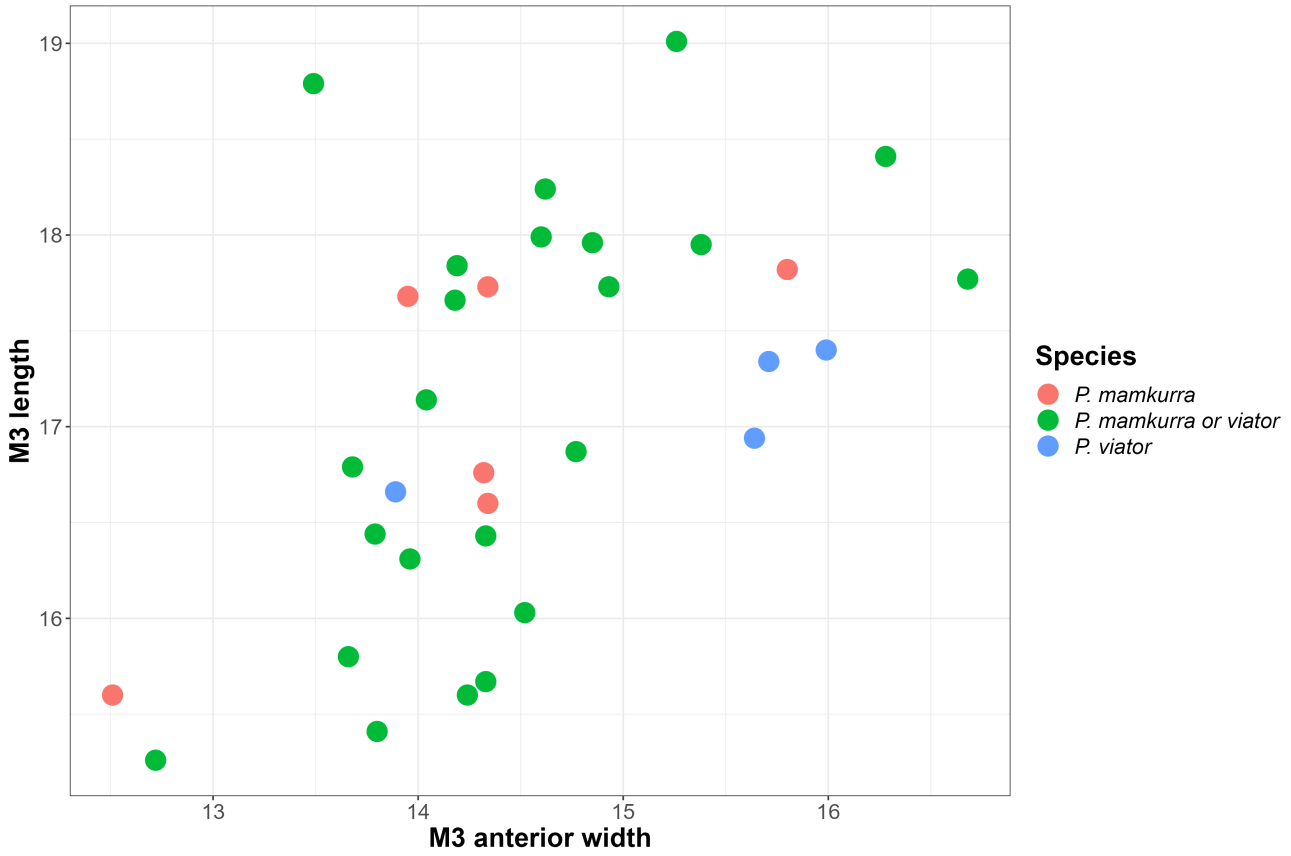

FIGURE 120. scatterplot of M3 anterior width versus length in specimens of *P. mamkurra* **sp. nov.**, *P. viator* **sp. nov.**, and specimens allocated to *P. mamkurra* **sp. nov.** or *viator* **sp. nov.**

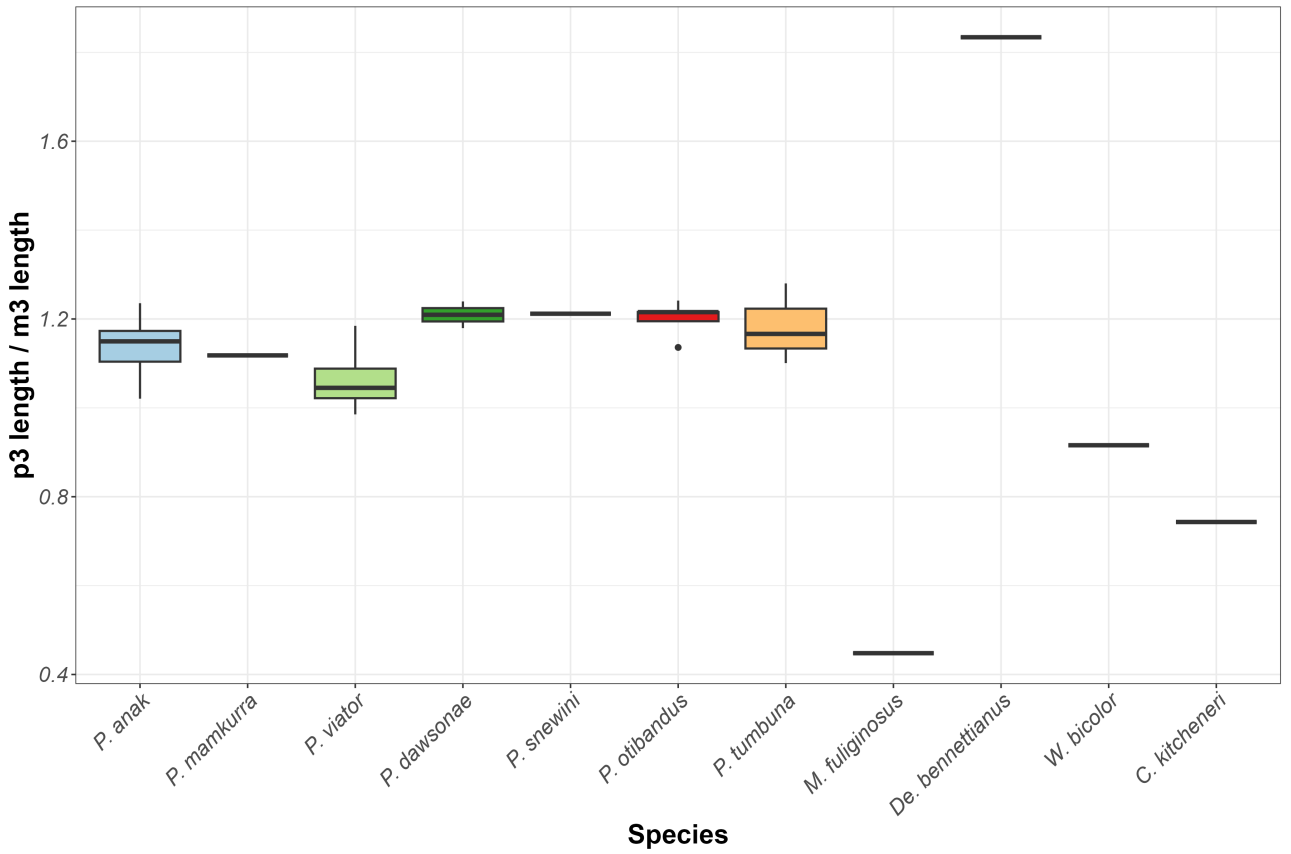

FIGURE 121. boxplot of p3 length divided by m3 length in specimens of *P. anak*, *P. mamkurra* **sp. nov.**, *P. viator* **sp. nov.**, *P. dawsonae* **sp. nov.**, *P. snewini*, *P. otibandus*, *P. tumbuna*, and four extrageneric taxa.

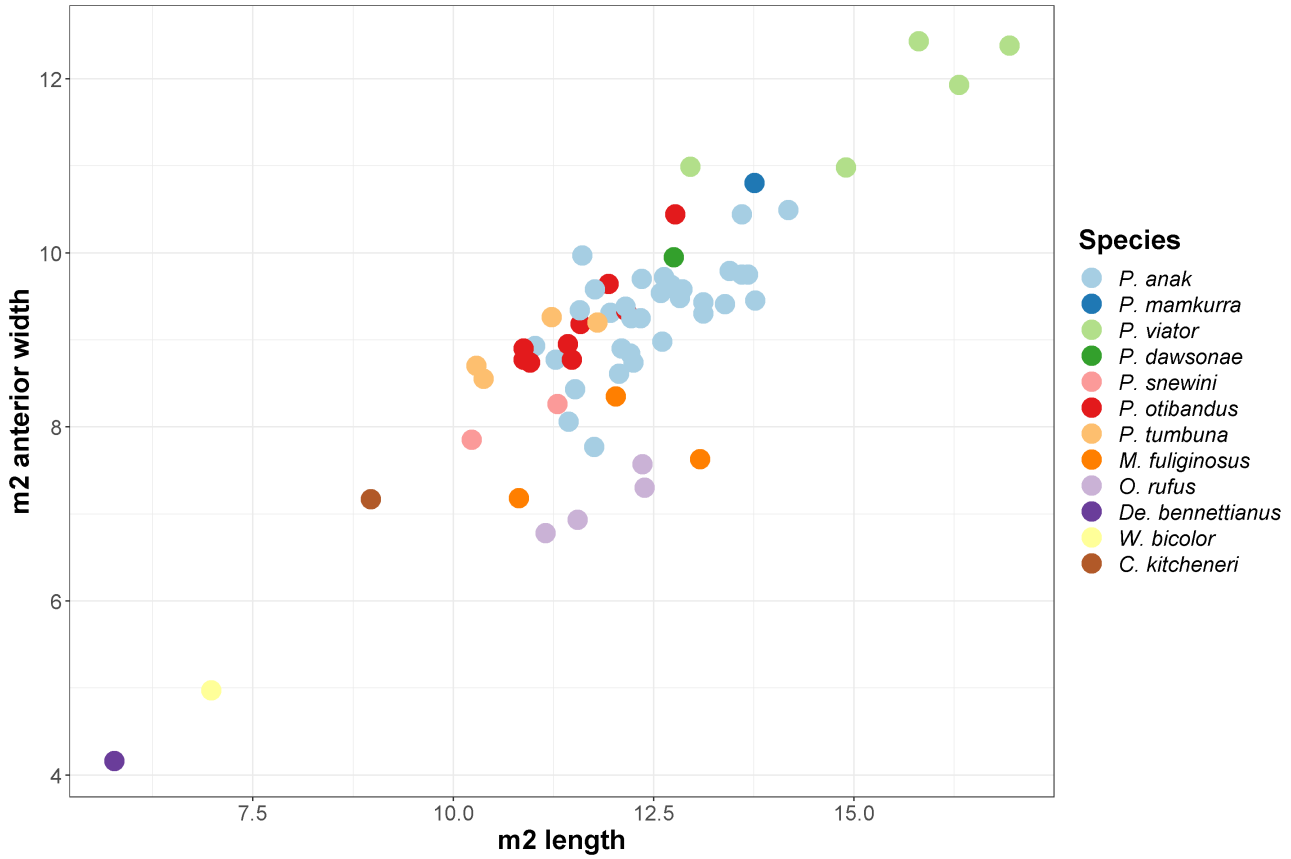

FIGURE 122. scatterplot of m2 length versus anterior width in specimens of *P. anak*, *P. mamkurra* **sp. nov.**, *P. viator* **sp. nov.**, *P. dawsonae* **sp. nov.**, *P. snewini*, *P. otibandus*, *P. tumbuna*, and five extrageneric taxa.

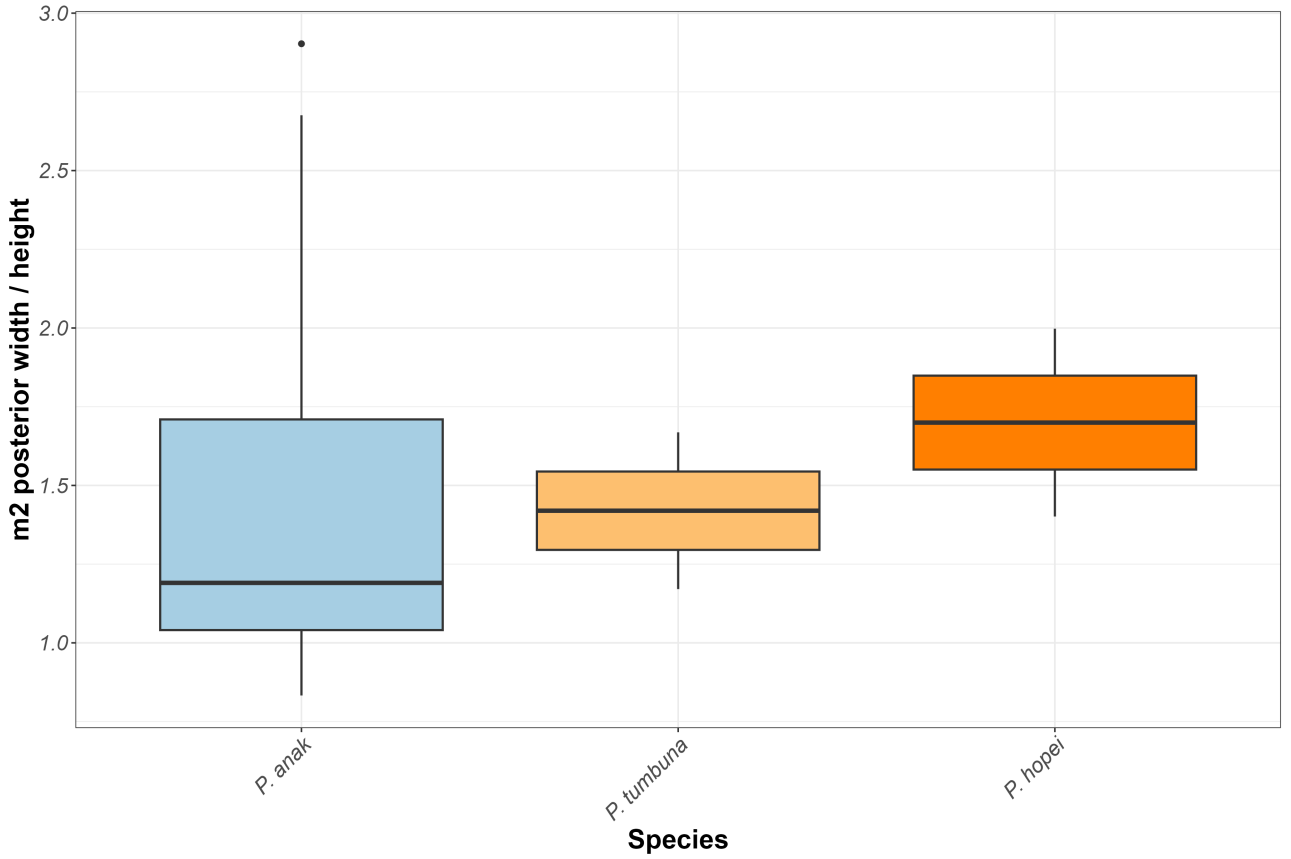

FIGURE 123. boxplot of m2 posterior width divided by posterior crown height in specimens of *P. anak*, *P. tumbuna*, and specimens previously allocated to *P. hopei*.

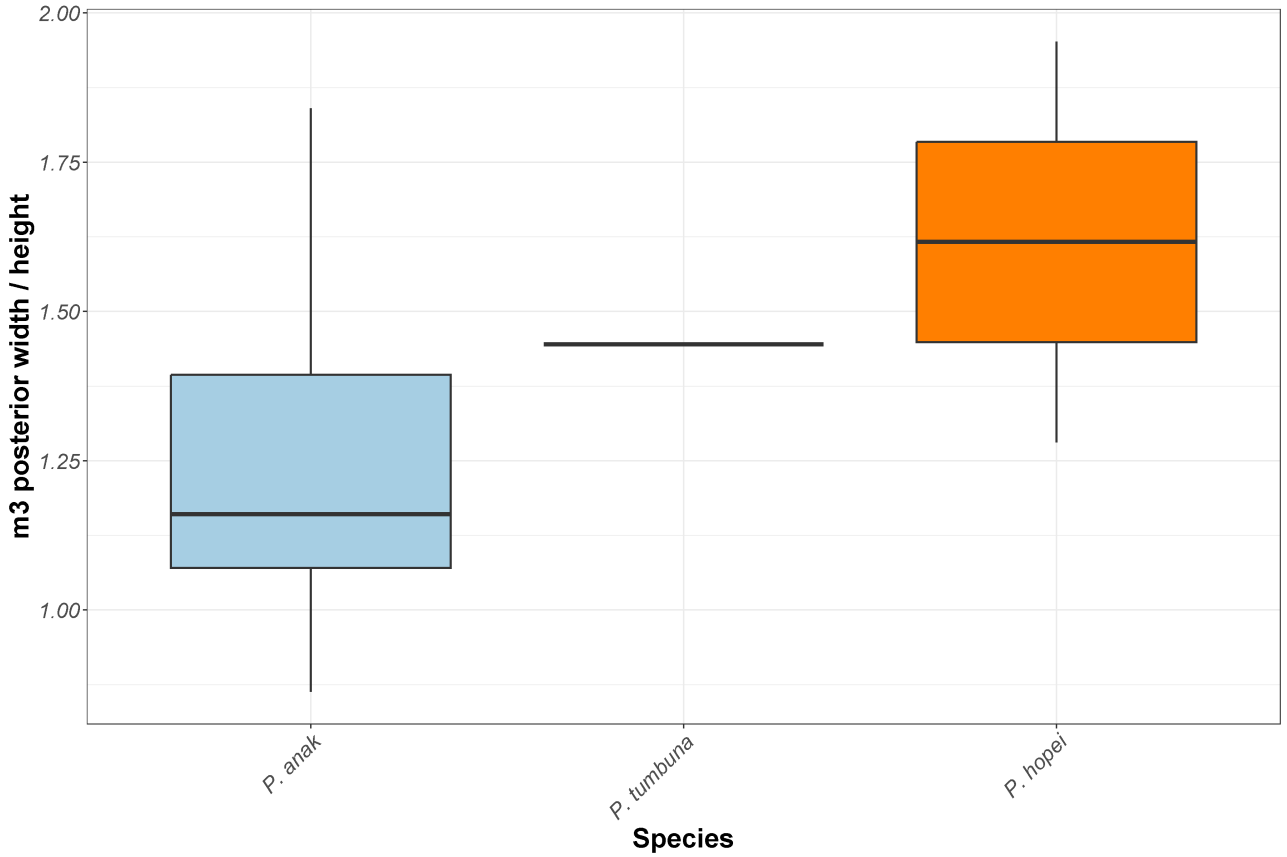

FIGURE 124. boxplot of m3 posterior width divided by posterior crown height in specimens of *P. anak*, *P. tumbuna*, and specimens previously allocated to *P. hopei*.

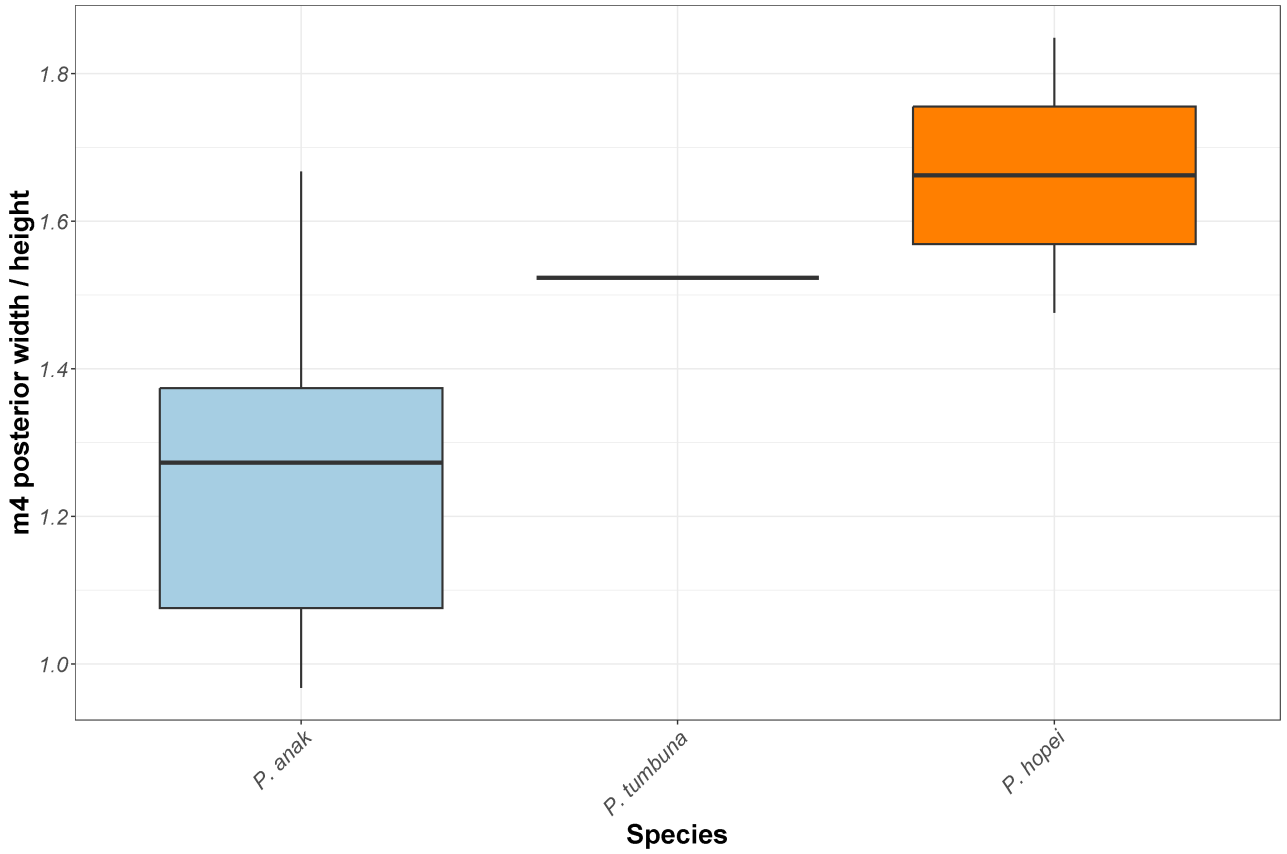

FIGURE 125. boxplot of m4 posterior width divided by posterior crown height in specimens of *P. anak*, *P. tumbuna*, and specimens previously allocated to *P. hopei*.

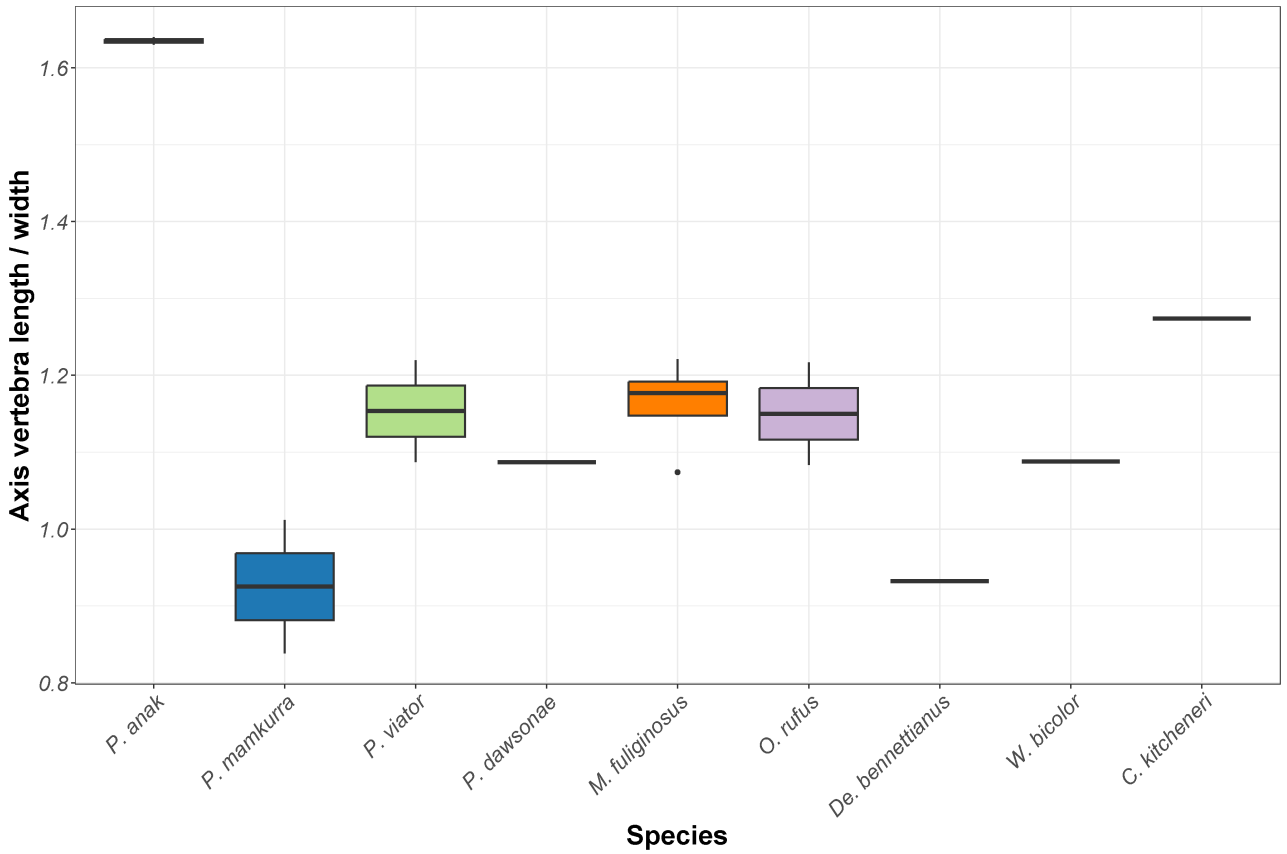

FIGURE 126. boxplot of axis vertebra (C2) length divided by width across cranial articular surfaces in specimens of *P. anak*, *P. mamkurra* **sp. nov.**, *P. viator* **sp. nov.**, *P. dawsonae* **sp. nov.**, and five extrageneric taxa.

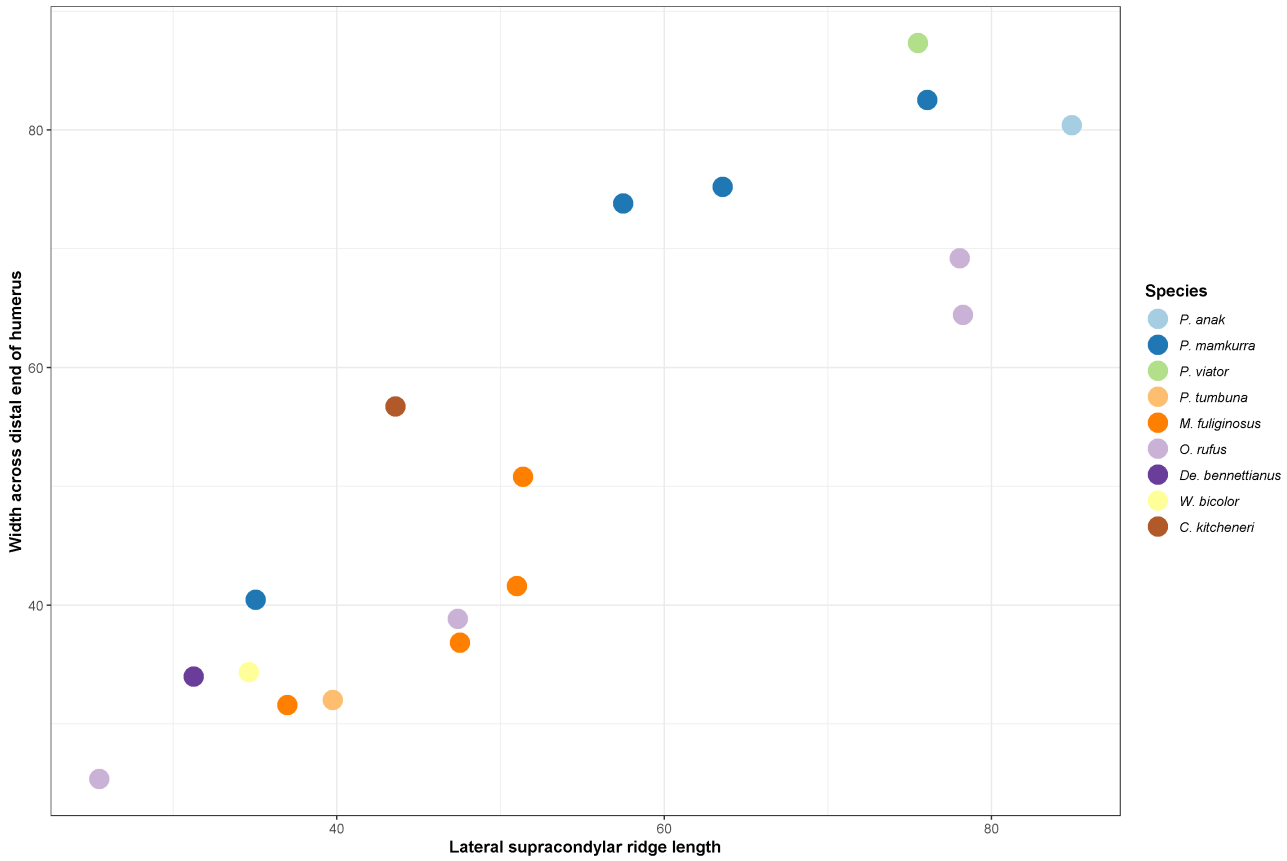

FIGURE 127. scatterplot of humerus supracondylar ridge length versus width across distal end in specimens of *P. anak*, *P. mamkurra* **sp. nov.**, *P. viator* **sp. nov.**, *P. tumbuna*, and five extrageneric taxa.

*Lower (*P. anak, P. tumbuna *and* P. hopei*)*

Figures 123–125: *Protemnodon anak* shows a wide range of m2, m3 and m4 posterior width relative to posterior lingual crown height compared to that shown by the specimens of *P. tumbuna* from Nombe Rockshelter and those historically assigned to *P. hopei*; in the m2, *P. tumbuna* has similar values to the centre of the range of *P. anak*, but are relatively slightly higher crowned in the m2 and slightly more so in the m4. *Protemnodon hopei* overlap with the higher values of *P. anak* and *P. tumbuna* in the m2, are mostly higher crowned than the other two taxa in the m3, and are slightly more so in the m4.

Axial skeleton

Figure 126: The axis vertebra of *P. anak* is the most elongate, and that of *P. mamkurra* **sp. nov.** is the shallowest and most robust. *Protemnodon dawsonae* **sp. nov.** and *P. viator* **sp. nov.** have a similarly proportioned axis vertebra to those of *M. fuliginosus*, *O. rufus* and *W. bicolor*, but are slightly shorter and broader than *C. kitcheneri*.

Forelimb

Figure 127: The dimensions of the humeri of species of *Protemnodon* fall into two semi-distinct groups spread along a growth series; *P. mamkurra* **sp. nov.**, *P. viator* **sp. nov.**, *C. kitcheneri* and *De. bennettianus* have wider humeral distal ends and shorter supracondylar ridges, and *P. anak*, *P. tumbuna*, *M. fuliginosus* and *O. rufus* possess narrower distal ends and longer supracondylar ridges.

Figure 128: The ulnae of the species of *Protemnodon* also fall into two groups spread along a growth series; *P. anak*, *P. viator* **sp. nov.**, *C. kitcheneri, W. bicolor* and *De. bennettianus* have a longer olecranon and a shorter ulna, while *O. rufus* has a shorter olecranon and a longer ulna.

Figure 129: *Protemnodon mamkurra* **sp. nov.** has the shortest olecranon relative to ulnar shaft height; *P. anak*, *P. otibandus* and *O. rufus* all have similar values, slightly lower than the remaining species. *Protemnodon viator* **sp. nov.** has the relatively longest olecranon of the species of *Protemnodon*, similar to *De. bennettianus* and *W. bicolor*.

Hindlimb

Figure 130: The species of *Protemnodon* are separated from the extrageneric taxa by their much wider iliac crest relative to caudal iliac spine length; of the extrageneric taxa, *De. bennettianus* and *W. bicolor* show the relatively broadest iliac crests. The ranges of the species of *Protemnodon* overlap almost completely; *P. mamkurra* **sp. nov.** shows the relatively narrowest iliac crest and *P. viator* **sp. nov.** shows the relatively broadest.

Figure 131: *Protemnodon mamkurra* **sp. nov.** and *P. viator* **sp. nov.** are separated from the extrageneric taxa by their relatively and absolutely larger acetabular diameter. The maximum ischiatic length for *P. mamkurra* **sp. nov.** and *P. viator* **sp. nov.** is slightly larger than that of *O. rufus*.

Figure 132: The femur of *P. viator* **sp. nov.** is shorter relative to shaft width than in other species of *Protemnodon*, comparable to the relative length of that of *C. kitcheneri*. That of *P. mamkurra* **sp. nov.** is relatively longer, similar to the values of the specimen of *De. bennettianus*. Relatively longer again is that of *P. anak*, which is similarly proportioned to the shorter specimens of *M. fuliginosus* and *O. rufus*. *Protemnodon tumbuna* has the relatively longest femur of the species of *Protemnodon*, proportionally similar to the longer specimens of *O. rufus*.

Figure 133: *Protemnodon viator* **sp. nov.** has a very high crural index (CI), similar to that of *O. rufus*. That of *P. anak* is lower, with a similar value to *M. fuliginosus* and *C. kitcheneri*. That of *P. mamkurra* **sp. nov.** is lower again, similar to *W. bicolor*. *Protemnodon tumbuna* has a low CI, close to that of *De. bennettianus*.

Figure 134: All species of *Protemnodon* have shorter, more robust tibiae than *M. fuliginosus* and *O. rufus*. *Protemnodon viator* **sp. nov.** and *P. snewini* have the most gracile tibiae of the species of *Protemnodon*; *P. anak* has similar values to *W. bicolor*. *Protemnodon tumbuna* has a robust tibia, but slightly less so than *P. mamkurra* **sp. nov.** and *P. otibandus.*

Figure 135: *Protemnodon mamkurra* **sp. nov.** has the broadest calcaneal head relative to calcaneal length of the genus, similar to the ratio seen in *De. bennettianus*. That of *P. otibandus* are relatively slightly narrower than all but the narrowest of *P. mamkurra* **sp. nov.**, similar to the broader head of *P. anak*, which is intermediate between *P. otibandus* and *P. viator* **sp. nov.** That of *P. viator* **sp. nov.** shows the relatively and absolutely narrowest head, with the narrowest specimens sharing similar proportions to the broadest of *M. fuliginosus*. The calcaneal heads of the extrageneric taxa are smaller than those of all species of *Protemnodon* except *P. otibandus*, which plots near to *M. fuliginosus*, *O. rufus* and *C. kitcheneri*, with a relatively slightly wider calcaneal head.

Figure 136: *Protemnodon otibandus* has a relatively shorter caudal end of the calcaneal tuberosity than those of the Australian Pleistocene species; *P. anak*, *P. mamkurra* **sp. nov.** and *P. viator* **sp. nov.** have similar caudal calcaneal tuberosity heights.

Figure 137: In terms of relative robustness, the fourth metatarsals of species of *Protemnodon* group together to the exclusion of those of *M. fuliginosus*, *O. rufus*, *De. bennettianus* and *W. bicolor*, which possess relatively narrower, more elongate fourth metatarsals. Metatarsal IV of *C. kitcheneri* has similar dimensions to the smaller species of *Protemnodon* but is relatively slightly narrower. Those of *P. otibandus* and *P. tumbuna* are similarly very short, the shortest of the species of *Protemnodon*; that of *P. snewini* has a similar width but is slightly longer. *Protemnodon anak* and *P. viator* **sp. nov.** have similar metatarsal IV lengths (100–125 mm), but that of *P. anak* is relatively wider. That of *P. mamkurra* **sp. nov.** is absolutely the longest of the species of *Protemnodon*, and is considerably wider than that of *P. viator* **sp. nov.** and slightly wider than that of *P. anak*. *Protemnodon dawsonae* **sp. nov.** is the absolutely widest, with a similar length to that of *P. anak* and the longest of *P. viator*.

Figure 138: The species of *Protemnodon* are separated from the extrageneric taxa by their absolutely wider fifth

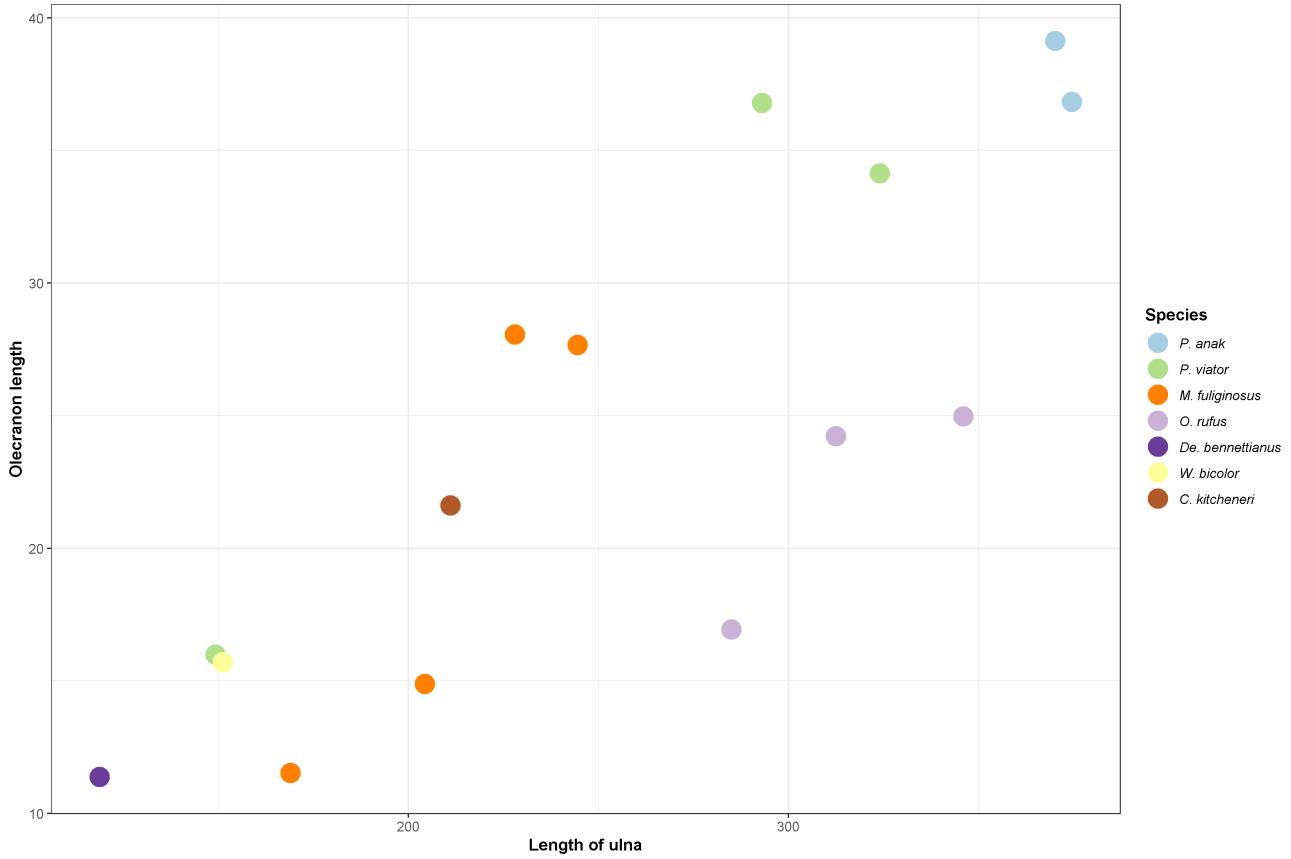

FIGURE 128. scatterplot of ulnar length versus olecranon length in specimens of *P. anak*, *P. viator* **sp. nov.**, and five extrageneric taxa.

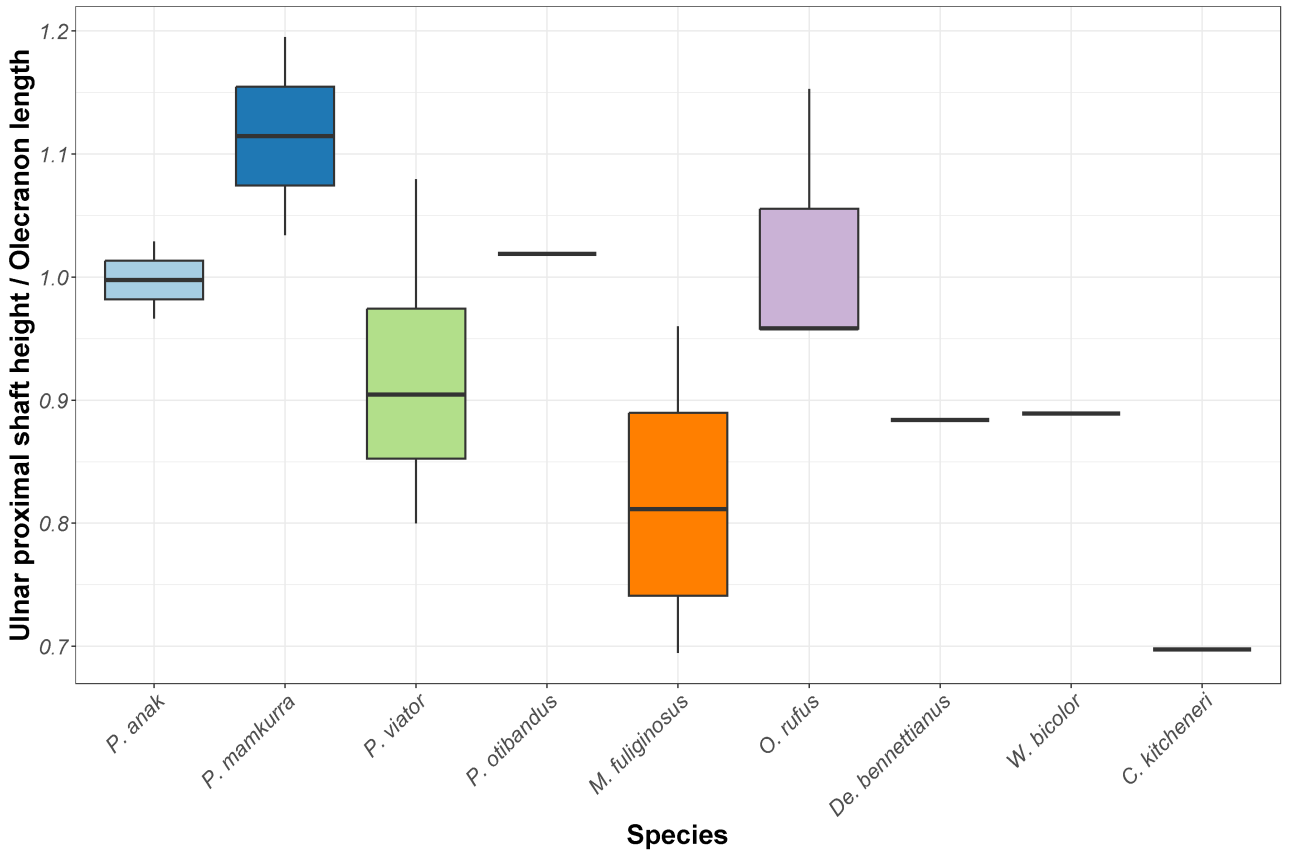

FIGURE 129. boxplot of ulnar proximal shaft height divided by olecranon length in specimens of *P. anak*, *P. mamkurra* **sp. nov.**, *P. viator* **sp. nov.**, *P. otibandus*, and five extrageneric taxa.

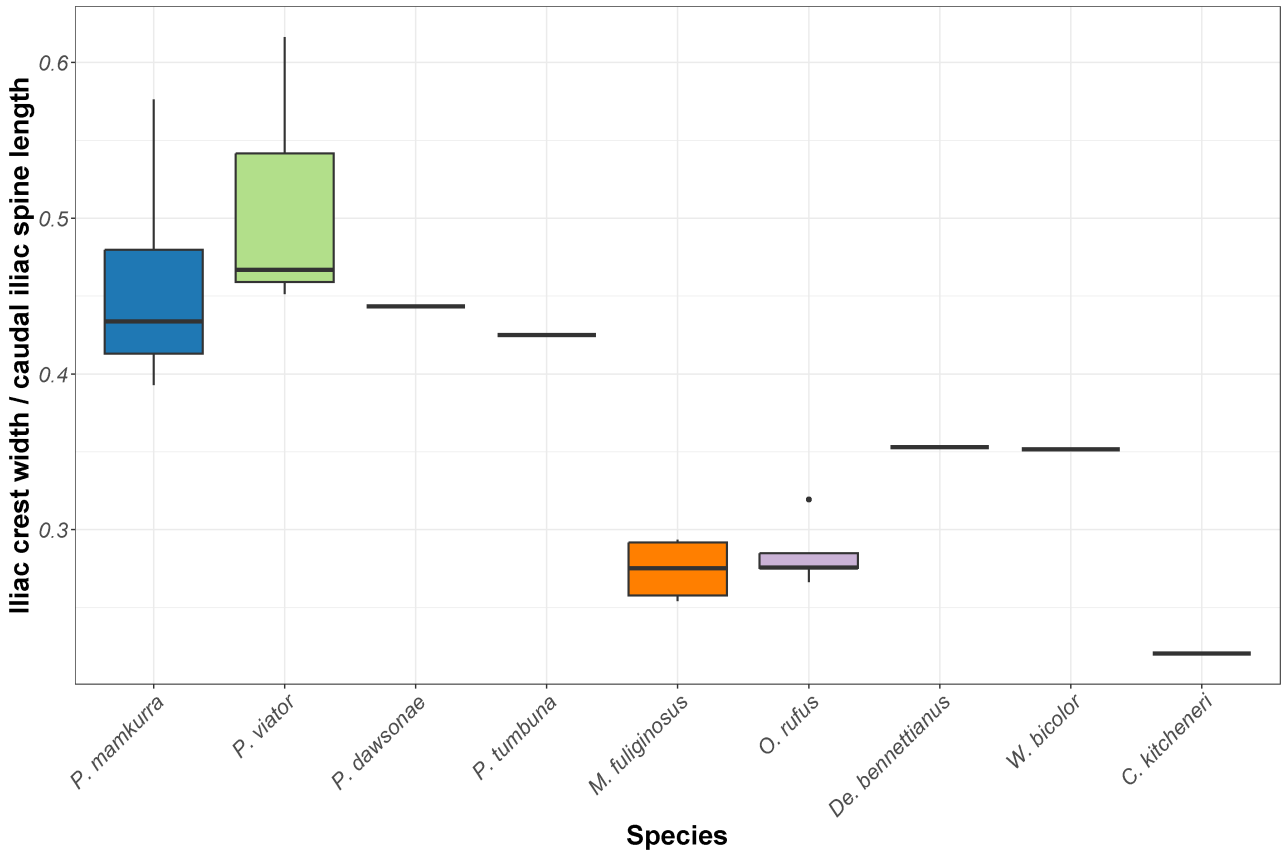

FIGURE 130. boxplot of iliac crest width divided by caudal iliac spine length in specimens of *P. mamkurra* **sp. nov.**, *P. viator* **sp. nov.**, *P. dawsonae* **sp. nov.**, *P. tumbuna*, and five extrageneric taxa.

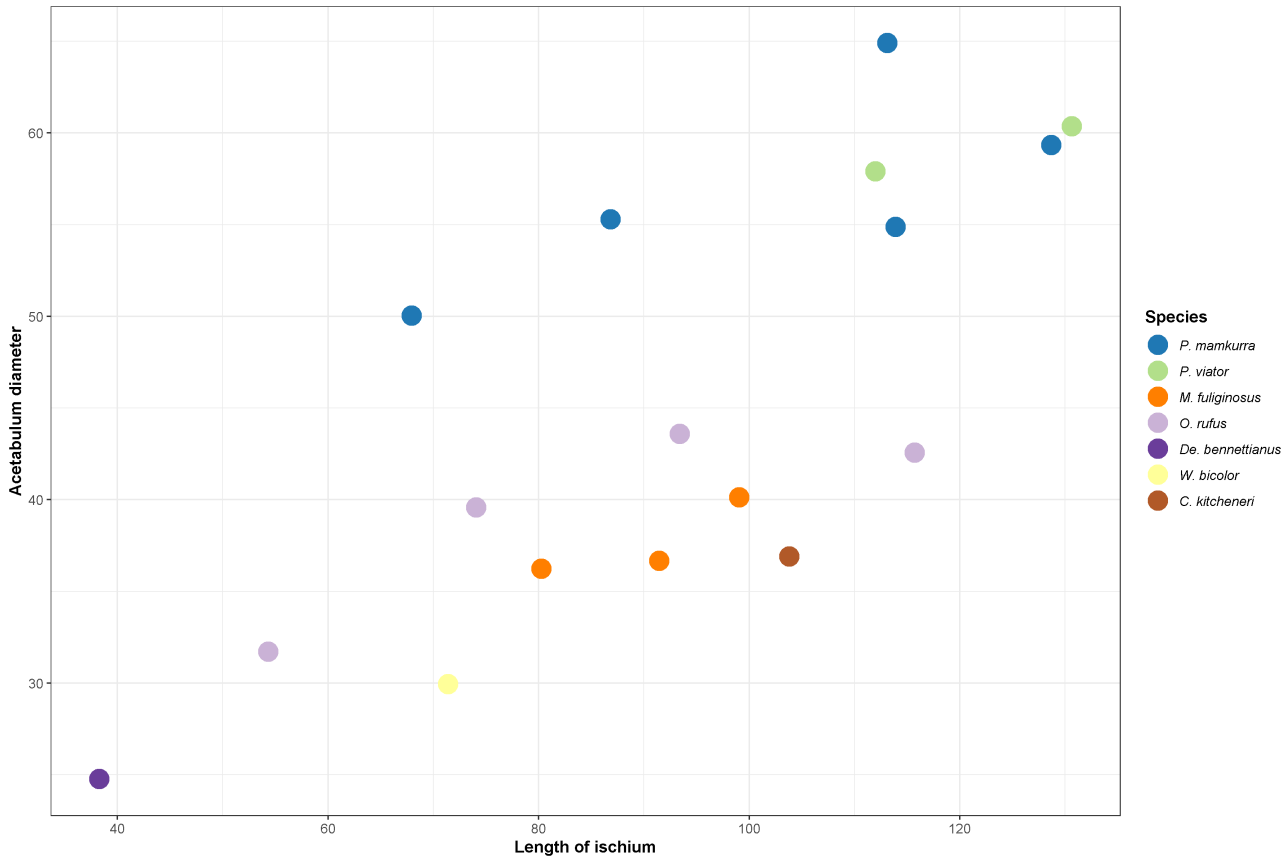

FIGURE 131. scatterplot of length of ischium versus acetabulum diameter in specimens of *P. mamkurra* **sp. nov.**, *P. viator* **sp. nov.**, and five extrageneric taxa.

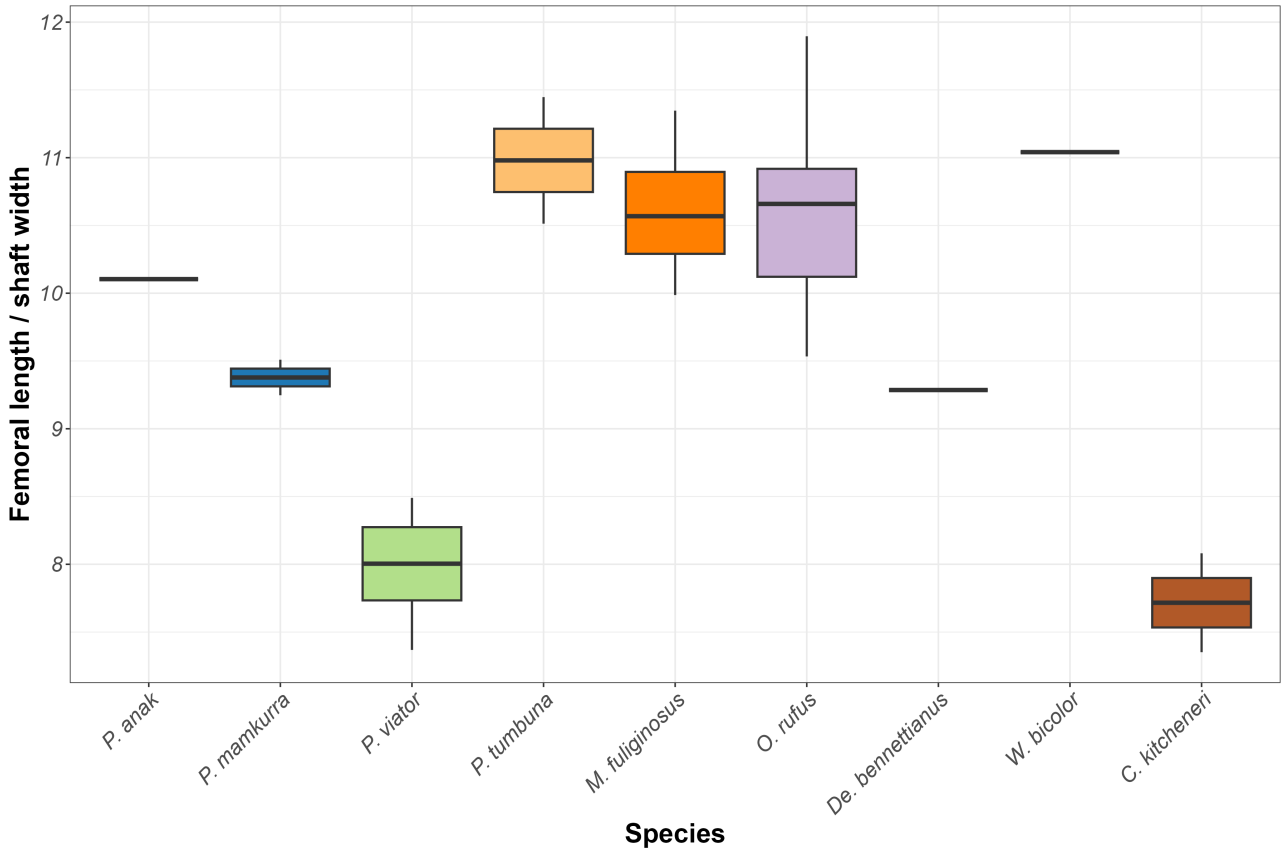

FIGURE 132. boxplot of femoral length divided by femoral shaft width in specimens of *P. anak*, *P. mamkurra* **sp. nov.**, *P. viator* **sp. nov.**, *P. tumbuna*, and five extrageneric taxa.

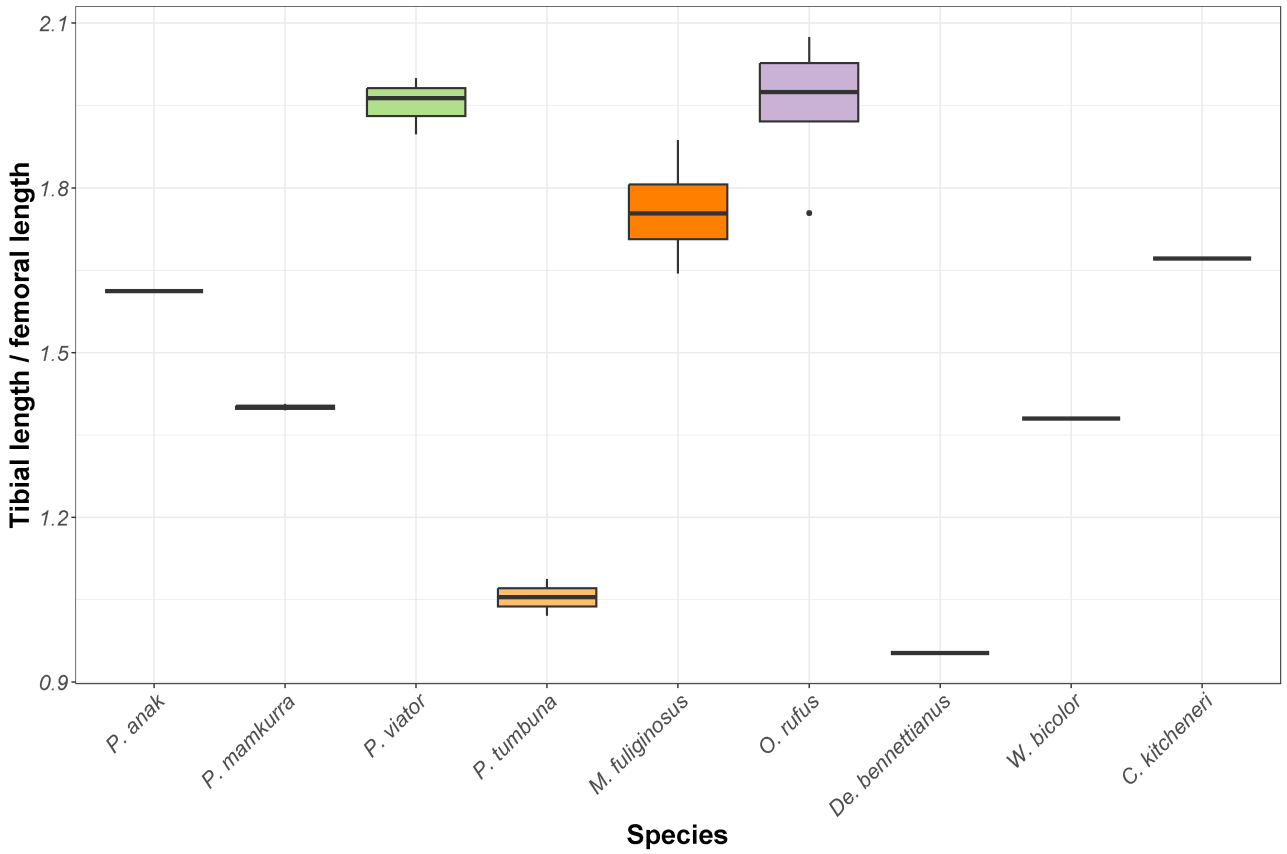

FIGURE 133. boxplot of the crural index (tibial length divided by femoral length) in specimens of *P. anak*, *P. mamkurra* **sp. nov.**, *P. viator* **sp. nov.**, *P. tumbuna*, and five extrageneric taxa.

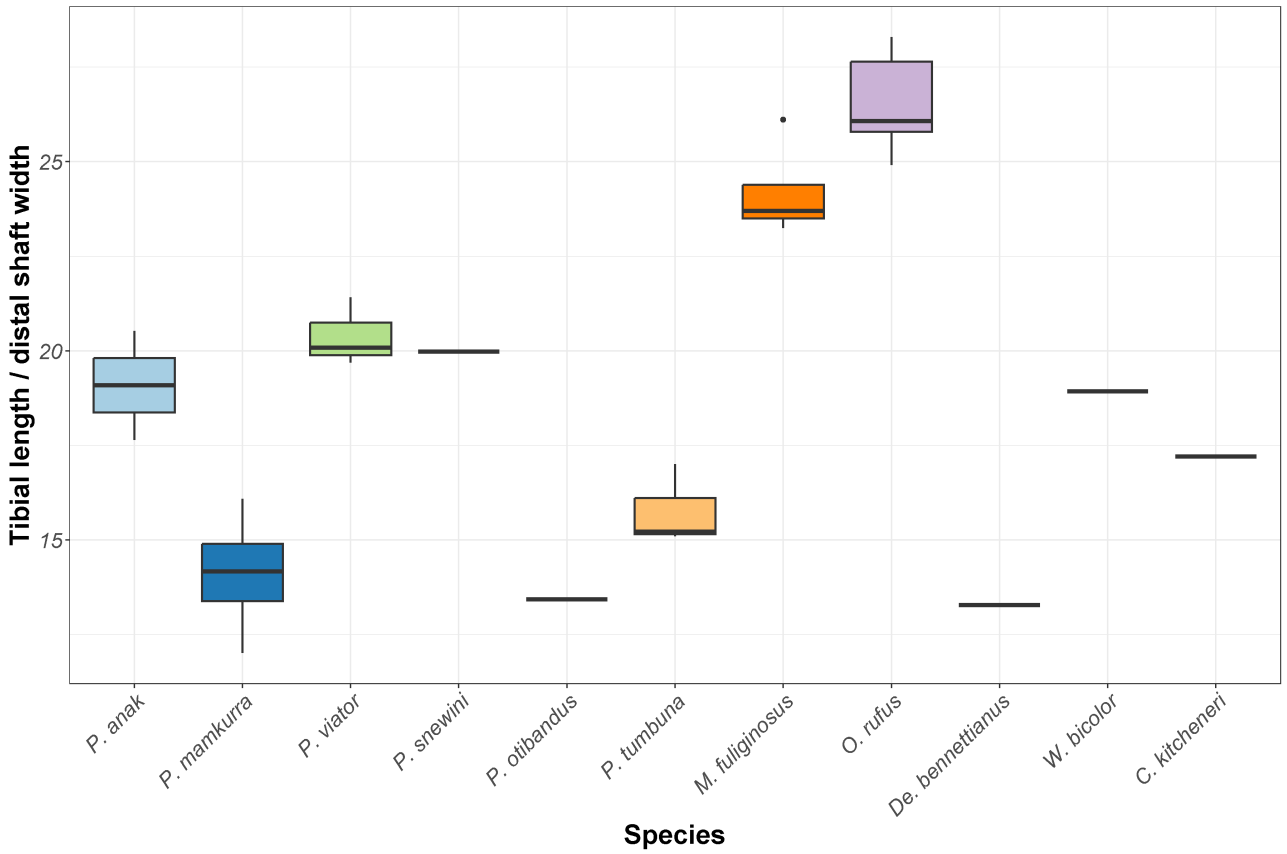

FIGURE 134. boxplot of tibial length divided by minimum distal shaft width in specimens of *P. anak*, *P. mamkurra* **sp. nov.**, *P. viator* **sp. nov.**, *P. snewini*, *P. otibandus*, *P. tumbuna*, and five extrageneric taxa.

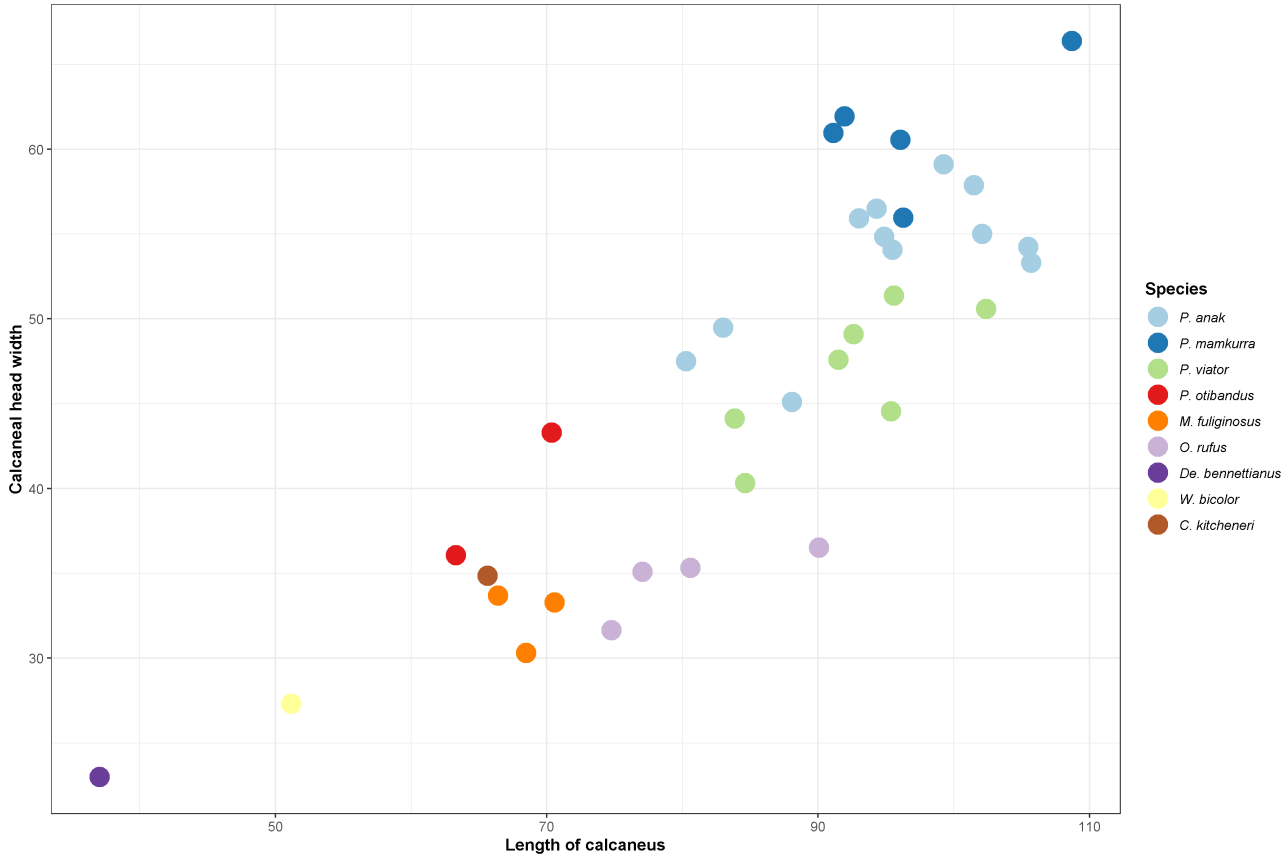

FIGURE 135. scatterplot of calcaneal craniocaudal length versus head width of calcaneal tuberosity in specimens of *P. anak*, *P. mamkurra* **sp. nov.**, *P. viator* **sp. nov.**, *P. otibandus*, and five extrageneric taxa.

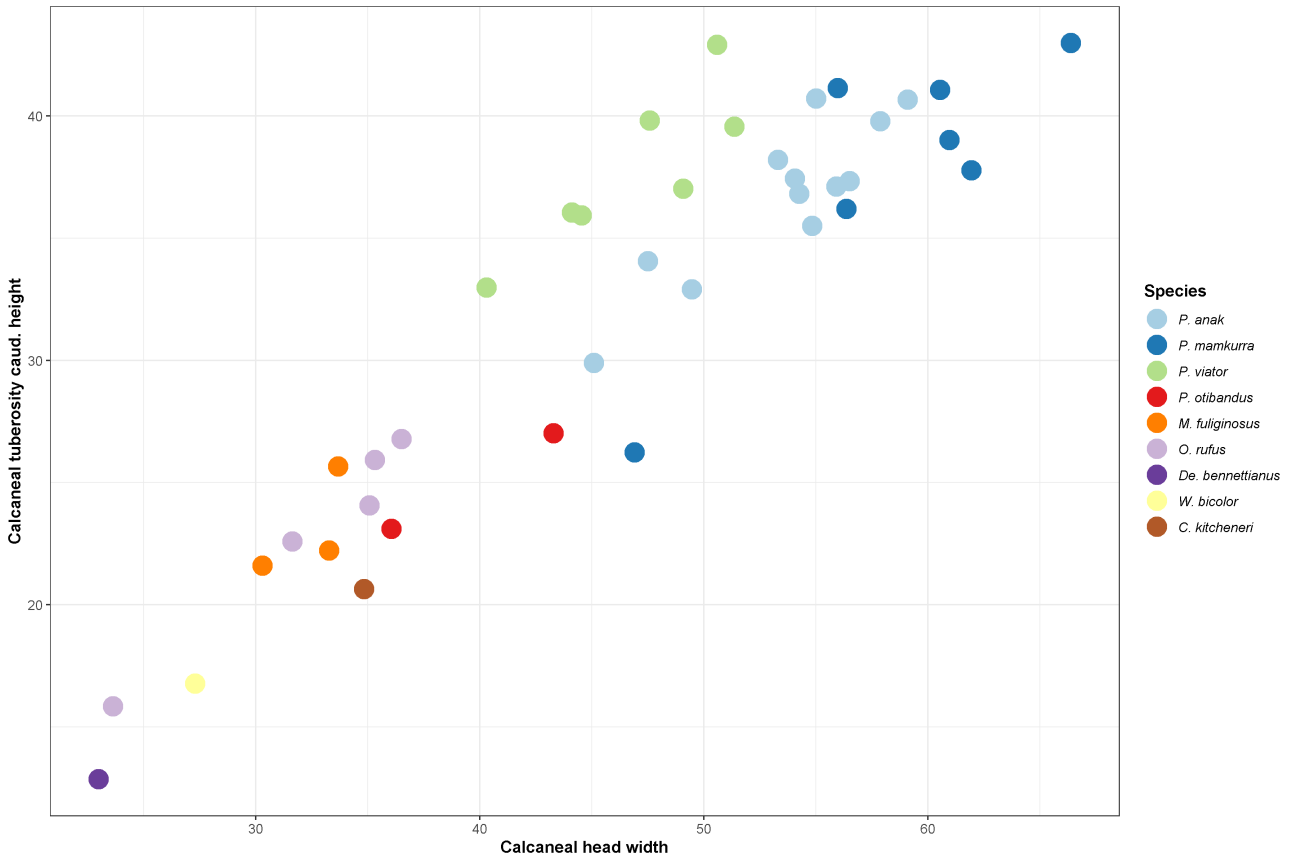

FIGURE 136. scatterplot of calcaneal proximal head width versus caudal height of calcaneal tuberosity in specimens of *P. anak*, *P. mamkurra* **sp. nov.**, *P. viator* **sp. nov.**, *P. otibandus*, and five extrageneric taxa.

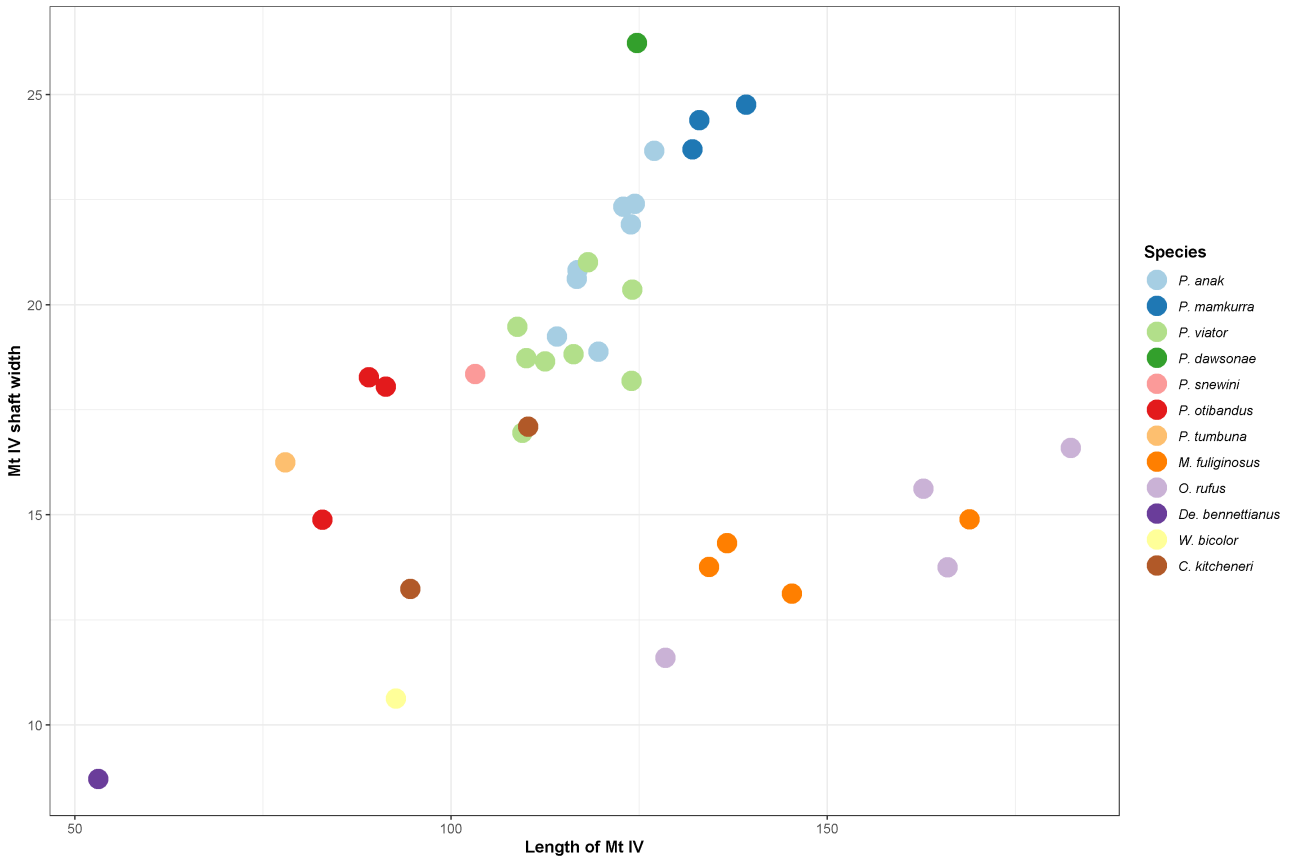

FIGURE 137. scatterplot of metatarsal IV length versus minimum shaft width (width of 'waist') in specimens of *P. anak*, *P. mamkurra* **sp. nov.**, *P. viator* **sp. nov.**, *P. dawsonae* **sp. nov.**, *P. snewini*, *P. otibandus*, *P. tumbuna*, and five extrageneric taxa.

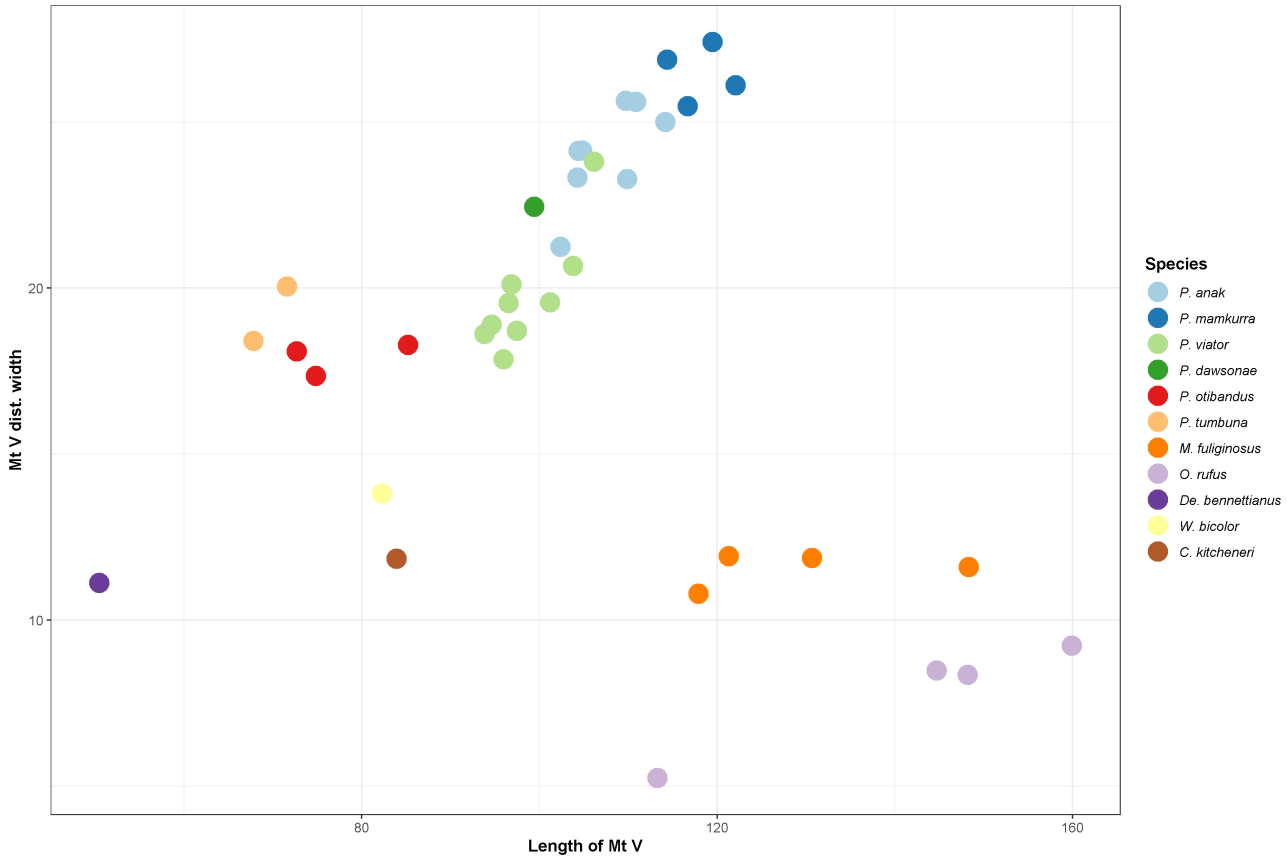

FIGURE 138. scatterplot of metatarsal V length versus distal end width in specimens of *P. anak*, *P. mamkurra* **sp. nov.**, *P. viator* **sp. nov.**, *P. dawsonae* **sp. nov.**, *P. snewini*, *P. otibandus*, *P. tumbuna*, and five extrageneric taxa.

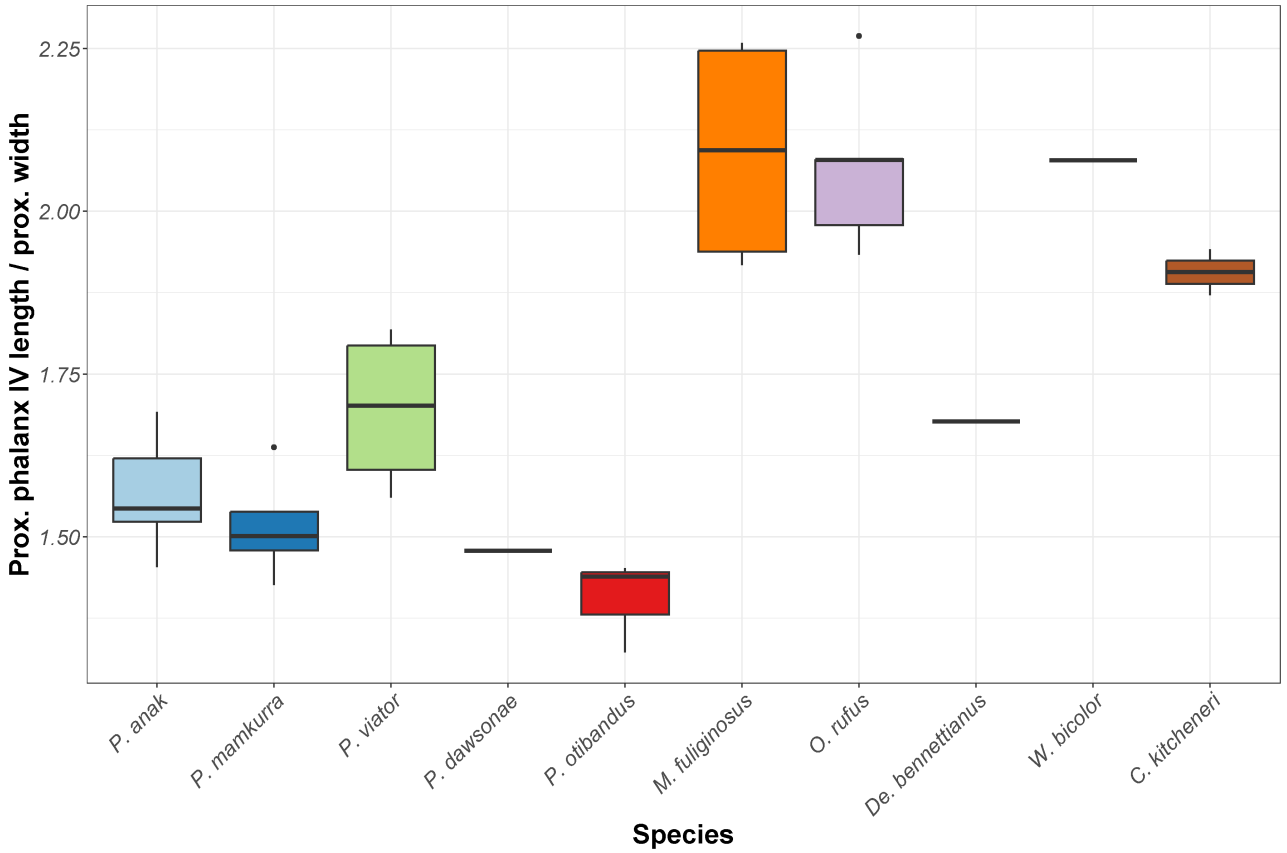

FIGURE 139. boxplot of proximal phalanx IV length divided by proximal width in specimens of *P. anak*, *P. mamkurra* **sp. nov.**, *P. viator* **sp. nov.**, *P. snewini*, *P. otibandus*, and five extrageneric taxa.

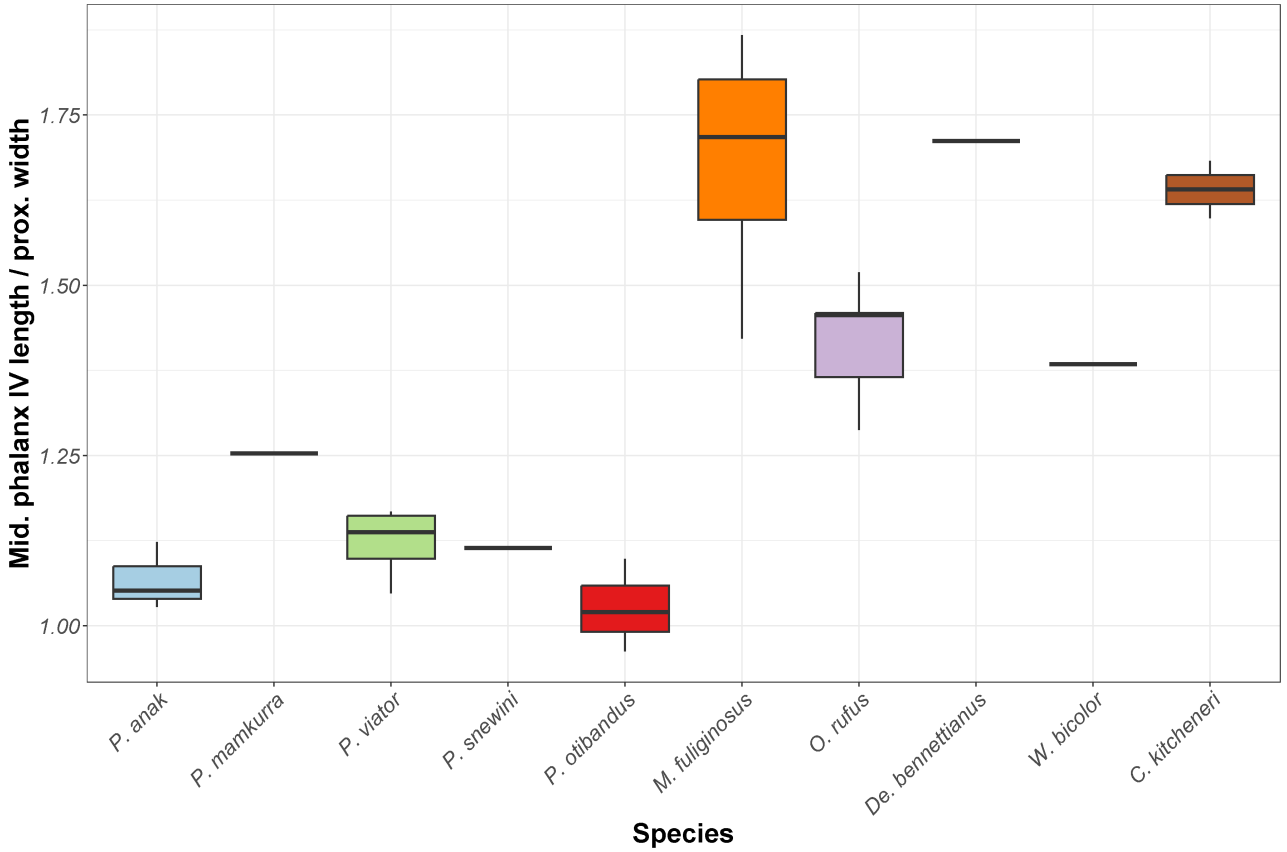

FIGURE 140. boxplot of middle phalanx IV length divided by proximal width in specimens of *P. anak*, *P. mamkurra* **sp. nov.**, *P. viator* **sp. nov.**, *P. snewini*, *P. otibandus*, and five extrageneric taxa.

metatarsals; those of *D. bennettianus* are relatively (but not absolutely) wider, while those of *M. fuliginosus*, *O. rufus*, *W. bicolor* and *C. kitcheneri* are relatively more elongate. *Protemnodon tumbuna* has the most robust metatarsal V, being slightly shorter and broader than that of *P. otibandus*. That of *P. viator* **sp. nov.** is the most gracile of the species of *Protemnodon*, absolutely shorter and narrower than that of *P. mamkurra* **sp. nov.**, and narrower than those of *P. anak* and *P. dawsonae* **sp. nov.** The fifth metatarsals of *P. anak* and *P. dawsonae* are similarly sized and proportioned, slightly shorter and narrower than that of *P. mamkurra* **sp. nov.**, which has the largest metatarsal V of the species of *Protemnodon*.

Figure 139: The species of *Protemnodon* have relatively wider fourth proximal pedal phalanges than the extrageneric taxa. The sole exception is *De. bennettianus*, which is similar in proportions to *P. viator*, which has the relatively narrowest fourth proximal pedal phalanx of the species of *Protemnodon*. Those of *P. mamkurra* **sp. nov.** and *P. dawsonae* **sp. nov.** are similarly proportioned, while that of *P. anak* is mostly relatively narrower. That of *P. otibandus* has the relatively widest values of the species of *Protemnodon*.

Figure 140: The species of *Protemnodon* also have relatively wider fourth middle pedal phalanges than the extrageneric taxa. *Protemnodon mamkurra* **sp. nov.** has the relatively longest fourth middle phalanx of the genus; that of *P. viator* is relatively broader, similar to *P. snewini* and mostly narrower than *P. anak*. *Protemnodon otibandus* has the relatively widest fourth middle pedal phalanges for the species of *Protemnodon*, with some specimens as wide as they are long.

Phylogenetic analysis

Parsimony analysis of the 12 species using TNT examined 3,771,334 rearrangements and returned three most parsimonious trees, which produced a strict consensus tree with length of 188 steps (Fig. 141). Within this tree, the seven species of *Protemnodon* herein recognised resolved as monophyletic, with low-moderate support from bootstrapping/jackknifing (65/57). *Wallabia bicolor* was very strongly supported (100/100) as the sister group to a clade containing *Protemnodon* + *C. kitcheneri* + *M. fuliginosus* + *O. rufus*. The grouping of *C. kitcheneri* as sister to a clade of *M. fuliginosus* + *O. rufus* was moderately supported (71/73). Within *Protemnodon*, *P. snewini* diverges basally with moderate support (66/70). Placement of *P. anak* as sister to a clade containing the remaining species of *Protemnodon* is moderately supported (63/67). The

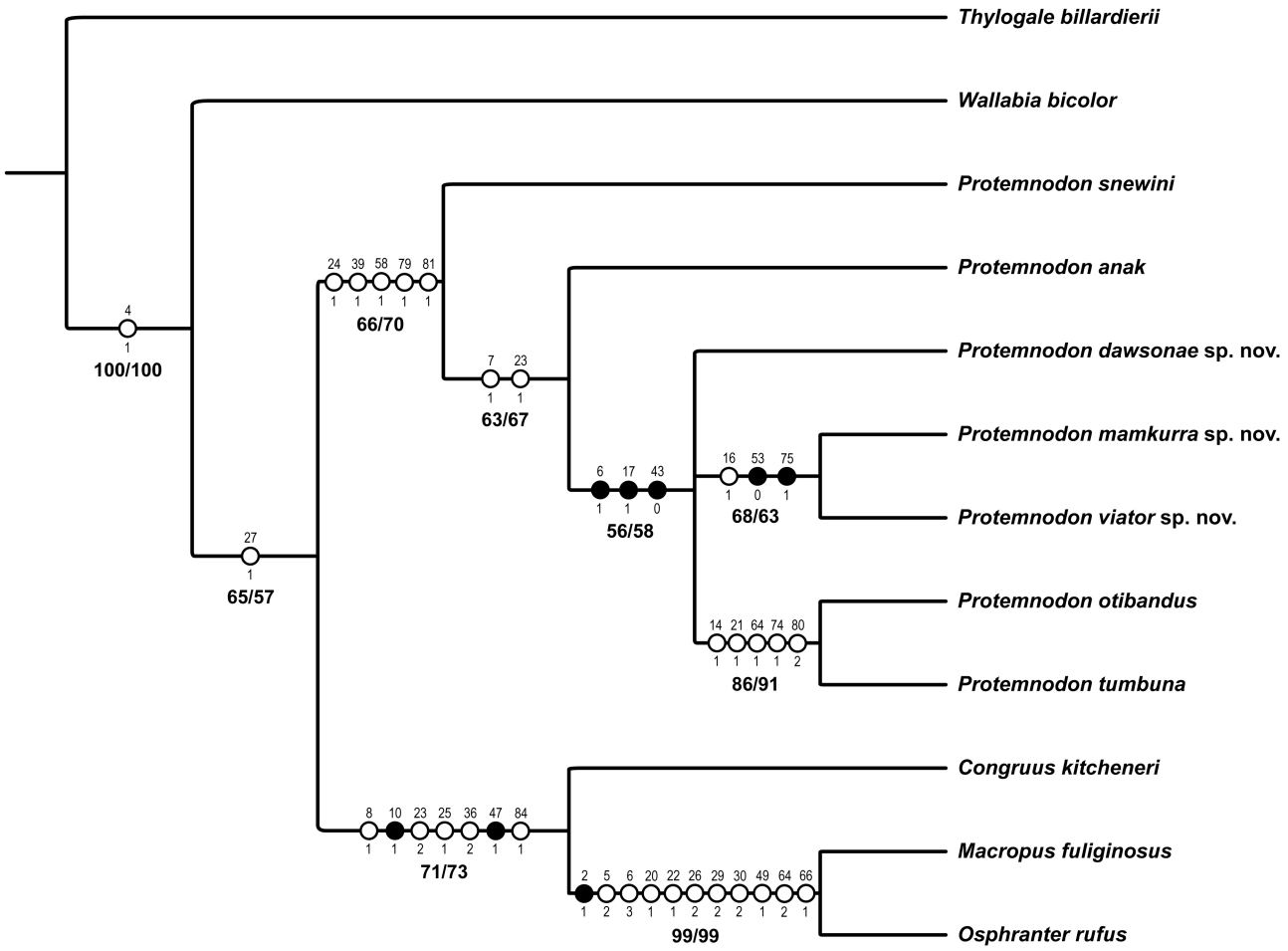

FIGURE 141. strict consensus tree (length = 194 steps) from a parsimony analysis showing the evolutionary relationships of the seven species of *Protemnodon* and the macropodin taxa *Wallabia bicolor*, *Congruus kitcheneri*, *Osphranter rufus* and *Macropus fuliginosus*, from 85 osteological characters (34 craniodental, 51 postcranial) with one outgroup taxon, *Thylogale billardierii*. Synapomorphies are represented by the black filled circles on branches; unambiguous (state not appearing anywhere else on tree) synapomorphies are indicated by black-outline unfilled circles. Branch support is indicated by the numbers beneath the branches (bootstrapping/jackknifing).

relationships of *P. dawsonae* **sp. nov.**, a moderately supported clade (68/63) containing *P. mamkurra* **sp. nov.** + *P. viator* **sp. nov.**, and a strongly supported pairing (83/88) of *P. otibandus* + *P. tumbuna* are unresolved, the three clades forming a trichotomy.

The exclusion of *W. bicolor* from the clade containing the species of *Protemnodon* + *C. kitcheneri* + *M. fuliginosus* + *O. rufus* is supported by plesiomorphic characters including: large, tall and narrow i1 (char. 18); large, oval palatine fenestra (character 27); a femur with a trochanteric fossa that extends distally past the lesser trochanter (char. 63); and a small, pointed proximolateral process on metatarsal V (char. 81). The grouping of *C. kitcheneri* with the clade of *M. fuliginosus* + *O. rufus* is supported by the following synapomorphies: short premolars relative to molar length (char. 8); lower molars lacking a premetacristid (char. 23); dorsally convex nasals (char. 25); a dentary with the anterior mental foramen situated closer to the base of the crown of the i1 than to the mandibular corpus (char. 36); and tall distal pedal phalanges IV with a distinct triangular dorsal peak in cross-section (char. 84).

In this analysis, the monophyly of *Protemnodon* is supported by the presence of five unambiguous synapomorphies: lower molars possessing a postcingulid (char. 24); a dentary with a deep medial pterygoid fossa with a high posterior margin (char. 39); a broad iliac blade (char. 58); a relatively robust metatarsal IV (char. 79); and a broad middle pedal phalanx IV (char. 81). In the clade containing *P. dawsonae* **sp. nov.** + *P. mamkurra* **sp. nov.** + *P. viator* **sp. nov.** + *P. otibandus* + *P. tumbuna*, the species share: a P3 with a high, elongate, smoothly dorsoventrally undulating lingual crest (char. 6); a dorsally deflected to straight i1 and diastema (char. 17); and a humerus with a broad distal facet (ulnar facet + capitulum) relative to the width across the humeral epicondyles (char. 43). These states are shared with *C. kitcheneri*, *W. bicolor*, and *T. billardierii*, respectively. The clade of *P. mamkurra* **sp. nov.** + *P. viator* **sp. nov.** displays a synapomorphic re-emergent stylar cusp C at the buccal

margin of the interloph valley of some upper molars (char. 16). *Protemnodon otibandus* + *P. tumbuna* form a clade defined by: their synapomorphic possession of a urocrista generally present on the metaloph of the M1–2 (char. 14); a small, rounded paracristid on the lower molars (char. 21); an elongate, mid-length to distally-situated quadratus tubercle on the femur (char. 64); a medially-displaced calcaneal head relative to the tuberosity (char. 74); and a robust metatarsal V (char. 80).

Protemnodon snewini is excluded from the clade containing the other species of *Protemnodon* due to its possession of the following character states that link it to both ancestral and more derived taxa. The small, broad and shallow posterolingual basin (char. 7) on the P3 of *P. snewini* shared with *W. bicolor*, *M. fuliginosus*, *O. rufus* and *C. kitcheneri*. The plesiomorphic lower molars of *P. snewini* with a weak, thin premetacristid (char. 23) are shared with *W. bicolor* and *T. billardierii*. The former shares a more gracile dentary (char. 34) with a more dorsally situated anterior mental foramen (char. 35) with *M. fuliginosus*, *O. rufus* and *C. kitcheneri*. Its short cnemial crest relative to tibial length (char. 67) is shared with all non-*Protemnodon* taxa in the analysis.

Distributions

Pliocene distributions (Fig. 142)

Protemnodon snewini is known to date only from the early Pliocene Bluff Downs LF of northeastern Australia (Fig. 142) (Bartholomai 1978; Mackness *et al.* 2000).

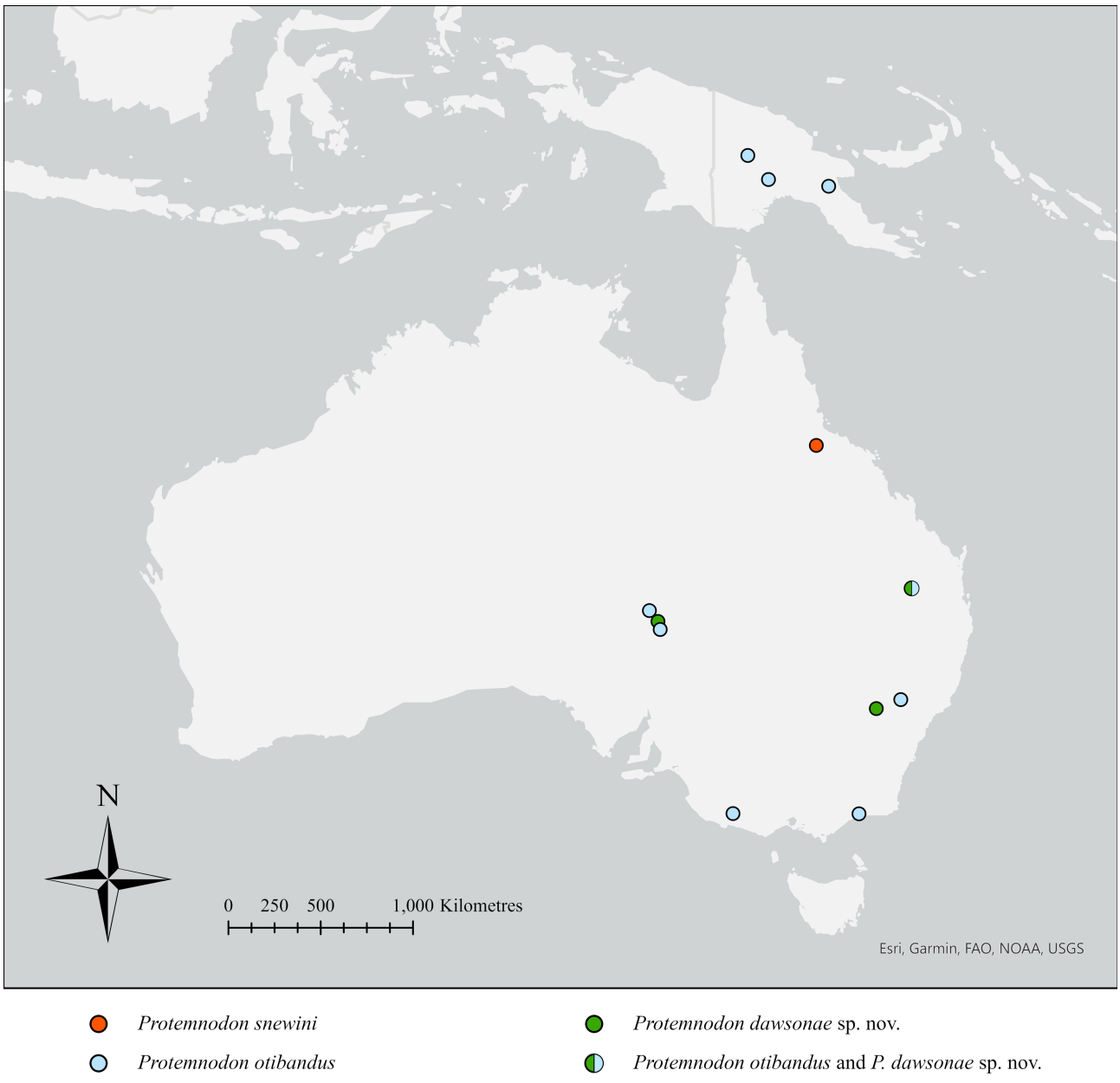

FIGURE 142. the localities in continental Australia yielding material of the three Pliocene species of *Protemnodon*: *P. snewini*, *P. dawsonae* **sp. nov.**, and *P. otibandus*.

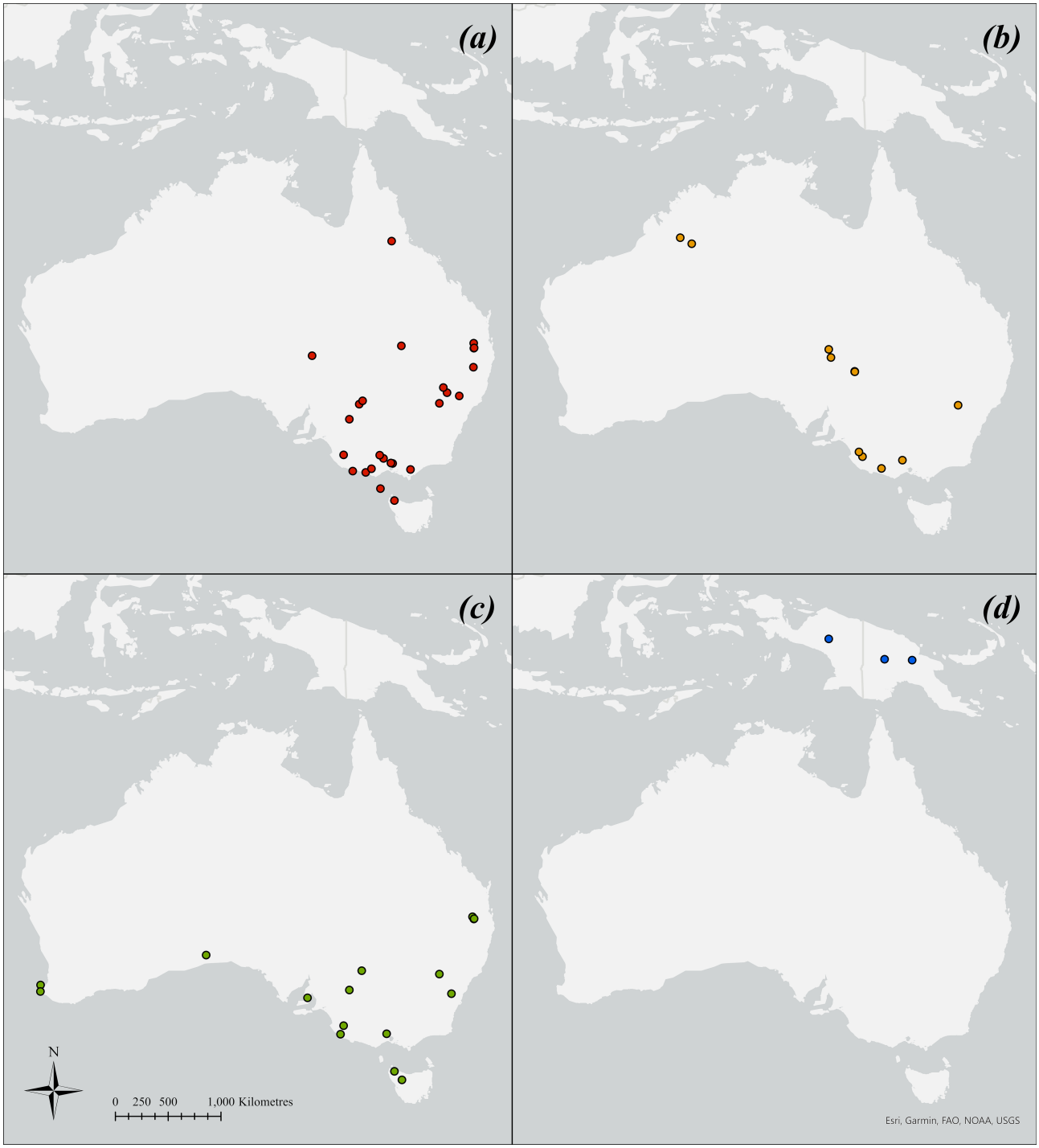

FIGURE 143. the localities in continental Australia yielding material of each of the four Pleistocene species of *Protemnodon*: (a) *P. anak*; (b) *P. viator* **sp. nov.**; (c) *P. mamkurra* **sp. nov.**; and (d) *P. tumbuna*.

Protemnodon dawsonae **sp. nov.** has been recorded from three assemblages (Fig. 142), the Kanunka LF of the Tirari Fm. in the eastern Lake Eyre Basin, which has been ascribed a late Pliocene age based on palaeomagnetic assessment of the entombing sediments (Tedford *et al.* 1992), and the Chinchilla and Big Sink LFs of central eastern Australia, which are biocorrelated with the Kanunka LF (Dawson *et al.* 1999; Louys & Price 2015). The species was not observed to co-occur with *P. otibandus* within any localities from the Tirari Fm.

Protemnodon otibandus is known from early and late Pliocene deposits. Specimens here tentatively allocated to *P.* sp. cf. *P. otibandus*, from the early Pliocene Hamilton LF in southwestern Victoria, may represent the earliest evidence of the genus. It is the only species of *Protemnodon* known to occur in both New Guinea and mainland Australia. The geographic range of the species extends through central eastern Papua New Guinea during the late Pliocene (Hoch & Holm 1986) and across the majority of eastern Australia, to the Nowa Nowa Arm of

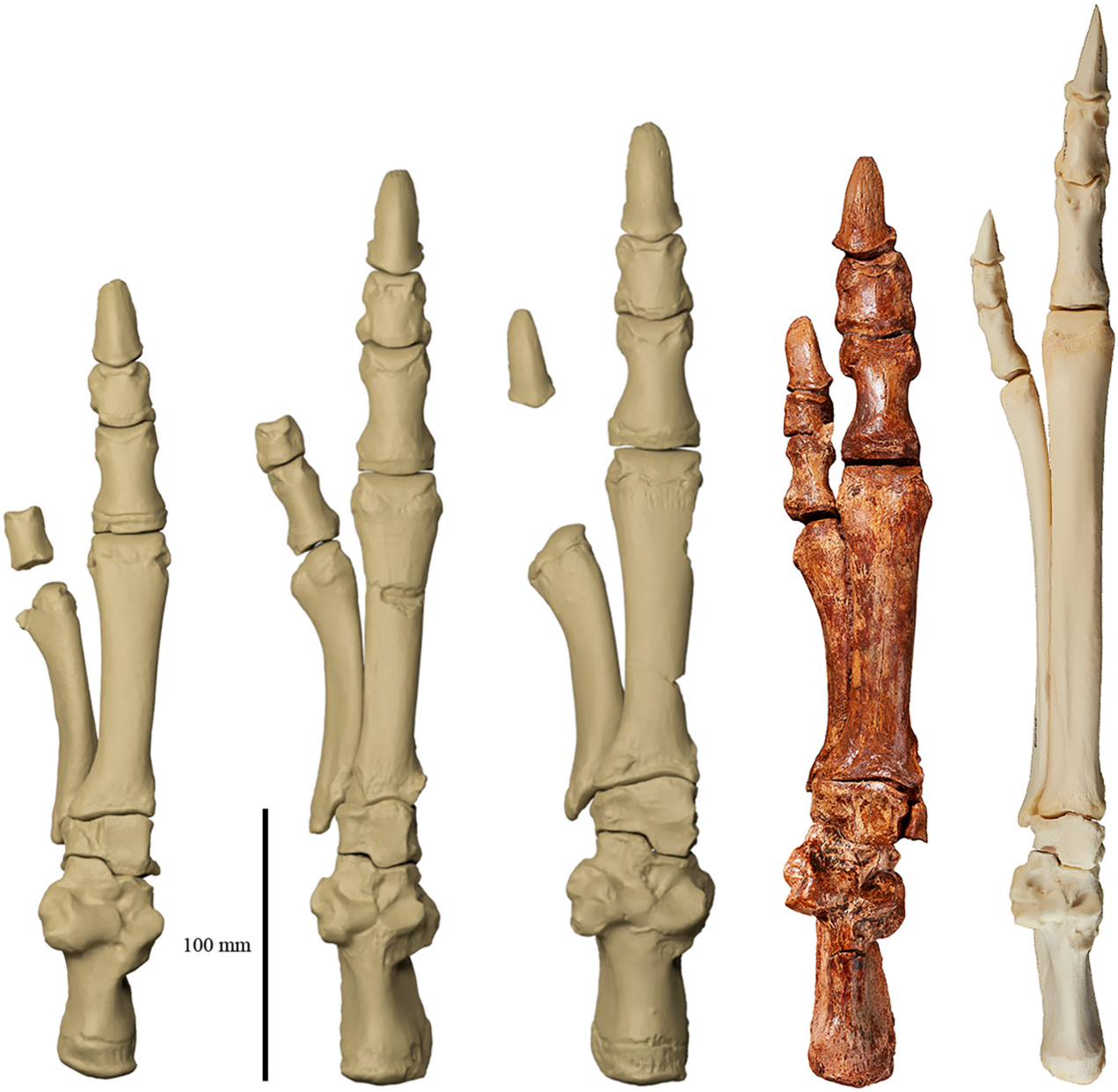

FIGURE 144. comparison of size and proportions of re-articulated partial left pedes of (from left to right): *P. otibandus*, UCMP 70584 (metatarsal V and proximal phalanx V mirrored); *P. anak*, NMV P39132 (calcaneus and middle phalanx V mirrored); *P. mamkurra* **sp. nov.**, SAMA P20810; *P. viator* **sp. nov.**, holotype SAMA P59552; and *M. fuliginosus*, FUR 266.

Lake Tyers (early Pliocene age from mollusc biocorrelation) (Darragh 1985) in the far southeast (Fig. 142). The distribution reaches west into the Lake Eyre Basin, with records at Lawson–Daily Quarry, Lake Palankarinna (mid-Pliocene) (Tedford *et al.* 1992) and Toolapinna Waterhole, Pompapillina Member (mid-Pliocene) (Tedford *et al.* 1992), on the Warburton River.

Pleistocene distributions (Fig. 143)

Protemnodon anak is known from early through late Pleistocene deposits. The earliest dated appearance of *P. anak* in the fossil record is in the early Pleistocene Nelson Bay LF. The youngest record of the species is ~54 ka from Site 51, Lake Victoria (Roberts *et al.* 2001). The species has a generally eastern range. It is not recorded from west of the Naracoorte Caves in the south, but extends into the Lake Eyre Basin. The northernmost record of *P. anak* is from Wyandotte Creek in northeastern Queensland (McNamara 1990). To the south, *P. anak* is known from King Island in the Bass Strait, and from Scotchtown Cave in northwestern Tasmania. The species is also known from sites across far southeastern Australia including the presumed early Pleistocene Morwell swamp and the late Pleistocene Lancefield swamp, and from numerous sites across eastern Australia (Fig. 143a).

Specimens of *P. viator* **sp. nov.** are present in middle to late Pleistocene deposits. The earliest evidence of the

species comes from Main Fossil Chamber, Victoria Fossil Cave (225 ka min. age) (Grün *et al.* 2001; Arnold *et al.* 2022), with a specimen found at a similar stratigraphic level to samples yielding dates of 478 ± 22 ka and 443 ± 32 ka (Grün *et al.* 2001). The youngest dated evidence of *P. viator* **sp. nov.** is from Lake Callabonna (deposition during drought starting about 48 ka) (McInerney *et al.* 2022) or from Spring Creek in southwestern Victoria (min. age 53.5 ka) (Gillespie *et al.* 2014). The material of species of *Protemnodon* from layer SU6B at Cuddie Springs, New South Wales (~50 ka min. age) (Grün *et al.* 2010), is here considered not to be *P. anak*, but belong to either *P. mamkurra* **sp. nov.** or *P. viator* **sp. nov.** The species is present in a small number of southeastern and eastern deposits, but has not been recorded from the Nullarbor Plain, from southwestern Australia and from Tasmania. It is most abundant in central Australian deposits, such as Lake Callabonna and Malkuni Waterhole, Cooper Creek. The species is known from the Canning Basin in the Kimberley region, marginally further north than Wyandotte Creek (Figs 2 & 143b), making it the only species of *Protemnodon* known from the entire northwest of Australia.

Protemnodon mamkurra **sp. nov.** is known from middle and late Pleistocene deposits. The earliest dated evidence of the species comes from Leaena's Breath Cave on the Nullarbor Plain (200–400 ka) (Prideaux *et al.* 2007) and Main Fossil Chamber, Victoria Fossil Cave (225 ka min. age) (Grün *et al.* 2001; Arnold *et al.* 2022). In the main pit of Main Fossil Chamber, specimens of *P. mamkurra* **sp. nov.** come from below, at and above the level of samples yielding dates of 478 ± 22 ka and 443 ± 32 ka (Grün *et al.* 2001). The youngest record is from Mt Cripps in northwestern Tasmania (41.5 ± 0.4 ka) (Gillespie *et al.* 2012). The species is found primarily in southern Australia, with a historic range apparently extending from the west coast of far southwestern Australia across the Nullarbor Plain to the Darling Downs and Wombeyan Caves in eastern Australia (Fig. 143c). *Protemnodon mamkurra* **sp. nov.** is the most common species of *Protemnodon* in the cave deposits of southeastern South Australia, and is found as far south as northwestern Tasmania. The Fossil Chamber deposit of Victoria Fossil Cave and the Wellington Caves are the only localities known to yield material of all three Pleistocene Australian species of *Protemnodon*.

The range of *P. tumbuna* reaches across late Pleistocene New Guinea from Nombe Rockshelter in Chimbu Province, eastern central PNG (Prideaux *et al.* 2022) to the West Baliem Valley in montane central Papua Province, West Papua (Fig. 143d) (Hope *et al.* 1993). It does not co-occur with any other species of *Protemnodon*, but does occur with *N. nombe* at Nombe Rockshelter (Flannery *et al.* 1983; Prideaux *et al.* 2022).

Discussion

Taxonomic implications

The genus *Protemnodon*, as redefined here, contains the following seven species: *P. anak*, *P. mamkurra* **sp. nov.**, *P. viator* **sp. nov.**, *P. tumbuna*, *P. dawsonae* **sp. nov.**, *P. otibandus* and *P. snewini*. *Protemnodon brehus*, *P. roechus* and *P. devisi* are deemed *nomina dubia*, while *P. chinchillaensis* is considered a junior synonym of *P. otibandus* and *P. hopei* a junior synonym of *P. tumbuna*.

Phylogenetic relationships

The identification of *P. snewini* as the most basal species of *Protemnodon* aligns well with its early Pliocene occurrence in the Bluff Downs LF of northeastern Australia (Bartholomai 1978; Mackness *et al.* 2000). Although *Protemnodon* material is also known from the ~4.5 Ma Hamilton LF in southeastern Australia (Flannery *et al.* 1992), the material is only tentatively allocated to *P.* sp. cf. *P. otibandus*. Together, these occurrences suggest a pre-Pliocene origin for the genus, consistent with molecular inferences (Cascini *et al.* 2019). *Protemnodon snewini* is characterised by a combination of plesiomorphic features (low-crowned cheek teeth, lower molars with a weak, thin premetacristid) and derived features (a gracile dentary with a dorsally situated anterior mental foramen, and a gracile tibia with short, strongly peaked cnemial crest).

The well-supported sister relationship between the Pliocene *P. otibandus* and Pleistocene *P. tumbuna* is unsurprising given that they inhabited New Guinea, and supports the suggestion that *P. otibandus* is the ancestor of *P. tumbuna* (see Flannery 1994). It is possible that a population of *P. otibandus* was able to disperse across a landbridge into New Guinea from the Australian mainland during a period of low sea level in the early Pliocene (Wilford & Brown 1994). Allopatric speciation may then have occurred following flooding of the Torres Strait in the mid–late Pliocene (Loutit & Kennett 1981; Rovere *et al.* 2014).

Though its relationship to *P. mamkurra* **sp. nov.** + *P. viator* **sp. nov.** and *P. otibandus* + *P. tumbuna* is unresolved here, the Pliocene *P. dawsonae* is considered a likely common ancestor of the Pleistocene *P. mamkurra* **sp. nov.** and *P. viator* **sp. nov.** because of dental similarities. Missing data are likely to have affected this lack of resolution, as only partial crania and partial pedes of *P. dawsonae* **sp. nov.** are known.

The general trend of increased body size and greater molar crown height within the Australian species of *Protemnodon* from the Pliocene to the Pleistocene conforms to the pattern observed within Macropodini during this period (Helgen *et al.* 2006; Couzens & Prideaux 2018). Within kangaroos, these attributes are correlated with adaptation to higher-fibre diets and the spread of more open habitats across the continent (Prideaux & Warburton 2010; Couzens & Prideaux 2018). The exception is the *P. otibandus* + *P. tumbuna* clade. As discussed below, the Pliocene *P. otibandus* was likely a low-geared bipedal hopper with a greater reliance on the forelimbs for locomotion than large modern kangaroos, while the Pleistocene *Protemnodon tumbuna* was even lower-geared, with its morphology suggesting facultative quadrupedality. This species has the most

divergent morphology relative to the inferred ancestral *Protemnodon* form.

Diet

There have been various investigations into the diets of the species of *Protemnodon*, producing varied results. Prior to the first in-depth analyses, they were asserted to be grazers by Bartholomai (1973), those of Pleistocene Australia were stated to be browsers (Flannery 1990b), and the New Guinean species were described as browsers based on molar crown heights (Flannery 1994; Flannery & Roberts 1999). The first dental carbon isotope analysis of species of *Protemnodon* was undertaken by Montanari *et al.* (2013) on material of *Protemnodon* sp. indet. from the Pliocene Chinchilla LF, and concluded that the specimens consumed primarily C3 browse with a small amount of C4 grasses. An analysis of the dental mesowear patterns of Plio-Pleistocene macropodids classified specimens of *Protemnodon roechus* from King's Creek, Darling Downs, as probable grazers or possible mixed-feeders (Butler *et al.* 2014). This material is considered here to belong to either *P. mamkurra* **sp. nov.** or *P. viator* **sp. nov.** An investigation of dental carbon isotope signatures at a generic level interpreted the specimens of *Protemnodon* from the late Pleistocene Cuddie Springs deposits (here allocated to *P. mamkurra* **sp. nov.** or *P. viator* **sp. nov.**) as having a preference for C3 browse, though with a more mixed diet than *Sthenurus*, and having eaten a more significant portion of brittle or woody plant material than *Macropus* (DeSantis *et al.* 2017). These studies may demonstrate variety in dietary niches among the Australian Pliocene and Pleistocene species of *Protemnodon*, and may also indicate substantial dietary plasticity within species.

There has been a historic reliance on comparison of dental morphologies in order to categorise extinct macropodid diets, which may have been misleading. A study of the dental microwear patterns of extant macropodoids suggested that many macropodoid taxa considered to have browsing dentition by landmark studies like Sanson (1978, 1980, 1989) are in fact mixed-feeders (Arman & Prideaux 2015). It was suggested that this resulted from a tendency of mixed feeders to have browser-grade dental morphology while in fact utilising a wider selection of food sources. This highlights the need for in-depth analyses of dietary signatures in extinct kangaroos. An analysis of the microwear patterns of the species of *Protemnodon* is definitely warranted.

Neck morphology

Protemnodon anak has craniocaudally elongate, relatively narrow cervical vertebrae, particularly the axis vertebra, which is longer relative to its width than in any other macropodine. For this reason, the species is unusual within the broader trends of neck elongation in mammals; C3–6 typically provide the increase in length, rather than the greatest increase occurring in the axis vertebra (Arnold *et al.* 2017). The cranial and caudal extremities of the centra of C2–7 are narrow and strongly caudoventrally projected, much more so than in other species of *Protemnodon*. Increased reach and flexibility in the neck region of herbivorous vertebrates is often an adaptation to facilitate feeding (Gunji & Endo 2019; Arnold 2021). It has been suggested that *P. anak* fed on foliage above body height (Den Boer 2018). We find evidence to support this. The ventral projection and angling of the cervical centra (Fig. 13) would result in elevation of the head, which could increase browsing height. The curvature of the vertebral articulations (both zygapophyseal and of the centra) would also greatly increase side to side flexibility. However, to more confidently ascertain the function of the intriguing cervical vertebrae of *P. anak*, it would be appropriate for a detailed examination of the neck musculature of an extant macropodine to be undertaken. The extinct Pleistocene kangaroo *Congruus kitcheneri* is the only other macropodine known to exhibit significant elongation of the centra of the cervical vertebrae (though to a lesser extent), an attribute suggested to have facilitated extended reaching and manoeuvring of the head and neck during arboreal browsing (Warburton & Prideaux 2021). As discussed above, further clarification of the diet of *P. anak* would inform any interpretation of neck adaptations.

The neck of *P. mamkurra* **sp. nov.** curves gently ventrally, particularly in the cranial part (C1–4), while the necks of *P. anak* and *P. viator* **sp. nov.** curve very slightly dorsally. The cervical vertebrae of *P. viator* **sp. nov.** are very similarly proportioned to those of *M. fuliginosus* and *O. rufus*, while *P. mamkurra* **sp. nov.** possesses a relatively very short neck, proportionally akin to that of species of *Dendrolagus* and *Petrogale*. The proportions of the axis vertebra of *P. dawsonae* **sp. nov.** are intermediate between those of *P. mamkurra* **sp. nov.** and *P. viator* **sp. nov.** This suggests that there may be a relationship linking shorter necks to lower-geared (that is, slower, and less efficient at higher speeds) macropodines, and mid-length necks to higher-geared macropodines (Fig. 126). The nature and cause of this relationship warrants in-depth investigation elsewhere.

Locomotion

Differences in postcranial morphology between the species of *Protemnodon* suggest a range of locomotory patterns, in line with recent assertions (Janis *et al.* 2023), but with greater diversity across the genus. Various diagnostic characteristics that help to unite species within *Protemnodon* are also clearly linked to structure and musculature that support powerful hindlimb extension and flexion and promote stability, particularly at the limb joints.

Locomotory use of the tail

When large macropodins move slowly, they utilise their tail as a fifth limb, combining with the forelimbs to form a tripod for support as the hindlimbs are simultaneously drawn forward (Frith & Calaby 1969). In this unique form of movement, called pentapedal locomotion ('punting') (Dawson & Taylor 1973), the proximal caudal vertebrae are flexed beneath the pelvis while the mid-distal vertebrae are pushed flat to the ground, forming the distinctive S-shape of the tail (Frith & Calaby 1969; Windsor & Dagg 1971;

Dawson & Taylor 1973). In more basal macropodines (except dorcopsins), the tail is dragged along the ground behind during slow quadrupedal locomotion (Windsor & Dagg 1971).

There is evidence to suggest that the species of *Protemnodon* utilised their tail for locomotion to varying degrees. All species of *Protemnodon* for which an ilium is known have a broad iliac crest for the origin of a large m. intertransversarius lateralis caudalis, which flexes the proximal caudal vertebrae beneath the sacrum during pentapedal locomotion (Warburton *et al.* 2012; Dawson *et al.* 2014). *Protemnodon mamkurra* **sp. nov.** and *P. viator* **sp. nov.** possess a similarly well-developed coccygeal fossa on the caudomedial ilium to that of *O. rufus* and *M. fuliginosus*. This fossa is the origin of the m. coccygeus, another major flexor that pulls the tail under the body during pentapedal movement (Dawson *et al.* 2014). Both the m. intertransversarius lateralis caudalis and the m. coccygeus insert to the distal component of the transverse processes of the proximal caudal vertebrae. These processes are as broad, deep and well-developed in *P. mamkurra* **sp. nov.** and *P. viator* **sp. nov.** as in *M. fuliginosus*, which implies that the flexors of the proximal tail were large. The m. sacrocaudalis ventralis lateralis, which originates ventrally on the transverse processes and the lateral part of the centrum and inserts to the tip of the transverse processes of Ca5 and continues to the tail tip, and the m. pubococcygeus, which originates on the cranial surface of the sacrum and inserts to the chevrons between the vertebrae distal to Ca12, are both identified as key extensors of the mid-distal region of the tail during pentapedal motion (Dawson *et al.* 2014). The sacrum of *P. anak* has broad transverse processes, particularly in the caudal section, with a similarly well-developed cranial surface to individuals of *O. rufus*, giving no suggestion of lesser mid-distal tail extensors than those seen in extant large macropodins. For these reasons, it is here considered probable that the large species *P. anak*, *P. mamkurra* **sp. nov.** and *P. viator* **sp. nov.** did indeed use the tail as a fifth limb during slow locomotion. One confounding factor is that males of *O. rufus* and species of *Macropus* also utilise the tail to form a tripod during fights with rival males (Ganslosser 1989), so male macropodines may exhibit larger tail musculature.

The crural index of extant macropodines is a good indicator of the use of pentapedal motion at slow speeds, with a mean of 1.71 in pentapedal versus 1.36 in non-pentapedal macropodines (Dawson *et al.* 2015). This is linked to the lower efficiency of elongate hindlimbs for quadrupedal motion in large macropodines (Dawson 1977; O'Connor *et al.* 2014). The crural indices of *P. viator* **sp. nov.** (~1.95) and *P. anak* (~1.61) (Fig. 133) are well within the bounds of the hindlimb proportions associated with pentapedality, implying that their tibiae were too long for quadrupedal locomotion to be efficient. Although its femur is not known, *P. snewini* also has a very elongate tibia and on this basis can probably be grouped with the pentapedal macropodines. The crural index of *P. mamkurra* **sp. nov.** is level with that of *W. bicolor* (1.39), While that of *P. tumbuna* (1.02) is slightly higher than that of *De. bennettianus* (Fig. 133). *Protemnodon tumbuna* is thus closer associated with the hindlimb proportions of non-pentapedal macropodines. There is a phylogenetic signal within pentapedality, with almost all living species within the crown group Macropodini utilising pentapedal locomotion (Dawson *et al.* 2015). There may also be an allometric factor at play, with larger, heavier kangaroos, even those with lower CIs, requiring support from the tail during low-speed locomotion. The phylogenetic position of *Protemnodon* is either at the base of the clade Macropodini or slightly more derived within the clade (Prideaux & Warburton 2010; Cascini *et al.* 2019; Westerman *et al.* 2022). As such, it is unclear whether the ancestral pattern for the species of *Protemnodon* would have been pentapedal or quadrupedal motion at slow speeds.

The Australian Pleistocene species of *Protemnodon* have caudal vertebral morphologies suggestive of differing levels of adaptation to tail use during high-speed hopping. In the 'floating' phase of bipedal hopping, in which the individual is off the ground, and the hindfeet have pushed off the substrate and are moving anteriorly from full posterior extent, the tail is curved upwards and actively raised. This provides a counterbalance for the body, moving the centre of gravity further caudally and preventing forward-pitching of the body upon landing (Baudinette 1989; Hopwood & Butterfield 1990; Baudinette 1994). This action necessitates strong extension of the lumbar spine and tail by muscular groups including the mm. sacrocaudalis dorsalis lateralis, which originates on the lower lumbar vertebrae and the sacrum and inserts to the mammillary processes of the proximal caudal vertebrae (Dawson *et al.* 2014). The presence of large mammillary processes on the proximal caudal vertebrae of *P. anak* and *P. viator* **sp. nov.** indicates that these two species required enlarged mm. sacrocaudalis dorsalis lateralis to support an extended tail during hopping. The mammillary processes on the proximal caudal vertebrae of *P. mamkurra* **sp. nov.** are relatively smaller, indicating a less developed mm. sacrocaudalis dorsalis lateralis. This suggests a comparatively reduced emphasis on use of the tail to aid hopping in *P. mamkurra* **sp. nov.** This may also suggest a reduced capability for sustained hopping, or, since during fast hopping more stress is put on the attachment areas (Biewener 1990), it could be an indicator of a lower speed of hopping to which they are adapted.

It has been suggested that large Pleistocene species of *Protemnodon* did not locomote pentapedally, based on features associated with the musculature of the sacrum and proximal caudal vertebrae (Jones *et al.* 2021). The large size of the sacrum of an unregistered specimen from the South Australian Museum that was referred to *P. brehus* was interpreted as suggesting significantly different forces in the hindlimbs compared to other kangaroos (Jones *et al.* 2021). The Ca1 of *P. anak* was described as lacking the morphological features seen by Dawson (2015) in large extant kangaroos that draw the tail under the body during pentapedal locomotion (Jones *et al.* 2021). Although we agree that the smaller *P. tumbuna* and *P. otibandus* quite possibly did not utilise pentapedal locomotion, it is argued

here that the inferred musculature of the caudal vertebrae, combined with other lines of evidence focussing on hindlimb proportions, form a stronger case that the larger species (*P. anak, P. mamkurra* **sp. nov.** and *P. viator* **sp. nov.**) most likely did undertake pentapedal movement as their primary low-speed locomotory mode.

Forelimbs

The species of *Protemnodon* have generally robust and muscular forelimbs, particularly the upper forelimb. The humeral proximal shaft is distinctly more robust and craniocaudally deeper than in other macropodines. This provides additional bracing against stresses in the sagittal plane, strengthening the humerus as the body moves over the forelimb during quadrupedal/pentapedal locomotion. A broad distal humerus provides additional structural support for the elbow joint (Jenkins Jr 1973). The deep humeral shaft and the broad lateral supracondylar ridge with pointed proximal peak facilitate the origins of a large m. brachialis and m. brachioradialis respectively, which flex the elbow (Hopwood 1974). The greater tubercle is tall and well-developed, for the insertions of the m. supraspinatus and m. infraspinatus, which perform abduction, stabilisation and rotation of the humerus, and the partial insertion of the m. pectoralis minor, which flexes the shoulder and stabilises the humerus. The lesser tubercle is also fairly large and tall, for the insertion of the m. subscapularis, which medially rotates and adducts the head of the humerus, and the m. coracobrachialis. These muscles provide support and stability as the body moves over the forelimb (Hopwood 1974; Warburton *et al.* 2011). The similar, though slightly weaker, development of the greater and lesser tubercles of the humerus in *M. fuliginosus* and *O. rufus* suggests that species of *Protemnodon* had fairly similar functional requirements to these modern species, though with more focus on stability and support for flexion and extension. This may have aided low-speed locomotion given the generally greater body mass of species of *Protemnodon* (Helgen *et al.* 2006).

We find the forearm of the species of *Protemnodon* to be muscular and fairly robust, stemming from a greater need for weight bearing during slow locomotion, or during bounding in the possibly quadrupedal *P. tumbuna*, as discussed below. The species of *Protemnodon* generally possess a fairly short, broad olecranon process. This allows for the insertion of large mm. triceps caput lateral medial et longum without the need for greater leverage from a more elongate olecranon (Warburton *et al.* 2011). Short, broad and dorsoventrally compressed proximal and middle manual phalanges are ubiquitous within *Protemnodon*. Broad phalanges may have provided additional support against transverse stresses during low-speed pentapedal and quadrupedal movement. The proximal and middle phalanges in particular have dorsally tilted proximal articular surfaces, suggesting a slightly greater degree of digitigrady than in species of *Macropus* or *Osphranter* (Gould, 1842).

Protemnodon anak

The forelimb of *P. anak* provides evidence of reinforcement to support slow-speed locomotion, as well as musculature possibly associated with intermale fighting, but does not appear to support the previous hypothesis of adaptations for overhead browsing. The forelimb of *P. anak* is known primarily from a large and muscular specimen (NMV P39105) that possesses the longest humerus, ulna and radius known for the genus and is here considered probably male due to its extreme forelimb dimensions. The deep, narrow bicipital groove would likely have constrained a large m. biceps brachii to flex the elbow. Similar to the condition seen in large males of *O. rufus*, this feature is likely associated with the need for powerful forelimb flexion during fighting between rival males for mates (Ganslosser 1989; Jarman 1989) as much as with locomotion. The ulna of *P. anak* is very deep and transversely compressed in its proximal component, providing greatest support against forces in the sagittal plane during low-speed locomotion. It could be expected, were *P. anak* adapted to overhead browsing, as was suggested Den Boer (2018), that this ability would manifest in forelimb adaptations, as in sthenurines. However, *P. anak* possesses a muscular forelimb more similar to that of *O. rufus*, showing no sign of overhead elevation in the morphology of the forelimb (Janis *et al.* 2020), and possess short digits, which would not extend browsing range.

Protemnodon mamkurra **sp. nov.**, *P. otibandus*, and *P. tumbuna*

Protemnodon mamkurra **sp. nov.** and *P. otibandus* have manual morphologies that suggest increased use of the forelimb for locomotion. These two species have a deeper carpal tunnel than *P. viator* **sp. nov.**, due mainly to the longer, curved palmar process of the hamatum. This provides for a larger m. flexor digitorum superficialis and m. flexor digitorum profundus, which flex the digits, providing forward propulsion, and stabilise the extended digits while the manus is bearing weight. The distal humerus and proximal ulna of *P. tumbuna* appears similar to that of *P. otibandus* in the degree of adaptation to forelimb use for locomotion, exhibiting a deep proximomedial flexor fossa on the ulna, which is the partial origin of the m. flexor carpi ulnaris and flexor digitorum profundus. These species were thus probably more reliant on their forelimbs for locomotion than *P. viator* **sp. nov.**

The functional purpose of the broad, palmarly curved, strongly dorsopalmarly compressed distal manual phalanges of *P. mamkurra* **sp. nov.** is unclear. Sthenurines, possess similarly curved, flattened distal manual phalanges with small flexor tubercles. These phalanges were hypothesised to be adapted for grasping foliage during browsing (Wells & Tedford 1995; Sears 2004), though sthenurine phalanges II–IV were far more elongate than those of *P. mamkurra* **sp. nov.** The short, robust proximal and middle phalanges of *P. mamkurra* **sp. nov.** are unlikely to have facilitated grasping in the manner of sthenurines. Their use may be fossorial, as has

been suggested based on robust ulnar morphology (Moore 2008). However, digging macropodoids such as the burrowing bettong, *Bettongia lesueur* (Quoy & Gaimard, 1824), have tall distal phalanges to provide support against the substrate, with enlarged flexor tubercles for the insertion of a powerful mm. flexor digitorum superficialis et profundus (Grand & Barboza 2001). The small phalangeal flexor tubercles of *P. mamkurra* **sp. nov.** suggest that the digits were not used for powerful digging in this manner. The possibility remains that the species engaged in scratch-digging, such as that undertaken by the bandicoot, *Isoodon fusciventer* (Gray, 1841). Ulnar robustness and the mass of the m. flexor carpi radialis and m. flexor digitorum superficialis covaried significantly in a study of forelimb anatomy in *I. fusciventer* (Martin *et al.* 2019). As discussed above, a deep carpal tunnel is present in *P. mamkurra* **sp. nov.** and would have facilitated the powerful flexion of these muscles. We deem it possible that *P. mamkurra* **sp. nov.** engaged in scratch-digging, perhaps to search for food items such as fungi.

The ulna of *P. tumbuna* (PM 25622) was described by Menzies & Ballard (1994) from a currently missing, near-complete specimen found in Haeapugua swamp in central PNG (Fig. 2), as follows: 'The ulna is a substantial bone and suggests rather longer and more powerful forelimbs than in extant terrestrial macropodids. The ratio of ulna length to tibia length in this specimen is 1:1.3 compared to 1:1.8 in a modern forest wallaby (*Dorcopsis luctuosa*), the same ratio in a modern grass wallaby ([*Notamacropus*] *agilis*) but 1:1.13 in a modern tree kangaroo (*Dendrolagus* sp.)… The ulna also shows some highly unusual features. It is flattened for most of its length and only becomes terete [rod-like and tapering] in its final quarter… The dorsal crest commences just before the centre of the bone and is deflected radially, forming quite a deep fossa for the ulnar origin of the m. flexor digitorum profundus' (Menzies & Ballard 1994, p. 129). This description illustrates that this individual of *P. tumbuna* possessed a long, muscular forelimb well adapted for use in quadrupedal locomotion. The transverse compression of the proximal shaft and the rod-like distal shaft described above seems very similar to the state we have observed in *P. anak*. As this may be a male individual and the species may be highly sexually dimorphic, we cannot be certain that this is the degree to which the forelimb musculature of both sexes was developed, though forest-dwelling macropodines typically display a lesser degree of sexual dimorphism than those that inhabit open habitats (Jarman 1989; Kaufmann 2015). Nonetheless, the description of the forelimb by Menzies & Ballard (1994) does lend itself to the view, supported by the morphology of the hindlimb elements explored further below, that *P. tumbuna* was particularly advanced in its adaptation to quadrupedal locomotion when compared to other species of *Protemnodon*.

Protemnodon otibandus has a particularly raised, elongate caudal ridge on the radius, likely for the partial origin of the m. abductor pollicis longus (m. extensor ossis metacarpus pollicus), which extends digits I–III in the extant large macropodin *Macropus giganteus* Shaw, 1790 (Hopwood 1974). This ridge could also be associated with the m. pronator teres and m. pronator quadratus and thus indicate a strong ability to pronate the manus (Warburton *et al.* 2011; Martin *et al.* 2019). The ridge is better developed than in *P. anak*, *P. viator* **sp. nov.**, *M. fuliginosus* and *O. rufus*, similar to that of *P. mamkurra* **sp. nov.** and *W. bicolor*. This could be related to greater use of the forelimb for locomotion, as the digits would be more regularly flexed and extended.

Protemnodon viator **sp. nov.**

Overall, the forelimb of *P. viator* **sp. nov.** is fairly similar to that of *P. mamkurra* **sp. nov.** The humerus of *P. viator* **sp. nov.** differs only very slightly from that of *P. mamkurra* **sp. nov.** Significant differences are present, however, in the distal forelimb elements. The ulna and radius of *P. viator* **sp. nov.** are considerably less robust than in *P. mamkurra* **sp. nov.**, suggesting less of a weight-bearing role, and perhaps less use overall as a means of locomotion. The ulna is more robust than that of *O. rufus* and *M. fuliginosus*, which is unsurprising considering the larger body mass of *P. viator* **sp. nov.** The ulna and radius give the impression of a forelimb requirement for locomotion and weight-bearing intermediate between the high-geared, gracile living macropodins and the lower-geared, more robust *P. mamkurra* **sp. nov.**

The prominent, proximally situated cranial ridge on the radius of *P. viator* **sp. nov.** may be for the partial origin of the m. abductor pollicis longus, which inserts to metacarpal I and extends the manus, the insertion of the m. pronator teres, which pronates the distal forelimb, and/or the partial origin of the m. flexor digitorum profundus, which inserts onto and flexes the digits (Hopwood 1974; Warburton *et al.* 2011). This ridge is fairly well-developed in all species of *Protemnodon* for which the proximal radius is known, but is slightly more distally situated than in *P. viator* **sp. nov.**, and lacks the eminence at the proximal end seen in this species. The purpose of this eminence is not certain; the cranial radial ridge is well-developed in species of *Dendrolagus*, associated with the need for powerful manual flexion during climbing (Warburton *et al.* 2011), though this is almost certainly not the case for the very large-bodied *P. viator* **sp. nov.** One possible explanation is that large forelimb flexor muscles are better developed in males of *P. viator* **sp. nov.**, as is the case with living macropodins, and particularly in the largest species, which inhabit more open environments (Warburton *et al.* 2013). In these species, during fights over mating rights, males strike and pull at the opponent's head and neck while standing tall (Ganslosser 1989), and the need for competitive advantage in these fights has been shown to drive significant dimorphism via positive allometry in the forelimb bones and musculature of males (Warburton *et al.* 2013; Richards *et al.* 2015). However, as the ridge is prominent proximally in the five known specimens, including in one considered probably female (SAMA P59552), this may not be the cause of the enlargement of this muscle attachment site in *P. viator* **sp. nov.**

Comparison with previous studies

Recent functional analyses of the humerus (Janis *et al.* 2020; Jones *et al.* 2021) demonstrated that the large Pleistocene species of *Protemnodon* were better-adapted to forelimb weight-bearing than large modern kangaroos. The large, craniomedially expanded greater tubercle of the humerus of *P. anak* was interpreted as facilitating the insertion of a larger m. supraspinatus than in most macropodids, though the origin of the m. supraspinatus, the supraspinous fossa on the scapula, was described as being similar in size to that of modern macropodids (Janis *et al.* 2020). The upper forelimb is known to be a highly sexually dimorphic area in macropodines (Jarman 1989; Richards *et al.* 2015), which may be a confounding factor when examining the development of the humeral musculature in fossil macropodids. Indeed, the m. supraspinatus has been identified as being considerably larger in *M. fuliginosus* males than in females (Warburton *et al.* 2013). Jones *et al.* (2021) undertook two-dimensional geometric morphometric analysis of the distal humeral articulation of *P. anak*, *P. otibandus* and an unregistered NHMUK partial humerus allocated therein to *P. brehus* (allocated here to *P.* sp. cf. *P. mamkurra*). Jones *et al*.'s (2021) PCA of the 2D proportions of the distal humerus of extinct kangaroos and numerous comparative marsupial taxa found that species of *Protemnodon* clustered with scansorial and terrestrial quadrupedal taxa immediately adjacent to saltatorial taxa, with a specimen of *P. anak* (NMV P39105, Fig. 20) falling on the margin between scansorial and saltatorial taxa. The distal humeri of these species of *Protemnodon* were interpreted therein as providing greater forelimb stability and capacity for weight-bearing, particularly in *P. anak*.

The results presented here generally support those of the above studies, insofar as, generally speaking, the species of *Protemnodon* do appear to have used their forelimbs for locomotion to a greater extent than modern large kangaroos, and may have utilised different locomotory modes between species. However, Janis *et al.* (2020) and Jones *et al.* (2021) interpret the slightly greater strength and stability of the forelimb of the Pleistocene Australian species of *Protemnodon* to suggest that they were predominantly quadrupedal. Increased forelimb musculature and support is also recognised by this study, but the morphology of the forelimbs is instead interpreted here as allometric scaling, reflecting a greater need for support and stability for a heavier kangaroo during pentapedal locomotion. The considerable mass of the Pleistocene Australian species of *Protemnodon*, the largest specimens of which may have been more than twice the mass (~166 kg) of a large adult male of the slender-limbed, high-geared, highly derived *O. rufus* and *M. fuliginosus* (~80 kg) , may have driven a need for increased stability and weight-bearing capacity in the forelimb. The differences in postcranial morphology highlighted here suggest that, just as with the extinct sthenurine kangaroos (Helgen *et al.* 2006), the Pleistocene Australian species of *Protemnodon* likely had differing ecological adaptations, and cannot be treated as a single palaeoecological unit.

Hindlimb

A large, robust ilium with a deep gluteal fossa, a deep caudal spine and a broad lateral spine is characteristic of the species of *Protemnodon* and is not seen in other large macropodines. The m. iliacus, a major hip flexor (Hopwood & Butterfield 1990; Warburton *et al.* 2012), arises from the iliac fossa and extends across the cranial surface of the very broad lateral iliac spine. On the opposing caudolateral face of the ilium, in the very broad and deeply concave gluteal fossa, the mm. gluteus profundus et minimus originate. Along with the m. gluteus medius, which originates from the medial component of the broad iliac crest, this very large muscle group inserts to the greater trochanter on its tip and lateral face and works to powerfully extend the hip joint (Warburton *et al.* 2012). The m. gemelli, which serves to medially rotate and abduct the femur at the hip joint, originates on the rugose, thickened caudodorsal face of the ischium, inserts to the large, elongate trochanteric fossa and was likely well-developed in species of *Protemnodon*. The m. vastus lateralis, part of the quadriceps group (mm. quadriceps femoris), which act primarily to flex the knee, is a large muscle originating from the distal part of the greater trochanteric ridge, the associated proximolateral ridge and the lateral part of the dorsal surface of the femoral proximal end (Hopwood & Butterfield 1990; Warburton *et al.* 2012); all of which are enlarged in species of *Protemnodon* compared to other macropodines. There is an emphasis in the morphology of the pelvis and femur on providing greater support for enlarged musculature that extends, flexes and, crucially, stabilises the hip and knee joints during the locomotion of a large, robust kangaroo.

The pes of the species of *Protemnodon* is also distinguished by: their calcaneus with large, medially projected sustentaculum tali; a robust metatarsal V; and a broad, dorsoplantarly compressed middle pedal phalanx IV (Fig. 144). The broad sustentaculum tali, which directs the passage of the m. flexor digitorum profundus tendon (Hopwood & Butterfield 1990), provides broader support for the plantar flexion of the pes outside of the sagittal plane to than is seen in high-speed hoppers like *O. rufus*. A particularly robust metatarsal V, peculiar among macropodins to species of *Protemnodon*, may provide support and transverse stability in the pes to accommodate for greater body mass.

Protemnodon tumbuna

Protemnodon tumbuna displays a hindlimb morphology that indicates a greater degree of adaptation to quadrupedal locomotion than the Pliocene *P. otibandus*. The crural index of *P. tumbuna* is low (1.02) (Fig. 133), equating to those of *Dorcopsulus vanheurni* and *Setonix brachyurus* (Quoy & Gaimard, 1830) and slightly higher than that of *De. bennettianus*. A lower CI is inferred to be associated with slower acceleration, less efficient hopping and a lower maximum speed (Murray 1991; Kear *et al.* 2008). Low-gearing is associated with denser-vegetated habitats in macropodines (Windsor & Dagg 1971). The femur has a quite distally situated and slightly medially displaced quadratus tubercle. The m. quadratus femoris, which

originates from the caudal surface of the ischiatic table and inserts to the quadratus tubercle, is a powerful extensor of the hip joint and is proximally situated in the higher-speed macropodins and relatively distal in less derived, lower-geared kangaroos such as species of *Dendrolagus* and *Dorcopsulus*. In species of *Dendrolagus*, the distally inserting m. quadratus femoris also plays a role in improved hip manoeuvrability (Warburton *et al.* 2012).

The tibia of *P. tumbuna* is distinctly short and robust, with a relatively more distally elongate cnemial crest, a thick, weakly raised proximolateral crest and broad, rounded intercondylar eminence, similar to species of *Dendrolagus*, *Dorcopsulus* and *Thylogale* Gray, 1837. The low, thick proximolateral crest, which separates and is the partial origin of the m. tibialis cranialis and m. popliteus, which act to dorsiflex the pes and flex the knee respectively (Hopwood & Butterfield 1990; Warburton *et al.* 2012), may indicate the smaller size of these muscles, providing a less efficient, less powerful hop. A relatively distally extensive cnemial crest indicates an m. tibialis cranialis with a more distally extensive muscle belly than in crown macropodins and other species of *Protemnodon*. The bellies of the hindlimb muscles are relatively short in the high-geared *Macropus giganteus* and considerably longer in the tree-kangaroo *Dendrolagus lumholtzi* Collett, 1884 (Hopwood & Butterfield 1990; Warburton *et al.* 2012). The long tendons of the major crurial muscles store and release elastic energy during hopping, and are thus of great importance for efficient locomotion (Alexander & Vernon 1975). Further, a more proximally situated muscle reduces the energy required to move the distal part of the limb by making the distal end lighter (Wickler *et al.* 2004). Large, proximally situated limb muscles with long tendons are also seen in high-speed cursorial vertebrates, such as the ostrich and the horse (Payne *et al.* 2005; Smith *et al.* 2006). The presence of shorter tendons and longer muscle bellies in the hindlimb musculature of *P. tumbuna* suggests that this species was not capable of a fast, efficient bipedal hop. This is in keeping with the findings of Kear *et al.* (2008).

The pes of *P. tumbuna* is quite specialised. The metatarsal V is very short, broad and robust, with a very small medial plantar tubercle and shallow plantar groove. The calcaneus is particularly odd, with a medially displaced and rotated head; a strongly convex and medially flared plantar surface; and a medially expanded or flared caudal epiphysis. A convex plantar surface is very unusual within Macropodinae and may indicate that *P. tumbuna* did not have a fully plantigrade stance (that is, calcaneus to distal phalanx in contact with the ground) at rest. The condition is present in some living dorcopsins, including *Dorcopsulus vanheurni*, which today inhabits the area around Nombe Rockshelter (Flannery 1990a). The medial flaring of the plantar surface and medial displacement of the head may suggest that the range of angles for the extension of the ankle by the m. plantaris and mm. gastrocnemius, which insert to the caudal epiphysis and plantar surface of the calcaneus, has broadened sufficiently to require support outside of the sagittal alignment typical of other macropodine hind feet. This may be linked to increased abduction of metatarsal V, being mirrored through broader support from the posterior of the pes. A medially flared caudal plantar surface and medially displaced calcaneal head are also seen in species of *Dorcopsulus* and *Se. brachyurus*. Species of *Dorcopsulus* and *Setonix* Lesson, 1842 are among the least specialised hoppers in Macropodinae, both exhibiting the greatest use of terrestrial quadrupedality, including quadrupedal bounding (Windsor & Dagg 1971). The calcaneal head displacement of *P. tumbuna* supports the locomotory inferences drawn from the ratios of the crural elements.

Protemnodon otibandus

The calcaneus and metatarsals IV and V of *P. otibandus* are short, broad, and robust, for slow movement with frequent changes of direction. The calcaneal tuberosity is relatively lower than in the larger Australian Pleistocene species, suggesting a lesser need for resistance to the forces from the gastrocnemial tendon in the sagittal plane. The calcaneus exhibits the condition of having the head slightly offset medially relative to the tuberosity, which suggests a change in the dominant force vector where the pes is rotated slightly laterally, to a lesser extent than in the Pleistocene *P. tumbuna*. This slight displacement perhaps indicates the beginning of a divergence from the typical sagittal alignment of the macropodine pes. The discovery of more complete crural material of *P. otibandus* would allow for more detailed investigation of the locomotory ability of this species.

Protemnodon viator **sp. nov.**

Adaptations for power and stability in the hindlimb are particularly apparent in *P. viator* **sp. nov.** In this species the ilium is largest and deepest, and the lesser trochanter is projected ventromedially from proximal end of the femur by the conjunction of the well-developed intertrochanteric crest and lesser trochanteric ridge. This area serves as the insertion point for the m. iliacus and m. psoas major, which are major flexors of the hip joint. The femoral proximal end is expanded laterally by a broader greater trochanteric ridge, giving rise to a larger proximolateral ridge than other species of *Protemnodon*. The crural index of *P. viator* **sp. nov.** is the highest among the species of *Protemnodon* (~1.95) (Fig. 133), close to that of *M. fuliginosus* (~1.75) and *O. rufus* (~1.98), and its relatively gracile tibia, metatarsals and calcaneus also point toward locomotory similarities with extant medium- and high-geared macropodins.

The hindlimbs of *P. viator* **sp. nov.** were seemingly adapted for efficient, long-distance hopping, in many ways similar to *M. fuliginosus* and *O. rufus*. The sustentaculum tali of *P. viator* **sp. nov.** is the least medially projected of the genus, providing support for the action of the m. flexor digitorum profundus chiefly in the sagittal plane. Corroborating this is a tall calcaneal tuberosity with a triangular cross-section, to provide greatest support for the plantar flexion of the pes by the mm. gastrocnemius in the sagittal plane, and a tall, narrow cuboid with a very deep, narrow plantar flexor tendon groove. The need for support principally in the sagittal plane is also visible in

the distal pedal phalanges IV and V, which are tall and narrow with a distinct, angular dorsal peak. Individuals of *O. rufus* are capable of travelling long distances (>300 km, Priddel *et al*. 1988b) in search of water, a behaviour which is more common in sub-adult males and during drought (Oliver 1986; Priddel *et al.* 1988a; Priddel *et al.* 1988b). Individuals of *P. viator* **sp. nov.** may have had a similar, though less extreme, capacity for vagility.

A study of the bone structure of the calcaneal tuberosity of large macropodids, with the genus *Protemnodon* represented by a specimen here allocated to *P. viator* **sp. nov.** (AMNH FM145501), demonstrated that *P. viator* **sp. nov.** lacked the extreme thickening of the cortical bone of the calcaneal tuberosity observed in *M. giganteus* or *M.* cf. *M. titan* Owen, 1838 (Wagstaffe *et al.* 2022). This was interpreted to imply a primarily quadrupedal mode of locomotion for this species. However, while it may be true that this would provide less support against the forces the tuberosity was exposed to by the gastrocnemial tendon, comparisons with extant taxa were not made for any mid- or low-geared bipedally hopping macropodines, only to the extremely efficient, long-distance hopper *M. giganteus*. As such, there is no demonstrated point at which the osteology of the calcaneal tuberosity definitively does not support bipedal hopping. So, we consider that this finding at most illustrates that *P. viator* **sp. nov.** was less well-adapted to high-speed hopping than *M. fuliginosus* in terms of its calcaneal tuberosity morphology, perhaps suggesting a slower-accelerating, mid-geared hopper.

Protemnodon mamkurra **sp. nov.**

The distinct differences between the relative hindlimb proportions of *P. mamkurra* **sp. nov.** and *P. viator* **sp. nov.**, species with remarkably similar craniodental morphologies, suggest that the two were adapted to quite different locomotory habits. *Protemnodon mamkurra* **sp. nov.** has a considerably lower crural index (~1.4) than *P. viator* **sp. nov.** (~1.9) (Fig. 133). The tibia is similar in robustness to that of *W. bicolor*. The calcaneus is robust, with a tall but rounded tuberosity in cross-section, providing support for the leverage and flexion of the pes in the transverse as well as sagittal plane. The cuboid is short and very broad, with a low, broad lateral plantar tubercle and broad, shallow flexor groove, also quite similar to the talus of *W. bicolor*. The distal pedal phalanges IV and V are broad with a rounded dorsal peak. This may indicate a slow, manoeuvrable hopping gait, as transverse support in the hindlimb and pes facilitates changes of direction when moving through dense undergrowth (Bishop 1997). The greater robustness of the metatarsal V may serve to spread the body weight more broadly during locomotion over a softer substrate (Roderick T. Wells, pers. comm. 2022) or brace against the greater lateral stresses associated with moving through a more closed habitat. Although little research has been undertaken into the role of the fifth metatarsal in macropodid locomotion, an unpublished study demonstrated that a robust metatarsal V increased the bending resistance of metatarsal IV (Wagstaffe 2018). If *P. mamkurra* **sp. nov.** was indeed a fairly robust, heavy kangaroo, a particularly robust fifth metatarsal providing additional support to the primary fourth digit would be expected. The proportions and hypothesised musculature of the hindlimb and pes of *P. mamkurra* **sp. nov.** suggest a locomotory style similar to those of woodland- and forest-dwelling macropodines like *Thylogale billardierii*, which utilise a slow quadrupedal gait and a faster bipedal hop with a low top-speed, with no fast quadrupedal bounding (Windsor & Dagg 1971; Dawson *et al.* 2015).

In macropodins, a high crural index is typically accompanied by elongate metatarsals to provide additional leverage against the calcaneal tuberosity for the plantar flexion of the pes and increase stride length during hopping, while in more plesiomorphic, slow-moving macropodines, a short and robust tibia is paired with fairly short metatarsals (Kear *et al.* 2008). Oddly, the low crural index is not accompanied by a shorter, more robust metatarsal IV in *P. mamkurra* **sp. nov.**, which instead possesses an absolutely longer metatarsal IV and V than both *P. anak* and *P. viator* **sp. nov.** Just a note for interest—it would be interesting to see if this was more similar to the proportions of juv protes, which might suggest a relatively recent evolution of Pmam via paedomorphosis.

Protemnodon anak

It is apparent in their crural and pedal proportions and morphology that individuals of *P. anak* were moderate in their hopping power and efficiency between the higher-geared *P. viator* and the lower-geared *P. mamkurra*. The crural index of *P. anak* is intermediate among macropodins, similar to that of *Osphranter robustus* Gould, 1841 and *Notamacropus agilis* (Gould, 1841), both mid-geared hoppers (Kear *et al.* 2008; Dawson *et al.* 2015). The large, gracile femur of *P. anak* has fairly large muscular attachment sites on the proximal, end but without the degree of specialisation and enlargement seen in *P. viator* **sp. nov.** The lateral trochlear crest is considerably more raised than the medial crest, a feature common in mid- and high-geared macropodins like *N. agilis* and species of *Macropus*, providing support to the outside of the knee joint during locomotion, as the fibula transmits force to the lateral side of the epiphysis (Wells & Tedford 1995). The tibia has a relatively longer cnemial crest than do specimens of *P. viator* **sp. nov.**, *P. snewini*, *O. rufus* and *M. fuliginosus*, providing for a longer-bellied m. gastrocnemius, for a less efficient hop than those higher-geared macropodins. The review by Janis *et al.* (2023) included a regression of tibia length versus body mass and concluded that the relatively slightly shorter tibia of *P. anak* would not have supported bipedal saltation to the degree seen in the high-geared, efficient crown macropodins, a view which is supported here.

Protemnodon dawsonae **sp. nov.**

Based on the more completely known *P. mamkurra* **sp. nov.** and *P. viator* **sp. nov.**, *P. dawsonae* **sp. nov.** appears to have been intermediate between these two species in terms of its locomotory abilities. Although the calcaneus of *P. dawsonae* **sp. nov.** is incompletely known, it possesses a calcaneal tuberosity with a robustness and

height that is intermediate between those of *P. mamkurra* **sp. nov.** and *P. viator* **sp. nov.** The metatarsals IV and V of *P. dawsonae* **sp. nov.** are large and elongate, more like those of *P. anak* and *P. mamkurra* **sp. nov.** than *P. viator* **sp. nov.** Critically, the crus of this species is not known. Its description would greatly aid understanding of the locomotion of *P. dawsonae* **sp. nov.**

Role of the middle phalanx IV

A very short, broad, dorsoplantarly compressed middle phalanx IV is characteristic of species of *Protemnodon*. Within Macropodinae, a short, broad middle phalanx IV is otherwise only observed in *O. rufus* and the Pliocene *Prionotemnus palankarinnicus* Stirton, 1955, though to a lesser degree than in the species of *Protemnodon*. This phalanx plays an important role in hopping, so its unique development in species of *Protemnodon* merits discussion here.

In macropodines, the distal fourth phalanx typically impacts the substrate first during hopping, followed by a pad under the proximal and middle fourth phalanges (Griffiths 1984; Hopwood & Butterfield 1990). The middle fourth phalanx directs and accommodates two major flexor tendons: the m. flexor digitorum profundus, which passes directly plantar to the middle fourth phalanx, between the proximal plantar tubercles, to insert to the flexor tubercle of the distal fourth phalanx; and another major digital flexor, the m. flexor digitorum superficialis, which passes along the plantar surface of the proximal fourth phalanx superficial to the m. flexor digitorum profundus and inserts to the plantomedial and plantolateral surfaces of the plantar tubercles of the middle fourth phalanx (Hopwood & Butterfield 1990; Warburton *et al.* 2012).

In addition to its robustness, the middle phalanx IV of the species of *Protemnodon* has particularly wide articular facets. The proximal facet is almost as wide as the margins of the plantar tubercles, instead of being considerably narrower, as in *O. rufus* and *Pri. palankarinnicus*. The distal facet is also considerably broader than in other macropodines, though the trochlea is shallower and less proximoplantarly extensive than in *M. fuliginosus* and *O. rufus*. With the presence of proximally projected plantar and dorsal margins of the proximal facet, the broad proximal facet of the middle phalanx forms a distinct 'saddle' shape, which is particularly resistant to dislocation (Hildebrand *et al.* 2001). Given that the species of *Protemnodon* are fairly robust and muscular kangaroos, it is possible that this broad, flattened phalanx developed as a means of securing the articulation of the fourth pedal phalanges under increased stress from additional body mass during hopping. Conversely, it is not a morphology that would indicate increased adaptation to lower-impact quadrupedal locomotion in species of *Protemnodon*.

Protemnodon anak exhibits a particularly broad proximal section of the middle pedal phalanx IV, with the plantar tubercles flared outward medially and laterally. These enlarged, almost bulbous plantar tubercles are similar to those present in *O. rufus*, though relatively larger. This may indicate the insertion of a larger m. flexor digitorum superficialis in these species, associated with a need for more powerful flexion of the fourth digit. In *P. viator* **sp. nov.** and *P. snewini* the well-developed plantar tubercles extend further distally along the transverse surfaces of the middle phalanx IV than in other species of *Protemnodon*, though the purpose of this adaptation is uncertain. In *P. mamkurra* **sp. nov.** and *P. otibandus*, the plantar tubercles are relatively smaller and more restricted to the proximal plantar region of the middle phalanx, similar to the state of the mid-geared *W. bicolor* and the low-geared *Dorcopsulus vanheurni*. This likely signals relatively less powerful flexion of the fourth digit, in keeping with the other morphological correlations of these two species with lower-geared macropodids, discussed above.

Summary of locomotory adaptations

Our findings broadly support those of previous studies, but improve understanding of variation in locomotory adaptations between different species and depth of understanding of ecomorphology within species. We suggest that the Australian species of *Protemnodon* were generally bipedal hoppers, and used pentapedal locomotion while moving slowly. The New Guinean *P. tumbuna* may have utilised a quadrupedal bound for high-speed locomotion to a greater degree than in other species of *Protemnodon*, bolstering the conclusions drawn by Kear *et al.* (2008). However, it is worth noting that all living macropodoids except *Hypsiprymnodon moschatus* have the ability to hop bipedally (Windsor & Dagg 1971; Baudinette 1989). This includes those regularly described as quadrupedal, such as species of *Potorous*, *Setonix brachyurus*, and species of *Dendrolagus* (Barrett 1943; Buchmann & Guiler 1974; Baudinette 1977, 1989). While species of *Protemnodon* do indeed demonstrate, to varying degrees, divergence from the limb morphology of the large, high-geared, extant macropodins like *O. rufus* and *M. fuliginosus*, these species are not necessarily the best yardstick for what is required morphologically, as a minimum, for a macropodine to hop. Species of *Osphranter* and *Macropus* are extremely well-adapted high-speed hoppers, and are unique among living mammals for their locomotory efficiency (Kram & Dawson 1998). Since it is the case that more basal macropodids with much less specialised hindlimb morphology than crown macropodins are also capable of sustained hop ping, and since the species of *Protemnodon*, with the possible exception of *P. tumbuna*, are apparently closer to the hindlimb morphology of the crown macropodins, it seems most likely that the species of *Protemnodon* hopped bipedally. These inferences from functional morphology are supported by phylogenetic and trace fossil evidence.

Body size and mass

The first study to do more than state an approximate mass for a species of *Protemnodon* was Helgen *et al.* (2006), who estimated the body masses of specimens of *Protemnodon* by establishing the relationship between

minimum femoral circumference and mass in extant macropodines. However, the revised taxonomy and changes to specimen allocations herein have altered the identities of several of the specimens used in that analysis, impacting the usefulness of the estimated masses of the Australian Pleistocene species. The study produced a mass estimate of ~166 kg for *P. roechus* based on the partial femur of NMV P26570 from Lake Victoria, New South Wales, which we allocate to *P. mamkurra* **sp. nov.** The mean mass estimate for *P. brehus* was 111 kg, from specimens including NMV P173087 from Spring Creek, which is here allocated to *P. viator* **sp. nov.** The mean mass estimate for *P. anak* was greater than that of *P. brehus* at 131 kg, but included the femur of SAMA P59549, the holotype of *P. mamkurra* **sp. nov.**

Wagstaffe *et al.* (2022) estimated the body masses of extinct macropodid taxa, including species of *Protemnodon*, by establishing the relationship between body masses and pedal dimensions of 64 extant macropodoid taxa, then extrapolating mass estimations to the same pedal measurements of the extinct taxa. The included specimen of *Protemnodon* sp. (AMNH FM145501 from Lake Callabonna, which we allocate to *P. viator* **sp. nov.**) was estimated to have weighed ~97 kg. The generic and specific taxonomic identities presented here will facilitate further study of the body mass ranges of the species of *Protemnodon*.

Palaeoecology

The Pliocene

Following the largely cool and dry climate of latest Miocene–earliest Pliocene, the early Pliocene of Australia was a period of fairly rapid warming and general increase in precipitation. There is evidence of aridification in the late Pliocene (Sniderman *et al.* 2016). C_4 grasslands became prominent in Australia for the first time during the early Pliocene and spread rapidly from around 3.5 Ma, starting in the northwest (Martin & McMinn 1994; Andrae *et al.* 2018). Northeastern Australia shows evidence of coastal araucarian rainforest and casuarinaceous sclerophyll forest through the Pliocene (Martin & McMinn 1993; Kershaw 1994). In the late Pliocene deposits at Chinchilla in eastern Australia, there is evidence of high rainfall and a mosaic of tropical rainforest, wetlands and grasslands (Montanari *et al.* 2013). Southeastern Australia was warm during the early Pliocene, cooling and becoming more variable in the late Pliocene, but maintaining generally much higher precipitation than modern levels (Gallagher *et al.* 2003). Although there is evidence of small resurgences of temperate rainforest, the vegetation in the bulk of the southeast was wet sclerophyll forest up until the latest Pliocene, when a drying climate drove the development of open woodlands and grasslands (Kershaw *et al.* 1994; Sniderman *et al.* 2007). Faunal correlations of the Big Sink LF at Wellington in central eastern New South Wales suggest mesic sclerophyll woodland/forest was present (Dawson *et al.* 1999). Pollen in early Pliocene sediments on the Grange Burn in southwestern Victoria indicates both gymnosperm-dominated temperate rainforest and wet and dry *Acacia*/Casuarinaceae-rich sclerophyll forests, with some grasses present (Macphail 1996, 1997). The faunal assemblage was interpreted as rainforest-adapted (Piper *et al.* 2006). The southern Australian coast during the early Pliocene was vegetated broadly by semi-arid and mesic grassy *Casuarina* and *Eucalyptus* woodlands, with areas of wet sclerophyll forest and rainforest (Benbow *et al.* 1995; Sniderman *et al.* 2016). In the late Pliocene, the vegetation of the Nullarbor began to aridify and open, with evidence of scrubby *Banksia* and Poaceae grasslands (Sniderman *et al.* 2016). In central Australia, evidence from near Lake Frome and Lake Eyre suggests arid scrubland, with open casuarinaceous sclerophyll forest, and wetlands and swamps not found in the area in the modern-day (Martin 1990, 1998). Despite generally increasing aridity, the region experienced brief warm, wet periods through the Pliocene (Benbow *et al.* 1995). Pliocene New Guinea was cool and humid, with faunal evidence from the late Pliocene Otibanda Fm. of savannah woodlands or possibly lowland rainforest (Plane 1967; Marshall & Beehler 2011).

The geographical range of *P. otibandus* extends from southeastern through eastern Australia to southeastern New Guinea, and inland to the Lake Eyre Basin (Fig. 142). The vegetation over the majority of this distribution ranged from wet and dry sclerophyllous woodlands and forests to rainforest. The Lake Eyre Basin is the most xeric extent of its range. Isotopic and palaeoclimatic evidence from the Pliocene Chinchilla Fm. in southeastern Queensland suggests that individuals of species of *Protemnodon* from the area, which we consider to include *P. otibandus*, shared similarities in diet with modern temperate and tropical kangaroo communities (Montanari *et al.* 2013). The range of *P. otibandus* is similar to that of *M. giganteus* (Caughley *et al.* 1983) and *W. bicolor* (Di Stefano *et al.* 2009; Cooke 2020) in its generally eastern distribution through predominantly mesic environments, though neither of these extant species extends into New Guinea (Maynes 1989). Comparison in vegetation preference and range could also be made to *Thylogale stigmatica* (Gould, 1860), which inhabits dense wet sclerophyll forests and subtropical and tropical rainforests from eastern Australia to southeastern New Guinea (Johnson & Vernes 2008). Functional morphological analysis paints *P. otibandus* as a low-geared bipedal hopper with a greater reliance on the forelimbs for locomotion than large modern kangaroos. This seems to fit well with the generally well-treed and mid- to high-rainfall environments that it inhabited.

Protemnodon snewini is known only from the early Pliocene Bluff Downs LF, central north Queensland (Figs 1 & 142). Based on tibial and pedal proportions and the proposed crural musculature, the species appears adapted to efficient bipedal hopping and similar in morphology to open-habitat macropodines. It has been suggested, based on the fauna of Allingham, that *P. snewini* inhabited open sclerophyll and open woodlands (Bartholomai 1978). An area of northeastern Australia including the fossil locality was considered to have been broadly mosaic rainforest with evidence of increasing presence of grasses during the

early Pliocene (Martin & McMinn 1993). The presence of the very large, grazing-specialised wombat *Ramsayia lemleyi* Archer, 1976 in the Bluff Downs LF (Archer & Wade 1976; Louys *et al.* 2022) implies a significant presence of grasses. Regardless, *P. snewini* is known only partially and from a single locality. The discovery of more complete material, or material from fossil localities with better understood palaeoenvironments would help to clarify the lifestyle and palaeohabitat of *P. snewini*.

Protemnodon dawsonae **sp. nov.** is distributed through the mid–late Pliocene of central eastern and central Australia (Fig. 142), which suggests a preference for semi-arid grassy woodlands to temperate woodlands and forest. The morphology of *P. dawsonae* **sp. nov.**, though quite incomplete, suggests it to be a robust, low- to mid-geared bipedal hopping kangaroo. Its range appears similar, though less extensive north and south, to that of the Pleistocene *P. anak* (Fig. 143a), and the modern *M. giganteus*. The fossil record for *P. dawsonae* **sp. nov.** is limited in its geographical range and by the paucity of postcranial material (forelimb and crus are unknown), which hobbles understanding of its palaeoecology. The fossil record is too incomplete to provide compelling evidence of competitive exclusion.

The Pleistocene

During the Pleistocene, an overall trend of increasing aridity prevailed over the bulk of Australia, but particularly in central and western Australia towards the end of the epoch (Fujioka *et al.* 2005; Nanson *et al.* 2008; McLaren & Wallace 2010). Eastern and southeastern Australia (from southeastern South Australia to southeastern Queensland) fluctuated between cooler glacial periods dominated by grassy *Eucalyptus* woodlands and open heathlands, and warmer interglacials promoting wet sclerophyll forest and temperate rainforest (Martin 1987; Kershaw *et al.* 1994; Lloyd & Kershaw 1997; Hughes *et al.* 2017; Weij *et al.* 2024). In the Darling Downs area in eastern Australia, the vegetation was composed of a mosaic of open sclerophyllous woodland, scrublands and grasslands (Price & Sobbe 2005; Price 2012). Central Australia, including the Lake Eyre Basin, was broadly semi-arid to arid, with desert grasslands, chenopod shrublands and open *Casuarina* and *Eucalyptus* woodlands dominating (Field *et al.* 2002; Martin 2006). During the middle–late Pleistocene the lakes in the Lake Eyre Basin were generally present, similar to those observed today following flood events, though not saline, with dramatic but temporary drying events occurring from around 160 ka (Cohen *et al.* 2012; Fu *et al.* 2017; Cohen *et al.* 2022). The Lake Eyre Basin occasionally experienced flood events that filled vast mega-lakes (Alley 1998; Fu *et al.* 2017). Vegetation in northeastern Australia was dominated by tropical rainforest, with evidence of high rainfall and mosaic grasslands and swamps (Gaffney & McNamara 1990; McNamara 1990; Kershaw 1994; Price 2012). The Nullarbor Plain experienced higher precipitation in the early Pleistocene than in the modern day and similar or slightly higher levels in the middle to late Pleistocene (Coede *et al.* 1990; Prideaux *et al.* 2007). With less widespread burning, the Nullarbor was more diversely vegetated and relatively well-treed, with a semi-arid mosaic of sclerophyll woodland and shrublands (Prideaux *et al.* 2007; Prideaux & Warburton 2008). In northern Tasmania, cool temperate rainforest of mainly *Nothofagus*, *Casuarina* and *Eucalyptus* remained fairly steadily present through the Pleistocene (Macphail *et al.* 1993).

At Nombe Rockshelter in the highlands of eastern New Guinea, very high-rainfall, mid-montane, *Nothofagus*-dominated rainforest prevailed through the late Pleistocene (Flannery *et al.* 1983; Prideaux *et al.* 2022). In West Baliem Valley in the montane west of New Guinea, vegetation fluctuated through late Pleistocene between sub-alpine herbfields and grasslands and upper-montane rainforest containing ferns and some *Nothofagus* (Flannery 1992a; Hope *et al.* 1993; Flannery 1999). There is evidence of lower temperatures than the modern day in late Pleistocene New Guinea, wherein the snow line fell periodically to ~1000 m lower, temperatures dropped to 2–6°C below modern averages, and montane vegetation was present at much lower altitudes (Heaney 1991; Flannery 1992a), with the treeline as low as 2200 m above sea level at the last glacial maximum (Walker & Flenley 1979).

Protemnodon anak, found across eastern Australia through the Pleistocene (Fig. 143a), is associated across the bulk of its range with what is currently mesic open and wet closed woodland habitats, extending into areas of tropical forest in the northeast and cool temperate forest in the southeast. The distribution of *P. anak* is similar to that of *M. giganteus* in the present-day (see Caughley *et al.* 1983). The extension of the distribution into Tasmania shows the tolerance of *P. anak* to cool temperatures, higher rainfall and dense forest. The absence of the species from the western half of Australia is possibly due to the xeric Nullarbor Plain and central western Australia acting as dispersal barriers, as they do for many modern taxa (Burbidge 1960; Keast 1981) including *M. giganteus* (Caughley *et al.* 1987). It is interesting that the environmental range of *P. anak* extended from the cool rainforests of northern Tasmania to the semi-arid Cooper Creek in southern central Australia. A possible modern analogue in this regard is *Macropus fuliginosus*, the western grey kangaroo, the range of which can extend from temperate open woodlands into arid central Australia along rivers and creeks, and further during flooding or high-rainfall years (Priddel 1988; Priddel *et al.* 1988a). The morphology and proportions of *P. anak* have been shown to align with that of mid-geared, bipedal-hopping forest- and woodland-adapted macropodines, which fits well with its distribution through open and closed woodlands and forests in mesic to high-rainfall areas. Its presence in central Australia may thus have implications for the late Pleistocene vegetation structure of these areas that are xeric today.

Protemnodon mamkurra **sp. nov.** shows a broad preference for cooler climates and southern areas, with a geographic distribution (Fig. 143c) similar to that of the modern *M. fuliginosus* (see Caughley *et al.* 1983). The habitat of *P. mamkurra* **sp. nov.** in middle and late

Pleistocene southeastern Australia was predominantly mesic grassy woodlands and closed *Eucalyptus* forests, including at the type locality, Green Waterhole Cave (Baird 1985; Newton 1988). The species has a strong presence in the middle Pleistocene Leaena's Breath Cave (400–200 ka, Prideaux *et al.* 2007) and Last Tree Cave (>101 ka, Prideaux *et al.* 2007) on the Nullarbor Plain. The range extends south into the high-rainfall, cool temperate rainforests of late Pleistocene northwestern Tasmania (Colhoun *et al.* 1999). Although this range of habitats may appear unlikely based on the distributions of modern large macropodids, it is perhaps not without precedent—*Simosthenurus occidentalis* (Glauert, 1910) has been found across southern Australia, from scrubby open woodlands in southwestern Australia to Mt Cripps, Tasmania, in the same deposit as material of *P. mamkurra* **sp. nov.** The distribution is also similar to that of *Metasthenurus newtonae* (Prideaux, 2000). The distribution of the robust *P. mamkurra* **sp. nov.** through temperate to cool, relatively well-wooded environments supports the interpretation of the limb proportions, morphology and suggested musculature as belonging to a low-geared kangaroo adapted to locomotion in dense vegetation.

Protemnodon viator **sp. nov.** inhabited predominantly inland, semi-arid and arid areas (Fig. 143b). These include the southeastern Kimberley region, which had sparsely treed grasslands and monsoonal tropical savannah in the middle and late Pleistocene (Wallis 2001; Pepper & Keogh 2014), and across the Lake Eyre Basin, which was broadly xeric during the Pleistocene, showing evidence of chenopod shrublands, open woodlands and grasslands, with increasing aridity and shrinking freshwater lakes in the late Pleistocene (Nanson *et al.* 1993; Alley 1998). The Cooper Creek area in the southeastern Lake Eyre Basin, where *P. viator* **sp. nov.** appears to have been fairly common during the late Pleistocene, was a mosaic of arid chenopod shrublands and semi-arid *Callitris* woodlands (Callen *et al.* 1986; Martin 1990; Alley 1998). The range of *P. viator* **sp. nov.** extended south to Spring Creek in the late Pleistocene. Though in a region considered to have broadly experienced high rainfall in this period (Flannery & Gott 1984; White & Flannery 1995) relative to the bulk of the distribution of this species, the Spring Creek assemblage has been characterised as having low, heathy vegetation with few trees (Flannery & Gott 1984) during a period of marked aridification across Australia (Cohen *et al.* 2012), and as such does not necessarily represent a departure from open habitat. *Protemnodon viator* **sp. nov.** exhibits a high degree of sexual dimorphism (to be further investigated in a separate publication), a characteristic which is more pronounced in large, vagile, social macropodines with a preference for open habitats (Jarman 1991). This species thus represents a large, fairly efficient and medium- to high-geared bipedal-hopping macropodine, possibly moving in groups (mobs), adapted to open habitats and xeric environments.

There are a few examples of sympatry and some evidence of possible competitive exclusion in the fossil records of the Australian Pleistocene species of *Protemnodon*. *Protemnodon anak*, *P. mamkurra* **sp. nov.** and *P. viator* **sp. nov.** all co-occur at Wellington Caves, but are only confirmed within the same deposit in the Main Fossil Chamber of Victoria Fossil Cave, Naracoorte (Figs 2 & 143). *Protemnodon anak* and *P. viator* **sp. nov.** do not occur together in a single layer, but each co-occurs in different layers with *P. mamkurra* **sp. nov.** *Protemnodon anak* and *P. mamkurra* **sp. nov.** co-occur in deposits at King Creek, near Clifton in the eastern Darling Downs (Figs 2 & 143). However, these specimens lack detailed provenance data and the co-occurrence is poorly constrained. *Protemnodon anak* and *P. viator* **sp. nov.** also co-occur in the Malkuni Waterhole deposit, Katipiri Fm. (130–100 ka, Callen & Nanson 1992), Cooper Creek. *Protemnodon viator* **sp. nov.** and *P. mamkurra* **sp. nov.** are only confirmed within the same deposit once, which may indicate that there was some direct competition between these two species resulting in mutual exclusion from certain habitats. It bears noting that there are multiple Australian Pleistocene sites from which solely dental material of species of *Protemnodon* has been collected, and which are constrained by the limited usefulness of dental characteristics in distinguishing *P. mamkurra* **sp. nov.** and *P. viator* **sp. nov.** As such, co-occurrence was possibly more common than it currently appears.

Protemnodon tumbuna inhabited eastern and western New Guinea (Fig. 143d), at altitudes of 1720 m (Nombe rockshelter) (Flannery *et al.* 1983), ~1500 m (Haeapugua) (Menzies & Ballard 1994), and 2800–2950 m (West Baliem Valley) (Flannery 1994), a broadly montane and sub-alpine distribution. The species likely inhabited mid- and upper-montane rainforest as well as the varied herbfields and grasslands above the treeline. With the interpretations of the limbs and pedal proportions and musculature of the species, combined with consideration of its palaeohabitats, *P. tumbuna* emerges as a robust, very low-geared kangaroo, adapted to a cool climate, high altitudes, high rainfall, and dense vegetation, most likely moving quadrupedally at slow speeds, hopping and/or quadrupedally bounding at higher speeds. Comparisons to modern taxa could be made, in terms of the inferred low-gearing, quadrupedality and habitat preferences of the species, to *Thylogale calabyi* Flannery, 1992b, a small, robust pademelon that inhabits sub-alpine grasslands and upper montane rainforests (Flannery 1992b; Helgen 2007).

Conclusion

The genus *Protemnodon* is united taxonomically by synapomorphies of the ilium and the middle pedal phalanx IV, as well as a combination of other craniodental and postcranial features. *Protemnodon* is found to contain seven species: *P. snewini*, *P. dawsonae* **sp. nov.** and *P. otibandus* from the Pliocene, and *P. anak*, *P. mamkurra* **sp. nov.**, *P. viator* **sp. nov.** and *P. tumbuna* from the Pleistocene. The early Pliocene *P. snewini* is a relatively early divergence within the genus. *Protemnodon anak* sits sister to a clade containing the remaining species. Forming a trichotomy within this clade are *P. dawsonae*

sp. nov., *P. mamkurra* **sp. nov.** + *P. viator* **sp. nov.**, and *P. otibandus* + *P. tumbuna*. The species are hypothesised to have ranged from relatively locomotively efficient, vagile, bipedal hopping kangaroos living in semi-arid and arid open woodlands, scrublands and grasslands, to robust, low-speed, more quadrupedal kangaroos adapted to densely vegetated, mesic and high-rainfall forests. While the Australian species display a general trend toward adaptations suited to open habitats, the New Guinean lineage suggests a movement toward greater adaptation to quadrupedality and closed, densely vegetated habitats. These findings provide a base for future study of the palaeoecology of the species of *Protemnodon* and of the possible causes and impacts of their extinction. Overall, this research also serves as an indicator of the depth of knowledge still untapped in the study of vertebrate palaeontology in Australia—although this genus has been known to science for nearly 150 years, we are just now beginning to understand its character, history and place in the late Cenozoic landscapes of Australia.

Acknowledgements

We would like to thank the following individuals and institutions for providing loans of or access to osteological specimens: David Stemmer, Mary-Anne Binnie and the South Australian Museum; Tim Ziegler and Melbourne Museum; Kenny Travouillon, Mikael Siversson and the Western Australian Museum; Matthew McCurry and the Australian Museum; Natalie Schroeder and Geoscience Australia; Tim Denham, Mary-Jane Mountain and the Australian National University; Scott Hocknull, Heather Janetzki and the Queensland Museum; David Maynard and the Queen Victoria Museum and Art Gallery; Jim Anamiato, Bulisa Iova and the Papua New Guinea National Museum and Art Gallery; Pat Holroyd, Kevin Padian and the University of California Museum of Paleontology; Amanda Millhouse and the Smithsonian; Jin Meng and the American Museum of Natural History; Pip Brewer and the Natural History Museum; and Ian Sobbe, for access to his private collection. We further thank Scott Hocknull for his detailed and constructive review of the manuscript, and thank an anonymous reviewer. Thanks to Lisa Nink for providing access to a specimen under her study. We thank Keith and Anita Cook (Maxim Foundation) for their help with fieldwork at Lake Callabonna, and thank the host of volunteers that have helped with fieldwork in the Lake Eyre and Lake Frome basins. IARK extends his thanks to the many people that supported him during his PhD, particularly his parents Greg and Nicole and his wife Rachel, and thanks Carey Burke for preparing much of the Lake Callabonna material, Grant Gully for help with focus-stacking, and Jacob Blokland for help with Illustrator. We acknowledge and thank the traditional custodians of the land from which the fossils were collected, including the representatives of the Pilatapa people of the Lake Callabonna area. We especially thank Robyn Campbell, Tara Bonney and the Bunganditj Language Reclamation Committee of the Burrandies Aboriginal Corporation, representing the Boandik people of southeastern South Australia, for their enthusiastic help in naming *Protemnodon mamkurra*.

Funding

This project was supported by: a Flinders University Research Scholarship; a Royal Society of South Australia Small Research Grant; grants from the Flinders University College of Science and Engineering, Flinders University Student Association, North American Paleontological Convention, and University of California Museum of Paleontology Welles Fund to IARK; a grant from the Australia Pacific Science Foundation (APSF 1709) to GJP, IARK and JDvZ; and grants from the Australian Research Council—DE130101133 to THW, DP180101913 to THW, L. Arnold and A. Chinsamy, and DP190103636 to GJP.

Author contributions

IARK, GJP, THW and ABC designed the study and collated the biogeographic data. IARK collected much of the scan data and all morphometric data, took the photographs, generated the scan images, and undertook the taxonomic descriptions, comparisons and analyses. JDvZ collected the remainder of the scan data. IARK, JDvZ, ABC and GJP contributed to the functional morphological and palaeobiological interpretations. IARK wrote the bulk of the manuscript, with all other authors contributing to the writing and editing.

References

Alexander, R.M. & Vernon, A. (1975) The mechanics of hopping by kangaroos (Macropodidae). *Journal of Zoology*, 177 (2), 265–303. https://doi.org/10.1111/j.1469-7998.1975.tb05983.x

Alley, N.F. (1998) Cainozoic stratigraphy, palaeoenvironments and geological evolution of the Lake Eyre Basin. *Palaeogeography, Palaeoclimatology, Palaeoecology*, 144 (1998), 239–263. https://doi.org/10.1016/S0031-0182(98)00120-5

Andrae, J., McInerney, F., Polissar, P., Sniderman, J., Howard, S., Hall, P. & Phelps, S. (2018) Initial expansion of C_4 vegetation in Australia during the late Pliocene. *Geophysical Research Letters*, 45 (10), 4831–4840. https://doi.org/10.1029/2018GL077833

Aplin, K.P. & Archer, M. (1987) Recent advances in marsupial systematics with a new syncretic classification. *In*: Archer, M. (ed.) *Possums and Opossums: Studies in Evolution*. Surrey Beatty and Sons and the Royal Zoological Society of New South Wales, Sydney, pp. 15–72.

Archer, M., Hand, S.J. & Godthelp, H. (1994) Patterns in the history of Australia's mammals and inferences about palaeohabitats. *In*: Hill, R.S. (ed.) *History of the Australian Vegetation: Cretaceous to Recent*. Cambridge University Press, Melbourne, pp. 80–103.

https://doi.org/10.20851/australian-vegetation-06

Archer, M. & Wade, M. (1976) Results of the Ray E. Lemley expeditions, part 1. The Allingham Formation and a new Pliocene vertebrate fauna from northern Queensland. *Memoirs of the Queensland Museum*, 17 (3), 379–397.

Arman, S.D. (2017) *Diets of the Macropodidae Inferred Through Dental Microwear Texture Analysis*. Thesis. Doctor of Philosophy, Flinders University, Adelaide, 243 pp. (unpublished)

Arman, S.D. & Prideaux, G.J. (2015) Dietary classification of extant kangaroos and their relatives (Marsupialia: Macropodoidea). *Austral Ecology*, 40 (8), 909–922. https://doi.org/10.1111/aec.12273

Arnold, L.J., Demuro, M., Power, R., Duval, M., Guilarte, V., Weij, R., Woodhead, J., White, L., Bourne, S. & Reed, E.H. (2022) Examining sediment infill dynamics at Naracoorte cave megafauna sites using multiple luminescence dating signals. *Quaternary Geochronology*, 70, 101301. https://doi.org/10.1016/j.quageo.2022.101301

Arnold, P. (2021) Evolution of the mammalian neck from developmental, morpho-functional, and paleontological perspectives. *Journal of Mammalian Evolution*, 28, 173–183. https://doi.org/10.1007/s10914-020-09506-9

Arnold, P., Amson, E. & Fischer, M.S. (2017) Differential scaling patterns of vertebrae and the evolution of neck length in mammals. *Evolution*, 71 (6), 1587–1599. https://doi.org/10.1111/evo.13232

Ayliffe, L.K., Prideaux, G.J., Bird, M.I., Grun, R., Roberts, R.G., Gully, G.A., Jones, R., Fifield, L.K. & Cresswell, R.G. (2008) Age constraints on Pleistocene megafauna at Tight Entrance Cave in southwestern Australia. *Quaternary Science Reviews*, 27, 1784–1788. https://doi.org/10.1016/j.quascirev.2008.07.008

Aziz-ur-Rahman, A. & McDougall, I. (1972) Potassium-Argon ages on the newer volcanics of Victoria. *Proceedings of the Royal Society of Victoria*, 85, 61–69.

Baird, R.F. (1985) Avian fossils from Quaternary deposits in 'Green Waterhole Cave', south-eastern South Australia. *Records of the Australian Museum*, 37, 353–370. https://doi.org/10.3853/j.0067-1975.37.1985.332

Barrett, C. (1943) *An Australian animal book*. Oxford University Press, Melbourne, 374 pp.

Bartholomai, A. (1973) The genus *Protemnodon* Owen (Marsupialia: Macropodidae) in the Upper Cainozoic deposits of Queensland. *Memoirs of the Queensland Museum*, 16 (3), 309–363.

Bartholomai, A. (1978) The Macropodidae (Marsupialia) from the Allingham Formation, northern Queensland. Results of the Ray E. Lemley expeditions, Part 2. *Memoirs of the Queensland Museum*, 18 (2), 127–143.

Baudinette, R. (1977) Locomotor energetics in a marsupial, *Setonix brachyurus*. *Australian Journal of Zoology,* 25, 423–428. https://doi.org/10.1071/ZO9770423

Baudinette, R.V. (1989) The biomechanics and energetics of locomotion in Macropodoidea. *In*: Grigg, G.C., Jarman, P.J. and Hume, I.D. (Eds.), *Kangaroos, Wallabies and Rat-kangaroos*. Surrey Beatty & Sons, Sydney, pp. 245–253.

Baudinette, R.V. (1994) Locomotion in macropoid marsupials: gaits, energetics and heat balance. *Australian Journal of Zoology*, 42, 103–123. https://doi.org/10.1071/ZO9940103

Beck, R.M.D., Voss, R.S. & Jansa, S.A. (2022) Craniodental morphology and phylogeny of marsupials. *Bulletin of the American Museum of Natural History*, 457 (1), 1–352. https://doi.org/10.1206/0003-0090.457.1.1

Belperio, A. & Fotheringham, D. (1990) Geological setting of two Quaternary footprint sites, western South Australia. *Australian Journal of Earth Sciences*, 37 (1), 37–42. https://doi.org/10.1080/08120099008727903

Benbow, M.C., Alley, N.F., Lindsay, M. & Greenwood, D.R. (1995) Geological history and palaeoclimate. *In*: Drexel, J.F. and Preiss, W.V. (Eds.), *The Geology of South Australia. Volume 2. The Phanerozoic*. Geological Survey of South Australia, Bulletin No. 54, Adelaide, pp. 208–217.

Biewener, A.A. (1990) Biomechanics of mammalian terrestrial locomotion. *Science*, 250 (4984), 1097–1103. https://doi.org/10.1242/jeb.105.1.147

Bishop, N. (1997) Functional anatomy of the macropodid pes. *Proceedings of the Linnean Society of New South Wales*, 117, 17–50.

Blender Online Community (2018) *Blender – a 3D modelling and rendering package*. 2.90.1 [http://www.blender.org]

Buchmann, C. & Guiler, E. (1974) Locomotion in the potoroo. *Journal of Mammology*, 55, 203–206. https://doi.org/10.2307/1379270

Burbidge, N.T. (1960) The phytogeography of the Australian region. *Australian Journal of Botany*, 8 (2), 75–211. https://doi.org/10.1071/BT9600075

Butler, K., Louys, J. & Travouillon, K. (2014) Extending dental mesowear analyses to Australian marsupials, with applications to six Plio-Pleistocene kangaroos from southeast Queensland. *Palaeogeography, Palaeoclimatology, Palaeoecology*, 408, 11–25. https://doi.org/10.1016/j.palaeo.2014.04.024

Callen, R. & Nanson, G. (1992) Formation and age of dunes in the Lake Eyre depocentres. Geologische Rundschau, 81 (2), 589–593. https://doi.org/10.1007/BF01828619

Callen, R.A., Dulhunty, J.D., Lange, R.T., Plane, M., Tedford, R.H., Wells, R.T. & Williams, D.L.G. (1986) *The Lake Eyre basin – Cainozoic sediments, fossil vertebrates and plants, landforms, silcretes and climatic implications*. Geological Society of Australia, Sydney, pp.

Carey, S.P., Camens, A.B., Cupper, M.L., Grün, R., Hellstrom, J.C., McKnight, S.W., Mclennan, I., Pickering, D.A., Trusler, P. & Aubert, M. (2011) A diverse Pleistocene marsupial trackway assemblage from the Victorian Volcanic Plains, Australia. *Quaternary Science Reviews*, 30 (5–6), 591–610. https://doi.org/10.1016/j.quascirev.2010.11.021

Cascini, M., Mitchell, K.J., Cooper, A. & Phillips, M.J. (2019) Reconstructing the evolution of giant extinct kangaroos: comparing the utility of DNA, morphology, and total evidence. *Systematic Biology*, 68 (3), 520–537. https://doi.org/10.1093/sysbio/syy080

Caughley, G., Grigg, G.C. & Short, J. (1983) How many kangaroos? *Search*, 14 (5–6), 151–152.

Caughley, G., Short, J., Grigg, G.C. & Nix, H. (1987) Kangaroos and climate: an analysis of distribution. *The Journal of Animal Ecology*, 751–761. https://doi.org/10.2307/4946

Celik, M., Cascini, M., Haouchar, D., Van Der Burg, C., Dodt, W., Evans, A.R., Prentis, P., Bunce, M., Fruciano, C. & Phillips, M.J. (2019) A molecular and morphometric assessment of the systematics of the *Macropus* complex clarifies the tempo and mode of kangaroo evolution. *Zoological Journal of the Linnean Society*, 186 (3), 793–812. https://doi.org/10.1093/zoolinnean/zlz005

Cignoni, P., Callieri, M., Corsini, M., M., D., Ganovelli, F. & Ranzuglia, G. (2008) MeshLab: an open-source mesh processing tool. *In*: Scarano, V., De Chiara, R. and Erra, U. (eds.), *Conference: Sixth Eurographics Italian Chapter Conference*, 129–136 pp. The Eurographics Association, Pisa, Italy. http://doi.org/10.2312/LocalChapterEvents/ItalChap/ItalianChapConf2008/129-136

Coede, A., Harmon, R.S., Atkinson, T.C. & Rowe, P.J. (1990) Pleistocene climatic change in southern Australia and its effect on speleothem deposition in some Nullarbor caves. *Journal of Quaternary Science*, 5 (1), 29–38. https://doi.org/10.1002/jqs.3390050104

Cohen, T., Nanson, G., Jansen, J.D., Jones, B., Jacobs, Z., Larsen, J., May, J.-H., Treble, P., Price, D. & Smith, A. (2012) Late Quaternary mega-lakes fed by the northern and southern river systems of central Australia: varying moisture sources and increased continental aridity. *Palaeogeography, Palaeoclimatology, Palaeoecology*, 356–357, 89–108. https://doi.org/10.1016/j.palaeo.2011.06.023

Cohen, T.J., Arnold, L.J., Gázquez, F., May, J.-H., Marx, S.K., Jankowski, N.R., Chivas, A.R., Garćia, A., Cadd, H., Parker, A.G., Jansen, J.D., Fu, X., Waldmann, N., Nanson, G.C., Jones, B.G. & Gadd, P. (2022) Late Quaternary climate change in Australia's arid interior: Evidence from Kati Thanda – Lake Eyre. *Quaternary Science Reviews*, 292, 107635. https://doi.org/10.1016/j.quascirev.2022.107635

Colhoun, E.A., Pola, J.S., Barton, C.E. & Heijnis, H. (1999) Late Pleistocene vegetation and climate history of Lake Selina, western Tasmania. *Quaternary International*, 57, 5–23. https://doi.org/10.1016/S1040-6182(98)00046-9

Collett, R. (1884) On some apparently new marsupials from Queensland. *Proceedings of the Zoological Society of London*, 52 (3), 381–389. https://doi.org/10.1111/j.1096-3642.1884.tb02840.x

Cooke, B.D. (2020) Swamp wallaby (*Wallabia bicolor*) distribution has dramatically increased following sustained biological control of rabbits. *Australian Mammalogy*, 42 (3), 321–328. https://doi.org/10.1071/AM19037

Cooke, B.N., Travouillon, K.J., Archer, M. & Hand, S.J. (2015) *Ganguroo robustiter*, sp. nov. (Macropodoidea, Marsupialia), a middle to early late Miocene basal macropodid from Riversleigh World Heritage Area, Australia. *Journal of Vertebrate Paleontology*, 35 (4), e956879. https://doi.org/10.1080/02724634.2015.956879

Couzens, A.M.C. & Prideaux, G.J. (2018) Rapid Pliocene adaptive radiation of modern kangaroos. *Science*, 362, 72–75. https://doi.org/10.1126/science.aas8788

Darragh, T.A. (1985) Molluscan biogeography and biostratigraphy of the Tertiary of southeastern Australia. *Alcheringa*, 9 (2), 83–116. https://doi.org/10.1080/03115518508618960

Dawson, L. (1985) Marsupial fossils from Wellington Caves, New South Wales; the historic and scientific significance of the collections in the Australia Museum, Sydney. *Records of the Australian Museum,* 37 (2), 55–69. https://doi.org/10.3853/j.0067-1975.37.1985.335

Dawson, L. (2001) Revision of *Protemnodon – Protemnodon devisi* and *Protemnodon chinchillaensis*: corrections to species concepts/descriptions as presented by Bartholomai (1973) (unpublished manuscript). *University of New South Wales*.

Dawson, L. (2004) A new fossil genus of forest wallaby (Marsupialia, Macropodinae) and a review of *Protemnodon* from eastern Australia and New Guinea. *Alcheringa: An Australasian Journal of Palaeontology,* 28, 275–290. https://doi.org/10.1080/03115510408619285

Dawson, L. & Flannery, T.F. (1985) Taxonomic and phylogenetic status of living and fossil kangaroos and wallabies of the genus *Macropus* Shaw (Macropodidae: Marsupialia), with a new subgeneric name for the larger wallabies. *Australian Journal of Zoology*, 33, 473–498. https://doi.org/10.1071/ZO9850473

Dawson, L., Muirhead, J. & Wroe, S. (1999) The Big Sink Local Fauna: a lower Pliocene mammalian fauna from the Wellington Caves complex, Wellington, New South Wales. *Records of the Western Australian Museum*, Supplement No. 57, 265–290.

Dawson, R.S. (2015) *Morphological correlates of pentapedal locomotion in kangaroos and wallabies (Family: Macropodidae)*. Thesis. University of Western Australia,

Dawson, R.S., Milne, N. & Warburton, N.M. (2014) Muscular anatomy of the tail of the western grey kangaroo, *Macropus fuliginosus*. *Australian Journal of Zoology*, 62 (2), 166–174. https://doi.org/10.1071/ZO13085

Dawson, R.S., Warburton, N.M., Richards, H.L. & Milne, N. (2015) Walking on five legs: investigating tail use during slow gait in kangaroos and wallabies. *Australian Journal of Zoology*, 63 (3), 192–200. https://doi.org/10.1071/ZO15007

Dawson, T.J. (1977) Kangaroos. *Scientific American*, 237 (2), 78–89. https://doi.org/10.1038/scientificamerican0877-78

--- (1989) Diets of macropodoid marsupials: general patterns and environmental influences. *In*: Grigg, G.C., Jarman, P.J. and Hume, I.D. (Eds.), *Kangaroos, Wallabies and Rat-kangaroos*. Surrey Beatty & Sons, Sydney, pp. 129–142.

Dawson, T.J. & Taylor, C.R. (1973) Energetic cost of locomotion in kangaroos. *Nature*, 246, 313–314. https://doi.org/10.1038/246313a0

De Vis, C.W. (1895) A review of the fossil jaws of the Macropodidae in the Queensland Museum. *Proceedings of the Linnean Society of New South Wales*, 10, 75–133.

Den Boer, W. (2018) *Evolutionary progression of the iconic Australasian kangaroos, rat-kangaroos, and their fossil relatives (Marsupialia: Macropodiformes)*. Thesis. Masters, Uppsala University, Uppsala, 105 pp. (unpublished)

DeSantis, L.R.G., Field, J.H., Wroe, S. & Dodson, J.R. (2017) Dietary responses of Sahul (Pleistocene Australia–New Guinea) megafauna to climate and environmental change. *Paleobiology*, 43 (2), 181–195. https://doi.org/10.1017/pab.2016.50

Desmarest, A. (1804) Tableau Méthodique des mammifères. *Nouveau Dictionnaire d'Histoire Naturelle*, 24, 5–58.

Desmarest, A. (1817) *Nouveau Dictionnaire d'Histoire Naturelle*.

25. Deterville, Paris, France, 477 pp.
Desmarest, A.G. (1822) *Mammalogie, ou, Description des espèces de mammifères*. 2. Chez Mme Veuve Agasse, Paris, France, 530 pp.
Di Stefano, J., York, A., Swan, M., Greenfield, A. & Coulson, G. (2009) Habitat selection by the swamp wallaby (*Wallabia bicolor*) in relation to diel period, food and shelter. *Austral Ecology,* 34 (2), 143–155. https://doi.org/10.1111/j.1442-9993.2008.01890.x
Etheridge, R. & Jack, R.L. (1892) Organic remains of the post-Tertiary period; extract from: The geology and palaeontology of Queensland and New Guinea. *Publications of the Geological Survey of Queensland,* 1 & 2 (92).
Field, J.H., Dodson, J.R. & Proccer, I.P. (2002) A late Pleistocene vegetation history from the Australian semi-arid zone. *Quaternary Science Reviews*, 21 (8–9), 1023–1037. https://doi.org/10.1016/S0277-3791(01)00057-9
Flannery, T.F. (1984) Re-examination of the Quanbun Local Fauna, a Late Cenozoic vertebrate fauna from Western Australia. *Records of the Western Australian Museum*, 11 (2), 119–128.
Flannery, T.F. (1989) A new species of *Wallabia* (Macropodinae: Marsupialia) from Pleistocene deposits in Mammoth Cave, southwestern Western Australia. Records of the Western Australian Museum, 14 (3), 299–307.
Flannery, T.F. (1990a) *Mammals of New Guinea*. Robert Brown and Associates, Brisbane, 568 pp.
Flannery, T.F. (1990b) Pleistocene faunal loss: implications of the aftershock for Australia's past and future. *Archaeology in Oceania*, 25 (2), 45–55. https://doi.org/10.1002/j.1834-4453.1990.tb00232.x
Flannery, T.F. (1992a) New Pleistocene marsupials (Macropodidae, Diprotodontidae) from subalpine habitats in Irian Jaya, Indonesia. *Alcheringa*, 16 (4), 321–331. https://doi.org/10.1080/03115519208619113
Flannery, T.F. (1992b) Taxonomic revision of the *Thylogale brunii* complex (Macropodidae: Marsupialia) in Melanesia, with description of a new species. *Australian Mammalogy*, 15 (1), 7–23. https://doi.org/10.1071/AM92002
Flannery, T.F. (1994) The fossil land mammal record of New Guinea: a review. Science in New Guinea, 20 (1), 39–48.
Flannery, T.F. (1999) The Pleistocene mammal fauna of Kelangurr Cave, central montane Irian Jaya, Indonesia. *Records of the Western Australia Museum*, 57, 341–350.
Flannery, T.F. & Archer, M. (1984) The macropodoids (Marsupialia) of the early Pliocene Bow Local Fauna, central eastern New South Wales. *The Australian Zoologist*, 21 (4), 357–383.
Flannery, T.F. & Gott, B. (1984) The Spring Creek locality, southwestern Victoria, a late surviving megafaunal assemblage. *The Australian Zoologist*, 21 (4), 385–422.
Flannery, T.F., Mountain, M.-J. & Aplin, K. (1983) Quaternary kangaroos (Macropodidae: Marsupialia) from Nombe Rock Shelter, Papua New Guinea, with comments on the nature of megafaunal extinctions in the New Guinea highlands. *Proceedings of the Linnean Society of New South Wales*, 107 (2), 77–99.
Flannery, T.F., Rich, T.H., Turnbull, W.D. & Lundelius Jr, E.L. (1992) The Macropodoidea (Marsupialia) of the early Pliocene Hamilton Local Fauna, Victoria, Australia. *Fieldiana*, (25), 1–37. https://doi.org/10.5962/bhl.title.3468
Flannery, T.F. & Roberts, R.G. (1999) Late Quaternary extinctions in Australasia: an overview. *In*: MacPhee, R.D.E. (ed.) *Extinctions in Near Time*. Kluwer Academic/Plenum Publishers, New York, pp. 239–255. https://doi.org/10.1007/978-1-4757-5202-1_10
Flower, W.H. (1867) On the development and succession of teeth in the Marsupialia. *Philosophical Transactions of the Royal Society,* 157, 631–641. https://doi.org/10.1098/rstl.1867.0020
Flower, W.H. (1884) *Catalogue of the specimens illustrating the osteology and dentition of vertebrated animals, recent and extinct, contained in the Museum of the Royal College of Surgeons of England. Part II. Class Mammalia other than man.* 2. Taylor and Francis, London, 779 pp. https://doi.org/10.5962/bhl.title.105637
Frith, H.J. & Calaby, J.H. (1969) *Kangaroos*. Cheshire, Melbourne, xiii, 209 pp.
Fu, X., Cohen, T.J. & Arnold, L.J. (2017) Extending the record of lacustrine phases beyond the last interglacial for Lake Eyre in central Australia using luminescence dating. *Quaternary Science Reviews*, 162, 88–110. https://doi.org/10.1016/j.quascirev.2017.03.002
Fujioka, T., Chappell, J., Honda, M., Yatsevich, I., Fifield, K. & Fabel, D. (2005) Global cooling initiated stony deserts in central Australia 2–4 Ma, dated by cosmogenic ^{21}Ne-^{10}Be. *Geology*, 33 (12), 993–996. https://doi.org/10.1130/G21746.1
Gaffney, E.S. & McNamara, G.C. (1990) A meiolaniid turtle from the Pleistocene of northern Queensland. *Memoirs of the Queensland Museum*, 28 (1), 107–113.
Gallagher, S.J., Greenwood, D.R., Taylor, D., Smith, A.J., Wallace, M.W. & Holdgate, G.R. (2003) The Pliocene climatic and environmental evolution of southeastern Australia: evidence from the marine and terrestrial realm. *Palaeogeography, Palaeoclimatology, Palaeoecology*, 193 (3–4), 349–382. https://doi.org/10.1016/S0031-0182(03)00231-1
Ganslosser, U. (1989) Agonistic behaviour in macropodoids – a review. *In*: Grigg, G.C., Jarman, P.J. and Hume, I.D. (Eds.), *Kangaroos, Wallabies and Rat-kangaroos*. Surrey Beatty & Sons, New South Wales, pp. 475–503.
Gillespie, R., Camens, A.B., Worthy, T.H., Rawlence, N.J., Reid, C., Bertuch, F., Levchenko, V. & Cooper, A. (2012) Man and megafauna in Tasmania: closing the gap. *Quaternary Science Reviews,* 37, 38–47. https://doi.org/10.1016/j.quascirev.2012.01.013
Gillespie, R., Wood, R., Fallon, S., Stafford Jr, T.W. & Southon, J. (2014) New 14C dates for Spring Creek and Mowbray Swamp megafauna: XAD-2 processing. *Archaeology in Oceania*, 50 (1), 43–48. https://doi.org/10.1002/arco.5045
Glauert, L. (1910) *Sthenurus occidentalis* (Glauert). *Bulletin of the Geological Survey of Western Australia*, 36, 53–69.
Goloboff, P.A., Farris, J.S. & Nixon, K.C. (2008) TNT, a free program for phylogenetic analysis. *Cladistics*, 24 (5), 774–786. https://doi.org/10.1111/j.1096-0031.2008.00217.x
Gould, J. (1841) *A Monograph of the Macropodidae, or Family of Kangaroos*. 1. John Gould, London, 184 pp. https://doi.org/10.5962/bhl.title.65990
Gould, J. (1863) *The Mammals of Australia*. 2. John Gould, London,

69 pp.
https://doi.org/10.5962/p.312827

Grand, T.I. & Barboza, P.S. (2001) Anatomy and development of the koala, *Phascolarctos cinereus*: an evolutionary perspective on the superfamily Vombatoidea. *Anatomy and Embryology*, 203 (3), 211–223.
https://doi.org/10.1007/s004290000153

Gray, J.E. (1821) On the arrangement of vertebrose animals. London Medical Repository, (15), 296–310.

Gray, J.E. (1837) Description of some new or little known Mammalia, principally in the British Museum collection. *Magazine of Natural History and Journal of Zoology, Botany, Mineralogy, Geology and Meteorology*, 1, 577–587.

Gray, J.E. (1841) Contributions towards the geographical distribution of the Mammalia in Australia, with notes on some recently discovered species, in a letter addressed to the Author. *In*: Grey, G. (ed.) *Journals of Two Expeditions of Discovery in North-west and Western Australia During the Years 1837, 38, and 39, Under the Authority of Her Majesty's Government. Describing many newly discovered, important, and fertile districts, with observations on the moral and physical condition of the aboriginal inhabitants, &c. &c.* T. & W. Boone, London, 397–414.

Griffiths, R.I. (1984) *Mechanical properties of an ankle extensor muscle in a freely hopping wallaby*. Thesis. Doctor of Philosophy, Monash University,

Grün, R., Eggins, S., Aubert, M., Spooner, N., Pike, A.W. & Müller, W. (2010) ESR and U-series analyses of faunal material from Cuddie Springs, NSW, Australia: implications for the timing of the extinction of the Australian megafauna. *Quaternary Science Reviews*, 29 (5–6), 596–610.
https://doi.org/10.1016/j.quascirev.2009.11.004

Grün, R., Moriarty, K.C. & Wells, R.T. (2001) Electron spin resonance dating of the fossil deposits in the Naracoorte Caves, South Australia. *Journal of Quaternary Science*, 16 (1), 49–59.
https://doi.org/10.1002/1099-1417(200101)16:1%3C49::AID-JQS570%3E3.0.CO;2-%23

Gunji, M. & Endo, H. (2019) Growth pattern and functional morphology of the cervical vertebrae in the Gerenuk (*Litocranius walleri*): the evolution of neck elongation in Antilopini (Bovidae, Artiodactyla). *Journal of Mammalian Evolution*, 26, 225–235.
https://doi.org/10.1007/s10914-017-9396-7

Heaney, L.R. (1991) A synopsis of climatic and vegetational change in Southeast Asia. *In*: Myers, N. (ed.) *Tropical Forests and Climate*. Springer, Dordrecht, pp. 53–61.
https://doi.org/10.1007/978-94-017-3608-4_6

Helgen, K.M. (2007) The mammal fauna of the Kaijende Highlands, Enga Province, Papua New Guinea. *In*: Richards, S.J. (ed.) *A rapid biodiversity assessment of the Kaijende Highlands, Enga Province, Papua New Guinea*. Conservation International, Arlington, pp. 52–68.

Helgen, K.M., Wells, R.T., Kear, B.P., Gerdtz, W.R. & Flannery, T.F. (2006) Ecological and evolutionary significance of sizes of giant extinct kangaroos. *Australian Journal of Zoology*, 54 (4), 293–303.
https://doi.org/10.1071/ZO05077

Hildebrand, M., Goslow, G.E. & Hildebrand, V. (2001) *Analysis of vertebrate structure*. 2. Wiley, New York, 656 pp.

Hoch, E. & Holm, P.M. (1986) New K/Ar age determinations of the Awe Fauna *Gangue*, Papua New Guinea: consequences for Papuaustralian Late Cenozoic biostratigraphy. *Modern Geology*, 10, 181–195.

Hocknull, S.A., Lewis, R., Arnold, L.J., Pietsch, T., Joannes-Boyau, R., Price, G.J., Moss, P., Wood, R., Dosseto, A. & Louys, J. (2020) Extinction of eastern Sahul megafauna coincides with sustained environmental deterioration. *Nature communications*, 11 (1), 1–14.
https://doi.org/10.1038/s41467-020-15785-w

Hocknull, S.A., Zhao, J.-x., Feng, Y.-x. & Webb, G.E. (2007) Responses of Quaternary rainforest vertebrates to climate change in Australia. *Earth and Planetary Science Letters*, 264 (1), 317–331.
https://doi.org/10.1016/j.epsl.2007.10.004

Hope, G.S., Flannery, T.F. & Boeardi (1993) A preliminary report of changing Quaternary mammal faunas in subalpine New Guinea. *Quaternary Research*, 40 (1), 117–126.
https://doi.org/10.1006/qres.1993.1062

Hopwood, P.R. (1974) The intrinsic musculature of the pectoral limb of the eastern grey kangaroo (*Macropus major* (Shaw) *Macropus giganteus* (Zimm)). *Journal of Anatomy*, 118 (3), 445–468.

Hopwood, P.R. & Butterfield, R.M. (1990) The locomotor apparatus of the crus and pes of the eastern grey kangaroo, *Macropus giganteus*. *Australian Journal of Zoology*, 38, 397–413.
https://doi.org/10.1071/ZO9900397

Horne, P. (1988) *"Fossil Cave" (5L81), underwater palaeontological and surveying project, 1987–88*. 1 p.

Hughes, P.J., Sullivan, M.E. & Hiscock, P. (2017) Palaeoclimate and human occupation in southeastern arid Australia. *Quaternary Science Reviews*, 163, 72–83.
https://doi.org/10.1016/j.quascirev.2017.03.014

Janis, C.M., Buttrill, K. & Figueirido, B. (2014) Locomotion in extinct giant kangaroos: were sthenurines hop-less monsters? *PloS one*, 9 (10), e109888.
https://doi.org/10.1371/journal.pone.0109888

Janis, C.M., Damuth, J., Travouillon, K.J., Figueirido, B., Hand, S.J. & Archer, M. (2016) Palaeoecology of Oligo-Miocene macropodoids determined from craniodental and calcaneal data. *Memoirs of Museum Victoria*, 73, 200–232.
https://doi.org/10.24199/j.mmv.2016.74.17

Janis, C.M., Napoli, J.G., Billingham, C. & Martín-Serra, A. (2020) Proximal humerus morphology indicates divergent patterns of locomotion in extinct giant kangaroos. *Journal of Mammalian Evolution*, 27 (4), 627–647.
https://doi.org/10.1007/s10914-019-09494-5

Janis, C.M., O'Driscoll, A.M. & Kear, B.P. (2023) Myth of the QANTAS leap: perspectives on the evolution of kangaroo locomotion. *Alcheringa: An Australasian Journal of Palaeontology*, 47 (4), 671–685.
https://doi.org/10.1080/03115518.2023.2195895

Jankowski, N.R., Gully, G.A., Jacobs, Z., Roberts, R.G. & Prideaux, G.J. (2016) A late Quaternary vertebrate deposit in Kudjal Yolgah Cave, south-western Australia: refining regional late Pleistocene extinctions. *Journal of Quaternary Science*, 31 (5), 538–550.
https://doi.org/10.1002/jqs.2877

Jarman, P.J. (1989) Sexual dimorphism in Macropodoidea. *In*: Grigg, G.C., Jarman, P.J. and Hume, I.D. (Eds.), *Kangaroos,*

Wallabies and Rat-kangaroos. Surrey Beatty & Sons, New South Wales, pp. 433–447.

Jarman, P.J. (1991) Social behavior and organization in the Macropodoidea. Advances in the Study of Behavior, 20, 1–50.
https://doi.org/10.1016/S0065-3454(08)60318-6

Jarman, P.J. & Phillips, C.M. (1989) Diets in a community of macropod species. *In*: Grigg, G.C., Jarman, P.J. and Hume, I.D. (Eds.), *Kangaroos, Wallabies and Rat-kangaroos*. Surrey Beatty & Sons, Sydney, pp. 143–149.

Jenkins Jr, F.A. (1973) The functional anatomy and evolution of the mammalian humero-ulnar articulation. *American Journal of Anatomy*, 137 (3), 281–297.
https://doi.org/10.1002/aja.1001370304

Johnson, P.M. & Vernes, K.A. (2008) Red-legged Pademelon: *Thylogale stigmatica*. *In*: Van Dyck, S. and Strahan, R. (Eds.), *The Mammals of Australia*. Reed New Holland, Sydney, pp. 397–400.

Jones, B., Martín-Serra, A., Rayfield, E.J. & Janis, C.M. (2021) Distal humeral morphology indicates locomotory divergence in extinct giant kangaroos. *Journal of Mammalian Evolution*, 29, 27–41.
https://doi.org/10.1007/s10914-021-09576-3

Kaufmann, J.H. (2015) The ecology and evolution of social organization in the kangaroo family (Macropodidae). *American Zoologist*, 14 (1), 51–62.
https://doi.org/10.1093/icb/14.1.51

Kear, B.P., Lee, M.S.Y., Gerdtz, W.R. & Flannery, T.F. (2008) Evolution of hind limb proportions in kangaroos (Marsupialia: Macropodoidea). *In*: Sargis, E.J. and Dagosto, M. (Eds.), *Mammalian Evolutionary Morphology: A Tribute to Frederick S. Szalay*. Springer Science, New York, pp. 25–35.
https://doi.org/10.1007/978-1-4020-6997-0_2

Keast, A. (1981) Distributional patterns, regional biotas and adaptation in the Australian biota: a synthesis. *In*: Keast, A. (ed.) *Ecological Biogeography of Australia*. Dr W. Junk, The Hague, pp. 1891–1997.
https://doi.org/10.1007/978-94-009-8629-9_68

Kerr, I.A.R. & Prideaux, G.J. (2022) A new genus of kangaroo (Marsupialia, Macropodidae) from the late Pleistocene of Papua New Guinea. *Transactions and Proceedings of the Royal Society of South Australia*, 146 (2), 295–318.
https://doi.org/10.1080/03721426.2022.2086518.

Kershaw, A. (1994) Pleistocene vegetation of the humid tropics of northeastern Queensland, Australia. *Palaeogeography, Palaeoclimatology, Palaeoecology*, 109 (2–4), 399–412.
https://doi.org/10.1016/0031-0182(94)90188-0

Kershaw, A.P., Martin, H.A. & McEwen Mason, J.R.C. (1994) The Neogene: a period of transition. *In*: Hill, R.S. (ed.) *History of the Australian Vegetation: Cretaceous to Recent*. Cambridge University Press, Melbourne, pp. 299–327.
https://doi.org/10.20851/australian-vegetation-13

Kirsch, J.A.W., Lapointe, F.-J. & Springer, M.S. (1997) DNA-hybridisation studies of marsupials and their implications for metatherian classification. *Australian Journal of Zoology*, 45 (3), 211–280.
https://doi.org/10.1071/ZO96030

Koungoulos, L.G., Flannery, T.F. & O'Connor, S. (2024) First record of *Protemnodon* (Macropodidae: Marsupialia) from Pleistocene lowland New Guinea. *Alcheringa: An Australasian Journal of Palaeontology*, 1–6.
https://doi.org/10.1080/03115518.2024.2304340

Kram, R. & Dawson, T.J. (1998) Energetics and biomechanics of locomotion by red kangaroos (*Macropus rufus*). *Comparative Biochemistry and Physiology Part B: Biochemistry and Molecular Biology*, 120 (1), 41–49.
https://doi.org/10.1016/S0305-0491(98)00022-4

Krefft, G. (1875) Remarks on Professor Owen's arrangement of the fossil kangaroos. Annals and *Magazine of Natural History 4th Series*, 15, 204–209.
https://doi.org/10.1080/00222937508681059

Lesson, R.P. (1842) *Nouveau tableau du règne animal: mammifères*. 1. A. Bertrand, Paris, 204 pp.

Linnaeus, C. (1758) Classis I: Mammalia. *Systema naturae per regna tria naturae: secundum classes, ordines, genera, species, cum characteribus, differentiis, synonymis, locis*. Laurentii Salvii, Stockholm, pp. 14–77.
https://doi.org/10.5962/bhl.title.542

Llamas, B., Brotherton, P., Mitchell, K.J., Templeton, J.E.L., Thomson, V.A., Metcalf, J.L., Armstrong, K.N., Kasper, M., Richards, S.M., Camens, A.B., Lee, M.S.Y. & Cooper, A. (2015) Late Pleistocene Australian marsupial DNA clarifies the affinities of extinct megafaunal kangaroos and wallabies. *Molecular Biology and Evolution*, 32 (3), 574–584.
https://doi.org/10.1093/molbev/msu338

Lloyd, P.J. & Kershaw, A.P. (1997) Late Quaternary vegetation and early Holocene quantitative climate estimates from Morwell Swamp, Latrobe Valley, south-eastern Australia. *Australian Journal of Botany*, 45 (3), 549–563.
https://doi.org/10.1071/BT96034

Long, J.A., Archer, M., Flannery, T. & Hand, S. (2002) *Prehistoric mammals of Australia and New Guinea: one hundred million years of evolution*. University of New South Wales Press, Kensington, 280 pp.

Loutit, T.S. & Kennett, J.P. (1981) New Zealand and Australian Cenozoic sedimentary cycles and global sea-level changes. *AAPG Bulletin*, 65 (9), 1586–1601.
https://doi.org/10.1306/03B59625-16D1-11D7-8645000102C1865D

Louys, J., Duval, M., Beck, R.M., Pease, E., Sobbe, I., Sands, N. & Price, G.J. (2022) Cranial remains of *Ramsayia magna* from the Late Pleistocene of Australia and the evolution of gigantism in wombats (Marsupialia, Vombatidae). *Papers in Palaeontology*, 8 (6), e1475.
https://doi.org/10.1002/spp2.1475

Louys, J. & Price, G.J. (2015) The Chinchilla Local Fauna: an exceptionally rich and well-preserved Pliocene vertebrate assemblage from fluviatile deposits of south-eastern Queensland, Australia. *Acta Palaeontologica Polonica*, 60 (3), 551–572.
https://doi.org/10.4202/app.00042.2013

Luckett, W.P. (1993) An ontogenetic assessment of dental homologies in therian mammals. *In*: Szalay, F.S., Novacek, M.J. and McKenna, M.C. (Eds.), *Mammal Phylogeny*. Springer-Verlag, New York, pp. 182–204.
https://doi.org/10.1007/978-1-4613-9249-1_13

Lydekker, R. (1887) *Mammalia in the British Museum (Natural History) Cromwell Road, S.W. Part 5. Containing the Group Tillodontia, the Orders Sirenia, Cetacea, Edentata, Marsupialia, Monotremata, and supplement*. 5. Taylor and

Francis, British Museum (Natural History), London, 339 pp.
Lydekker, R. (1894) *A handbook to the Marsupialia and Monotremata*. XVI. W. H. Allen and Co., London, 302 pp. https://doi.org/10.5962/bhl.title.14336
Lydekker, R. (1896) *A handbook to the Marsupialia and Monotremata*. XV. Edward Lloyd, London, 320 pp. https://doi.org/10.5962/bhl.title.15228
MacFadden, B.J., Whitelaw, M.J., McFadden, P. & Rich, T.H. (1987) Magnetic polarity stratigraphy of the Pleistocene section at Portland (Victoria), *Australia. Quaternary Research*, 28 (3), 364–373. https://doi.org/10.1016/0033-5894(87)90004-4
Mackness, B.S., Whitehead, P.W. & McNamara, G.C. (2000) New Potassium-Argon basalt date in relation to the Pliocene Bluff Downs Local Fauna, northern Australia. *Australian Journal of Earth Sciences,* 47 (4), 807–811. https://doi.org/10.1046/j.1440-0952.2000.00812.x
Macphail, M., Jordan, G. & Hill, R. (1993) Key periods in the evolution of the flora and vegetation in western Tasmania. I. The Early–Middle Pleistocene. *Australian Journal of Botany*, 41 (6), 673–707. https://doi.org/10.1071/BT9930673
Macphail, M.K. (1996) Neogene environments in Australia, 1: re-evaluation of microfloras associated with important early Pliocene marsupial remains at Grange Burn, southwest Victoria. *Review of Palaeobotany and Palynology*, 92, 307–328. https://doi.org/10.1016/0034-6667(95)00113-1
Macphail, M.K. (1997) Late Neogene climates in Australia: fossil pollen-and spore-based estimates in retrospect and prospect. *Australian Journal of Botany*, 45 (3), 425–464. https://doi.org/10.1071/BT96052
Maddison, W.P. & Maddison, D.R. (2021) *Mesquite: a modular system for evolutionary analysis*. 3.70
Mahoney, J.A. & Ride, W.D.L. (1975) Index to the genera and species of fossil Mammalia described from Australia and New Guinea between 1838 and 1968 (including citations of type species and primary type specimens). *Special Publication of the Western Australian Museum*, 6, 1–250.
Marshall, A.J. & Beehler, B.M. (2011) *Ecology of Indonesian Papua Part One*. 6. Periplus Editions (HK) Limited, London, 784 pp.
Martin, H.A. (1987) The Cainozoic history of the vegetation and climate of the Lachlan River Region, New South Wales. *Proceedings of the Linnean Society of New South Wales*, 109, 214–257.
Martin, H.A. (1990) The palynology of the Namba Formation in the Wooltana-1 bore, Callabonna Basin (Lake Frome), South Australia, and its relevance to the Miocene grasslands in central Australia. *Alcheringa*, 14, 247–255. https://doi.org/10.1080/03115519008619058
Martin, H.A. (1998) Late Cretaceous-Cainozoic palynology of the Poonarunna No. 1 well, central Australia. *Transactions of the Royal Society of South Australia*, 122 (3), 89–138.
Martin, H.A. (2006) Cenozoic climatic change and the development of the arid vegetation in Australia. *Journal of Arid Environments*, 66 (3), 533–563. https://doi.org/10.1016/j.jaridenv.2006.01.009
Martin, H.A. & McMinn, A. (1993) Palynology of sites 815 and 823: the Neogene vegetation history of coastal northeastern Australia. *In*: McKenzie, J.A., Davies, P.J. and Palmer-Julson, A. (Eds.), *Proceedings of the Ocean Drilling Program, Scientific Results*. Pp. 115–125. https://doi.org/10.2973/odp.proc.sr.133.218.1993
Martin, H.A. & McMinn, A. (1994) Late Cainozoic vegetation history of north-western Australia, from the palynology of a deep sea core (ODP Site 765). *Australian Journal of Botany*, 42, 95–102. https://doi.org/10.1071/BT9940095
Martin, M.L., Travouillon, K.J., Sherratt, E., Fleming, P.A. & Warburton, N.M. (2019) Covariation between forelimb muscle anatomy and bone shape in an Australian scratch-digging marsupial: comparison of morphometric methods. *Journal of Morphology*, 280 (12), 1900–1915. https://doi.org/10.1002/jmor.21074
Mather, E.K., Lee, M.S.Y., Fusco, D.A., Hellstrom, J. & Worthy, T.H. (2023) Pleistocene raptors from cave deposits of South Australia, with a description of a new species of *Dynatoaetus* (Accipitridae: Aves): morphology, systematics and palaeoecological implications. *Alcheringa: An Australasian Journal of Palaeontology*, 48, 134–167. https://doi.org/10.1080/03115518.2023.2268780
Maynes, G.M. (1989) Zoogeography of the Macropodoidea. *In*: Grigg, G.C., Jarman, P.J. and Hume, I.D. (Eds.), *Kangaroos, Wallabies and Rat-kangaroos*. Surrey Beatty & Sons, Sydney, pp. 47–66.
McInerney, P.L., Arnold, L.J., Burke, C., Camens, A.B. & Worthy, T.H. (2022) Multiple occurrences of pathologies suggesting a common and severe bone infection in a population of the Australian Pleistocene giant, *Genyornis newtoni* (Aves, Dromornithidae). *Papers in Palaeontology,* 8 (1), e1415. https://doi.org/10.1002/spp2.1415
McLaren, S. & Wallace, M.W. (2010) Plio-Pleistocene climate change and the onset of aridity in southeastern *Australia. Global and Planetary Change*, 71 (1–2), 55–72. https://doi.org/10.1016/j.gloplacha.2009.12.007
McNamara, G.C. (1990) The Wyandotte Local Fauna: a new, dated, Pleistocene vertebrate fauna from northern Queensland. *Memoirs of the Queensland Museum*, 28 (1), 285–297.
McNamara, J.A. (1994) A new fossil wallaby (Marsupialia; Macropodidae) from the south east of South Australia. *Records of the South Australian Museum*, 27 (2), 111–115.
Menzies, J.I. & Ballard, C. (1994) Some new records of Pleistocene megafauna from New Guinea. *Science in New Guinea*, 20 (2, 3), 113–139.
Mitchell, D.R., Sherratt, E., Ledogar, J.A. & Wroe, S. (2018) The biomechanics of foraging determines face length among kangaroos and their relatives. *Proceedings of the Royal Society B*, 285 (1881), 20180845. https://doi.org/10.1098/rspb.2018.0845
Montanari, S., Louys, J. & Price, G.J. (2013) Pliocene paleoenvironments of southeastern Queensland, Australia inferred from stable isotopes of marsupial tooth enamel. *PloS One*, 8 (6), e66221. https://doi.org/10.1371/journal.pone.0066221
Moore, L. (2008) *Functional morphology and palaeoecology of extinct macropodoids, sthenurines and* Protemnodon *spp. (Marsupialia; Diprotodontia)*. Thesis. B.Sc. (Hons), Flinders University, Adelaide, 96 pp. (unpublished)
Müller, S. (1840) Bijdragen tot de Kennis van Nieuw-Guinea.

In: Temminck, C.J. (ed.) *Verhandlingen over de natuurlijke Geschiedenis der Nederlandische Overzeesche Bezittingen, Door de Leden der Natuurkundige Commissie in Indie en Andere Schrijvers. Zoologie.* S & J. Luchtmans and C. C. van der Hoek, Leiden, 80 pp.

Murray, P.F. (1991) The Pleistocene megafauna of Australia. *In*: Rich, P.V., Monaghan, J.M., Baird, R.F. and Rich, T.H. (Eds.), *Vertebrate Palaeontology of Australia*. Pioneer Design Studio, Melbourne, pp. 1071–1164.

Nanson, G.C., Page, K.J., Callen, R.A. & Price, D.M. (1993) Evidence for changes in the climate and moisture regime of Australia over the past 60 ka. *Quaternary palaeoclimatic mapping: A proticol for Australia*, Quaternary Australasia, Monash University, 69 pp.

Nanson, G.C., Price, D.M., Jones, B.G., Maroulis, J.C., Coleman, M., Bowman, H., Cohen, T.J., Pietsch, T.J. & Larsen, J.R. (2008) Alluvial evidence for major climate and flow regime changes during the middle and late Quaternary in eastern central Australia. *Geomorphology*, 101 (1–2), 109–129. https://doi.org/10.1016/j.geomorph.2008.05.032

Newton, C.A. (1988) *A taphonomic and palaeoecological analysis of the Green Waterhole (5L81), a submerged Late Pleistocene bone deposit in the lower southeast of South Australia*. Thesis. B.Sc. (Hons), Flinders University, Adelaide, 106 pp. (unpublished)

O'Connor, S.M., Dawson, T.J., Kram, R. & Donelan, J.M. (2014) The kangaroo's tail propels and powers pentapedal locomotion. *Biology letters*, 10 (7), 20140381. https://doi.org/10.1098/rsbl.2014.0381

Oliver, A.J. (1986) *Social organisation and dispersal in the red kangaroo*. Thesis. Murdoch University,

Osborne, R.A.L. (1997) Rehabilitation of the Wellington Caves Phosphate Mine: implications for Cainozoic stratigraphy. *Proceedings of the Linnean Society of New South Wales*, 117, 175–180.

Owen, R. (1838) Fossil Marsupialia from the caves of Wellington Valley. *In*: Mitchell, T.L. (ed.) *Three expeditions into the interior of eastern Australia, with descriptions of the recently explored region of Australia Felix, and of the present colony of New South Wales*. T. & W. Boone, London, pp. 359–363.

Owen, R. (1874) On the fossil mammals of Australia, Part VIII. Family Macropodidae: genera *Macropus*, *Osphranter*, *Phascolagus*, *Sthenurus* and *Protemnodon*. *Philosophical Transactions of the Royal Society,* 164, 245–288. https://doi.org/10.1098/rstl.1874.0008

Owen, R. (1876) On the fossil mammals of Australia, Part X. Family Macropodidae: mandibular dentition and parts of the skeleton of *Palorchestes*; additional evidences of *Macropus titan*, *Sthenurus* and *Procoptodon*. *Philosophical Transactions of the Royal Society*, 166, 197–223. https://doi.org/10.1098/rstl.1876.0008

Owen, R. (1877) *Researches on the fossil remains of the extinct mammals of Australia; with a notice of the extinct marsupials of England*. 1. J. Erxleben, London, 522 pp. https://doi.org/10.5962/bhl.title.77375

Palmer, T.S. (1904) Index generum mammalum. *North American Fauna*, (23), 984. https://doi.org/10.3996/nafa.23.0001

Payne, R.C., Hutchinson, J.R., Robilliard, J.J., Smith, N.C. & Wilson, A.M. (2005) Functional specialisation of pelvic limb anatomy in horses (*Equus caballus*). *Journal of Anatomy*, 206 (6), 557–574. https://doi.org/10.1111/j.1469-7580.2005.00420.x

Pepper, M. & Keogh, S.J. (2014) Biogeography of the Kimberley, Western Australia: a review of landscape evolution and biotic response in an ancient refugium. *Journal of Biogeography*, 41 (8), 1443–1455. https://doi.org/10.1111/jbi.12324

Peters, K.J., Saltré, F., Friedrich, T., Jacobs, Z., Wood, R., McDowell, M., Ulm, S. & Bradshaw, C.J.A. (2019) FosSahul 2.0, an updated database for the Late Quaternary fossil records of Sahul. *Scientific Data*, 6 (1), 272. https://doi.org/10.1038/s41597-019-0267-3

Piper, K.J. (2016) The Macropodidae (Marsupialia) of the early Pleistocene Nelson Bay Local Fauna, Victoria, Australia. *Memoirs of Museum Victoria*, 74, 233–253. https://doi.org/10.24199/j.mmv.2016.74.18

Piper, K.J., Fitzgerald, E.M.G. & Rich, T.H. (2006) Mesozoic to Early Quaternary mammal faunas of Victoria, south-east Australia. *Palaeontology*, 49 (6), 1237–1262. https://doi.org/10.1111/j.1475-4983.2006.00595.x

Plane, M. (1972) A New Guinea fossil macropodid (Marsupialia) from the marine Pliocene of Victoria, Australia. *Memoirs of the National Museum of Victoria*, 33, 33–36. https://doi.org/10.24199/j.mmv.1972.33.03

Plane, M.D. (1967) Stratigraphy and vertebrate fauna of the Otibanda Formation, New Guinea. *Bulletin of the Bureau of Mineral Resources, Geology and Geophysics, Australia*, 86, 1–64.

Pledge, N.S. (1980) Macropodid skeletons, including *Simosthenurus* Tedford, from an unusual "drowned cave" deposit in the south east of South Australia. *Records of the South Australian Museum*, 18 (6), 131–141.

Pledge, N.S. (1990) The Upper Fossil Fauna of the Henschke Fossil Cave, Naracoorte, South Australia. *Memoirs of the Queensland Museum*, 28 (1), 247–262.

Pledge, N.S. (1992) The Curramulka local fauna: a new late Tertiary fossil assemblage from Yorke Peninsula, South Australia. *The Beagle: Records of the Museums and Art Galleries of the Northern Territory*, 9 (1), 115–142. https://doi.org/10.5962/p.263122

Price, G.J. (2012) Plio-Pleistocene climate and faunal change in central eastern Australia. *Episodes*, 35 (1), 160–165. https://doi.org/10.18814/epiiugs/2012/v35i1/015

Price, G.J. & Sobbe, I.H. (2005) Pleistocene palaeoecology and environmental change on the Darling Downs, southeastern Queensland, Australia. *Memoirs of the Queensland Museum*, 51 (1), 171–201. https://doi.org/10.5281/zenodo.6390297

Priddel, D. (1988) Habitat utilisation by sympatric red kangaroos *Macropus rufus* and western grey kangaroos *M. fuliginosus*, in western New South Wales. Australian. *Wildlife Research*, 15, 413–421. https://doi.org/10.1071/WR9880413

Priddel, D., Shepherd, N. & Wellard, G. (1988a) Home ranges of sympatric red kangaroos *Macropus rufus* and western grey kangaroos *M. fuliginosus*, in western New South Wales. Australian. *Wildlife Research*, 15, 405–411. https://doi.org/10.1071/WR9880405

Priddel, D., Wellard, G. & Shepherd, N. (1988b) Movements of

sympatric red rangaroos, *Macropus rufus*, and western grey kangaroos, *Macropus fuliginosus*, in western New South Wales. *Wildlife Research*, 15 (3), 339–346. https://doi.org/10.1071/WR9880339

Prideaux, G.J. (2000) *Simosthenurus newtonae* sp. nov., a widespread sthenurine kangaroo (Diprotodontia: Macropodidae) from the Pleistocene of southern and eastern Australia. *Records of the South Australian Museum*, 33 (1), 1–15.

Prideaux, G.J. (2004) Systematics and evolution of the sthenurine kangaroos. *University of California Publications in Geological Sciences*, 146, 1–623. https://doi.org/10.1525/california/9780520098459.001.0001

Prideaux, G.J. (2006) *Mid-Pleistocene vertebrate records: Australia*. *Encyclopedia of Quaternary Science.*, pp.

Prideaux, G.J., Kerr, I.A.R., van Zoelen, J.D., Grün, R., van der Kaars, S., Oertle, A., Douka, K., Grono, E., Barron, A., Mountain, M.-J., Westaway, M.C. & Denham, T. (2022) Re-evaluating the evidence for late-surviving megafauna at Nombe rockshelter in the New Guinea highlands. *Archaeology in Oceania*, 57 (3), 223–248. https://doi.org/10.1002/arco.5274

Prideaux, G.J., Long, J.A., Ayliffe, L.K., Hellstrom, J.C., Pillans, B., Boles, W.E., Hutchinson, M.N., Roberts, R.G., Cupper, M.J., Arnold, L.J., Devine, P.D. & Warburton, N.M. (2007) An arid-adapted middle Pleistocene vertebrate fauna from south-central Australia. *Nature*, 445, 422–425. https://doi.org/10.1038/nature05471

Prideaux, G.J. & Warburton, N.M. (2008) A new Pleistocene tree-kangaroo (Diprotodontia: Macropodidae) from the Nullarbor Plain of south-central Australia. *Journal of Vertebrate Paleontology,* 28 (2), 463–478. https://doi.org/10.1671/0272-4634(2008)28[463:ANPTDM]2.0.CO;2

Prideaux, G.J. & Warburton, N.M. (2010) An osteology-based appraisal of the phylogeny and evolution of kangaroos and wallabies (Macropodidae: Marsupialia). Zoological Journal of the Linnean Society, 159 (4), 954–987. https://doi.org/10.1111/j.1096-3642.2009.00607.x

Quoy, J.R.C. & Gaimard, P. (1830a) "*Kangurus brachyurus*". *In*: Lesson, A., Quoy, J.R.C., Gaimard, P., de Boisduval, J.B.A.C. and Richard, A. (Eds.), *Voyage de la corvette l'Astrolabe exécuté par ordre du roi: pendant les années 1826–1827 & 1828–1829*. J. Tastu, Paris, pp. 114–116.

Quoy, J.R.C. & Gaimard, P. (1830b) Zoologie. *In*: Dumont d'Urville, J.-S.b.-C.s. (ed.) *Voyage de Decouvertes de l'Astrolabe: exécuté par ordre du Roi, pendant les années 1826-1827-1828-1829*. Imprimerie Royale, Paris, pp. 1–527. https://doi.org/10.5962/bhl.title.96961

Raven, H.C. (1929) Kangaroo. *Encyclopaedia Brittanica, 14th ed.,* pp. 254–255.

Richards, H.L., Grueter, C.C. & Milne, N. (2015) Strong arm tactics: sexual dimorphism in macropodid limb proportions. *Journal of Zoology*, 297 (2), 123–131. https://doi.org/10.1111/jzo.12264

Roberts, R.G., Flannery, T.F., Ayliffe, L.K., Yoshida, H., Olley, J.M., Prideaux, G.J., Laslett, G.M., Baynes, A., Smith, M.A., Jones, R. & Smith, B.L. (2001) New ages for the last Australian megafauna: continent-wide extinction about 46,000 years ago. *Science*, 292, 1888–1892. https://doi.org/10.1126/science.1060264

Rovere, A., Raymo, M.E., Mitrovica, J., Hearty, P.J., O'Leary, M. & Inglis, J. (2014) The mid-Pliocene sea-level conundrum: glacial isostasy, eustasy and dynamic topography. *Earth and Planetary Science Letters,* 387, 27–33. https://doi.org/10.1016/j.epsl.2013.10.030

RStudio Team (2020) *RStudio: Integrated Development for R*.

Sanson, G.D. (1978) The evolution and significance of mastication in the Macropodidae. *Australian Mammalogy*, 2 (1), 23–28. https://doi.org/10.1071/AM78003

Sanson, G.D. (1980) The morphology and occlusion of the molariform cheek teeth in some Macropodinae (Marsupialia: Macropodidae). *Australian Journal of Zoology*, 28, 341–365. https://doi.org/10.1071/ZO9800341

Sanson, G.D. (1989) Morphological adaptations of teeth to diets and feeding in the Macropodoidea. *In*: Grigg, G.C., Jarman, P.J. and Hume, I.D. (Eds.), *Kangaroos, Wallabies and Rat-kangaroos*. Surrey Beatty and Sons, Sydney, pp. 151–168.

Sears, K.E. (2004) Role of development in the evolution of the scapula of the giant sthenurine kangaroos (Macropodidae: Sthenurinae). *Journal of Morphology*, 265 (2), 226–236. https://doi.org/10.1002/jmor.10353

Shaw, G. (1790) *The Naturalist's Miscellany*. 1. Nodder & Co., London, 253 pp. https://doi.org/10.5962/bhl.title.79941

Simpson, G.G. (1930) Post-Mesozoic Marsupialia. *Fossilium Catalogus. 1: Animalia Part 47*. W. Junk, Berlin, 87 pp.

Smith, N., Wilson, A., Jespers, K.J. & Payne, R. (2006) Muscle architecture and functional anatomy of the pelvic limb of the ostrich (*Struthio camelus*). *Journal of Anatomy*, 209 (6), 765–779. https://doi.org/10.1111/j.1469-7580.2006.00658.x

Sniderman, J.K., Pillans, B., O'Sullivan, P.B. & Kershaw, A.P. (2007) Climate and vegetation in southeastern Australia respond to Southern Hemisphere insolation forcing in the late Pliocene–early Pleistocene. *Geology*, 35 (1), 41–44. https://doi.org/10.1130/G23247A.1

Sniderman, J.K., Woodhead, J.D., Hellstrom, J., Jordan, G.J., Drysdale, R.N., Tyler, J.J. & Porch, N. (2016) Pliocene reversal of late Neogene aridification. *Proceedings of the National Academy of Sciences of the United States of America*, 113 (8), 1999–2004. https://doi.org/10.1073/pnas.1520188113

Stirton, R.A. (1963) A review of the macropodid genus *Protemnodon*. *University of California Publications in Geological Sciences*, 44 (2), 97–162.

Tate, G.H.H. (1948) Results of the Archbold Expeditions. No. 59. Studies on the anatomy and phylogeny of the Macropodidae (Marsupialia). *Bulletin of the American Museum of Natural History*, 91 (2), 233–351.

Tate, G.H.H. & Archbold, R. (1937) Results of the Archbold Expeditions, No. 16: some marsupials of New Guinea and Celebes. *Bulletin of the American Museum of Natural History*, 73, 331–476.

Tedford, R.H. (1967) The fossil Macropodidae from Lake Menindee, New South Wales. *University of California Publications in Geological Sciences*, 64, 1–165.

Tedford, R.H., Wells, R.T. & Barghoorn, S.F. (1992) Tirari Formation and contained faunas, Pliocene of the Lake Eyre Basin, South Australia. The Beagle: *Records of the Museums and Art Galleries of the Northern Territory*, 9 (1), 173–193.

https://doi.org/10.5962/p.263124
Travouillon, K., Cooke, B., Archer, M. & Hand, S. (2014) Revision of basal macropodids from the Riversleigh World Heritage Area with descriptions of new material of *Ganguroo bilamina* Cooke, 1997 and a new species. *Palaeontologia Electronica*, 17 (1), 1–34.
https://doi.org/10.26879/402
Trouessart, E.L. (1904) *Catalogus Mammalium tam viventium quam fossilium. Quinquennale supplementum, anno 1904*. 1. R. Friedlander and Son, Berlin, 929 pp.
https://doi.org/10.5962/bhl.title.61820
Troughton, E.L.G. (1957) The kangaroo family: brush wallabies. *Australian Museum Magazine*, (12), 186–192.
Turnbull, W.D., Lundelius Jr, E.L. & Archer, M. (2003) Chapter 18: dasyurids, perameloids, phalangeroids, and vombatoids from the Early Pliocene Hamilton Fauna, Victoria, Australia. *Bulletin of the American Museum of Natural History*, 279, 513–540.
https://doi.org/10.1206/0003-0090(2003)279%3C0513:C%3E2.0.CO;2
Turney, C.S., Flannery, T.F., Roberts, R.G., Reid, C., Fifield, L.K., Higham, T.F., Jacobs, Z., Kemp, N., Colhoun, E.A. & Kalin, R.M. (2008) Late-surviving megafauna in Tasmania, Australia, implicate human involvement in their extinction. *Proceedings of the National Academy of Sciences, United Statess of America,* 105 (34), 12150–12153.
https://doi.org/10.1073/pnas.0801360105
Wagstaffe, A.Y. (2018) *The biomechanics of kangaroo feet: hopping for a better resolution*. Thesis. University of Bristol, Bristol, 115 pp. (unpublished)
Wagstaffe, A.Y., O'Driscoll, A.M., Kunz, C.J., Rayfield, E.J. & Janis, C.M. (2022) Divergent locomotor evolution in "giant" kangaroos: evidence from foot bone bending resistances and microanatomy. *Journal of Morphology*, 283 (3), 313–332.
https://doi.org/10.1002/jmor.21445
Walker, D. & Flenley, J.R. (1979) Late Quaternary vegetational history of the Enga Province of upland Papua New Guinea. *Philosophical Transactions of the Royal Society of London. B, Biological Sciences*, 286 (1012), 265–344.
https://doi.org/10.1098/rstb.1979.0034
Wallis, L.A. (2001) Environmental history of northwest Australia based on phytolith analysis at Carpenter's Gap 1. *Quartenary International*, 83–85, 103–117.
https://doi.org/10.1016/S1040-6182(01)00033-7
Warburton, N., Travouillon, K. & Camens, A. (2019) Skeletal atlas of the Thylacine (*Thylacinus cynocephalu*s). *Palaeontologia Electronica*, 22.2.29A, 1–56.
https://doi.org/10.26879/947
Warburton, N.M. (2009) Comparative jaw muscle anatomy in kangaroos, wallabies, and rat-kangaroos (Marsupialia: Macropodoidea). *The Anatomical Record*, 292 (6), 875–884.
https://doi.org/10.1002/ar.20905
Warburton, N.M., Bateman, P.W. & Fleming, P.A. (2013) Sexual selection on forelimb muscles of western grey kangaroos (Skippy was clearly a female). *Biological Journal of the Linnean Society,* 109 (4), 923–931.
https://doi.org/10.1111/bij.12090
Warburton, N.M., Harvey, K.J., Prideaux, G.J. & O'Shea, J.E. (2011) Functional morphology of the forelimb of living and extinct tree-kangaroos (Marsupialia: Macropodidae). *Journal of Morphology,* 272 (10), 1230–1244.
https://doi.org/10.1002/jmor.10979
Warburton, N.M. & Prideaux, G.J. (2021) The skeleton of *Congruus kitcheneri*, a semiarboreal kangaroo from the Pleistocene of southern Australia. *Royal Society Open Science*, 8 (3), 202–216.
https://doi.org/10.1098/rsos.202216
Warburton, N.M., Yakovleff, M. & Malric, A. (2012) Anatomical adaptations of the hind limb musculature of tree kangaroos for arboreal locomotion (Marsupialia: Macropodinae). *Australian Journal of Zoology*, 60 (4), 246–258.
https://doi.org/10.1071/ZO12059
Webb, S.D. (2008) Megafauna demography and late Quaternary climatic change in Australia: A predisposition to extinction. *Boreas*, 37, 329–345.
https://doi.org/10.1111/j.1502-3885.2008.00026.x
Weij, R., Sniderman, J.K., Woodhead, J.D., Hellstrom, J.C., Brown, J.R., Drysdale, R.N., Reed, E., Bourne, S. & Gordon, J. (2024) Elevated Southern Hemisphere moisture availability during glacial periods. *Nature*, 626 (7998), 319–326.
https://doi.org/10.1038/s41586-023-06989-3
Wells, R.T. & Tedford, R.H. (1995) *Sthenurus* (Macropodidae: Marsupialia) from the Pleistocene of Lake Callabonna, South Australia. *Bulletin of the American Museum of Natural History*, 225, 1–111.
Westerman, M., Loke, S., Tan, M.H. & Kear, B.P. (2022) Mitogenome of the extinct Desert 'rat-kangaroo' times the adaptation to aridity in macropodoids. *Scientific Reports*, 12 (1), 5829.
https://doi.org/10.1038/s41598-022-09568-0
White, J.P. & Flannery, T.F. (1995) Late Pleistocene fauna at Spring Creek, Victoria: a re-evaluation. *Australian Archaeology*, 40, 13–17.
https://doi.org/10.1080/03122417.1995.11681541
Whitelaw, M.J. (1991) Magnetic polarity stratigraphy of the Fisherman's Cliff and Bone Gulch vertebrate fossil faunas from the Murray Basin, New South Wales, Australia. *Earth and Planetary Science Letters*, 104, 417–423.
https://doi.org/10.1016/0012-821X(91)90219-8
Wickler, S.J., Hoyt, D.F., Clayton, H.M., Mullineaux, D.R., Cogger, E.A., Sandoval, E., McGuire, R. & Lopez, C. (2004) Energetic and kinematic consequences of weighting the distal limb. *Equine Veterinary Journal*, 36 (8), 772–777.
https://doi.org/10.2746/0425164044848046
Wilford, G.E. & Brown, P.J. (1994) Maps of Late Mesozoic-Cenozoic Gondwana break-up: some palaeogeographic implications. *In*: Hill, R.S. (ed.) *History of the Australian Vegetation: Cretaceous to Recent*. Cambridge University Press, Melbourne, 5–13.
https://doi.org/10.20851/australian-vegetation-02
Wilson, J.T. & Hill, J.P. (1897) Observations on the development and succession of the teeth in *Perameles*. *Quarterly Journal of Microscopic Science*, 2 (156), 427–588.
https://doi.org/10.1242/jcs.s2-39.156.427
Windsor, D.E. & Dagg, A.I. (1971) The gaits of the Macropodinae (Marsupialia). *Journals of Zoology*, 163 (2), 165–175.
https://doi.org/10.1111/j.1469-7998.1971.tb04530.x
Woodburne, M.O. (1984) Families of marsupials: relationships, evolution and biogeography. *Studies in Geology, Notes for a Short Course*, 8, 48–71.
https://doi.org/10.1017/S0271164800000889

Comparative figures

The following figures facilitate direct comparison between significant and diagnostic elements of different species of *Protemnodon*. Elements have been included if they are diagnostic, known from three or more species of *Protemnodon*, and can be shown isolated (*i.e.* are not preserved articulated).

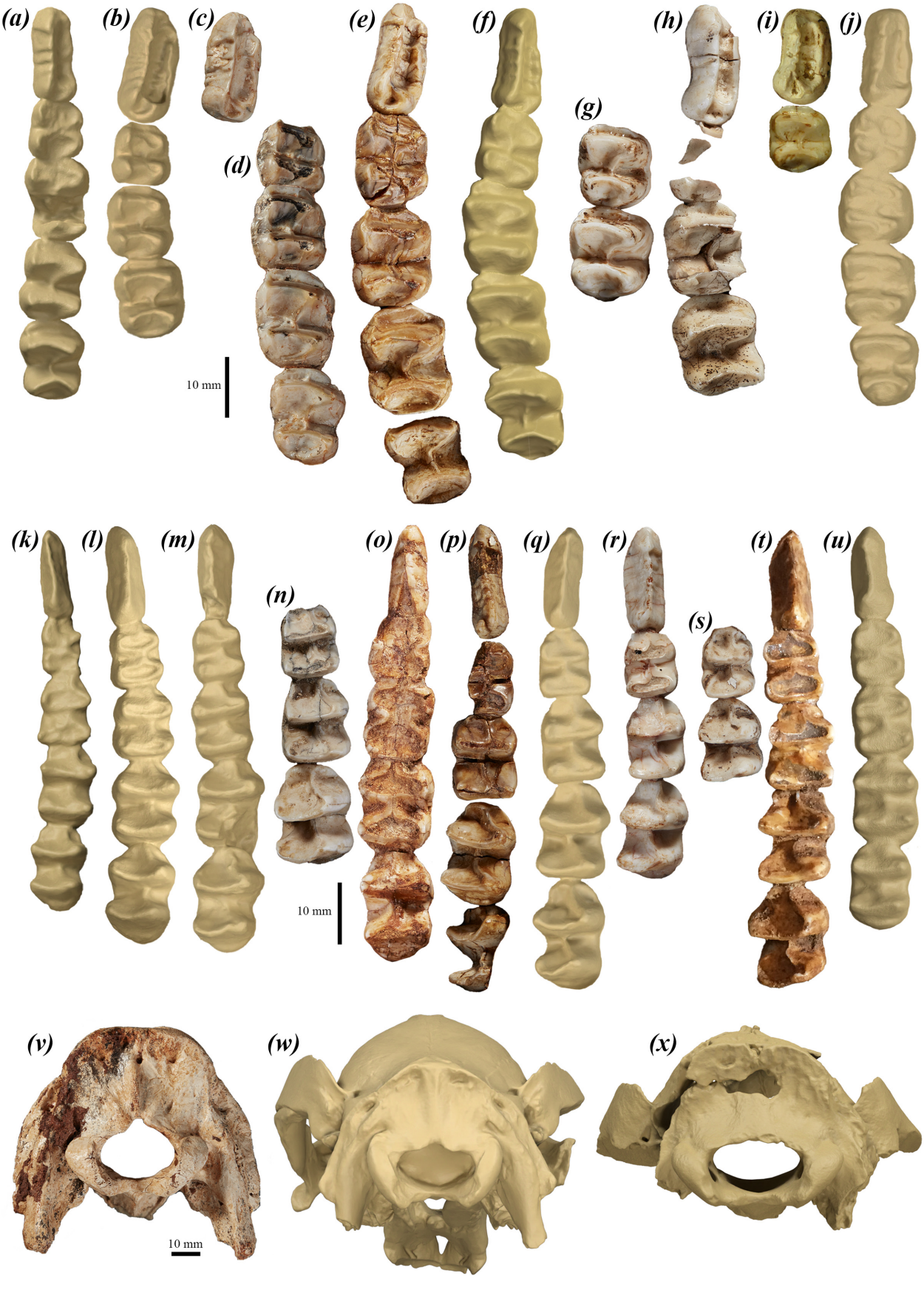

APPENDIX FIGURE 1. comparison of (a–j) right upper and (k–u) right lower cheek teeth in occlusal view, and (v–x) crania in posterior view of the species of *Protemnodon*. (a) scan of P3–M4 of *P. snewini* paratype QM F9074; (b) scan of P3–M3 of *P. otibandus* paratype UCMP 69857 (mirrored); (c) P3 of *P. dawsonae* **sp. nov.** paratype AM F161923 (mirrored); (d) M1–4 of *P. dawsonae* **sp. nov.** holotype AM F161915; (e) P3–M3 and partially erupted M4 of *P. viator* **sp. nov.** paratype SAMA P59548 (mirrored); (f) scan of *P. anak* IS V122; (g) M1–M2 of *P. mamkurra* **sp. nov.** paratype SAMA P28163 (mirrored); (h) P3, partial M1 and M2–M3 of *P. mamkurra* **sp. nov.** holotype SAMA P59549; (i) P3–M1 of *P. tumbuna* holotype PNG 83-40-8; (j) scan of *P. tumbuna* AM F83613 (*P. hopei* holotype); (k) scan of p3–m4 of *P. snewini* holotype QM F9061; (l) scan of p3–m4 of *P. otibandus* holotype CPC 6771; (m) scan of p3–m4 of *P. dawsonae* **sp. nov.** paratype AM F69858; (n) m1–m3 of *P. viator* **sp. nov.** paratype SAMA P53836 (mirrored); (o) p3–m4 of *P. viator* **sp. nov.** paratype SAMA P59550 (mirrored); (p) p3–m3 and partially erupted m4 of *P. viator* **sp. nov.** paratype SAMA P59548 (mirrored); (q) scan of p3–m4 of *P. anak* QM F3017; (r) p3–m3 of *P. anak* UCMP 57375; (s) m1–m2 of *P. mamkurra* **sp. nov.** paratype SAMA P28163; (t) p3–m4 of *P. mamkurra* **sp. nov.** SAMA P59547; (u) scan of p3–m4 of *P. tumbuna* AM F83612 (*P. hopei* paratype). (v) *P. mamkurra* **sp. nov.** SAMA P59553; (w) scan of *P. anak* IS V122; (x) scan of *P. viator* **sp. nov.** NMV P42526.

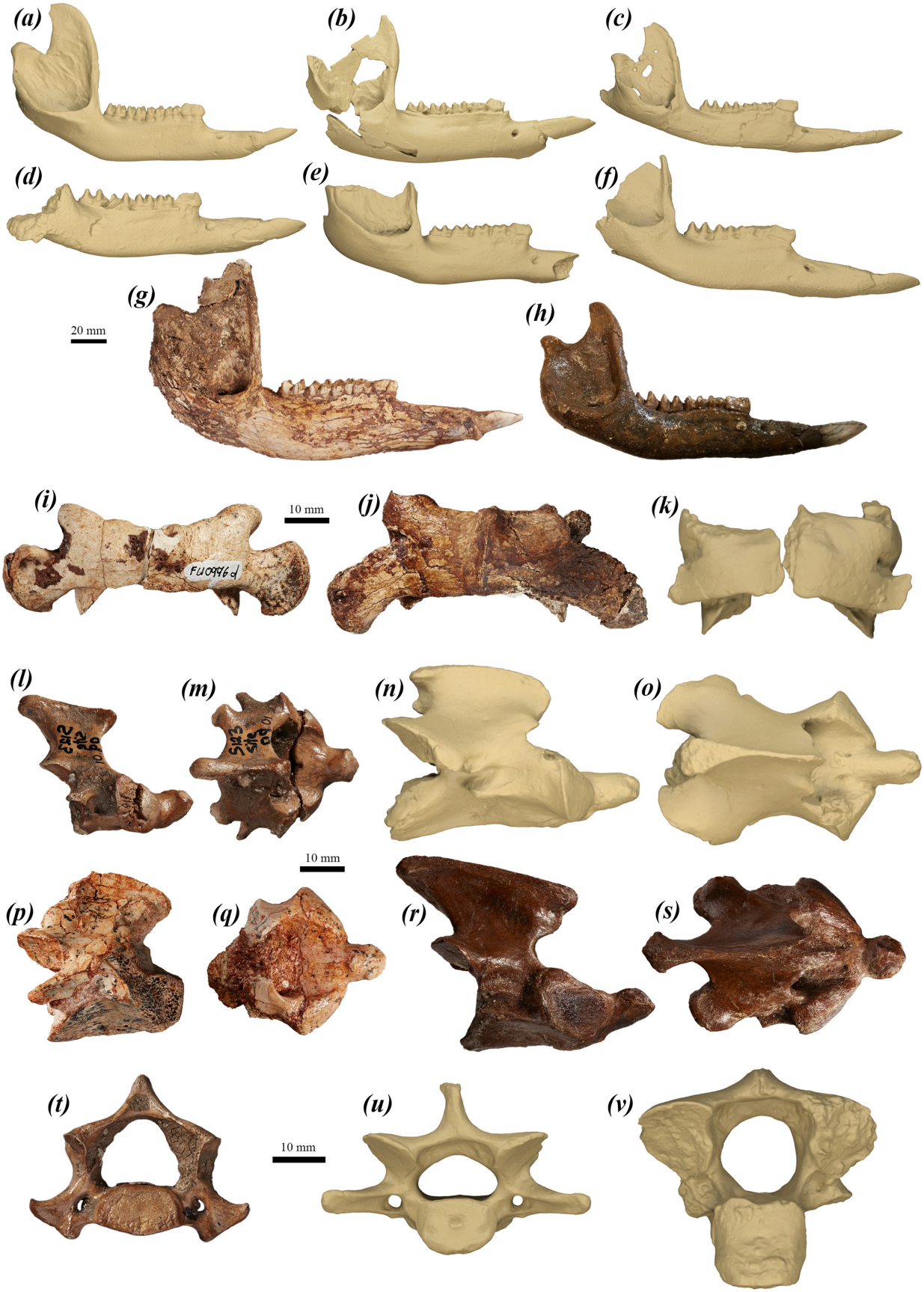
(a)
(b)
(c)
(d)
(e)
(f)
(g)
20 mm
(h)
(i)
10 mm
(j)
(k)
(l)
(m)
(n)
(o)
10 mm
(p)
(q)
(r)
(s)
(t)
10 mm
(u)
(v)

APPENDIX FIGURE 2. comparison of right dentaries (a–h) and cervical vertebrae (i–v) of the species of *Protemnodon*. (a) scan of *P. otibandus* holotype CPC 6771; (b) scan of *P. tumbuna* paratype PNG 82-40-20 (mirrored); (c) scan of *P. snewini* holotype QM F9061; (d) scan of *P. dawsonae* **sp. nov.** paratype AM F69858; (e) scan of *P. tumbuna* AM F83612 (*P. hopei* paratype); (f) scan of *P. anak* NMV P39105 (mirrored); (g) *P. viator* **sp. nov.** paratype SAMA P59550 (mirrored); and (h) *P. mamkurra* **sp. nov.** SAMA P59547. (i–k) atlas vertebrae C1 in dorsal view; (i) *P. mamkurra* **sp. nov.** SAMA P59553; (j) *P. viator* **sp. nov.** paratype SAMA P59550; (k) scan of *P. anak* NMV P39105.5. (l–s) axis vertebrae C2 in right lateral and dorsal views; (l–m) juvenile *P. mamkurra* **sp. nov.** paratype SAMA P28163 (mirrored); (n–o) scan of *P. anak* NMV P39101.4; (p) *P. dawsonae* **sp. nov.** paratype AM F161914; (q) *P. dawsonae* **sp. nov.** paratype AM F161920; (r–s) *P. viator* **sp. nov.** SAMA P54629. (t) juvenile cervical vertebra C7 of paratype SAMA P28163 in caudal view; (u) scan of cervical vertebra C3 of *P. tumbuna* AM F113144 in caudal view; (v) scan of partial cervical vertebra C5 of *P. anak* NMV P39101.5 in caudal view.

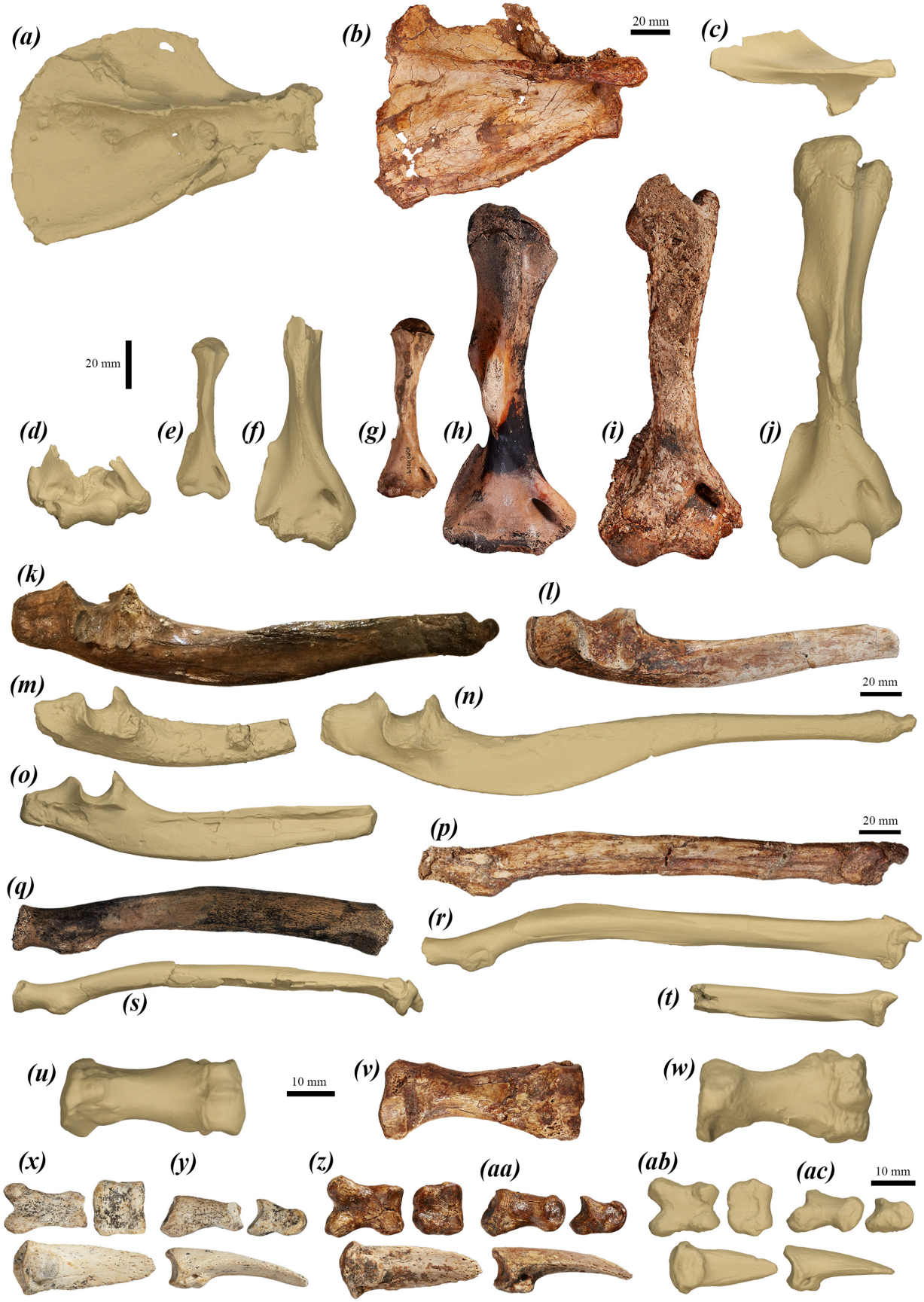
(a)
(b)
20 mm
(c)
20 mm
(d)
(e)
(f)
(g)
(h)
(i)
(j)
(k)
(l)
20 mm
(m)
(n)
(o)
20 mm
(p)
(q)
(r)
(s)
(t)
(u)
10 mm
(v)
(w)
(x)
(y)
(z)
(aa)
(ab)
(ac)
10 mm

APPENDIX FIGURE 3. comparison of right pectoral girdle and forelimb elements of the species of *Protemnodon*. (a–c) scapulae in dorsolateral view; (a) scan of *P. anak* NMV; (b) *P. viator* **sp. nov.** paratype SAMA P59550 (mirrored); (c) scan of juvenile *P. mamkurra* **sp. nov.** QVM2001 GFV39. (d–j) humeri in cranial view; (d) scan of *P. otibandus* UCMP 70059; (e) scan of juvenile *P. tumbuna* AM F113142; (f) scan of *P. tumbuna* AM F113171; (g) juvenile *P. mamkurra* **sp. nov.** paratype SAMA P28163 (mirrored); (h) *P. mamkurra* **sp. nov.** holotype SAMA P59549 (mirrored); (i) *P. viator* **sp. nov.** paratype SAMA P59550 (mirrored); (j) scan of *P. anak* NMV P39105. (k–o) ulnae in lateral view; (k) *P. mamkurra* **sp. nov.** SAMA P59546; (l) *P. viator* **sp. nov.** paratype SAMA P53836 (mirrored); (m) scan of *P. tumbuna* NCA-M71-9; scan of *P. anak* NMV P39105 (mirrored); (o) scan of *P. otibandus* UCMP 70059. (p–t) radii in medial view; (p) *P. viator* **sp. nov.** paratype SAMA P59550; (q) *P. mamkurra* **sp. nov.** holotype SAMA P59549 (mirrored); (r) scan of *P. anak* NMV P39101.47 (mirrored); (s) scan of *P. otibandus* UCMP 70059; scan of *P. tumbuna* AM F88925. (u–w) fourth metacarpals in palmar view; (u) scan of *P. mamkurra* **sp. nov.** WAM 02.7.11 (mirrored); (v) *P. viator* **sp. nov.** holotype SAMA P59552; (w) scan of *P. anak* NMV P39105. (x–ac) proximal, middle and distal fourth manual phalanges in palmar and lateral views; (x–y) *P. mamkurra* **sp. nov.** SAMA P20810 (middle phalanx III); (z–aa); *P. viator* **sp. nov.** holotype SAMA P59552; (ab–ac) scan of *P. anak* NMV P39105.

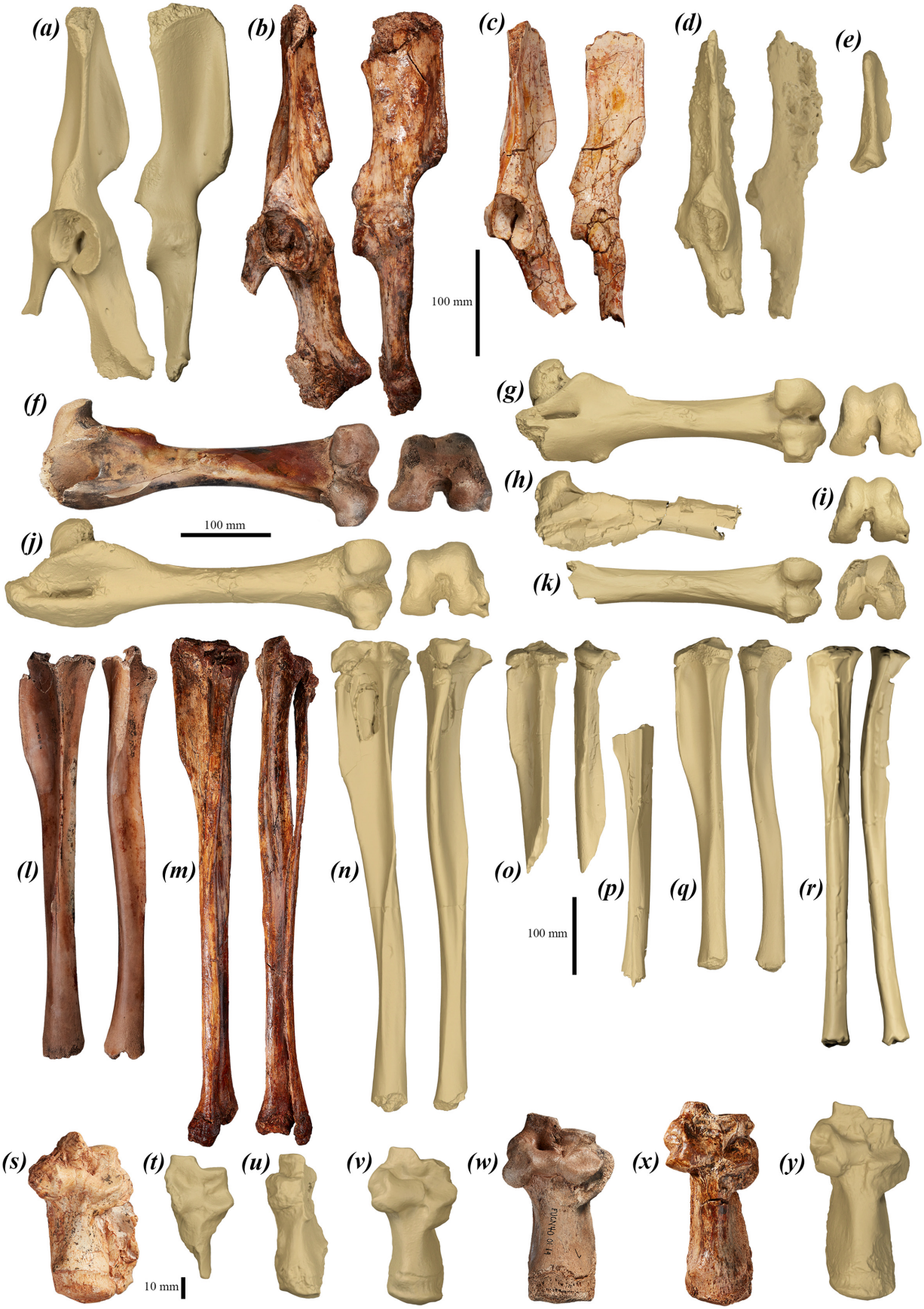
(a)
(b)
(c)
(d)
(e)
100 mm
(f)
(g)
(h)
(i)
100 mm
(j)
(k)
(l)
(m)
(n)
(o)
(p)
(q)
(r)
100 mm
(s)
(t)
(u)
(v)
(w)
(x)
(y)
10 mm

APPENDIX FIGURE 4. comparison of left pelvic girdle and hindlimb elements of species of *Protemnodon*. (a–e) partial pelves; (a) scan of *P. mamkurra* **sp. nov.** holotype SAMA P59549 in lateral and caudodorsal views (mirrored); (b) *P. viator* **sp. nov.** paratype SAMA P59550 in lateral and caudodorsal views; (c) *P. dawsonae* **sp. nov.** UCMP 156881 in lateral and caudodorsal views (mirrored); (d) scan of *P. tumbuna* AM F113140 (mirrored); (e) scan of *P. tumbuna* AM F113143 (mirrored). (f–k) femora in ventral and distal views; (f) *P. mamkurra* **sp. nov.** holotype SAMA P59549; (g) scan of *P. viator* **sp. nov.** NMV P173087; (h) scan of *P. otibandus* UCMP 45344 (mirrored); (i) scan of *P. otibandus* UCMP 70066; (j) scan of *P. anak* NMV P159917; (k) scan of *P. tumbuna* AM F88924. (l–r) tibiae in lateral and cranial views; (l) *P. mamkurra* **sp. nov.** holotype SAMA P59549; (m) *P. viator* **sp. nov.** paratype SAMA P59550; (n) scan of *P. anak* NMV P39101.41 (mirrored); (o) scan of *P. otibandus* UCMP 70584; (p) scan of *P. otibandus* UCMP 70584 (mirrored); (q) scan of *P. tumbuna* AM F88923; (r) scan of *P. snewini* QM F9075. (s–y) calcanei in dorsal view; (s) *P. dawsonae* **sp. nov.** paratype AM F161913 (mirrored); (t) scan of *P. tumbuna* AM F88929; (u) scan of *P. tumbuna* NCA-H71-9 (mirrored); (v) scan of *P. otibandus* UCMP 70584; (w) *P. mamkurra* **sp. nov.** holotype SAMA P59549; (x) *P. viator* **sp. nov.** holotype SAMA P59552; (y) scan of *P. anak* NMV P39105.87 (mirrored).

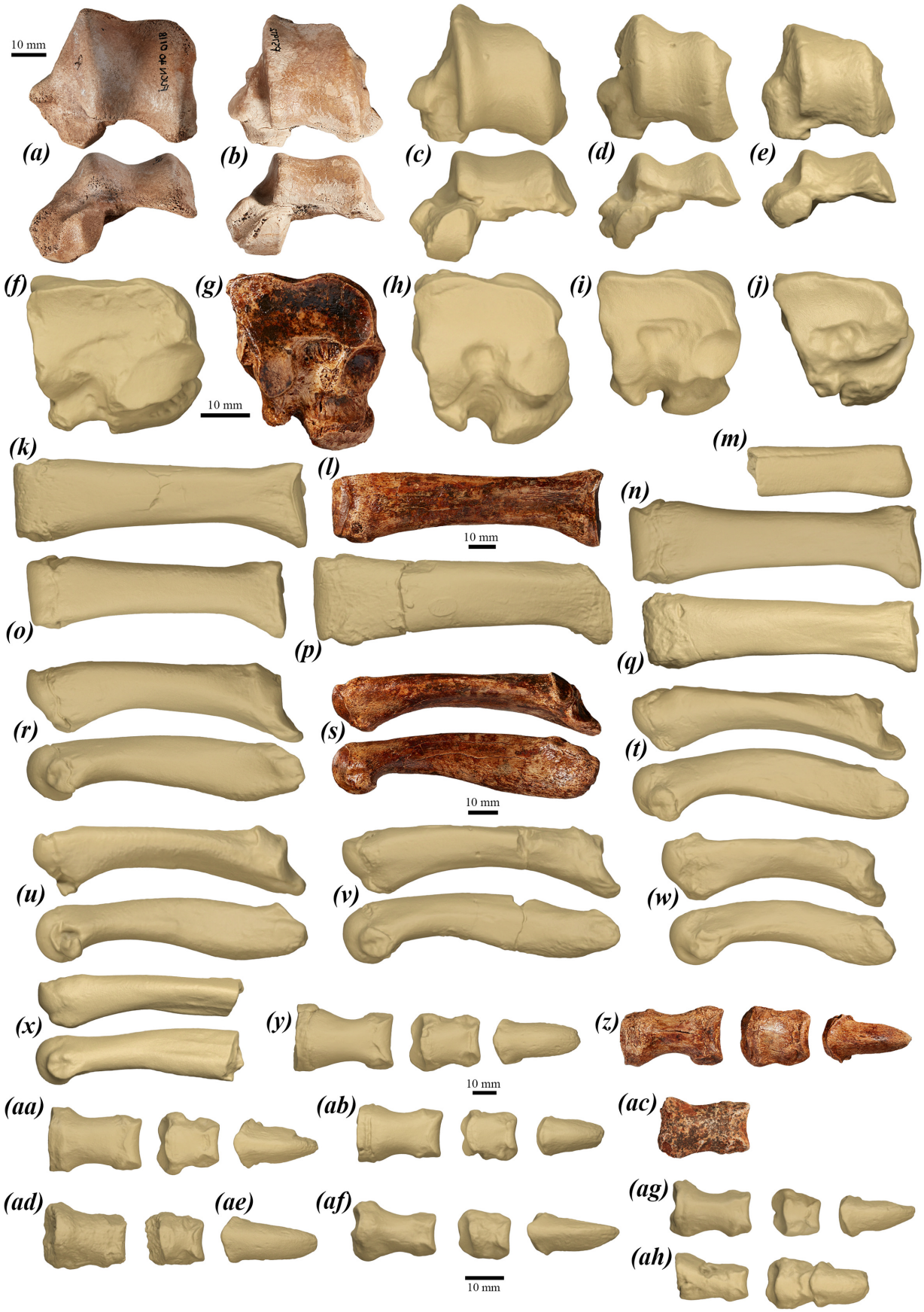
10 mm
(a)
(b)
(c)
(d)
(e)
(f)
(g)
10 mm
(h)
(i)
(j)
(k)
(l)
10 mm
(m)
(n)
(o)
(p)
(q)
(r)
(s)
10 mm
(t)
(u)
(v)
(w)
(x)
(y)
10 mm
(z)
(aa)
(ab)
(ac)
(ad)
(ae)
(af)
10 mm
(ag)
(ah)

APPENDIX FIGURE 5. comparison of pedal elements of species of *Protemnodon*. (a–e) left tali in dorsal and cranial views; (a) *P. mamkurra* **sp. nov.** holotype SAMA P59549 (mirrored); (b) *P. viator* **sp. nov.** SAMA P57972 (mirrored); (c) scan of *P. anak* NMV P39118; (d) scan of *P. otibandus* UCMP 45250; (e) scan of *P. snewini* QM F9076. (f–j) left cuboids in distal view; (f) scan of *P. mamkurra* **sp. nov.** SAMA P20810 (mirrored); (g) *P. viator* **sp. nov.** holotype SAMA P59552; scan of *P. anak* NMV P39132; (i) scan of *P. otibandus* UCMP 70078; (j) scan of *P. snewini* QM F9076. (k–q) left fourth metatarsals; (k) scan of *P. mamkurra* **sp. nov.** SAMA P59541; (l) *P. viator* **sp. nov.** holotype SAMA P59552; (m) scan of *P. tumbuna* AM F88930; (n) scan of *P. anak* NMV P209937; (o) scan of *P. otibandus* UCMP 70585; (p) scan of *P. dawsonae* **sp. nov.** paratype AM F106039; (q) scan of *P. snewini* QM F9075. (r–x) left fifth metatarsals in dorsal and lateral views; (r) scan of *P. mamkurra* SAMA P20810; (s) *P. viator* holotype SAMA P59552; (t) scan of *P. anak* NMV P39105.91 (mirrored); (u) scan of *P. otibandus* UCMP 70585 (mirrored); (v) scan of *P. dawsonae* **sp. nov.** AM F106040; (w) scan of *P. tumbuna* NCA-071 (mirrored); (x) scan of *P. snewini* QM F9076. (y–ac) proximal, middle and distal fourth pedal phalanges in dorsal view; (y) scan of *P. mamkurra* **sp. nov.** SAMA P20810; (z) *P. viator* **sp. nov.** holotype SAMA P59552; (aa) scan of *P. anak* NMV P39105; (ab) scan of *P. otibandus* UCMP 70585; *P. dawsonae* **sp. nov.** paratype AM F161916. (ad–ag) right proximal, middle and distal fifth pedal phalanges in dorsal view; (ad) scan of *P. mamkurra* **sp. nov.** WAM 02.7.11; (ae) scan of *P. mamkurra* **sp. nov.** SAMA P20810; (af) scan of *P. anak* NMV P39105; (ag) scan of *P. viator* **sp. nov.** NMNH 498886; (ah) scan of *P. otibandus* UCMP 45247.

Additional tables

Taxonomic analysis

TABLE 1. details of comparative and reference specimens used in taxonomic analysis.

Species	Specimen number	Locality	Age	Element
Congruus kitcheneri	WAM 02.7.12	Leaena's Breath Cave, WA	Middle Pleistocene	Partial cranium & skeleton
C. kitcheneri	WAM 02.7.21	Flightstar Cave, WA	Middle Pleistocene	Partial juvenile skeleton
Macropus fuliginosus	FUR 270	Near Terowie, SA	Modern	Complete skeleton
M. fuliginosus	FUR 267	SA	Modern	Partial cranium & skeleton
M. fuliginosus	FUR 094	Kangaroo Island, SA	Modern	Complete skeleton
M. fuliginosus	FUR K3	No data	Modern	Complete skeleton
M. fuliginosus	FUR 144	No data	Modern	Complete skeleton
Thylogale billardierii	FUR 395	Avenue River, TAS	Modern	Cranium & partial skeleton
T. billardierii	FUR 389	Near Guildford, TAS	Modern	Cranium & partial skeleton
T. billardierii	FUR 111	Avenue River, TAS	Modern	Complete skeleton
T. billardierii	FUR 213	Austral Creek, TAS	Modern	Cranium & partial skeleton
Wallabia bicolor	SAMA M21355	Near Port MacDonnell, SA.	Modern	Postcranial skeleton
W. bicolor	FUR 345	Columboola, NSW	Modern	Cranium & mandible

Phylogenetic analysis

TABLE 2. details of specimens used for character scoring in phylogenetic analysis.

Species	Specimen number	Locality	Age	Element
Congruus kitcheneri	WAM 02.7.12	Leaena's Breath Cave, WA	Middle Pleistocene	Partial cranium & skeleton
C. kitcheneri	WAM 02.7.21	Flightstar Cave, WA	Middle Pleistocene	Partial juvenile skeleton
Macropus fuliginosus	FUR 270	Near Terowie, SA	Modern	Complete skeleton
M. fuliginosus	FUR 267	SA	Modern	Partial cranium & skeleton
M. fuliginosus	FUR 094	Kangaroo Island, SA	Modern	Complete skeleton
M. fuliginosus	FUR K3	No data	Modern	Complete skeleton
M. fuliginosus	FUR 144	No data	Modern	Complete skeleton
Thylogale billardierii	FUR 395	Avenue River, TAS	Modern	Cranium & partial skeleton
T. billardierii	FUR 389	Near Guildford, TAS	Modern	Cranium & partial skeleton
T. billardierii	FUR 111	Avenue River, TAS	Modern	Complete skeleton
T. billardierii	FUR 213	Austral Creek, TAS	Modern	Cranium & partial skeleton
Wallabia bicolor	SAMA M21355	Near Port MacDonnell, SA.	Modern	Postcranial skeleton
W. bicolor	FUR 345	Columboola, NSW	Modern	Cranium & mandible

TABLE 3. characters and states scored for the phylogenetic analysis, with details of origin and/or effect of each character.

#	Character description	Character states	Details
1	I1 shape	Slightly broadened from subcylindrical (0); markedly broadened (1).	Most of the species of *Protemnodon* have a broad, anteroposteriorly compressed I1, while *P. otibandus* does not. Adapted slightly from Prideaux & Warburton (2010) to better target the variation among species of *Protemnodon*.
2	Maximum width of I1 relative to maximum length of I3	Narrower (0); broader (1).	Adapted from Prideaux & Warburton (2010).
3	Cleft in main crest of P3/p3 immediately posterior to anterior peak	Present (0); absent (1).	*Thylogale billardierii* and some dendrolagins have a variable cleft in the main crest of the P3/p3 immediately posterior to a high anterior peak. From Prideaux & Warburton (2010).
4	P3 ridgelets on main crest	Buccal face with 2–4 low to very low, rounded ridgelets (0); buccal and lingual faces with 3–4 raised, angular ridgelets (1); absent (2).	The number and morphology of the dorsoventrally aligned ridgelets on the buccal and lingual surfaces of the main crest of the P3 varies within *Protemnodon*. With reference to Stirton (1963) and Bartholomai (1973).
5	P3 lingual crest	Very short, curves rapidly to base of main crest, not extending past midpoint of main crest (0); high, smoothly dorsoventrally undulating, extends at least to lingual margin of anterior cusp (1); mid-height and jagged, extends from posterolingual basin to ridgelet ascending from second main crest cuspule (2); very short, extends along whole lingual margin, separated into distinct anterior and posterior moieties (3); very low, extends along whole lingual margin (4).	The presence and morphology of the lingual crest (cingulum) and lingual basin varies across Macropodinae and within *Protemnodon*.
6	P3 posterolingual basin	Very small, narrow and shallow (0); large, broad and deep (1); small, broad and shallow (2).	Although the P3 of *W. bicolor* is quite similar to that of most of the species of *Protemnodon*, the relative size and shape of its posterior basin differs.
7	Premolar length relative to M3/m3	Subequal to slightly longer (0); slightly shorter (1); much shorter (2).	The length of the permanent premolar relative to that of the molars generally decreases upward through Macropodini. *Protemnodon* maintain a large premolar despite this trend.

...Continued on the next page

TABLE 3. (Continued)

#	Character description	Character states	Details
8	Forelink on precingulum and protoloph of M1–2	Thin, raised, extends from midpoint of precingulum, merges into anterior face of loph (0); very slight to absent (1).	The forelink (preprotocrista) on the precingulum of the upper molars is variably present across Macropodini, but is absent from most species of *Protemnodon*.
9	Preparacrista on M1–2	Moderately developed (0); low, thin, slight (1); absent (2).	The preparacrista leads from the buccal edge of the precingulum along the anterobuccal margin of the protoloph to the paracone. It is generally larger in more basal macropodines and varies in size among species of *Protemnodon*.
10	Postparacrista development and morphology	Very weak to weak, positioned lingual to buccal margin of protoloph and curving lingually (0); very weak to weak, short, straight, positioned lingual to buccal margin of protoloph, deflected slightly lingually and merging into protoloph (1); straight, moderately high, extends along posterobuccal margin of protoloph (2); weak, positioned lingual to buccal margin of protoloph, curving lingually from paracone, recurving to buccal margin and lingually again into interloph valley (3); absent (4).	The postparacrista extends from the paracone into the interloph valley. Its development, curvature and position relative to the buccal margin of the protoloph vary among macropodines and among species of *Protemnodon*.
11	Premetacrista development	Absent to very weak (0); weak to moderately developed, extends to metacone (1).	Premetacrista reaches from base of postparacrista in buccal component of interloph valley to metacone.
12	Urocrista (postlink) on M1–2 metaloph	Absent (0); mostly present (1).	Urocrista, a small crest on posterior face of metaloph, perpendicular to metaloph crest, is variably present on anterior upper molars of *P. otibandus* and *P. tumbuna*.
13	Cuspule (‘tuberculation’) sometimes present on lingual extremity of interloph valley	Absent (0); present as a slight ridge to a small, triangular cuspule (1).	Small cuspule occasionally present on lingual margin of interloph valley of upper molars of *P. mamkurra*, *P. viator* and *P. dawsonae*. Varies from a slight swelling on posterolingual base of protoloph to a small, pointed enamel eminence. With reference to Bartholomai (1973).

...Continued on the next page

TABLE 3. (Continued)

#	Character description	Character states	Details
14	Stylar cusp C (re-emergent cuspule) at buccal margin of interloph valley	Absent (0); present (1).	A small cuspule, possibly a re-emergent stylar cusp C, is occasionally present on buccal margin of interloph valley of upper molars of *P. mamkurra* and *P. viator*. Varies from a slight swelling to a small, pointed cuspule on posterobuccal base of protoloph.
15	Angle of i1 relative to alveolar row	Procumbent (0); dorsally deflected or straight (1).	Most macropodins have a variably ventrally deflected diastema and i1 on dentary.
16	i1 morphology	Large, deep and narrow (0); large to very large, broad (1); small, shallow, narrow (2).	The ancestral state of the i1 is large, tall and transversely compressed, and relative size and shape continue to vary across Macropodini.
17	i1 ventrolingual enamel crest	Thin and flared (0); absent to thick and low (1).	Most macropodins possess a thin, variably raised ventrolingual enamel crest on i1, but in *P. dawsonae* crest is reduced to a low, thick ridge. It is completely absent in *P. mamkurra* and *P. tullochorum*, instead with a thick, smooth, rounded ventrolingual lip.
18	Development of lingual component of paracristid on m2–4	Large, anterolingually projected (0); small, rounded (1).	Paracristid extends anteriorly from protoconid towards anterior margin of trigonid before bifurcating into lingual and buccal components. Lingual component wraps around anterolingual margin of trigonid valley, projecting variably anterolingually.
19	Premetacristid	Weak, thin (0); moderately developed, broad (1); absent (2).	Premetacristid extends anteriorly or anterobuccally from metaconid along anterolingual margin of protolophid to merge into lingual component of anterior base of paracristid.
20	Postcingulid	Absent or very slight bulge (0); present, usually as a distinct stepped shelf (1).	Identified by Owen (1874) and others as a feature of *Protemnodon*. Arisen independently in various basal macropodines, but is not common in macropodins.
21	Masseteric process	Very small to small, pointed (0); Large, broad, and straight to anteriorly curved (1); very long, straight and narrow (2).	Masseteric process, on lateral side of cranium beneath the orbit, is the site of origin of m. masseter superficialis (Warburton 2009), which elevates, protracts and medially rotates mandible. Character targets species of *Protemnodon*, though masseteric process of *P. snewini* is not known.
22	Palatine vacuities	Very large, oval (0); absent, or scattered and very small (1).	Palatine vacuities refer to foramina (excluding anterior palatine) in the palatine bone between the posterior molars. *Wallabia* and *Thylogale* have very large, oval vacuities, while they are absent in *Congruus* and all four species of *Protemnodon* for which this area is preserved. With reference to Stirton (1963).

...Continued on the next page

TABLE 3. (Continued)

#	Character description	Character states	Details
23	Foramen ovale and anterior ridge	Narrow, shallow anteroposterior groove meets anterior of foramen (0); broad, shallow anteroposterior groove meets anterior of foramen (1); raised, narrow anteroposterior ridge meets foramen on medial margin (2).	The foramen ovale is a small foramen on the basicranium, passing through the alisphenoid near its medial edge, immediately posterolateral to the pterygoid fossa. This foramen is met on its medial edge by a thin, anteroposteriorly-aligned ridge in *Protemnodon*.
24	Postglenoid process shape and orientation	Deep and rounded in lateral view, obliquely aligned in ventral view (0); squarish in lateral view, obliquely aligned in ventral view (1); thin in lateral view, broad and transversely aligned in ventral view (2).	The postglenoid process, which projects ventrally from the squamosal at the posterior base of the zygomatic arch, varies in size across Macropodidae (Prideaux & Warburton 2010). Its shape and orientation in ventral view are similarly variable. 'Oblique alignment' refers to the state where the anterior surface of the postglenoid is tilted medially.
25	Size and lateral projection of anterior process of ectotympanic relative to external auditory meatus in ventral view	Anterior process larger and more laterally projected (0); subequal in size and lateral projection (1).	In species of *Protemnodon*, *C. kitcheneri* and *M. fuliginosus*, the ectotympanic has a moderately sized anterior component which projects from the base of the external auditory meatus and abuts the posteromedial margin of the postglenoid process. In *T. billardierii*, this anterior process is somewhat larger relative to the size of the EAM.
26	Posterior projection of occipital condyles in lateral view	Subequal or less posteriorly projected than occipital and nuchal crest (0); project well beyond posterior margin of occipital and nuchal crest (1).	The occipital condyles of species of *Protemnodon* are fairly large, and project posteriorly when viewed laterally, visible in their projection past the occipital and nuchal crest.
27	Maximum occipital width relative to height	Taller than wide (0); wider than high (1).	From Prideaux and Warburton (2010).
28	Foramen magnum size relative to occipital size in posterior view	Small (0); large (1).	From Prideaux and Warburton (2010).
29	Mandibular corpus	Deep and robust (0); shallow and gracile (1).	More basal macropodines and most species of *Protemnodon* have a deep/tall and robust mandibular corpus, while a shallower/shorter and more gracile one is more typical of *Macropus* and *Osphranter*.

...Continued on the next page

TABLE 3. (Continued)

#	Character description	Character states	Details
30	Dorsoventral position of anterior mental foramen on dentary	On lateral face of diastema, ventral to dorsal margin (0); on or immediately adjacent to dorsal margin of diastema (1).	The position of the anterior mental foramen (often just 'mental foramen'; here differentiated from the posterior mental foramen present in more basal macropodines) relative to the dorsal margin of the diastema on its lateral surface. This foramen is more dorsally situated in crown macropodins *Macropus*, *Notamacropus* and *Osphranter*, as well as *C. kitcheneri* and *P. snewini*.
31	Anteroposterior position of anterior mental foramen on dentary relative to p3 and to base of crown of i1	Closer to p3/mandibular corpus (0); closer to base of crown of i1 (1).	Position of anterior mental foramen relative to posterior margin of i1 and anterior margin of p3. The foramen is more posteriorly situated in more basal macropodines like *Dendrolagus*, and more anteriorly in crown macropodins like *M. fuliginosus*.
32	Buccinator sulcus	Very shallow, extends from beneath p3 to m1/m2 margin (0); shallow, extends from beneath p3 at least to m2/m3 margin (1).	The buccinator sulcus (labial groove) is a groove near the alveolar margin on the lateral surface of the mandibular corpus, for the partial insertion of the m. buccinator. Its length and depth varies among macropodines.
33	Posterior component of masseteric fossa on dentary	Shallow, with lateral ridge very low or absent (0); deep, bounded by thin, raised lateral ridge (1).	The masseteric fossa is a long, deep fossa situated posterolaterally on the dentary, for the insertion of the m. masseter profundus (deep masseter), which elevates and retracts the mandible (Warburton 2009). The depth of the posterior component and the morphology of its lateral margin differs between species of *Protemnodon* and other macropodins.

...Continued on the next page

TABLE 3. (Continued)

#	Character description	Character states	Details
34	Height of posterior margin of mandibular fossa relative to mandibular condyle	Low to moderate (0); high (1).	The mandibular fossa is a deep, broad fossa on the posteromedial surface of the dentary, the posterior component of which is for the insertion of the m. pterygoid medialis (Warburton 2009). The posterior margin of this fossa extends medially into the angular process, and its height relative to the position of the mandibular condyle and the height of the alveolar margin varies among Macropodini.
35	Caudomedial projection of humeral head from shaft	Marked (0); slight (1).	The degree of caudomedial projection of the humeral head relative to the proximal shaft. Greater in *Wallabia* and *Protemnodon*.
36	Proximal humeral shaft morphology	Shallow and more gracile (0); deep and robust, distinctly deepens proximally (1).	The robustness of the humeral shaft between the pectoral crest and the proximal end. That of *Protemnodon* is more robust and craniocaudally deeper, and deepens toward the proximal end.
37	Supracondylar foramen shape and size relative to thickness of medial supracondylar bridge	Very flattened oval, large to very large (0); flattened oval, very small to small (1); round to slightly flattened oval, large (2).	The supracondylar foramen passes beneath the medial supracondylar bridge on the distal end of the humerus. Size and shape of the foramen relative to the medial supracondylar bridge varies among macropodines.
38	Medial supracondylar bridge continues up as low, broad ridge to distal extremity of pectoral crest	Present (0); absent (1).	Medial supracondylar bridge, in some species of macropodine, extends towards the peak of the pectoral crest as a low, broad ridge or elongate swelling, which deepens the distal shaft of the humerus.
39	Width of distal articular facet of humerus relative to width across epicondyles	Broad (0); narrow (1).	Width of the distal articular facet of the humerus (ulnar and radial facets) relative to the total width of the distal end of the humerus (width between the medial and lateral epicondyles).
40	Olecranon development (length of ulna divided by olecranon length)	Moderate (6–7) (0); short (>7) (1); elongate (<6) (2).	The olecranon process is the 'lever arm' of the ulna, protruding posteriorly from the behind the humeral articulation. Measured from centre of humeral articulation to posterior/distal tip of olecranon.
41	Olecranon shape in lateral view (including epiphysis)	Straight, tapers craniocaudally to tip (0); straight, untapered (1); cranially deflected, untapered to slightly craniocaudally tapered (2).	Shape and angle of the olecranon varies among macropodines; best described in lateral view.

...Continued on the next page

TABLE 3. (Continued)

#	Character description	Character states	Details
42	Depth of proximomedial flexor fossa on ulna	Gently to moderately concave (0); deeply concave (1).	The proximomedial flexor fossa extends anteriorly and posteriorly from beneath humeral articulation on medial side of ulna. Fossa is the partial origin for the flexor muscle group, which act to flex manus and digits (Warburton *et al.* 2011).
43	Degree of transverse compression of proximal ulnar shaft	Moderate (0); low (1); very high (2).	The degree of transverse compression (i.e. height relative to width) of ulnar shaft between humeral articulation and midway to distal epiphysis.
44	Cross-sectional shape of distal shaft of ulna	Round (0); tall and oval (1).	Shape of distal half of shaft of ulna in cross-section. Varies among macropodines.
45	Cross-sectional shape of distal shaft of radius	Oval, dorsoventrally compressed (0); round, not compressed (1).	Adapted from Prideaux and Warburton (2010).
46	Facet for metacarpal V on metacarpal IV	Faces distally (0); faces laterally (1).	The metacarpal IV articulates with metacarpal V on the lateral side of the proximal end. Though typically a single facet facing laterally, the metacarpal IV of *P. anak*, *W. bicolor* and *T. billardierii* have a lateral facing facet on a projection at the proximal end, and a second semi-continuous facet facing distally on the distal face of the projection.
47	Peak and height of shaft of distal manual phalanges	Not dorsopalmarly compressed, with a rounded-triangular dorsal peak (0); very tall, with strong triangular peak (1); moderately to strongly dorsopalmarly compressed, with dorsal surface rounded to very slightly rounded-triangular (2).	The distal manual phalanges differ between species of *Protemnodon* and other macropodines in their height and in the strength of the peak on the dorsal surface, which varies from absent/rounded and smoothly convex to distinctly pointed and triangular in cross-section.
48	Curvature of shaft of distal manual phalanges	Strongly palmarly curved (0); moderately palmarly curved (1); no palmar curvature (2).	Viewed laterally/medially, distal manual phalanges of macropodines exhibit varying degrees of palmar (ventral) curvature in the shaft.
49	Relative size of flexor tubercle of distal manual phalanges II–IV	Small, fairly narrow compared to proximal end (0); large, broad (1).	The flexor tubercle projects palmarly from the proximal end of the distal manual phalanges, for insertion of tendons of m. flexor digitorum profundus, which flexes digits. Size in lateral view relative to the rest of the phalanx, while width gauged in palmar view relative to body of phalanx.

...Continued on the next page

TABLE 3. (Continued)

#	Character description	Character states	Details
50	Axis vertebra length to width index	Low (<1.05) (0); moderate (1.05–1.35) (1); high (>1.35) (2).	Length of axis vertebra (C2), from tip of dens to middle of dorsal margin of caudal extremity of body, divided by maximum width between lateral margins of the cranial articular surfaces.
51	Morphology of spinous process of axis vertebra	Much deeper than arch, due to elongate caudal projection (0); subequal to slightly deeper than arch, with very slight caudal projection (1).	Spinous process of axis vertebra is elongate relative to body in some macropodines, with caudal end extending well beyond caudal extremity of body.
52	Number of thoracic: lumbar vertebrae	13:6 (0); 14:5 (1).	Number of thoracic and lumbar vertebrae differs between *C. kitcheneri* and *P. tullochorum* and other macropodines, the former two having 14 thoracic and five lumbar vertebrae instead of the usual 13 and six. Proportionate number of vertebrae not known for other species of *Protemnodon*.
53	Cranial iliac spine	Well-developed, extends close to or reaches distal end of ilium (0); a low, swollen, proximal ridge (1).	The cranial iliac spine projects cranially from iliac blade, extends to iliac crest (distal end) of ilium as a distinct crest in most macropodines, but present as a narrow proximal swelling in *Protemnodon*.
54	Iliac blade width (maximum width across lateral spine to medial side of ilium)	Narrow (0); broad (1).	The lateral iliac spine projects laterally from iliac blade, extends from acetabulum to the iliac crest. In cranial view, width of the blade, which includes lateral iliac spine, is much greater in species of *Protemnodon* due to a broad iliac spine, than in other macropodines.
55	Alignment of ilium and ischium in lateral view	Aligned, without deflection at acetabulum (0); ischium deflected caudodorsally relative to angle of ilium (1).	Viewed laterally, axis of ilium and ischium are aligned (i.e. form a 180-degree angle) in some species of macropodine, including *P. tumbuna*, though more typically axis of ilium is caudodorsally tilted relative to that of ischium.
56	Position of rectus tubercle on ilium	Distinctly separate from acetabular rim (0); adjacent to or abutting acetabular rim (1).	Rectus tubercle is an enlarged, rugose tubercle situated at proximal base of lateral iliac spine, facing laterally, for origin of m. rectus femoris, which is a major knee extensor and hip flexor (Hopwood & Butterfield 1990; Warburton *et al.* 2013). Its position relative to acetabulum varies among macropodines. Adapted from Prideaux & Warburton (2010).
57	Iliopubic eminence at junction of ilium and pubis	Long, well-developed, square in outline (0); short, broad (1).	Iliopubic eminence, partial origin of m. pectineus (Warburton *et al.* 2013), projects craniomedially from pubis at its junction with craniomedial base of ilium. Size and shape of eminence varies across Macropodidae, and is particularly short and broad in species *Protemnodon*. From Prideaux & Warburton (2010).

...Continued on the next page

TABLE 3. (Continued)

#	Character description	Character states	Details
58	Morphology of lesser trochanter of femur and confluence of intertrochanteric crest and lesser trochanteric ridge in ventral view	Forms peak of gently medially rounded crest (0); forms peak of distinctly triangular crest (1).	Lesser trochanter of femur projects medially beneath femoral head, sitting at confluence of intertrochanteric crest and lesser trochanteric ridge, which extends distally along the medioventral surface of the proximal end. In *P. tullochorum*, lesser trochanter is more strongly projected, and intertrochanteric crest and lesser trochanteric ridge are both more raised and straighter, such that lesser trochanter sits at tip of a triangular process beneath femoral head. In other compared taxa the crest and ridge are weaker and gently medially convex.
59	Development of proximolateral ridge (lateral edge of greater trochanteric ridge)	Large, raised, projected and dorsolaterally curved ridge (0); slightly raised, dorsolaterally curved ridge (1); lateral face of proximal end of femur slightly rugose (2).	Proximolateral ridge is formed by lateral projection of greater trochanteric ridge on proximal end of femur. This ridge is origin of m. vastus lateralis (a major knee flexor) (Warburton *et al.* 2012), and varies in size among Macropodinae.
60	Distal extent of lesser trochanteric ridge	Distal to that of proximolateral ridge (0); subequal to that of proximolateral ridge (1).	Lesser trochanteric ridge extends variably distally along femoral shaft among macropodines; measured relative to distal extent of proximolateral ridge.
61	Distal extent of trochanteric fossa relative to peak of lesser trochanter	Distal to lesser trochanter (0); level with lesser trochanter (1); proximal to lesser trochanter (2).	Trochanteric fossa extends variably anteriorly along proximal end of femur among macropodines; measured relative to position of lesser trochanter.
62	Size and position of quadratus tubercle on ventral femoral shaft	Large, oval, elongate and proximally extensive (0); elongate, situated at or past midpoint of shaft and distally extensive (1); small, oval, raised, clearly demarcated and immediately proximal to midpoint of shaft (2); elongate, rugose, situated at midpoint of shaft on medioventral surface (3).	Quadratus tubercle, insertion for major femoral extensor m. quadratus femoris (Hopwood & Butterfield 1990), is situated on ventral surface of femoral shaft, with relative proximodistal position varying among macropodines.
63	Femoral shaft in dorsal view	Straight (0); bowed medially (1).	Femoral shaft of *C. kitcheneri* bows medially, while other macropodines have a straight shaft.
64	Relative heights of trochlear crests of femur in distal view	Subequal in height (0); lateral crest significantly higher (1).	The trochlear crests are dorsal eminences on distal epiphysis of femur, for articulation with tibia. Their relative heights vary among macropodines.
65	Position of lateral gastrocnemial fossa on lateral epicondyle of femur	Closer to distal margin of condyle (0); central or closer to proximal margin of condyle (1).	Lateral gastrocnemial fossa, situated on lateral epicondyle of the distal femur, is partial origin of m. gastrocnemius lateralis, a major plantar flexor of pes (Hopwood & Butterfield 1990; Warburton *et al.* 2013). In species of *Protemnodon* it is situated centrally on lateral epicondyle or closer to proximal margin of distal epiphysis than distal margin.
66	Relative length of cranial tibial crest (tibial crest length divided by length of tibia without epiphyses)	Short (<0.21) (0); intermediate (0.21–0.26) (1); long (>0.26) (2).	Length of cranial tibial crest (from proximal extremity of crest, where it abuts proximal epiphysis, to distal peak) divided by tibial length without epiphyses. Adapted from Prideaux & Warburton (2010).

...Continued on the next page

TABLE 3. (Continued)

#	Character description	Character states	Details
67	Proximolateral crest on tibia	Low and thin (0); low and thick (1); raised and thin (2).	Proximolateral crest on tibia extends along lateral surface from proximal epiphysis to around midpoint of shaft, then merging smoothly into distal shaft. Height and thickness of this crest vary between species of *Protemnodon*, particularly in distal component.
68	Calcaneal tuberosity length and height	Short, subequal to slightly longer than head length (0); considerably longer than head length (1).	Calcaneal tuberosity is longer in higher-geared macropodins; increases in length towards crown macropodins. Caudal surface is site of insertion for major pedal flexors e.g. Mm. gastrocnemius.
69	Calcaneal tuberosity cross-sectional shape at caudal end	Broader than high (0); narrower than high (1).	As above. Tall and narrow shape is an indicator of higher-gearing.
70	Relative width of calcaneus-talus articulation	Intermediate (0.4–0.45) (0); narrow (<0.4) (1); wide (>0.45) (2).	From Prideaux & Warburton (2010).
71	Medial displacement of calcaneal head relative to calcaneal tuberosity	Absent (0); present (1).	*Protemnodon otibandus*, *P. tumbuna* and some dorcopsins have a medially displaced calcaneal head relative to the tuberosity, an adaptation providing more support for the flexion of the pes outside the typical sagittal plane of macropodines.
72	Caudal component of fibular facet on calcaneus	Slightly caudally projected, convex, slightly higher than lateral talar facet, with distinct circular margin (0); caudolaterally projected, low relative to lateral talar facet, margins indistinct (1); convex, unprojected, level with–slightly higher than lateral talar facet and with margins indistinct (2).	Fibular facet on calcaneus is subdivided into a cranial and caudal component, partially separated by a dorsolateral groove or fossa. Shape and projection of the caudal component varies among species of *Protemnodon*, as does distinctness of the margin or edge of the articular surface of the caudal component.
73	Navicular facet on talar head	Small, short (0); large, tall, caudoplantarly extensive (1).	Greater contact between the navicular and the talus aids ankle stability during locomotion.
74	Tubercle medioplantar to medial malleolus on talar head	Present (0); absent (1).	Distinct rugose tubercle projects plantomedially from beneath the medial malleolus on the navicular head in *P. otibandus* and *T. billardierii*.
75	Height of talar trochlear crests	Subequal (0); medial crest higher (1).	Adapted from Prideaux & Warburton (2010).
76	Dorsal and plantar cuboid facets on metatarsal IV	Confluent (0); separated by shallow transverse fossa (1).	In some macropodines, proximal facet of metatarsal IV, which articulates with cuboid, has a separate larger dorsal and smaller plantar facet, separated by a shallow transverse fossa or groove. Others have a single continuous facet with a small plantolateral fossa partially separating dorsal and plantar components.

...Continued on the next page

TABLE 3. (Continued)

#	Character description	Character states	Details
77	Metatarsal IV relative robustness	Gracile (7.5–10) (0); robust (<7.5) (1); very gracile (>10) (2).	Maximum length divided by minimum width across shaft of metatarsal IV produces relative robustness, which is lower (i.e. more robust) in species of *Protemnodon*.
78	Size and plantar projection of proximal plantar tubercle on metatarsal IV	Small (0); large (1).	Proximal plantar tubercle projects plantarly from proximal end of metatarsal IV. Proximal surface of plantar tubercle is covered by plantar cuboid facet, while larger plantodistal surface is covered by the facet for the proximal plantar sesamoid. In species of *Protemnodon* and in *C. kitcheneri*, an enlarged, plantarly-projected proximal plantar tubercle articulates with a large proximal plantar sesamoid.
79	Metatarsal V relative robustness	Moderate (4–6) (0); gracile (>6) (1); robust (<4) (2).	Length of metatarsal V divided by width across plantar surface of distal end.
80	Size and shape of proximal lever arm on metatarsal V in medial view	Small and pointed (0); well developed, rounded (1); very small (2).	Proximal lever arm projects proximally and slightly laterally from proximal end of metatarsal V. In species of *Macropus* and *Osphranter*, lever arm is very reduced, while in species of *Protemnodon* and *C. kitcheneri* it is large and rounded in lateral view.
81	Medial plantar tubercle on metatarsal V	Absent to very small and covered proximally by cuboid facet (0); rounded and caudomedially projected, cuboid facet not covering proximal surface of tubercle (1).	Medial plantar tubercle is a small projection on medial corner of proximal end of metatarsal V, abutting or covered by cuboid facet. Size, shape and degree of overlap with cuboid facet vary between species of *Protemnodon*.
82	Middle pedal phalanx IV	Narrow, gently dorsoplantarly compressed (0); broad, strongly dorsoplantarly compressed (1); elongate, narrow, not dorsoplantarly compressed (2).	Middle pedal phalanx IV of *Protemnodon* is synapomorphic in its absolute and relative breadth and strong dorsoplantar compression.
83	Proximal plantar tubercles of middle pedal phalanx IV	Broad and low, unflared mediolaterally (0); broad and low, distinctly flared and thickened mediolaterally (1); narrow, well-developed plantarly, come to broad point, unflared mediolaterally (2).	Proximal plantar (flexor) tubercles of middle pedal phalanx of *P. anak* and *W. bicolor* are relatively very broad with medial-lateral flaring, resulting in a very broad proximal end.

...Continued on the next page

TABLE 3. (Continued)

#	Character description	Character states	Details
84	Shaft of distal pedal phalanx IV	Broad, with rounded-triangular peak (0); tall, with sharp triangular peak (1); broad, gently dorsoventrally compressed, dorsal surface with very slight peak to smoothly rounded (2).	Distal pedal phalanges differ between species of *Protemnodon* and other macropodines in their height and in strength of peak on dorsal surface, which varies from rounded and smoothly convex to distinctly pointed and triangular in cross-section.
85	Curvature of shaft of distal pedal phalanx IV	Straight/not curved plantarly (0); curved gently to moderately plantarly (1); curved slightly dorsally before curving moderately plantarly toward tip (2).	Shaft of distal pedal phalanx IV is variable in its plantar/dorsoplantar curvature. Gauged in lateral view.

Supplementary Data

Supplementary Materials. The following supporting information can be downloaded with the DOI links provided.

Character Matrix—https://doi.org/10.6084/m9.figshare.25441243
Measurement dataset—https://doi.org/10.6084/m9.figshare.25441240